

**Structural Determination of Highly
Flexible Oxylipin Natural Products
via Computationally-Guided
Synthesis**

Liam A. McLean

PhD Thesis

2019

Author Declaration

This thesis is the result of the author's original research. It has been composed by the author and has not been previously submitted for examination which has led to the award of a degree.

The copyright of this thesis belongs to the author under the terms of the United Kingdom Copyrights Acts as qualified by University of Strathclyde Regulation 3.50. Due acknowledgment must always be made of the use of any material contained in, or derived from, this thesis.

Liam A. McLean

16/08/2019

Abstract

A programme of work to further our research towards the total synthesis of (–)-mucosin, a highly flexible oxylipin, has been carried out. This resulted in the investigation of multiple synthetic strategies to afford the desired natural product. These strategies all involved the use of the Kerr group's magnesium bisamide-mediated asymmetric deprotonation methodology as an efficient transformation to introduce asymmetry in our synthesis, and to facilitate the synthesis towards (–)-mucosin. Additionally, the group's magnesium carbon-centered base technology was employed in this work, to aid in delivering the natural product.

Following publications from independent researchers, there was strongly compelling evidence suggesting (–)-mucosin had been incorrectly assigned. Considering this, computational chemistry was employed to allow us to propose a probable structure for (–)-mucosin by comparing calculated NMR spectral data with the experimental data available in the chemical literature. Multiple quantitative approaches towards assigning probabilities to possible candidate structure were assessed.

Having evaluated the performance of computational chemistry in predicting the structure of conformationally-flexible oxylipins, work then focused on employing this on the natural product, dictyosphaerin. Dictyosphaerin, an oxylipin structure bearing two flexible sidechains, has never had its relative stereochemistry proposed, prior to this work. Using computational chemistry, we were able to propose probable candidate structures for dictyosphaerin, before embarking on our synthetic work. Using a convergent strategy, employing multiple organometallic mediated transformations, a route towards dictyosphaerin was quickly established. Upon the synthesis of dictyosphaerin methyl ester, and comparison of our experimental data to that collected during the isolation, we were able to provide strong evidence in favour of our computationally proposed structure.

Acknowledgements

Initially, I would like to give my utmost thanks to Professor William J. Kerr for taking me on as a PhD student and for giving me such an interesting research project to allow me to develop as a chemist. I am incredibly grateful for all the opportunities you have given me.

I would like to thank Dr David M Lindsay for his day-to-day support within the laboratory and always being available to talk about chemistry and discuss strategy when moving forward. Additionally, I am hugely grateful to you for taking the time to meticulously read through this thesis, and for your help in shaping it into a piece of work that I am proud of. I am also thankful to Dr Laura Paterson for her day-to-day support, helpful suggestions and advice regarding chemistry.

I would like to say thanks to all the Kerr group members, past and present, that have helped create the experience I have had during my PhD. I wish you all the best in your future endeavours. I would like to extend special thanks to Gary Knox, Adele Queen and Raymond Chung. Gary, I could not have asked for a better friend throughout my PhD. Thank you for being available to discuss chemistry with me in the lab, and during unsociable hours. Outside of the lab, you've always been a good friend to me. I have enjoyed our conversations and our somewhat questionable humour. Adele, it was always great to work in the adjacent hood to you, and to fight over the custody of Mega-Büchi. Importantly, you have always been kind to me and have always cared about my wellbeing, for this, I am incredibly grateful. Raymond, my total synthesis "brother-in-arms", it has been great to have someone who understands the unique challenges of total synthesis. I will always appreciate you being in the lab on the weekend, particularly for our discussions regarding steaks.

A special thanks goes to Craig Irving, for his dedication to running the fantastic NMR service available at the University of Strathclyde. Thank you for always being helpful, even on a Friday evening when my sample has, once again, got stuck just as you have left for the weekend. Additionally, I will miss our in-depth discussions on almost any topic.

Professor Glenn Burley, thank you for all your insightful conversations on chemistry and for all your less insightful conversations.

Thanks also goes to Dr Andrew Sutherland at the University of Glasgow, who has been helpful in supplying chemicals and allowing me access to equipment when there was an issue at the University of Strathclyde.

I would like to extend thanks to Dr Sebastien Campos and Dr Gemma White, for helping to make my three-month placement at GlaxoSmithKline, Stevenage a fulfilling experience.

Finally, I will never be able to thank my family enough for all the love and support throughout my life. I have always looked up to your drive to work hard, no matter how unreasonable it may have seemed to other people. I could not have asked for a better mum, dad and brother.

Abbreviations

Ac	acetyl
Aq	aqueous
BBN	9-borabicyclo(3.3.1)nonane
Bn	benzyl
BPi	bis(pinacolato)diboron
Bu	butyl
C	centrosymmetric
cm	centimetre
CMAE	corrected mean absolute error
Cp	cyclopentadienyl
CV	column volume
D	dextrorotatory
DCM	dichloromethane
DEAL	diethyl aluminium
<i>Di</i> CE	diastereomeric <i>in silico</i> chiral elucidation
DIPA	di- <i>iso</i> -propylamine
DIPT	di- <i>iso</i> -propyl tartrate
DFT	density functional theory
(DHQD) ₂ PHAL	hydroquinidine 1,4-phthalazinediyl diether
DMAP	4-dimethylaminopyridine
DMF	<i>N,N</i> -dimethylformamide
DMPU	1,3-dimethyl-3,4,5,6-tetrahydro-2(1 <i>H</i>)-pyrimidinone
DMSO	dimethyl sulfoxide

DPEN	1,2-diphenyl-1,2-ethylenediamine
Dppf	1,1'-ferrocenediyl-bis(diphenylphosphine)
d.r.	diastereomeric ratio
E	electrophile
ee	enantiomeric excess
EQ	external quench
eq	equivalents
e.r.	enantiomeric ratio
ESI	electrospray ionisation
Et	ethyl
FTIR	Fourier transform <i>infra</i> -red
g	grams
GIAO	gauge-independent atomic orbital
h	hours
HSQC	heteronuclear single quantum coherence
HMBC	heteronuclear multiple bond correlation
HMDS	hexamethyldisilazane
HMPA	hexamethylphosphoramide
HPLC	high performance liquid chromatography
HRMS	high resolution mass spectrometry
IPA	<i>iso</i> -propylalcohol
<i>i</i> Pr	<i>iso</i> -propyl
IR	<i>infra</i> -red
IQ	internal quench

Ipc	<i>iso</i> -pinocampheyl
L	levorotatory
LiAlH ₄	lithium aluminium hydride
LDA	lithium di- <i>iso</i> -propylamide
M	molar
MAE	mean absolute error
MCMC	Monte Carlo multiple minimum
Me	methyl
Mes	mesityl
mg	milligrams
MHz	megahertz
min	minutes
mL	millilitres
MMFF	Merck molecular force field
mmol	millimoles
m.p.	melting point
Ms	methanesulfonyl
NMR	nuclear magnetic resonance
	s singlet
	d doublet
	dd doublet of doublets
	dt doublet of triplets
	t triplet
	q quartet

	p	pentet
	sept	septet
	m	multiplet
NOESY		nuclear overhauser spectroscopy
PCM		polarisable continuum model
Ph		phenyl
ppm		parts per million
rt		room temperature
R.T.		retention time
TBS		<i>tert</i> -butyldimethylsilane
^t Bu		<i>tert</i> -butyl
THF		tetrahydrofuran
TBAF		tetra- <i>n</i> -butylammonium fluoride
TES		triethylsilyl
Tf		triflyl
TLC		thin layer chromatography
TMS		trimethylsilyl
Ts		tosyl
UV		ultraviolet

Contents

Author Declaration	i
Abstract	ii
Acknowledgements	iii
Abbreviations	v
Chapter One	1
1.1. Introduction.....	1
1.1.1. Asymmetric Synthesis.....	1
1.1.2. Transition States in an Asymmetric Process.....	6
1.1.3. Asymmetric Deprotonation Chemistry of Ketones	9
1.1.4. Chiral Lithium Amide Chemistry	11
1.1.5. Chiral Magnesium Amide Chemistry.....	16
1.1.6. Metal-Mediated Deprotonations	19
1.1.7. (–)-mucosin	23
1.1.8. Previous Work Within the Kerr Group	39
1.1.9. Proposed Work.....	43
1.2. Results and Discussion	49
1.2.1. Synthesis of Key Bicyclic Ketone Intermediate 72	49
1.2.2. Synthesis of the Allyl Bromide Intermediate 126	50
1.2.3. Application of Magnesium-Bisamides in Asymmetric Deprotonation	57
1.2.4. sp^2 - sp^3 cross-coupling	65
1.2.5. Investigation of a Cross-Metathesis Strategy	74
1.2.6. sp^3 - sp^3 cross-coupling	85
1.3. Conclusions.....	92
1.4. Experimental	99
1.4.1. Synthesis of Key Bicyclic Ketone Intermediate 72	100
1.4.2. Synthesis of the Allyl Bromide Intermediate 126	104
1.4.3. Application of Magnesium-Bisamides in Asymmetric Deprotonation Chemistry 112	
1.4.4. sp^2 - sp^3 cross-coupling	128
1.4.5. Investigation of a Cross-Metathesis Strategy	142
1.4.6. sp^3 - sp^3 cross-coupling	156

1.5. References	163
Chapter Two	168
2.1. Introduction	168
2.1.1. Calculation of NMR Chemical Shifts	168
2.1.2. Elatenyne	170
2.1.3. DP4	172
2.1.4. DP4+	174
2.1.5. DP4.2	176
2.1.6. DiCE	178
2.1.7. Proposed Work	179
2.2. Results and Discussion	181
2.3. Conclusion	195
2.4. Experimental	197
2.4.1. Details of Computational Methods	197
2.4.2. Details of Statistical Analysis	199
2.4.3. Tables of Calculated Isotropic Shielding Constants and Probabilities	202
2.5. References	209
Chapter Three	213
3.1. Introduction	214
3.1.1. Dictyosphaerin	214
3.1.2. Proposed Work	214
3.2. Results and Discussion	218
3.2.1. DP4 Analysis of Dictyosphaerin	218
3.2.2. Synthesis of the Enol Triflate	222
3.2.3. Synthesis of the Boronic Ester	228
3.2.4. Completing the Convergent Strategy	239
3.2.5. Structural Determination of Dictyosphaerin	242
3.3. Conclusion	249
3.4. Future Work	255
3.5. Experimental	256
3.5.1. Details of Computational Methods	256
3.5.2. Details of Statistical Analysis	257
3.5.3. Tables of Calculated Shielding Tensors and Probabilities	260

3.5.4.	Synthesis of the Enol Triflate.....	265
3.5.5.	Synthesis of the Boronic Ester.....	278
3.5.6.	Completing the Convergent Strategy.....	304
3.5.7.	Structural Determination of Dictyosphaerin.....	308
3.6.	References.....	324

Chapter One

Towards the Total Synthesis of (–)-Mucosin

1.1. Introduction

1.1.1. Asymmetric Synthesis

Chirality is an important feature of biologically active systems. Many vital components of life, such as DNA and proteins, are present as a single enantiomer and can only carry out their biological function as a specific enantiomer. Additionally, considering chirality when designing new pharmaceuticals is important to enhance potency and avoid potential undesired side-effects. As such, the control of chirality in chemical synthesis has been a heavily studied area of chemical research. Achieving effective stereocontrol during synthesis, requires the introduction of a chiral environment in a chemical transformation. A number of strategies exist within the chemical literature to allow for the creation of a chiral environment to allow for the synthesis of molecules with high enantio-purity.

1st Generation Asymmetric Synthesis

Control of the formation of a new stereocentre within a molecule is typically carried out using four different methods, which are divided up into “generations”.¹ The 1st generation of asymmetric synthesis - chiral pool - employs starting materials with the stereochemical information already set in place. These materials are abundant in nature and can come, for example, in the form of amino acids, sugars or terpenes (Figure 1). Manipulation of such so called “chiral pool” starting materials using achiral reagents can provide easy integration of stereochemical information into the desired product. Having said this, manipulation of chiral pool materials can also involve long syntheses, i.e. the use of sugars in synthetic routes usually involves laborious protecting group strategies and various redox steps, throughout which the chemist has to ensure that the stereochemical integrity remains intact.

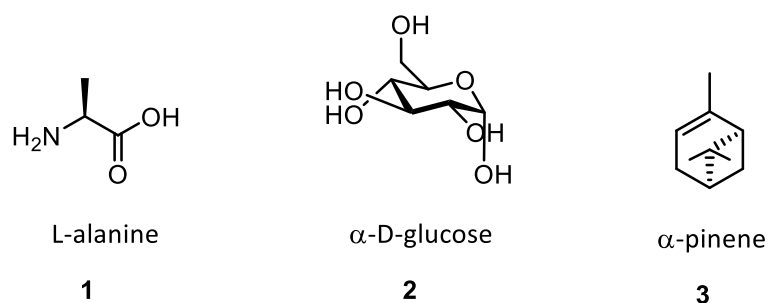
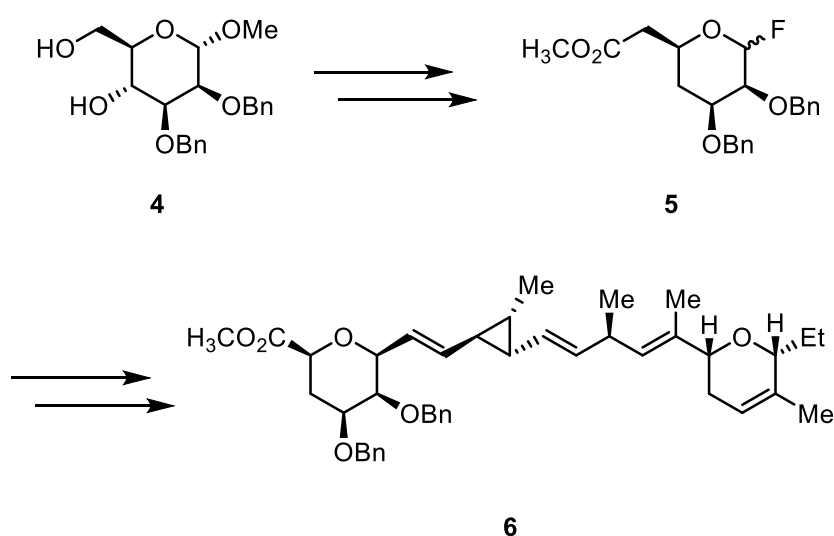


Figure 1 - Examples of chiral pool materials

The total synthesis of (+)-ambruticin **6**, a carbohydrate derivative with nine stereocentres, by Kende *et al.* is an example of an asymmetric synthesis involving a sugar from the chiral pool.² The synthesis

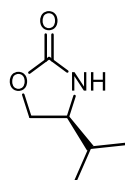
involved nine transformations from methyl α -glucopyranoside **4** to afford the fluorinated compound **5** (Scheme 1). These transformations resulted in the loss of multiple chiral centres from the starting material and the bulk of the chemical manipulations consisted of protecting group chemistry and redox chemistry. Despite this, Kende and co-workers were able to access (+)-ambruticin **6** over 32 steps using a convergent synthetic strategy by drawing from the chiral pool. Despite being a readily available source of stereochemically-rich materials, the use of compounds from the chiral pool has drawbacks. Typically, the use of chiral pool materials in synthesis requires multiple synthetic transformations to be useful to the synthetic chemist. Additionally, these synthetic transformations often include atom-inefficient protecting group strategies and can result in the loss of stereocentres from the chosen chiral pool starting material.



Scheme 1 - Use of sugars in the total synthesis of (+)-Ambruticin

2nd Generation Asymmetric Synthesis

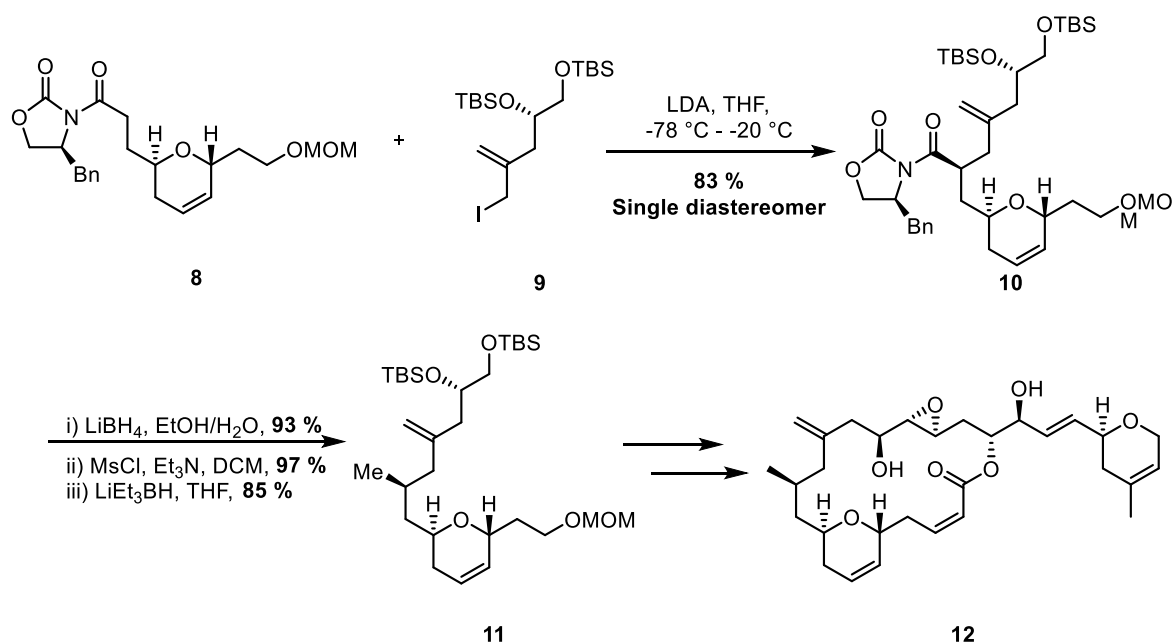
To overcome the pitfalls of 1st generation asymmetric synthesis, 2nd generation asymmetric synthesis involves the use of chiral auxiliaries. A chiral auxiliary is a group that can be attached to a molecule to direct the stereochemical outcome of subsequent reactions, before being removed. An important aspect in the design of chiral auxiliaries is that they must be easy to attach, as well as to remove and recover. An example of a chiral auxiliary, and one of the most widely used, is the Evans oxazolidinone (Figure 2). The use of oxazolidinone auxiliaries has been employed to facilitate highly diastereoselective alkylation, aldol, and Diels Alder transformations.³



7

Figure 2 - An example of an Evans' oxazolidinone chiral auxiliary

The use of an Evans auxiliary is showcased in the synthesis of the C₁-C₁₆ fragment of Laulimalide **12**, a marine toxin from the Indonesian sponge, *Hyattella sp.*⁴ Nishiyama and Shimizu employed an Evans auxiliary to facilitate the convergent synthesis of **11** *via* a stereoselective alkylation (Scheme 2). The stereoselective alkylation allowed the transformation of **8** to the single diastereomer **10** in a high yield of 83 %, highlighting the utility of chiral auxiliaries in asymmetric synthesis. Subsequently, through clever manipulation of the oxazolidone Nishiyama *et al.* were able to remove the auxiliary by cleavage to the corresponding alcohol, which is then converted into the methyl group required at the C-30 stereogenic centre, present in Laulimalide **12**.⁴ Due to the wide scope of chemistry involving the use of auxiliaries, it would be challenging to do the area justice within this review, however, many excellent reviews highlight the elegant chemistry in this area.³



Scheme 2 - Partial synthesis of Laulimalide facilitated with chiral auxiliaries

Chiral auxiliaries are still employed in synthesis today but being able to induce stereochemistry *via* the use of chiral reagents would provide a more elegant route into the synthesis of stereogenic centres.

3rd Generation Asymmetric Synthesis

3rd generation asymmetric synthesis involves the use of chiral reagents. This strategy avoids the need to synthesise chiral auxiliaries, attach them to molecules which may have taken great synthetic effort to prepare, perform the desired transformation and then remove the chiral auxiliary. All of these steps reduce the overall yield of a synthetic route, which is undesirable to the chemist. An example of a transformation involving a chiral reagent is the Paterson aldol reaction. The Paterson aldol transformation involves the use of chiral boron reagent **13** to allow highly enantioselective aldol reactions to be performed.⁵ Despite the success of 3rd Generation methods, these all involve the use of stoichiometric quantities of expensive chiral reagents.

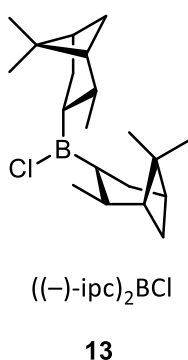
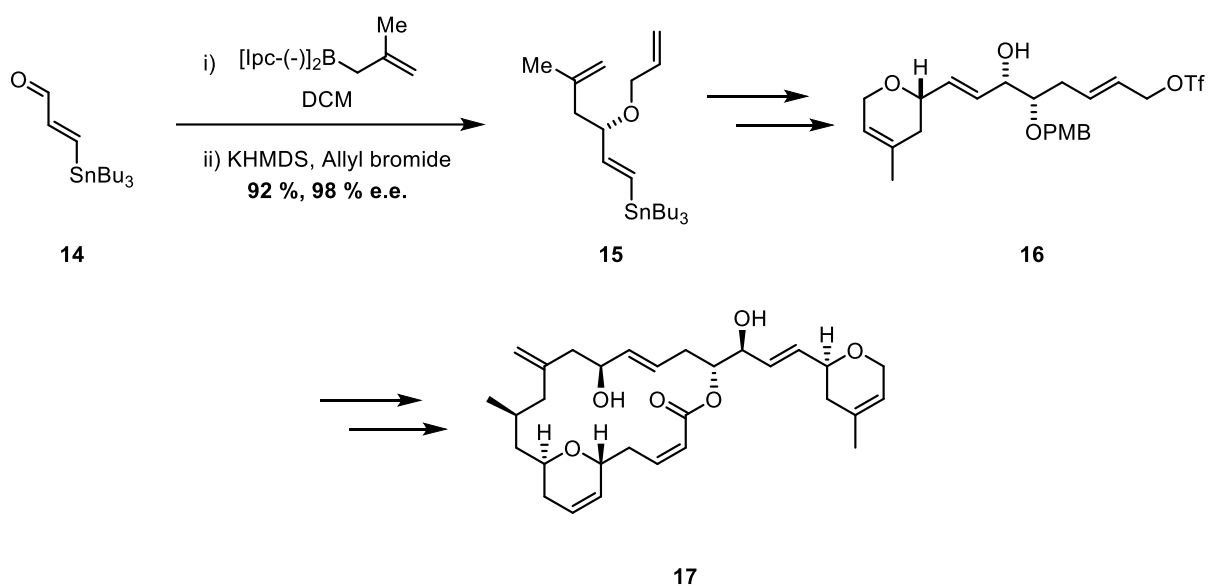


Figure 3 - An example of a chiral reagent utilised in the Paterson Aldol

Following on from the previously mentioned partial synthesis of laulimalide **12** by Nishiyama *et al.*, an alternative strategy by Nelson *et al.*, in 2002, employed Brown's crotylation methodology to successfully achieve a formal synthesis of laulimalide **12**.⁶ The asymmetric crotylation and subsequent etherification delivered triene **15** in excellent yield and enantioselectivity (Scheme 3). Following subsequent transformations, fragment **16** was delivered, and through a convergent synthetic strategy, allowed for the synthesis of laulimalide over 16 steps with an overall yield of 5.4%.⁶ Nelson's elegant synthesis highlights the effectiveness that 3rd generation, reagent-controlled stereochemical induction can have in the synthesis of advanced chiral intermediates.



Scheme 3 - Application of chiral reagents in the formal synthesis of Lualimalide

4th Generation Asymmetric Synthesis

The development of catalytic chiral synthesis became immensely popular as it overcame the need to use stoichiometric quantities of chiral reagents. The use of catalytic asymmetric synthesis is known as the 4th generation of asymmetric synthesis. The Sharpless asymmetric dihydroxylation is an excellent example of a 4th generation method, whereby sub-stoichiometric quantities of a chiral ligand-bound OsO_4 complex is used to asymmetrically dihydroxylate olefins (Figure 4).⁷

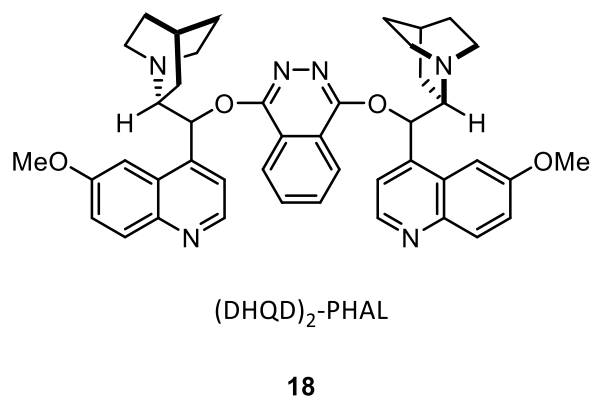
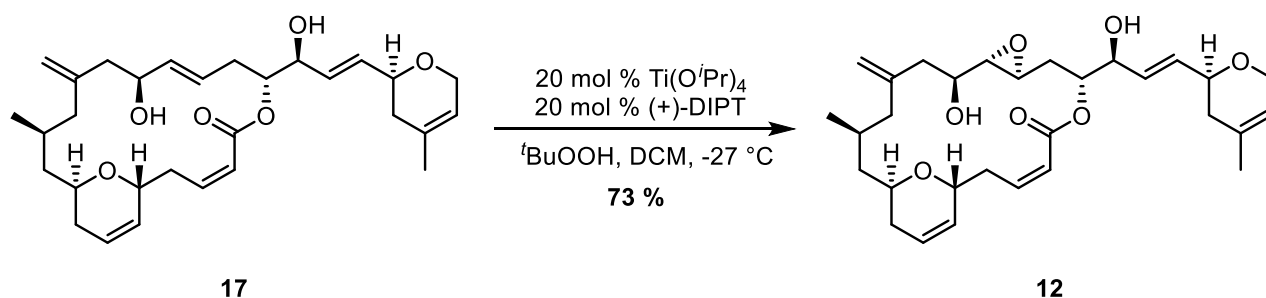


Figure 4 - Chiral ligand used in Sharpless' asymmetric dihydroxylation

Paterson's total synthesis of Lualimalide **12** concludes with an example of 4th generation asymmetric synthesis methodology (Scheme 4).⁸ The final epoxidation reaction in Paterson's synthesis is mediated by a catalytic Sharpless epoxidation. Employing sub-stoichiometric quantities of both the metal and ligand, and stoichiometric quantities of the *tert*-butyl hydroperoxide, Paterson effectively furnished

lailimalide **12** in an excellent 73 % yield. This example is remarkable considering the precursor has six olefins which could be epoxidised, two of which are allylic alcohols, for which Sharpless epoxidation methodology is selective. Paterson's synthetic sample was shown to be identical to the natural product when compared to the physical and spectroscopic data Higa *et al.* had obtained from the authentic sample.⁹

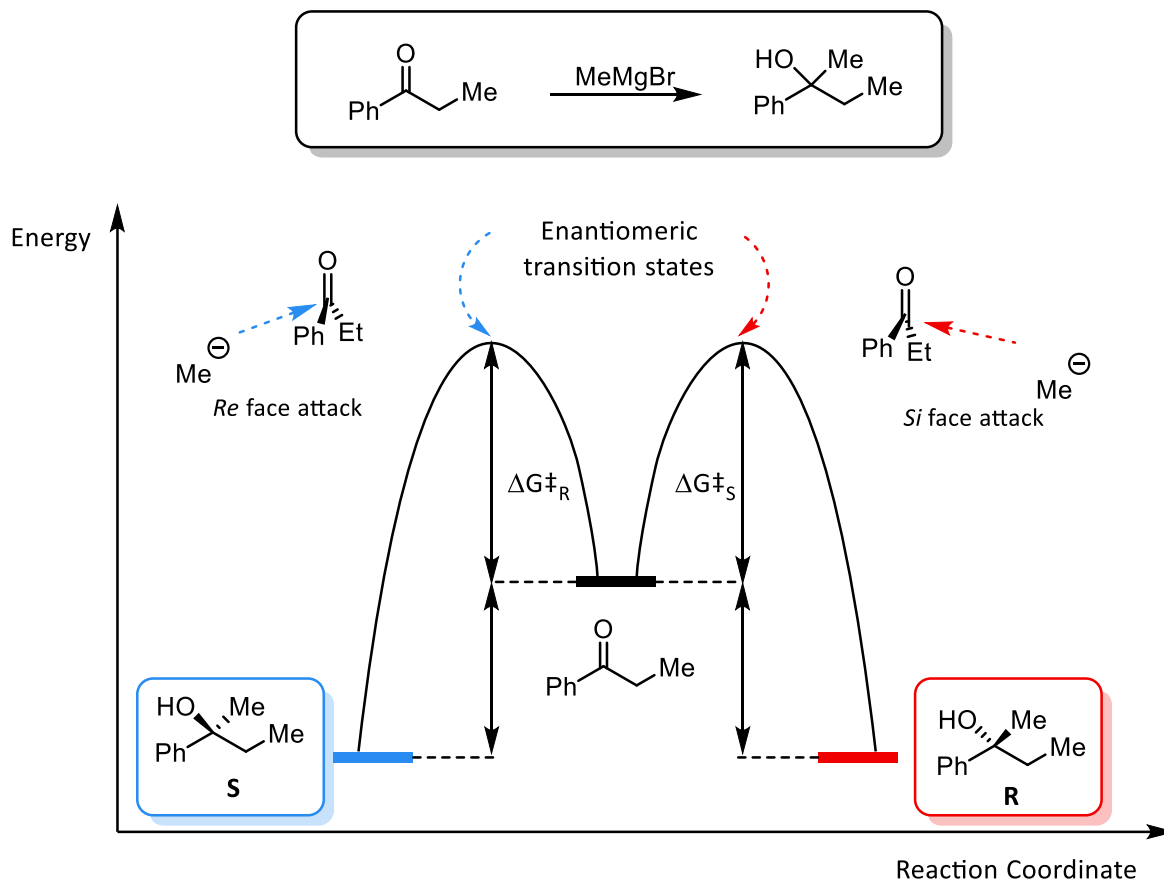


Scheme 4 - Catalytic asymmetric epoxidation utilised in the total synthesis of lailimalide

1.1.2. Transition States in an Asymmetric Process

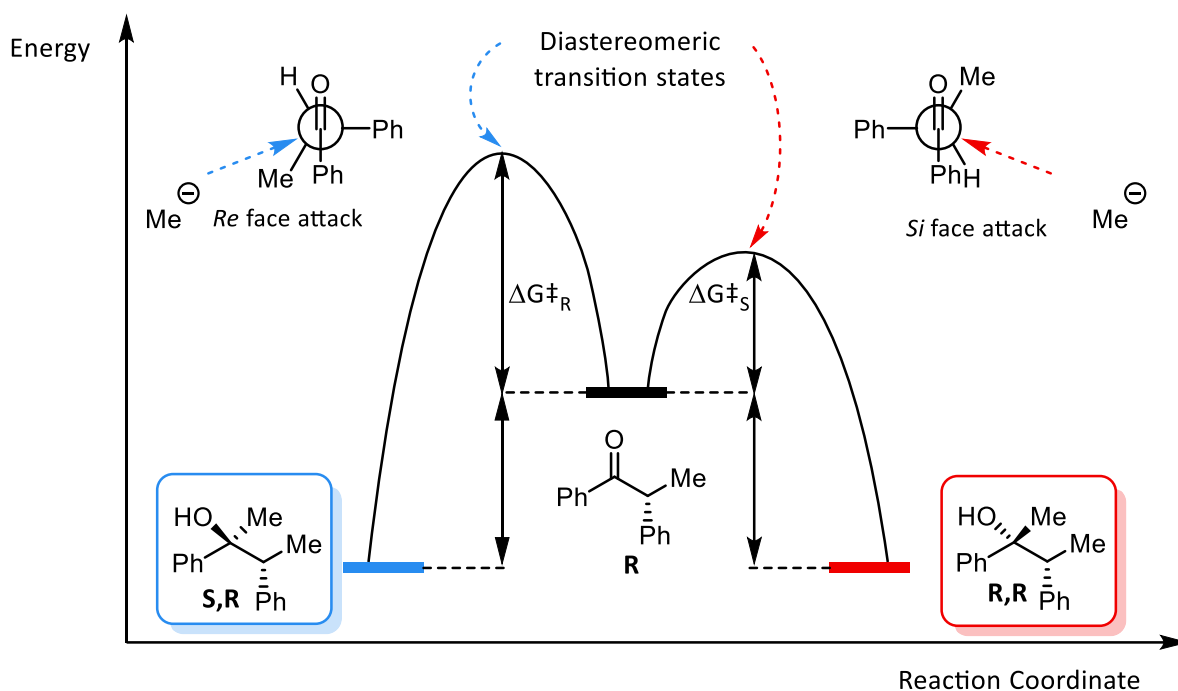
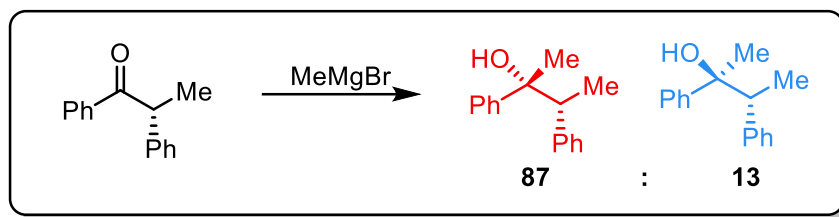
Diastereomeric Transition States

In order to understand how asymmetry can arise in a chemical transformation, we need to understand the transition states involved in the reaction coordinates. In the example of a nucleophilic addition to a prochiral ketone, there are two possible approaches the nucleophile can make. The nucleophile can attack from either the *Re* or the *Si* face and in the case of a prochiral ketone, either attack has no energetic preference as the transition states are in fact mirror images of one another, hence “enantiomeric transition states”.¹⁰ Therefore the nucleophilic attack on a prochiral ketone affords a racemic mixture of the corresponding product (Scheme 5).



Scheme 5 - An example reaction with enantiomeric transition states throughout the reaction coordinate

In a stereoselective process, such as a nucleophilic attack of a chiral ketone, diastereomeric products are now possible. Diastereomeric products are possible due to a stereoselective process proceeding through “diastereomeric transition states” which are not equal in energy and do in fact lead to a diastereomeric mixture of products.¹⁰ In the case of a nucleophilic attack on a chiral ketone, the nucleophile prefers the least hindered approach to the ketone, as shown by the Newman projections (Scheme 6). In this example, the nucleophile prefers *Si* face attack and hence the transition state involving a *Si* face attack is in fact lower in energy than the transition state involving *Re* face attack. This is an example of the Curtin-Hammett principle, which states that it is the relative energies of the transition states that control selectivity and not the relative energies of the starting materials.¹⁰



Scheme 6 - An example reaction with enantiomeric transition states throughout the reaction coordinate

The relationship between the ΔG^\ddagger and enantioselectivity can be further illustrated mathematically. If we understand that a stereoisomeric ratio is the ratio between the rate constants of the respective diastereomeric pathways, a rate constant can be expressed by the Arrhenius equation:

$$k = Ae^{\frac{-\Delta G^\ddagger}{RT}}$$

k = rate constant
 A = pre-exponential factor
 ΔG^\ddagger = free energy of activation
 R = gas constant
 T = temperature

Equation 1 - Arrhenius Equation

Substituting the Arrhenius equation into the stereoisomeric ratio, illustrates that the enantiomeric or diastereomeric ratio is proportional to the difference in Gibbs free energy between the two

diastereomeric transition states. It also highlights that the enantiomeric or diastereomeric ratio is inversely proportional to the temperature.

$$\text{e. r. or d. r.} = \frac{k_R}{k_S} = e^{\frac{-(\Delta G^\ddagger_R - \Delta G^\ddagger_S)}{RT}} = e^{\frac{-\Delta\Delta G^\ddagger}{RT}}$$

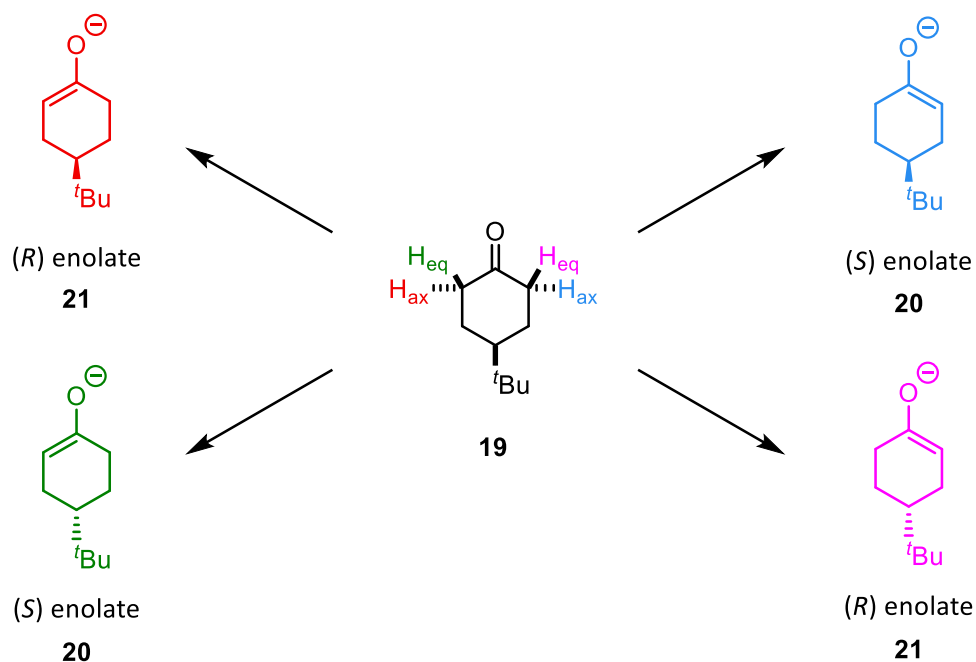
Equation 2 - Stereoisomeric ratios described using the Arrhenius equation

Practically, this means that a stereoselective reaction run at a decreased temperature should give a higher enantiomeric excess than the respective control reaction.

1.1.3. Asymmetric Deprotonation Chemistry of Ketones

Use of Conformationally Locked Ketones

The asymmetric deprotonation of conformationally locked ketones has been heavily researched within our laboratories, due to its utility in transforming various prochiral ketone substrates into chiral products. This asymmetric process is underpinned by the differentiation of four different protons α to the ketone. In the example of 4-*tert*-butylcyclohexanone **19**, there is a stereoelectronic preference for the axial protons to be deprotonated over the equivalent equatorial protons (Scheme 7).



Scheme 7 - Products resulting from the deprotonation of 4-*tert*-butylcyclohexanone

4-*tert*-Butylcyclohexanone **19** has become a benchmark substrate in asymmetric deprotonation methodology. As shown in Scheme 7, the deprotonation of 4-*tert*-butylcyclohexanone could proceed through the deprotonation of four different protons, the axial and equatorial protons α to the ketone, resulting in either the (*R*) or (*S*)-enolate. However, the large 4-*tert*-butyl group prevents the ring from flipping due to its strong preference to be equatorial, resulting in a conformationally locked ring system. The conformationally locked ring system ensures that only the axial protons, and not the equatorial ones after a “ring-flip”, can be deprotonated in preference to the equatorial protons due to the nature of the electronics in the ring system (Figure 5).

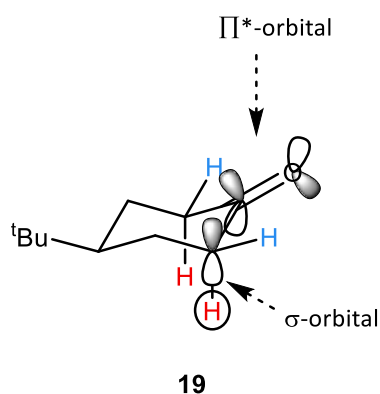
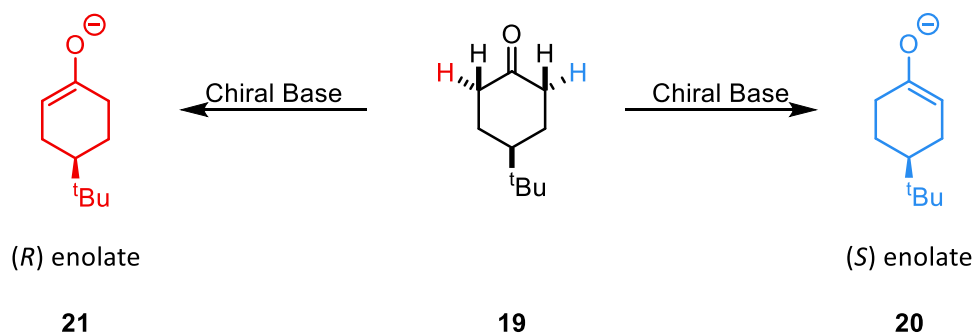


Figure 5 - 4-*tert*-butylcyclohexanone depicting orbital overlap with axial protons

As shown in Figure 5, the π^* – orbital of the carbonyl moiety overlaps favourably with the σ orbital of the axial C-H bond. This overlap makes the axial protons α to the ketone more acidic and thus more susceptible to deprotonation.¹¹ This electronic preference in 4-*tert*-butylcyclohexanone **19** gives a preference for the axial protons. Therefore, when a chiral environment is introduced, for example using a chiral base, diastereomeric transition states are induced, allowing further discrimination over the two individual axial protons and, thus, the preferential formation of one enantiomeric enolate over another (Scheme 8).



Scheme 8 - Potential enolates formed from a deprotonation

In asymmetric deprotonation chemistry, 3rd generation asymmetric synthesis has dominated with the use of chiral lithium amide chemistry, where the amine ligand is the source of the chiral environment in the transformation. Chiral lithium amide chemistry was developed independently by Koga and Simpkins.^{12,13} In our laboratories, the use of magnesium amide bases has overcome some of the drawbacks of chiral lithium amide chemistry, which will be discussed in further detail within the following sections of this report.

1.1.4. Chiral Lithium Amide Chemistry

Initial developments of Chiral Lithium Amide Chemistry

The first report of the asymmetric deprotonation of a prochiral ketone using a chiral lithium amide was by Koga *et. al.*, in 1986.¹² In Koga's initial publication he described the use of twelve different chiral lithium amide bases, where all of the corresponding amines were designed around a similar core and their substituents were varied (Figure 6).

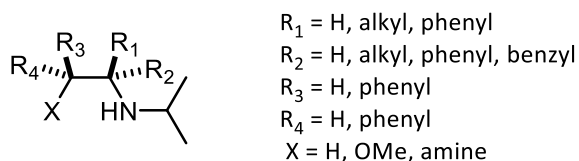
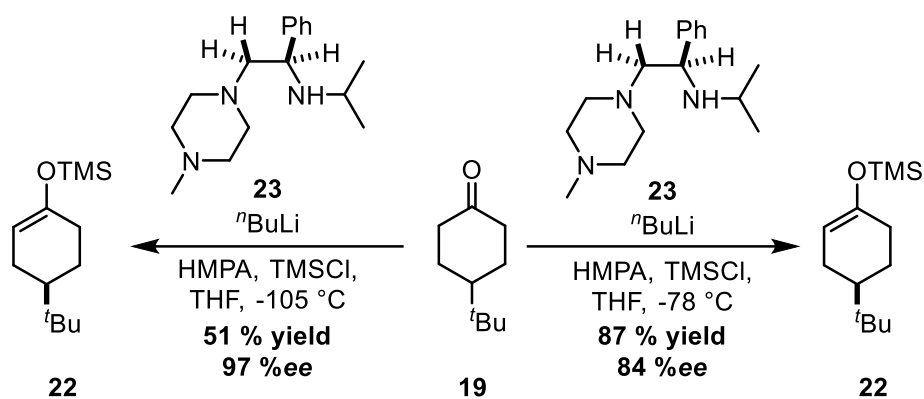


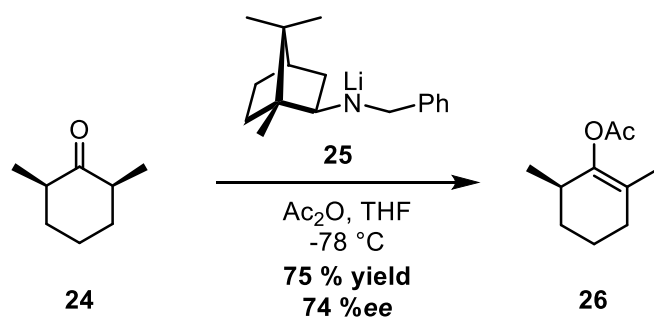
Figure 6 - Amines designed by Koga *et al.* for utilisation in chiral lithium amide chemistry

Koga's twelve chiral amines were employed in asymmetric deprotonation reactions of **19** involving an internal quench procedure with TMSCl, and it was found that chiral amine **23** gave the best results, with an 87 % yield and an enantiomeric excess of 84 % (Scheme 9). Additionally, upon performing this reaction at a reduced temperature of -105 °C, it was shown that the enantiomeric excess increased to an impressive 97 %. This increase in enantiomeric excess fits with the inversely proportional relationship between temperature and enantiomeric excess (*vide supra*).¹² Despite the initial success of Koga's methodology, drawbacks included the requirement of HMPA as an additive, which has shown to be highly carcinogenic and its use in industry is banned.¹⁴ Additionally, Koga's requirement to cool to -105 °C to achieve high enantiomeric excess is an expensive hindrance in practical terms.



Scheme 9 - Koga et al. best results using chiral lithium amide chemistry

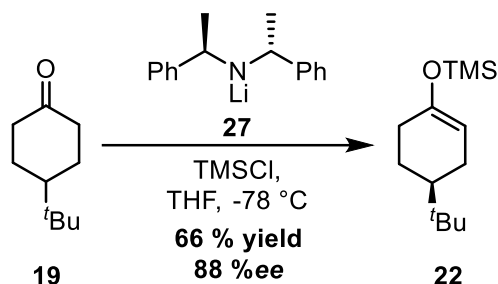
Another researcher in the field of asymmetric deprotonation, who also published work in 1986, was Nigel S. Simpkins.¹³ His initial work in this area involved the desymmetrisation of 2,6-dimethylcyclohexanone **24**, employing amine bases without a chelating heteroatom, differing from Koga's protocol (Scheme 10). The Simpkins methodology diverged from Koga's in several ways: (i) there was no requirement for additives such as HMPA; (ii) the resulting lithium enolates were quenched with Ac_2O , *via* an external quench procedure, which allowed for a more straightforward determination of enantiomeric excess by ^1H NMR analysis; and (iii) the most successful lithium amide was derived from camphor. In comparison to Koga's work, the Simpkins' methodology delivers lower yields and a lower enantiomeric excess but as previously stated circumvents the need for highly toxic additives (Scheme 10).



Scheme 10 - Simpkins' use of homochiral amines in lithium amide chemistry

Following his initial publication, in 1989 Simpkins expanded his chiral amine base scope to include a C_2 symmetric base **27**, and amended his quench protocol to an internal quench with TMSCl (Scheme 11). Another major change in this methodology was the choice of ketone substrate. To allow a direct comparison with Koga's work he opted for 4-*tert*-butylcyclohexanone **19** as the prochiral ketone to desymmetrise.¹⁵

As shown below, Simpkins's methodology offered slightly higher enantiomeric excess over Koga's work but had a detrimental impact on the yield, giving only a 66 % yield, compared to Koga's best yield of 87 %.^{12,15}

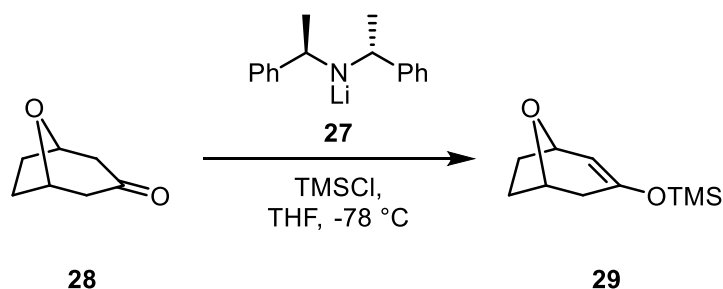


Scheme 11 - Simpkins' use of C₂ symmetric amines in lithium amide chemistry

From comparison of both Simpkins's and Koga's respective methodologies it could be suggested that the addition of HMPA increases the reactivity of lithium amide bases, as shown by the increased yield observed in Koga's work.

The Effect of Additives on Asymmetric Deprotonations

In 1991, Simpkins continued to extend his methodology to include the asymmetric deprotonation of oxabicyclooctanone systems, such as **28** (Scheme 12).¹⁶ By 1993, he showed that, depending on the electrophilic quench technique varying degrees of enantiomeric excess could be achieved. As shown below, using an internal quench technique, whereby the electrophile is present in the reaction mixture from the beginning, gave a good yield and enantiomeric excess (Table 1, Entry 1). Alternatively, employing an external quench protocol, where stoichiometric amounts of the lithium enolate is generated in the reaction mixture and then quenched with an appropriate electrophile, good yields were obtained, but with a significantly diminished enantiomeric induction (Table 1, Entry 2). However, Simpkins did note that, with the use of an external quench protocol and LiCl as additive, which is produced continually using an internal quench, analogous results to the internal quench were obtained (Table 1, Entry 3).



Scheme 12 – Simpkins' work on oxabicyclooctanone systems

Table 1 - Results from Simpkins' work regarding alternative quench techniques

Entry	Quench	Additive	Yield (%)	ee (%)
1	IQ	-	78	82
2	EQ	-	81	33
3	EQ	LiCl (0.1 equiv)	75	84

Following these results, Simpkins hypothesised that the aggregation states of the lithium amide species influenced the performance of the lithium amide in asymmetric deprotonation reactions. This preliminary hypothesis came with a note of caution, as Simpkins himself noted that there are a number of ionic and neutral species present in solution that could be influencing the outcome of this reaction. With this in mind, Simpkins proposed four possible aggregation species of the lithium amide in solution: the homo-dimer **30**, and three mixed aggregates, involving lithium enolate **31**, lithium chloride **32** or TMSCl **33**.¹⁷

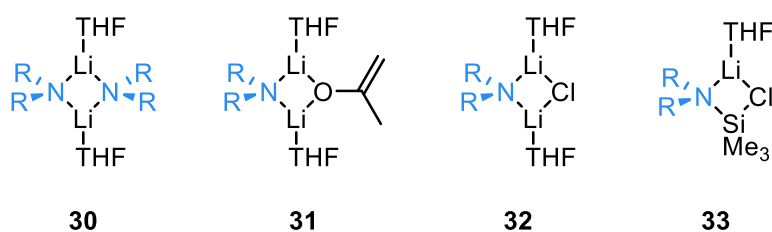
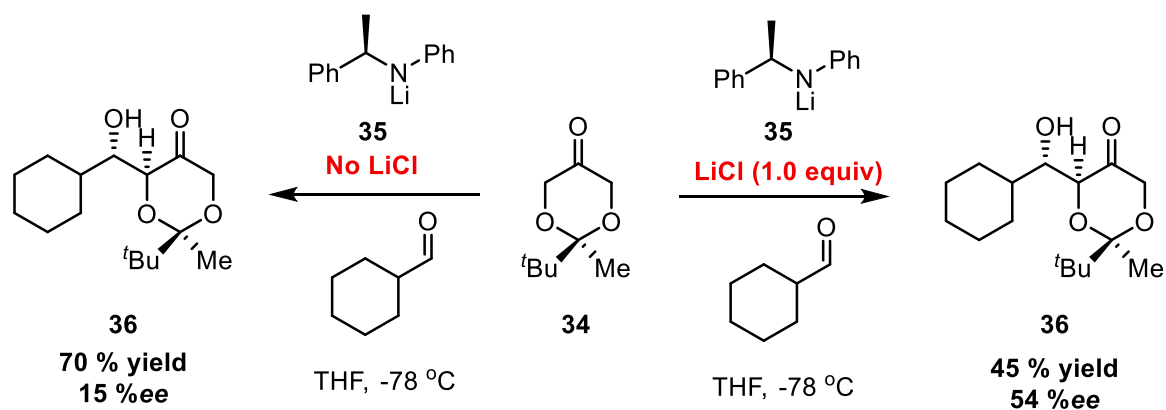


Figure 7 - Simpkins' postulated lithium aggregates

Similar results in relation to the above have been shown by other researchers, such as Marek Majewski.¹⁸ In 1995, through the development of a one-pot asymmetric deprotonation/aldol methodology, he noted that the enantioselectivity of the process was increased by the addition of LiCl before the substrate was added. As shown below, the desymmetrisation of dioxanone **34**, followed by an *in situ* aldol reaction in the presence of no LiCl, gave very limited enantioselective induction. In contrast, the presence of one equivalent of LiCl afforded moderate enantiomeric excess, albeit with reduced yields (Scheme 13).



Scheme 13 - Majewski's work highlighting the effect of LiCl additives

This result, combined with results Simpkins obtained in 1993, gives stronger credence to the hypothesis that LiCl affects the aggregation state.

Further evidence regarding the effect of Li salts on the selectivity of chiral lithium amide-mediated asymmetric deprotonations was shown in Koga's work. Through the use of ^6Li and ^{15}N NMR experiments, Koga portrayed how LiCl affects the solution state aggregation states of lithium amides.¹⁹ Indeed, Koga's work was based on Collum's previous identification of four possible lithium amide aggregates in solution; lithium amide monomer **37**, homo dimer **38** and two possible mixed aggregates **39** and **40** (Figure 8).^{20,21}

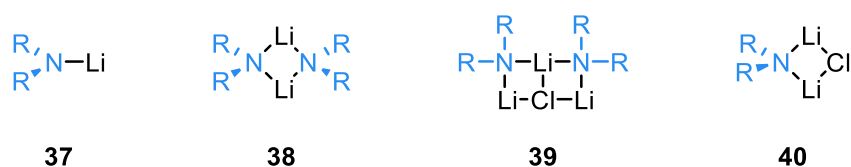


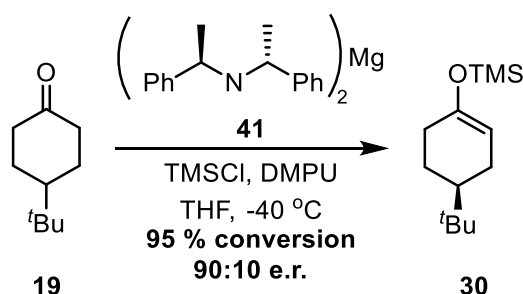
Figure 8 - Koga's proposed lithium aggregates

Koga showed that when no additive was present, only the monomer **37** and homo dimer **38** were present, which results in low enantioselectivity. In the presence of LiCl (0.6 equiv.), the formation of new peaks in the ^6Li and ^{15}N NMR spectra were detected, which correspond to the mixed aggregate species **39** and **40**.¹⁹ Through this work, Koga has inarguably shown that through careful control of the aggregation states in lithium amide asymmetric deprotonation reactions, an increase in enantioselectivity can be achieved.

1.1.5. Chiral Magnesium Amide Chemistry

Improving upon Chiral Lithium Amide Chemistry

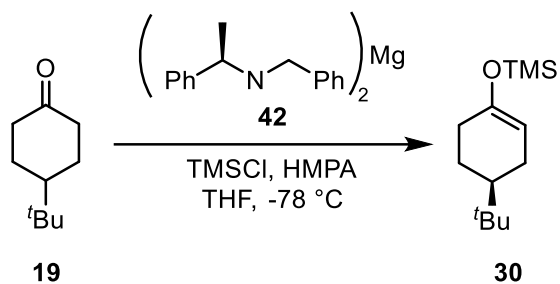
Despite the developed understanding in the field of lithium amide-mediated asymmetric deprotonations of conformationally locked prochiral ketones, there remained pitfalls that were intrinsic to this chemistry. Specifically, the complex mixture of aggregation states present with lithium amides in solution often give inconsistent reactivities and selectivities. In addition to this, there have been no reports of acceptable enantioselectivities being obtained without the requirement for very low temperatures. Running an asymmetric deprotonation at $-78\text{ }^{\circ}\text{C}$ or even $-100\text{ }^{\circ}\text{C}$ is achievable in the academic laboratory setting. However, in industry, running reactions at temperatures below $-40\text{ }^{\circ}\text{C}$ has an estimated additional cost of about £250,000 per annum per batch tonne process.²² Therefore, there remained a gap in the literature for a milder asymmetric deprotonation methodology that could operate independent of cryogenic temperatures. In 2011, asymmetric deprotonation methodology was developed within our laboratories using chiral magnesium amides, providing excellent enantiomeric ratios at $-40\text{ }^{\circ}\text{C}$. As shown in Scheme 14, the use of chiral bisamide **41** allowed the generation of silyl enol ether **22** in an excellent 95 % conversion and 90:10 e.r.²²



Scheme 14 - Kerr labs magnesium amide asymmetric deprotection

Initial Developments with a Homochiral Magnesium Amide Base

In the initial publication from the Kerr research team, a homochiral amine was employed in the formation of a magnesium bisamide **41** which was subsequently applied to mediate the desymmetrisation of 4-tert-butylcyclohexanone **19** using TMSCl as the electrophile and HMPA as an additive (Scheme 15, Table 2).²³



Scheme 15 - Magnesium-mediated asymmetric deprotonation with homochiral amines

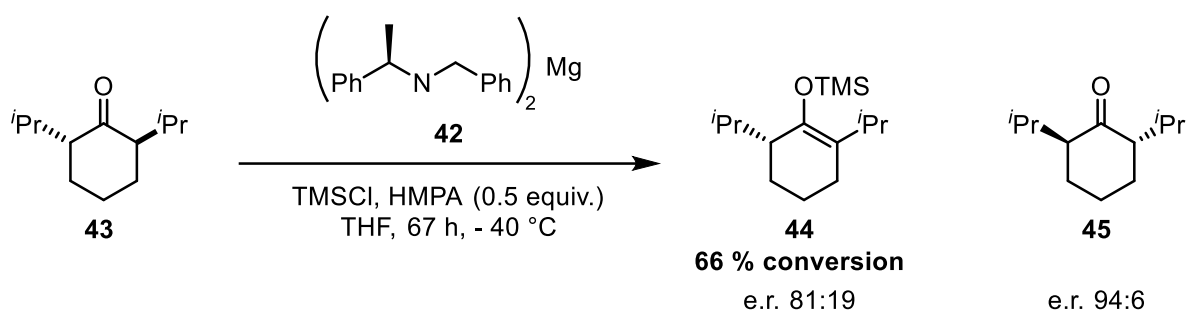
Table 2 - Optimisation of asymmetric deprotonation with homochiral amines

Entry	HMPA (equiv)	Conversion (%)	Enantiomeric ratio (e.r.) (S):(R)
1	0	33	90:10
2	0.5	82	91:9
3	1	94	86:14
4	2	26	86:14

As shown in Table 2, this chiral magnesium amide methodology provided consistently high enantiomeric ratios with and without additives such as HMPA, although the conversion was significantly hindered without an additive, suggesting that HMPA is increasing the reactivity of the chiral magnesium amide (Table 2, Entry 1 vs Entries 2-4). Although HMPA has shown to be effective in delivering good selectivities it should be noted that HMPA is considered highly toxic. With this in mind, Kerr *et al.* have also shown that no loss in selectivity is observed when switching from HMPA to DMPU.^{23,24}

Kinetic resolution of 2,6-Disubstituted Cyclohexanones with a Homochiral Magnesium Amide Base

Whilst research within the Kerr laboratories was focused on the asymmetric deprotonation of prochiral ketones, a novel kinetic resolution of *trans*-2,6-disubstituted cyclohexanones was developed employing the homochiral magnesium amide base **42**.²⁵

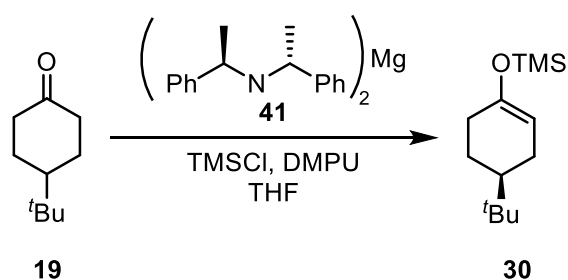


Scheme 16 - Kinetic resolution of 2,6-disubstituted ketones

As shown in Scheme 16, upon treating 2,6-di-*iso*-propylcyclohexanone **43** with homochiral magnesium amide **42** and trapping with TMSCl for 67 hours, both the TMS enol ether **44** and remaining ketone **45** are returned, optically enriched. In particular, the returned ketone **45** exhibited an excellent 94:6 e.r. This result highlights the utility of chiral magnesium amides for the kinetic resolution of racemic ketones. To date, no further work has been developed within the group in the area of kinetic resolution with magnesium bisamides, highlighting a potential area for future research.

The Development and Application of a C₂ Symmetric Magnesium Amide Base

In 2011, the Kerr laboratories reported a further development in their magnesium amide chemistry by employing a C₂ symmetric chiral amine **41** (Scheme 17).²² The use of the C₂ symmetric chiral amine afforded higher enantioselectivities than the previous homochiral amine methodology, along with excellent conversions. Additionally, the excellent substitution of HMPA for DMPU in this methodology increases the appeal of using magnesium bisamides, due to the exclusion of toxic reagents. This publication also showcased the increased thermal stability of the developed magnesium bisamide-mediated asymmetric deprotonation chemistry, displaying good selectivities even at room temperature, as shown in Table 3.



Scheme 17 – Magnesium-mediated asymmetric deprotonation with C₂ symmetric amines

Table 3 - The effect of temperature variance on magnesium-mediated asymmetric deprotonation

Entry	Temperature (°C)	Conversion (%)	Enantiomeric ratio (e.r.) (S):(R)
1	-78	97	94:6
2	-60	93	92:8
3	-40	95	90:10
4	-20	97	88:12
5	0	93	86:14
6	23	89	75:25

Considering the maturity of this methodology, research within the Kerr team has recently been centred on employing this methodology as a key transformation in the total synthesis of a natural product and it is this programme of work that will be the focus of this report.

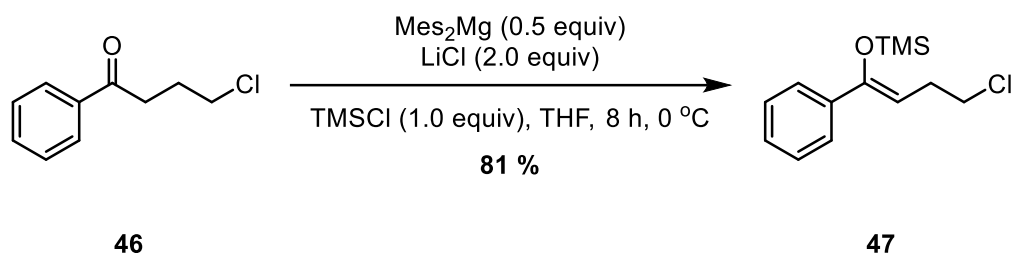
1.1.6. Metal-Mediated Deprotonations

Deprotonation of acidic C—H bonds is a key procedure in generating carbon nucleophiles for use in synthesis. Lithium di-*iso*-propyl amide (LDA) has long been the golden standard base used in deprotonations α to ketones. The reasons behind its success is the control of reactivity making it selective towards acidic protons. This reactivity is curtailed by the sterically encumbering di-*iso*-propyl amine, the di-*iso*-propyl groups prevents the amine from reacting *via* nucleophilic pathways. Despite LDA's well established chemistry and widespread use, drawbacks to the chemistry do exist. Typically when using LDA, the reactions are carried out at -78 °C due to its highly reactive nature.²⁶ It is also possible to observe undesired side reactions such as reductions of α -substituted ketones observed by Burke et al.²⁷ Another intrinsic flaw of lithium amide chemistry is the requirement for stoichiometric quantities of metal and amine.²⁶ Since the early 2000s, work within our laboratories has focused on magnesium-mediated deprotonation chemistries in order to overcome some of the drawbacks of lithium amide chemistry.

Development of Milder Metal Base Technology

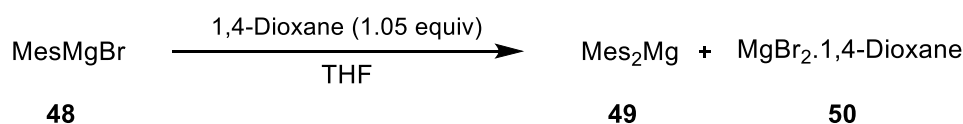
In 2000, Kerr *et al.* described an asymmetric deprotonation methodology employing the use of a magnesium amide, which displayed an improvement over the current lithium amide methodologies at the time (*vide supra*).²³ An additional advancement in deprotonation chemistry came in 2007, through the use of dimesityl magnesium as a base in the deprotonation of ketones. The optimum

conditions for this transformation were at a temperature of 0 °C, with only 0.5 equivalents of dimesityl magnesium, as shown in Scheme 18.



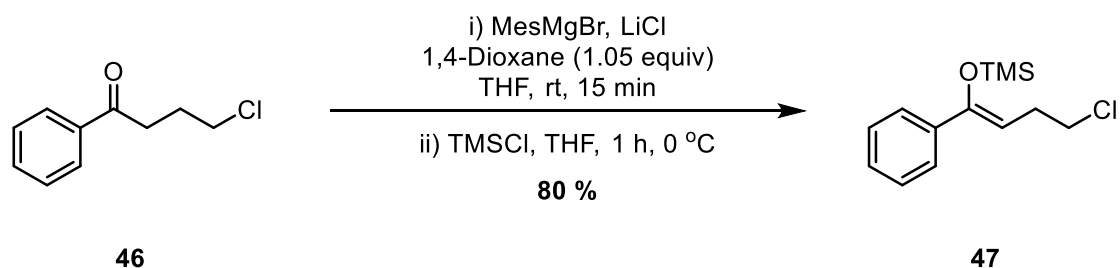
Scheme 18 - Optimised conditions for dimesityl magnesium mediated deprotonation

The deprotonation of ketone **46** highlights the mild nature of dimesityl magnesium as when the same substrate is subjected to a deprotonation with LDA, only elimination products were observed.²⁶ In 2008, research within our laboratories sought to improve upon this carbon-centred magnesium base methodology further. As the chemistry stood in 2007, pre-formation of the dimesityl magnesium was required before the addition of this reagent to the reaction mixture.²⁶ Taking advantage of the Schlenk equilibrium, a one-pot procedure was developed, involving the use of stoichiometric mesityl magnesium bromide **48** which forms the desired dimesityl magnesium **49** upon addition of 1,4-dioxane, as shown in Scheme 19.



Scheme 19 - Formation of Mes_2Mg

The pre-formation of dimesityl magnesium **49** at room temperature, followed by subsequent cooling to 0 °C before the addition of the desired ketone substrate and TMSCl provided a successful one-pot procedure which reduced the labour intensity of the methodology developed in 2007.²⁸

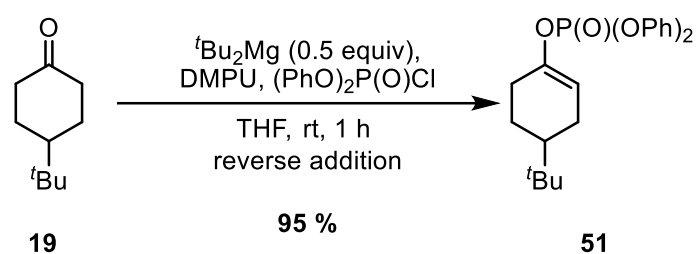


Scheme 20 - Optimised conditions for deprotonation mediated by an in-situ formation of Mes_2Mg

Further to the already described magnesium-based deprotonation methodologies, Kerr *et al.* reported the use of di-*tert*-butylmagnesium as an alternative base, which offered increased atom efficiency over the mesitylene variant.²⁹ Di-*tert*-butylmagnesium could be prepared and used in subsequent reactions or prepared and used *in situ*, as also shown with dimesityl magnesium.^{29,28}

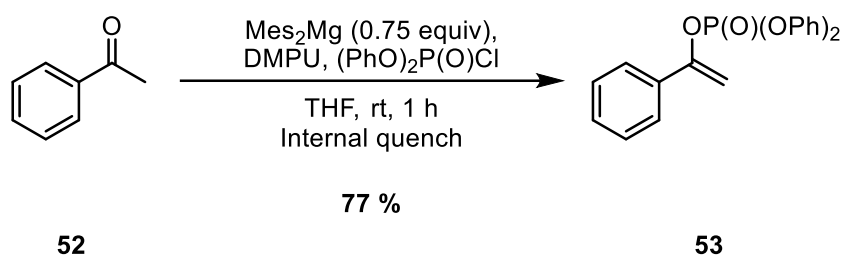
Recent Utility of Magnesium Carbon-Centred Bases

Having developed a magnesium carbon-centred base deprotonation methodology, work within our laboratory looked to showcasing the utility of such protocols. In 2015, Kerr and co-workers demonstrated the use of magnesium carbon-centred bases in allowing access to enol phosphates.³⁰ The optimised conditions in the synthesis of enol phosphates from cyclic ketones is shown in Scheme 21.



Scheme 21 - Magnesium carbon centred base protocol to synthesise enol phosphates

This method utilised a reverse addition protocol in which the base was slowly added to the reaction mixture, containing electrophile and ketone **19**, to prevent by-product formation between the magnesium base and the reactive phosphoryl chloride electrophile. This procedure proved successful with cyclic ketones, as highlighted with the synthesis of enol phosphate **51** in a 95 % yield, but proved troublesome with the more sensitive acetophenone derivatives. It was hypothesised this was due to the high reactivity of $t\text{Bu}_2\text{Mg}$ and that the increased steric bulk and lower basicity of Mes_2Mg would temper the reactivity of the base, and allow access to the acetophenone derivatives. The optimised conditions for the synthesis of enol phosphates from acetophenone derivatives using Mes_2Mg are shown in Scheme 22.



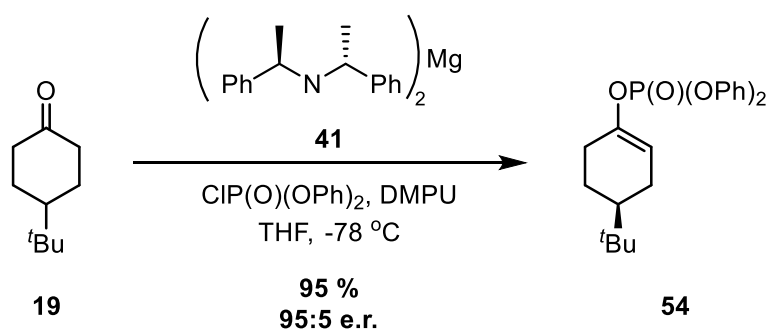
Scheme 22 - The use of Mes_2Mg to allow access to enol phosphates from acetophenone

The conditions displayed in Scheme 22, using the milder Mes_2Mg , allowed access to the enol phosphates from aryl methyl ketones; which proved non-trivial with the use of $^t\text{Bu}_2\text{Mg}$. The use of the milder base also allowed the less labour-intensive internal quench procedure to be utilised as possible by-products resulting from the reaction of the base with phosphoryl chloride were mitigated. The inclusion of this particular electrophile further enhances the utility of magnesium carbon centred bases, as enol phosphates have been shown to be useful coupling partners in cross coupling chemistry. Notably, Cheng et al. discussed the use of aryl phosphates as a pseudo-halide in nickel-catalysed Suzuki coupling methodology.³¹ The applications of enol phosphates in synthesis has been extensively discussed in a review, by Sellars.³²

To summarise, work within our laboratories have previously shown that carbon-centred magnesium bases offer an improvement in some deprotonation reactions when compared to LDA. The success of carbon-centred magnesium bases is due to their milder nature in comparison to lithium amides.

Chiral Enol Phosphates

In addition to the previously discussed formation of achiral enol phosphates from cyclic ketones and acetophenone substrates, the generation of chiral enol phosphates has also been explored *via* asymmetric deprotonation methodology.³³ In an analogous method to the desymmetrisation of ketones to form chiral silyl enol ethers, the generation of a chiral enol phosphate from 4-*tert*butyl cyclohexanone **19** is highlighted below in Scheme 23.



Scheme 23 – Synthesis of chiral enol phosphates

When employing the well-established magnesium bisamide **41** in the asymmetric deprotonation of ketone **19** followed by the subsequent quench with diphenyl phosphoryl chloride, the respective enol phosphate **54** was obtained in an excellent yield of 95 % and an excellent enantiomeric ratio of 95:5. This addition to the Kerr asymmetric deprotonation methodology is significant as the enol phosphate functional group allows for further derivatisation by cross-coupling reactions. Indeed, this was exemplified in the total synthesis of (*S*)-Sporochnol, highlighting the utility of asymmetric deprotonation technology in the synthesis of complex natural products.³³

1.1.7. (–)-mucosin

With Kerr's research towards the development of mild and efficient asymmetric deprotonation reactions ongoing, we looked to the oxylipin natural product (–)-mucosin as a platform for evaluating the utility of our chemistry in complex molecule synthesis (Figure 9).

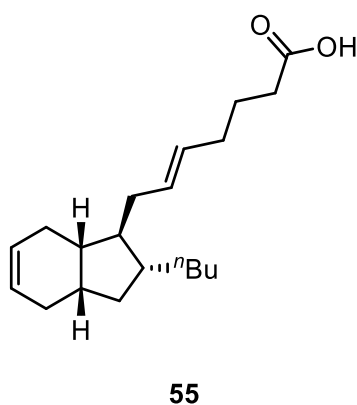


Figure 9 – Proposed structure of (–)-Mucosin

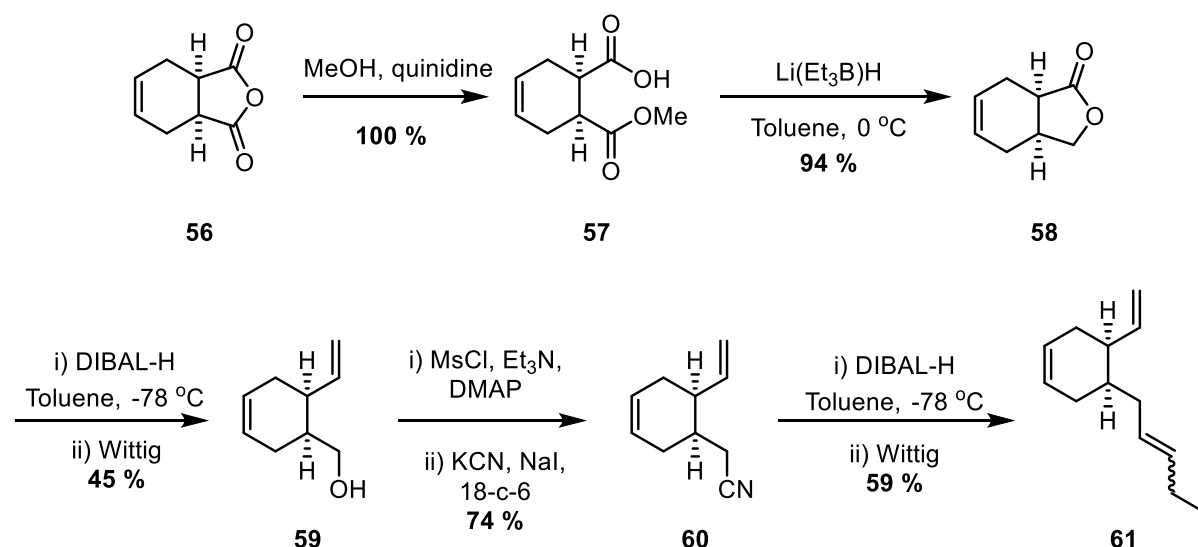
Isolation and Characterisation

(–)-Mucosin **55** was first isolated in 1997 from the *Reniera mucosa*, a marine sponge found in the Mediterranean. Upon isolation, Casapullo *et al.* characterised (–)-mucosin **55** with the use of 2D NMR

experiments, which allowed the assignment of the olefin geometry and the relative stereochemistry around the core of the molecule.³⁴ Structurally, (–)-mucosin incorporates an unusual bicyclo[4.3.0]nonene with four contiguous stereocentres, which presents a unique synthetic challenge for the chemist.

Total Synthesis of (+)-mucosin

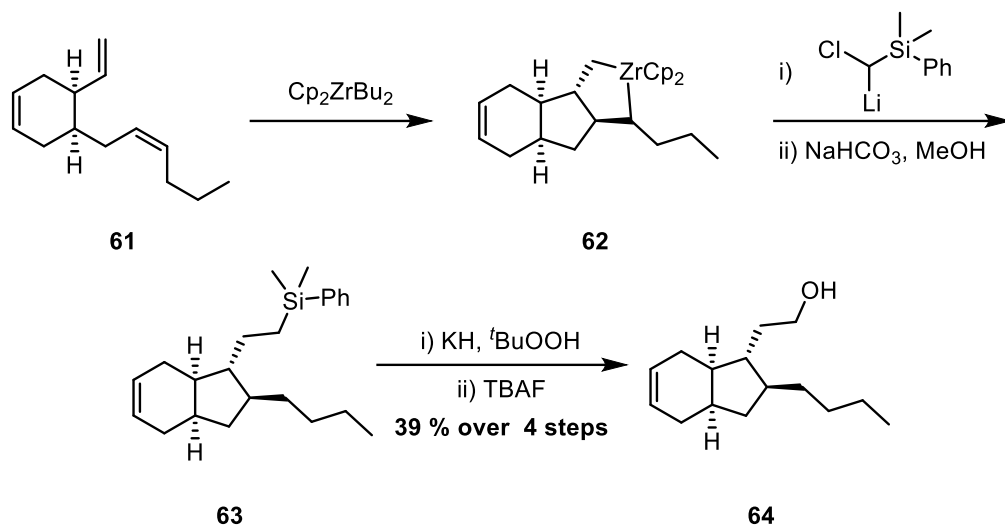
The synthesis of the antipode of our targeted natural product was completed in 2012 by Whitby *et al.*³⁵ Their synthetic strategy involved the interesting use of a Zr-promoted bicyclisation of a 1,6-diene as their key step, chemistry that was developed originally by Negishi.³⁶ This step allowed control over the four contiguous stereocentres in mucosin **55**. Key to the success of their route was the efficient synthesis of the requisite triene **61**. This was achieved as shown in Scheme 24, starting from the commercially available tetrahydrophthalic acid anhydride **56**. An asymmetric ring opening, mediated by quinidine, afforded the diacid monoester **57** in 100 % yield, which, upon a selective reduction with Super-Hydride®, gave lactone **58**. Upon a partial reduction of lactone **58**, the corresponding lactol was prepared, which underwent a Wittig olefination to afford alcohol **59** in 45 % yield. Mesylation and a subsequent S_N2 displacement with KCN gave the cyano product **60** in 74 % yield. Finally, a DIBAL-H partial reduction and subsequent Wittig reaction gave the desired triene **61** as a 4:1 mixture of *Z*:*E* isomers in 59 % yield.



Scheme 24 - Whitby *et al.* synthetic route into the triene precursor

With a synthetic route in place for the synthesis of the intermediate **61**, the key step of the synthetic route was then explored (Scheme 25). Treatment of triene **61** with Cp₂ZrⁿBu₂ delivered zirconacycle **62**. Subsequent *in situ* insertion with a silyl carbenoid into the zirconacycle **62** afforded the silyl

species **63**. Tamao-Fleming oxidation delivered alcohol **64** as a 2.7:1 mixture of diastereomers from the starting triene **61** in a 39 % yield over 4 steps. This elegant strategy allowed for the synthesis of the core of (+)-mucosin, embedding the four contiguous stereocentres.



Scheme 25 - Whitby *et al.* Synthetic route towards (+)-mucosin

In order to gain an understanding of the stereoselectivity of the central Zr-mediated bicyclisation, Whitby *et al.* probed the stability of possible zirconacycles in this synthetic route. Through the use of Density Function Theory (DFT) calculations, four possible zirconacycle isomers **62a-d** were identified as accessible structures in the Zr-mediated bicyclisation by calculating their relative energies which allowed for an assessment of their relative stabilities. (Figure 10).

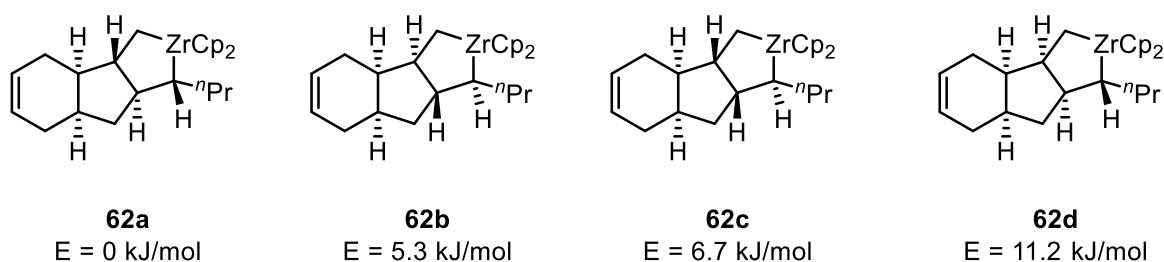
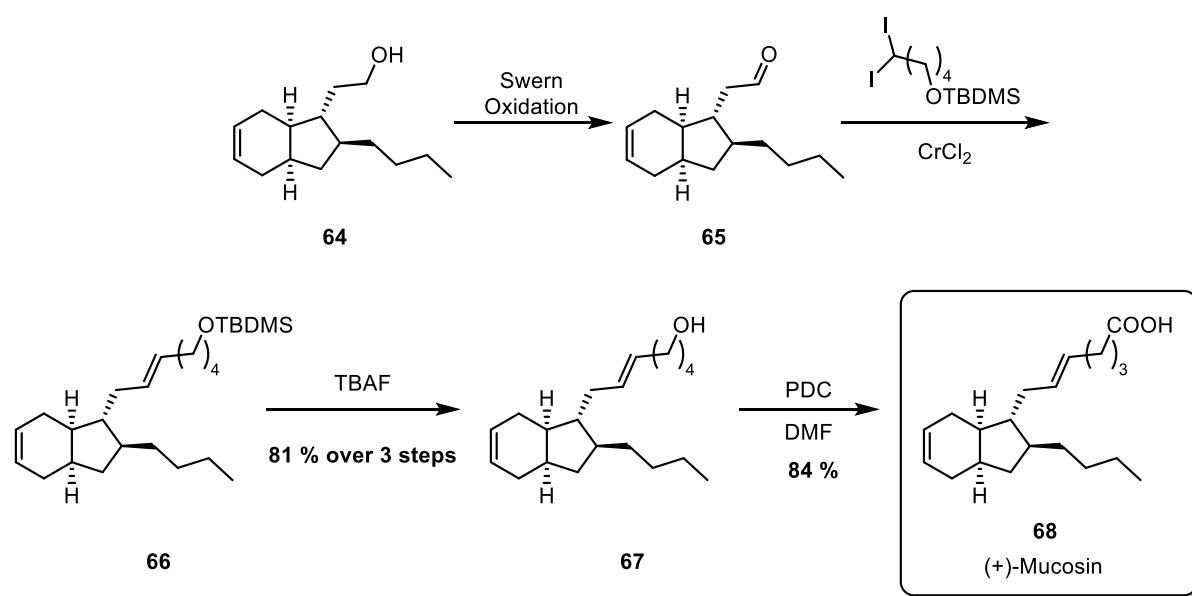


Figure 10 - Possible Zirconacycle epimers and their relative calculated energies

Through reaction monitoring *via* gas chromatography (GC), Whitby was able to employ kinetic and thermodynamic control in the reaction in order to bias the ratios obtained in the product mixtures. It was discovered that after 1.25 hours at room temperature the isomer ratio was 26:68:4:2 (**62a:62b:62c:62d**) whereas after 0.5 hours at 65 °C the isomer ratio was 63:24:11:2 (**62a:62b:62c:62d**). Through subsequent derivatisation of a model system, it was shown that the

product obtained under thermodynamic conditions had the correct relative stereochemistry to be taken forth in Whitby's synthetic route towards (+)-mucosin.

The final steps towards the oxylipin mucosin, albeit the opposite enantiomer of the natural target, were carried out using classical synthetic transformations (Scheme 26). Following a Swern oxidation, aldehyde **65** was obtained and subjected directly to a Takai Olefination. The silyl group was removed using tetra-butylammonium fluoride (TBAF) to afford alcohol **67** in 81 % over 3 steps. Finally, Whitby obtained (+)-mucosin **68** from alcohol **67** *via* oxidation. Overall, Whitby's synthetic route afforded (+)-mucosin **68** in a 7 % yield over 14 steps.³⁵

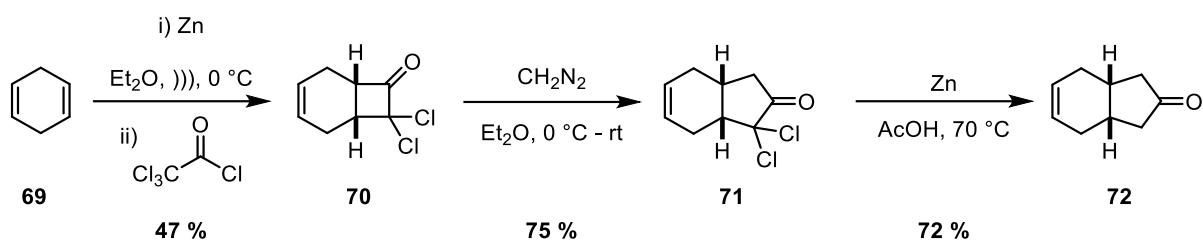


Scheme 26- Remaining steps in Whitby *et al.* synthetic route towards (+)-mucosin

Despite an elegant synthesis of (+)-mucosin **68**, work towards the synthesis of the natural antipode (–)-mucosin **55** had not been reported, within the chemical literature. It was envisioned that methodology within the Kerr group could be employed to complete the first total synthesis of (–)-mucosin.

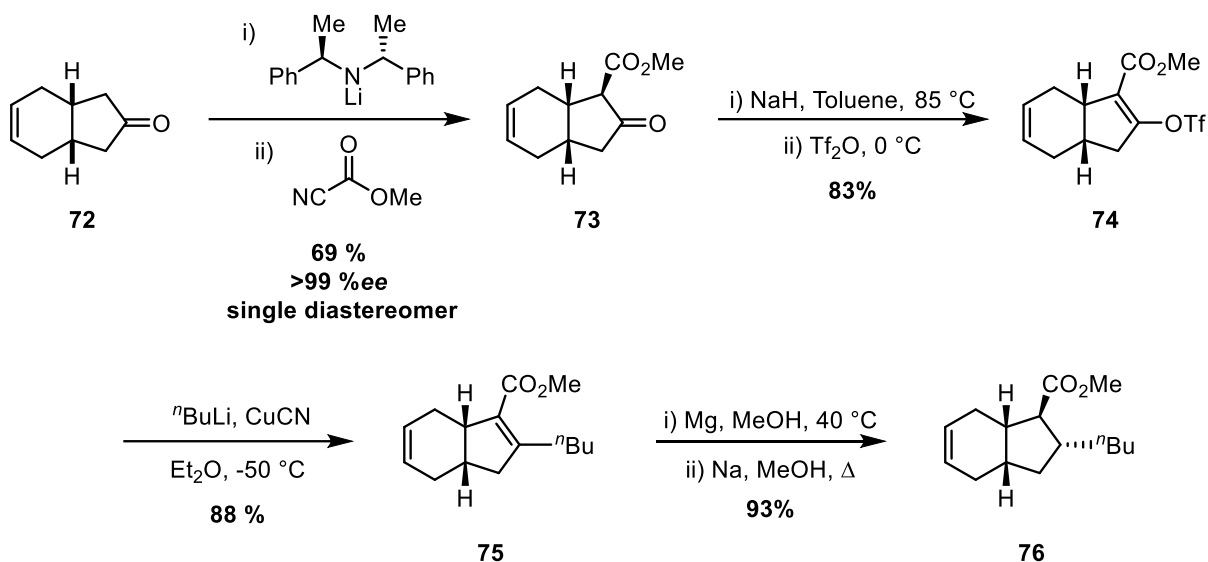
Total Synthesis of *cis*-mucosin

In 2016, whilst our work within the Kerr laboratories towards (–)-mucosin was underway, Stenstrøm and co-workers published their total synthesis of *cis*-mucosin, the previously proposed structure for (–)-mucosin **55**.³⁷ Their strategy involved the desymmetrisation of ketone **75**. Ketone **75** was synthesised as shown below in Scheme 27.



Scheme 27 - Stenstrøm's synthesis of ketone **72**

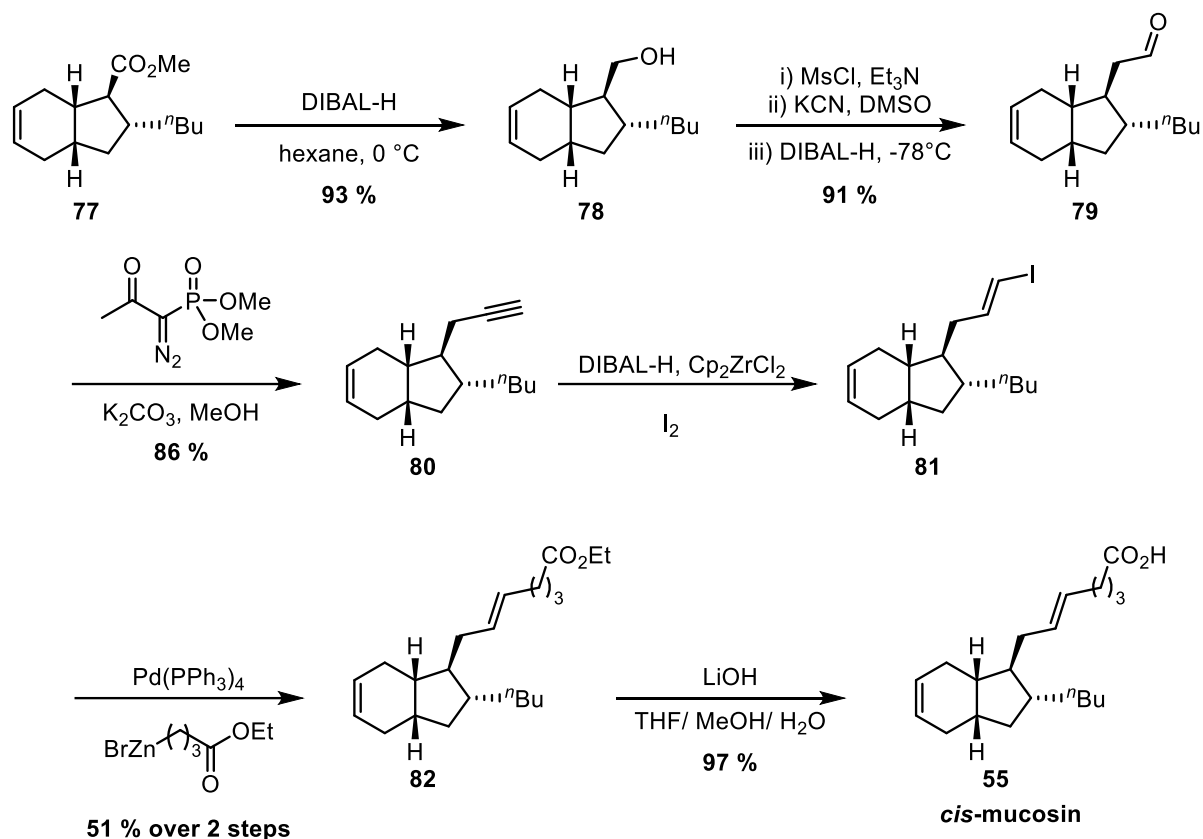
Starting from cyclohexadiene **69**, a zinc-mediated [2+2] cycloaddition with trichloroacetyl chloride afforded dichloroketone **70** in a moderate yield of 47 %. A ring expansion of **70** with diazomethane allowed for the formation of dichloro cyclopentanone **71** in a yield of 75 %. Finally, a zinc-mediated dehalogenation afforded the required ketone **72** in 72 %. Overall, the synthesis of ketone **72** was achieved in three steps with an overall yield of 25 %. Having synthesised ketone **72**, Stenstrøm *et al.* focused on installing the two side-chains of *cis*-mucosin **55** (Scheme 28).



Scheme 28 - Desymmetrisation of ketone **72** and installation of the *n*-butyl chain

Employing a chiral lithium amide base followed by a quench with Mander's reagent, β -ketoester **73** was afforded in a good yield of 69 % as in >99 % *ee* and diastereomer, following recrystallisation. Upon forming enol triflate **74** in an 83 % yield, the previously defined stereochemical information was scrambled, however a subsequent cuprate addition followed by elimination gave ester **75** with the *n*-butyl side-chain in place, in a good yield of 88 %. The reduction of the α,β -unsaturated ester **75** proceeded with magnesium turnings in methanol to give a 2:1 mixture of epimers. Following an epimerisation with sodium methoxide, a single diastereomer of ester **76** was obtained in a 93 % yield

from α,β -unsaturated ester **75**. With all four contiguous stereocentres installed, synthetic efforts then focused on extending the side-chain bearing the carboxylic acid (Scheme 29).



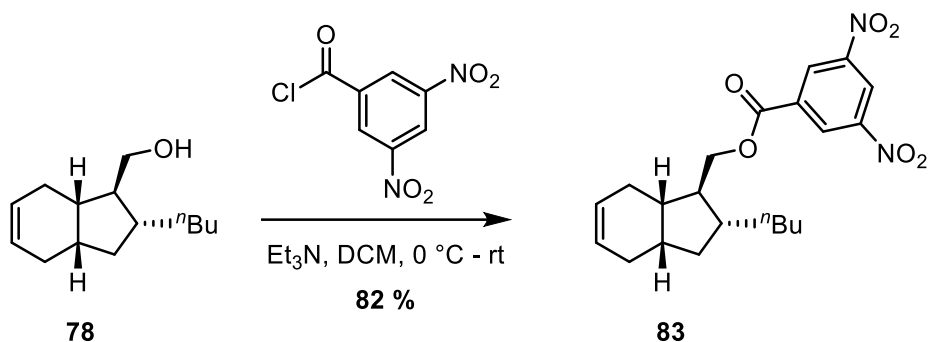
Scheme 29 – Stenstrøm's synthesis of (-)-mucosin

Methyl ester **77** was reduced to alcohol **78** in a 93 % yield. With alcohol **78** in hand, a homologation procedure involving a mesylation, S_N2 displacement with KCN and nitrile reduction afforded aldehyde **79** in an excellent yield of 91 %. Subsequently, a Seyferth-Gilbert homologation employing the Ohira-Bestmann reagent allowed for the synthesis of alkyne **80** in an 86 % yield. *In situ* formation of Schwartz's reagent allowed for hydrozirconation of alkyne **80** and, upon quenching with iodine, (*E*)-vinyl iodide **81** was formed selectively. Subsequently, the vinyl iodide was subjected to a Negishi cross-coupling with the commercially available alkyl zinc bromide to give the ethyl ester **82** in a 51 % yield over two steps from alkyne **80**. Stenstrøm then employed a simple hydrolysis to unveil the carboxylic acid and afford *cis*-mucosin **55** in a 97 % yield. Overall, Stenstrøm's synthesis afforded *cis*-mucosin in an overall yield of 4 % over 18 steps. In comparison to Whitby and co-workers' synthetic route, Stenstrøm's route proves to be longer and lower yielding overall. However, upon synthesis of the methyl ester of *cis*-mucosin **55**, it was noted that multiple ^{13}C NMR signals were different to that of both the reported data from the original isolation and from Whitby's synthesis. (Table 4).

Table 4 - Comparison of ^{13}C NMR data for methyl ester of *cis*-mucosin 55

Casapullo <i>et al.</i>	Whitby <i>et al.</i>	Stenstrøm <i>et al.</i>
174.2	174.2	174.2
130.0	130.3	130.4
129.8	129.8	129.9
127.0	127.3	126.3
127.0	127.1	126.1
52.1	52.2	51.4
51.4	51.4	51.0
47.1	47.2	44.0
42.1	42.3	40.3
39.9	40.1	38.1
36.7	37.0	37.7
36.5	36.74	37.1
36.4	36.68	34.9
33.2	33.4	33.4
32.0	32.4	31.9
31.7	31.9	31.0
31.5	31.6	27.8
30.7	30.7	27.7
24.5	24.7	24.8
22.6	22.9	22.9
13.8	14.1	14.1

As shown above in Table 4, multiple ^{13}C resonances, highlighted in bold, are shown to differ by a significant margin. Additionally, the optical rotation of the material synthesised by Stenstrøm gave an $[\alpha]_{\text{D}} = -9.8^\circ$, which is, again, significantly different to that of the optical rotation obtained from Casapullo's isolation, which gave a value of $[\alpha]_{\text{D}} = -35.5$.³⁴ Despite these differences, Stenstrøm and co-workers obtained a crystal structure of intermediate **83**, which contained all four contiguous stereocentres in accordance with the relative stereochemistry Casapullo originally assigned (Scheme 30, Figure 11).



Scheme 30 - Synthesis of dinitro benzoate **83**

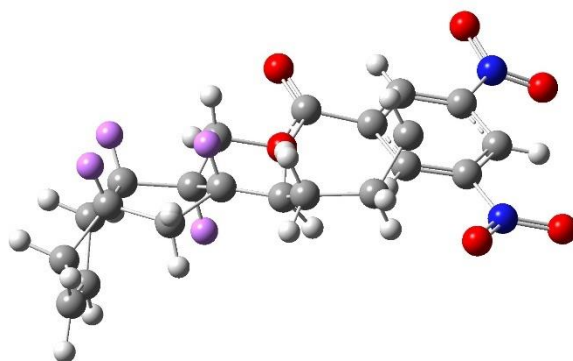


Figure 11 - Crystal Structure

As shown by Figure 11, Stenstrøm's synthesis has afforded the fused *cis*- ring junction and the substituents on the core in a *syn,anti*- geometry, as proposed by Casapullo in their original characterisation. This crystal structure, in conjunction with the discrepancies in the ^{13}C NMR resonances and the significant difference observed in the optical rotation, suggests that the original assignment of (–)-mucosin was incorrect. This presents a rare situation in natural product chemistry, where the original structure of the isolated material is confirmed *via* synthesis and then subsequently thrown into uncertainty following further syntheses.

This ambiguity in the assignment of (–)-mucosin, presents an opportunity for our group to not only synthesise the originally assigned structure and confirm Stenstrøm's findings, but also establish the correct structure of (–)-mucosin, either by synthesis or other means.

Synthesis of *exo*-mucosin

In 2017, Stenstrøm and co-workers continued their synthetic campaign to elucidate the true structure of the oxylipin (–)-mucosin and targeted the synthesis of so-called *exo*-mucosin **84**, bearing a *cis*-bridgehead and the appendages in an *anti,anti*- geometry.(Figure 12).³⁸

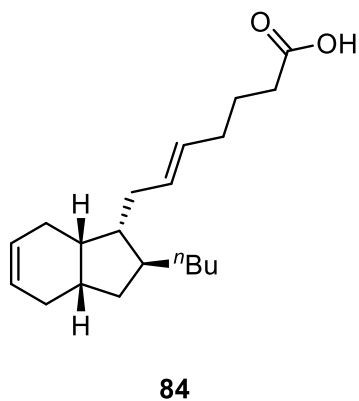
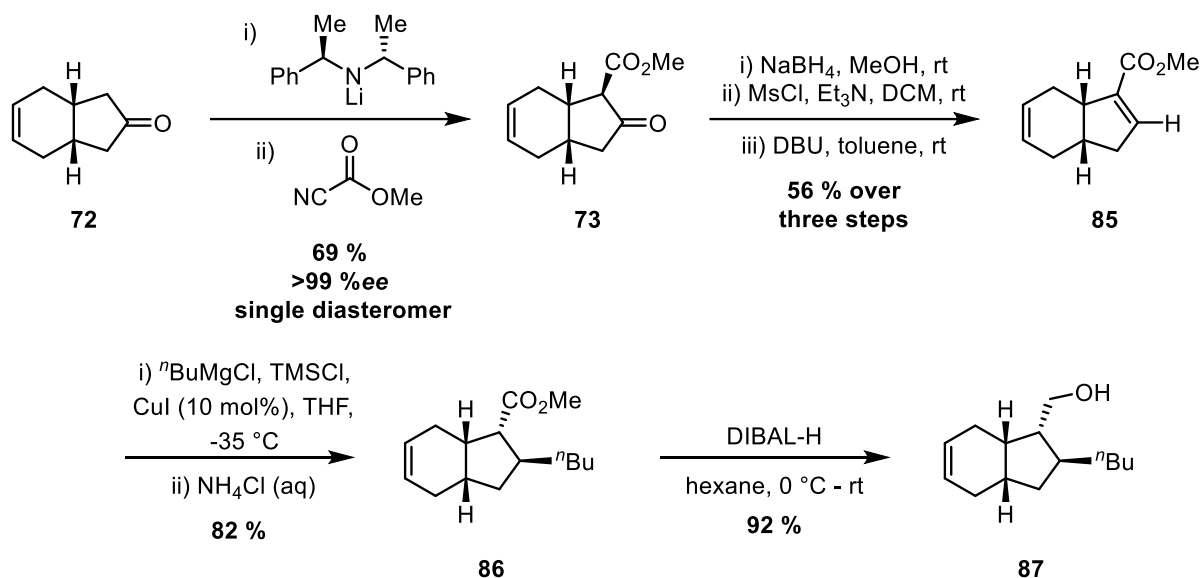


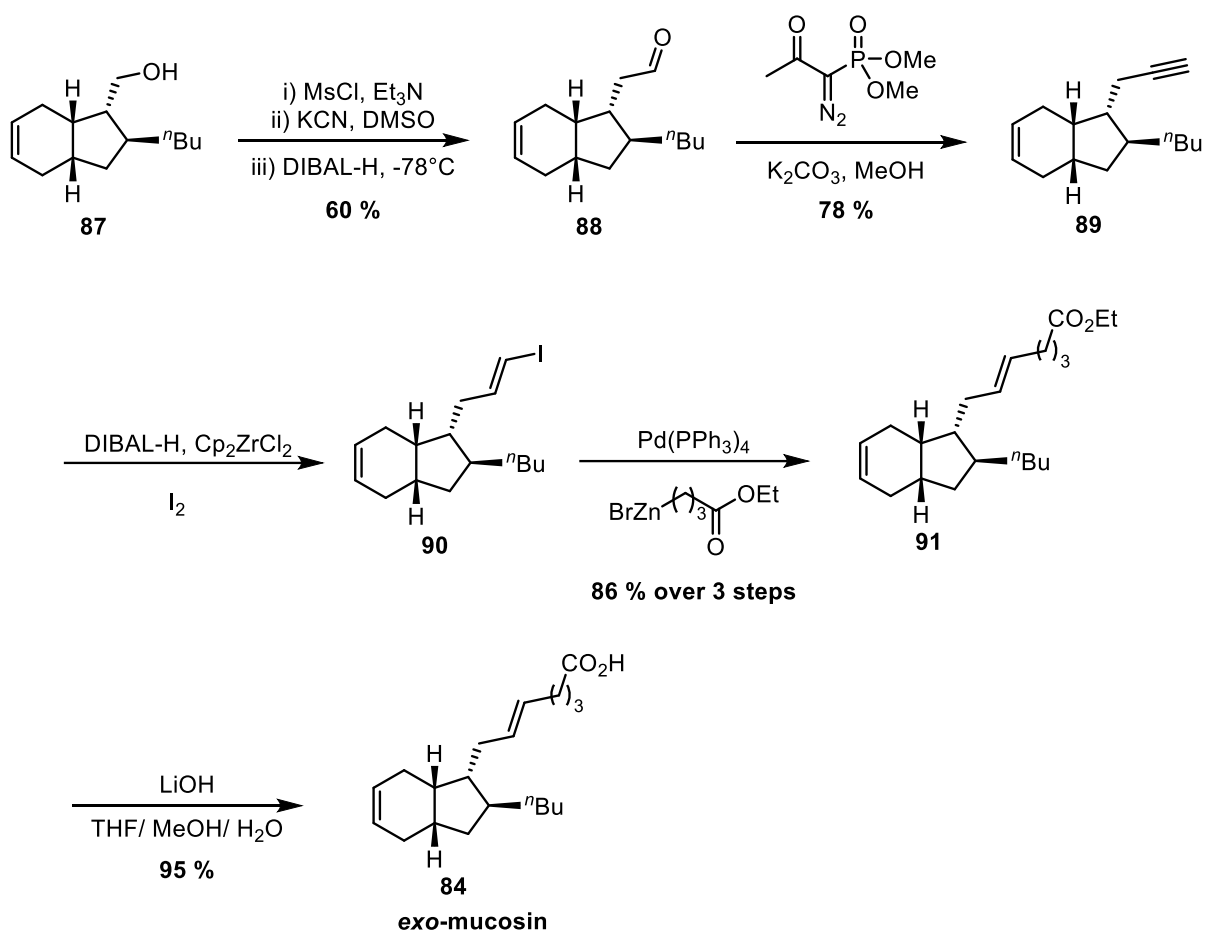
Figure 12 - *exo*-mucosin

Having already developed a route in their previous publication for the synthesis of *cis*-mucosin **55**, only slight modifications in the synthetic approach were required to achieve the synthesis of *exo*-mucosin **84** (Scheme 31).



Scheme 31 - Towards the synthesis of *exo*-mucosin

As described previously, the β -ketoester **73** was synthesised *via* desymmetrisation of ketone **72** and subsequent quench with Mander's reagent. The β -ketoester **73** was then reduced to give the alcohol, followed by a mesylation and elimination procedure to give the desired α,β -unsaturated ester **85** in a 56 % yield over three steps. Installation of the *n*butyl chain was carried out *via* a Cu(I)-catalysed conjugate addition to give the desired ester **86** in an 82 % yield. Subsequent reduction of the ester **86** gave the alcohol **87** in a 92 % yield and from here the route towards *exo*-mucosin **84** was very similar to the previously developed route in Stenstrøm's synthesis of *cis*-mucosin **55** (Scheme 32).



Scheme 32 - Stenstrøm's synthesis of exo-mucosin

With alcohol **87** prepared, the homologation procedure involving a mesylation, S_N2 displacement with KCN and nitrile reduction was employed and afforded aldehyde **88** in a good yield of 60 %. Subsequently, a Seyferth-Gilbert homologation employing the Ohira-Bestmann reagent allowed for the synthesis of alkyne **89** in an 78 % yield. *In situ* formation of Schwartz's reagent allowed for hydrozirconation of alkyne **89** and, upon quenching with iodine, (*E*)-vinyl iodide **90** was formed selectively. Subsequently, the vinyl iodide was subjected to a Negishi cross-coupling with the commercially available alkyl zinc bromide to give the ethyl ester **91** in an 86 % yield over three steps from alkyne **89**. Finally, a hydrolysis unveiled the carboxylic acid delivering *exo*-mucosin **84** in a 95 % yield. The methyl ester of *exo*-mucosin was synthesised and the spectroscopic data was again compared the original. The ^{13}C NMR spectra from *exo*-mucosin **84** also did not match the data obtained from the isolation or from Whitby's total synthesis (Table 5).

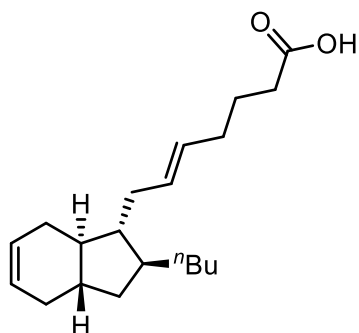
Table 5 - ¹³C comparison table

Casapullo <i>et al.</i>	Whitby <i>et al.</i>	Stenstrøm <i>et al.</i>	Exo-mucosin
174.2	174.2	174.2	174.2
130.0	130.3	130.4	131.2
129.8	129.8	129.9	129.0
127.0	127.3	126.3	125.3
127.0	127.1	126.1	125.1
52.1	52.2	51.4	51.6
51.4	51.4	51.0	51.4
47.1	47.2	44.0	41.3
42.1	42.3	40.3	37.2
39.9	40.1	38.1	36.2
36.7	37.0	37.7	35.5
36.5	36.74	37.1	35.4
36.4	36.68	34.9	33.4
33.2	33.4	33.4	33.0
32.0	32.4	31.9	31.9
31.7	31.9	31.0	31.0
31.5	31.6	27.8	26.9
30.7	30.7	27.7	24.7
24.5	24.7	24.8	23.0
22.6	22.9	22.9	21.7
13.8	14.1	14.1	14.1

With the two *cis*-bridgehead containing isomers of (–)-mucosin synthesised and characterised, Stenstrøm had narrowed down the search for the correct stereoisomer. Additionally, Stenstrøm had, previously, discounted the *cis*- containing stereoisomers with *syn*- appendages due to the unfavourable steric penalty involved in placing two large groups *syn* to each other

Structural Elucidation and Total Synthesis of (–)-mucosin

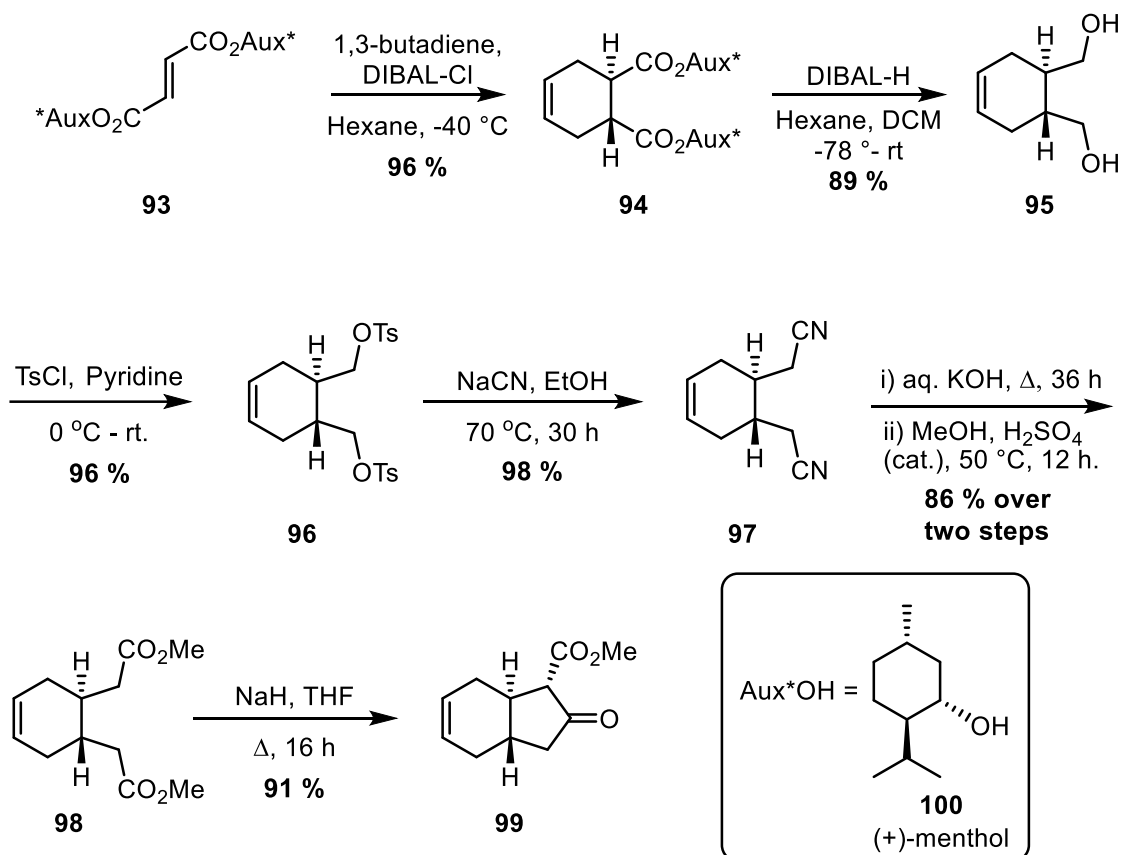
As our own work towards the structural elucidation and total synthesis of (–)-mucosin was in its later stages, in 2018, Stenstrøm published their revision of the structure of (–)-mucosin.³⁹ Having previously suggested that the *cis*- bridgehead within (–)-mucosin might be unfavourable, through their previous work and with the doubts this had raised in the proposed biosynthesis (*vide infra*), Stenstrøm now proposed that (–)-mucosin had the structure **92** as shown in Figure 13, containing a *trans*-bridgehead and the appendages in a *syn,anti*- geometry.



92

Figure 13 - Stenstrøm's proposed structure of (-)-mucosin

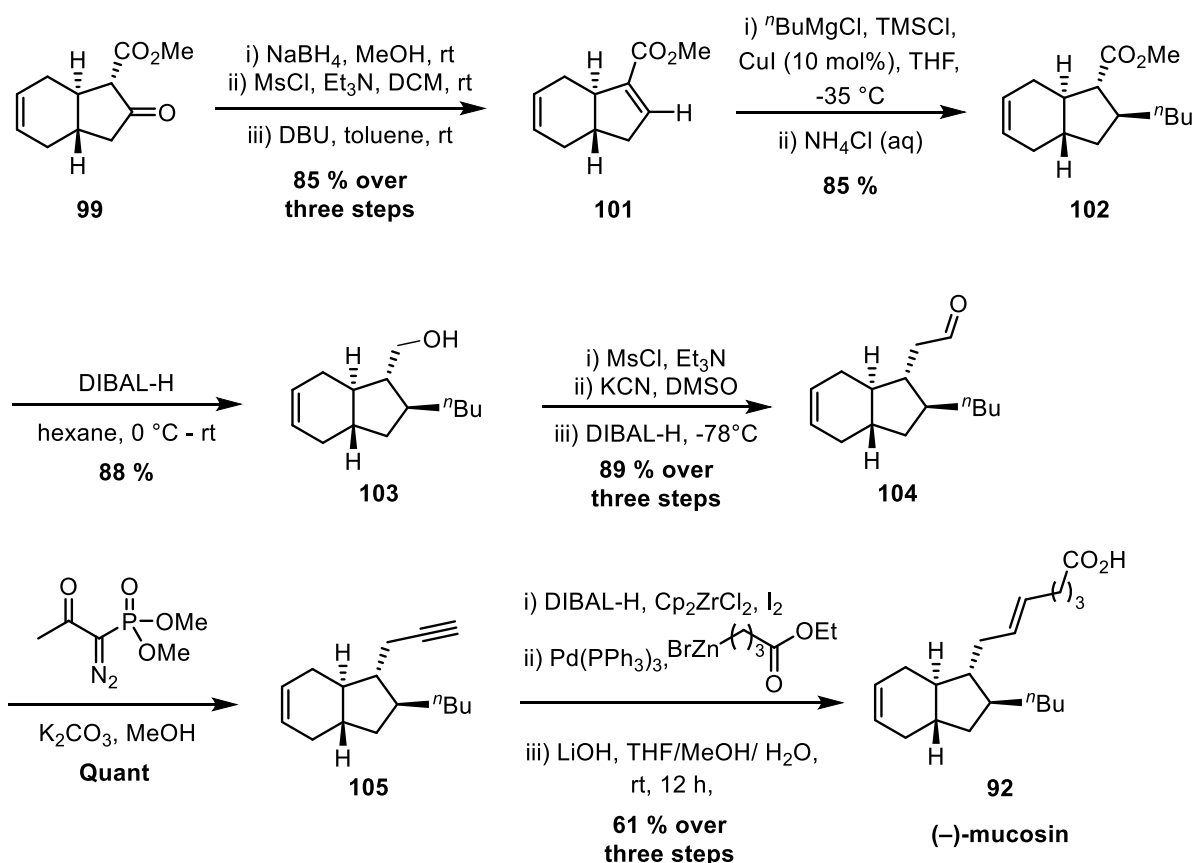
Their strategy towards this newly proposed target did not include an asymmetric deprotonation as the asymmetry inducing step but, instead, a chiral auxiliary-mediated asymmetric Diels-Alder reaction, as described in Scheme 33.



Scheme 33 - Synthesis of trans-bridgehead

The initial step is an asymmetric Diels-Alder reaction which not only constructs the cyclohexene ring present in mucosin, but also sets the stereochemistry at the bridgehead. Through the use of (+)-menthol **100** as the chiral auxiliary, the desired six-membered ring **94** is afforded in an excellent

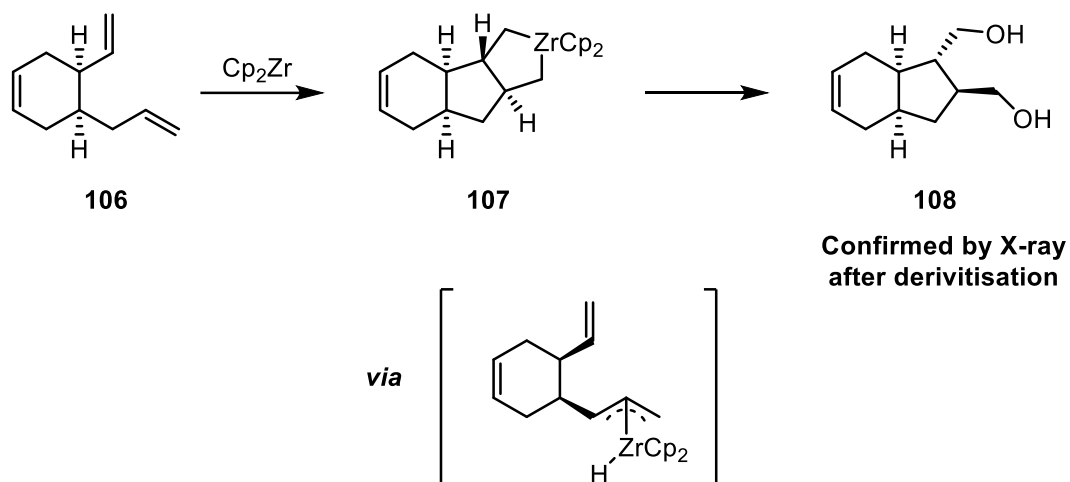
96 % yield. Following a reduction to the diol **95** using DIBAL-H in an 89 % yield, the dinitrile compound **97** is synthesised *via* a tosylation and subsequent S_N^2 displacement with sodium cyanide in 96 % and 98 % yields, respectively. Hydrolysis of dinitrile **97** followed by acid-catalysed esterification allowed access to the diester **98** in 86 % yield over two steps. Finally, a Dieckmann condensation gives the desired β -ketoester **99** in an excellent 91 % yield. With Stenstrøm's synthesis of the β -ketoester **99** featuring the *trans*-bridgehead, complete, the remaining synthesis is undertaken in a very similar fashion to the previously reported syntheses of the other mucosin stereoisomers.^{37,38}



Scheme 34 - Synthesis of (-)-mucosin

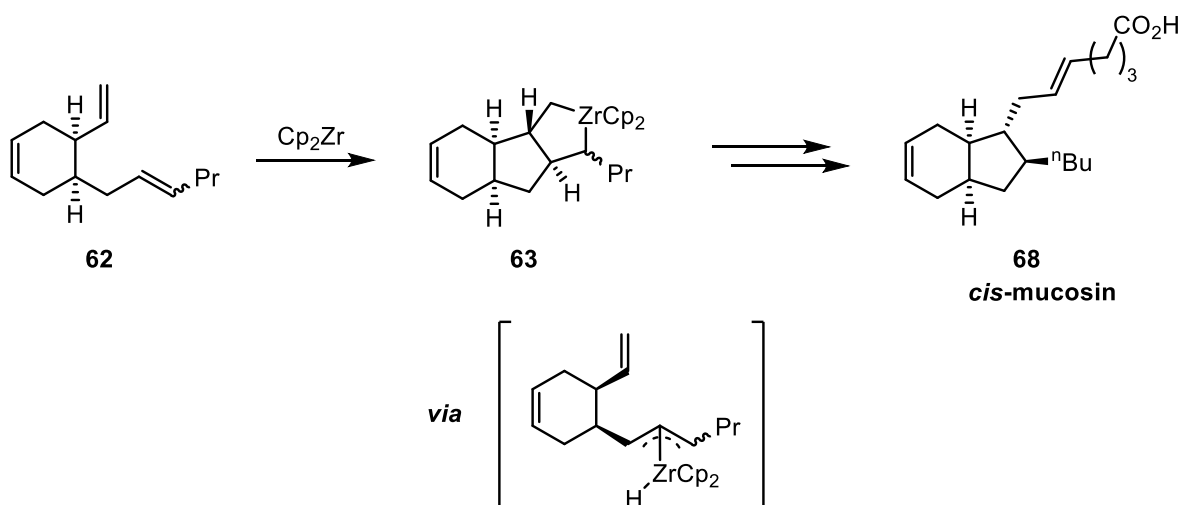
Synthesis of the α,β -unsaturated ester **101** proceeds from the β -ketoester **99** in an 85 % yield using a reduction, mesylation and then elimination strategy utilised in Stenstrøm's previous synthetic works. Installation of the *n*butyl chain is carried out *via* a Cu(I)-catalysed conjugate addition to give the desired stereoisomer **102** as the major product. The remaining appendage of (-)-mucosin was constructed by the previously documented strategy involving installation of an alkyne from aldehyde **104** *via* a Seyferth-Gilbert homologation in a quantitative yield. The alkyne was then subjected to hydrozirconation, iodination, and Negishi cross-coupling. Ester hydrolysis then delivered (-)-mucosin in 61 % over four steps. Upon synthesis of the methyl ester of (-)-mucosin Stenstrøm reported

matching data to the material isolated from *Reniera mucosa* strongly suggesting the structure of (-)-mucosin was that indicated in Figure 13. With an alternative structure of (-)-mucosin now proposed, it became increasingly evident that Whitby and co-workers had unwittingly made the correct natural product during their total synthesis but had assigned the incorrect structure to this product.³⁵ Stenstrøm *et al.* suggests this is a result of being misled by the triene system **106** they used to model their co-cyclisation which ultimately sets the stereochemistry in Whitby's synthesis (Scheme 35).³⁹



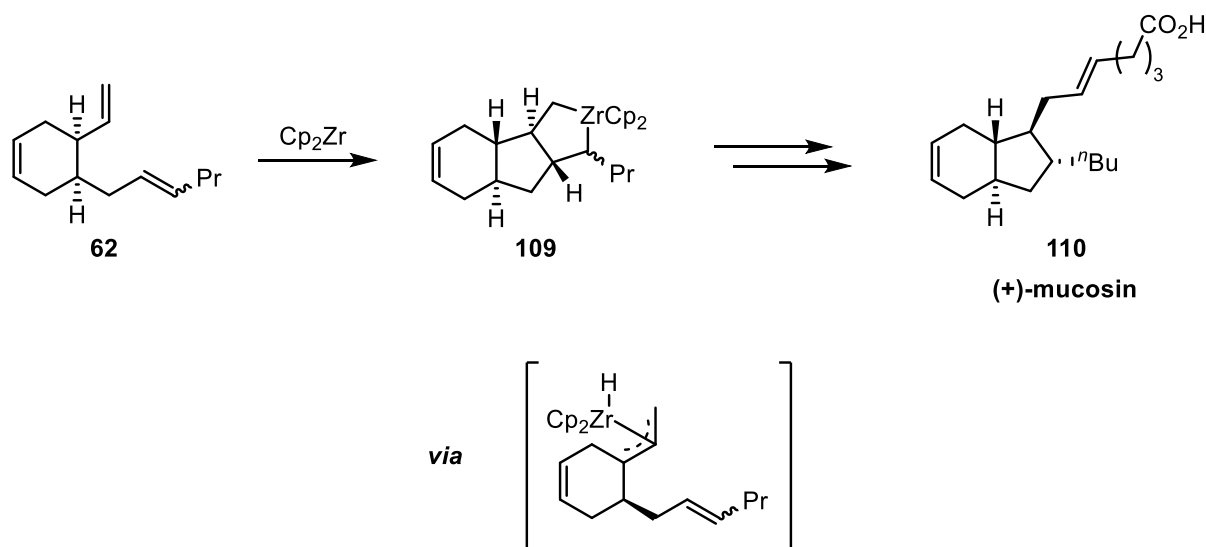
Scheme 35 - Whitby's model system

As confirmed by X-ray crystallography, the model system **106** does appear to undergo the co-cyclisation to form the 5,6-fused ring systems with a *cis*-ring junction. However, in Whitby's real system, reaction of **62** via the methylene allyl group, co-cyclisation should give the desired stereochemistry for *cis*-mucosin **68**, as shown in Scheme 36.



Scheme 36 - Whitby's real system reacting via the methylene allyl group

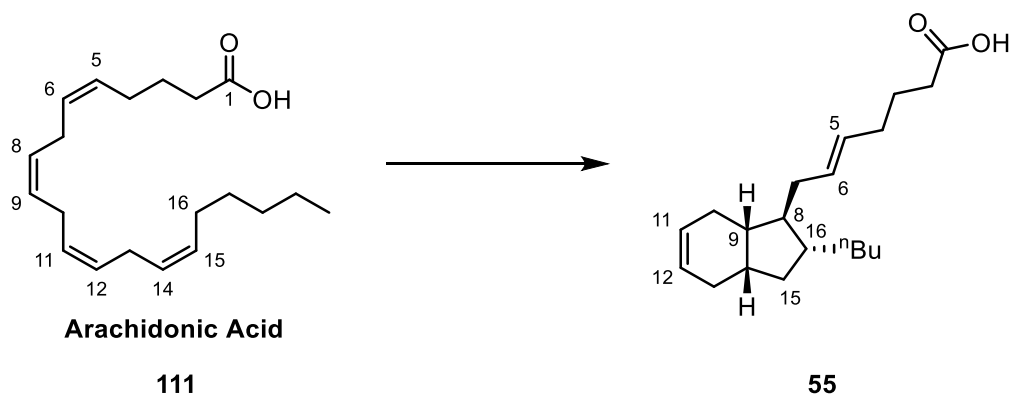
It is suggested that the 1,2-disubstituted olefin on the triene **62**, is bulky enough, such that the methine allyl group can compete with the Zr-catalyst in the stereo-determining co-cyclisation implemented in Whitby's synthesis. Structurally, this competition is inconsequential as reaction *via* the methylene or methine allyl groups will yield the, skeletally similar, 5,6 ring system. Conversely, preferential co-ordination of the methine allyl group could cause scrambling of the stereochemistry at the would-be bridgehead *via* β -hydride elimination (Scheme 37). The resulting scrambling is a plausible hypothesis as to how Whitby came to erroneously synthesise the enantiomer of the natural product, (-)-mucosin.



Scheme 37 - Whitby's real system reacting *via* methine allyl group

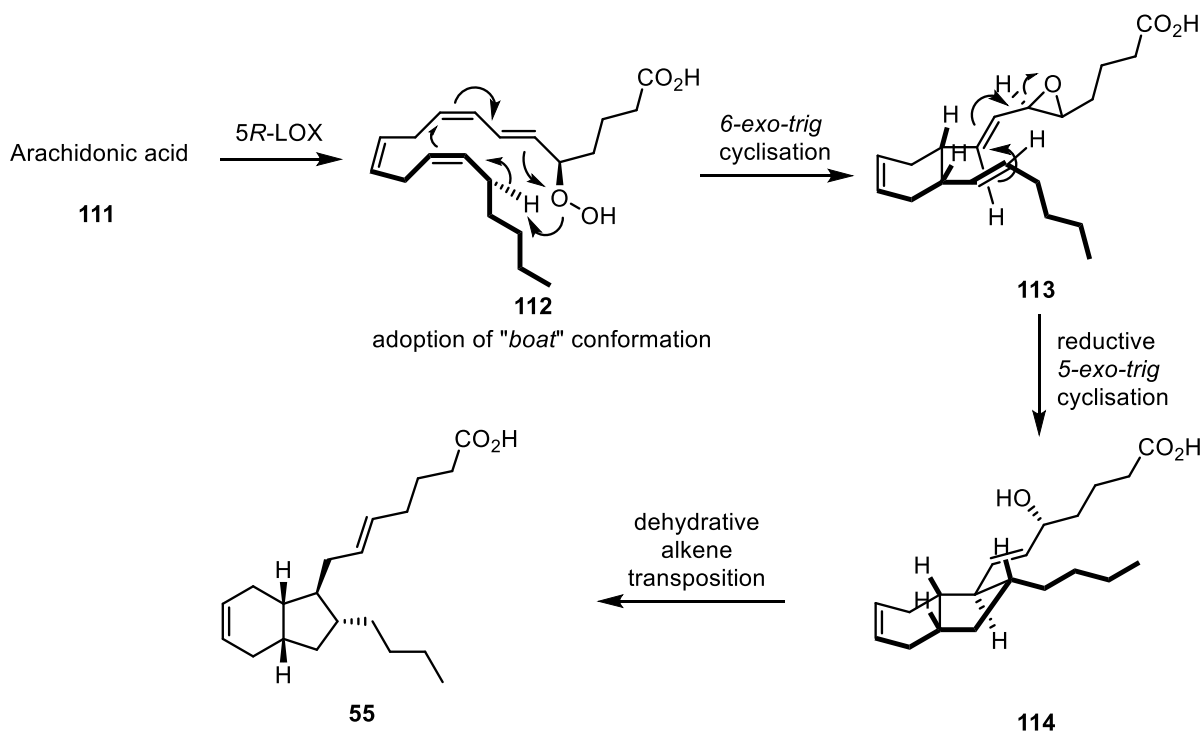
Biosynthesis

To date, there have been no published studies towards the elucidation of the biosynthesis of the oxylipin (-)-mucosin. Despite this, Casapullo *et al.* have proposed that it is possible that mucosin is derived from arachidonic acid **111**, similar to other eicosanoids such as prostaglandin E1.⁴⁰ As shown in Scheme 38, Casapullo's proposal consists of a cyclisation between C8 and C16, and an isomerisation of the C₅-C₆ olefin, to afford (-) mucosin **55**.³⁴



Scheme 38 - Caspullo et al. proposed biosynthesis of (-)-mucosin

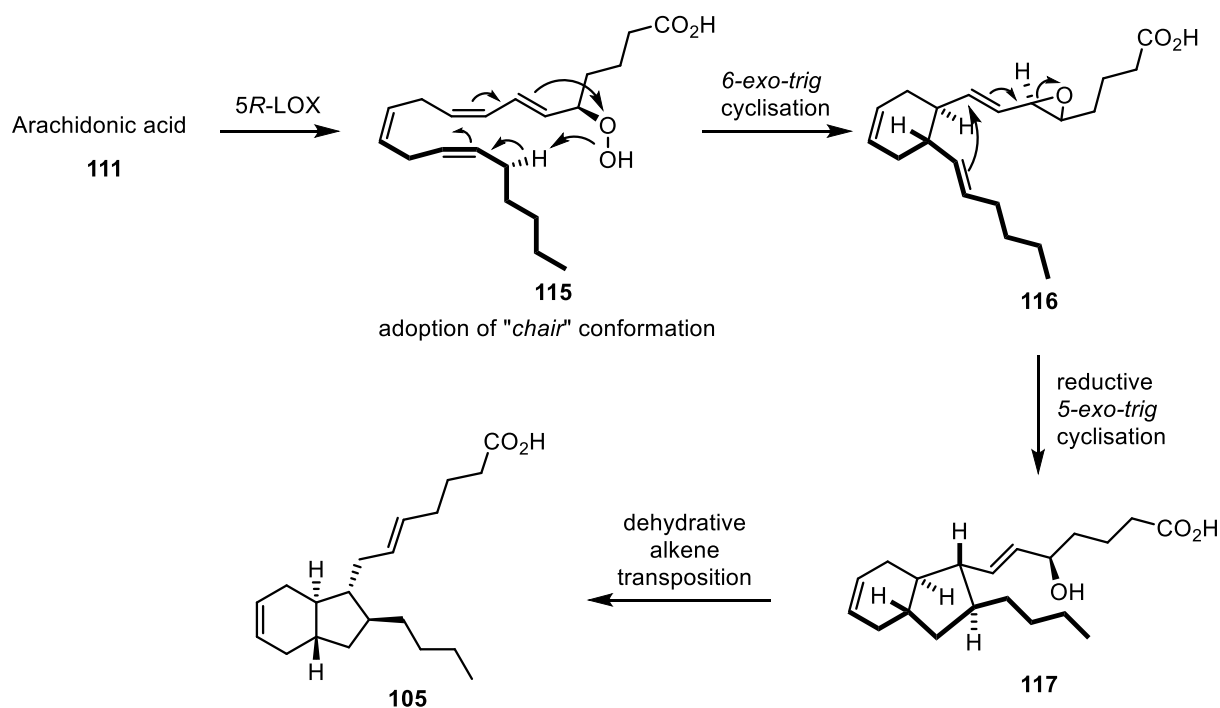
In addition, Stenstrøm *et al.* proposed a possible biosynthesis of the postulated structure of (-)-mucosin **55**, based on a survey of the enzymes known to operate on arachidonic acid (Scheme 39).³⁹



Scheme 39 - Proposed biosynthesis of (-)-mucosin

Stenstrøm *et al.* proposed that polyene arachidonic acid **111** undergoes an asymmetric peroxidation catalysed by 5-lipoxygenase (5-LOX), to **112** followed by a 6-*exo-trig* cyclisation to give the epoxide **113**. The fused ring system is then completed *via* a reductive 5-*exo-trig* cyclisation of the vinylic epoxide **113** to give the allylic alcohol **114**, which is then removed following a dehydrative alkene transposition, to give the proposed structure of (-)-mucosin **55**. Stenstrøm had noted that the macrocyclic transition state involved in the 6-*exo-trig* cyclisation of **112** would likely proceed through

a “boat” conformation over the “chair” conformation of **115**, leading to the proposed *syn* stereochemistry, with respect to the bridgehead protons, in the cyclisation. With this in mind, Stenstrøm proposed that the *trans*-ring junction was thus more likely and proposed an alternative structure for (–)-mucosin **105** (Scheme 40).³⁹

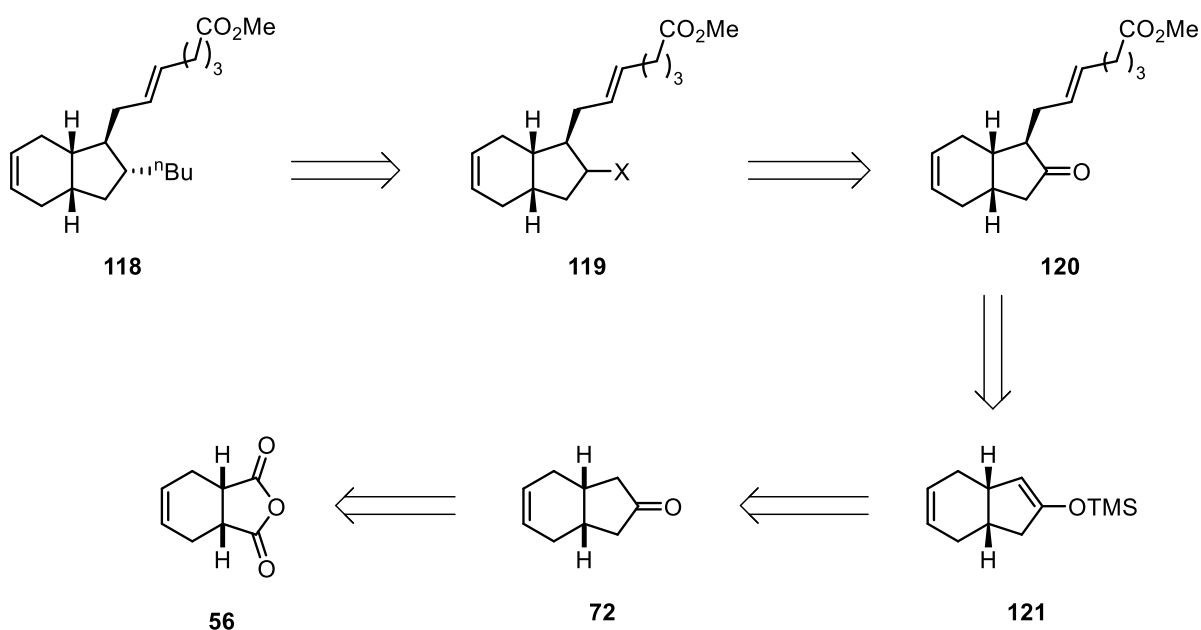


Scheme 40 - Alternative biosynthesis of (–)-mucosin

The synthetic story of (–)-mucosin highlights an interesting case in total synthesis in which the proposed structure was incorrectly confirmed by Whitby and co-workers and brought back into question by subsequent synthesis from an independent research group. Through the synthesis of several stereoisomers, whilst our own synthetic work was being carried out, Stenstrøm *et al.* produced a compelling case for the correct structure of (–)-mucosin.

1.1.8. Previous Work Within the Kerr Group

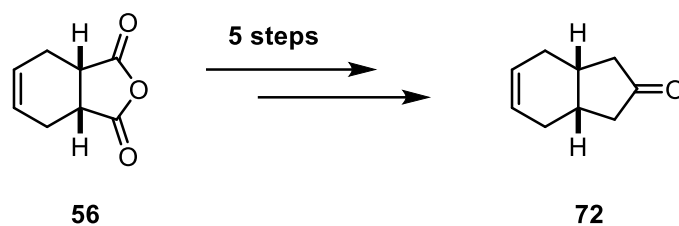
With *cis*-mucosin identified as the target natural product to showcase the Kerr group’s developing asymmetric deprotonation methodology, a retrosynthetic route was devised by Linsey Bennie and furthered by Tina Weber, researchers within the Kerr group. (Scheme 41).^{41,42}



Scheme 41- (-)-mucosin retrosynthesis

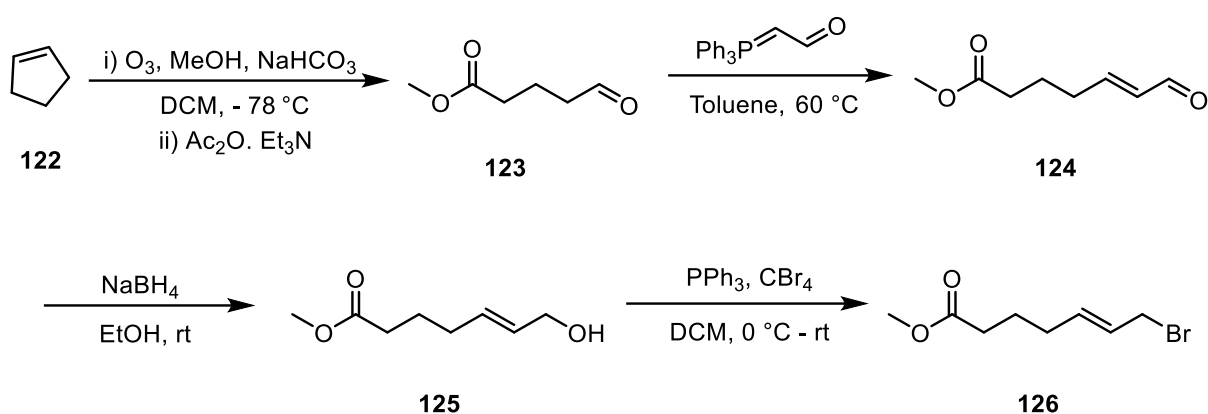
From the methyl ester of (-)-mucosin **118** it was anticipated that the ⁿbutyl chain could be installed late stage, through either a displacement or coupling reaction with a halide or pseudohalide **119**. Such a leaving group would be installed from the reduction of ketone **120** and further manipulation *via* Appel or sulfonylation chemistry. The central transformation in our proposed synthesis is **72-121** *via* asymmetric deprotonation, and enol ether formation, followed by a deprotection and allylation with an allyl bromide variant of the ester sidechain. This would embed the desired stereochemistry for the natural product. Ketone **72** can be ultimately synthesised in five steps from the bicyclic anhydride **56** which is available commercially at an affordable price, as shown by Mundy *et al.*⁴³

With a retrosynthetic route in place the first stage of the synthetic strategy towards (-)-mucosin was the synthesis of the ketone **72**, the precursor for our key asymmetric deprotonation methodology. The previous synthesis towards ketone **72** (Scheme 42) was based on protocols designed by Mundy *et al.*⁴³ Despite these well-established protocols, some modifications were made including a mesylation instead of a tosylation and decarboxylative cyclisation being mediated by acetic anhydride and sodium acetate as an alternative to Mundy's original barium hydroxide mediated cyclisation.



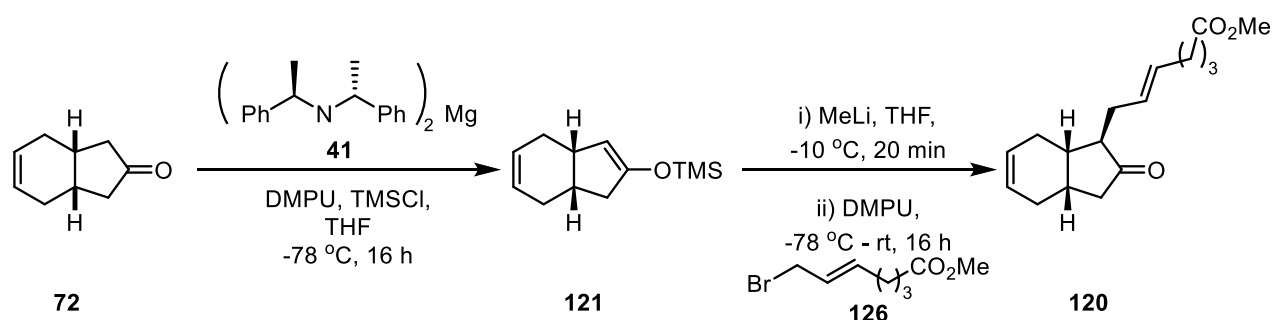
Scheme 42 - Synthetic route towards key ketone intermediate

With an established synthetic sequence in place for ketone **72** focus turned to the synthesis of allylic bromide **126**, the key compound that is necessary for the introduction of the side-arm of the natural target (Scheme 43).



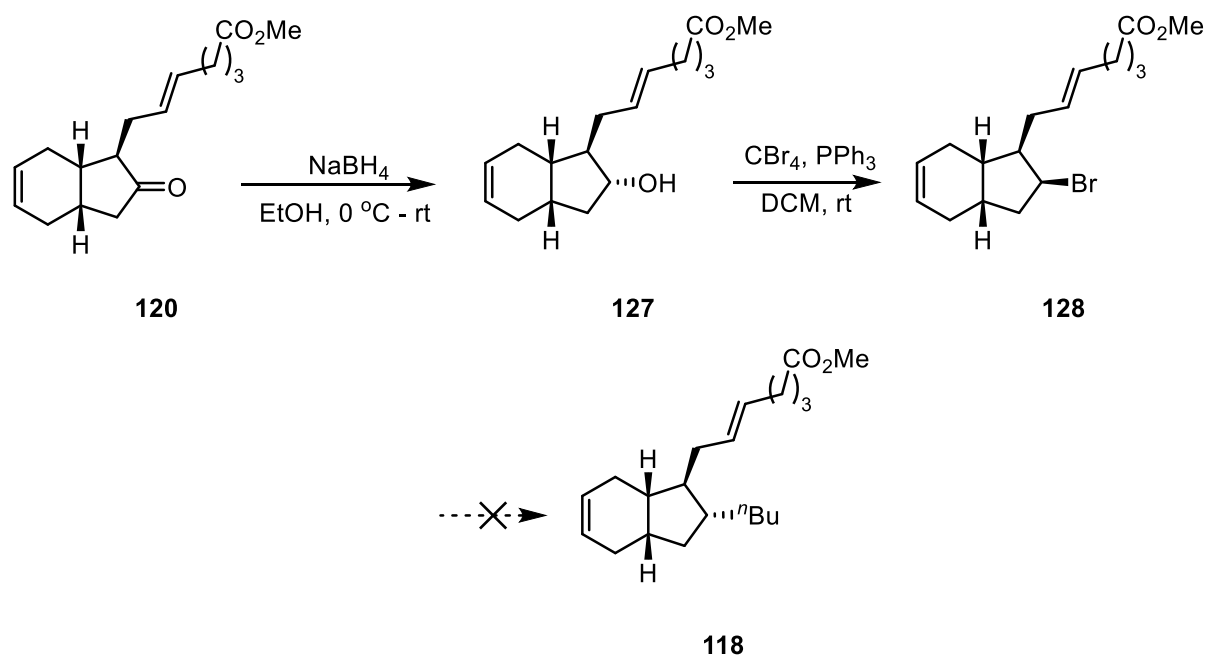
Scheme 43 - Synthetic route towards allylic bromide side chain

The short sequence developed to synthesise **126** commenced with the ozonolysis of cyclopentene **122** and subsequent treatment with acetic anhydride and triethylamine to afford aldehyde **123**. Subsequently, aldehyde **123** was then subjected to a Wittig olefination to afford enal **124**. Sequential treatment of enal **124** with sodium borohydride delivered the desired allylic alcohol **125**. Finally, subjecting allylic alcohol **125** to an Appel reaction furnished a route into the key allylic bromide side-chain **126**. With both convergent components in hand, the focus of the research with the team turned to the application of magnesium-bisamide based asymmetric deprotonation methodology as shown below (Scheme 44).



Scheme 44 - Asymmetric deprotonation and subsequent convergent synthetic step

Asymmetric deprotonation of ketone **72** has proven challenging in the past due to the hydrolytically unstable nature of trimethylsilyl (TMS) protecting groups. Despite this, using the group's developed asymmetric deprotonation methodology, isolation of the TMS enol ether **121** proved possible in high yields and, more importantly, in high enantiomeric ratios. With access to the TMS enol ether **121**, subsequent deprotonation to provide the lithium enolate which was treated *in situ* with allylic bromide **126** to give ketone **120** in 70 % yield. Impressively, this transformation was found to proceed stereoselectively as the *cis*-bridgehead of TMS enol ether **121** creates a concave and convex face. The convex face is the more favourable face for a molecule such as allylic bromide **126** to approach due to the reduced steric demand compared to the concave face. With the bulk of (–)-mucosin in place, the remaining work has focused on the installation of the final *n*-butyl side chain. The final efforts towards (–)-mucosin **55** are detailed in Scheme 45.

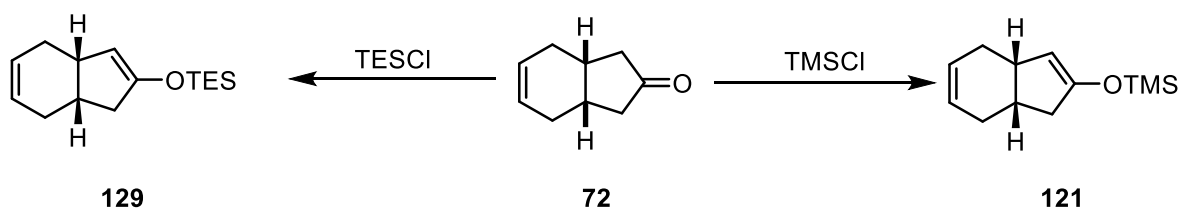


Scheme 45 - Towards the total synthesis of (–)-mucosin

With the three contiguous stereocentre ketone **120** in place, an S_N2 displacement to insert the n -butyl chain seemed an attractive synthetic strategy to follow. With concave face in ketone **120**, caused by the *cis*-bridgehead, a simple reduction of ketone **120** gave the desired alcohol **127** as a single diastereomer in a high yield of 85 %. The stereo inversion caused by the subsequent Appel reaction gave the corresponding bromide **121** in a prime position for a S_N2 displacement to occur with a butyl anion to give the methyl ester of (-)-mucosin **118**. Unfortunately, to date, no success has been achieved with the use of Grignard reagents or butyllithium-based protocols due to their preference to react with the methyl ester than with the sterically more challenging secondary bromide. As a result, work towards the total synthesis of (-)-mucosin **55** had stopped at this stage.

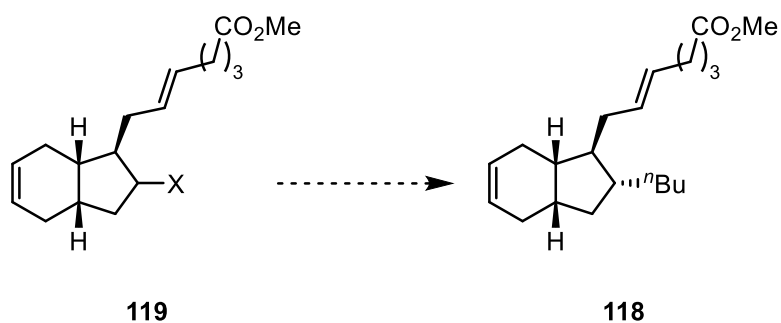
1.1.9. Proposed Work

With much of the route towards (-)-mucosin **55** in place, it was proposed to follow the procedures already in place to gain access to the advanced intermediate **121**. Having said this, the inclusion of an alternative silyl protecting group in the allylation procedure will be investigated. A hydrolytically robust silyl enol ether, such as a TES enol ether, could avoid the difficulty of handling capricious TMS enol ethers. Experiments will be carried out to determine whether the TES silyl enol ether **129** is a synthetically tractable precursor to the allylation or if the more sensitive TMS silyl enol ether **121** is the preferred precursor.



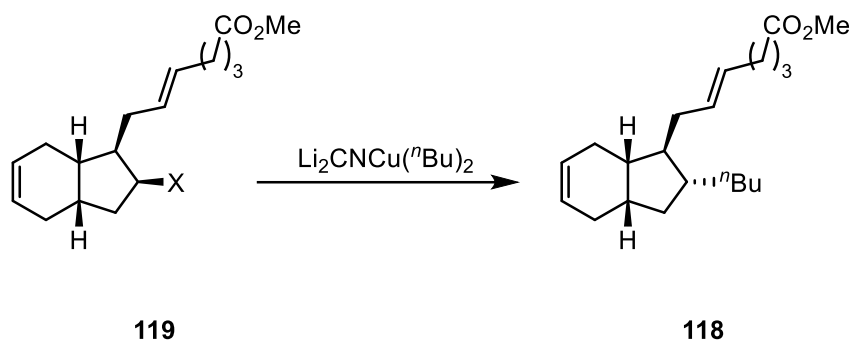
Scheme 46 - Possible enolate protecting group strategies.

Once intermediate **121**, or a derivative thereof, has been synthesised, investigations towards the final alkylation, to afford us the methyl ester of (-)-mucosin **118**, will be undertaken (Scheme 47).



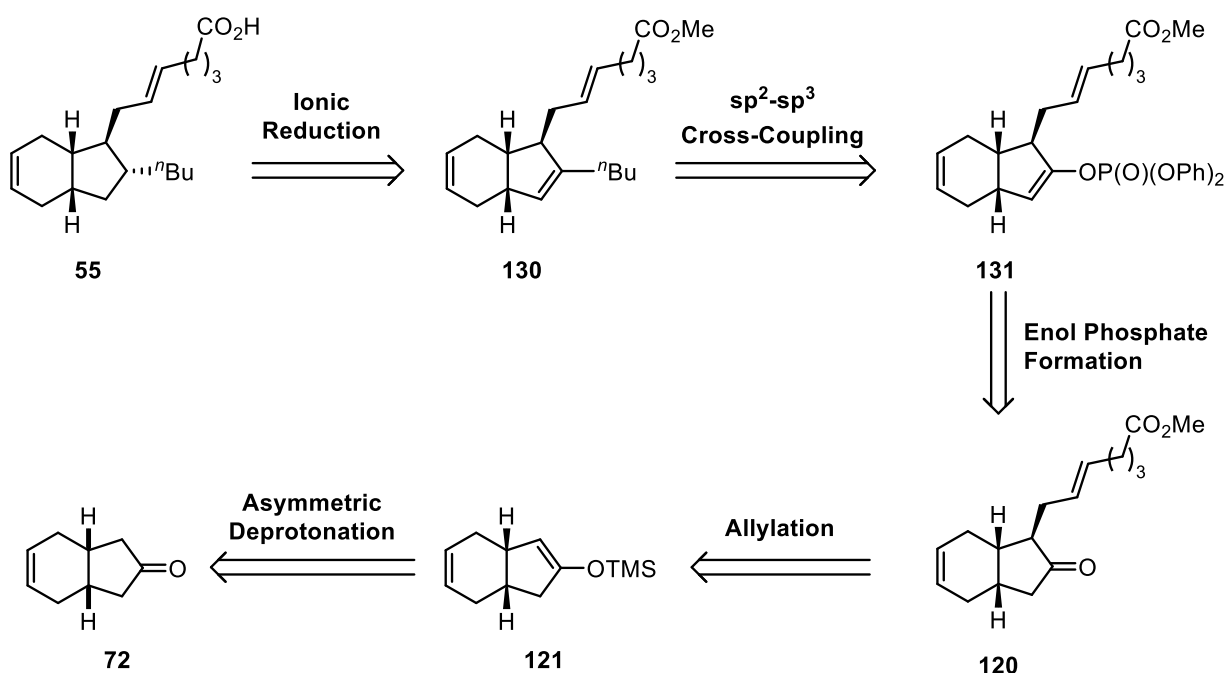
Scheme 47 - Envisioned route towards (-)-mucosin

Initial work will revisit the previously attempted application of Lipshutz organocuprate chemistry and investigate in further detail the outcome of this transformation (Scheme 48). It has been previously hypothesised that the organocuprate was attacking the methyl ester and not the sterically more challenging secondary bromide.⁴² If the methyl ester proves problematic, it may be beneficial to increase the steric demand around the ester by changing to an *iso*-propyl ester for example, or altering the ester moiety *via* reduction.



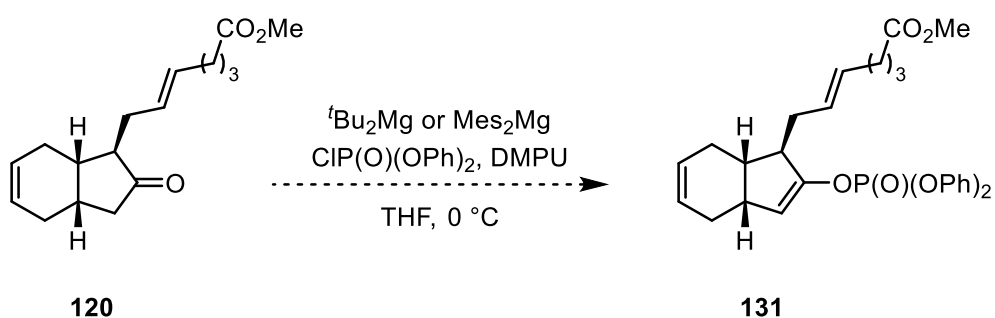
Scheme 48 - Potential use of Lipshutz chemistry

Should the Lipshutz chemistry prove unfruitful, an alternative strategy would be attempted to allow for the synthesis of (-)-mucosin **55**. This strategy outlined in the retrosynthetic route below in Scheme 49.



Scheme 49 - Proposed Retrosynthesis

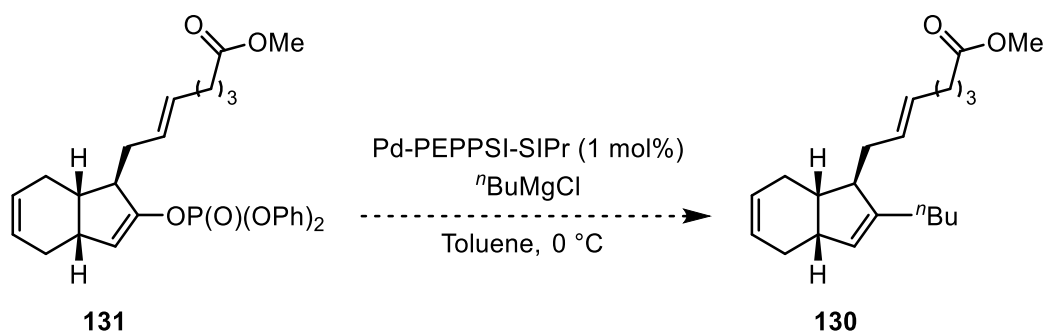
From (–)-mucosin, preceding the final hydrolysis, an ionic reduction could be employed to selectively remove the trisubstituted double-bond, in methyl ester **130**. To gain access to methyl ester **130**, an $\text{sp}^2\text{-sp}^3$ cross-coupling could be utilised to install the *n*-butyl side chain in (–)-mucosin after ketone **120** had a suitable pseudohalide such as an enol phosphate installed. Ketone **120** is synthesised from the previous route towards (–)-mucosin **55**. Having shown efficient access to ketone **120**, the main challenge of this proposed route will be installing an effective coupling partner and subsequently screening $\text{sp}^2\text{-sp}^3$ cross-coupling conditions. In order to facilitate an $\text{sp}^2\text{-sp}^3$ cross-coupling, an enol phosphate **131** could be accessed using chemistry recently published within the group, as shown in Scheme 50.³⁰



Scheme 50 - Enol phosphate synthesis

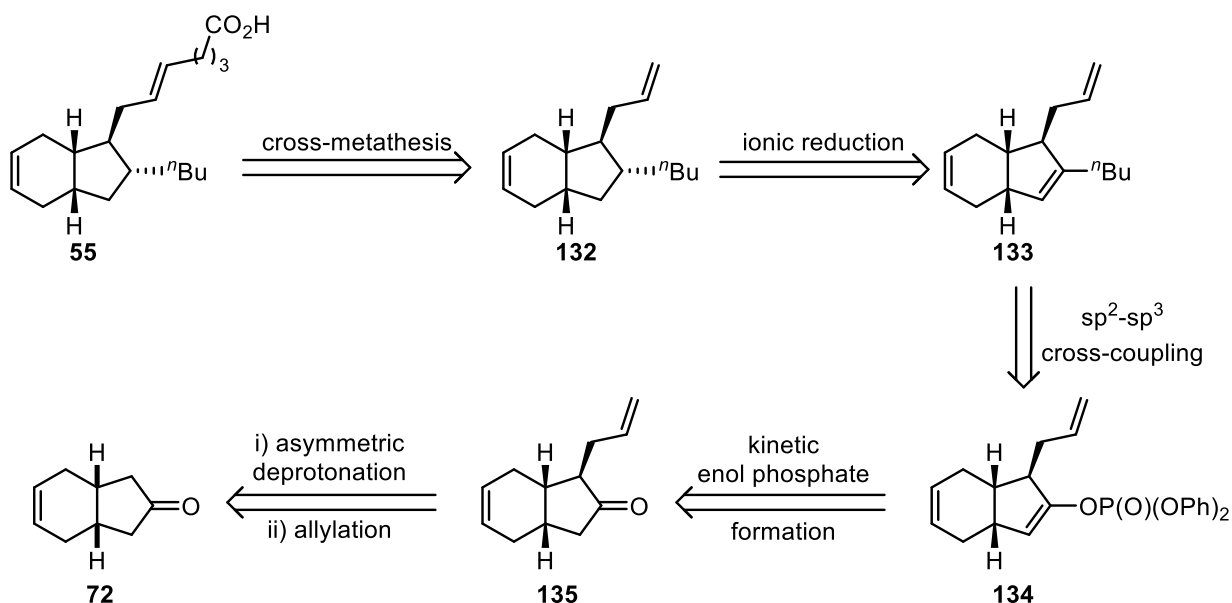
Once access to enol phosphate **131** is achieved, the next synthetic step to tackle would be the $\text{sp}^2\text{-sp}^3$ cross-coupling. We envisage, employing unpublished work from our own laboratory in which

Pd-PEPPSI-SIPr catalyses the Kumada reaction between enol phosphates and an alkyl Grignard reagent, as described in Scheme 51.³³



Scheme 51 - Use of in-house developed Pd-PEPPSI catalysed Kumada coupling

Optimising the Kumada cross-coupling could prove challenging due the inherent reactivity of ester functional groups in the presence of Grignard reagents. If this does prove to become an unsurmountable challenge, introducing or unveiling the ester group at a later stage in the synthesis would be preferential. A modification of the previously described strategy could involve a cross-metathesis as shown in Scheme 52.

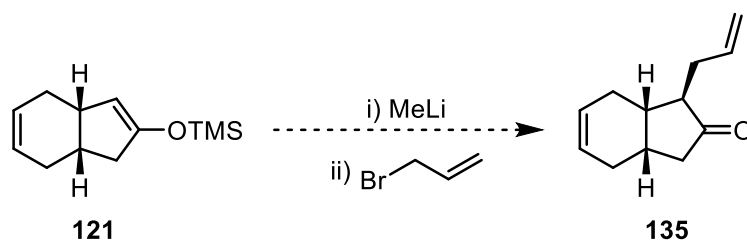


Scheme 52 - Proposed Retrosynthesis

From *cis*-mucosin, it is thought that the alkene portion bearing the acid functionality could be introduced late stage by a cross-metathesis from diene **132**. An ionic reduction, which favours the reduction of the more substituted olefin, could be employed to obtain diene **133**. Triene **133** could be furnished from the cross-coupling of *n*-butyl Grignard and enol phosphate **134**.

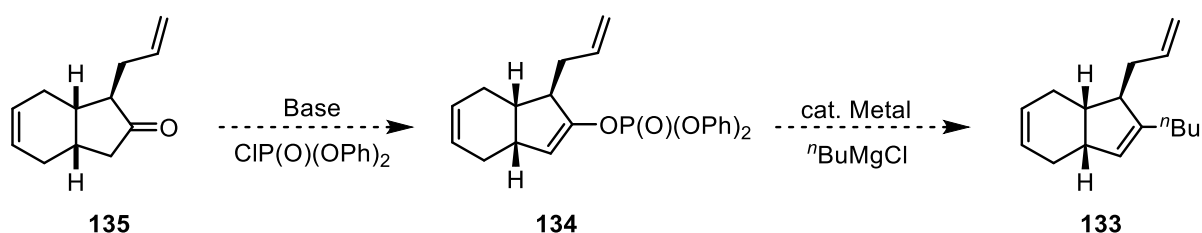
Utilising chemistry developed within our group, it is envisioned that enol phosphate **134** could be synthesised from ketone **135**. Using chemistry previously employed in the route towards (-)-mucosin, allyl-bearing ketone **135** would be the product of an asymmetric deprotonation and allylation procedure from the key ketone intermediate **72**.

With ketone **72** having previously shown competency in an asymmetric deprotonation reaction, the first step would be to ensure the efficiency of the allylation procedure, as shown in Scheme 53.



Scheme 53 – Allylation

The reaction above would ensure the positioning of three of the four required stereocentres, and hence future synthetic effort would then focus towards installing the ⁿbutyl side chain that features in (-)-mucosin **55**. The proposed route for installation of the ⁿbutyl side chain is shown in Scheme 54.

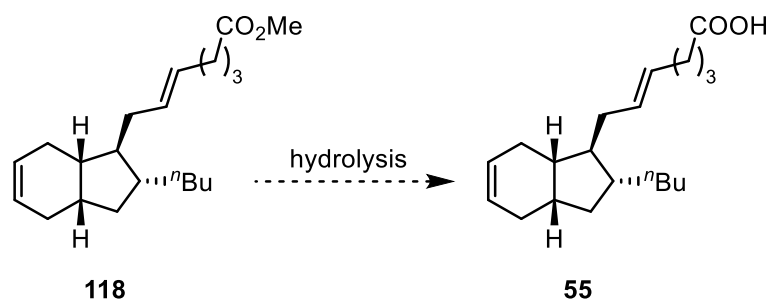


Scheme 54 - Installation of the ⁿbutyl side chain

The formation of enol phosphate **134** could proceed using previously published work within our laboratory. Having established the synthesis of enol phosphate **134**, work would then focus on producing triene **133** *via* a metal-mediated cross-coupling. It is here that the opportunity to use our in-house developed Pd-PEPSSI-SIPr cross-coupling methodology could be taken. If an sp^2 - sp^3 cross-coupling is successful in installing the ⁿbutyl chain, a challenging ionic reduction needs to be optimised on hydrocarbon **133** to allow only the reduction of the trisubstituted olefin. Typically, triethylsilane and trifluoroacetic acid are employed in ionic reductions such as in the 1991 synthesis of estrone.^{44,45}

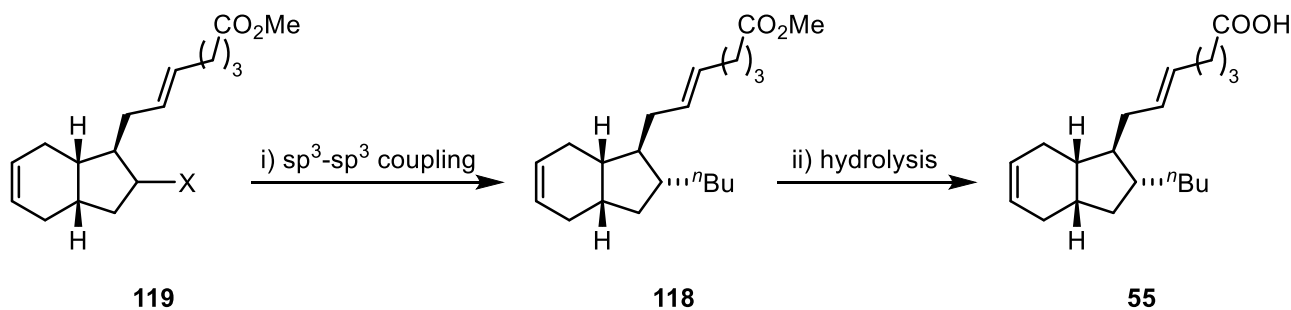
If the ionic reduction proves successful and access to the methyl ester **118** is achieved, it would be at this point that comparison to Casapullo's optical rotation and NMR characterisation would be undertaken. This would ensure that our proposed synthetic route has allowed access to (-)-mucosin

55. If our characterisation corroborated the data obtained by Stenstrøm, it is possible that one or more stereocentres of the natural product has been misassigned. If this is indeed the case, further work will need to be undertaken to redesign the route to allow for the synthesis of the correct stereoisomer of (–)-mucosin **55**. Once the correct stereoisomer of the methyl ester is obtained, a hydrolysis to yield (–)-mucosin **55** would be the final step (Scheme 55).



Scheme 55 - Hydrolysis to afford (–)-mucosin

Finally, if access to (–)-mucosin does prove challenging *via* the previously detailed strategies, recent literature has described examples of sp^3 - sp^3 cross-coupling reactions (Scheme 56).^{46,47} Alkyl-alkyl cross coupling would provide an interesting route towards the desired product, but is likely to require redesigning of the route already in place to obtain the correct stereochemistry.

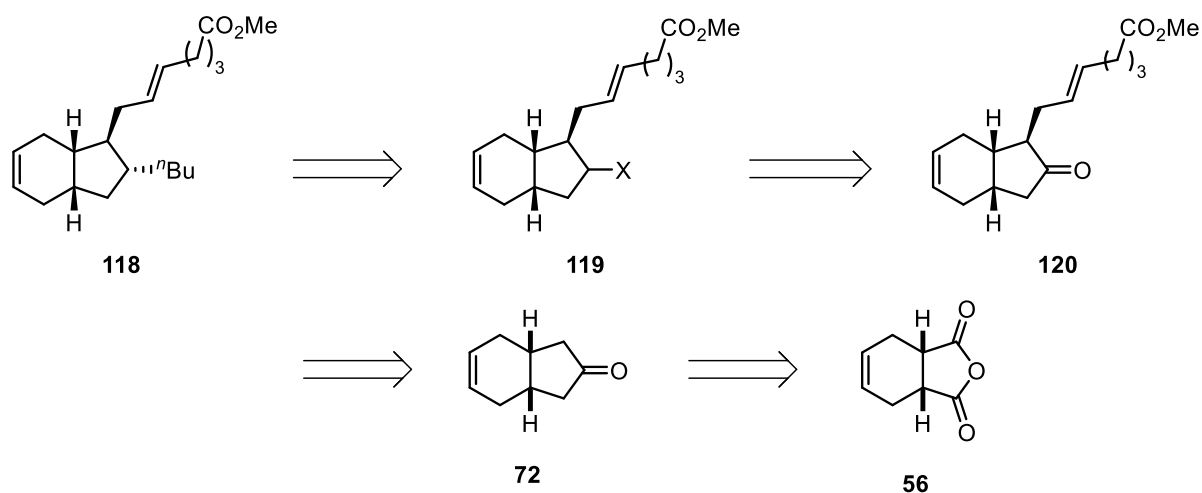


Scheme 56 - Proposed strategy to yield (–)-mucosin via sp^3 - sp^3 cross-coupling

1.2. Results and Discussion

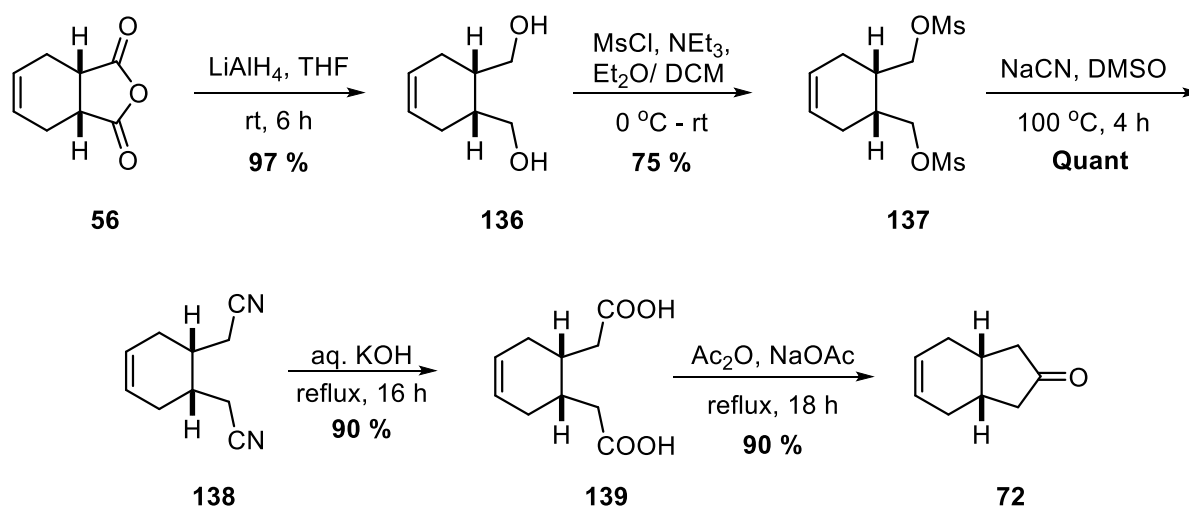
1.2.1. Synthesis of Key Bicyclic Ketone Intermediate **72**

As previously discussed, the initial synthetic target towards the synthesis of (-)-mucosin is bicyclic ketone **72**, as highlighted below (Scheme 57).



Scheme 57- Retrosynthesis of (-)-mucosin

It has previously been shown within Kerr laboratories that the desired ketone **72** can be accessed in a high yield of 51 %, over 5 steps, from the commercially available *cis*-1,2,3,6-tetrahydrophthalic anhydride **56**.^{41,42} As such, the synthesis of the key ketone intermediate **72** was synthesised as described in Scheme 58.

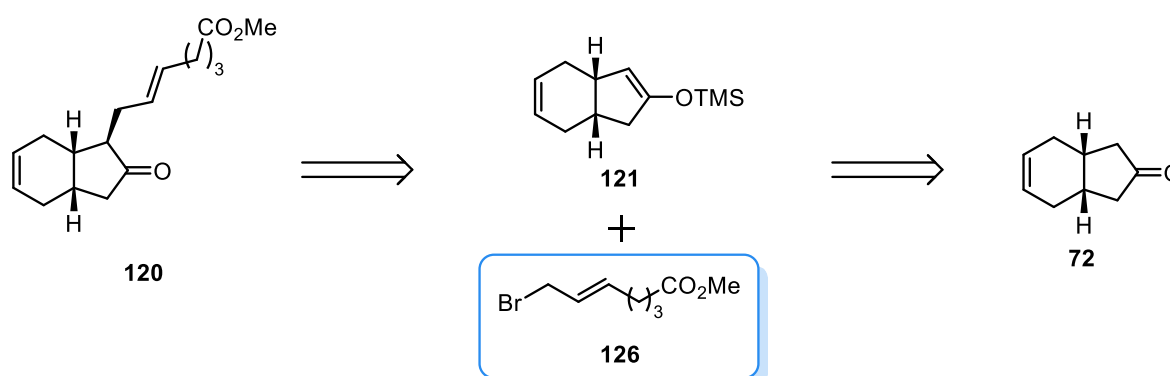


Scheme 58 - Synthesis of ketone **72**

Reduction of the anhydride **56** to the diol **136** proceeded efficiently when LiAlH₄ was employed, giving an excellent 97 % yield. With the diol **136** in hand, the homologation procedure commenced with mesylation, which proceeded in 75 % yield, followed by an S_N2 displacement with NaCN, furnished the dinitrile compound **138** in a quantitative yield. Hydrolysis of the dinitrile **138** with aqueous KOH afforded the diacid **139** in an excellent 90 % yield. Finally, the key ketone intermediate **72** was synthesised *via* a Dieckmann condensation of diacid **139**. To summarise, the synthesis of the key bicyclic ketone intermediate **72** was achieved using a modified version of Mundy's protocols and this afforded the desired bicyclic ketone **72** in an overall yield of 59 % over 5 steps; an excellent improvement on Mundy's reported literature yield of 12 % over 5 steps. As a synthetic route to a key intermediate, our developed protocols are operationally facile and high yielding overall. Additionally, it is important to note that only the final step requires column chromatography, significantly reducing time spent on purification and increasing the appeal of this optimised synthetic sequence.

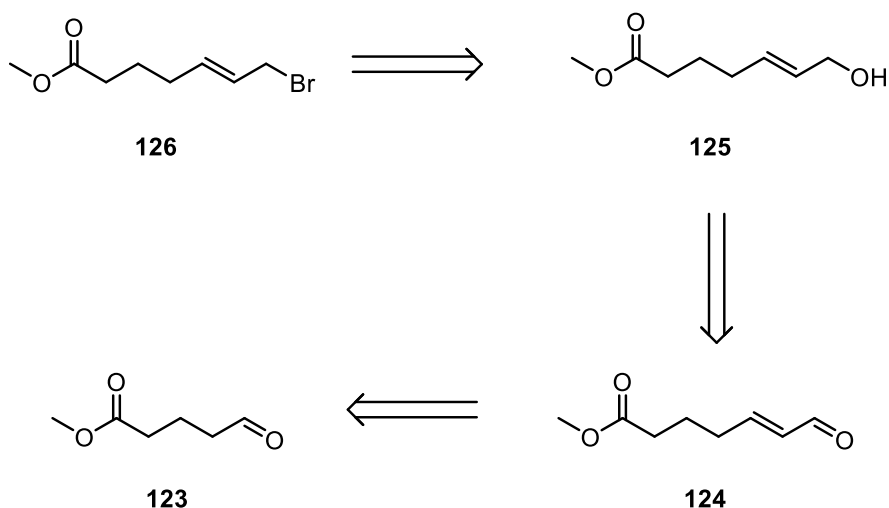
1.2.2. Synthesis of the Allylic Bromide Intermediate **126**

Having established the synthetic route towards the key ketone intermediate **72**, the core of the natural product target, attention focused on the requisite allylic bromide side chain **126** as highlighted in Scheme 59.



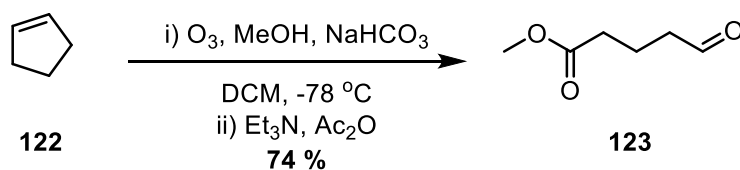
Scheme 59 - Retrosynthesis highlighting allylic bromide

As previously discussed, it was envisioned that **126** could be afforded directly from alcohol **125** *via* an Appel reaction. In turn, allylic alcohol **125** would be provided from the reduction of enal **124**, which ultimately could be prepared from compound **123** (Scheme 60).



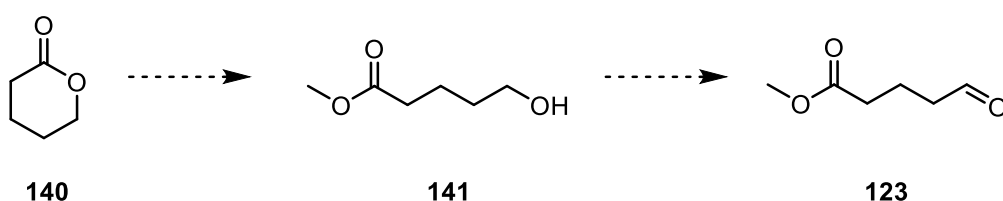
Scheme 60 - Retrosynthesis of the allylic bromide

The synthesis of aldehyde **123** was previously carried out within our laboratories *via* the ozonolysis of cyclopentene **122** with high yields (Scheme 61).⁴² Having said this, due to technical issues involving our ozonolysis equipment, an alternative route towards aldehyde **123** had to be devised in order to move forward.



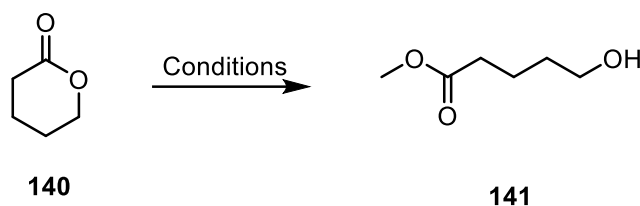
Scheme 61 - Ozonolysis of cyclopentene

The newly proposed synthesis of aldehyde **123** involved the ring opening of δ -valerolactone **140**, followed by an oxidation, as shown below in Scheme 62.



Scheme 62 - Proposed synthesis of aldehyde 123

Two methods could be employed for the ring opening of δ -valerolactone **140**, involving either basic or acidic conditions. Both protocols were attempted initially, and, pleasingly, acidic conditions proved very successful (Scheme 63, Table 6). Strangely, no product was observed at all when treating **140** with Et₃N in MeOH.

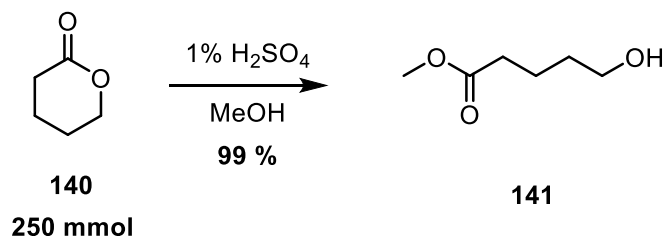


Scheme 63 - Ring opening of δ -valerolactone

Table 6- Initial results from the ring opening of δ -valerolactone

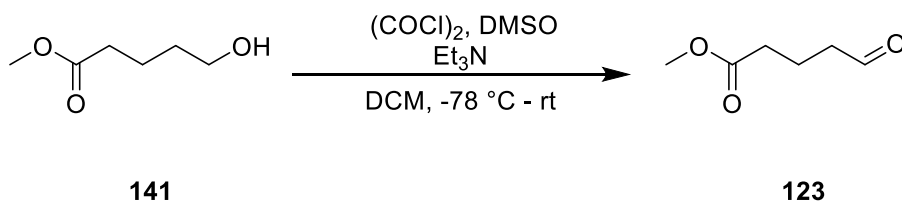
Entry	Conditions	Scale (mmol)	Yield (%)
1	1 % H ₂ SO ₄ in MeOH	4.99	80
2	3 % Et ₃ N in MeOH	4.99	-

Pleasingly, on repeating the acidic protocol on large scale, near quantitative yields were obtained, allowing effective access to large quantities of alcohol **141**, as documented in Scheme 64.



Scheme 64 - Large-scale hydrolysis

With efficient access to large quantities of alcohol **141** established, work focused upon oxidation of **141** to afford aldehyde **123**. It was thought that employing a Swern oxidation would prove successful (Scheme 65, Table 7).



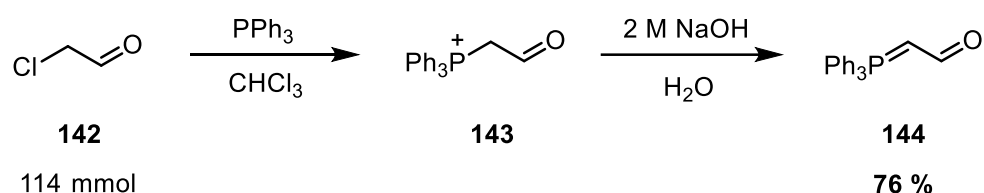
*Scheme 65 - Swern oxidation of alcohol **141***

Table 7- Swern oxidation

Entry	Scale (mmol)	Yield (%)
1	45.4	78
2	90.9	95

Due to the exothermic nature of the individual additions in a Swern oxidation, and its known poor thermal temperament, an internal thermometer was used to monitor the temperature throughout the various additions. Ensuring the internal temperature of the reaction never reached above $-72\text{ }^{\circ}\text{C}$, along with using freshly distilled dimethylsulfoxide (DMSO), proved essential to achieving the high yields shown in entries 1 and 2 of Table 7. Initially, a good yield of 78% was achieved, as shown by entry 1 in Table 7. Upon an increase in scale, gratifyingly, column chromatography allowed purification of the desired aldehyde **123** with no observed degradation to give an excellent 95 % yield as shown by entry 2 in Table 7.

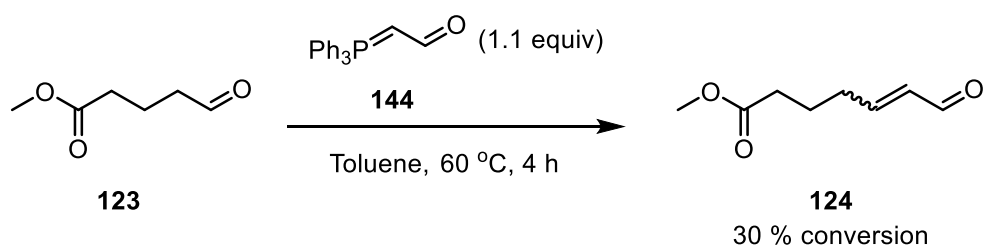
Having established the ring opening of δ -valerolactone **140**, followed by a Swern oxidation to afford aldehyde **123**, the next step in the synthetic sequence consisted of a Wittig reaction to afford enal **124**. In order to perform the Wittig reaction, significant quantities of the stabilised ylide **137** were required. The preparation of ylide **137** is detailed in Scheme 66 below.



Scheme 66 - Formation of stabilised ylide 144

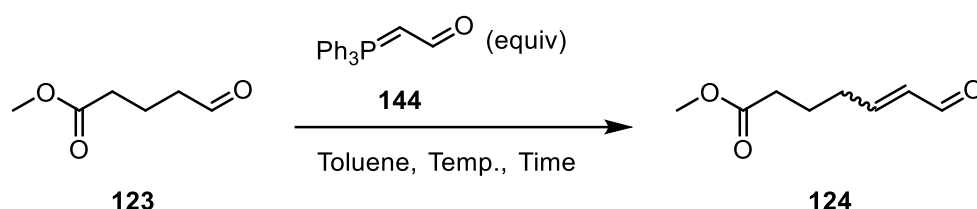
Following procedures developed by Huefner *et al.* stabilised ylide **144** was easily synthesised in large quantities.⁴⁸ It should be highlighted that the best quality ylide was obtained when the crude product was triturated with hot toluene. Interestingly, upon NMR spectral analysis the *cis* and *trans* conformers of ylide **144** are observed (see experimental for details).

With significant quantities of both aldehyde **123** and stabilised ylide **144** in hand, the subsequent Wittig reaction could be attempted. Initially, we employed conditions that had been previously reported as successful within our research team (Scheme 67).⁴¹



Scheme 67 - Initial attempted Wittig reaction

Unfortunately, TLC monitoring of this reaction proved ineffective, as both the starting material and desired product had the same retention factor (R_f). Having said this, monitoring using ^1H NMR spectroscopy provided sufficient information to quantify the conversion of the reaction. Unfortunately, only 30 % conversion was achieved in the first attempt (Scheme 67). Following this, optimisation was carried out, initially based on the assumption that increasing the equivalents of ylide **144** would increase the conversion towards the desired enal **124** (Scheme 68, Table 8).

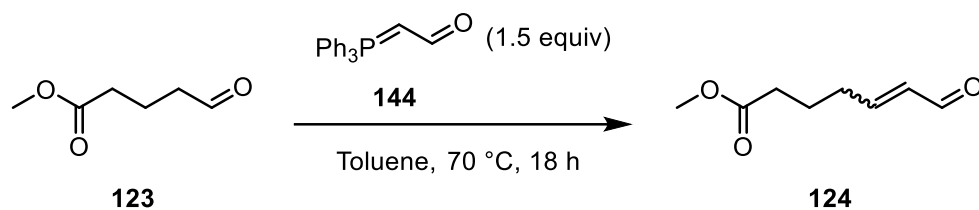


Scheme 68 - Wittig reaction optimisation

Table 8- Optimisation of Wittig reaction

Entry	Ylide (equiv)	Time (h)	Temperature	SM present (%)	Yield (%)	E:Z
1	1.5	18	70	10	52	9:1
2	2.5	18	70	11	58	9:1
3	3.0	18	70	10	54	9:1
4	3.5	18	70	10	67	9:1
5	4.0	18	70	10	64	9:2
6	1.5	64	70	0	56	7:3

As documented in Entries 1-5 in Table 8, increasing the equivalents of the stabilised ylide did not affect the conversion to the desired product. As shown by Entry 6 in Table 8, increasing the reaction length did lead to complete conversion to the desired enal product **124** but, unfortunately, caused significant isomerisation of the olefin. Indeed, the isomerisation was not favourable considering the required *E* geometry for the target molecule. It was hypothesised that the isomerisation observed as a result of extended reaction times could be due to the light sensitivity to enal **124**. With this in mind, the Wittig reaction was carried out with the exclusion of light, as shown in Scheme 69, Table 9.

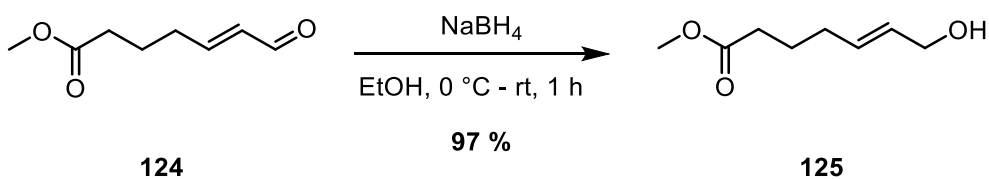


Scheme 69 - Wittig reaction in the dark

Table 9 - Wittig reaction results in the dark

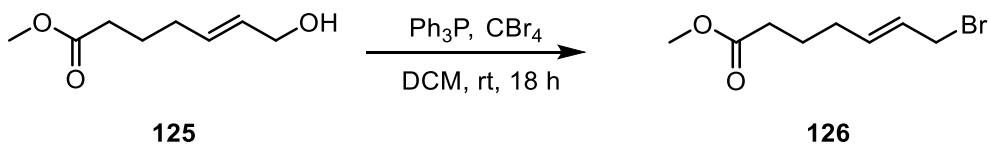
Entry	Scale (mmol)	Yield (%)	E:Z
1	7.68	50	92:8
2	46.1	68	92:8

Pleasingly, carrying out the reaction in the dark not only reduced the amount of isomerisation, but also allowed the reaction to be carried out using a lower number of equivalents of ylide **144** (Table 9, Entry 1). Further success was achieved when increasing the scale, which delivered a good yield of the desired enal **124** at 68 % (Table 9, Entry 2). With enal **124** material in hand, the selective reduction of the aldehyde functionality to give allylic alcohol **125** was undertaken (Scheme 70).



Scheme 70 - Reduction of enal

The reduction of enal **124** proceeded in excellent yields. Having achieved success in the penultimate transformation toward the allylic bromide chain **126**, the final Appel was initially attempted using the Appel reaction conditions already commonly utilised, within our team (Scheme 71, Table 10).

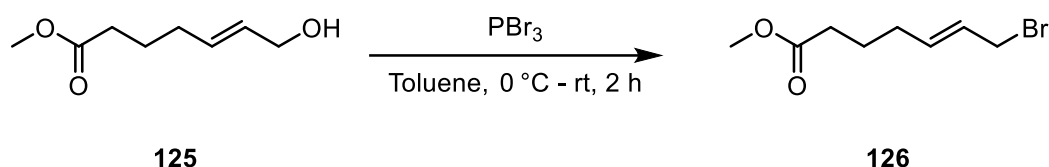


Scheme 71 - Appel reaction using carbontetrabromide

Table 10 - Results from Appel reaction using carbon tetrabromide

Entry	Scale (mmol)	Yield (%)
1	0.50	67
2	2.46	55
3	3.80	53

Employing Appel conditions using carbon tetrabromide and triphenylphosphine, pleasingly, afforded the desired allylic bromide **126**, however only in moderate yields (Table 10). When compared to the previously reported yield of 85 %, ⁴¹ this proved disappointing. No further improvement was observed with the use of recrystallized carbon tetrabromide and triphenylphosphine (Table 10, Entry 3). Despite now having the fully functionalised side chain for our synthesis, we continued to optimise the bromination reaction by attempting the transformation using phosphorous tribromide (Scheme 72, Table 11).



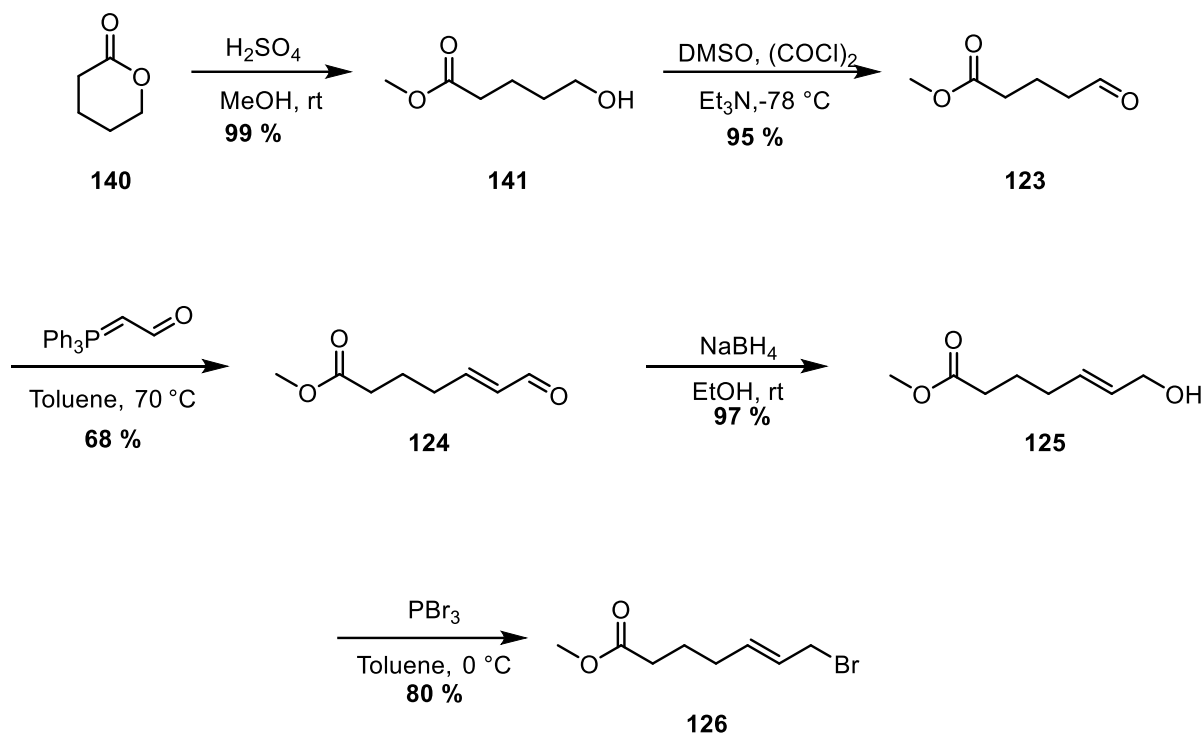
Scheme 72 – Bromination reaction using phosphorous tribromide

Table 11 - Results from bromination reaction using phosphorous tribromide

Entry	Scale (mmol)	Yield (%)
1	3.90	80
2	20.2	67

Pleasingly, good yields were obtained using this protocol with the highest yield obtained being 80 % (Table 11, Entry 1). Unfortunately, a slight reduction in yield was observed upon an increase in scale as shown in (Table 11, Entry 2). Nonetheless, this procedure allowed synthesis of multigram quantities of the desired allylic bromide side chain **126**.

To summarise, the synthesis of the allylic bromide side chain has been successfully completed *via* the modification and optimisation of the original procedures already in place at the outset of the project. These modifications afforded the desired allylic bromide **126** in 50 % over five steps (Scheme 73) whereas the previously reported synthesis, detailed in Scheme 43, afforded the desired product **126** in 41 % over four steps.

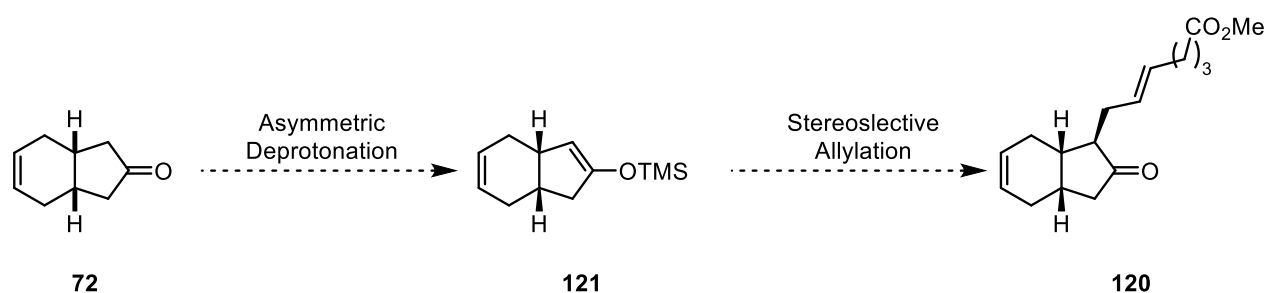


Scheme 73 - Overall synthesis of the allylic bromide side chain

At this stage, both key fragments for mucosin have been prepared efficiently, and in sufficient quantities to investigate the key asymmetric deprotonation reaction and subsequent allylation to begin the assembly of the natural product structure.

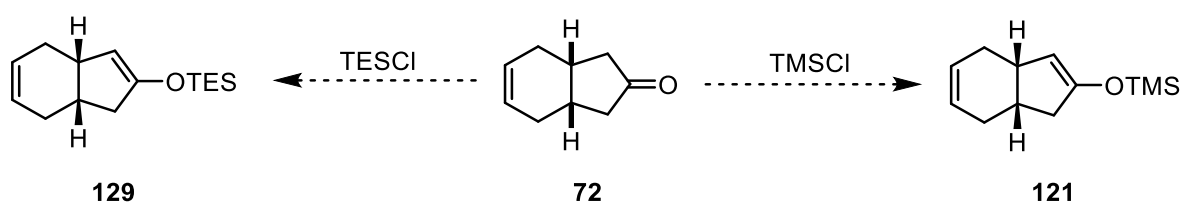
1.2.3. Application of Magnesium-Bisamides in Asymmetric Deprotonation

Having efficiently prepared both key fragments for the proposed synthesis of (–)-mucosin **55**, studies towards the union of these two fragments were now undertaken. As shown in Scheme 74, the C–C bond formation proceeds *via* an initial asymmetric deprotonation, followed by electrophilic trapping, to generate **120**. Indeed, chemistry from the Kerr group, employing magnesium bisamide chemistry is a suitable strategy for our target synthesis. Following this, electrophilic trapping of TMS enol ether **121** with allylic bromide chain **126** would afford the desired late stage intermediate **120** (Scheme 75).



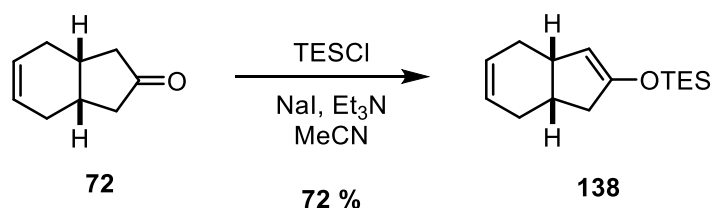
Scheme 74 - Proposed convergent synthesis of late stage intermediate 120

Due to the hydrolytically unstable nature of TMS enol ethers, it was decided that the asymmetric deprotonation would be carried out concurrently with the use of a TMS protecting group and the more robust TES protecting group (Scheme 75).



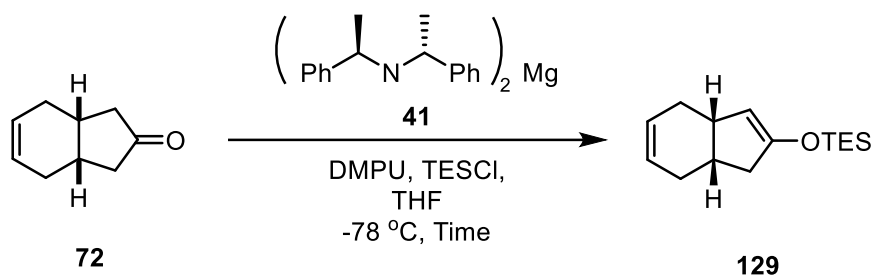
Scheme 75 - Protecting group strategies

Due to the greater inherent stability of a TES protecting group, work was initially carried out towards the TES protected enol ether **129**. At first, a racemic sample of the product **138** was synthesised to probe the formation of the TES enol ether. Additionally, the racemic silyl enol ether will allow the determination of the enantiomeric ratio of the subsequent asymmetric deprotonation by chiral HPLC. Using Finkelstein type conditions to allow the *in situ* formation of TESI which offers increased electrophilicity in comparison to TESCl, a racemic sample of the enol ether was synthesised (Scheme 76).



Scheme 76 - Synthesis of racemic sample

The racemic silyl enol ether was made in a 72 % yield. Having synthesised the racemic silyl enol ether, the asymmetric synthesis of TES silyl enol ether **129** was attempted using the magnesium bisamide **41**, as shown in Scheme 77, Table 12. Bisamide **41** was prepared from the corresponding amine (see experimental section for full details).



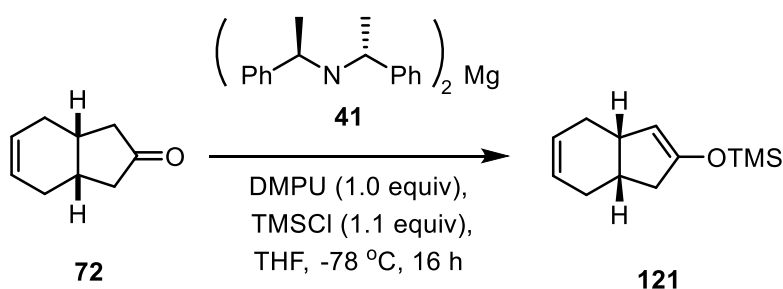
Scheme 77 - Asymmetric deprotonation trapping with TESCO

Table 12 - Results from the asymmetric deprotonation and TESCO trapping

Entry	Scale (mmol)	Additive	Time (h)	Yield (%)	e.r.
1	0.79	DMPU (1.0 equiv)	1	20	n/a
2	0.79	DMPU (2.0 equiv)	1	51	n/a
3	2.40	DMPU (2.0 equiv)	3	65	94:6

As shown in Table 12, initial results proved disappointing when only using one equivalent of DMPU to obtain a meagre yield of 20 % (Entry 1). An increase in yield to 51 % was observed when increasing the DMPU equivalents as shown in Entry 2. Additionally, an increase in scale afforded an increase in yield to give the desired TES enol ether **129** in 65 % yield. Following the analysis by chiral HPLC, the enantiomeric ratio of the TES enol ether **129** from the asymmetric deprotonation was determined to be 94:6 as shown in Table 12, Entry 3.

With a procedure towards the synthesis of the TES enol ether **138**, the synthesis of the inherently more unstable TMS enol ether **121** was attempted. Using conditions which had been optimised for the synthesis of the TMS enol ethers within our research group, the asymmetric deprotonation of **72** was attempted, trapping with TMS chloride (Scheme 78, Table 13).



Scheme 78 - Asymmetric deprotonation to afford TMS enol ether 121

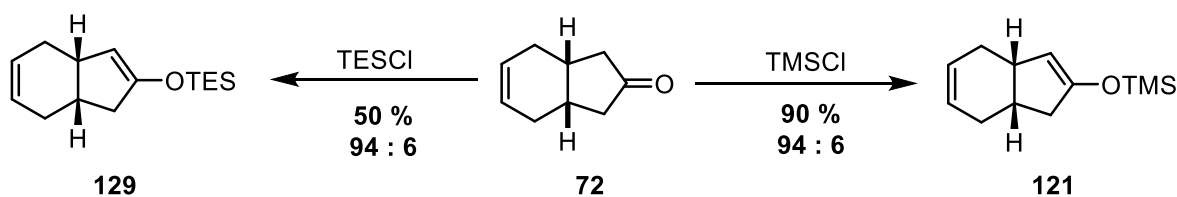
Table 13 - TMS enol ether **121** results

Entry	Scale (mmol)	Purification	Yield (%)	e.r.
1	0.80	Silica (oven dried)	-	-
2	4.20	Silica (oven dried)	86 ^a	95:5
3	4.20	Silica (oven dried)	90 ^a	94:6

a) column dimensions \varnothing 55 mm x 50 mm

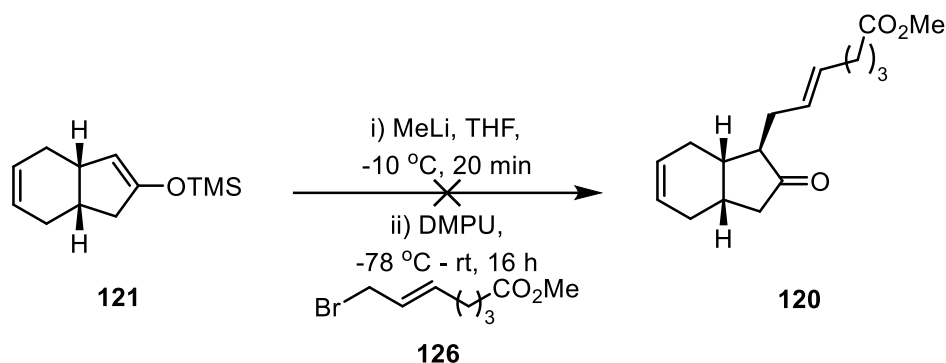
Pleasingly, conversion was observed from the initial attempt at the asymmetric deprotonation. Unfortunately, upon purification using oven-dried silica, no product was afforded and returned only the starting ketone (Table 13, Entry 1). This led to the hypothesis that the TMS enol ether **121** was hydrolysing on the silica column. It was envisioned that use of a short silica column with a fast flow rate would prevent the TMS enol ether **121** from hydrolysing. This method would require the correct balance of column dimensions to achieve a good separation but not cause any degradation of the desired product *via* contact with the silica stationary phase. Gratifyingly, after trialling various column dimensions, as shown by Entry 2 in Table 13, a good yield of 86 % was achieved with a silica column of a 55 mm diameter and a height of 50 mm. After comparison with a racemic sample of the product by chiral HPLC, the TMS enol ether **121** had been formed in an excellent enantiomeric ratio of 95:5. To add to this success, upon increasing the scale of the reaction, an excellent yield of 90 % was achieved, with an excellent enantiomeric ratio of 94:6 (Table 13, Entry 3). This optimisation highlighted that the correct column conditions can allow the chemist to achieve high isolated yields of these inherently unstable TMS enol ethers.

In summary, two different methods of trapping a reactive enolate have been developed namely as the TMS or TES enol ether species (Scheme 79). Notably, purification of the capricious TMS enol ether **121** has been further optimised to allow reliable isolation. At the current stage, the TMS enol ether **121** can be viewed as the more attractive intermediate to take forward due to the ability to achieve an excellent yield of 90 % upon isolation. Further work could be attempted to improve the yield of the TES enol ether **129**, possibly by using column dimensions like that utilised with the TMS enol ether.



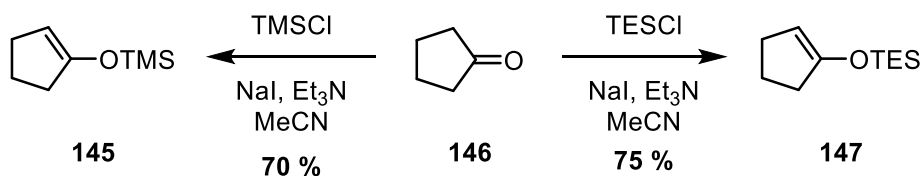
Scheme 79 - Results from the asymmetric deprotonation

Having established proficiency in the asymmetric synthesis and isolation of silylated ethers **121** and **129**, the focus of the project turned to the subsequent electrophilic quench with allyl bromide **126**. Unfortunately, an initial attempt, using MeLi and a DMPU additive failed (Scheme 80).



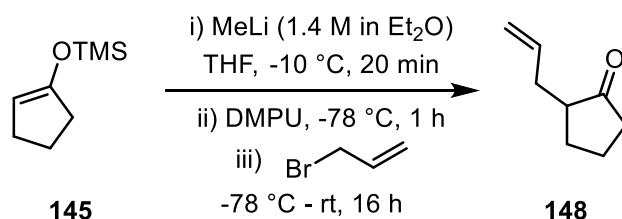
Scheme 80 - Failed allylation

As both starting materials involved in this transformation require a significant synthetic investment, it seemed sensible to trial this transformation with a commercially available test substrate. Cyclopentanone **146** was selected as a suitable test substrate and allyl bromide was chosen as the electrophilic quench. As such, the respective TMS and TES silyl enol ethers were synthesised from cyclopentanone **146** (Scheme 81). In both cases, good yields were obtained.



Scheme 81 - Formation of the silyl enol ether test substrates

With good quantities of each test substrate in hand, initial testing commenced, employing the TMS enol ether **145**. The conditions are described in Scheme 82 below and the results displayed in Table 14.

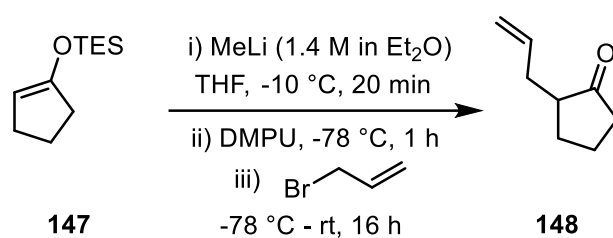


Scheme 82 - Test allylation on TMS enol ether 145

Table 14 - Results from test allylation on TMS enol ether **145**

Entry	Scale (mmol)	Yield (%)
1	0.6	0
2	0.6	72

The initial attempt proved unsuccessful, and returned cyclopentanone **146**, presumably from deprotection then subsequent quench by water, either from moisture within the reagents or from the aqueous work-up. To eliminate the possibility that the TMS enol ether **145** contained small quantities of water, which would prevent the reaction from proceeding, the TMS enol ether **145** was diluted with plenty of chloroform to allow for azeotropic removal of water. Following this drying of the starting substrate, a yield of 72 % was obtained, as shown in Entry 2 in Table 14. This highlights the need for rigorously anhydrous conditions to allow the allylation to proceed. With confidence in the lithium enolate formation and electrophilic quench, the procedure was applied to the TES enol ether **147**, as shown in Scheme 83, with the results documented in Table 15.



Scheme 83- Test allylation of TES enol ether **147**

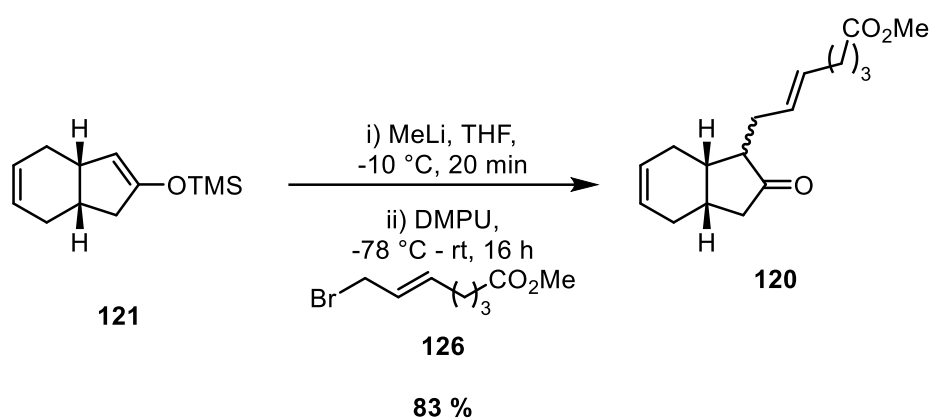
Table 15 - Results from test allylation on TES enol ether **147**

Entry	Scale (mmol)	Yield (%)
1	0.6	10 ^a
2	0.6	73 ^b

a) 20 mins enolate formation, b) 2 h enolate formation

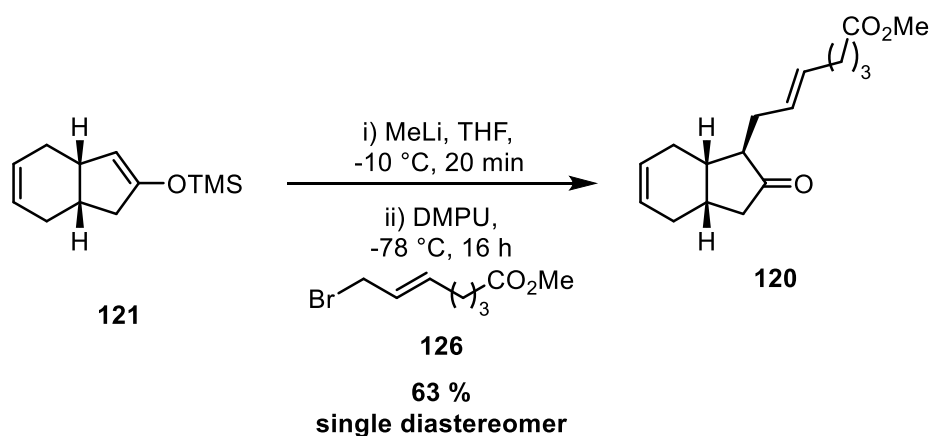
Disappointingly, initial results using the above procedure only afforded 10 % of the desired product as shown by Entry 1 in Table 15. It was thought that the more stable TES protecting group would be more resistant to enolate formation using MeLi as compared to the facile enolate formation observed by the TMS enol ether **145**. In order to circumvent this issue, a longer enolate formation time was applied, to hopefully solve this issue. As a result, allowing the enolate formation to occur over two hours, followed by an electrophilic quench, gave an excellent yield of 73 % considering literature precedent for similar transformations.⁴⁹ Having achieved a successful result, using the TES enol ether **147** test

substrate, it was anticipated that application of this procedure to the (–)-mucosin **55** synthesis would proceed effectively. Using the conditions described in Scheme 84, ensuring strictly anhydrous conditions and thorough distillation or drying of all starting materials and reagents, we were pleased to achieve excellent yields of our advanced intermediate **120** (Scheme 84).



Scheme 84 - Successful allylation

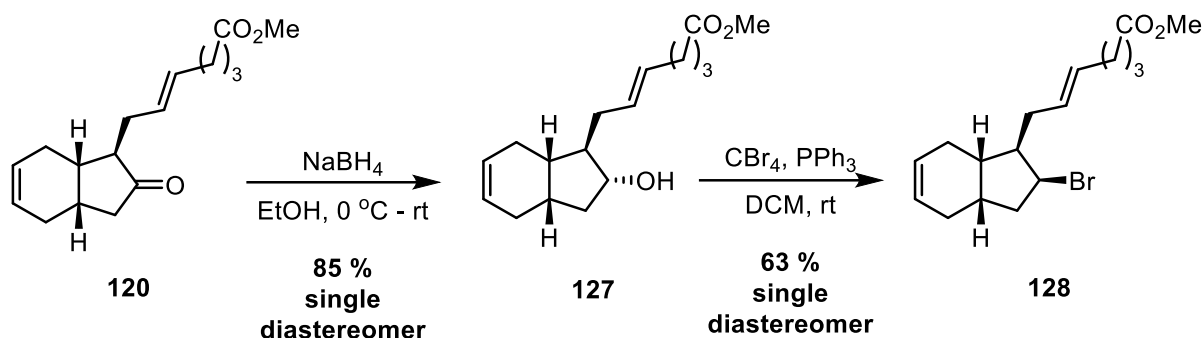
Pleasingly, an initial high yield of 83 % was obtained using the TMS enol ether **121** as the starting substrate due to the competence. Unfortunately, the allylation did not proceed diastereoselectively as indicated by the ^{13}C NMR spectrum. However, due to the qualitative nature of ^{13}C NMR, no quantification of the diastereoselectivity of the transformation could be extrapolated at this point. Despite this, it is possible that holding the electrophilic quench at $-78\text{ }^{\circ}\text{C}$, as opposed to allowing it to warm to room temperature, could allow better diastereoselectivity, as shown in Scheme 85.



Scheme 85 - Stereoselective allylation

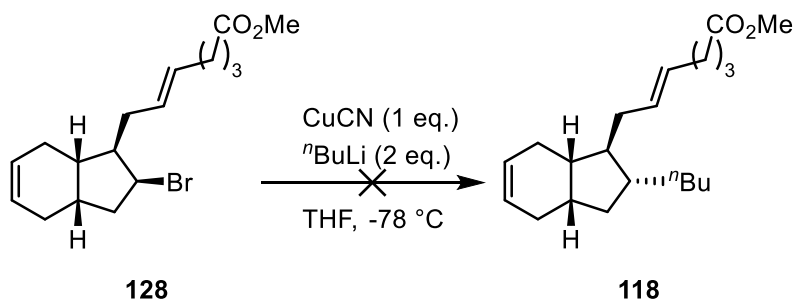
Indeed, performing the electrophilic quench at a sustained low temperature of $-78\text{ }^{\circ}\text{C}$ furnishes the desired allylated ketone **120** as a single diastereomer, albeit in a reduced yield of 63 %. With the three contiguous stereocentres present in ketone **120** in place, an $\text{S}_{\text{N}}2$ displacement to insert the n -butyl chain

seemed an attractive synthetic strategy to follow. Conversion of the ketone **120** to the corresponding bromide, required for the desired S_N2 displacement, was carried out in a stereoselective fashion *via* a reduction and subsequent Appel reaction, as described in Scheme 86.



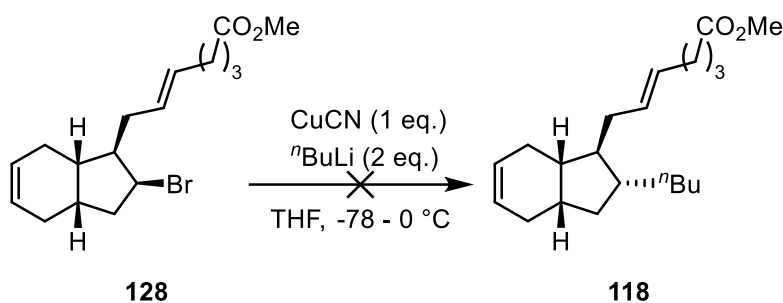
Scheme 86 - Synthesis of bromide (128)

With the concave face in ketone **120**, caused by the *cis*-bridgehead, a simple reduction of ketone **120** gave the desired alcohol **127** as a single diastereomer in a high yield of 85 %. The stereoinversion resulting from the subsequent Appel gave the corresponding bromide **128** in a good yield of 63 %; in a prime position for a S_N2 displacement to occur with a n butyl nucleophile to give the methyl ester of (–)-mucosin **118**. Typically, Lipshutz cyanocuprate chemistry is implemented in the displacement of secondary alkyl bromides or iodides in a stereoinvertive manner. Accordingly, S_N2 displacement was attempted on alkyl bromide **128** as shown in Scheme 87.



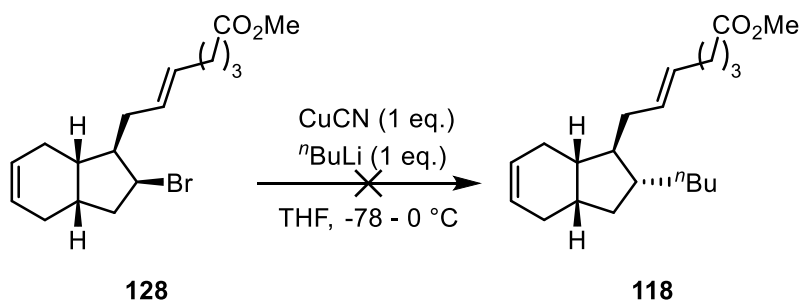
Scheme 87 - Higher-order cyanocuprate chemistry

Surprisingly, no reaction was observed at $-78\text{ }^\circ\text{C}$ and the starting material was recovered. Indeed, the chemical literature shows that the reaction at secondary alkyl bromides might require elevated temperatures compared to the same reaction carried out on a secondary alkyl iodide.⁵⁰ With this in mind, the same reaction was attempted, and the reaction was allowed to warm to $0\text{ }^\circ\text{C}$ (Scheme 88).



Scheme 88 - Higher-order cyanocuprate chemistry with warming

Unfortunately, warming of the reaction resulted only in decomposition of the secondary bromide **128**. It is possible that the *n*butyl nucleophile could preferentially attack the ester, present in the secondary bromide **128**, if the desired reaction centre proves sterically inaccessible, due to the concave nature of the ring system. Accordingly, lower-order cyanocuprates were also examined, in order to probe whether reactive organocuprates could prevent unproductive side reactions from occurring (Scheme 89).

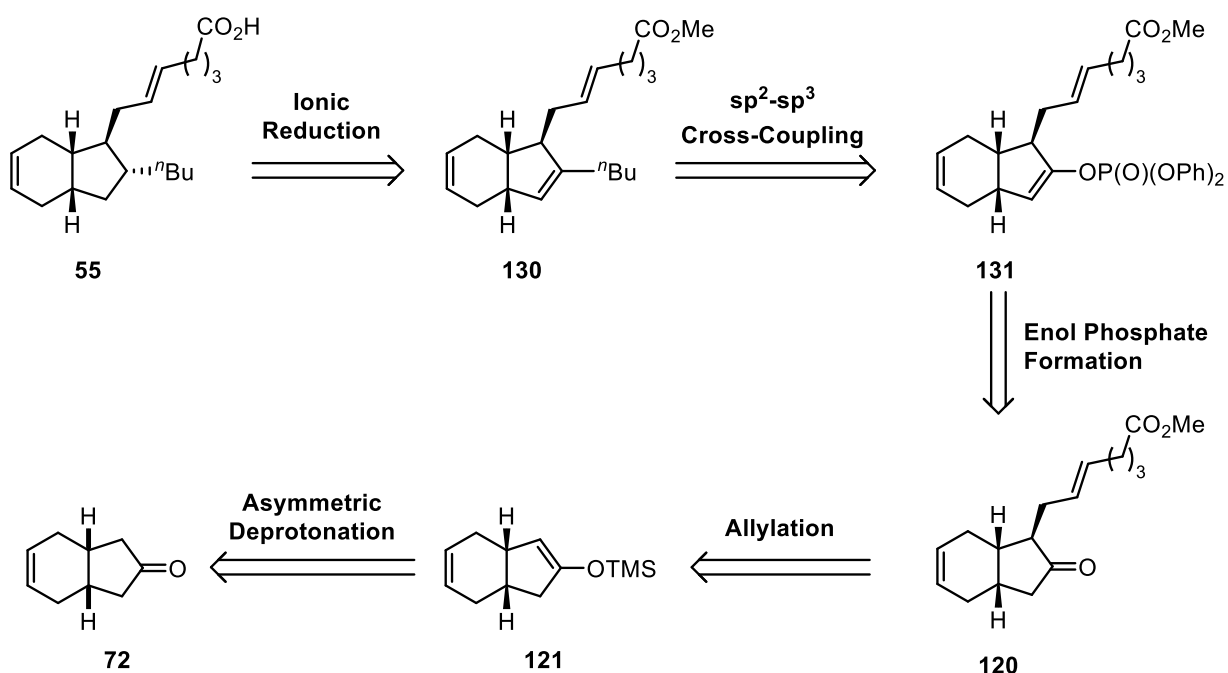


Scheme 89 - Lower-order cyanocuprate chemistry with warming

Unsurprisingly, no desired reaction was observed, and no starting bromide **128** could be recovered. At this stage the secondary alkyl bromide **128** was considered relatively inaccessible, compared to the accessible ester moiety, for the desired reactivity to occur and a change in strategy was now being deliberated.

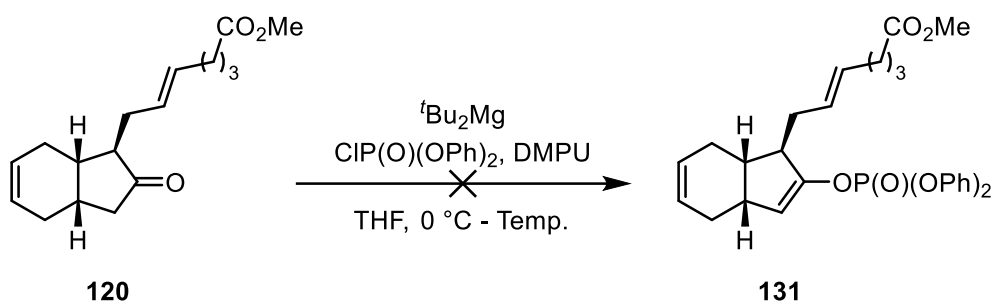
1.2.4. $\text{sp}^2\text{-sp}^3$ cross-coupling

Having demonstrated the difficulties using late-stage alkylation with high-order cyanocuprate chemistry, a new strategy was developed to allow the synthesis of (–)-mucosin **55**. The new strategy is described in the retrosynthetic route below in Scheme 90.



Scheme 90 - Proposed Retrosynthesis

It has previously been shown within Kerr laboratories that the carbon centred magnesium base, $t\text{Bu}_2\text{Mg}$, can facilitate the formation of enol phosphates from their respective ketones.³⁰ As such, the enol phosphate formation conditions were applied to the proposed synthetic route of (-)-mucosin **55**, as shown below in Scheme 91, Table 16.

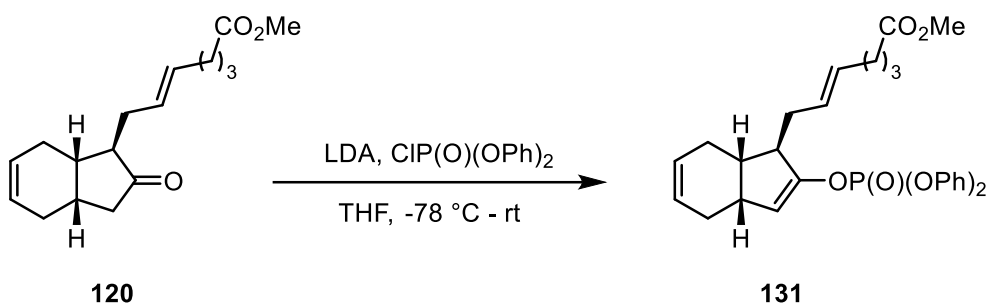


Scheme 91 - Enol phosphate formation

Table 16 - Results from enol phosphate formation

Entry	Temperature (°C)	Result
1	rt	No reaction, 93 % SM recovered
2	30	No reaction, 82 % SM recovered
3	40	No reaction, 87 % SM recovered

Surprisingly, the enol phosphate formation did not proceed on ketone **120**, and the majority of starting material **120** was recovered from the reaction attempt (Table 16, Entry 1). With this result in hand, attempts were made to increase the efficiency of the reaction by increasing the temperature (Table 16, Entries 2 and 3). Despite the increase in temperature, the enol phosphate formation proved unyielding when using the carbon-centred magnesium base, ^tBu₂Mg. As such, the widely used, and stronger, base LDA, was then employed instead of ^tBu₂Mg, as shown below (Scheme 92, Table 17)

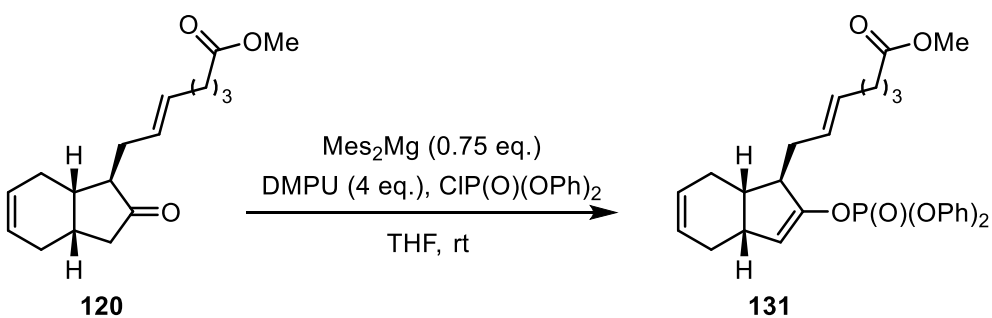


Scheme 92 - Enol phosphate formation employing LDA

Table 17 – Results from LDA mediated enol phosphate formation

Entry	Scale (mmol)	Result
1	0.11	No reaction, 83 % SM recovered
2	0.29	No reaction, 90 % SM recovered

Unfortunately, the desired enol phosphate **131** was not formed, and the starting material was once again recovered (Table 17, Entry 1). The reaction was then performed on larger scale, but the same result was observed with the starting material **120** being returned (Table 17, Entry 2). At this stage, an alternative carbon-centred magnesium base, Mes₂Mg, was then utilised in the surprisingly challenging formation of enol phosphate **131** (Scheme 93, Table 18). Indeed, Mes₂Mg has been shown to work well in the formation of enol phosphates from acetophenone substrates, where ^tBu₂Mg does not perform.³⁰



Scheme 93 - Enol phosphate formation employing Mes₂Mg

Table 18 - Results from Mes_2Mg mediated enol phosphate formation

Entry	Scale (mmol)	Yield (%)
1	0.18	44
2	1.08	55

Pleasingly, Mes_2Mg proved an effective base for the formation of enol phosphate **131** delivering the product in a yield of 44 % (Table 18, Entry 1). Upon an increase in scale, an increase in the yield of the desired enol phosphate **131** to 55 % was observed (Table 18, Entry 2). Additionally, it should be noted that no epimerisation of the stereocentre bearing the sidechain was observed. However, upon purification of enol phosphate **131**, a side-product was observed and isolated. The side-product had an almost identical ^1H NMR profile to enol phosphate **131**, except for the integral of the methyl ester being approximately half, with respect to the rest of the molecule, and a new distinctive peak observed at $\delta = 3.46$ ppm. With this preliminary data in hand, it was proposed that the desired enol phosphate **131** had undergone an undesired Claisen condensation, to give keto-ester **149** (Figure 14).

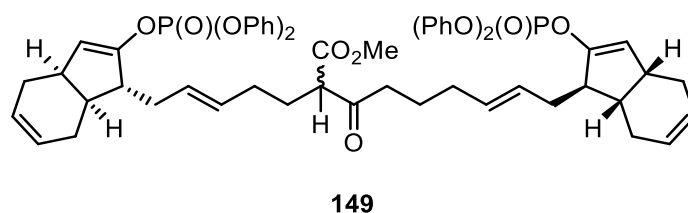
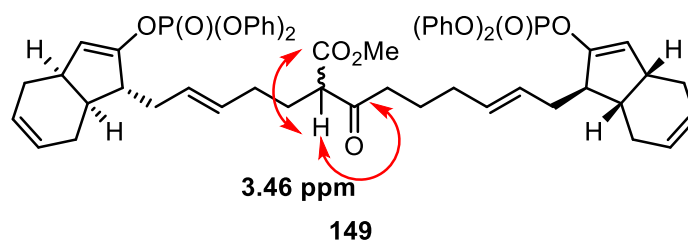


Figure 14 - Claisen condensation side-product

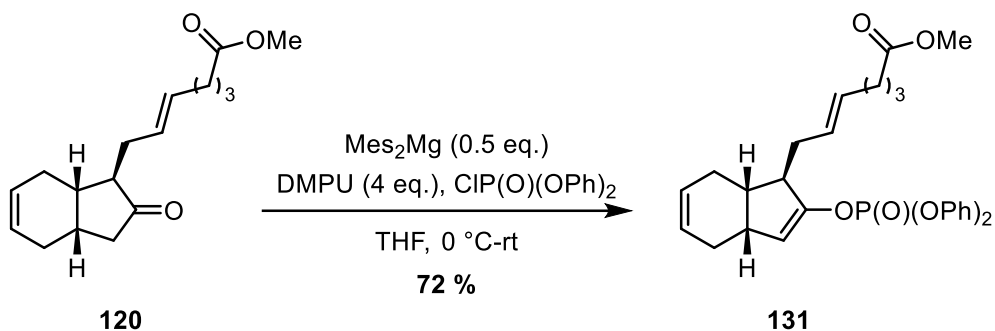
Upon analysing the data gathered from 2D NMR experiments, a correlation between the peak at $\delta = 3.46$ ppm and the ^{13}C signals correlating to a ketone and ester was observed. This HMBC correlation gave further credence to the proposed structure of side-product **149**. With the ^1H , ^{13}C and HMBC NMR experimental data in hand, HRMS data confirmed the mass of the proposed structure of side-product **149** (Figure 15).



HRMS (ESI) m/z calculated for $\text{C}_{29}\text{H}_{33}\text{O}_6\text{P}$ $[\text{M}+\text{H}]^+$: 985.3846. Found: 985.3854

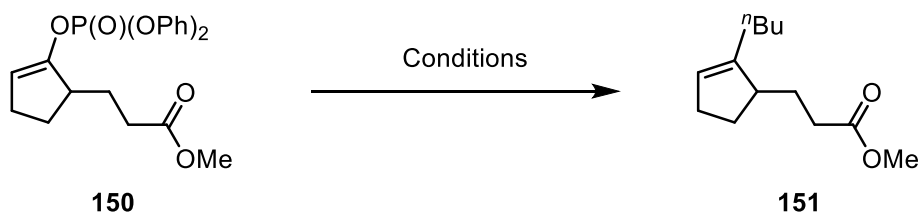
Figure 15 - Claisen condensation side-product highlighting HMBC correlations

Having identified the side-product from the enol phosphate formation, it was proposed that using equimolar quantities of base, along with reduced temperature, would prevent the formation of this side-product and potentially result in an increased yield of **131**. As shown in Scheme 94, use of just 0.5 equivalents of Mes_2Mg provided a high yield of the desired enol phosphate **131**, by reducing the potential for undesired Claisen condensation.



Scheme 94 - Modified enol phosphate formation conditions

With efficient access towards enol phosphate **131** established, the key $\text{sp}^2\text{-sp}^3$ cross coupling became the next synthetic challenge. In the first instance, a screen of varying cross-coupling conditions on test substrate **150**, the synthesis of which is described within the Experimental Section, was performed (Scheme 95, Table 19).



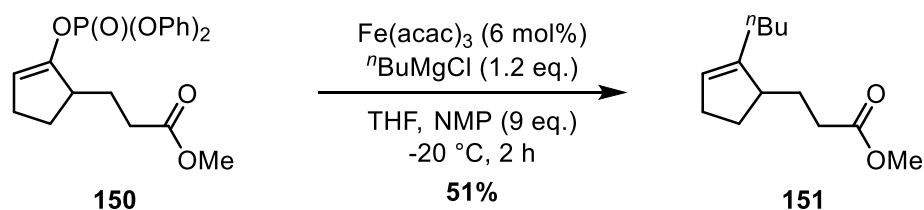
Scheme 95 - Cross-coupling screen

Table 19 - Cross-coupling conditions screen results

Entry	Conditions	Qualitative Assessment
1	Pd-PEPPSI-SIPr (1 mol%), ⁿ BuMgCl (1.5 eq.), Toluene, 0 °C, 16 h	Cross-coupling, undesired addition into ester indicated.
2	Pd-PEPPSI-SIPr (1 mol%), ⁿ BuMgCl (1.0 eq.), Toluene, 0 °C, 16 h	Cross-coupling, undesired addition into ester, starting material indicated.
3	Pd-PEPPSI-SIPr (1 mol%), ⁿ BuZnCl (1.5 eq.), Toluene, 0 °C, 16 h	No reaction indicated
4	Pd-PEPPSI-SIPr (1 mol%), ⁿ BuZnCl (1.5 eq.), Toluene, 70 °C, 16 h	No cross coupling indicated, undesired addition into ester, starting material present.
5	Fe(acac) ₃ (3 mol%), ⁿ BuMgCl (1.2 eq.), THF, NMP (9 eq.), -20 °C, 2 h	Desired product and starting material present
6	Fe(acac) ₃ (6 mol%), ⁿ BuMgCl (1.2 eq.), THF, NMP (9 eq.), -20 °C, 2 h	Desired product indicated
7	Pd - PEPPSI-SIPr (1 mol%), ⁿ BuMgCl (1.5 eq.), THF, NMP (9 eq.), 0 °C, 2 h	Trace product observed

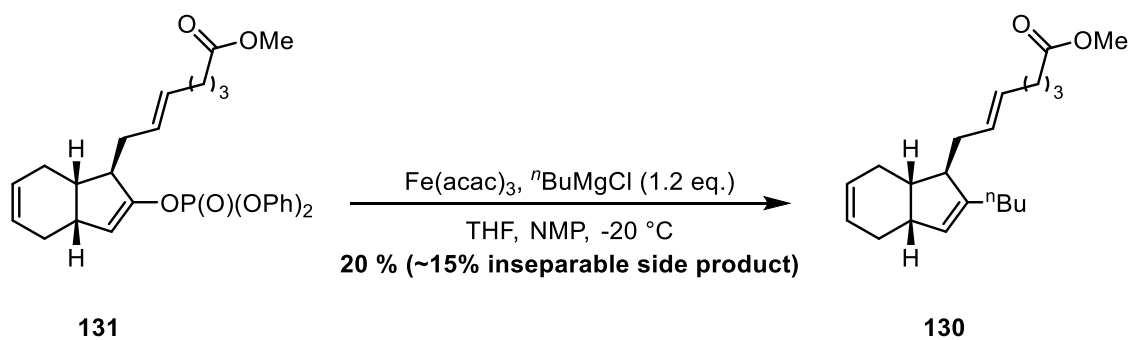
Initially, in-house developed Pd-PEPPSI-SIPr catalysed Kumada conditions³³ were attempted on test substrate **150** and, by ¹H NMR spectroscopic analysis, cross-coupling was observed along with undesired addition into the ester functionality (Table 19, Entry 1). In an effort to avoid the undesired addition into the ester, the equivalents of ⁿBuMgCl were reduced. As a result of lowering the equivalents of Grignard reagent, incomplete conversion of starting material was observed, along with the previously observed undesired ester addition (Table 19, Entry 2). It became evident at this point that the use of such reactive Grignard reagents was likely incompatible with the accessible methyl ester in our substrate. A strategy to temper the reactivity of the organometallic reagent was to exchange for the alkylzinc chloride equivalent. However, simply exchanging ⁿBuMgCl for ⁿBuZnCl proved ineffective when employed with Pd-PEPPSI-SIPr, even at elevated temperatures (Table 19, Entries 3 and 4). Gratifyingly, employing Cahiez's iron-catalysed Kumada conditions, which have been shown to tolerate methyl esters, allowed for cross-coupling to be achieved without an undesired addition into the ester functionality, albeit with starting material remaining (Table 19, Entry 5). Pleasingly, increasing the amount of Fe(acac)₃ used led to complete conversion of the starting material (Table 19, Entry 6). Indeed, it was thought that the THF/NMP solvent system was responsible for the chemoselectivity observed in the iron-catalysed Kumada conditions and, with this in mind, the previously discussed Pd-PEPPSI-SIPr catalysed conditions were employed with a THF/NMP solvent system (Table 19, Entry 7). Unfortunately, this resulted in no conversion of the starting material at all;

suggesting that the THF/NMP solvent system was incompatible with the Pd-PEPSI catalyst system. Following on from the positive initial screening, the optimal conditions (Table 19, Entry 6) were repeated on a larger scale to allow for an isolated yield to be obtained (Scheme 96).



Scheme 96 - Isolated yield from Iron-catalysed cross-coupling

The screened cross-coupling conditions allowed for the synthesis of the desired product **151** from test substrate **150** in a 51 % isolated yield. With this result in hand, the conditions were then applied to the enol phosphate **131**, as required in our synthesis towards (–)-mucosin (Scheme 97).



Scheme 97 - Cross-coupling with enol phosphate 131

Incongruously, when applying the previously used conditions, a lower isolated yield of the desired product **130** was observed, along with an inseparable side-product which, at this point, was unidentifiable. Effort was made to optimise this cross-coupling to increase the yield of the desired product **130** and simultaneously reduce the yield of the inseparable side-product (Table 20).

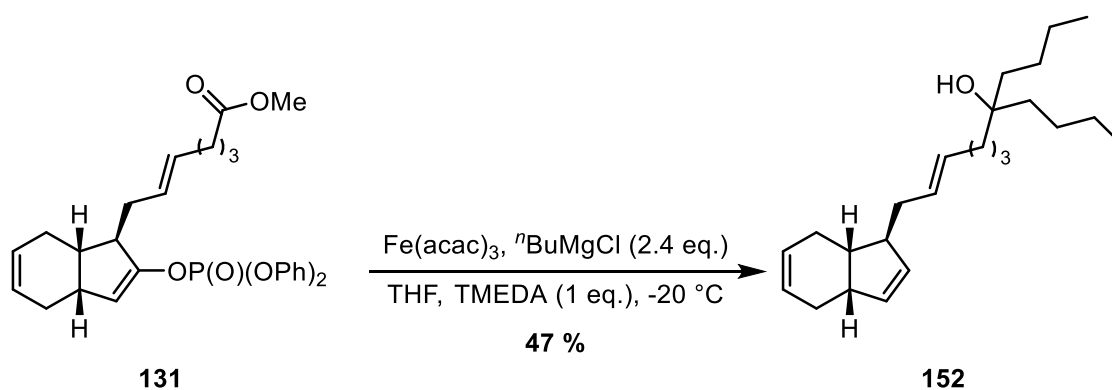
Table 20 - Optimisation table for cross-coupling of enol phosphate **131**

Entry	Scale (mmol)	Concentration (M)	ⁿ BuMgCl eq.	Yield (%)
1	0.1	0.5	2.4	28 (~23% inseparable side-product)
2^a	0.1	0.5	2.4	-
3	0.1	0.05	2.4	66 (~40% inseparable side-product)
4^b	0.1	0.05	2.4	16 (~32% inseparable side-product)

a) Et₂O/NMP as solvent system, b) degassed solvent

Initially, an increase in the equivalents of ⁿBuMgCl from the original 1.2 equivalents to 2.4 equivalents afforded an increase of yield the desired product, however, this time with a corresponding increase in yield of the undesired side-product (Table 20, Entry 1). A switch in the solvent system from THF to Et₂O, surprisingly, led to complete precipitation of the reaction mixture upon addition of ⁿBuMgCl (Table 20, Entry 2). Reverting to THF as the solvent of choice, the concentration of the reaction was diluted ten-fold, which led to an increase in the isolated yield of the reaction but also an increase in the amount of side-product isolated (Table 20, Entry 3). Unfortunately, the use of degassed solvent hindered the formation of the desired product with a greater proportion of the unidentified side-product being isolated (Table 20, Entry 4).

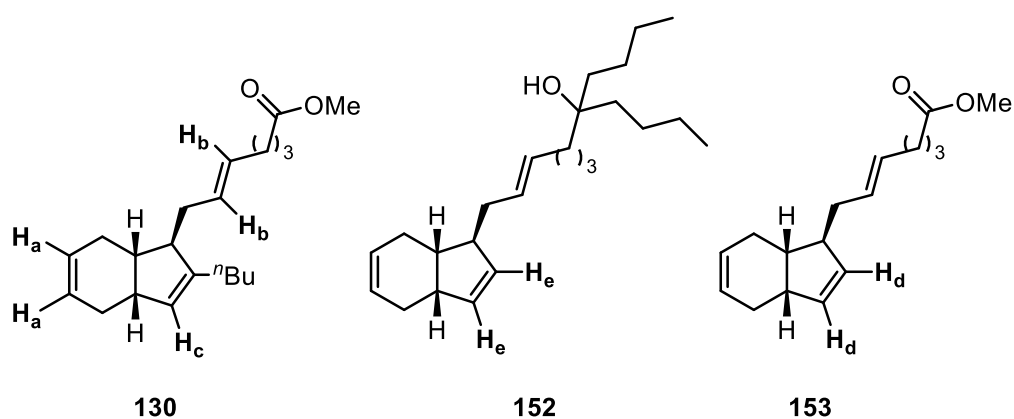
TMEDA is frequently employed in iron-catalysed cross-coupling to suppress off-cycle pathways and therefore give efficient access to the desired material.^{51,52} The use of TMEDA in our iron-catalysed cross-coupling as an additive was thus examined (Scheme 98).



Scheme 98 - Iron cross-coupling employing TMEDA as an additive

Surprisingly, the desired product **130** was not isolated but the sole species isolated in a 47 % yield, was in fact the product of proto-dephosphorylation and addition of ⁿBuMgCl to the ester moiety, **152**.

The ^1H NMR spectrum of the usual mixture of products obtained from the iron-cross coupling reaction was compared with the proto-dephosphorylation product **152** (Scheme 99, Figure 16). Upon comparing the ^1H NMR profiles to that of the usual mixture of compounds obtained from the iron cross-coupling reactions thus far, it was noticed that the proto-dephosphorylation product **152** shared a similar chemical shift, $\delta = 5.62$ ppm, H_e with that of the unidentified peak H_d . Based on this, it was proposed that the side-product in the iron-catalysed cross-coupling reactions was likely to be the proto-dephosphorylation product **153**. At this point, optimisation of this iron cross-coupling was halted, and a new strategy was sought.



Scheme 99 - Compounds isolated from Iron cross-coupling reactions

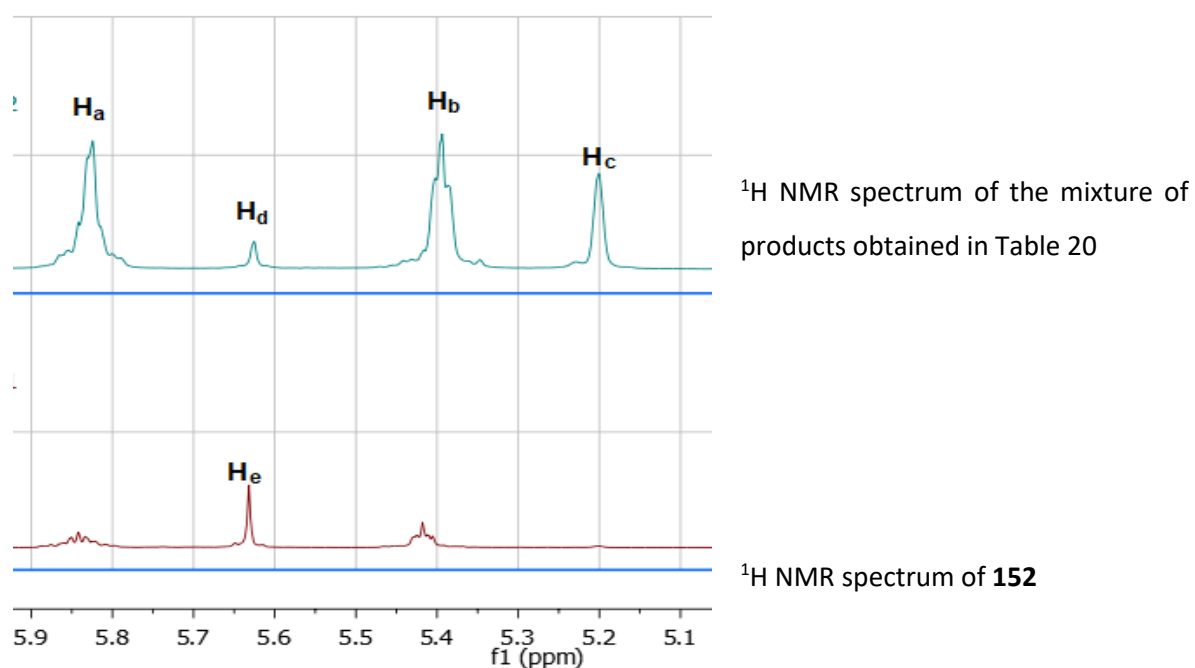
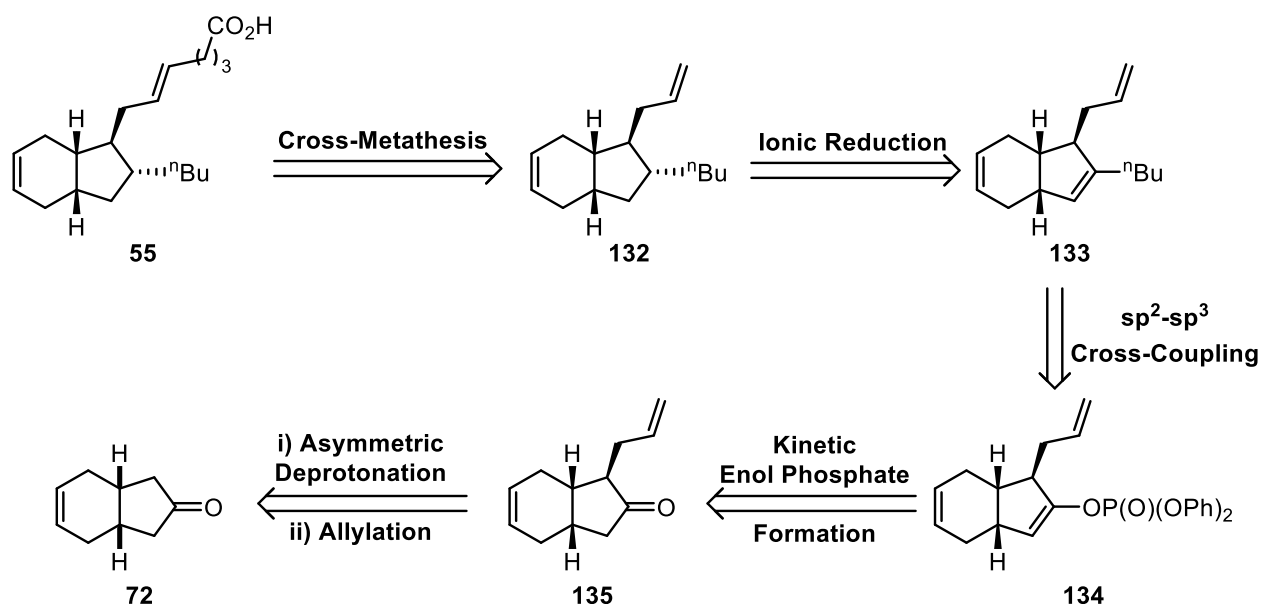


Figure 16 - Stacked ^1H NMR spectra

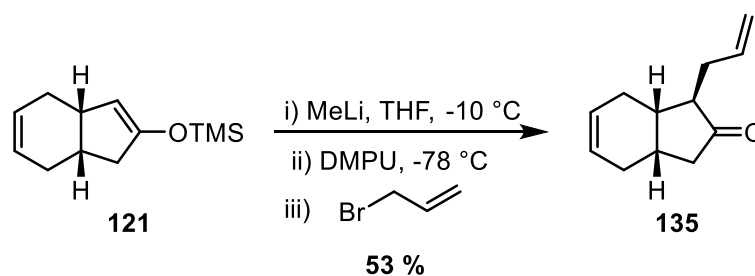
1.2.5. Investigation of a Cross-Metathesis Strategy

As mentioned previously, efforts to install the desired butyl group within (-)-mucosin was presenting a significant challenge. Indeed, this has been attributed to the presence of a methyl ester group in our substrate. As such, a new synthetic strategy towards (-)-mucosin **55** was devised. The newly developed retrosynthetic route is shown in Scheme 100.



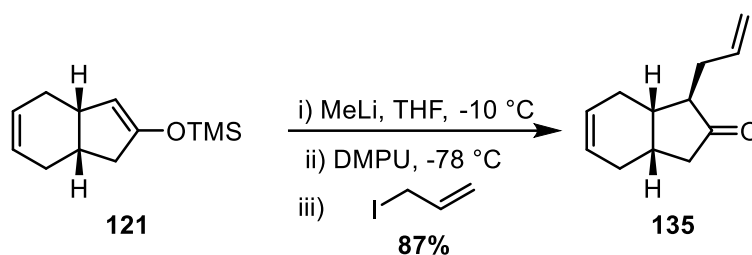
Scheme 100 - Proposed Retrosynthesis

The first synthetic challenge of the newly devised strategy is the allylation of previously prepared silyl enol ether **121** to afford allylated ketone **135**. As such, the allylation was carried out using MeLi and allyl bromide as the electrophile (Scheme 101). As has been shown before, the allylation proceeded in only a moderate 53% yield of the desired product **135**, which was isolated as a single diastereomer.



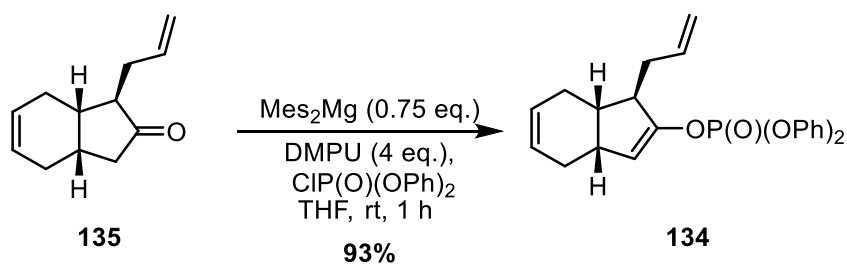
Scheme 101 - Allylation of silyl enol ether **121** with allyl bromide

In order to increase the yield of the desired product formation, allyl iodide was employed as a more reactive electrophile in the same allylation procedure (Scheme 102).



*Scheme 102 - Alkylation of silyl enol ether **121** with allyl iodide*

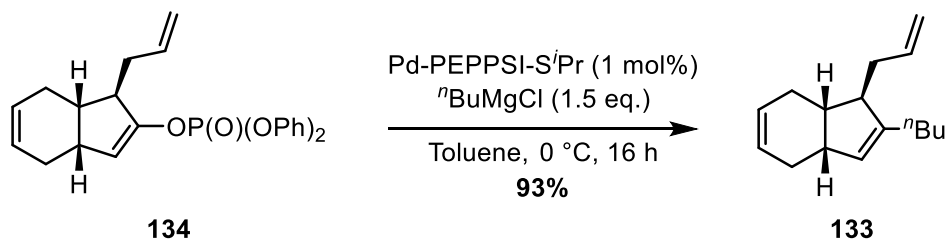
Pleasingly, the use of allyl iodide greatly improved the yield of the desired product **135**, whilst retaining the same stereoselectivity previously observed using allyl bromide. The alkylation procedure proved to be reproducible when using freshly distilled allyl iodide, which was necessary due to its inherent photo- and thermal-instability. Having gained efficient access to ketone **135**, the formation of enol phosphate **134** became the next target (Scheme 103), installing the key functional group for the downstream cross-coupling reaction.



*Scheme 103 - Enol phosphate **134** formation*

Upon employing Mes₂Mg as the base for the enol phosphate formation, the desired compound **134** was synthesised in an excellent yield of 93 %. Importantly, no epimerisation of the allyl side chain was observed by ¹H or ¹³C NMR spectroscopy.

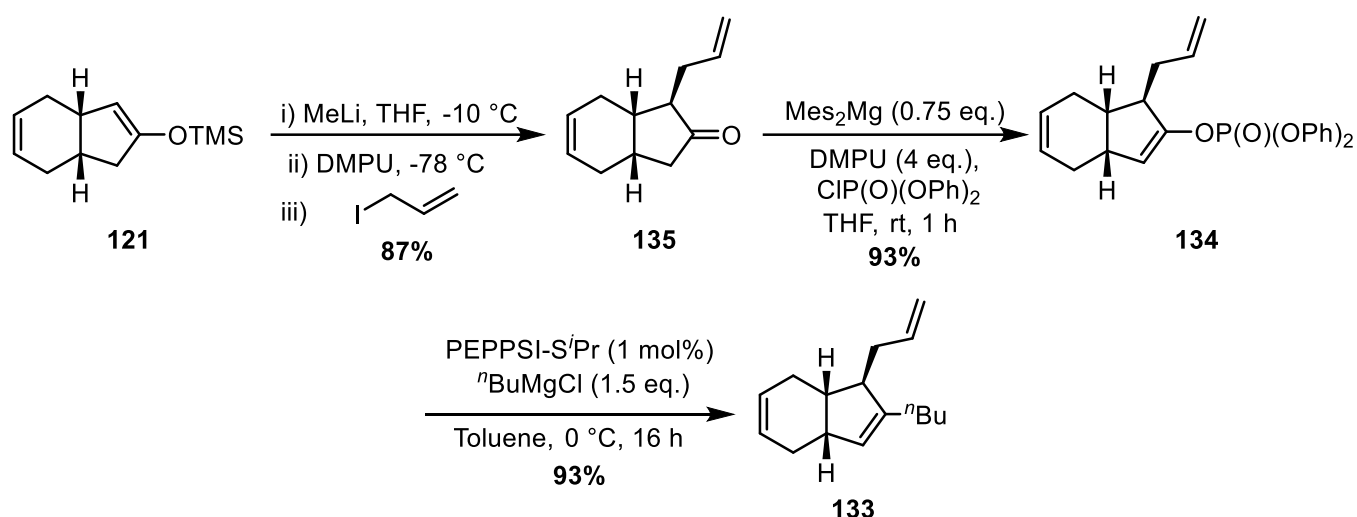
With a single diastereomer of enol phosphate **134** in hand, installation of the ⁿbutyl appendage, *via* cross-coupling, was the next challenge. As planned, our in-house Pd-PEPPSI-SⁱPr-catalysed Kumada protocol seemed to be a sensible first choice, as enol phosphate **134** does not contain the ester functional group that previously proved incompatible with the use of Grignard reagents (Scheme 104).



Scheme 104 – Pd-catalysed Kumada cross-coupling.

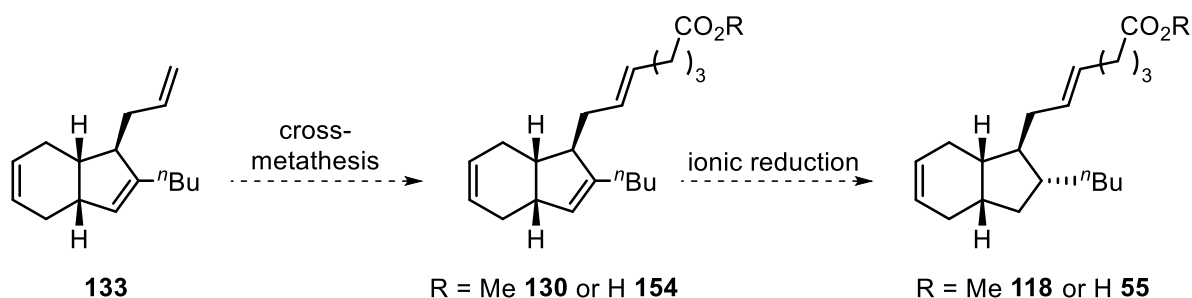
Gratifyingly, the desired triene **133** was obtained in an excellent yield of 93 % using only 1 mol% of catalyst. This result highlights the utility of Kerr group methodology to facilitate challenging C—C bond formation in a complex natural product synthesis. This key result, provided for the first time, an advanced mucosin intermediate with the desired butyl side chain.

To summarise, triene **133** has been synthesised using multiple steps developed within the Kerr group including the magnesium-mediated asymmetric deprotonation reaction required to synthesise starting silyl enol ether **121**. Notably, a change to a more reactive electrophile (allyl iodide) allowed for an efficient allylation in a procedure which has typically been capricious in our hands. Additionally, the use of our mild organometallic base chemistry has allowed for exclusive formation of the kinetic enol phosphate **134** with no indication of racemisation. Finally, a novel C—C bond forming process has been utilised in the synthesis of triene **133** which has the core aspects of (–)-mucosin **55** in place. Overall, triene **133** was synthesised in three steps from silyl enol ether **121** with an overall yield of 75%, and as a single diastereomer.



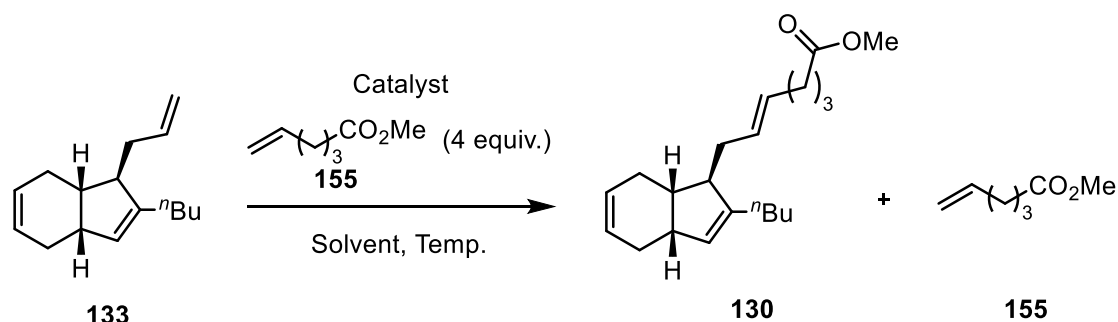
Scheme 105 - Synthesis of triene **133**

Having established the synthetic route towards the triene **133**, research now focused on installing the remaining skeletal framework of (–)-mucosin **55**. Initially, it was proposed that the cross-metathesis would be the first synthetic step to be attempted which, indeed, could prove challenging as our triene system was inclusive of a strained five membered endocyclic olefin (Scheme 106).



Scheme 106 - Initial cross-metathesis strategy

Optimisation of the cross-metathesis of triene **133** began with using Grubbs 2nd generation catalyst and four equivalents of alkene **155** (Scheme 107, Table 21).



Scheme 107 - Cross metathesis optimisation

Table 21 - Results

Entry	Catalyst	Solvent	Temperature (°C)	Time (h)	Product ratio 130 : 155	E:Z
1	Grubbs II (6 mol%)	DCM	Δ	2	1:2	4:1
2	Grubbs II (6 mol%)	DCM	Δ	16	1:1	4:1

Unfortunately, upon purification, it was observed that cross-metathesis partner **155** was inseparable from the desired product **130** and a 2:1 mixture of the desired product with alkene **155** was obtained (Table 21, Entry 1). In an attempt to increase the ratio of desired product with respect to the re-isolated alkene **155**, the reaction was allowed to run for a longer time period. Indeed, we expected that this would force dimer formation of alkene **155**, the product of which was separable from the desired product **130**. However, after an extended run the mixture was isolated as 1:1 ratio of desired product **130** to alkene **155** (Table 21, Entry 2). It should be noted that in the first two cases the *E:Z* ration of product **130** was 4:1. A change in solvent to toluene allowed an increase in the temperature of the reaction. Unfortunately, when running the reaction at 60 °C and 110 °C no product was observed at all (Table 22, Entries 1 and 2).

Table 22 – Results

Entry	Catalyst	Solvent	Temperature (°C)	Time (h)	Product ratio 130 : 155	E:Z
1	Grubbs II (6 mol%)	Toluene	60	16	N/A	N/A
2	Grubbs II (6 mol%)	Toluene	110	16	N/A	N/A

Having shown that toluene, at an elevated temperature, was an unsuitable solvent for this intermolecular cross-metathesis, a variety of commonly employed catalysts were screened using DCM as the reaction medium (Scheme 107, Table 23).

Table 23 - Catalyst Screen

Entry	Catalyst	Solvent	Temperature (°C)	Time (h)	Product ratio 130 : 155	E:Z
1	Grubbs I (6 mol%)	DCM	Δ	16	1:1.2	11:9
2	Grubbs II (18 mol%)	DCM	Δ	16	1:2	4:1
3	Hoveyda-Grubbs II (6 mol%)	DCM	Δ	16	1:1	4:1
4	Hoveyda-Grubbs II (18 mol%)	DCM	Δ	16	1:1	4:1

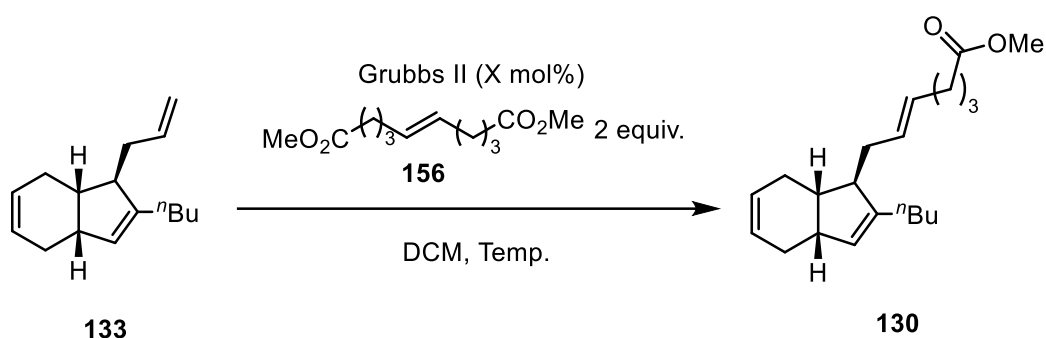
Unsurprisingly, Grubbs 1st generation catalyst gave an unfavourable E:Z ratio in comparison to the Grubbs 2nd generation catalyst, albeit with a similar product ratio (Table 23, Entry 1). Employing Grubbs 2nd generation catalyst with an increased catalyst loading unexpectedly led to no improvement in the ratio of desired product to the undesired remaining cross metathesis partner **155** (Table 23, Entry 2). Hoveyda-Grubbs 2nd generation catalyst also gave no improvement on the ratio of products isolated or the E:Z ratio (Table 23, Entry 3). Additionally, increasing the catalyst loading of Hoveyda-Grubbs 2nd generation catalyst led to no improvement in the reaction profile (Table 23, Entry 4).

The final attribute of the intermolecular cross-metathesis reaction with alkene **155** to be modified was the concentration of the reaction itself (Scheme 107, Table 24).

Table 24 - Concentration screen

Entry	Catalyst	Solvent	Temperature (°C)	Conc. (M)	Time (h)	Product ratio 130 : 155	E:Z
1	Grubbs II (6 mol%)	DCM	Δ	0.06	16	N/A	N/A
2	Grubbs II (6 mol%)	DCM	Δ	0.24	16	5:2	4:1

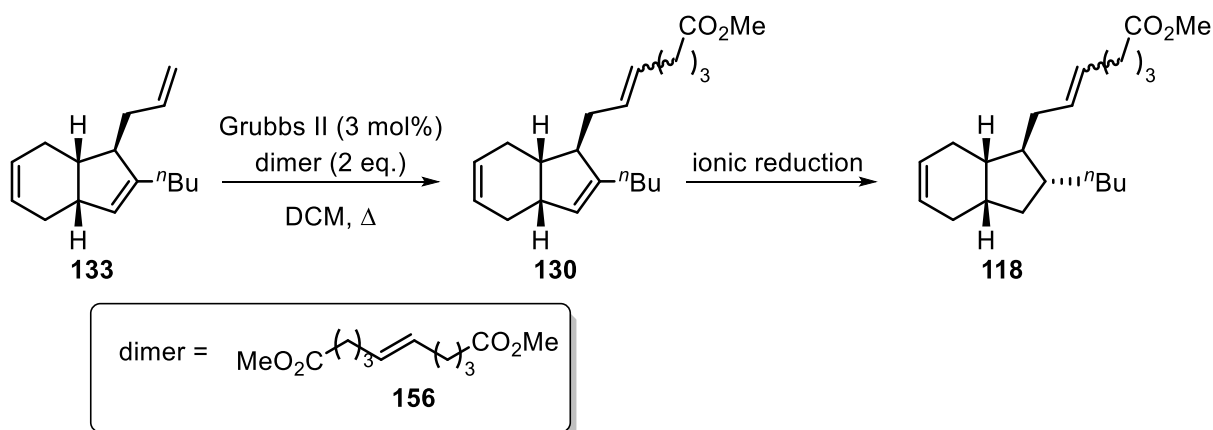
Frustratingly, when attempting the cross-metathesis between triene **133** and cross-metathesis partner **155** at half the typical concentration, no product was observed (Table 24, Entry 1). This indicated how sensitive intermolecular cross-metathesis processes are to changes in their concentration. Subsequently, increasing the concentration by a factor of two led to a switch in the product ratio, in comparison to the result from Table 21, Entry 2, whilst retaining the *E:Z* ratio. It became evident that optimising the reaction to force the formation of dimer **156** was challenging. To circumvent the requirement of the reaction to form its dimer, dimer **156** was independently synthesised then employed in the cross-metathesis with triene **133** (Scheme 108).

Scheme 108 - Intermolecular cross-metathesis with dimer **156**Table 25 - Results from cross-metathesis with dimer **156**

Entry	Catalyst Loading (mol %)	Temperature (°C)	Time (h)	Yield (%)	E:Z
1	6	Δ	16	77	4:1
2	3	Δ	16	74	4:1
3	6	rt	16	60	4:1
4	3	Δ	2	66	4:1

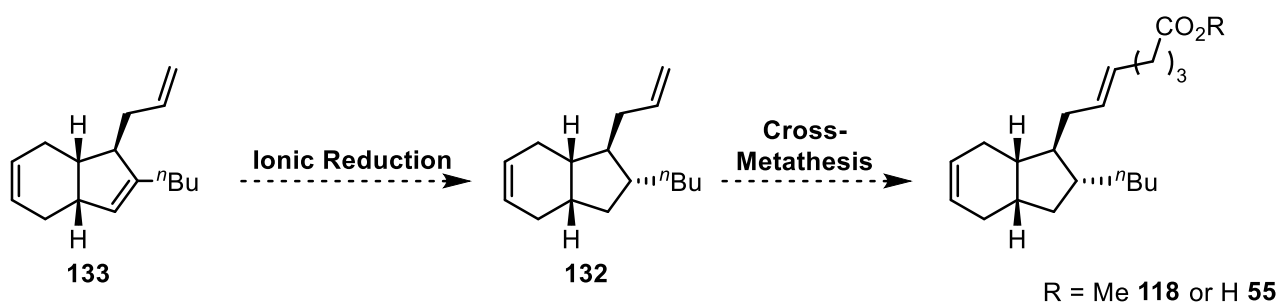
Gratifyingly, employing the dimer **156** did allow for clean isolation of methyl ester **130** in a 77% yield with an *E:Z* ratio of 4:1 (Table 25, Entry 1). In an effort to improve the reaction conditions further, the catalyst loading was dropped to 3 mol%, which gave a slight decrease in yield and successfully retained the *E:Z* ratio (Table 25, Entry 2). Reverting to 6 mol% catalyst loading and reducing the reaction

temperature to room temperature led to a significant reduction in the yield of methyl ester **130**, indicating that the reaction is more sensitive to a change in temperature than catalyst loading (Table 25). Finally, reducing the time of the reaction to just two hours resulted in a slight reduction in yield to 66% with no change in the *E:Z* ratio. Unfortunately, separation of the *E:Z* isomers could not be achieved. Regardless, with access to a very late stage intermediate towards the natural target, the final ionic reduction was attempted, which would deliver an advanced intermediate in the Stenstrom synthesis, whereby analytical data can be compared.



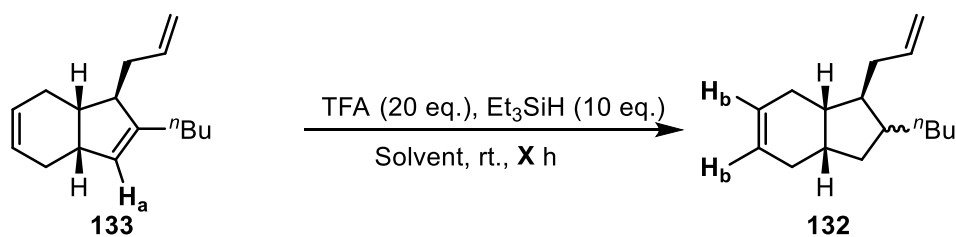
Scheme 109 – Route to methyl ester of (–)-mucosin

Having said this, with methyl ester **118** being a mixture of *E:Z* isomers, it became evident that analysing the outcome of any ionic reduction could prove very challenging. It is possible that the ionic reduction would not proceed diastereoselectively, which would then give a potential of four stereoisomers as a mixture; in a compound which is already challenging to analyse. With this in mind, it was decided to change the strategy to perform the ionic reduction before the previously optimised cross-metathesis (Scheme 110) and tackle the separation of the resulting *E:Z* mixture at the final stage.



Scheme 110 - Re-ordered strategy for accessing (–)-mucosin **55**

As such, initial attempts at the ionic reduction of triene **133** were carried out with superstoichiometric quantities of both trifluoroacetic acid and triethylsilane in toluene (Scheme 111, Table 26).



Scheme 111 - Ionic reduction optimisation

Table 26 - Optimisation with toluene as the solvent

Entry	Solvent	Time (h)	Consumption H _a (%)	Conversion to H _b (%)	Presence of Side Product (Y/N)
1	Toluene	1	42	24	N
2	Toluene	2.5	58	32	N
3	Toluene	6	61	27	N

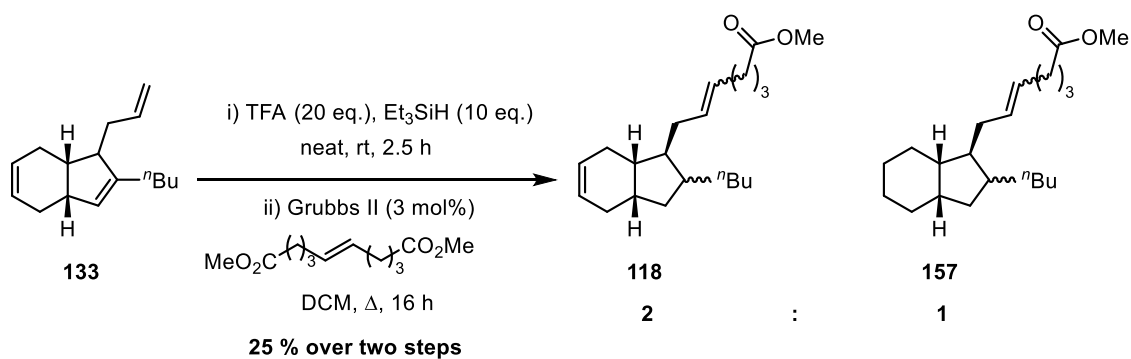
Initially, allowing the reaction to run for only an hour led to 42 % consumption of starting material **133** by analysing the integral at $\delta = 5.27 - 5.20$ ppm, in the ^1H NMR spectrum. Unfortunately, in these cases, starting material **133** does not cleanly convert to the desired diene product **132** with only 24 % of the desired material being observed by analysing the integral at $\delta = 5.67$ ppm, in the ^1H NMR spectrum (Table 26, Entry 1). Increasing the time of the reaction did allow for further consumption of the starting material, however, unfortunately, only a slight increase was observed in the formation of the desired product **132**, in comparison to the one hour run (Table 26, Entry 2 and 3). Having considered toluene as the reaction medium, a small solvent screen was performed employing conventional solvents for an ionic reduction – DCM and 2-nitropropane – and other solvents not typically employed (Scheme 111, Table 27).

Table 27 - Ionic reduction solvent screen

Entry	Solvent	Time (h)	Consumption H _a (%)	Conversion to H _b (%)	Presence of Side Product (Y/N)
1	DCM	2.5	94	0	Y
2	EtOAc	2.5	42	0	Y
3	THF	2.5	38	0	Y
4	2-nitropropane	2.5	48	0	N
5	Neat	2.5	100	79	N

Using DCM as a solvent in the ionic reduction of **133** led to almost complete consumption of starting material but it was not obvious what the material had converted to, with a new peak at $\delta \sim 5.8$ ppm being observed (Table 27, Entry 1). Unfortunately, due to the nature of the compounds (exceedingly non-polar), separation and analysis of the various constituents of the mixture was not possible. Changing the reaction medium to EtOAc led to only 42 % consumption of the starting material with, again, no evidence of the desired reaction occurring (Table 27, Entry 2). A similar result was observed when utilising THF as the solvent with only 38 % consumption of the starting material by ¹H NMR analysis, and no evidence of the desired reaction occurring. The use of 2-nitropropane in the ionic reduction of **133**, again, led to a moderate consumption of the starting material but no evidence for the conversion to the desired product **132**, by ¹H NMR. Surprisingly, performing the ionic reduction of **133** with no solvent at all led to complete consumption of the starting triene **133** and a good 79 % conversion to the desired product **132**. Pleasingly, no evidence of a side-product was observed by ¹H NMR analysis.

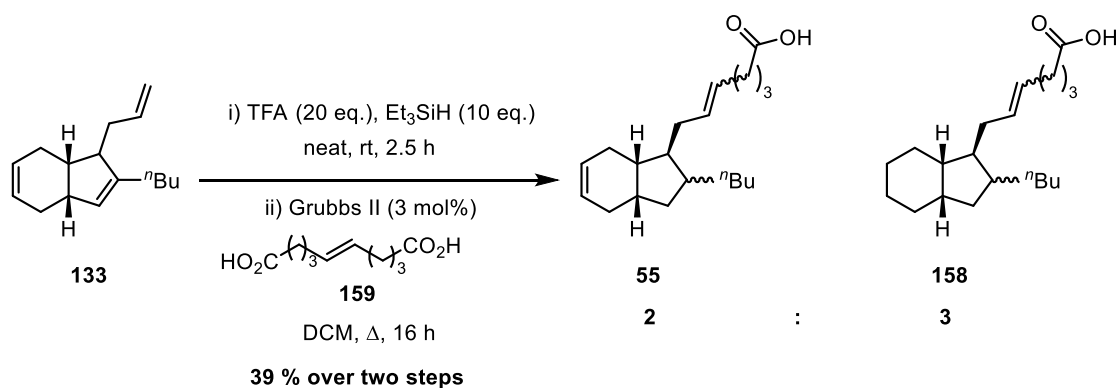
Having shown that the ionic reduction could proceed without the requirement of a reaction solvent, work was undertaken to complete the synthesis of (–)-mucosin by carrying out the ionic reduction and cross-metathesis in sequence without isolating the intermediate diene **132** (Scheme 112).



Scheme 112 - Synthesis of the methyl ester of (-)-mucosin **118**

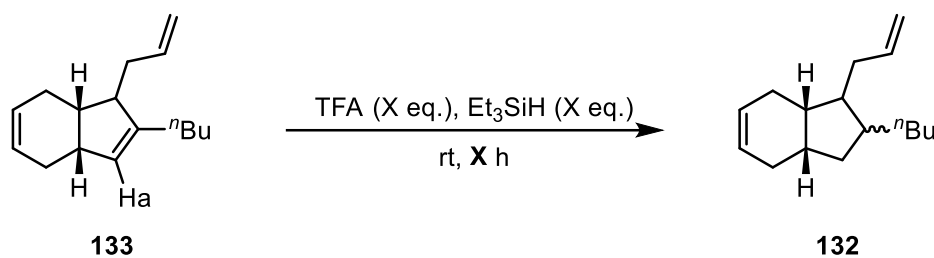
Employing previously optimised conditions for both the ionic reduction and the cross-metathesis led to the isolation of a 2:1 mixture of the methyl ester of (-)-mucosin **118** and the dihydro methyl ester of (-)-mucosin **157** in a 25 % yield over the two steps.

In addition, the cross-metathesis procedure was modified to include the use of diacid **159**, to allow direct access to (-)-mucosin **55** without the requirement for a hydrolysis step (Scheme 113).



Scheme 113 - Synthesis of (-)-mucosin

Unfortunately, but as expected, switching the dimer to **159** gave a mixture of (-)-mucosin **55** and the dihydro mucosin **158** in a 39% yield over the two steps, confirmed by ¹H NMR and HRMS. Despite a valiant attempt to furnish the final natural product target **55**, it is evident that over-reduction in the ionic reduction is prevalent. With this knowledge, work focused on circumventing the undesired over-reduction and the unidentified side product that has, thus far, inconsistently plagued this transformation. Further work was carried out, including modifying the stoichiometries of the acid and silane and reducing the time the reaction was carried out for (Scheme 114, Table 28).



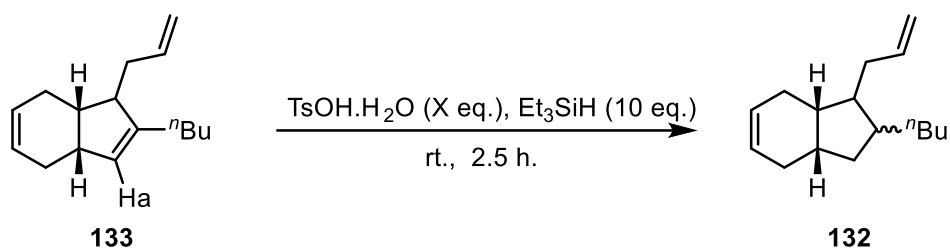
Scheme 114 - Ionic reduction optimisation

Table 28 - Ionic reduction optimisation results

Entry	TFA (eq.)	Et ₃ SiH (eq.)	Time (h)	Consumption of H _a	Appearance of unidentified side product
1	20	10	2.5	100	Yes
2	10	10	2.5	100	Yes
3	5	10	2.5	100	Yes
4	20	20	2.5	100	Yes
5	20	40	2.5	100	Yes
6	20	10	1	100	Yes
7	20	10	0.5	100	Yes
8	5	10	0.5	100	Yes

Initially, using the standard conditions of 20 equivalents of TFA and 10 equivalents of Et₃SiH, complete consumption of the starting material **133** was observed but additionally, an undesired side-product was also observed by ¹H NMR spectroscopy (Table 28, Entry 1). Understanding that carrying out a reaction in super-stoichiometric TFA is likely to cause product degradation, efforts to reduce the TFA loading were also attempted but proved unfruitful as the unidentified side product was still present after the reaction (Table 28, Entries 2 and 3). It was considered that the formation of a tertiary carbocation was likely to be the source of an undesired reaction occurring, increasing the silane concentration could facilitate a faster quenching of the reactive carbocation. Unfortunately, despite using up to 40 equivalents of the reducing silane, the undesired side-product still persisted throughout the reaction (Table 28, Entries 4 and 5). Attempts were then made to reduce the time that the triene **133** was subjected to the harsh conditions in order to achieve a cleaner reaction profile. Reducing the time from 2.5 hours to, ultimately, 30 minutes did allow for complete consumption of the starting material **133** as observed by ¹H NMR but the reaction mixture also contained the inseparable side-product (Table 28, Entries 6 and 7). Finally, combining the reduced reaction times with reduced TFA loading was also unsuccessful at affording a clean reaction mixture (Table 28, Entry 8). It has also been

reported in literature that *p*-tolylsulfonic acid can be used as an alternative acid in the ionic reduction. As a result, *p*-tolylsulfonic acid was implemented in the ionic reduction of triene **133** (Scheme 115, Table 29).



Scheme 115 - Ionic reduction employing p-tolylsulfonic acid

Table 29 - Results from employing p-tolylsulfonic acid in the ionic reduction of 133

Entry	TsOH.H ₂ O (eq.)	Et ₃ SiH (eq.)	Solvent	Consumption of H _a	Appearance of unidentified side product
1	20	10	Neat	0	No
2	40	10	Neat	0	No
3	20	10	DCM	0	No
4	20	10	2-nitropropane	0	No

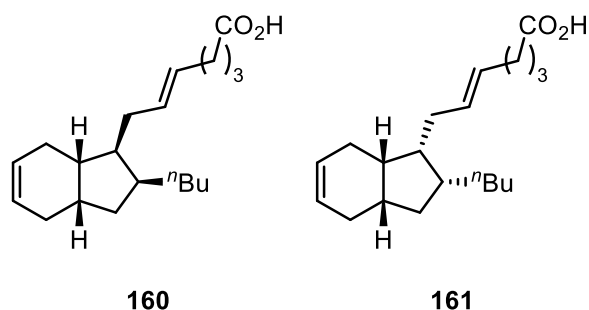
Carrying out the ionic reduction in a neat fashion proved unsuccessful, and it was thought that due to the lack of solubility of *p*-tolylsulfonic acid in either the triene **133** or silane that it was unlikely for a successful reaction to occur. Considering this, the reaction was then tried with two different solvents employed in ionic reductions, namely, DCM and 2-nitropropane. Neither DCM nor 2-nitropropane allowed for any reaction to occur, despite the acid being soluble in both solvents. At this point, *p*-tolylsulfonic acid appeared to be non-productive in the ionic reduction of triene **133**.

Ultimately, the ionic reduction of triene **133** has proven difficult to analyse and control, despite a number of reactions investigating the use of different solvents, stoichiometries of the reagents and alternative acidic reagents. Due to these difficulties and further development in the (–)-mucosin story by Stenstrøm *et al.* (*vide supra*) and from our preliminary computational results (*vide infra*) a change in strategy was sought.

1.2.6. sp³-sp³ cross-coupling

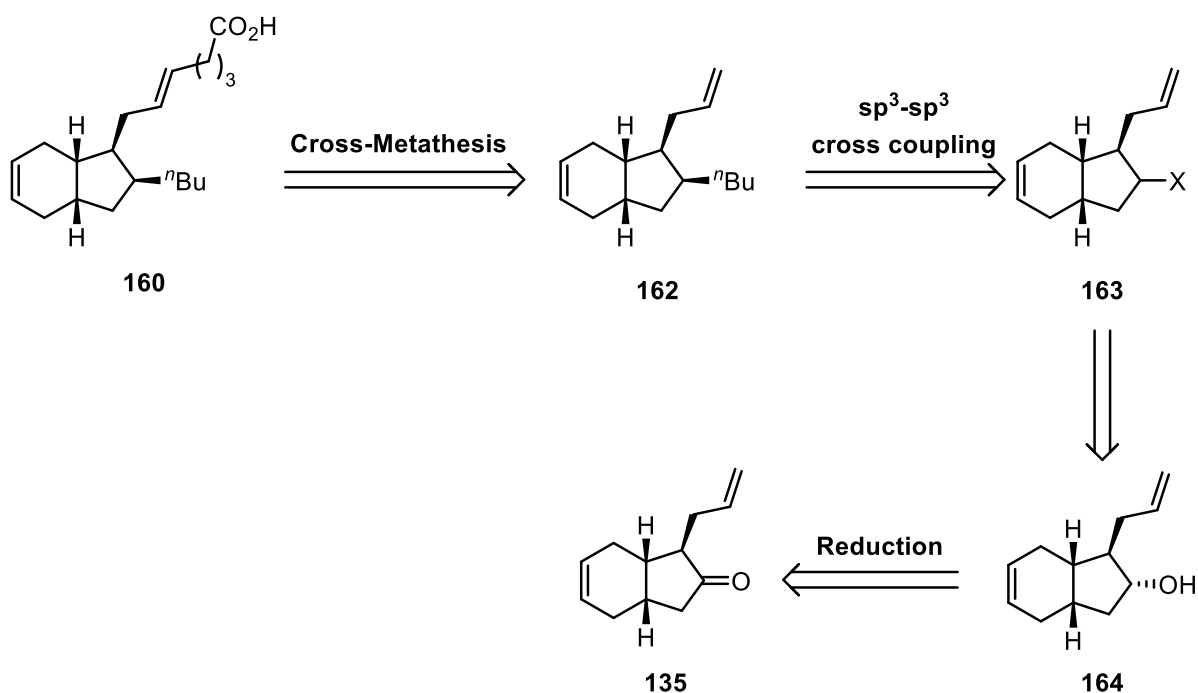
Despite our attempts to achieve the synthesis of the originally proposed structure of (–)-mucosin **55**, it was becoming increasingly obvious through Stenstrøm's published works, within the chemical literature, that the structure of (–)-mucosin had been misassigned. In order to synthesise the correct

stereoisomer of (-)-mucosin, computational prediction was sought, which is described in full within this thesis in Chapter 2 (*vide infra*). Of the four compounds containing a *cis*-bridgehead, computational prediction suggested that structure **160** or **161** were the most likely candidates for the structure of (-)-mucosin.



Scheme 116 - Computationally proposed structures of (-)-mucosin

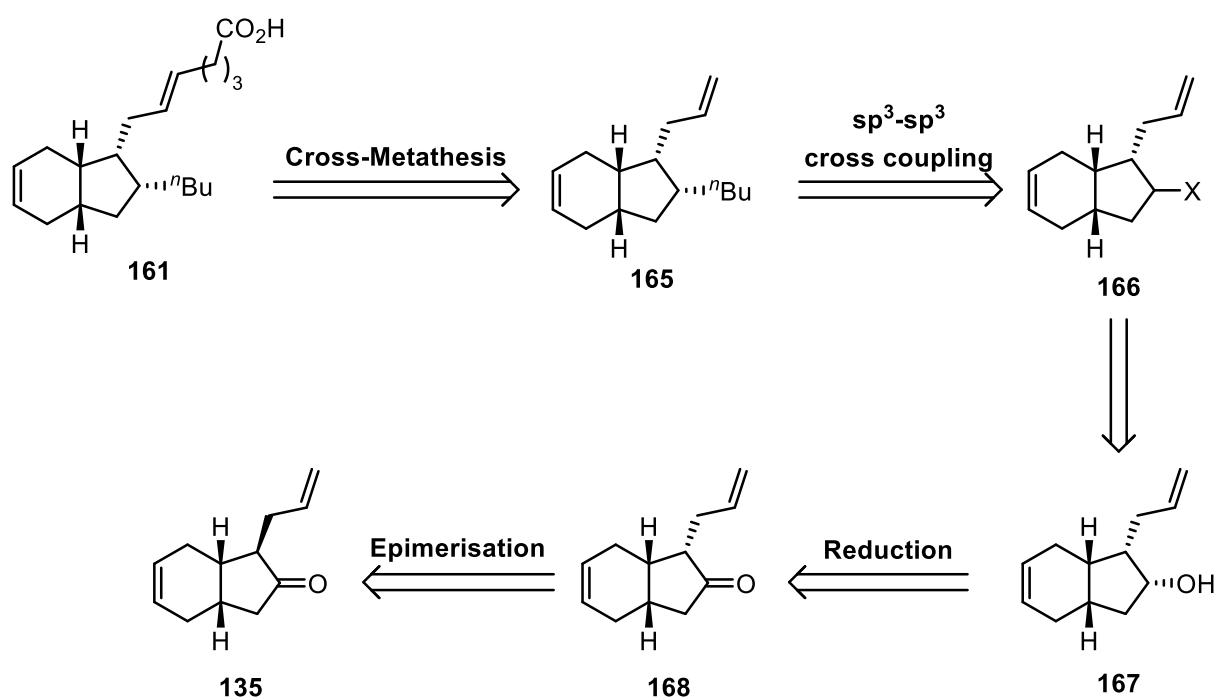
Unusually, both of these proposed structures have the side chains in a *syn*- relationship to one another. The planned strategy for synthesising these structures is detailed in Scheme 117 and Scheme 118.



Scheme 117 - Proposed retrosynthesis

From proposed structure **160** it is thought that the alkene portion bearing the acid functionality could be introduced, late stage, by a cross-metathesis from diene **162**. An sp^3 - sp^3 cross-coupling could install the *n*butyl appendage from a compound containing an appropriate electrophile, **163**. Electrophile **163**

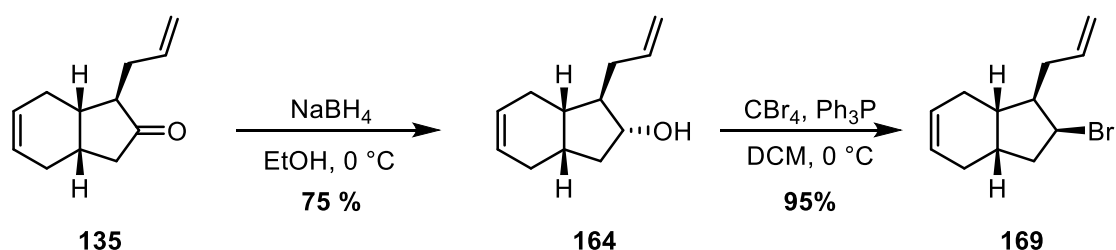
could be synthesised from alcohol **164**. Utilising a stereoselective reduction of allyl-bearing ketone **135**, allowed access to alcohol **164**. Using chemistry previously employed in the route towards (-)-mucosin, allyl-bearing ketone **135** would be the product of an asymmetric deprotonation and allylation procedure from the key ketone intermediate **72**.



Scheme 118 - Proposed retrosynthesis

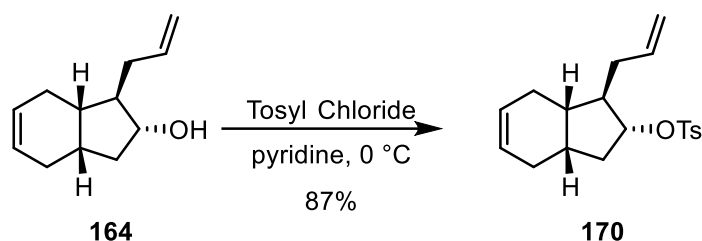
To gain access to the alternative structure **161**, a similar strategy as previously described would be performed. However, to access the epimer at the carbon bearing the allyl side chain, an epimerisation of the allyl-bearing ketone **135** would be required.

In order to explore the feasibility of an $\text{sp}^3\text{-sp}^3$ cross-coupling on a complex intermediate in this natural product synthesis, two substrates were initially targeted for synthesis – an alkyl bromide and alkyl tosylate. These substrates were both made from the previously synthesised allyl-bearing ketone **135**.



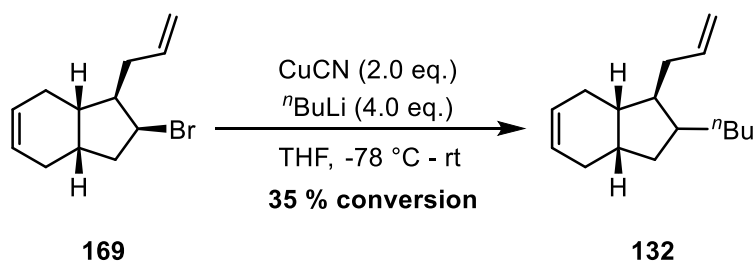
Scheme 119 - Synthesis of alkyl bromide

Reduction of the allyl ketone **135** with NaBH₄ gave the desired secondary alcohol **164**, as a single diastereomer, after column chromatography in a 75 % yield. The secondary alcohol **164** was then subjected to standard Appel bromination conditions which furnished the desired secondary alkyl bromide **169** in an excellent 95 % yield. With the desired alkyl bromide **169** synthesised, work then focused on synthesising the desired alkyl tosylate **170** (Scheme 120).



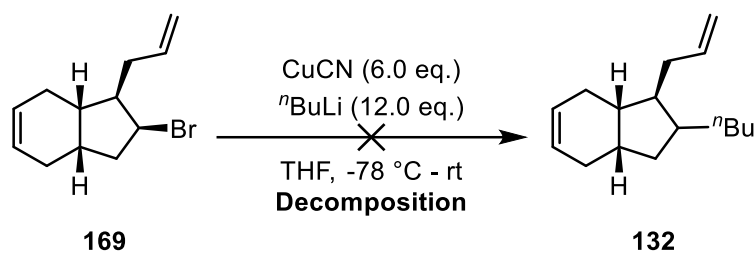
Scheme 120 - Synthesis of alkyl tosylate

Pleasingly, the alkyl tosylate **170** was readily synthesised from the previously prepared secondary alcohol **164** in an excellent yield of 87 %. With both the alkyl tosylate **170** and alkyl bromide **169** in hand, we now have access to two substrates bearing suitable electrophiles for our proposed sp³-sp³ cross couplings. Initially, it was decided to attempt the previously trialled higher-order cyanocuprate chemistry, as shown in Scheme 121, as the tosylate **170** and bromide **169** lack the previously problematic carboxylate functional group.



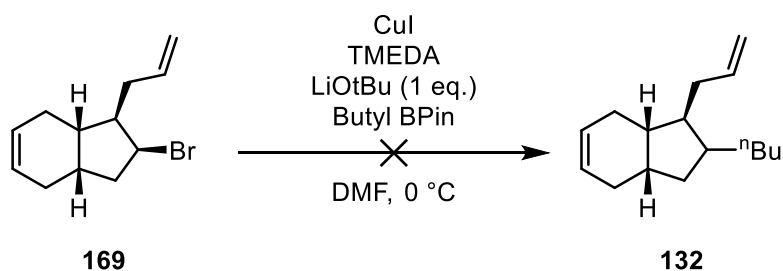
Scheme 121 - Higher-order cyanocuprate chemistry on alkyl bromide

Preliminary subjection of the alkyl bromide **169** to the cyanocuprate chemistry, yielded a promising result of 35 % conversion by ¹H NMR spectroscopy. Due to the inseparable nature of the alkyl bromide starting material **169** and the hydrocarbon product **132**, the material was resubjected to the reaction conditions. Unfortunately, this ultimately led to the decomposition of the material and no recognisable species could be identified. A final attempt using Lipshutz cyanocuprate chemistry was carried out with three times the stoichiometry to circumvent any need for crude material resubjection and potentially allow for isolation of only the desired product **132** (Scheme 122).



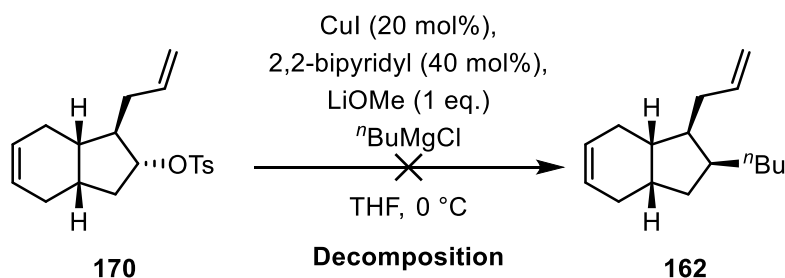
Scheme 122 - Higher-order cyanocuprate on alkyl bromide

Unfortunately, despite the starting material being consumed, no discernable products could be identified by ^1H NMR spectroscopy. At this point, the Lipshutz higher-order cyanocuprate chemistry was abandoned and other cross-coupling methodologies were sought in order to afford the desired alkylation. Within the chemical literature, there are documented methods of successfully performing $\text{sp}^3\text{-sp}^3$ cross-couplings which circumvent the issues of β -hydride elimination typically associated with Pd-catalysed cross coupling involving sp^3 nucleophiles or electrophiles.⁵³ With this in mind, work focused on implementing recent Cu-catalysed Suzuki and Kumada methodologies. Initially, a Cu-catalysed Suzuki-Miyaura reaction with the secondary alkyl bromide **169** and a butyl pinacol boronic ester was explored in an attempt to afford the desired alkylation (Scheme 123).



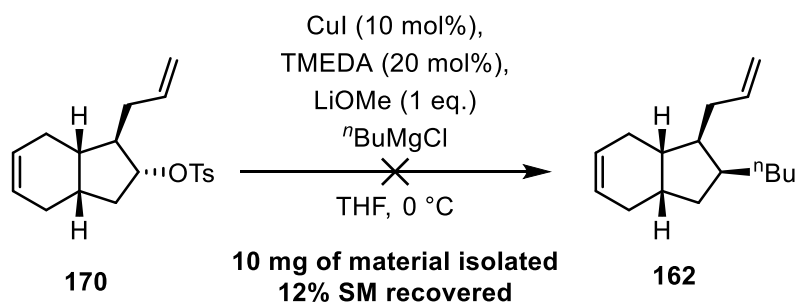
Scheme 123 - Cu-catalysed Suzuki-Miyaurai reaction on alkyl bromide

The $\text{sp}^3\text{-sp}^3$ Cu-catalysed Suzuki-Miyaura reaction with the alkyl secondary bromide **169** resulted in decomposition of the starting material and no discernible products could be identified. Following this result, Cu-catalysed Kumada cross-coupling were then attempted. We have shown previously that alkyl Grignard reagents are well-tolerated in these cross-coupling methodologies, and with this consideration it was hoped that the alkyl electrophiles **169** and **170** could be tolerated in the Kumada conditions shown below in Scheme 124.⁵⁴



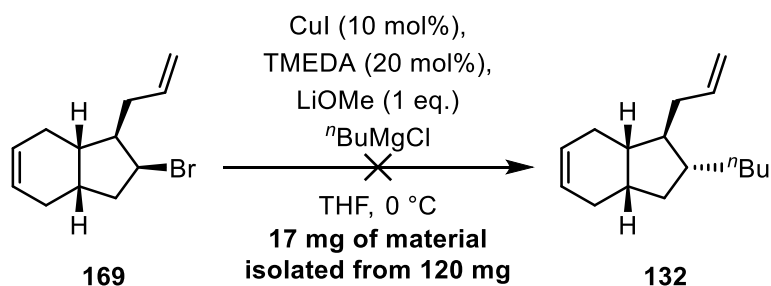
Scheme 124 - Cu-catalysed Kumada with 2,2-bipyridine ligand

Using 2,2-bipyridyl as a ligand in this Cu-catalysed Kumada reaction, with the alkyl tosylate **170** proved unsuccessful as no product **162** or starting material **170** could be recovered. Fortunately, following a search of the chemical literature, similar conditions were discovered being employed in the convergent synthesis of Phthioceranic Acid.⁵⁵ These modified Kumada conditions were applied to the alkyl tosylate **170** (Scheme 125).



Scheme 125 – Cu-catalysed Kumada using TMEDA as a ligand

Substituting the bipyridyl ligand for TMEDA proved somewhat successful as a minimal amount of the desired product could be identified by ¹H NMR spectroscopy. However, upon isolation of what was thought to be the desired product **162**, it appeared to co-elute alongside another, unidentifiable, side-product. No further optimisation was carried out in an attempt to circumvent the formation of this side-product. The Cu-catalysed Kumada was also attempted on the alkyl bromide **169** (Scheme 126).



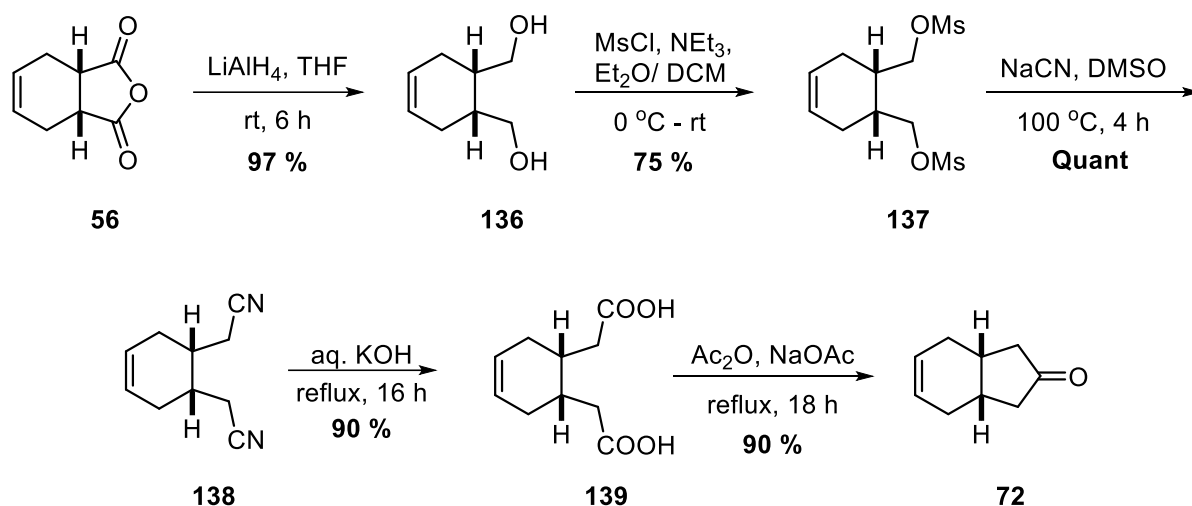
Scheme 126 - Cu-catalysed Kumada using TMEDA as a ligand on the alkyl bromide

Unsurprisingly, the Cu-catalysed Kumada on the alkyl bromide **169** also appeared to show desired product by ^1H NMR spectroscopy but after attempted purification the material could not be isolated cleanly. Additionally, the Cu-catalysed Kumada reactions with both the alkyl tosylate **170** and the alkyl bromide **169** suffered from poor mass balance, which the root cause of could not be identified.

At this stage in the research programme, Stenstrøm had identified the correct structure of (–)-mucosin (*vide supra*) and as a result, our work towards the total synthesis of (–)-mucosin was ceased. The attempts at employing a late-stage $\text{sp}^3\text{-sp}^3$ cross-coupling on complex natural products exemplifies the need for further development and understand of $\text{sp}^3\text{-sp}^3$ cross coupling, particularly on substrates bearing an α -substituent to the reaction centre.

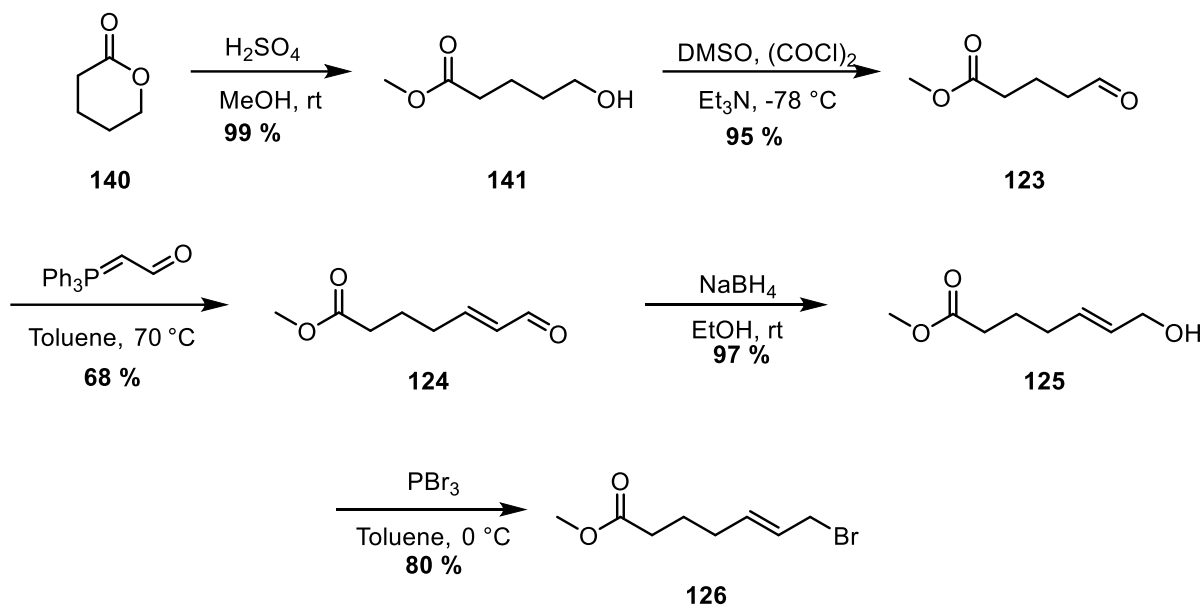
1.3. Conclusions

To conclude, synthetic efforts towards the total synthesis of the originally proposed structure of oxylipin (-)-mucosin **55** have been extensive. By employing a convergent strategy, the initial synthesis of the key ketone intermediate **72** proved successful and large quantities were obtained in 59 % yield over 5 steps (Scheme 127).



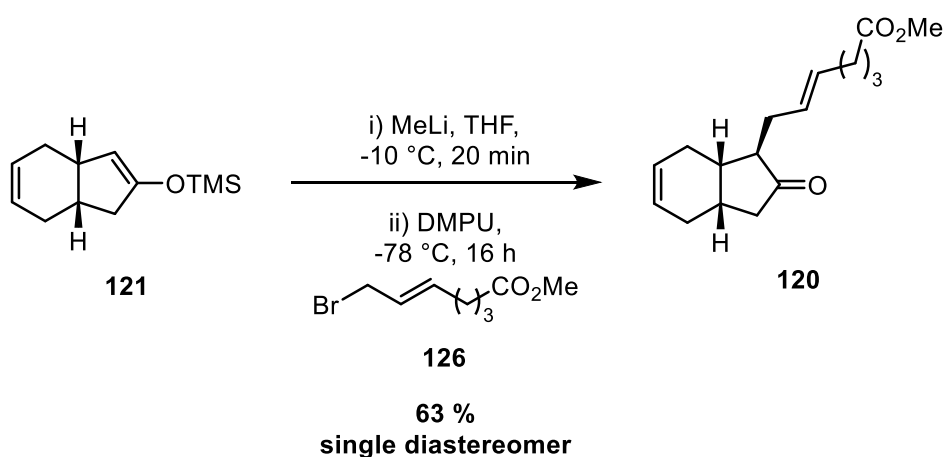
Scheme 127 - Synthesis of ketone **72**

Having synthesised the desired ketone intermediate **72**, work to access the allylic bromide side-chain **126** commenced. Due to technical limitations, a new route towards aldehyde **123** was devised and allowed for successful access to multigram quantities in extremely high yields (Scheme 128). This alternative ring opening/ oxidation procedure offered improvement over the previous ozonolysis of cyclopentene. The subsequent Wittig reaction proved challenging, but, after extending the reaction times and excluding light from the reaction mixture, excellent yields of the *E*-alkene **124** were afforded. Following a selective reduction of the carbonyl portion of enal **124**, allylic alcohol **125** was delivered in near quantitative yields. The final step towards allylic bromide **126** used PBr_3 as opposed to CBr_4 and PPh_3 , which allowed for a simpler procedure and a higher yield. Overall, the synthesis of the allylic bromide side chain **126** proceeded over five steps in an overall yield of 50 %.



Scheme 128 - Synthesis of allylic bromide side chain 126

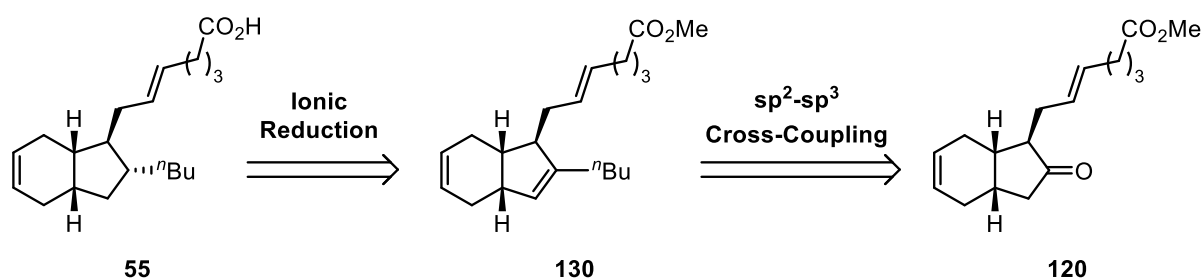
Efforts towards the utilisation of asymmetric deprotonation chemistry developed within Kerr labs came with its own challenges, as the resulting TMS enol ether **121** proved difficult to isolate and handle. Despite these difficulties, through judicious choice in isolation conditions, robust and repeatable column chromatography conditions were developed and have been recorded to allow isolation of similar compounds in any future studies. With careful isolation, TMS enol ether **121** was isolated in a high yield of 90 % with an extremely high e.r. of 94:6. Prior drying of the TMS enol ether **121** allowed for effective allylation, in a high yield of up to 63 % as a single diastereomer (Scheme 129).



Scheme 129- Allylation

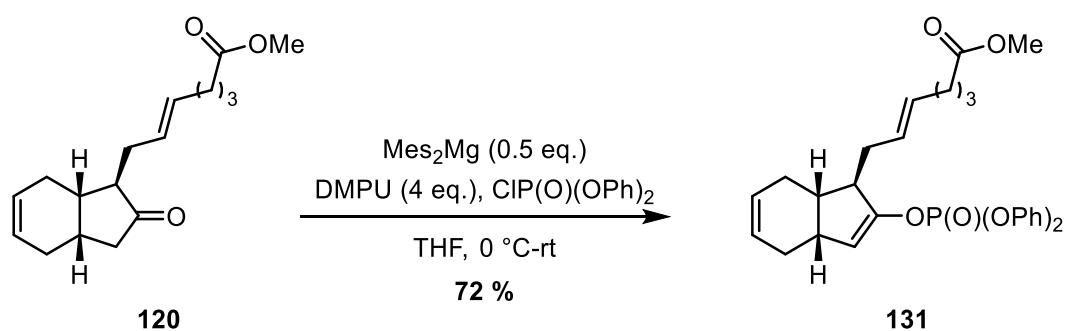
Having constructed three of the contiguous stereocentres present in (–)-mucosin, work then focused on the installation of the final appendage, the *n*-butyl chain. Multiple strategies were attempted in

order to install the butyl chain. Initially, installation of an alkyl bromide to allow for a direct displacement *via* Lipshutz higher-order cyanocuprate chemistry proved unfruitful. The desired alkylation could not be achieved with the use of several cyanocuprate procedures. At this point, the use of a range of butyl nucleophiles appeared incompatible with the ester moiety. Despite this, it was proposed, as shown in Scheme 130, that (–)-mucosin could be accessed from an ionic reduction from triene **130**, which could be furnished from ketone **120**.



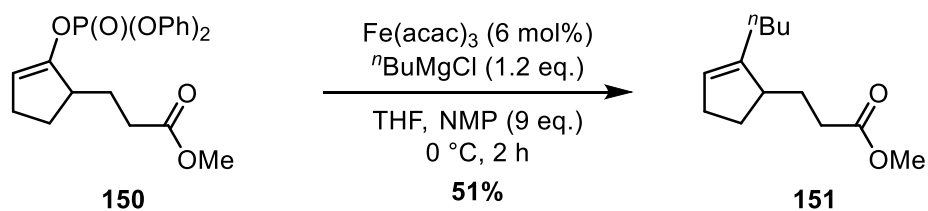
Scheme 130 - Ionic reduction strategy

In order to access cross-coupled product **130**, ketone **120** had to be converted into a functional group that would act as a leaving group in a cross-coupling reaction. Adapting previously published group methodology allowed access to enol phosphate **131** in a good yield of 72 % (Scheme 131).



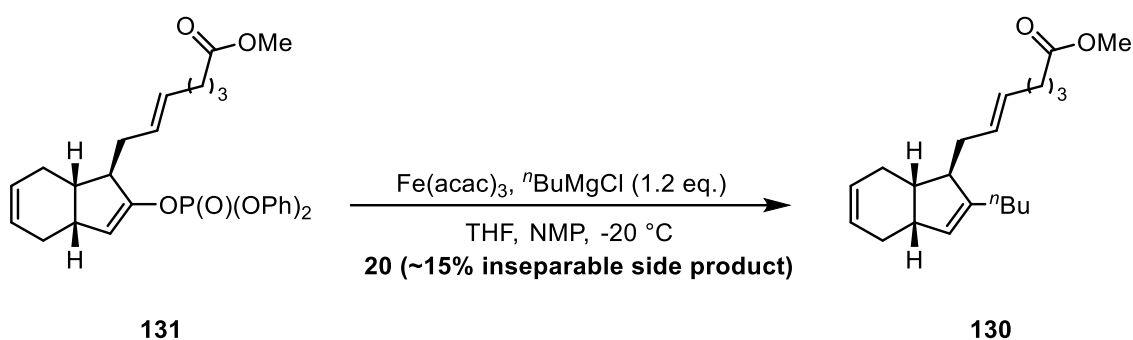
Scheme 131 - Optimised enol phosphate formation

Pleasingly, no epimerisation of the group bearing the appending chain was observed, highlighting the ability of carbon-centred magnesium bases to perform kinetic deprotonations even at 0 °C. Identification of the Claisen condensation product **149** aided in improving this reaction as steps were taken to mitigate this by-product. With efficient access to the single diastereomer of enol phosphate **131**, work then focused on the cross-coupling of enol phosphate **131**. Initially, Kerr group Kumada conditions developed specifically for the cross-coupling of enol phosphates were employed. Unfortunately, the use of Grignard reagents proved unsuitable with the highly accessible methyl ester. Despite this, iron-catalysed cross-coupling proved successful with Grignard reagents in the presence of esters leading to selective cross-coupling on model substrate **150** (Scheme 132).



Scheme 132 - Isolated yield from Iron-catalysed cross-coupling

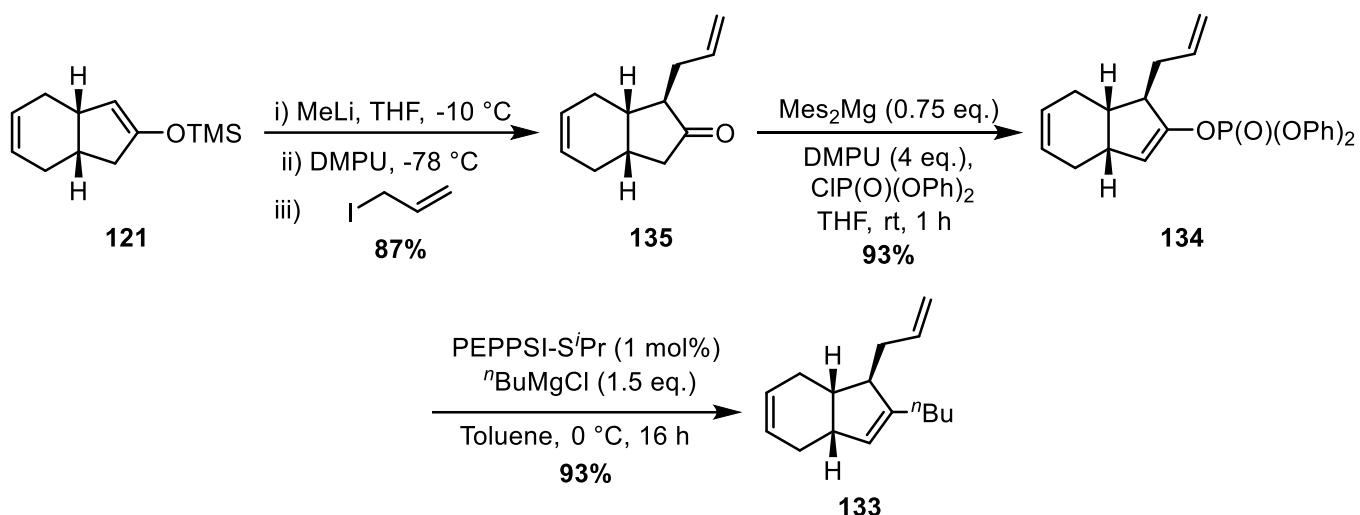
Despite the success obtained with these conditions, application to enol phosphate **131** proved difficult (Scheme 133). After a number of optimisation reactions, the desired product was only ever obtained in low yields and with an inseparable by product; which was later determined to be the proto-dephosphorylation product **147**.



Scheme 133 – Iron-catalysed cross-coupling

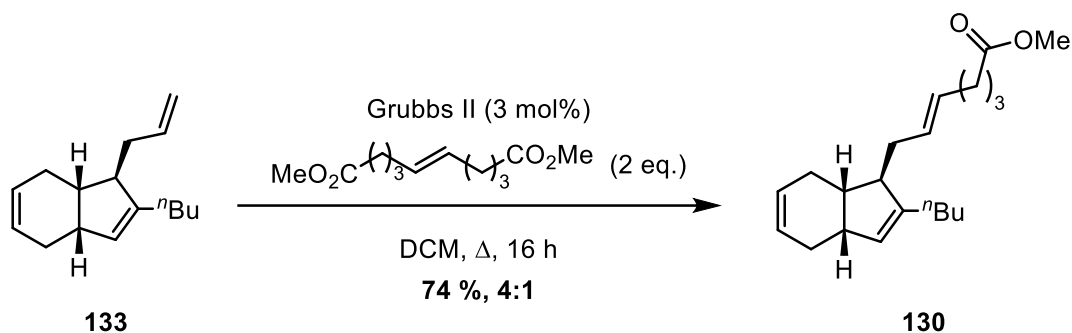
Optimisation of this cross-coupling proved unfruitful, in removing the undesired proto-dephosphorylation product **153** and at this point the newly devised strategy was abandoned. It is possible that $\text{sp}^2\text{-sp}^3$ cross coupling could be used to install the n butyl group on the core of (–)-mucosin **55**, however, the methyl ester group would need to be removed or protected to allow more robust chemistries to be employed.

By removing the methyl ester group, present in the previous intermediates, the formation of enol phosphate **134** proceeded more efficiently than has been shown previously. Additionally, the use of more traditional cross-coupling methodology led to the efficient and high yielding synthesis of triene **133**, with an overall yield of 75 % over three steps from silyl enol ether **121** (Scheme 134).



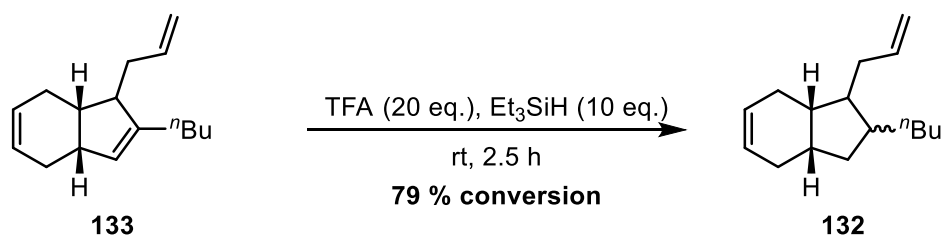
Scheme 134 - Synthesis of triene **133**

Having gained efficient access to triene **133**, work focused on the optimisation of the intermolecular cross-metathesis to obtain methyl ester **130**. This proved challenging as the polarity of product and starting material **133** were inseparable. This was overcome by employing the dimer of the methyl ester olefin **156**, allowing for a more trivial isolation of methyl ester in a good 74% yield utilising only 3 mol% of Grubbs 2nd generation catalyst.



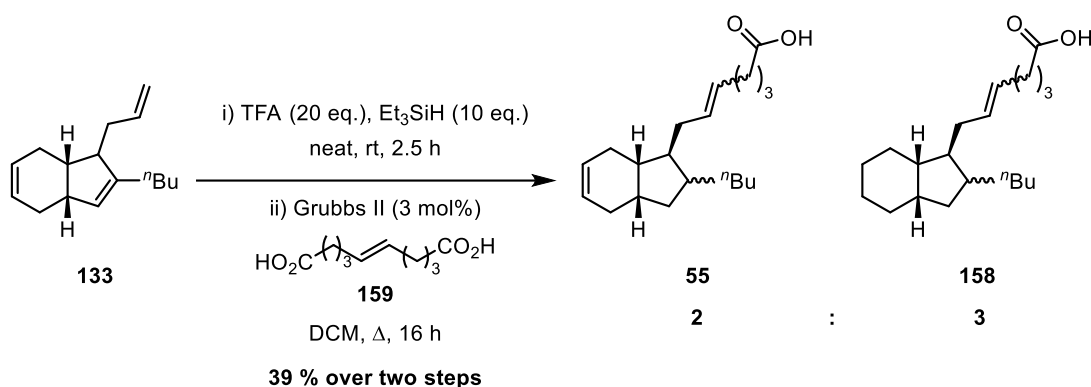
Scheme 135 - Optimised cross-metathesis conditions

Despite this success, issues with the *E:Z* ratio of the newly formed olefin would have made analysis of the subsequent ionic reduction extremely challenging. With this in consideration, the ionic reduction was then carried out on triene **133** to obtain diene **132**, prior to the cross-metathesis.



Scheme 136 - Ionic reduction of triene 133

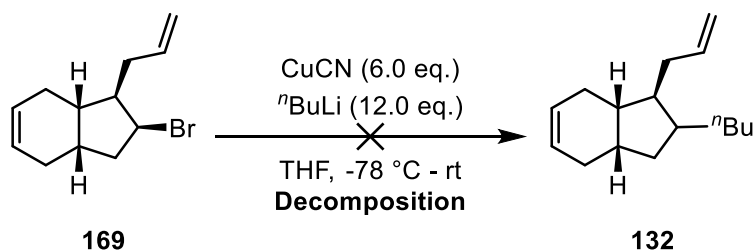
Having, seemingly, optimised the ionic reduction on triene **133**, work then focused on synthesising *cis*-mucosin **55** from triene **133**.



Scheme 137 - Synthesis of (-)-mucosin

Upon isolation and analysis of *cis*-mucosin it was found by ¹H NMR analysis that the material was a mixture of both the desired product **55** and dihydro mucosin **158**. Unfortunately, due to the complexity of a mixture containing potentially over forty different carbon nuclei, a potential mixture of *E:Z*, and a possibility of two diastereomers. Additionally, the ionic reduction suffered from a lack of reproducibility and effectively resulted in the discontinuation of this strategy.

Having shown that the cross-metathesis can skeletally allow access to the acid-bearing side-chain of (-)-mucosin, We hypothesised that an sp³-sp³ cross coupling on an allyl-bearing core, featuring an appropriate electrophile e.g. alkyl bromide **169**, could allow for the seemingly elusive alkylation.



Scheme 138 - Attempted alkylation of alkyl bromide

The previously employed higher-order cyanocuprate conditions did appear to allow limited conversion to the desired product but due, to the inseparable nature of the alkyl bromide **169** and alkylated product **132**, further resubmissions of the crude material had to be carried out. Upon further resubmissions, no discernible products could be identified by ^1H NMR spectroscopy. Following on, further $\text{sp}^3\text{-sp}^3$ cross-couplings were attempted including Cu-catalysed Suzuki-Miyaura and Kumada couplings. Unfortunately, these methodologies proved problematic due to either decomposition of the starting material or poor mass balance. Due to the untenable nature of these procedures and the further development of the (-)-mucosin story by external researchers, research within our lab towards the total synthesis was halted and work refocused on an alternative oxylipin natural product target.

1.4. Experimental

Reagents

All reagents were obtained from commercial suppliers and used without further purification, unless otherwise stated. All reactions were carried out under an inert, dry argon atmosphere, unless otherwise stated. Purification was carried out according to standard laboratory methods.⁵⁶

- Dry Et₂O, and PhMe were obtained from an Innovative Technology, Pure Solv, SPS-400-5 solvent purification system. All other solvents were used as purchased unless required dry, wherein distillation under argon, and over calcium hydride, was performed prior to use.
- MeLi was obtained as a solution in Et₂O, and standardised using diphenyl acetic acid in THF.⁵⁶
- ⁿBu₂Mg was obtained as a solution in Et₂O and standardised using iodine and LiCl in THF.⁵⁷
- Petroleum ether refers to the petroleum ether fraction in the boiling point (b.p.) range 40-60 °C unless otherwise stated.
- Tetrahydrofuran was dried by heating to reflux over sodium wire, using benzophenone ketyl as an indicator, then distilled under nitrogen.
- Dichloromethane was dried by heating to reflux over calcium hydride then distilled under nitrogen.

Instrumentation and Data

Thin layer chromatography was carried out using Merck silica gel plates coated with fluorescent indicator UV254 and was analysed using a Mineralight UVGL-25 lamp or developed using a vanillin or potassium permanganate solution.

Flash column chromatography was carried out using Prolabo silica gel (230-400 mesh).

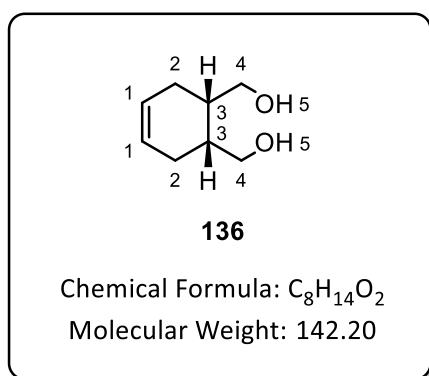
Melting points were obtained (uncorrected) on a Gallenkamp Griffin melting point apparatus.

IR spectra were obtained on a Shimadzu IR Affinity-1 Spectrophotometer machine and data are reported in cm⁻¹ unless stated otherwise.

¹H, ¹³C NMR and ³¹P NMR spectra were recorded on a Bruker DPX spectrometer at 400 MHz, 101 MHz and 162 MHz, respectively. ¹H NMR spectra were also recorded on a Bruker DPX spectrometer at 600 MHz. Unless otherwise stated, chemical shifts are reported in ppm. Coupling constants are reported in Hz and refer to ³J_{HH} interactions unless stated otherwise.

1.4.1. Synthesis of Key Bicyclic Ketone Intermediate 72

Preparation of ((1*R*,2*S*)-cyclohex-4-ene-1,2-diyl)dimethanol.^{41,42}



Scheme 58:

The reaction was carried out as documented in the literature procedure.^{41,42}

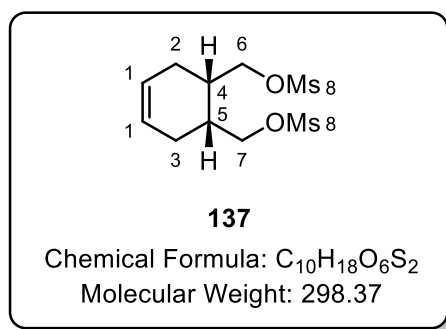
To a flame-dried flask fitted with a condenser was added distilled THF (600 mL), which was allowed to cool in an ice-bath, before the addition of LiAlH₄ (20.0 g, 527.0 mmol) to give a grey suspension. To the resulting suspension, a solution of *cis*-1,2,3,6-tetrahydrophthalic anhydride **56** (40.0 g, 262 mmol) in THF (200 mL) was added in a dropwise manner, and the resulting mixture was allowed to warm to room temperature with stirring for 6 h. After this time, the reaction mixture was quenched by addition of a saturated aqueous solution of Na₂SO₄ until the reaction mixture turned from a grey suspension to a white suspension. The white solid was filtered, and the filtrate was concentrated *in vacuo* to give the diol **136** (36.1 g, 254 mmol, 97 % yield) as a colourless oil.

IR (neat, cm⁻¹): 3318, 2917, 2836, 1772, 1768, 1681, 1673, 1614, 1431.

¹H NMR (400 MHz, Chloroform-*d*): δ 5.80 – 5.47 (m, 2H, H-1), 3.75 – 3.55 (m, 6H, H-4, H-5), 2.30 – 1.95 (m, 6H, H-2, H-3).

¹³C NMR (101 MHz, Chloroform-*d*): δ 125.5, 63.9, 37.8, 26.9.

Preparation of ((1R,2S)-cyclohex-4-ene-1,2-diyl)bis(methylene) dimethanesulfonate.^{41,42}



Scheme 58:

The reaction was carried out as documented in the literature procedure.^{41,42}

To a solution of diol **136** (25 g, 175 mmol) in DCM (180 mL) and Et₂O (600 mL) was added Et₃N (75 mL, 393 mmol) followed by MsCl (32.5 mL, 420 mmol) dropwise at 0 °C. The reaction mixture was then allowed to warm to room temperature and stirred for 18 h. The reaction mixture was concentrated *in vacuo* to leave an orange residue which was then dissolved in DCM and H₂O. The layers were separated, and the organic phase was washed with brine, and then subsequently dried over Na₂SO₄ and filtered. The resulting solvent was removed *in vacuo* to give a yellow oil, which was triturated with MeOH to provide the dimesylate **137** (39.2 g, 131 mmol) as a white solid.

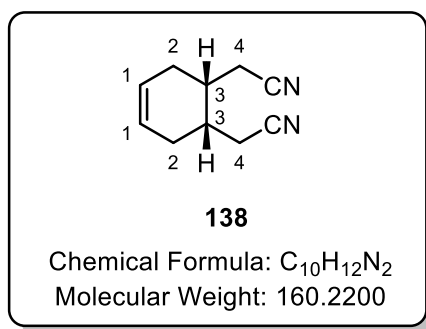
M.p.: 79-81 °C, lit.⁵⁸: 81-82 °C

IR ν (neat, cm⁻¹): 3030, 2915, 2848, 2246, 1766, 1676, 1424.

¹H NMR (400 MHz, Chloroform-*d*) δ 5.69 (s, 2H, H-1), 4.30 (dd, *J* = 10.0, 7.1 Hz, 2H, H-7 or H-6), 4.18 (dd, *J* = 10.0, 7.0 Hz, 2H, H-7 or H-6), 3.05 (s, 6H, H-8), 2.53 – 2.38 (m, 2H, H-4 and H-5), 2.34 – 2.22 (m, 2H, H-2 or H-3), 2.06 – 1.93 (m, 2H, H-2 or H-3).

¹³C NMR (101 MHz, Chloroform-*d*): δ 124.3, 69.4, 36.9, 33.5, 25.5.

Preparation of 2,2'-((1R,2S)-cyclohex-4-ene-1,2-diyl)diacetonitrile.^{41,42}



Scheme 58:

The reaction was carried out as documented in the literature procedure.^{41,42}

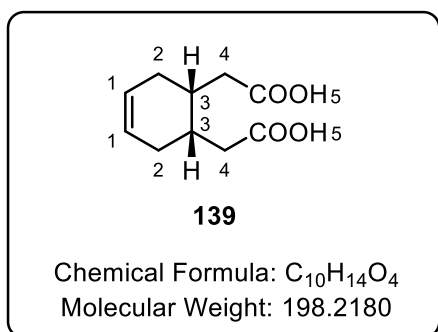
Under an argon atmosphere, a flame-dried flask fitted with a condenser, was charged with NaCN (25.0 g, 510 mmol) and a solution of **137** (39.0 g, 130 mmol) in freshly distilled DMSO (400 mL). The resulting mixture was heated to 100 °C and allowed to stir for 18 h. After this time, the reaction mixture was allowed to cool to room temperature and had water (1 L) added. The mixture was then extracted with EtOAc and the combined organic phases were dried over Na₂SO₄ and filtered. The filtrate was concentrated *in vacuo* to yield the dinitrile **138** (20.8 g, 130 mmol, Quantitative) as a brown oil.

IR ν (neat, cm⁻¹): 1424, 1443, 1652, 2247, 2848, 2915, 3031.

¹H NMR (400 MHz, Chloroform-*d*): δ 5.69 (s, 2H, H-1), 2.37 (m, 8H, H-2, H-4), 2.09 – 1.96 (m, 2H, H-3).

¹³C NMR (101 MHz, Chloroform-*d*): δ 123.9, 117.9, 32.6, 28.1, 18.0.

Preparation of 2,2'-((1R,2S)-cyclohex-4-ene-1,2-diyl)diacetic acid.^{41,42}



Scheme 58:

The reaction was carried out as documented in the literature procedure.^{41,42}

Dinitrile **138** (19 g, 119 mmol) was added to a solution of aq. 30 % KOH (140 mL) and the mixture was heated to reflux with vigorous stirring for 18 h. The reaction mixture was then allowed to cool in an ice bath, after which concentrated HCl was added dropwise until the pH \approx 2. The precipitated solid thus formed was filtered off and dried in the vacuum oven to yield the diacid **139** (21.3 g, 107 mmol, 90 % yield) as a white solid.

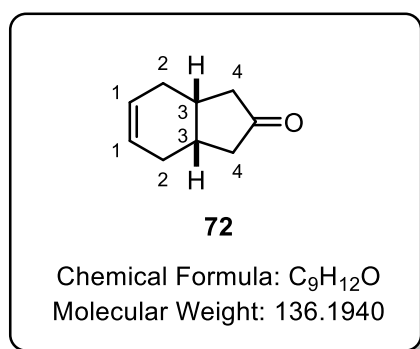
M.p.: 156-158 °C. lit.⁴¹: 156-158 °C

IR (neat, cm⁻¹): 1408, 1681, 3031.

¹H NMR (400 MHz, CD₃OD): δ 5.75 – 5.56 (m, 2H, H-1), 2.53 – 2.12 (m, 8H, H-2 and H-4), 1.97 – 1.64 (m, 2H, H-3).

¹³C NMR (101 MHz, CD₃OD): δ 175.1, 124.4, 34.1, 32.2, 28.4

Preparation of (3*aR*,7*aS*)-1,3,3*a*,4,7,7*a*-hexahydro-2*H*-inden-2-one.^{41,42}



Scheme 58:

The reaction was carried out as documented in the literature procedure.^{41,42}

A flame-dried flask, fitted with a condenser, was charged with diacid **139** (3.4 g, 17.2 mmol) to which was added distilled Ac₂O (50 mL). The resulting mixture was heated to reflux, with stirring, under argon for 2.5 h. After this time, NaOAc (7.0 g, 85.4 mmol) was added and the resulting mixture was allowed to continue to reflux, with stirring, under argon for a further 16 h. The reaction mixture was then cooled to room temperature, quenched with an aqueous saturated NaHCO₃ solution and extracted with Et₂O. The combined organic phases were concentrated *in vacuo* to give an orange oil. The orange oil was purified *via* column chromatography, eluting the silica gel column with 40 % Et₂O/petroleum ether. The appropriate fractions were combined and concentrated *in vacuo* to yield the ketone **72** (2.1 g, 15.4 mmol, 90 % yield) as a colourless oil.

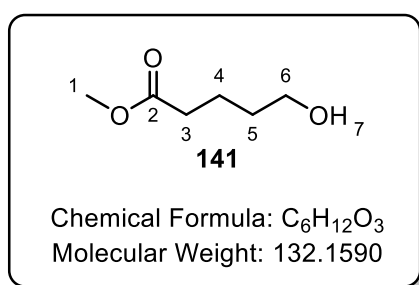
IR (neat, cm^{-1}): 2899, 1735.

^1H NMR (400 MHz, Chloroform-*d*) δ 5.77 – 5.62 (m, 2H, H-1), 2.48 – 2.39 (m, 2H, aliphatic protons), 2.36 – 2.24 (m, 4H, aliphatic protons), 2.12 – 2.01 (m, 2H, aliphatic protons), 1.92 – 1.79 (m, 2H, aliphatic protons).

^{13}C NMR (101 MHz, Chloroform-*d*) δ 219.1, 124.1, 44.2, 31.8, 25.8.

1.4.2. Synthesis of the Allyl Bromide Intermediate 126

Preparation of methyl 5-hydroxypentanoate.⁵⁹



General Procedure:

The reaction was carried out as documented in the literature procedure.^{60, 61}

To a 1 % H_2SO_4 in MeOH solution was added δ -valerolactone **140**. The resulting reaction mixture was allowed to heat to reflux and stir under an atmosphere of argon for 18 h. The reaction mixture was removed from the heat and allowed to cool in an ice-bath, after which Na_2CO_3 was added until the pH was approximately 7. DCM and water were added to the mixture and the layers separated. The aqueous layer was extracted with further DCM and the organic extracts were collected and combined. The combined organic phases were concentrated *in vacuo* to provide the alcohol **141** as a colourless oil.

Following the **General Procedure**, data are presented as a) volume of 1 % H_2SO_4 in MeOH, b) amount and mmol of δ -valerolactone **140**, and c) yield of methyl 5-hydroxypentanoate **141**.

Table 6, Entry 1

a) 10 mL, b) 500 mg, 4.99 mmol, c) 399 mg, 3.99 mmol, 80 % yield.

Scheme 64

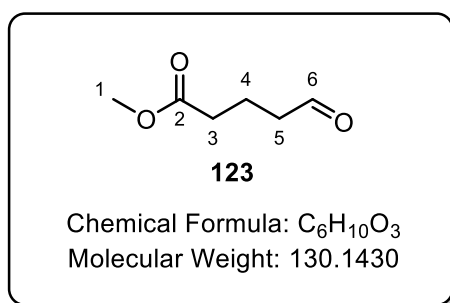
a) 25 g, 250.0 mmol, b) 25 g, 250.0 mmol, c) 32.7 g, 248.5mmol, 99 % yield.

IR ν (neat, cm^{-1}): 1728, 2873, 2951, 3435.

^1H NMR (400 MHz, Chloroform-*d*): δ 3.68 (s, 3H, H-1), 3.67 – 3.63 (m, 2H, H-6), 2.37 (t, $J = 7.3$ Hz, 2H, H-3), 1.79 (s, 1H, H-7), 1.73 (m, 2H, H-4 or H-5), 1.61 (m, 2H, H-4 or H-5).

^{13}C NMR (101 MHz, Chloroform-*d*): δ 173.7, 61.7, 51.0, 33.1, 31.5, 20.6.

Preparation of methyl 5-oxopentanoate.⁶⁰



General Procedure:

The reaction was carried out as documented in the literature procedure.⁶⁰

To a flame-dried flask, fitted with an internal thermometer, and under an atmosphere of argon, was added DCM (volume a) and oxalyl chloride and the mixture was cooled to -78 °C with stirring. To another flame-dried flask was added DCM (volume c) and DMSO under an atmosphere of argon. The DCM/DMSO mixture was added dropwise to the oxalyl chloride-containing reaction vessel ensuring that the internal temperature remained below -72 °C on completion of the addition, the resulting reaction mixture was allowed to stir for a further 15 min at -78 °C. A solution of **141** in DCM (volume f) was added dropwise to the reaction mixture, again, ensuring that the internal temperature remained below -72 °C, and the resulting reaction mixture was allowed to stir for a further 1 h at -78 °C. The reaction mixture was quenched with a dropwise addition of Et_3N , again ensuring a < -72 °C internal temperature, and the resulting reaction mixture was allowed to gradually warm to room temperature. The reaction mixture was diluted with DCM and washed with aq. sat. NH_4Cl . The organic phases were separated, collected and subsequently dried over Na_2SO_4 then filtered. The filtrate was concentrated *in vacuo* to give an orange oil. The crude product was either applied to a silica column and eluted with 50 % Et_2O / petroleum ether to give the aldehyde **123** as a colourless oil.

Following the above **General Procedure**, data are presented as a) volume of DCM, b) amount and mmol of oxalyl chloride, c) volume of DCM, d) volume and mmol of DMSO, e) amount and mmol of **141**, f) volume of DCM, g) amount and mmol of Et₃N h) method of purification, and i) amount, mmol and yield of methyl 5-oxopentanoate **123**.

Table 7, Entry 1

a) 30 mL, b) 6 mL, 70.0 mmol, c) 30 mL, d) 9 mL, 127 mmol, e) 6.00 g, 45.4 mmol, f) 15 mL, g) 45 mL, 323 mmol, h) column chromatography, and i) 4.60 g, 35.4 mmol, 78 % yield.

Table 7, Entry 2

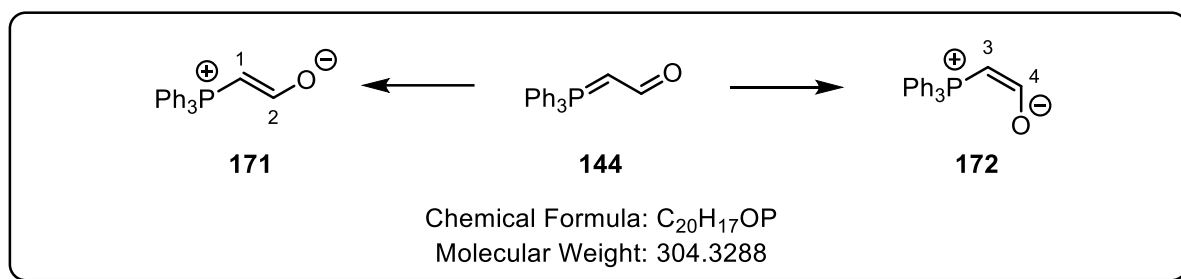
a) 60 mL, b) 12 mL, 139.9 mmol, c) 60 mL, d) 18 mL, 253 mmol, e) 12.0 g, 90.9 mmol, f) 30 mL, g) 90 mL, 645 mmol, h) column chromatography, and i) 11.2 g, 86.1 mmol, 95 % yield.

IR ν (neat, cm⁻¹): 2953, 2831, 1720.

¹H NMR (400 MHz, Chloroform-*d*) δ 9.74 (t, J = 1.2 Hz, 1H, H-6), 3.64 (s, 3H, H-1), 2.50 (td, J = 7.2, 1.2 Hz, 2H, H-5), 2.35 (t, J = 7.3 Hz, 2H, H-3), 1.92 (p, J = 7.2 Hz, 2H, H-4).

¹³C NMR (101 MHz, Chloroform-*d*) δ 201.0, 172.8, 51.1, 42.3, 32.4, 16.8.

Preparation of 2-(triphenylphosphanylidene)acetaldehyde.⁴⁸



Scheme 66

The reaction was carried out as documented in the literature procedure.⁴⁸

Chloroacetylaldehyde in H₂O (50% w/w) (18 mL, 114 mmol) was suspended in chloroform (400 mL) and the reaction vessel was fitted with distillation apparatus. The mixture was heated to reflux, which allowed the water to be distilled off as an azeotrope (57 °C). To the resulting solution was added triphenylphosphine (26.3 g, 100 mmol) and the resulting solution was heated to reflux with stirring for 18 h. After this time, the reaction mixture was allowed to cool and water was added. The aqueous layer was separated, collected, and subsequently treated with 2 M NaOH solution, until a yellow precipitate was formed. The precipitate was filtered, collected, and triturated with hot toluene. The resulting pink solid was dried in a vacuum oven to give the ylide **144** as a pink solid (23.1 g, 76 mmol, 76 % yield).

M.p.: decomposed above 185 °C. lit.⁴⁸: decomposed above 187 °C

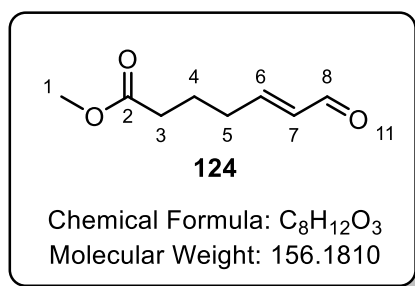
IR (neat, cm⁻¹): 1550, 1573, 2765, 3327.

¹H NMR (400 MHz, Chloroform-*d*): δ 8.98 (*trans*) (dd, ³J_{PH} = 38.2, ³J_{HH} = 3.5 Hz, 1H, H-2), 8.24 (*cis*) (dd, ³J_{PH} = 10.8, ³J_{HH} = 3.6 Hz, 1H, H-4), 7.82 – 7.41 (m, 15H, ArH), 4.10 (*cis*) (dd, ²J_{PH} = 19.3, ³J_{HH} = 10.8 Hz, 1H, H-3), 3.69 (*trans*) (dd, ²J_{PH} = 24.6, ³J_{HH} = 3.5 Hz, 1H, H-1).

¹³C NMR (101 MHz, Chloroform-*d*) δ 181.7 (t, *J* = 8.6 Hz), 133.3 (d, *J* = 9.9 Hz), 133.1 (d, *J* = 10.1 Hz), 132.9 (d, *J* = 2.3 Hz), 132.4 (d, *J* = 2.6 Hz), 129.2 (d, *J* = 12.4 Hz), 129.0 (d, *J* = 12.3 Hz), 126.5 (d, *J* = 90.6 Hz), 126.0 (d, *J* = 90.1 Hz), 56.6 (d, *J* = 110.5 Hz), 54.9 (d, *J* = 99.8 Hz).

³¹P NMR (162 MHz, Chloroform-*d*): δ (*cis*) 18.9, (*trans*) 14.94.

Preparation of methyl (*E*)-7-oxohept-5-enoate.⁶²



General Procedure:

The reaction was carried out as documented in the literature procedure.^{41,42}

To a solution of **123** in toluene was added ylide **144**, and the resulting mixture was heated to 70 °C, with stirring, for the allotted time. Conversion was established by ¹H NMR spectroscopy analysis. Once full conversion was reached, the reaction mixture was allowed to cool to room temperature and petroleum ether was added, to give a yellow mixture. This mixture was filtered through Celite® to give a yellow solution, which was concentrated *in vacuo* to give a red residue. The residue was purified *via* column chromatography, eluting with 50 % Et₂O/Petroleum ether. The appropriate fractions were combined and concentrated *in vacuo* to yield the enal **124** as a yellow oil.

Following the above **General Procedure**, data are presented as a) amount and mmol of **123**, b) volume of toluene, c) amount and mmol of **144**, d) reaction time, e) amount, mmol and yield of methyl (*E*)-7-oxohept-5-enoate **124**, and f) ratio of *E*:*Z* isomers.

Table 8, Entry 1

a) 200 mg, 1.54 mmol, b) 10 mL, c) 700 mg, 2.30 mmol, d) 18 h, e) 124.9 mg, 0.80 mmol, and 52 % yield f) 9:1.

Table 8, Entry 2

a) 200 mg, 1.54 mmol, b) 10 mL, c) 1.15 g, 3.83 mmol, d) 18 h, e) 139.0 mg, 0.89 mmol, and 58 % yield f) 9:1.

Table 8, Entry 3

a) 200 mg, 1.54 mmol, b) 10 mL, c) 1.40 g, 4.60 mmol, d) 18 h, e) 129.6 mg, 0.83 mmol, and 54 % yield f) 9:1.

Table 8, Entry 4

a) 200 mg, 1.54 mmol, b) 10 mL, c) 1.64 g, 5.37 mmol, d) 18 h, e) 160.9 mg, 1.03 mmol, and 67 % yield
f) 9:1.

Table 8, Entry 5

a) 200 mg, 1.54 mmol, b) 10 mL, c) 1.86 g, 6.12 mmol, d) 18 h, e) 160.9 mg, 0.99 mmol, and 64 % yield
f) 9:2.

Table 8, Entry 6

a) 200 mg, 1.54 mmol, b) 10 mL, c) 700 mg, 2.3 mmol, d) 64 h, e) 134.3 mg, 0.86 mmol, and 56 % yield
f) 7:3.

Table 9, Entry 1 (Foil covered reaction)

a) 1.00 g, 7.68 mmol, b) 50 mL, c) 3.5 g, 11.5 mmol, d) 18 h, e) 0.60 g, 3.84 mmol, and 50 % yield f)
92:8.

Table 9, Entry 2 (Foil covered reaction)

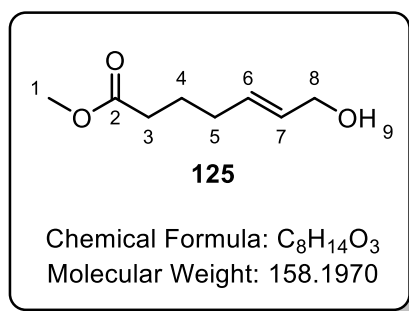
a) 6.00 g, 46.1 mmol, b) 300 mL, c) 21.0 g, 69.1 mmol, d) 18 h, e) 4.89 g, 31.3 mmol, and 68 % yield f)
92:8.

IR (neat, cm^{-1}): 2951, 1730, 1683, 1637.

^1H NMR (400 MHz, Chloroform-*d*): δ 9.52 (d, $J = 7.8$ Hz, 1H, H-8), 6.83 (dt, $J = 15.6, 6.7$ Hz, 1H, H-6),
6.14 (ddt, $J = 15.6, 7.8, ^4J = 1.5$ Hz, 1H, H-7), 3.69 (s, 3H, H-1), 2.42 – 2.35 (m, 4H, H-5 and H-3), 1.87 (p,
 $J = 7.4$ Hz, 2H, H-4).

^{13}C NMR (101 MHz, Chloroform-*d*) δ 193.3, 172.8, 156.5, 133.0, 51.1, 32.6, 31.4, 22.5.

Preparation of methyl (*E*)-7-hydroxyhept-5-enoate.⁴²



Scheme 70

The reaction was carried out as documented in the literature procedure.^{41,42}

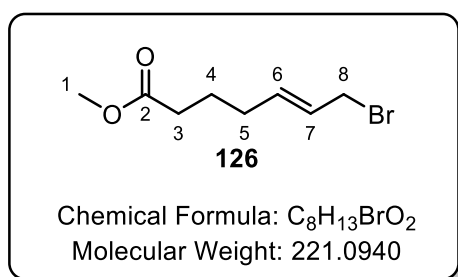
To a mixture of NaBH₄ (42 mg, 1.10 mmol) and EtOH (10 mL) stirring under an atmosphere of argon, at 0 °C, was added a solution of aldehyde **124** (160 mg, 1.01 mmol) in EtOH (10 mL) in a dropwise manner. After the addition, the solution was allowed to slowly warm to room temperature over 1 h, after which, the reaction mixture was cooled to 0 °C and carefully quenched by the addition of H₂O until no further effervescence was observed. The resulting mixture was further diluted with H₂O and extracted with DCM. The collected organics were combined, dried over Na₂SO₄, and filtered to give a yellow solution which then was concentrated *in vacuo* to give the allylic alcohol **125** (160.9 mg, 0.99 mmol, 97 % yield) as a pale-yellow oil.

IR (neat, cm⁻¹): 1730, 2864, 2927, 3342.

¹H NMR (600 MHz, Chloroform-*d*): δ 5.71 – 5.64 (m, 2H, H-6 and H-7), 4.12 – 4.07 (m, 2H, H-8), 3.68 (s, 3H, H-1), 2.33 (t, *J* = 7.4 Hz, 2H, H-3), 2.14 – 2.08 (m, 2H, H-5), 1.74 (p, *J* = 7.5 Hz, 2H, H-4), 1.56 (s, 1H, H-9).

¹³C NMR (151 MHz, Chloroform-*d*): δ 174.0, 131.7, 130.1, 63.6, 51.5, 33.4, 31.5, 24.2.

Preparation of methyl (*E*)-7-bromohept-5-enoate.^{42,41}



General Procedure A:

The reaction was carried out as documented in the literature procedure.^{41,42}

To a flame-dried flask, was added CBr₄, alcohol **125** and DCM (volume c), and the resulting mixture was allowed to cool in an ice-bath to approximately 0 °C. To the cooled mixture was added a solution of PPh₃ in DCM (volume e) *via* syringe pump over 40 min. The resulting solution was then allowed to stir for 16 h, at room temperature, under an atmosphere of argon, after which Et₂O was added until the formation of a white precipitate had ceased. The resulting mixture was filtered, the filtrate collected, and the solvent removed *in vacuo* to give an orange residue. The residue was loaded onto silica, applied to a silica column and eluted with 20 % Et₂O/petroleum ether. The appropriate fractions were combined and concentrated *in vacuo* to give the allylic bromide **126** as a colourless oil.

Following the above **General Procedure A**, data are presented as a) amount and mmol of CBr₄ (commercial or recrystallised), b) amount and mmol of **125**, c) volume of DCM, d) amount and mmol of PPh₃ (commercial or recrystallised), e) volume of DCM and f) amount, mmol and yield of methyl (*E*)-7-bromohept-5-enoate **126**.

Table 10, Entry 1

a) 250 mg, 0.75 mmol, commercial b) 79.1 mg, 0.5 mmol, c) 1.5 mL, d) 200 mg, 0.76 mmol, commercial e) 1.5 mL, and f) 75.2 mg, 0.34 mmol, 67 %

Table 10, Entry 2

a) 1.36 g, 4.1 mmol, commercial b) 390 mg, 2.46 mmol, c) 6 mL, d) 1.1 g, 4.2 mmol, commercial e) 6 mL, and f) 300 mg, 1.36 mmol, 55 %

Table 10, Entry 3

a) 2.3 g, 6.9 mmol, recrystallised b) 600 mg, 3.80 mmol, c) 12 mL, d) 2 g, 7.6 mmol, recrystallised e) 12 mL, and f) 400 mg, 1.81 mmol, 47 %

General Procedure B:

To a flame-dried flask was added a solution of alcohol **125** in toluene, and the solution cooled to 0 °C, with stirring, under an atmosphere of argon. To the solution was added PBr₃ in a dropwise manner, and the resulting reaction mixture was allowed to warm to room temperature over 2 h. The reaction mixture was cooled again to 0 °C and was slowly quenched with sat. aq. NaHCO₃ until no further effervescence was observed. The mixture was diluted further with H₂O and extracted with Et₂O. The

collected organic phases were combined, dried over Na₂SO₄ and filtered to yield a yellow solution, which subsequently, was concentrated *in vacuo* to give a yellow residue. The residue was applied to a silica column and eluted with 20 % Et₂O/Petroleum ether. The appropriate fractions were combined, and the solvent was concentrated *in vacuo* to deliver a pale yellow oil, which was further purified by distillation (85 °C/ 0.5 mbar) to give the allylic bromide **126** as a colourless oil.

Following the above **General Procedure B**, data are presented as a) amount and mmol of **125**, b) volume of toluene, c) amount and mmol of PBr₃, and d) amount, mmol and yield of methyl (*E*)-7-bromohept-5-enoate **126**.

Table 11, Entry 1

a) 540 mg, 3.41 mmol, b) 10 mL, c) 0.28 mL, 2.95 mmol, and d) 600 mg, 2.71 mmol, 80 % yield.

Table 11, Entry 2

a) 3.20 g, 20.2 mmol, b) 90 mL, c) 1.80 mL, 19.0 mmol, and d) 3.00 g, 13.6 mmol, 67 % yield.

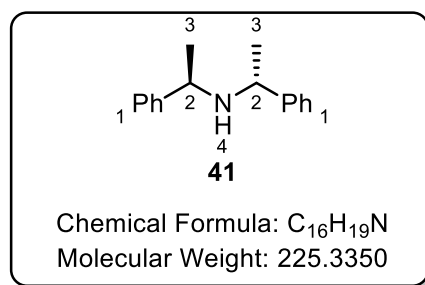
IR (neat, cm⁻¹): 1730, 2949.

¹H NMR (400 MHz, Chloroform-*d*) δ 5.76 – 5.71 (m, 2H, H-6 and H-7), 3.94 (d, *J* = 6.1 Hz, 2H, H-8), 3.68 (s, 3H, H-1), 2.32 (t, *J* = 7.5 Hz, 2H, H-3), 2.17 – 2.07 (m, 2H, H-5), 1.75 (p, *J* = 7.5 Hz, 1H, H-4).

¹³C NMR (101 MHz, Chloroform-*d*) δ 173.3, 134.6, 126.9, 51.0, 32.7, 32.6, 30.8, 23.5.

1.4.3. Application of Magnesium-Bisamides in Asymmetric Deprotonation Chemistry

Preparation of (*R*)-bis((*R*)-1-phenylethyl)amine.^{63,64}



The reaction was carried out as documented in the literature procedure.⁶⁴

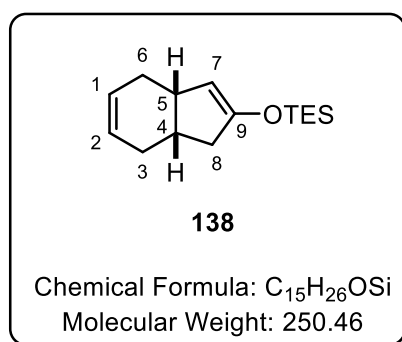
To a mixture of acetophenone (19.2 mL, 165.0 mmol) and (*R*)-1-phenylethan-1-amine (21.3 mL, 164.2 mmol) was added Ti(OⁱPr)₄ (150 mL, 495 mmol) and the resulting mixture was allowed to stir for 30 min at room temperature. Following this, the reaction mixture was transferred to a Parr hydrogenation apparatus. To the reaction mixture was added palladium on carbon (0.72 g, 10 % Pd) and EtOAc (100 mL) and the resulting mixture was subjected to an atmosphere of H₂ (8 bar) with vigorous stirring for 48 h. After this time, reaction mixture was diluted with EtOAc and water to give a white suspension. The resulting suspension was filtered through a plug of Celite® and the filter cake was washed with further EtOAc. The filtrate was then concentrated *in vacuo* to give an orange oil (¹H NMR spectroscopic analysis showed complete conversion to the product with a d.r. of 86:14, as determined by δ 3.81 (q, *J* = 6.5 Hz, 0.28H) and 3.54 (q, *J* = 6.7 Hz, 1.72H)). The orange oil was dissolved in EtOAc and the resulting solution treated with conc. HCl until a white precipitate was formed, which was filtered and collected. This process was repeated until no more white solid precipitated. The collected white solid was combined and recrystallised with boiling *iso*-propanol. The mother liquor was reduced *in vacuo* to give a white solid (¹H NMR spectroscopic analysis showed only one diastereoisomer was present, as determined by 3.54 (q, *J* = 6.7 Hz, 2H) .)). The white solid was then treated with 2M NaOH solution and extracted with EtOAc. The collected organic phases were combined, dried over Na₂SO₄, and reduced *in vacuo* to yield the amine **41** as a colourless oil (18.1 g, 80.5 mmol, 49 %).

IR (neat, cm⁻¹): 3080, 3059, 3022, 2958, 2922, 2186, 1490.

¹H NMR (400 MHz, Chloroform-*d*): δ 7.43 – 7.21 (m, 10H, H-1), 3.56 (q, *J* = 6.7 Hz, 2H, H-2), 1.32 (d, *J* = 6.7 Hz, 6H, H-3).

¹³C NMR (101 MHz, Chloroform-*d*): δ 145.4, 127.9, 126.3, 126.2, 54.6, 24.5.

Preparation of triethyl((3a,4,7,7a-tetrahydro-1*H*-inden-2-yl)oxy)silane.⁶⁵



Scheme 76

The reaction was carried out as documented in the literature procedure.⁶⁵

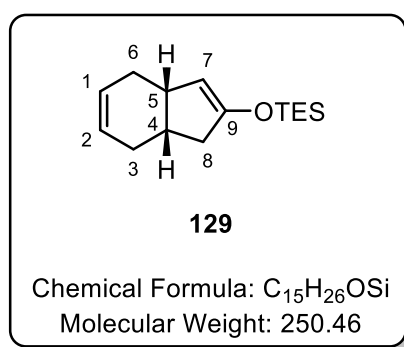
A flask was charged with NaI (0.75 g, 5.0 mmol), then flamed-dried under vacuum and allowed to cool under argon. The NaI was dissolved in MeCN (8 mL) and the resulting solution was cooled in an ice-bath with stirring. To the clear solution, triethylsilyl chloride (0.94 mL, 5.6 mmol) was added dropwise, after which, ketone **72** (0.5 mL, 4.2 mmol) was added dropwise, forming a white precipitate. To the reaction mixture was added Et₃N (0.5 mL, 4.9 mmol) dropwise, which produced a brownish mixture. The resulting mixture was allowed to warm to room temperature and was stirred for a further 6 h. The reaction mixture then had *n*-hexane (8 mL) added. The resulting phases were separated, and the *n*-hexane collected. The MeCN was further extracted with *n*-hexane (2 x 40 mL). The collected *n*-hexane extracts were combined, and concentrated *in vacuo* to give the TES enol ether **138** as clear oil (756 mg, 3.02 mmol, 72 %).

IR ν (neat, cm⁻¹): 2954, 2932, 2910, 2875, 1647.

¹H NMR (400 MHz, Chloroform-*d*) δ 5.93 – 5.82 (m, 2H, H-1 and H-2), 4.59 (dd, *J* = 3.7, 1.8 Hz, 1H, H-7), 2.84 – 2.72 (m, 1H, H-5), 2.56 – 2.37 (m, 2H, ring protons), 2.26 – 2.14 (m, 2H, ring protons), 2.04 – 1.76 (m, 3H, ring protons), 1.00 (t, *J* = 7.9 Hz, 9H, Si(CH₂CH₃)₃), 0.70 (q, *J* = 7.7 Hz, 6H, Si(CH₂CH₃)₃).

¹³C NMR (101 MHz, Chloroform-*d*) δ 154.0, 128.3, 127.5, 107.4, 40.7, 39.0, 32.8, 28.5, 28.4, 6.1, 4.3.

Preparation of triethyl(((3a*S*,7a*S*)-3a,4,7,7a-tetrahydro-1*H*-inden-2-yl)oxy)silane.⁶⁶



General Procedure:

The reaction was carried out as documented in the literature procedure.⁶⁶

To a flame-dried Schlenk tube fitted with a Suba-Seal[®] was added ⁿBu₂Mg (1.0 M in heptane) and the heptane was evaporated under vacuum to produce a white residue, which was dissolved in THF. To the resulting solution was added amine **41**, and a reflux condenser was fitted to the Schlenk tube. The reaction mixture was heated to reflux, with stirring, under an atmosphere of argon for 1.5 h. The reaction mixture was taken off heating and allowed to cool to room temperature prior to being cooled to -78 °C using a dry ice/acetone bath. The reflux condenser was quickly switched with a Suba-Seal[®] and then DMPU, was added to the mixture followed by triethylsilyl chloride. Following this, a solution of ketone **72** in THF was added to the mixture *via* a syringe pump over 1 h. Once the addition was complete, the reaction mixture was stirred at -78 °C for a further 16 h. The reaction mixture was quenched with a saturated aqueous solution of NaHCO₃ and then extracted with Et₂O. The collected organic phases were combined, dried over Na₂SO₄, and evaporated *in vacuo* to give a colourless residue. The residue was absorbed onto silica and applied to a silica column, eluting with 5% Et₂O/petroleum ether. The appropriate fractions were combined then reduced *in vacuo* to give the TES enol ether **129** as a colourless oil.

Following the above **General Procedure**, data are presented as a) volume and mmol of 1.0 M MgⁿBu₂ in heptane, b) volume of THF, c) volume and mmol of amine **41**, d) volume and mmol of DMPU, e) amount and mmol of TESCl, f) volume and mmol of ketone **72**, g) volume of THF, h) time, i) amount, mmol and yield of triethyl(((3aS,7aS)-3a,4,7,7a-tetrahydro-1H-inden-2-yl)oxy)silane **129**, and j) enantiomeric ratio.

Table 12, Entry 1

a) 1.00 mL, 1.00 mmol, b), 10 mL, c) 0.42 mmol, 2.00 mmol, d) 60 μL, 0.5 mmol, e) 0.17 mL, 0.101 mmol, f) 0.1 mL, 0.8 mmol, g) 2 mL, h) 1 h, i) 40.0 mg, 0.16 mmol, 20 % yield, and j) N/A

Table 12, Entry 2

a) 1.00 mL, 1.00 mmol b), 10 mL, c) 0.42 mmol, 2.00 mmol, d) 0.12 mL, 1.0 mmol, e) 0.17 mL, 0.10 mmol, f) 0.1 mL, 0.80 mmol, g) 2 mL, h) 1 h, i) 102 mg, 0.41 mmol, 51 % yield, and j) N/A

Table 12, Entry 3

a) 3.00 mL, 3.00 mmol, b), 30 mL, c) 1.26 mmol, 6.00 mmol, d) 0.36 mL, 3.0 mmol, e) 0.51 mL, 0.30 mmol, f) 0.3 mL, 2.40 mmol g) 6 mL, h) 3 h, i) 110 mg, 0.44 mmol, 65 % yield, and j) 94:6

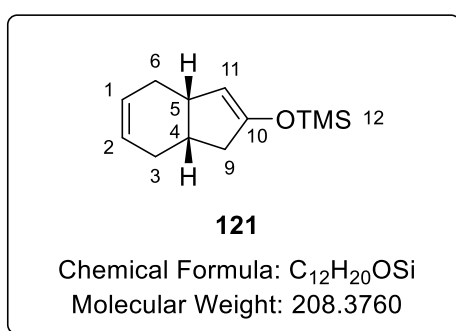
IR ν (neat, cm⁻¹): 2954, 2932, 2910, 2875, 1647.

^1H NMR (400 MHz, Chloroform-*d*) δ 5.93 – 5.82 (m, 2H, H-1 and H-2), 4.59 (dd, $J = 3.7, 1.8$ Hz, 1H, H-7), 2.84 – 2.72 (m, 1H, H-5), 2.56 – 2.37 (m, 2H, ring protons), 2.26 – 2.14 (m, 2H, ring protons), 2.04 – 1.76 (m, 3H, ring protons), 1.00 (t, $J = 7.9$ Hz, 9H, $\text{Si}(\text{CH}_2\text{CH}_3)_3$), 0.70 (q, $J = 7.7$ Hz, 6H, $\text{Si}(\text{CH}_2\text{CH}_3)_3$).

^{13}C NMR (101 MHz, Chloroform-*d*) δ 154.0, 128.3, 127.5, 107.4, 40.7, 39.0, 32.8, 28.5, 28.4, 6.1, 4.3.

Chiral HPLC: Chiracel OJ column, 100 % Hexane, 210 nm, 0.40 ml/min, $\text{RT}_1 = 14.77$ min and $\text{RT}_2 = 15.93$ min. $\text{RT}_1 = 94\%$ $\text{RT}_2 = 6\%$.

Preparation of trimethyl(((3*aS*,7*aS*)-3*a*,4,7,7*a*-tetrahydro-1*H*-inden-2-yl)oxy)silane.^{41,42}



General Procedure:

The reaction was carried out as documented in the literature procedure.^{41,42}

To a flame-dried Schlenk tube fitted with a Suba-Seal[®] was added $^n\text{Bu}_2\text{Mg}$ (1.0 M in heptane) and the heptane was evaporated under vacuum leave a white residue, which was dissolved in THF. To the resulting solution was added amine **41**, and a reflux condenser was fitted to the Schlenk tube. The reaction mixture was heated to reflux, with stirring, and under an atmosphere of argon for 1.5 h. The reaction mixture was taken off heating and allowed to cool to room temperature prior to being cooled to $-78\text{ }^\circ\text{C}$ using a dry ice/acetone bath. The reflux condenser was quickly switched with a Suba-Seal[®] and then DMPU, followed by trimethylsilyl chloride were added to the mixture. Following this, a solution of ketone **72** in THF was added to the mixture *via* a syringe pump over 1 h. Once the addition was complete, the reaction mixture was stirred at $-78\text{ }^\circ\text{C}$ for a further 16 h. The reaction mixture was quenched by addition of a saturated aqueous solution of NaHCO_3 and then extracted with Et_2O . The collected organic phases were combined, dried over Na_2SO_4 , and evaporated *in vacuo* to give a colourless residue. The residue was absorbed onto silica and applied to a silica column eluting with 5% Et_2O /petroleum ether. The appropriate fractions were combined and reduced *in vacuo* to give the TMS enol ether **121** as a colourless oil.

Following the above **General Procedure**, data are presented as a) volume and mmol of 1.0 M Mg^nBu_2 in heptane, b) volume of THF, c) volume and mmol of amine **41**, d) volume and mmol of DMPU, e) amount and mmol of TESCl, f) volume and mmol of ketone **72**, g) volume of THF, h) time, i) amount, mmol and yield of triethyl(((3aS,7aS)-3a,4,7,7a-tetrahydro-1H-inden-2-yl)oxy)silane **121**, and j) enantiomeric ratio.

Table 13, Entry 1

a) 1.00 mL, 1.00 mmol, b), 10 mL, c) 0.42 mmol, 2.00 mmol, d) 0.12 mL, 1.0 mmol, e) 0.13 mL, 0.10 mmol, f) 0.1 mL, 0.8 mmol, g) 2 mL, h) 1 h, i) 0 mg, 0 mmol, 0 % yield, and j) N/A.

Table 13, Entry 2

a) 5.00 mL, 5.00 mmol, b), 50 mL, c) 2.10 mL, 10.00 mmol, d) 0.60 mL, 5.0 mmol, e) 0.65 mL, 5.05 mmol, f) 0.5 mL, 4.20 mmol, g) 10 mL, h) 5 h, i) 717 mg, 3.44mmol, 86 % yield, and j) 95:5.

Table 13, Entry 3

a) 5.00 mL, 5.00 mmol, b), 50 mL, c) 2.10 mL, 10.00 mmol, d) 0.60 mL, 5.0 mmol, e) 0.65 mL, 5.05 mmol, f) 0.5 mL, 4.20 mmol, g) 10 mL, h) 5 h, i) 750 mg, 3.60mmol, 90 % yield, and j) 94:6.

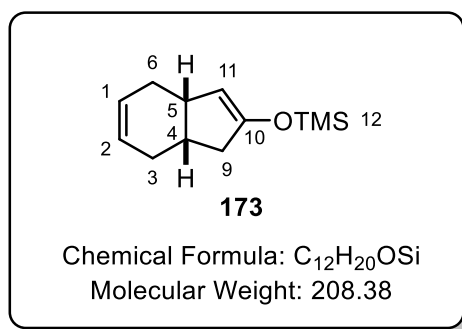
IR (neat, cm^{-1}): 3032, 2956, 2924, 2837, 1643 cm^{-1} .

^1H NMR (600 MHz, Chloroform-*d*): δ 5.76 – 5.56 (m, 2H, H-1 and H-2), 4.36 (s, 1H, H-11), 2.62 – 2.46 (m, 1H, H-5), 2.36 – 2.14 (m, 2H, ring protons), 2.05 – 1.91 (m, 2H, ring protons), 1.79 – 1.74 (m, 1H, ring proton), 1.68 (d, $J = 16.5$ Hz, 1H, ring proton), 1.59 (d, $J = 16.8$ Hz, 1H, ring proton), -0.00 (s, 9H, H-12).

^{13}C NMR (151 MHz, Chloroform-*d*): δ 154.1, 128.7, 128.0, 108.1, 41.2, 39.4, 33.2, 29.0, 28.8, 0.0.

Chiral HPLC: Chiracel OJ column, 100 % Hexane, 210 nm, 0.45 ml/min, $\text{RT}_1 = 13.78$ min and $\text{RT}_2 = 14.50$ min. $\text{RT}_1 = 95$ % $\text{RT}_2 = 5$ %.

Preparation of trimethyl((3a,4,7,7a-tetrahydro-1H-inden-2-yl)oxy)silane.⁶⁵



The reaction was carried out as documented in the literature procedure.⁶⁵

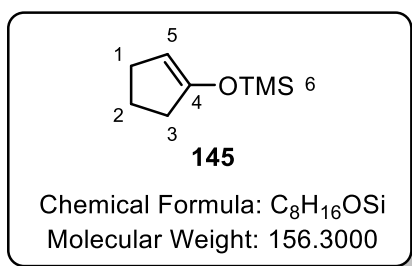
A flask was charged with NaI (0.75 g, 5.0 mmol), then flamed-dried under vacuum, and allowed to cool under argon. The NaI was dissolved in MeCN (8 mL) and the resulting solution was cooled in an ice-bath with stirring. To the clear solution, trimethylsilyl chloride (0.71 mL, 5.6 mmol) was added dropwise, after which, ketone **72** (0.5 mL, 4.2 mmol) was added dropwise, forming a white precipitate. To the reaction mixture was added Et₃N (0.5 mL, 4.9 mmol) dropwise, which produced a brownish mixture. The resulting mixture was allowed to warm to room temperature and was stirred for a further 6 h. The reaction mixture then had *n*-hexane (8 mL) added. The resulting phases were separated, and the *n*-hexane collected. The MeCN was further extracted with *n*-hexane (2 x 40 mL). The collected *n*-hexane extracts were combined, and concentrated *in vacuo* to give the TMS enol ether **173** as clear oil (569 mg, 2.73 mmol, 65 %).

IR (neat, cm⁻¹): 3032, 2956, 2924, 2837, 1643.

¹H NMR (600 MHz, Chloroform-*d*): δ 5.76 – 5.56 (m, 2H, H-1 and H-2), 4.36 (s, 1H, H-11), 2.62 – 2.46 (m, 1H, H-5), 2.36 – 2.14 (m, 2H, ring protons), 2.05 – 1.91 (m, 2H, ring protons), 1.79 – 1.74 (m, 1H, ring proton), 1.68 (d, *J* = 16.5 Hz, 1H, ring proton), 1.59 (d, *J* = 16.8 Hz, 1H, ring proton), -0.00 (s, 9H, H-12).

¹³C NMR (151 MHz, Chloroform-*d*): δ 154.1, 128.7, 128.0, 108.1, 41.2, 39.4, 33.2, 29.0, 28.8, 0.0.

Preparation of (cyclopent-1-en-1-yloxy)trimethylsilane.^{65,67}



Scheme 81

The reaction was carried out as documented in the literature procedure.⁶⁵

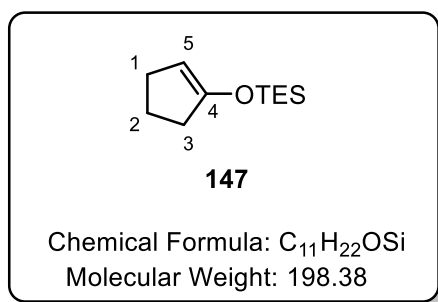
A flask was charged with NaI (4.2 g, 28.0 mmol), then flamed-dried under vacuum, and allowed to cool under argon. The NaI was dissolved in MeCN (40 mL) and the resulting solution was cooled in an ice-bath with stirring. To the clear solution, trimethylsilyl chloride (4.0 mL, 31.3 mmol) was added dropwise, followed by, ketone **146** (2.1 mL, 23.7 mmol) was added dropwise, forming a white precipitate. To the reaction mixture was then added Et₃N (2.8 g, 27.7 mmol) dropwise, which produced a brownish mixture. The resulting mixture was allowed to warm to room temperature and then stirred for a further 6 h. The reaction mixture then had *n*-hexane (40 mL) added. The resulting phases were separated, and the *n*-hexane collected. The MeCN was further extracted with *n*-hexane (2 x 40 mL). The collected *n*-hexane extracts were combined, concentrated *in vacuo* to give the TMS enol ether **145** as colourless oil (2.59 g, 16.6 mmol, 70 %).

IR (neat, cm⁻¹): 2954, 2899, 2848, 1643.

¹H NMR (400 MHz, Chloroform-*d*) δ 4.64 (m, 1H, H-5), 2.34 – 2.24 (m, 4H, H-1 and H-3), 1.88 (m, 2H, H-2), 0.26 – 0.20 (m, 9H, H-6).

¹³C NMR (101 MHz, Chloroform-*d*) δ 154.5, 101.6, 33.0, 28.2, 20.8, -0.5.

Preparation of (cyclopent-1-en-1-yloxy)triethylsilane.^{65,68}



The reaction was carried out as documented in the literature procedure.⁶⁵

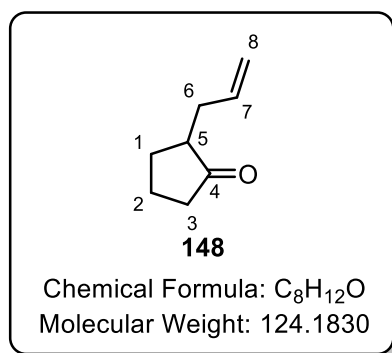
A flask was charged with NaI (4.2 g, 28.0 mmol), then flamed-dried under vacuum, and allowed to cool under argon. The NaI was dissolved in MeCN (40 mL) and the resulting solution was cooled in an ice-bath with stirring. To the clear solution, triethylsilyl chloride (5.25 mL, 31.3 mmol) was added dropwise, followed by, ketone **146** (2.1 mL, 23.7 mmol) was added dropwise, forming a white precipitate. To the reaction mixture was then added Et₃N (2.8 g, 27.7 mmol) dropwise, which produced a brownish mixture. The resulting mixture was allowed to warm to room temperature and then stirred for a further 6 h. The reaction mixture then had *n*-hexane (40 mL) added. The resulting phases were separated, and the *n*-hexane collected. The MeCN was further extracted with *n*-hexane (2 x 40 mL). The collected *n*-hexane extracts were combined, then concentrated *in vacuo* to give the TES enol ether **147** as a colourless oil (3.5 g, 17.7 mmol, 75 %).

IR (neat, cm⁻¹): 2953, 2910, 2875, 2848, 1643.

¹H NMR (400 MHz, Chloroform-*d*): δ 4.65 (s, 1H, H-5), 2.28 (t, *J* = 7.4 Hz, 4H, H-1 and H-3), 1.92 – 1.83 (m, 2H, H-2), 1.00 (t, *J* = 7.9 Hz, 9H, COSi(CH₂CH₃)₃), 0.70 (q, *J* = 7.7 Hz, 6H, COSi(CH₂CH₃)₃).

¹³C NMR (101 MHz, Chloroform-*d*): δ 154.8, 101.5, 33.0, 28.2, 20.9, 6.1, 4.3.

Preparation of 2-allylcyclopentan-1-one.^{69,70}



General Procedure:

The reaction was carried out as documented in the literature procedure.^{41,42}

An oven-dried Schlenk tube was allowed to cool under an argon atmosphere and then flame-dried under vacuum, before, once again, being allowed to cool under an argon atmosphere. This cycle was repeated three times. To the now cool Schlenk tube was then added silyl enol ether **145** or **147** and THF. The resulting clear solution was cooled to -10 °C, with stirring, before the dropwise addition of MeLi (1.4 M in Et₂O). After this, the resulting solution was allowed to stir at -10 °C for the allocated time. The resulting solution was then cooled to -78 °C before the addition of DMPU, and the reaction mixture was allowed to stir at -78 °C for a further 60 min. To the resulting mixture was added allyl bromide at -78 °C, after which the reaction mixture was allowed to gradually warm to room temperature overnight. The resulting yellow solution was quenched by addition of a saturated aqueous solution of NH₄Cl and extracted with Et₂O. The organic phases were collected, combined and dried over Na₂SO₄. The resulting solution was concentrated *in vacuo* to provide the crude mixture as a colourless liquid. The crude material was then applied to a silica column and eluted with 10 % Et₂O/petroleum ether (40-60 °C) (2CV), 20 % Et₂O/petroleum ether (40-60 °C) (2CV), and then 30 % Et₂O/petroleum ether (40-60 °C) (2CV). The appropriate fractions were combined and concentrated *in vacuo* to give the allyl cyclopentanone **148** as a colourless oil.

Following the above **General Procedure**, data are presented as a) amount and mmol of **145** or **147**, b) volume of THF, c) volume and mmol of MeLi (1.4 M in Et₂O), d) time, e) volume and mmol of DMPU, f) volume and mmol of allyl bromide, and g) amount, mmol and yield of 2-allylcyclopentan-1-one **148**.

Table 14, Entry 1

a) **145**, 96.0 mg, 0.6 mmol, b) 3 mL, c) 0.40 mL, 0.56 mmol, d) 20 min, e) 0.24 mL, 1.98 mmol, f) 69 μL, 0.80 mmol, and g) 0 mg, 0 mmol, 0 % yield.

Table 14, Entry 2

a) **145**, 96.0 mg, 0.6 mmol (freshly distilled, 49 °C @ 15 mbar), b) 3 mL, c) 0.40 mL, 0.56 mmol, d) 20 min, e) 0.24 mL, 1.98 mmol, f) 69 µL, 0.80 mmol, and g) 54 mg, 0.43 mmol, 72 % yield.

Table 15, Entry 1

a) **147**, 119.0 mg, 0.6 mmol (freshly distilled, 100 °C @ 20 mbar), b) 3 mL, c) 0.40 mL, 0.56 mmol, d) 20 min, e) 0.24 mL, 1.98 mmol, f) 69 µL, 0.80 mmol, and g) 7.50 mg, 0.06 mmol, 10 % yield.

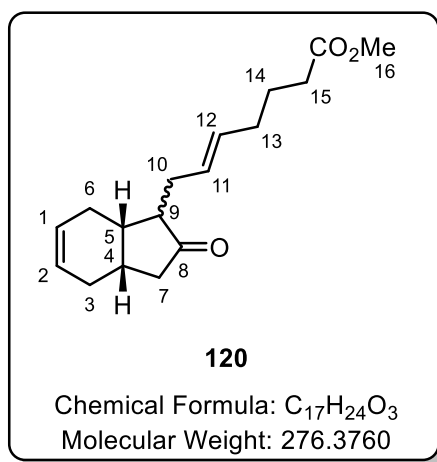
Table 15, Entry 2

a) **147**, 119.0 mg, 0.6 mmol (freshly distilled, 100 °C @ 20 mbar), b) 3 mL, c) 0.40 mL, 0.56 mmol, d) 2 h, e) 0.24 mL, 1.98 mmol, f) 69 µL, 0.80 mmol, and g) 54.4 mg, 0.44 mmol, 73 % yield.

IR ν (neat, cm^{-1}): 2960, 2873, 1735.

^1H NMR (400 MHz, Chloroform-*d*): δ 5.85 – 5.72 (m, 1H, H-7), 5.12 – 5.02 (m, 2H, H-8), 2.57 – 2.50 (m, 1H, protons), 2.39 – 2.30 (m, 1H, aliphatic protons), 2.27 – 2.06 (m, 5H, aliphatic protons), 1.88 – 1.74 (m, 1H, aliphatic protons), 1.65 – 1.59 (m, 1H, aliphatic protons).

^{13}C NMR (101 MHz, Chloroform-*d*): δ 220.1, 135.4, 115.9, 48.1, 37.7, 33.4, 28.6, 20.2.

Preparation of methyl (*E*)-7-((1*R*,3*aS*,7*aS*)-2-oxo-2,3,3*a*,4,7,7*a*-hexahydro-1*H*-inden-1-yl)hept-5-enoate.⁴²**General Procedure:**

The reaction was carried out as documented in the literature procedure.^{41,42}

An oven-dried Schlenk tube was allowed to cool under an argon atmosphere and then flame-dried under vacuum, before, once again, being cooled under an argon atmosphere. This cycle was repeated three times. To the now cool Schlenk tube was added silyl enol ether **121** and THF. The resulting clear solution was cooled to -10 °C, with stirring, before the dropwise addition of MeLi (1.4 M in Et₂O). After this, the resulting solution was allowed to stir at -10 °C for 20 min. The resulting solution was then cooled to -78 °C before the addition of DMPU, and the reaction mixture was allowed to stir at -78 °C for a further 60 min. To the resulting mixture was added allylic bromide **126** at -78 °C, after which the reaction mixture was allowed to gradually warm to room temperature overnight. The resulting yellow solution was quenched by addition of a saturated aqueous solution of NH₄Cl and extracted with Et₂O (x3). The organic extracts were collected, combined and dried over Na₂SO₄. The resulting solution was concentrated *in vacuo* to provide the crude mixture as a colourless liquid. The crude was then applied to a silica column and eluted with 10 % Et₂O/petroleum ether (40-60 °C) (2CV), 20 % Et₂O/petroleum ether (40-60 °C) (2CV), and 30 % Et₂O/petroleum ether (40-60 °C) (2CV). The appropriate fractions were combined and concentrated *in vacuo* to yield the allylated ketone **120** as a colourless oil.

Following the above **General Procedure**, data are presented as a) amount and mmol of **121**, b) volume of THF, c) volume and mmol of MeLi (1.4 M in Et₂O), d) volume and mmol of DMPU, e) amount and mmol of **126**, and h) amount, mmol and yield of methyl (*E*)-7-((1*R*,3*aS*,7*aS*)-2-oxo-2,3,3*a*,4,7,7*a*-hexahydro-1*H*-inden-1-yl)hept-5-enoate **120**.

Scheme 80

a) 100 mg, 0.48 mmol, b) 3 mL, c) 0.33 mL, 0.45 mmol, d) 0.44 mL, 1.92 mmol e) 20 min, f) 0.23 mL, 1.92 mmol g) 159 mg, 0.72 mmol, h) 0 mg, 0 mmol, 0 % yield.

Scheme 84

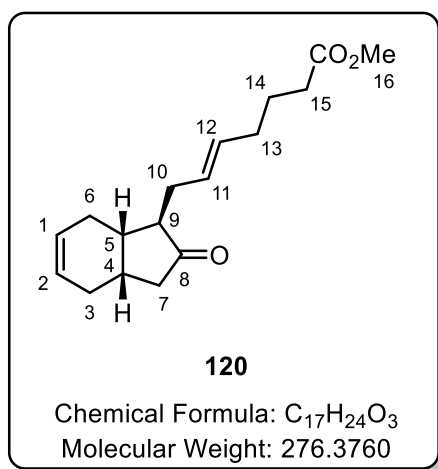
a) 300 mg, 1.26 mmol, b) 9 mL, c) 0.99 mL, 1.35 mmol, d) 1.32 mL, 5.04 mmol e) 20 min, f) 0.69 mL, 5.76 mmol, g) 475 mg, 2.16 mmol, and h) 290 mg, 1.05 mmol, 83 % yield.

IR ν (neat, cm⁻¹): 3020, 2958, 2902, 2835, 1734.

¹H NMR (400 MHz, Chloroform-*d*): δ 5.78 – 5.60 (m, 2H, H-1 and H-2) 5.52 – 5.25 (m, 2H, H-11 and H-12), 3.66 (s, 3H, H-16), 2.54 – 1.85 (m, 14H, aliphatic protons), 1.77 – 1.57 (m, 3H, aliphatic protons).

¹³C NMR (101 MHz, Chloroform-*d*) δ 220.5, 219.2, 174.1, 132.0, 131.8, 130.6, 129.0, 127.9, 125.1, 124.7, 124.5, 57.8, 57.1, 53.3, 51.5, 50.9, 49.7, 46.3, 41.1, 37.1, 36.1, 33.9, 33.4, 31.9, 31.9, 31.1, 29.8, 27.6, 27.2, 26.2, 25.4, 24.7, 22.9, 22.2.

Preparation of methyl (*E*)-7-((1*R*,3*aS*,7*aS*)-2-oxo-2,3,3*a*,4,7,7*a*-hexahydro-1*H*-inden-1-yl)hept-5-enoate.⁴²



Scheme 85

The reaction was carried out as documented in the literature procedure.^{41,42}

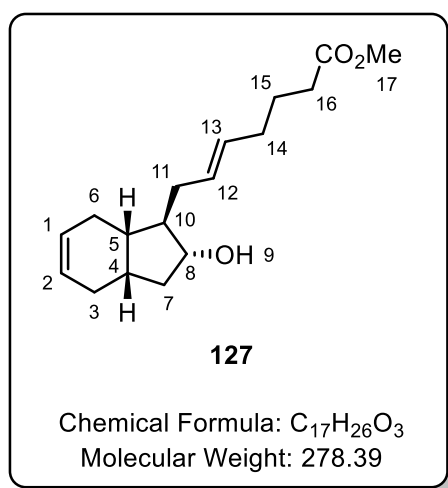
An oven-dried Schlenk tube was allowed to cool under an argon atmosphere and then flame-dried under vacuum, before, once again, being cooled under an argon atmosphere. This cycle was repeated three times. To the now cool Schlenk tube was added silyl enol ether **121** and THF. The resulting clear solution was cooled to -10 °C, with stirring, before the dropwise addition of MeLi (1.4 M in Et₂O). After this, the resulting solution was allowed to stir at -10 °C for 20 min. The resulting solution was then cooled to -78 °C, before the addition of DMPU, and the reaction mixture was then allowed to stir at -78 °C for a further 60 min. To the resulting mixture was added allylic bromide **126** at -78 °C, after which the reaction mixture was allowed to stir at -78 °C overnight. The resulting yellow solution was quenched by the addition of a saturated aqueous solution of NH₄Cl and extracted with Et₂O (x3). The organic extracts were collected, combined and dried over Na₂SO₄. The resulting solution was concentrated *in vacuo* to provide the crude mixture as a colourless liquid. The crude was then applied to a silica column which was subsequently eluted with 10 % Et₂O/petroleum ether (40-60 °C) (2CV), 20 % Et₂O/petroleum ether (40-60 °C) (2CV), and 30 % Et₂O/petroleum ether (40-60 °C) (2CV). The appropriate fractions were combined and concentrated *in vacuo* to yield the allylated ketone **120** as a colourless oil.

IR ν (neat, cm⁻¹): 3020, 2958, 2902, 2835, 1734.

¹H NMR (400 MHz, Chloroform-*d*) δ 5.73 – 5.64 (m, 2H, H-1 and H-2), 5.49 – 5.32 (m, 2H, H-11 and H-12), 3.67 (s, 3H, H-16), 2.40 – 2.00 (m, 14H, aliphatic protons), 1.74 – 1.63 (m, 3H, aliphatic protons).

^{13}C NMR (101 MHz, Chloroform-*d*) δ 220.0, 173.6, 131.3, 127.3, 124.6, 124.0, 51.0, 50.3, 45.8, 36.5, 32.8, 31.3, 30.5, 29.2, 26.6, 24.9, 24.1.

Preparation of methyl (E)-7-((1*R*,2*R*,3*aS*,7*aS*)-2-hydroxy-2,3,3*a*,4,7,7*a*-hexahydro-1*H*-inden-1-yl)hept-5-enoate.⁴²



Scheme 86

The reaction was carried out as documented in the literature procedure.⁴⁴

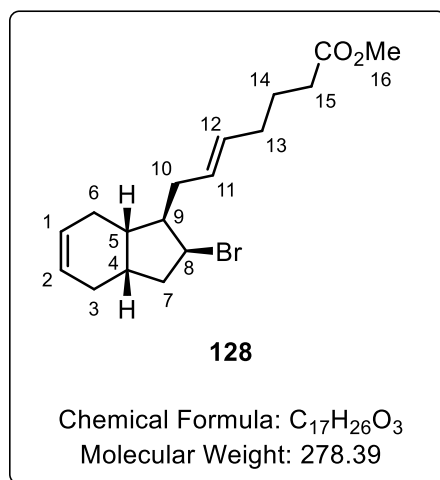
A flame-dried flask was charged with NaBH_4 (91 mg, 2.4 mmol), which was suspended in EtOH (6 mL) and cooled to 0 °C under argon with stirring. To the resulting suspension was added, dropwise, a solution of **120** (250 mg, 0.9 mmol) in EtOH (6 mL), and the resulting reaction mixture was allowed to warm to room temperature over 1 h. The reaction mixture was once again cooled to 0 °C and quenched by the addition of water until no further effervescence was observed. The resulting mixture was extracted with DCM (x3). The collected organic extracts were combined, dried over Na_2SO_4 , filtered and the filtrate was concentrated *in vacuo* to yield the secondary alcohol **127** as a colourless oil (214 mg, 0.77 mmol, 85 %, as a single diastereomer).

IR (neat, cm^{-1}): 3419, 3018, 2904, 2837, 1735.

^1H NMR (400 MHz, Chloroform-*d*): δ 5.82 – 5.63 (m, 2H, H-1 and H-2), 5.58 – 5.40 (m, 2H, H-12 and H-13), 3.99 – 3.90 (m, 1H, H-8), 3.73 – 3.63 (m, 3H, H-17), 2.42 – 1.88 (m, 13H, aliphatic protons), 1.81 – 1.44 (m, 5H, aliphatic protons and H-9).

^{13}C NMR (101 MHz, Chloroform-*d*) δ 173.7, 130.3, 129.6, 126.1, 125.4, 77.5, 51.9, 51.0, 40.6, 40.0, 35.3, 32.9, 32.8, 31.4, 27.5, 25.8, 24.1.

Preparation of methyl (E)-7-((1R,2S,3aS,7aS)-2-bromo-2,3,3a,4,7,7a-hexahydro-1H-inden-1-yl)hept-5-enoate.⁴²



Scheme 86

The reaction was carried out as documented in the literature procedure.⁴⁴

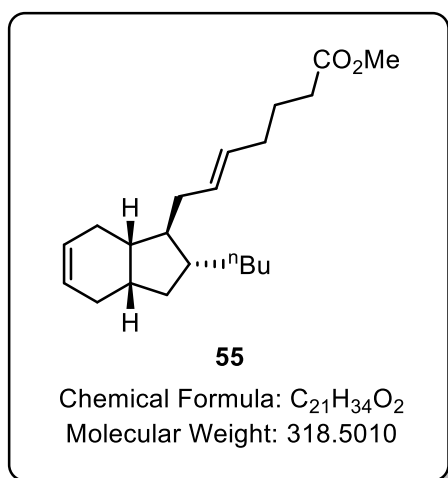
To a stirred solution of alcohol **127** (65 mg, 0.24 mmol) in DCM (3 mL) was added CBr₄ (118 mg, 0.36 mmol) and the solution was allowed to cool to 0 °C. Subsequently, a solution of triphenylphosphine (94 mg, 0.36 mmol) in DCM (4 mL) was added dropwise and the reaction solution was then allowed to warm to room temperature. After 16 h, Et₂O was added, resulting in the formation of a white precipitate. The precipitate was filtered, and the filtrate concentrated *in vacuo* to give a brown oil. The crude was applied to a silica column and eluted with 10 % Et₂O/Petroleum ether (3 CV). The appropriate fractions were combined and had the solvent was removed *in vacuo* to give the secondary bromide **128** (52 mg, 0.15 mmol, 63 % yield) as a colourless oil.

IR ν (neat, cm⁻¹): 3032, 2966, 2870, 1724.

¹H NMR (400 MHz, Chloroform-*d*) δ 6.00 – 5.88 (m, 2H, H-1 and H-2), 5.61 – 5.34 (m, 2H, H-11 and H-12), 4.53 (t, *J* = 4.2 Hz, 1H, H-8), 3.69 (s, 3H, H-16), 2.74 – 2.59 (m, 1H, Aliphatic protons), 2.43 – 2.28 (m, 4H, Aliphatic protons), 2.26 – 1.98 (m, 7H, Aliphatic protons), 1.95 – 1.65 (m, 4H, Aliphatic protons), 1.56 – 1.43 (m, 1H, Aliphatic protons).

¹³C NMR (101 MHz, Chloroform-*d*) δ 174.2, 130.9, 129.4, 129.2, 62.1, 52.3, 51.6, 44.3, 40.1, 35.3, 35.1, 33.5, 32.0, 27.8, 25.9, 24.7. Resonances for the two carbons of the ring olefin overlap, hence 16 resonances are observed and not 17 resonances.

Attempted Synthesis of methyl (*E*)-7-((1*S*,2*R*,3*aS*,7*aS*)-2-butyl-2,3,3*a*,4,7,7*a*-hexahydro-1*H*-inden-1-yl)hept-5-enoate.



General Procedure

CuCN was placed in a flame-dried two-necked flask and THF (1mL) was added. The resulting slurry was cooled to -78 °C and *n*butyllithium (2.5 M in hexanes) was added dropwise. The heterogeneous mixture was allowed to warm to 0 °C at which temperature it was stirred for a further 1-2 min and then recooled to -78 °C. To the now turbid mixture was added the alkyl bromide **128** (90 mg, 0.32 mmol) as a solution in THF (1 mL), and the reaction mixture stirred at the appropriate temperature. The reaction mixture was quenched by the addition of 10 % concentrated NH₄OH /saturated NH₄Cl solution and extracted with Et₂O (3x). The combined organic extracts were then dried over Na₂SO₄, filtered and concentrated *in vacuo* to give a brown oil. The crude material was then analysed by ¹H NMR spectroscopy.

Following the above **General Procedure**, data are presented as (a) amount and mmol of CuCN, (b) *n*butyllithium, (c) temperature and, (d) ¹H NMR analysis.

Scheme 87

(a) 57 mg, 0.64 mmol (b) 0.50 mL, 1.24 mmol, (c) -78 °C and, (d) Only starting material observed.

Scheme 88

(a) 57 mg, 0.64 mmol (b) 0.50 mL, 1.24 mmol, (c) 0 °C and, (d) No starting material was observed and none of the desired product was observed.

Scheme 89

(a) 57 mg, 0.64 mmol (b) 0.25 mL, 0.64 mmol, (c) 0 °C and, (d) No starting material was observed and none of the desired product was observed.

1.4.4. sp^2 - sp^3 cross-coupling

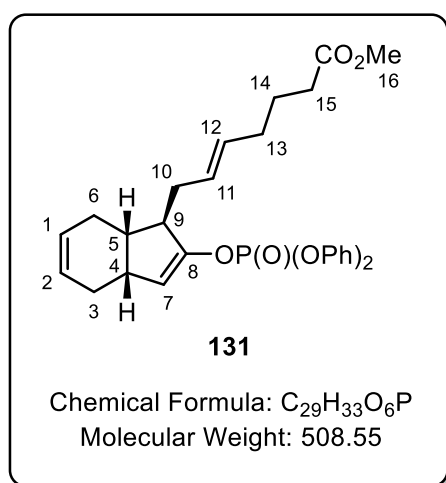
Synthesis of di-*tert*-butylmagnesium.²⁹

To a flame-dried flask equipped with a stirrer bar, was added a solution of *t*BuMgBr (1.0 M in THF) and the reaction vessel was cooled in an ice-bath under an atmosphere of argon. Freshly distilled 1,4-dioxane was then added dropwise to the solution, resulting in the formation of a white precipitate, and the reaction mixture was allowed to stir for 3 h. The reaction mixture was then filtered under an inert atmosphere to give a pale brown solution of *t*Bu₂Mg (~0.3 M in THF when titrated with I₂ in a saturated THF/LiCl solution).⁵⁷

Synthesis of dimesitylmagnesium.²⁶

To a flame-dried flask equipped with a stirrer bar, was added a solution of MesMgBr (1.0 M in THF) and the reaction vessel was cooled in an ice-bath under an atmosphere of argon. Freshly distilled 1,4-dioxane was then added dropwise to the solution, resulting in the formation of a white precipitate, and the reaction mixture was allowed to stir for 3 h. The reaction mixture was then filtered under an inert atmosphere to give a pale brown solution of Mes₂Mg (~0.3 M in THF when titrated with I₂ in a saturated THF/LiCl solution).⁵⁷

Preparation of methyl (*E*)-7-((1*R*,3*aR*,7*aS*)-2-((diphenoxyphosphoryl)oxy)-3*a*,4,7,7*a*-tetrahydro-1*H*-inden-1-yl)hept-5-enoate.



General Procedure A:

The reaction was carried out as documented in the literature procedure.³⁰

To a flame-dried schlenk flask was added ketone **120** as a solution in THF. DMPU and diphenylphosphoryl chloride were then added and the reaction mixture was allowed to stir for 5 min at the allotted temperature, before the dropwise addition of Mes₂Mg in THF. The resulting reaction mixture was then allowed to stir for a further 16 h, after which time the reaction mixture was quenched by the addition of a saturated aqueous NaHCO₃ solution. The resulting mixture was extracted with Et₂O (x3) and the collected organic extracts were combined, dried over Na₂SO₄ and filtered to give a colourless solution. The resulting solution was concentrated *in vacuo* to give a colourless residue, which was applied to a silica column and eluted with 30 % Et₂O/ Petroleum ether. The appropriate fractions were combined, and the solvent was removed *in vacuo*.

Following **General Procedure A**, data are presented as (a) amount and mmol of ketone **120**, (b) volume of THF, (c) volume and mmol of DMPU, (d) volume and mmol of diphenylphosphoryl chloride, (e) temperature, (f) volume and mmol of ^tBu₂Mg in THF, (g) amount and mmol of enol phosphate **131** isolated, and (h) amount and mmol of starting material **120** recovered.

Table 16, Entry 1

(a) 110 mg, 0.42 mmol, (b) 4 mL, (c) 0.19 mL, 1.60 mmol, (d) 0.11 mL, 0.50 mmol, (e) 0 °C, (f) 0.54 mL, 0.46 M, 0.25 mmol, (g) n/a, and (h) 101 mg, 0.37 mmol, 93 % recovered starting material.

Table 16, Entry 2

(a) 110 mg, 0.42 mmol, (b) 4 mL, (c) 0.19 mL, 1.60 mmol, (d) 0.03 mL, 0.18 mmol, (e) 30 °C, (f) 0.54 mL, 0.46 M, 0.25 mmol, (g) n/a, and (h) 34 mg, 0.12 mmol, 82 % recovered starting material.

Table 16, Entry 3

(a) 40 mg, 0.15 mmol, (b) 2 mL, (c) 0.07 mL, 0.60 mmol, (d) 0.03 mL, 0.18 mmol, (e) 40 °C, (f) 0.28 mL, 0.46 M, 0.075 mmol, (g) n/a, and (h) 35 mg, 0.13 mmol, 87 % recovered starting material.

General Procedure B:

A flame-dried schlenk flask charged with a solution of di-*iso*-propylamine in THF at -78 °C, was added ⁿBuLi (2.2 M in hexanes) was added to the reaction mixture and allowed to stir for 5 min. A solution of ketone **41** in THF was added dropwise at -78 °C, followed by addition of diphenylphosphoryl chloride. The reaction mixture was then allowed to stir for 5 min at 78 °C, before being warmed to room

temperature. The resulting reaction mixture was stirred for a further 1 hr, after which the reaction was quenched by the addition of a saturated aqueous NaHCO₃ solution. The resulting mixture was extracted with Et₂O (x3) and the collected organic extracts were combined, dried over Na₂SO₄ and filtered to give a colourless solution. The resulting solution was concentrated *in vacuo* to give a clear residue which was applied to a silica column and eluted with 30 % Et₂O/Petroleum ether. The appropriate fractions were combined, and the solvent was removed *in vacuo*.

Following **General Procedure B**, data are presented as (a) volume and mmol of diisopropylamine, (b) volume of THF, (c) volume and mmol of ⁿBuLi, (d) amount and mmol of ketone, (e) volume of THF, (f) volume and mmol of diphenylphosphoryl chloride, and (g) amount and mmol of starting material **120** recovered.

Table 17, Entry 1

(a) 0.015 mL, 0.11 mmol, (b) 0.5 mL, (c) 0.05 mL, 0.11 mmol, (d) 30 mg, 0.11 mmol, (e) 0.5 mL, (f) 0.03 mL, 0.12 mmol, and (g) 25 mg, 0.09 mmol, 82 % recovered starting material

Table 17, Entry 2

(a) 0.04 mL, 0.29 mmol, (b) 3 mL, (c) 0.13 mL, 0.29 mmol, (d) 80 mg, 0.29 mmol, (e) 3 mL, (f) 0.08 mL, 0.35 mmol, and (g) 72 mg, 0.26 mmol, 90 % recovered starting material.

General Procedure C:

The reaction was carried out as documented in the literature procedure.³⁰

To a flame-dried schlenk flask was added ketone **120** as a solution in THF, followed by DMPU and diphenylphosphoryl chloride. The mixture was allowed to stir for 5 min at the allotted temperature before the dropwise addition of a solution of Mes₂Mg in THF. The resulting reaction mixture was then allowed to stir for a further 1 h, after which time the reaction mixture was quenched by the addition of a saturated aqueous NaHCO₃ solution. The resulting mixture was extracted with Et₂O (x3), and the organic extracts were combined, dried over Na₂SO₄ and filtered to give a colourless solution. The resulting solution was concentrated *in vacuo* to give a colourless residue, which was applied to a silica column and eluted with 30 % Et₂O/Petroleum ether. The appropriate fractions were combined, and the solvent was removed *in vacuo* to give the enol phosphate **131** as a colourless oil.

Following **General Procedure C**, data are presented as (a) amount and mmol of ketone **120**, (b) volume of THF, (c) volume and mmol of DMPU, (d) volume and mmol of diphenylphosphoryl chloride, (e)

temperature, (f) volume and mmol of Me_2Mg in THF, (g) amount, mmol and yield of enol phosphate **131** isolated, and (h) amount, mmol and yield of side product **149** isolated.

Table 18, Entry 1

(a) 50 mg, 0.18 mmol, (b) 2 mL, (c) 0.09 mL, 0.72 mmol, (d) 0.06 mL, 0.27 mmol, (e) rt., (f) 0.67 mL, 0.21 M, 0.14 mmol, (g) 40 mg, 0.08 mmol, 44 % yield, and (h) n/a.

Table 18, Entry 2

(a) 300 mg, 1.08 mmol, (b) 12 mL, (c) 0.54 mL, 4.32 mmol, (d) 0.36 mL, 1.27 mmol, (e) rt., (f) 4.02 mL, 0.21 M, 0.84 mmol, (g) 302 mg, 0.59 mmol, 55 % yield, and (h) 152 mg, 0.15 mmol, 29 %.

Scheme 94

(a) 190 mg, 0.69 mmol, (b) 7 mL, (c) 0.33 mL, 2.76 mmol, (d) 0.14 mL, 0.69 mmol, (e) 0 °C, (f) 1.67 mL, 0.21 M, 0.35 mmol, (g) 253 mg, 0.50 mmol, 72 % yield, and (h) n/a.

IR ν (neat, cm^{-1}): 1589, 1660, 1734, 2841, 2916, 3032.

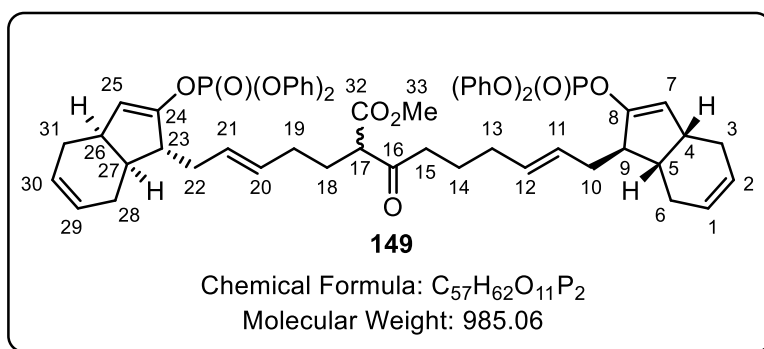
^1H NMR (400 MHz, Chloroform-*d*): δ 7.37 (t, $J = 7.9$ Hz, 4H, ArH), 7.28 – 7.17 (m, 6H, ArH), 5.95 – 5.81 (m, 2H, H-1 and H-2), 5.44 – 5.30 (m, 3H, H-7, H-11 and H-12), 3.68 (s, 3H, H-16), 2.87 – 2.78 (m, 1H, aliphatic ring protons), 2.30 (t, $J = 7.6$ Hz, 2H, H-15), 2.26 – 2.23 (m, 1H, aliphatic protons), 2.22 – 2.09 (m, 3H, aliphatic protons), 2.08 – 1.99 (m, 3H, aliphatic protons), 1.95 – 1.86 (m, 1H, aliphatic protons), 1.85 – 1.77 (m, 1H, aliphatic protons), 1.69 (p, $J = 7.2$ Hz, 2H, H-14).

^{13}C NMR (101 MHz, Chloroform-*d*) δ 173.6, 150.5 (d, $^2J_{\text{CP}} = 10.4$ Hz), 150.0 (d, $^3J_{\text{CP}} = 7.2$ Hz), 130.9, 129.3, 128.4, 127.7 (d, $^3J_{\text{CP}} = 7.5$ Hz), 125.0, 119.6 (apt, $^3J_{\text{CP}} = 4.3$ Hz), 114.3, 114.3, 51.0, 50.2 (d, $^3J_{\text{CP}} = 6.0$ Hz), 38.2, 37.8, 34.3, 32.8, 31.4, 28.0, 27.4, 24.1.

^{31}P NMR (162 MHz, Chloroform-*d*) δ -17.6.

HRMS (ESI) m/z calculated for $\text{C}_{29}\text{H}_{34}\text{O}_6\text{P}$ $[\text{M}+\text{H}]^+$: 509.2093. Found: 509.2094.

Preparation of methyl (*E*)-9-((1*R*,3*aR*,7*aS*)-2-((diphenoxyphosphoryl)oxy)-3*a*,4,7,7*a*-tetrahydro-1*H*-inden-1-yl)-2-((*E*)-5-((1*S*,3*aS*,7*aR*)-2-((diphenoxyphosphoryl)oxy)-3*a*,4,7,7*a*-tetrahydro-1*H*-inden-1-yl)pent-3-en-1-yl)-3-oxonon-7-enoate.



Isolated as a side product from the above deprotonation reaction (Table 18, Entry 2)

IR ν (neat, cm⁻¹): 1658, 1712, 1741, 2879, 2922, 3032.

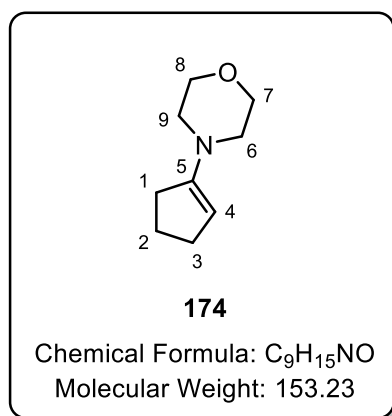
¹H NMR (400 MHz, Chloroform-*d*) δ 7.37 (t, *J* = 8.6 Hz, 8H, ArH), 7.28 – 7.16 (m, 12H, ArH), 5.93 – 5.80 (m, 4H, H-1, H-2, H-29 and H-30), 5.37 (m, 6H, H-7, H-11, H-12, H-20, H-21, H-25), 3.71 (s, 3H, H-33), 3.46 (t, *J* = 7.0 Hz, 1H, H-17), 2.86 – 2.78 (m, 2H, aliphatic protons), 2.58 – 2.39 (m, 4H, aliphatic protons), 2.30 – 2.12 (m, 8H, aliphatic protons), 2.08 – 1.76 (m, 12H, aliphatic protons), 1.63 (p, *J* = 7.3 Hz, 2H, aliphatic protons).

¹³C NMR (101 MHz, Chloroform-*d*) δ 204.5, 169.7, 150.5 (d, ²*J*_{CP} = 7.1 Hz), 150.4 (d, ²*J*_{CP} = 7.6 Hz), 150.0 (d, ³*J*_{CP} = 7.0 Hz), 131.1, 130.3, 129.3, 128.4, 128.3, 127.7, 127.5, 125.0, 119.6 (apt, ³*J*_{CP} = 3.7 Hz), 114.5 (d, ³*J*_{CP} = 3.4 Hz), 114.3 (d, ³*J*_{CP} = 3.4 Hz), 57.6, 51.8, 50.2 (apt, ³*J*_{CP} = 6.2 Hz), 40.8, 38.2, 37.8, 34.2, 31.3, 29.8, 28.0, 27.4, 22.7.

³¹P NMR (162 MHz, Chloroform-*d*) δ -17.6.

HRMS (ESI) *m/z* calculated for C₅₇H₆₃O₁₁P₂ [M+H]⁺: 985.3846. Found: 985.3854.

Synthesis of 4-(cyclopent-1-en-1-yl)morpholine.⁷¹



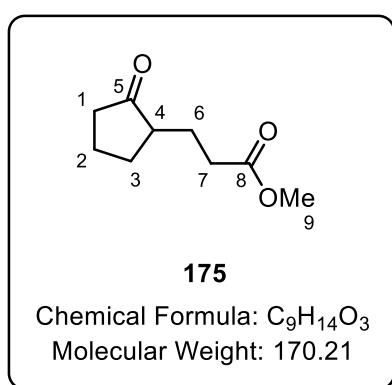
The reaction was carried out as documented in the literature procedure.⁷¹

To a reaction vessel fitted with a Dean-Stark apparatus was added cyclopentanone (5.0 g, 59.4 mmol), morpholine (6.1 g, 70.0 mmol) and toluene (30 mL). The reaction mixture was heated to reflux for 3.5 h under an atmosphere of argon. The resulting mixture had the solvent removed *in vacuo* to give a brown residue which was then subjected to distillation under vacuum (110 °C/ 20 mbar) to give the enamine **174** (5.95 g, 38.8 mmol, 65 % yield) as a colourless oil.

¹H NMR (400 MHz, Chloroform-*d*) δ 4.47 (s, 1H, H-4), 3.77 – 3.72 (m, 4H, H-7 and H-8), 2.92 – 2.87 (m, 4H, H-6 and H-9), 2.41 – 2.31 (m, 4H, H-1 and H-3), 1.95 – 1.85 (m, 2H, H-2).

¹³C NMR (101 MHz, Chloroform-*d*) δ 151.3, 97.9, 66.2, 48.6, 30.8, 29.8, 22.0.

Synthesis of methyl 3-(2-oxocyclopentyl)propanoate.⁷¹



The reaction was carried out as documented in the literature procedure.⁷¹

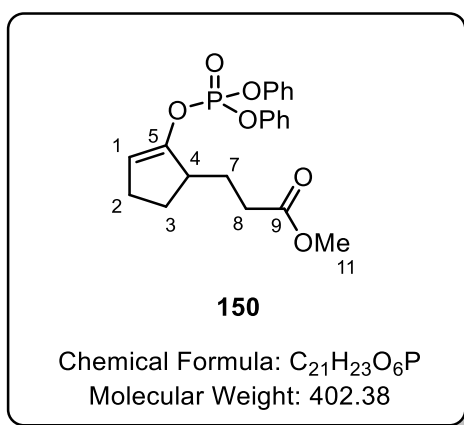
To a flame dried three-necked flask was added **174** (1.0 g, 6.5 mmol), distilled 1,4-dioxane (2 mL) and methyl acrylate (1.2 mL, 13 mmol). The resulting solution was heated to reflux under an atmosphere of argon and stir for 3.5 h. After which water (1 mL) was added and the reaction mixture was allowed to stir at reflux for a further 1 h. The resulting reaction mixture was allowed to cool after which the solvent was removed *in vacuo* to give a colourless residue. The residue was applied to a silica column and eluted with (20 % Et₂O/ Petroleum ether) (4 CV) and (30 % Et₂O/ Petroleum ether) (4 CV). The appropriate fractions were combined and had the solvent removed *in vacuo* to give the keto ester **175** (705 mg, 4.1 mmol, 63 % yield) as a colourless oil.

¹H NMR (400 MHz, Chloroform-*d*) δ 3.72 – 3.66 (m, 3H, H-9), 2.51 – 2.41 (m, 2H), 2.38 – 2.19 (m, 2H), 2.19 – 1.98 (m, 4H), 1.88 – 1.72 (m, 1H), 1.70 – 1.48 (m, 2H).

¹³C NMR (101 MHz, Chloroform-*d*) δ 219.9, 173.2, 51.1, 47.7, 37.5, 31.4, 29.0, 24.4, 20.1.

HRMS (ESI) *m/z* calculated for C₉H₁₄O₃ [M+H]⁺: 171.1016. Found: 171.1013.

Synthesis of methyl 3-(2-((diphenoxyphosphoryl)oxy)cyclopent-2-en-1-yl)propanoate.



The reaction was carried out as documented in the literature procedure.³⁰

To a flame-dried Schlenk tube was added ^tBu₂Mg (0.33 M, 1.51 mL, 0.5 mmol), THF (10 mL), diphenyl phosphoryl chloride (0.21 mL, 1.01 mmol) and DMPU (0.24 mL, 2 mmol) under an atmosphere of argon, and the mixture was stirred at 0 °C for 5 min. Subsequently, ketone **175** (170 mg, 1 mmol) was added as a solution in THF (1 mL) over 1 h *via* syringe pump. The resulting reaction mixture was allowed to warm to room temperature over 16 h, after which the reaction mixture was quenched by addition of a saturated solution of NaHCO₃ and extracted with Et₂O (3x). The collected organic extracts were combined, dried over Na₂SO₄, filtered and the solvent was concentrated *in vacuo* to give the

crude product as a colourless oil. The crude material was further purified *via* column chromatography eluting with 20 % Et₂O/Petroleum ether (4 CV) and 30 % Et₂O/Petroleum ether (4 CV). The appropriate fractions were combined, and the solvent was concentrated *in vacuo* to give the enol phosphate **150** (204 mg, 0.51 mmol, 51 % yield) as a colourless oil.

IR ν (neat, cm⁻¹): 1589, 1654, 1733, 2859, 2949.

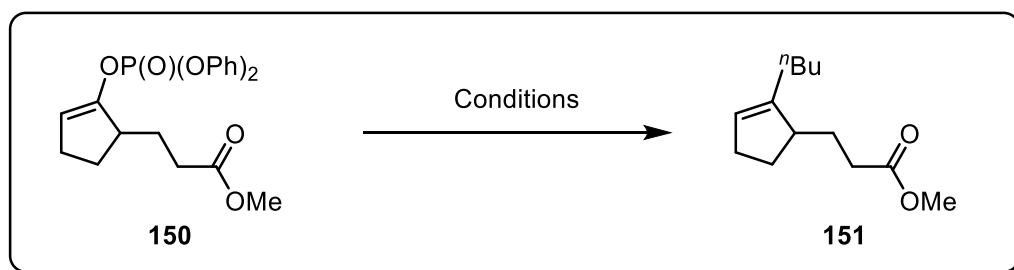
¹H NMR (400 MHz, Chloroform-*d*) δ 7.42 – 7.33 (m, 4H, ArH), 7.28 – 7.20 (m, 6H, ArH), 5.53 – 5.45 (m, 1H, H-1), 3.67 (s, 3H, H-11), 2.80 – 2.69 (m, 1H, aliphatic protons), 2.39 – 2.22 (m, 4H, aliphatic protons), 2.20 – 2.07 (m, 1H, aliphatic protons), 2.02 – 1.87 (m, 1H, aliphatic protons), 1.67 – 1.50 (m, 2H, aliphatic protons).

¹³C NMR (101 MHz, Chloroform-*d*) : δ 173.3, 150.9 (d, ²J_{CP} = 10.4 Hz), 150.0 (d, ²J_{CP} = 7.3 Hz), 129.3, 125.0, 119.6 (d, ³J_{CP} = 4.8 Hz), 110.0 (d, ⁴J_{CP} = 4.3 Hz), 51.0, 42.2 (d, ⁴J_{CP} = 6.2 Hz), 30.9, 27.4, 26.7, 26.4.

³¹P NMR (162 MHz, Chloroform-*d*) δ -17.6.

HRMS (ESI) *m/z* calculated for C₂₁H₂₄O₆P [M+H]⁺ : 403.1310. Found: 403.1312,

Screening cross-coupling conditions for methyl 3-(2-butylcyclopent-2-en-1-yl)propanoate.



General Procedure A:

The reaction was carried out as documented in the literature procedure.³³

To a solution of enol phosphate **150** (25 mg, 0.06 mmol) in toluene (0.25 mL) and additive, was added PEPSI-SiPr (0.45 mg, 7 μ mol) and the resulting mixture was allowed to stir for 5 min at 0 °C under an atmosphere of argon. After 5 min, *n*butylmagnesium chloride was added to the reaction mixture and the resulting yellow solution was allowed to stir for 16 h at 0 °C. The reaction mixture was quenched by addition of a saturated aqueous solution of NH₄Cl and then extracted with Et₂O (3x). The organic extracts were then combined, dried over Na₂SO₄, filtered and the solvent was removed *in vacuo* to give a clear residue. The clear residue then analysed by ¹H NMR spectroscopy.

Following **General Procedure A**, data are presented as (a) amount and mmol of additive, (b) volume and mmol of *n*-butyl magnesium chloride in Et₂O, and (c) result.

Table 19, Entry 1

(a) n/a, (b) 0.1 mL, 1.9 M, 0.19 mmol (c) Cross-coupling indicated by ¹H NMR from consumption of the signal at δ 5.54 (m) and the appearance of a new peak at δ 5.37 (m). Undesired addition into ester was indicated by the consumption of the signal at 3.65 (s) and the appearance of a new peak at 0.93 (t, *J* = 7.4 Hz), indicative of the CH₃ of a butyl group.

Table 19, Entry 2

(a) n/a, (b) 0.07 mL, 1.9 M, 0.13 mmol, and (c) cross-coupling indicated by ¹H NMR from partial consumption of the signal at δ 5.54 (m) and appearance of a new peak at δ 5.37 (m). Undesired addition into ester was indicated by the consumption of the signal at 3.65 (s) and the appearance of a new peak at 0.93 (t, *J* = 7.4 Hz), indicative of the CH₃ of a butyl group.

Table 19, Entry 7

(a) NMP, 0.06 mL, 0.6 mmol, (b) 0.07 mL, 1.9 M, 0.13 mmol, and (c) Trace product indicated by appearance of a new peak at δ 5.37 (m).

General Procedure B:

To a solution of enol phosphate **150** (25 mg, 0.06 mmol) in toluene (0.25 mL), was added Pd-PEPSSI-SiPr (0.45 mg, 7 μmol) and the resulting mixture was allowed to stir for 5 min at 0 °C under an atmosphere of argon. After 5 min, *n*-butylzinc chloride was added to the reaction mixture and the resulting yellow solution was allowed to stir for 16 h at the reported temperature. The reaction was quenched by addition of a saturated aqueous solution of NH₄Cl and extracted with Et₂O (3x). The combined organic extracts were dried over Na₂SO₄, filtered and the solvent was removed *in vacuo* to give a clear residue. The clear residue then analysed by ¹H NMR spectroscopy.

Following **General Procedure B**, data are presented as (a) volume and mmol of *n*-butyl zinc chloride in Et₂O, (b) temperature, and (c) result.

Table 19, Entry 3

(a) 0.07 mL, 1.07 M, 0.075 mmol, (b) 0 °C, and (c) No change to the ¹H NMR profile of the starting enol phosphate **150** was observed.

Table 19, Entry 4

(a) 0.07 mL, 1.07 M, 0.075 mmol, (b) 70 °C, and (c) No cross-coupling observed due to no consumption at δ 5.54 (m) being observed, consumption at 3.65 (s) was observed corresponding to addition into the ester along with the appearance of 0.93 (t, J = 7.4 Hz) indicative of the CH₃ of a butyl group.

General Procedure C:

The reaction was carried out as documented in the literature procedure.⁷²

A flame-dried flask was charged with Fe(acac)₃, and a solution of enol phosphate **150** (25 mg, 0.06 mmol) in THF (0.06 mL) and NMP (0.06 mL, 0.6 mmol) was added. The mixture was subsequently cooled to -20 °C and allowed to stir for 5 mins. A solution of *n*-butyl magnesium chloride in Et₂O (0.04 mL, 1.9 M, 0.075 mmol) was added dropwise over 5 min, resulting in a dark brown solution, and the resulting reaction mixture was then allowed to stir for 2 h. The reaction mixture was quenched by addition of 2 M HCl, and allowed to warm to room temperature. The mixture was extracted with Et₂O (3x) and the collected organic extracts, were combined, dried over Na₂SO₄ and filtered to give a colourless residue. The colourless residue then analysed by ¹H NMR spectroscopy.

Following **General Procedure C**, data are presented as (a) amount and mmol of Fe(acac)₃ and (b) result.

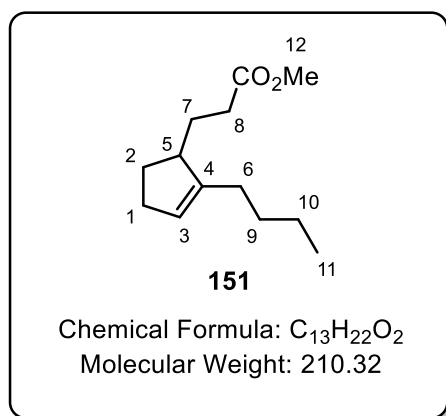
Table 19, Entry 5

(a) 0.66 mg, 1.86 μ mol, 3 mol%, and (b) Cross-coupling indicated by ¹H NMR from partial consumption of the peak at δ 5.54 ppm (m) and the appearance of a new peak at δ 5.37 ppm (m). No undesired addition into ester was indicated as no reduction of the peak at δ 3.65 ppm (s) was observed. Additionally, the appearance of δ 0.93 ppm (t, J = 7.4 Hz) indicative of the CH₃ of a butyl group was observed.

Table 19, Entry 6

(a) 1.32 mg, 3.72 μ mol, 6 mol%, and (b) Cross-coupling indicated by ¹H NMR from partial consumption of the peak at δ 5.54 (m) and the appearance of a new peak at δ 5.37 (m). No undesired addition into ester was indicated as no reduction of the peak at δ 3.65 (s) was observed. Additionally, the appearance of δ 0.93 (t, J = 7.4 Hz) indicative of the CH₃ of a butyl group was observed.

Preparation of methyl 3-(2-butylcyclopent-2-en-1-yl)propanoate.



Scheme 96

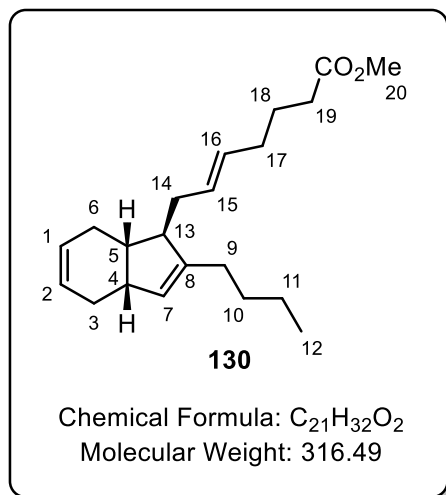
The reaction was carried out as documented in the literature procedure.⁷²

A flame-dried flask was charged with Fe(acac)₃ (10.0 mg, 28 μmol) and a solution of enol phosphate **150** (190 mg, 0.47 mmol) in THF (0.5 mL) was added. NMP (0.41 mL, 4.23 mmol) was added and the mixture was subsequently cooled to -20 °C and allowed to stir for 5 mins. A solution of *n*-butyl magnesium chloride in Et₂O (0.28 mL, 1.9 M, 0.56 mmol) was added dropwise over 5 min, resulting in a dark brown solution, and the reaction mixture was allowed to stir for 2 h. The reaction mixture was quenched by the addition of 2 M HCl, and allowed to warm to room temperature. The mixture was extracted with Et₂O (3x) and the collected organic extracts were combined, dried over Na₂SO₄ and filtered to give a colourless solution. The solution was concentrated *in vacuo* to give a colourless residue which was applied to a silica column and eluted with 5 % Et₂O/Petroleum ether. The appropriate fractions were combined and had the solvent removed *in vacuo* to give the ester **151** (51 mg, 2.38 mmol, 51 % yield) as a colourless oil.

¹H NMR (400 MHz, Chloroform-*d*) δ 5.37 (m, 1H, H-3), 3.70 (s, 3H, H-12), 2.56 (m, 1H, H-5), 2.45 – 2.15 (m, 4H, aliphatic protons), 2.15 – 1.89 (m, 4H, aliphatic protons), 1.54 – 1.24 (m, 6H, aliphatic protons), 0.93 (t, *J* = 7.2 Hz, 3H, H-11).

¹³C NMR (101 MHz, Chloroform-*d*) δ 174.0, 146.4, 123.2, 51.0, 45.5, 31.5, 30.3, 29.3, 29.0, 28.2, 28.1, 22.2, 13.5.

Preparation of methyl (E)-7-((1R,3aR,7aS)-2-butyl-3a,4,7,7a-tetrahydro-1H-inden-1-yl)hept-5-enoate.



General Procedure:

The reaction was carried out as documented in the literature procedure.⁷²

A flame-dried flask was charged with Fe(acac)₃, to which was added enol phosphate **131** as a solution of THF and NMP. The mixture was subsequently cooled to -20 °C and allowed to stir for 5 mins. A solution of *n*-butyl magnesium chloride in Et₂O was added dropwise over 5 min, resulting in a dark brown solution, and the reaction mixture was allowed to stir for 2 h. The reaction mixture was quenched by the addition of 2M HCl, and allowed to warm to room temperature. The mixture was extracted with Et₂O (3x) and the collected organic extracts, were combined, dried over Na₂SO₄ and filtered to give a colourless residue. The colourless residue was concentrated *in vacuo* to give a clear residue which was applied to a silica column and eluted with 5 % Et₂O/ Petroleum ether. The appropriate fractions were combined and the solvent was removed *in vacuo* to give the ester **130** as a colourless oil.

Following the above **General Procedure**, data are presented as (a) amount and mmol of Fe(acac)₃, (b) amount and mmol of enol phosphate **131**, (c) solvent and volume of solvent, (d) volume and mmol of NMP, (e) volume and mmol of *n*-butyl magnesium chloride in Et₂O, (f) mass isolated, and (g) percentage of side product as determined by ¹H NMR analysis δ = 5.56 ppm.

Scheme 97

(a) 1.7 mg, 4.8 μmol, 6 mol%, (b) 40 mg, 0.08 mmol, (c) THF, 90 μL, (d) 80 μL, 0.8 mmol, (e) 85 μL, 0.96 mmol, (f) 5 mg, 15 μmol, 20% yield, and (g) 15%.

Table 20, Entry 1

(a) 2.1 mg, 6 μ mol, 6 mol%, (b) 50 mg, 0.1 mmol, (c) THF, 0.1 mL, (d) 90 μ L, 0.9 mmol, (e) 0.12 mL, 0.24 mmol, (f) 9 mg, 28 μ mol, 28% yield, and (g) 23%.

Table 20, Entry 2

(a) 2.1 mg, 6 μ mol, 6 mol%, (b) 50 mg, 0.1 mmol, (c) Et₂O, 0.1 mL, (d) 90 μ L, 0.9 mmol, (e) 0.12 mL, 0.24 mmol, (f) n/a, and (g) n/a.

Table 20, Entry 3

(a) 2.1 mg, 6 μ mol, 6 mol%, (b) 50 mg, 0.1 mmol, (c) THF, 1 mL, (d) 0.9 mL, 9 mmol, (e) 0.12 mL, 0.24 mmol, (f) 28 mg, 66 μ mol, 66% yield, and (g) 40%.

Table 20, Entry 4

(a) 2.1 mg, 6 μ mol, 6 mol%, (b) 50 mg, 0.1 mmol, (c) degassed THF, 1 mL, (d) 0.9 mL, 9 mmol, (e) 0.12 mL, 0.24 mmol, (f) 5 mg, 16 μ mol, 16% yield, and (g) 32%.

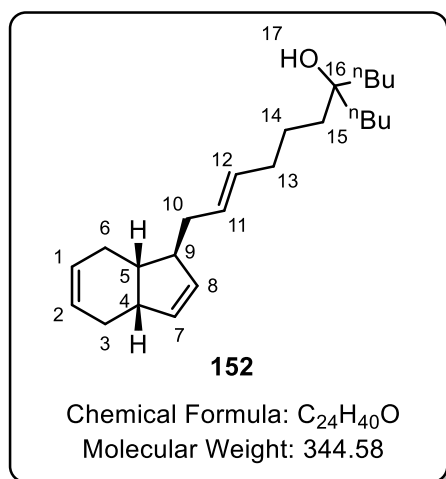
IR ν (neat, cm⁻¹): 1718, 1734, 2856, 2927, 2953.

¹H NMR (400 MHz, Chloroform-*d*) δ 5.94 – 5.75 (m, 2H, H-1 and H-2), 5.42 (m, 2H, H-15 and H-16), 5.23 (m, 1H, H-7), 3.69 (m, 3H, H-20), 2.85 – 2.71 (m, 1H, H-4), 2.46 – 1.63 (m, 16H, aliphatic protons), 1.49 – 1.25 (m, 4H, H-10 and H-11), 0.92 (t, *J* = 7.2, 3H, H-12) ppm.

¹³C NMR (101 MHz, Chloroform-*d*) δ 173.7, 145.8, 129.8, 129.4, 128.2, 128.1, 127.9, 53.4, 50.9, 40.2, 34.9, 32.9, 31.5, 29.2, 28.4, 27.5, 24.2, 22.1, 13.5 ppm. Two ¹³C resonances are missing due to overlapping signals.

HRMS (ESI) *m/z* calculated for C₂₁H₃₃O₂ [M+H⁺]: 317.2475. Found: 317.2478.

Preparation of (E)-5-butyl-11-((1S,3aS,7aS)-3a,4,7,7a-tetrahydro-1H-inden-1-yl)undec-9-en-5-ol.



Scheme 98

A flame-dried flask was charged with Fe(acac)₃ (2.1 mg, 6 μmol), to which was added enol phosphate **131** (50 mg, 0.1 mmol) in a solution of THF (0.5 mL) and TMEDA (0.14 mL, 0.9 mmol). The mixture subsequently cooled to -20 °C and allowed to stir for 5 mins. A solution of ⁿbutyl magnesium chloride in Et₂O (0.39 mL, 1.9 M, 0.24 mmol) was added dropwise over 5 min, resulting in a dark brown solution, and the resulting reaction mixture was allowed to stir for 2 h. The resulting reaction mixture was quenched by addition of 2 M HCl, and allowed to warm to room temperature. The mixture was extracted with Et₂O (3x) and the collected organic extracts, were combined, dried over Na₂SO₄ and filtered to give a clear solution. The clear solution had was concentrated *in vacuo* to give a clear residue which was applied to a silica column and eluted with 5 % Et₂O/Petroleum ether. The appropriate fractions were combined and concentrated *in vacuo* to give the tertiary alcohol **152** (15 mg, 47 μmol, 47 % yield) as a colourless oil.

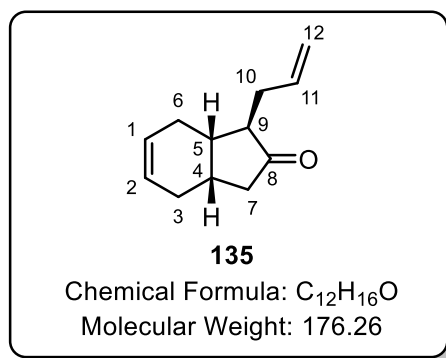
¹H NMR (400 MHz, Chloroform-*d*) δ 5.94 – 5.78 (m, 2H, H-1 and H-2), 5.73 – 5.59 (m, 2H, H-7 and H-8), 5.52 – 5.36 (m, 2H, H-11 and H-12), 2.93 – 2.79 (m, 1H, H-4 or H-9), 2.43 – 2.30 (m, 1H, H-4 or H-9), 2.27 – 1.90 (m, 7H, aliphatic protons), 1.86 – 1.73 (m, 1H, aliphatic protons), 1.60 (s, 1H, H-17), 1.49 – 1.26 (m, 16H, aliphatic protons), 1.12 (s, 1H, aliphatic protons), 0.93 (t, *J* = 7.2 Hz, 6H, terminal CH₃).

¹³C NMR (101 MHz, Chloroform-*d*) δ 135.1, 133.5, 130.8, 128.6, 127.9, 127.6, 73.9, 52.1, 42.2, 40.7, 38.5, 38.3, 37.3, 32.6, 27.4, 27.2, 25.2, 23.0, 22.8.

HRMS (ESI) *m/z* calculated for C₂₄H₄₄NO [M+NH₄⁺]: 362.3417. Found: 362.3420.

1.4.5. Investigation of a Cross-Metathesis Strategy

Preparation of (1*R*,3*aS*,7*aS*)-1-allyl-1,3,3*a*,4,7,7*a*-hexahydro-2*H*-inden-2-one.



General Procedure:

An oven-dried Schlenk tube was allowed to cool under an argon atmosphere and then flame-dried under vacuum before, once again, being cooled under an argon atmosphere. This cycle was repeated three times. To the now cooled, Schlenk tube was added silyl enol ether **121** and THF. The resulting clear solution was cooled to -10 °C, with stirring, before the dropwise addition of MeLi. After this, the resulting solution was allowed to stir at -10 °C for 20 min. The resulting solution was then cooled to -78 °C before the addition of DMPU, and further stirring at -78 °C for 60 min. To the resulting mixture was added the electrophile at -78 °C, after which time the reaction mixture was allowed to gradually warm to room temperature overnight. The resulting yellow solution was quenched with a saturated aqueous solution of NH₄Cl and extracted with Et₂O (x3). The organic extracts were collected, combined and dried over Na₂SO₄. The resulting solution was filtered, and the solvent was removed *in vacuo* to provide the crude mixture as a colourless liquid. The crude was applied to a silica column, and subsequently eluted with 5 % Et₂O/Petroleum ether (2CV) and then 10 % Et₂O/Petroleum ether (2CV). The appropriate fractions were combined and concentrated *in vacuo* to yield the allylated ketone **135** as a colourless oil.

Following the above **General Procedure**, data are presented as (a) amount and mmol of silyl enol ether **121**, (b) volume of THF, (c) volume and mmol of MeLi, (d) volume and mmol of DMPU, (e) electrophile, and (f) isolated yield of **135**.

Scheme 101

(a) 300 mg, 1.44 mmol, (b) 7 mL, (c) 0.9 mL, 1.6 M in Et₂O, 1.44 mmol, (d) 0.7 mL, 5.76 mmol, (e) allyl bromide, 0.25 mL, 2.9 mmol, and (f) 136 mg, 0.77 mmol, 53% yield.

Scheme 102

(a) 660 mg, 3.1 mmol, (b) 15 mL, (c) 1.9 mL, 1.6 M in Et₂O, 3.1 mmol, (d) 1.55 mL, 12.4 mmol, (e) allyl iodide, 0.57 mL, 6.2 mmol, and (f) 477 mg, 2.71 mmol, 87% yield.

IR ν (neat, cm⁻¹): 1639, 1736, 2833, 2899, 3023, 3073.

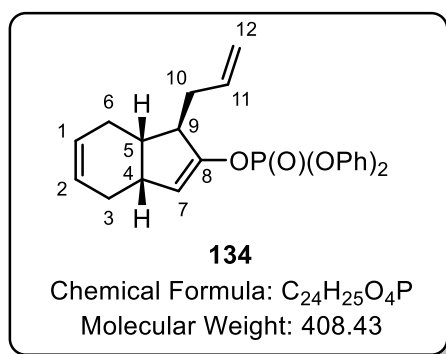
¹H NMR (400 MHz, Chloroform-*d*) δ 5.83 – 5.66 (m, 3H, H-1, H-2 and H-11), 5.12 – 5.01 (m, 2H, H-12), 2.46 – 2.00 (m, 10H, aliphatic protons), 1.77 – 1.64 (m, 1H, aliphatic protons).

¹³C NMR (101 MHz, Chloroform-*d*) δ 219.8, 135.1, 124.5, 123.9, 116.4, 50.0, 45.7, 36.7, 31.9, 29.2, 26.6, 24.8.

HRMS (ESI) *m/z* calculated for C₁₃H₁₆O [M]⁺: 176.1201. Found: 176.1200.

R_f = 0.3 (5 % Et₂O/Petroleum ether).

Preparation of (1*R*,3*aR*,7*aS*)-1-allyl-3*a*,4,7,7*a*-tetrahydro-1*H*-inden-2-yl diphenyl phosphate.



Scheme 103

The reaction was carried out as documented in the literature procedure.³⁰

To a flame-dried Schlenk flask was added ketone **135** (300 mg, 1.7 mmol) as a solution in THF (17 mL), DMPU (0.85 ml, 6.8 mmol) and diphenylphosphoryl chloride (0.39 mL, 1.9 mmol). The mixture was allowed to stir for 5 min before the dropwise addition of Mes₂Mg (4 ml, 1.2 mmol, 0.3 M in THF). The resulting reaction mixture was allowed to stir for 1 h, after which the reaction mixture was quenched by the addition of a saturated aqueous NaHCO₃ solution. The resulting mixture was extracted with Et₂O (x3) and the collected organic extracts were combined, dried over Na₂SO₄ and filtered to give a colourless solution. The resulting solution was concentrated *in vacuo* to give a clear residue, which was applied to a silica column and eluted with 10% Et₂O/Petroleum ether (2 CV) then 20 %

Et₂O/Petroleum ether (2 CV). The appropriate fractions were combined and had the solvent removed *in vacuo* to give the enol phosphate **134** (647 mg, 1.58 mmol, 93 %) as a colourless oil.

IR ν (neat, cm⁻¹): 1539, 1639, 1654, 2835, 2918, 3032, 3068.

¹H NMR (400 MHz, Chloroform-*d*) δ 7.41 – 7.34 (m, 4H, ArH), 7.28 – 7.20 (m, 6H, ArH), 5.95 – 5.84 (m, 2H, H-1 and H-2), 5.75 (ddt, $J = 17.2, 10.2, 7.1$ Hz, 1H, H-11), 5.39 (dd, $J = 3.2, {}^4J_{PH} = 1.5$ Hz, 1H, H-7), 5.08 – 4.98 (m, 2H, H-12), 2.89 – 2.80 (m, 1H, aliphatic protons), 2.49 – 2.41 (m, 1H, aliphatic protons), 2.37 – 2.29 (m, 1H, aliphatic protons), 2.28 – 2.06 (m, 4H, aliphatic protons), 1.97 – 1.87 (m, 1H, aliphatic protons), 1.86 – 1.77 (m, 1H, aliphatic protons).

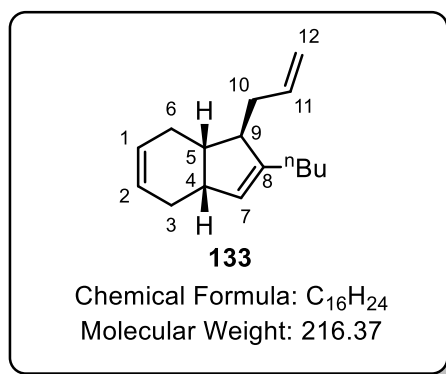
¹³C NMR (101 MHz, Chloroform-*d*) δ 150.4 (d, ${}^2J_{CP} = 10.5$ Hz), 150.0 (d, ${}^2J_{CP} = 7.4$ Hz), 135.4, 129.3, 128.4, 127.7, 125.0, 119.6 (t, ${}^3J_{CP} = 4.5$ Hz), 116.1, 114.4 (d, ${}^3J_{CP} = 3.9$ Hz), 49.9 (d, ${}^3J_{CP} = 6.1$ Hz), 38.3, 37.8, 35.7, 28.0, 27.4.

³¹P NMR (162 MHz, Chloroform-*d*) δ -17.6.

HRMS (ESI) m/z calculated for C₂₄H₂₆O₄P [M+H]⁺: 409.1569. Found: 409.1569.

R_f = 0.32 (20 % Et₂O/Petroleum ether)

Preparation of (1*R*,3*aR*,7*aS*)-1-allyl-2-butyl-3*a*,4,7,7*a*-tetrahydro-1*H*-indene.



Scheme 104

To a solution of enol phosphate **134** (501 mg, 1.22 mmol) in toluene (11 mL), was added Pd-PEPSSI-SiPr (9.2 mg, 14 μ mol), and the resulting mixture was allowed to stir for 5 min at 0 °C under an atmosphere of argon. After 5 min, ⁿbutylmagnesium chloride (6.6 mL, 1.80 mmol, 0.27 M) was added to the reaction and the resulting yellow solution was allowed to stir for 16 h at 0 °C. The reaction mixture was quenched by the addition of a saturated aqueous solution of NH₄Cl and extracted with

Et₂O (3x). The combined organic extracts were dried over Na₂SO₄, filtered and the solvent was removed *in vacuo* to give a clear residue. The residue was loaded onto silica and applied to a silica column, which was eluted with 100% Petroleum ether (2CV). The appropriate fractions were combined to give the triene **133** (245 mg, 1.13 mmol, 93 % yield) as a colourless oil.

IR ν (neat, cm⁻¹): 1637, 2835, 2856, 2870, 2924.

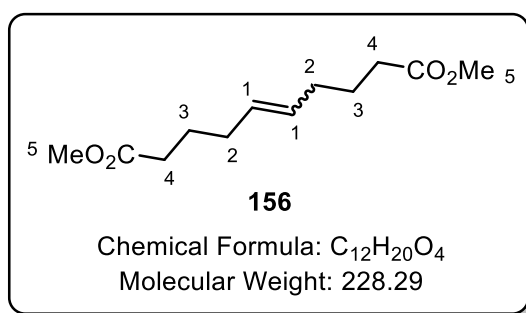
¹H NMR (400 MHz, Chloroform-*d*) δ 5.93 – 5.73 (m, 3H, H-1, H-2 and H-11), 5.27 – 5.20 (m, 1H, H-7), 5.09 – 4.99 (m, 2H, H-12), 2.87 – 2.75 (m, 1H, H-4), 2.34 – 1.74 (m, 10H, aliphatic protons), 1.55 – 1.31 (m, 4H, butyl chain CH₂x2), 0.93 (t, *J* = 7.2 Hz, 3H, terminal CH₃).

¹³C NMR (101 MHz, Chloroform-*d*) δ 145.7, 137.0, 128.3, 128.0, 127.8, 115.1, 53.1, 40.8, 40.3, 36.3, 29.2, 28.4, 28.2, 27.5, 22.1, 13.5.

HRMS (ESI) *m/z* calculated for C₁₆H₂₄ [M-H]⁺: 215.1800. Found: 215.1801.

R_f = 1.00 (100% Petroleum ether)

Preparation of (*EZ*)-dimethyl-dec-5-enedioate.⁷³



A flame-dried flask fitted with reflux condenser was charged with Grubbs 1st generation catalyst (192 mg, 0.23 mmol), to which was added a solution of alkene **155** (455 mg, 3.5 mmol), in DCM (10 mL). The mixture was then stirred for 72 h at reflux. The solution was then allowed to cool and had the solvent was removed *in vacuo* to give a black residue. The black residue was then applied to a silica column and eluted with 100 % Petroleum ether (2 CV) then 5 % Et₂O/ Petroleum ether (3 CV). The appropriate fractions were combined, and the solvent was removed *in vacuo* to give the diester **156** (360 mg, 1.58 mmol, 90 % yield) as a colourless oil.

IR ν (neat, cm⁻¹): 1734, 2908, 2949.

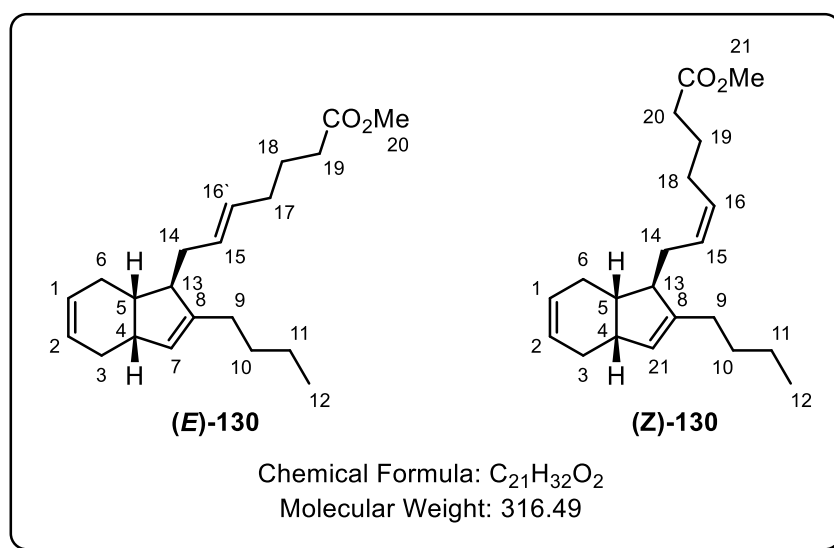
^1H NMR (400 MHz, Chloroform-*d*) δ 5.43 – 5.33 (m, 2H, H-1), 3.66 (s, 6H, H-5), 2.29 (t, $J = 7.7$ Hz, 4H, H-4), 2.09 – 1.98 (m, 4H, H-2), 1.68 (p, $J = 7.2$ Hz, 4H, H-3).

^{13}C NMR (101 MHz, Chloroform-*d*) δ 173.6, 129.7, 129.1, 51.0, 32.9, 31.4, 26.0, 24.1. (Three extra signals were observed due to a small unquantifiable amount of the *Z* isomer)

HRMS (ESI) m/z calculated for $\text{C}_{12}\text{H}_{21}\text{O}_4$ $[\text{M}+\text{H}]^+$: 229.1436. Found: 229.1434.

$R_f = 0.50$ (20% Et_2O /Petroleum ether)

Preparation of methyl (*EZ*)-7-((1*R*,3*aR*,7*aS*)-2-butyl-3*a*,4,7,7*a*-tetrahydro-1*H*-inden-1-yl)hept-5-enoate.



General Procedure A:

A flame-dried flask fitted with reflux condenser was charged with the catalyst, then a solution of triene **133** was added, and the reaction mixture stirred for 5 min under an atmosphere of argon. After 5 min, alkene **155** was added and the resulting solution was warmed to the allotted temperature for the stated reaction time. The solution was then allowed to cool and the solvent was removed *in vacuo* to give a dark residue. The residue was then applied to a silica column and eluted with 100 % Petroleum ether (2 CV) and 2.5 % Et_2O /Petroleum ether (3 CV). The appropriate fractions were combined and the solvent removed *in vacuo* to give the desired product **130** as a colourless oil. On analysis the product was obtained as a mixture with starting alkene **155**.

Following **General Procedure A**, data are presented as (a) catalyst, (b) amount and mmol of triene **133**, (c) solvent, (d) volume and mmol of alkene **155**, (e) temperature, (f) reaction time, (g) Product ratio **130:155** and h) *E:Z* ratio of newly formed olefin.

Table 21, Entry 1

(a) Grubbs 2nd generation, 4.7 mg, 6 μmol , (b) 20 mg, 93 μmol , (c) DCM, 0.75 mL, (d) 52 μL , 0.37 mmol, (e) Δ , (f) 2 h, (g) 1:2 and, (h) 4:1.

Table 21, Entry 2

(a) Grubbs 2nd generation, 4.7 mg, 6 μmol , (b) 20 mg, 93 μmol , (c) DCM, 0.75 mL, (d) 52 μL , 0.37 mmol, (e) Δ , (f) 16 h, (g) 1:1 and, (h) 4:1.

Table 22, Entry 1

(a) Grubbs 2nd generation, 4.7 mg, 6 μmol , (b) 20 mg, 93 μmol , (c) Toluene, 0.75 mL, (d) 52 μL , 0.37 mmol, (e) 60 $^{\circ}\text{C}$, (f) 16 h, (g) N/A and, (h) N/A.

Table 22, Entry 2

(a) Grubbs 2nd generation, 4.7 mg, 6 μmol , (b) 20 mg, 93 μmol , (c) Toluene, 0.75 mL, (d) 52 μL , 0.37 mmol, (e) Δ , (f) 16 h, (g) N/A and, (h) N/A.

Table 23, Entry 1

(a) Grubbs 1st Generation, 4.9 mg, 6 μmol , (b) 20 mg, 93 μmol , (c) DCM, 0.75 mL, (d) 52 μL , 0.37 mmol, (e) Δ , (f) 16 h, (g) 1:1.2 and, (h) 11:9.

Table 23, Entry 2

(a) Grubbs 2nd generation, 13.8 mg, 18 μmol , (b) 20 mg, 93 μmol , (c) DCM, 0.75 mL, (d) 52 μL , 0.37 mmol, (e) Δ , (f) 16 h, (g) 1:2 and, (h) 4:1.

Table 23, Entry 3

(a) Hoveyda-Grubbs 2nd generation, 3.8 mg, 6 μmol , (b) 20 mg, 93 μmol , (c) DCM, 0.75 mL, (d) 52 μL , 0.37 mmol, (e) Δ , (f) 16 h, (g) 1:1 and, (h) 4:1.

Table 23, Entry 4

(a) Hoveyda-Grubbs 2nd generation, 11.3 mg, 18 μmol , (b) 20 mg, 93 μmol , (c) DCM, 0.75 mL, (d) 52 μL , 0.37 mmol, (e) Δ , (f) 16 h, (g) 1:1 and, (h) 4:1.

Table 24, Entry 1

a) Grubbs 2nd generation, 4.7 mg, 6 μ mol, (b) 20 mg, 93 μ mol, (c) DCM, 1.5 mL, (d) 52 μ L, 0.37 mmol, (e) Δ , (f) 16 h, (g) N/A and, (h) N/A.

Table 24, Entry 2

(a) Grubbs 2nd generation, 4.7 mg, 6 μ mol, (b) 20 mg, 93 μ mol, (c) DCM, 0.38 mL, (d) 52 μ L, 0.37 mmol, (e) Δ , (f) 16 h, (g) 5:2 and, (h) 4:1.

General Procedure B:

A flame-dried flask fitted with reflux condenser was charged with Grubbs 2nd generation catalyst, to which was added a solution of triene **133** in DCM and the reaction mixture stirred for 5 min under an atmosphere of argon. After 5 min, dimer **156** was added and the resulting solution was warmed to the allocated temperature for the stated reaction time. The solution was then allowed to cool, and the solvent was removed *in vacuo* to give a dark residue. The residue was then applied to a silica column and eluted with 100 % Petroleum ether (2 CV) and 2.5 % Et₂O/Petroleum ether (3 CV). The appropriate fractions were combined, and the solvent was removed *in vacuo* to give the desired product **130** as a colourless oil.

Following **General Procedure B**, data are presented as (a) amount and mmol of Grubbs 2nd generation catalyst, (b) amount and mmol of triene **133**, (c) volume of DCM, (d) amount and mmol of dimer **156**, (e) temperature, (f) reaction time, (g) amount, mmol and yield of methyl ester **130**, and (h) *E:Z* ratio of newly formed olefin.

Table 25, Entry 1

(a) Grubbs 2nd generation, 4.7 mg, 6 μ mol, (b) 20 mg, 93 μ mol, (c) DCM, 0.75 mL, (d) 43 mg, 0.18 mmol, (e) Δ , (f) 16 h, (g) 23 mg, 73 μ mol 77 % yield and, (h) 4:1.

Table 25, Entry 2

(a) Grubbs 2nd generation, 2.4 mg, 3 μ mol, (b) 20 mg, 93 μ mol (c) DCM, 0.75 mL (d) 43 mg, 0.18 mmol, (e) Δ , (f) 16 h, (g) 22 mg, 70 μ mol, 74 % yield and, (h) 4:1.

Table 25, Entry 3

(a) Grubbs 2nd generation, 4.7 mg, 6 μ mol, (b) 20 mg, 93 μ mol, (c) DCM, 0.75 mL, (d) 43 mg, 0.18 mmol, (e) room temperature, (f) 16 h, (g) 18 mg, 57 μ mol, 60 % yield and, (h) 4:1.

Table 25, Entry 4

(a) Grubbs 2nd generation, 2.4 mg, 3 μ mol, (b) 20 mg, 93 μ mol, (c) DCM, 0.75 mL, (d) 43 mg, 0.18 mmol, (e) Δ , (f) 2 h, (g) 20 mg, 63 μ mol, 66 % yield and, (h) 4:1.

IR ν (neat, cm^{-1}): 1718, 1734, 2856, 2927, 2953.

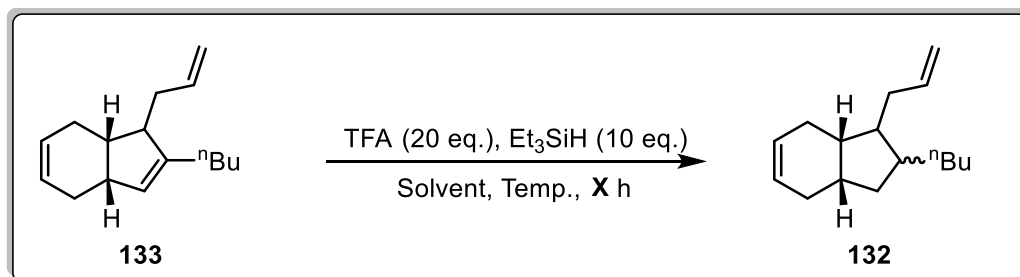
^1H NMR (400 MHz, Chloroform-*d*) δ 5.90 – 5.78 (m, 2H, H-1 and H-2), 5.48 – 5.35 (m, 2H, H-15 and H-16), δ 5.26 – 5.24 (m, 0.2H, H-21), 5.23-5.21 (m, 0.8H, H-7), 3.69 (s, 3H, H-20), 2.86 – 2.45 (m, 1H, aliphatic ring proton), 2.33 (m, 3H, aliphatic protons), 2.26 – 1.93 (m, 10H, aliphatic protons), 1.88 – 1.67 (m, 2H aliphatic protons), 1.43 – 1.24 (m, 4H, aliphatic chain protons), 0.92 (t, $J = 7.2$ Hz, 3H, H-12).

^{13}C NMR (101 MHz, Chloroform-*d*) δ 173.7, 146.6, 145.8, 130.2, 129.8, 129.4, 129.1, 128.8, 128.8, 128.2, 128.1, 127.9, 126.6, 53.4, 50.9, 45.8, 44.7, 40.8, 40.5, 40.2, 34.9, 33.0, 32.9, 31.9, 31.5, 29.5, 29.2, 28.4, 28.2, 28.2, 27.5, 27.5, 26.2, 24.4, 24.2, 22.1, 22.0, 13.5.

HRMS (ESI) m/z calculated for $\text{C}_{21}\text{H}_{33}\text{O}_2$ $[\text{M}+\text{H}]^+$: 317.2475. Found: 317.2478.

$R_f = 0.3$ (2.5% Et_2O /Petroleum ether)

Ionic Reduction Screen



General Procedure A:

To a mixture of triene **133** (11 mg, 53 μ mol) in the specified solvent and Et_3SiH (85 μL , 530 μ mol) was added TFA (80 mL, 1.06 mmol) and the reaction was allowed to stir under an atmosphere of nitrogen for the allocated time. After the allocated time, the reaction mixture was quenched by the addition of a saturated aqueous solution of NaHCO_3 and extracted with Et_2O (3x). The collected organic extracts were dried with Na_2SO_4 , filtered and the solvent was removed *in vacuo*. The crude material was then analysed by ^1H NMR spectroscopy.

Following **General Procedure A**, data are presented as (a) solvent, (b) allocated time, (c) % consumption of H_a, (d) conversion to H_b **132** and, (e) presence of side product.

Table 26, Entry 1

(a) Toluene, 1.8 mL, (b) 1 h, (c) 42 %, (d) 24 %, and, (e) not observed.

Table 26, Entry 2

(a) Toluene, 1.8 mL, (b) 2.5 h, (c) 58 %, (d) 32 % and, (e) not observed.

Table 26, Entry 3

(a) Toluene, 1.8 mL, (b) 6 h, (c) 61 %, (d) 27 % and, (e) not observed.

Table 27, Entry 1

(a) DCM, 1.8 mL, (b) 2.5 h, (c) 94 %, (d) 0 % and, (e) observed.

Table 27, Entry 2

(a) EtOAc, 1.8 mL, (b) 2.5 h, (c) 42 %, (d) 0 %, and (e) observed.

Table 27, Entry 3

(a) THF, 1.8 mL, (b) 2.5 h, (c) 38 %, (d) 0 %, and (e) observed.

Table 27, Entry 4

(a) 2-nitropropane, 1.8 mL, (b) 2.5 h, (c) 48 %, (d) 0 %, and (e) not observed.

Table 27, Entry 5

(a) neat, 1.8 mL, (b) 2.5 h, (c) 100 %, (d) 79 %, and (e) not observed.

General Procedure B:

To a mixture of triene **133** (22 mg, 106 μmol) and Et₃SiH was added TFA, and the reaction mixture was allowed to stir under an atmosphere of nitrogen for the allotted time. After the allocated time, the reaction mixture was quenched with a saturated aqueous solution of NaHCO₃ and extracted with Et₂O (3x). The collected organic extracts were dried with Na₂SO₄, filtered and the solvent was removed *in vacuo*. The crude material was then analysed by ¹H NMR spectroscopy.

Following **General Procedure B**, data are presented as (a) volume and mmol of Et₃SiH, (b) volume and mmol of TFA (c) allocated time, (d) % consumption of H_a **133**, and, (e) presence of side product.

Table 28, Entry 1

(a) 0.17 mL, 1.06 mmol (b) 0.16 mL, 2.12 mmol (c) 2.5 h, (d) 100 % and, (e) observed.

Table 28, Entry 2

(a) 0.17 mL, 1.06 mmol (b) 85 μ L, 1.06 mmol (c) 2.5 h, (d) 100 % and, (e) observed.

Table 28, Entry 3

(a) 0.17 mL, 1.06 mmol (b) 43 μ L, 0.503 mmol (c) 2.5 h, (d) 100 % and, (e) observed.

Table 28, Entry 4

(a) 0.34 mL, 2.12 mmol (b) 0.16 mL, 2.12 mmol (c) 2.5 h, (d) 100 % and, (e) observed.

Table 28, Entry 5

(a) 0.68 mL, 4.24 mmol (b) 0.16 mL, 2.12 mmol (c) 2.5 h, (d) 100 % and, (e) observed.

Table 28, Entry 6

(a) 0.17 mL, 1.06 mmol (b) 0.16 mL, 2.12 mmol (c) 1 h, (d) 100 % and, (e) observed.

Table 28, Entry 7

(a) 0.17 mL, 1.06 mmol (b) 0.16 mL, 2.12 mmol (c) 0.5 h, (d) 100 % and, (e) observed.

Table 28, Entry 8

(a) 0.17 mL, 1.06 mmol (b) 43 μ L, 0.503 mmol (c) 0.5 h, (d) 100 % and, (e) observed.

General Procedure C:

To a mixture of triene **133** (22 mg, 106 μ mol) and Et₃SiH (0.17 mL, 1.06 mmol) in the specified solvent was added TsOH.H₂O and the reaction mixture was allowed to stir under an atmosphere of nitrogen for 2.5 h. After the allocated time, the reaction mixture was quenched by the addition of a saturated aqueous solution of NaHCO₃ and extracted with Et₂O (3x). The collected organic extracts were dried with Na₂SO₄, filtered and the solvent was removed *in vacuo*. The crude material was then analysed by ¹H NMR spectroscopy.

Following **General Procedure C**, data are presented as (a) solvent, (b) volume and mmol of TFA (c) % consumption of H_a **133**, and, (d) presence of side product.

Table 29, Entry 1

(a) n/a (b) 365 mg, 2.12 mmol, (c) 0 % and, (d) not observed.

Table 29, Entry 2

(a) n/a (b) 730 mg, 4.24 mmol, (c) 0 % and, (d) not observed.

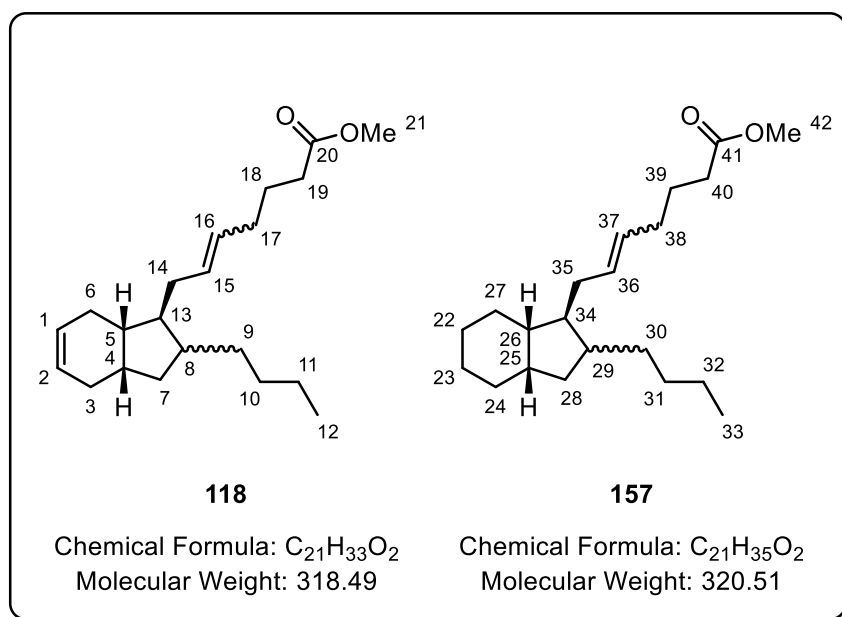
Table 29, Entry 3

(a) DCM, 1.8 mL (b) 365 mg, 2.12 mmol, (c) 0 % and, (d) not observed.

Table 29, Entry 4

(a) 2-nitropropane, 1.8 mL (b) 365 mg, 2.12 mmol, (c) 0 % and, (d) not observed.

Preparation of a mixture of methyl 5-((1S,3aS,7aS)-2-butyl-2,3,3a,4,7,7a-hexahydro-1H-inden-1-yl)-3,3-dimethyl-3-pent-3-enoate and methyl 5-((1S,3aS,7aS)-2-butyloctahydro-1H-inden-1-yl)-3,3-dimethyl-3-pent-3-enoate.



Scheme 112

To a mixture of triene **133** (44 mg, 212 μ mol) and Et_3SiH (0.34 mL, 2.12 mmol) was added TFA (0.32 mL, 4.24 mmol) and the reaction was allowed to stir under an atmosphere of nitrogen for the allocated time. After the allocated time, the reaction mixture was quenched by the addition of a saturated aqueous solution of $NaHCO_3$ and extracted with Et_2O (3x). The collected organic extracts were dried with $NaSO_4$, filtered and the solvent was removed *in vacuo*. The crude material was then dissolved in

DCM (1.5 mL), transferred to an oven-dried flask fitted with a reflux condenser to which was added dimer **91** (96 mg, 424 μmol) and Grubbs 2nd generation catalyst (5.5 mg, 6.5 μmol). The reaction mixture was allowed to stir at reflux under an atmosphere of nitrogen for 16 h. After this time, the reaction mixture was allowed to cool, and the solvent was removed *in vacuo* to give a dark residue. The dark residue was then applied to a silica column and eluted with 100 % Petroleum ether (2 CV) then 2.5 % Et₂O/ Petroleum ether (3 CV). The appropriate fractions were combined and had the solvent removed *in vacuo* to give the mixture of products described in the title (17 mg, 53 μmol , 25 % yield, 2:1 **118:157** mixture) as a clear oil.

IR ν (neat, cm^{-1}): 1739, 1778, 2852, 2918, 2951.

¹H NMR (400 MHz, Chloroform-*d*) δ 5.79 – 5.58 (m, 1.3H, H-1 and H-2), 5.55 – 5.27 (m, 2H, H-15, H-16, H-36 and H-37), 3.68 (s, 3H, H-21 and H-42), 2.40 – 2.20 (m, 2H, aliphatic protons), 2.19 – 0.98 (m, 21.7H, aliphatic protons), 0.89 (m, 3H, H-12 and H-33).

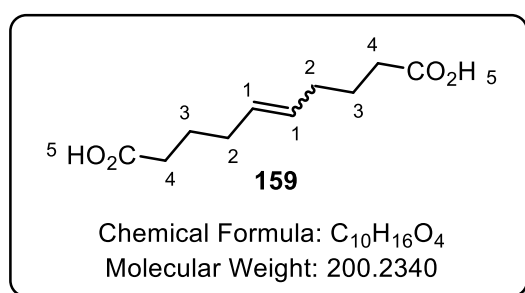
¹³C NMR (101 MHz, Chloroform-*d*) δ 174.3, 130.7, 130.4, 129.9, 129.7, 128.6, 127.5, 127.4, 127.2, 126.8, 126.4, 52.3, 51.8, 51.5, 47.3, 44.7, 43.1, 42.4, 41.9, 40.2, 37.1, 36.8, 36.5, 33.6, 33.5, 32.5, 32.2, 32.1, 32.0, 31.7, 31.0, 30.9, 30.8, 26.7, 26.6, 26.5, 24.9, 24.8, 23.0, 14.2.

HRMS (ESI) m/z calculated for **118** C₂₁H₃₄O₂ [M+H]⁺: 319.2637. Found: 319.2637.

HRMS (ESI) m/z calculated for **157** C₂₁H₃₆O₂ [M+H]⁺: 321.2767. Found: 321.2784.

R_f(mixture) = 0.27 (2.5% Et₂O/ Petroleum ether)

Preparation of (*E/Z*)-dec-5-enedioic acid.



To a flask charged with diester **156** (360 mg, 1.58 mmol) was added THF (6 mL), MeOH (6 mL), H₂O (3 mL) and then LiOH (1.3 g, 55 mmol) and the resulting mixture was allowed to stir for 1 h. After 1 h, 1 M aqueous solution of hydrochloric acid was added dropwise, until pH \approx 2, and the reaction mixture was then extracted with Et₂O (3x). The collected organic extracts were dried with Na₂SO₄, filtered and

the solvent was removed *in vacuo* to give a colourless residue. The colourless residue was then applied to a silica column and then eluted with 80 % Et₂O/Petroleum ether (5 CV). The appropriate fractions were combined, and the solvent was removed *in vacuo* to give the diacid **159** (270 mg, 1.35 mmol, 85 % yield) as a white solid.

M.p.: 99-101 °C

IR ν (neat, cm⁻¹): 1685, 2601, 2819, 2937 (br).

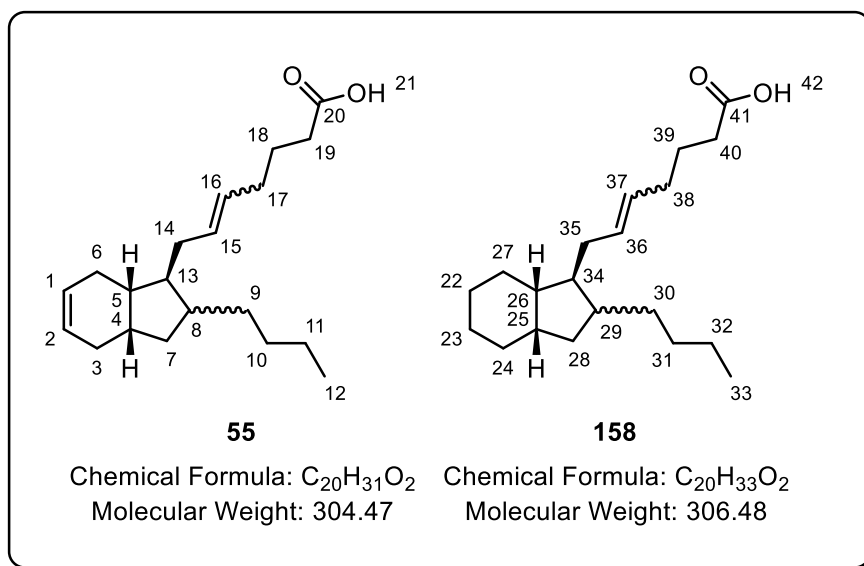
¹H NMR (400 MHz, Chloroform-*d*) δ 11.15 (s, 2H, H-5), 5.58 – 5.26 (m, 2H H-1), 2.48 – 2.23 (m, 4H, H-4), 2.17 – 2.02 (m, 4H, H-2), 1.83 – 1.66 (m, 4H, H-3).

¹³C NMR (101 MHz, Chloroform-*d*) δ 179.7, 129.7, 129.1, 32.8, 31.3, 25.9, 24.0, 23.8. (Three extra signals were observed due to a small unquantifiable amount of the *Z* isomer)

HRMS (ESI) *m/z* calculated for C₁₀H₁₅O₄ [M-H]⁺: 199.0976. Found: 199.0979.

R_f = 0.3 (80% Et₂O/ Petroleum ether)

Preparation of a mixture of 5-((1*S*,3*aS*,7*aS*)-2-butyl-2,3,3*a*,4,7,7*a*-hexahydro-1*H*-inden-1-yl)-3,3-dimethyl-3,5-pent-3-enoic acid and 5-((1*S*,3*aS*,7*aS*)-2-butyl-2,3,3*a*,4,7,7*a*-hexahydro-1*H*-inden-1-yl)-3,3-dimethyl-3,5-pent-3-enoic acid.



Scheme 113

To a mixture of triene **133** (44 mg, 212 μmol) and Et_3SiH (0.34 mL, 2.12 mmol) was added TFA (0.32 mL, 4.24 mmol) and the reaction was allowed to stir under an atmosphere of nitrogen for the allotted time. After the allocated time, the reaction mixture was quenched by the addition of a saturated aqueous solution of NaHCO_3 and extracted with Et_2O (3x). The collected organic extracts were dried with Na_2SO_4 , filtered and the solvent removed *in vacuo*. The crude material was then dissolved in DCM (1.5 mL) and, transferred to an oven-dried flask fitted with a reflux condenser to which was added dimer **159** (85 mg, 424 μmol) and Grubbs 2nd generation catalyst (5.5 mg, 6.5 μmol). The reaction mixture was then heated to reflux under an atmosphere of nitrogen for 16 h. After this time, the reaction mixture was allowed to cool, and the solvent was removed *in vacuo* to give a dark residue. The dark residue was then applied to a silica column and eluted with 100 % Petroleum ether (2 CV), 20 % Et_2O /Petroleum ether (3 CV) and 50% Et_2O /1% acetic acid/Petroleum ether (2 CV). The appropriate fractions were combined, and the solvent was removed *in vacuo* to give the mixture of products described in the title (23 mg, 78 μmol , 39 % yield, 2:3 **55:158** mixture) as a clear oil.

^1H NMR (400 MHz, Chloroform-*d*) δ 5.68 (m, 0.85H, H-1 and H-2), 5.56 – 5.33 (m, 2H, H-15, H-16, H-36 and H-37), 2.49 – 1.09 (m, 25.15H, aliphatic protons), 1.01 – 0.82 (m, 3H, terminal, H-12 and H-33).

^{13}C NMR (101 MHz, Chloroform-*d*) δ 180.0, 137.5, 130.9, 130.7, 130.6, 129.8, 129.7, 129.5, 127.4, 127.2, 52.3, 51.8, 51.6, 51.5, 50.6, 49.9, 47.3, 44.7, 44.5, 42.4, 42.4, 42.0, 40.2, 38.0, 37.2, 37.1, 37.0, 36.8, 36.5, 34.9, 33.5, 33.4, 33.4, 33.3, 33.0, 32.5, 32.2, 32.0, 31.9, 31.9, 31.7, 31.1, 31.0, 30.9, 30.8, 30.4, 26.6, 26.5, 24.7, 24.6, 24.5, 24.5, 23.0, 23.0, 14.2.

IR ν (neat, cm^{-1}): 1705, 2853, 2872, 2916, 2935, 3016 (br).

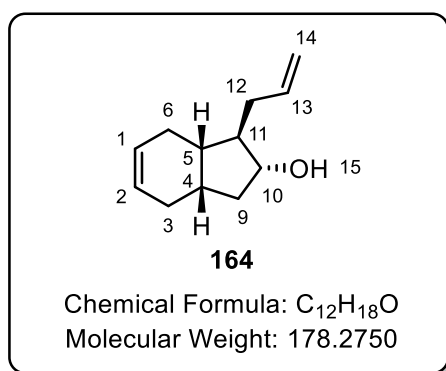
HRMS (ESI) m/z calculated for $\text{C}_{21}\text{H}_{30}\text{O}_2$ $[\text{M}-\text{H}]^-$: 303.2330. Found: 303.2329.

HRMS (ESI) m/z calculated for $\text{C}_{21}\text{H}_{32}\text{O}_2$ $[\text{M}-\text{H}]^-$: 305.2480. Found: 305.2484.

R_f (mixture) = 0.35 (50% Et_2O / 1% acetic acid/Petroleum ether)

1.4.6. sp^3 - sp^3 cross-coupling

Preparation of (1*R*,2*R*,3*aS*,7*aS*)-1-allyl-2,3,3*a*,4,7,7*a*-hexahydro-1*H*-inden-2-ol.



Scheme 119

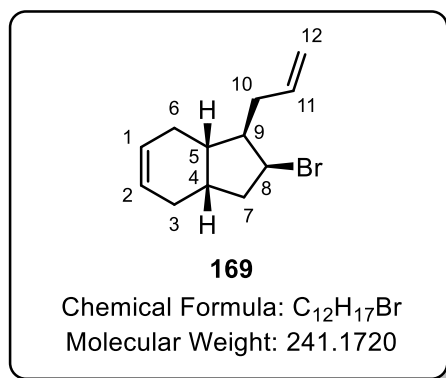
A flame dried flask was charged with NaBH₄ (118 mg, 3.12 mmol) which was suspended in EtOH (10 mL) and the mixture was cooled to 0 °C under argon with stirring. To the resulting suspension was added, dropwise, a solution of ketone **135** (275 mg, 1.56 mmol) in EtOH (10 mL) and the resulting reaction mixture was allowed to warm to room temperature over 1 h. The reaction mixture was once again cooled to 0 °C and quenched with water until no further effervescence was observed. The resulting mixture was extracted with DCM (3x). The collected organic extracts were combined, dried over Na₂SO₄, filtered and the filtrate was concentrated *in vacuo* to yield the secondary alcohol **164** (209 mg, 1.17 mmol, 75 % yield) as a colourless oil.

¹H NMR (400 MHz, Chloroform-*d*) δ 6.01 – 5.84 (m, 1H, H-13), 5.81 – 5.68 (m, 2H, H-1 and H-2), 5.19 – 5.02 (m, 2H, H-14), 4.01 – 3.92 (m, 1H, H-10), 2.39 – 2.30 (m, 1H, Aliphatic protons), 2.28 – 1.92 (m, 7H, Aliphatic protons), 1.76 – 1.61 (m, 3H, Aliphatic protons), 1.43 (dt, *J* = 12.8, 5.6 Hz, 1H, Aliphatic protons).

¹³C NMR (101 MHz, Chloroform-*d*) δ 137.8, 126.7, 126.0, 116.2, 78.2, 52.1, 41.2, 40.6, 37.3, 33.4, 28.2, 26.4.

HRMS (ESI) *m/z* calculated for C₁₂H₁₈O [*M*]: 178.1358. Not Found. However, fragment C₁₂H₂₀O₂ calculated [*M*+H₂O]⁺: 196.1696. Found: 196.1697. The fragment corresponds to the hydration of an olefin within the molecule.

Preparation of (1R,2S,3aS,7aS)-1-allyl-2-bromo-2,3,3a,4,7,7a-hexahydro-1H-indene.



Scheme 119

To a stirred solution of alcohol **164** (250 mg, 1.4 mmol) in DCM (6 mL) was added CBr₄ (696 mg, 2.1 mmol) and the solution was allowed to cool to 0 °C. Subsequently, a solution of triphenylphosphine (550 mg, 2.1 mmol) in DCM (6.5 mL) was added dropwise and the reaction solution was then allowed to warm to room temperature. After 16 h, Et₂O was added, resulting in a white precipitate. The precipitate was filtered, and the filtrate was concentrated *in vacuo* to give a brown oil. The crude was applied to a silica column and eluted with 100% petroleum ether and the appropriate fractions were combined and had the solvent removed *in vacuo* to give the secondary bromide **169** (321 mg, 1.33 mmol, 95 % yield) as a colourless oil.

IR ν (neat, cm⁻¹): 659, 1639 2837, 2922, 3034, 3074.

¹H NMR (400 MHz, Chloroform-*d*) δ 6.02 – 5.89 (m, 2H, H-1 and H-2), 5.82 (ddt, $J = 17.2, 10.2, 7.0$ Hz, 1H, H-11), 5.16 (ddt, $J = 17.1, ^4J = 2.1, ^2J = 1.5$ Hz, 1H, H-12), 5.09 – 5.00 (m, 1H, H-12), 4.55 (t, $J = 4.3$ Hz, 1H, H-8), 2.78 – 2.60 (m, 1H, Aliphatic proton), 2.43 – 2.05 (m, 7H, Aliphatic protons), 1.98 – 1.74 (m, 3H, Aliphatic protons).

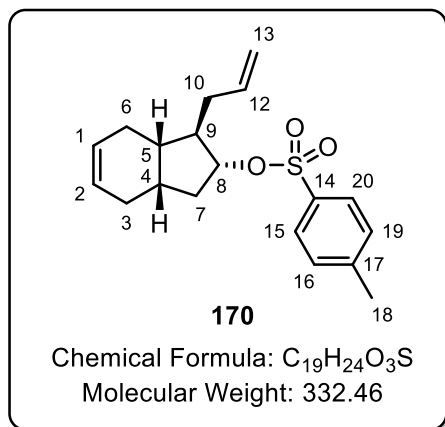
¹³C NMR (101 MHz, Chloroform-*d*) δ 136.3, 128.8, 128.6, 115.6, 61.3, 51.3, 43.7, 39.6, 35.8, 34.7, 27.2, 25.3.

HRMS (ESI) m/z calculated for C₁₂H₁₈⁷⁹Br [M+H]⁺: 255.0385. Found: 255.0392.

HRMS (ESI) m/z calculated for C₁₂H₁₈⁸¹Br [M+H]⁺: 257.0365. Found: 257.0374.

R_f = 1.00 (100% Petroleum ether)

Preparation of (1R,2R,3aS,7aS)-1-allyl-2,3,3a,4,7,7a-hexahydro-1H-inden-2-yl 4-methylbenzenesulfonate.



Scheme 120

The reaction was carried out as documented in the literature procedure.⁵⁴

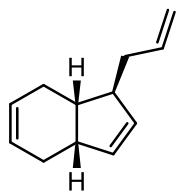
To a stirred solution of alcohol **164** (320 mg, 1.8 mmol) in pyridine (1 mL) was added tosyl chloride (412 mg, 2.16 mmol) portion wise at 0 °C. The reaction was allowed to warm to room temperature overnight and was diluted with Et₂O. The organic layer was then washed with 2M HCl (2x) and water (2x) and subsequently dried over Na₂SO₄, filtered and the solvent removed *in vacuo* to give a yellow oil. The yellow oil was applied to a silica column and eluted with 10 % Et₂O/ Petroleum ether. The appropriate fractions were combined and had the solvent removed *in vacuo* to give the tosylate **170** (520 mg, 1.57 mmol, 87 % yield) as a colourless oil.

IR ν (neat, cm⁻¹): 1595, 1642, 2838, 2918, 3021, 3070.

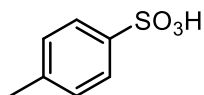
¹H NMR (400 MHz, Chloroform-*d*) δ 7.80 (d, *J* = 8.3 Hz, 2H, ArH), 7.35 (d, *J* = 8.1 Hz, 2H, ArH), 5.75 – 5.50 (m, 3H, H-1, H-2 and H-12), 4.96 – 4.81 (m, 2H, H-13), 4.60 (dt, *J* = 8.0, 5.1 Hz, 1H, H-8), 2.47 (s, 3H, H-18), 2.22 – 1.91 (m, 9H, aliphatic Protons), 1.74 – 1.63 (m, 2H, aliphatic Protons).

¹³C NMR (101 MHz, Chloroform-*d*) δ 144.0, 134.8, 133.8, 129.2, 127.4, 125.2, 124.6, 116.4, 86.4, 48.5, 37.9, 34.7, 32.8, 26.4, 25.2, 21.1 (1 resonance missing due to overlapping signals).

HRMS (ESI) *m/z* calculated for C₁₉H₂₄O₃S [M]: 332.1446. Not Found. However, fragment C₁₂H₁₇ calculated [M+H]⁺: 161.1330. Found: 161.1335. Additionally, fragment C₇H₉SO₃ calculated [M+H]⁺: 173.0272. Found 173.0277. This fragment corresponding to the elimination of the tosylate group within the molecule.



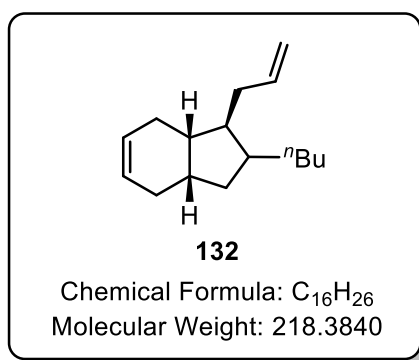
Chemical Formula: C₁₂H₁₆
Exact Mass: 160.1252



Chemical Formula: C₇H₈O₃S
Exact Mass: 172.0194

R_f = 0.32 (10% Et₂O/ Petroleum ether)

Attempted Synthesis of (1S,2R,3aS,7aS)-1-allyl-2-butyl-2,3,3a,4,7,7a-hexahydro-1H-indene.



CuCN was placed in a dry two-necked flask and THF (1mL) was added. The resulting slurry was cooled to -78 °C and *n*butyllithium was added dropwise. The heterogeneous mixture was allowed to warm to 0°C, at which temperature it was stirred for a further 1-2 min and then recooled to -78°C. To the now turbid mixture was added the alkyl bromide **169** (90 mg, 0.37 mmol) as a solution in THF (1 mL) and the mixture stirred at 0 °C. The mixture was quenched by the addition of 10 % concentrated NH₄OH /saturated NH₄Cl solution and extracted with Et₂O (3x). The combined organic extracts were then subsequently dried over Na₂SO₄, filtered and the solvent concentrated *in vacuo* to give a brown oil. The brown oil was then analysed by ¹H NMR spectroscopy.

Following **General Procedure A**, data are presented as (a) amount and mmol of CuCN, (b) THF (c) amount and mmol of *n*butyllithium, and, (d) ¹H NMR analysis.

Scheme 121

(a) 51 mg, 0.58 mmol (b) 0.44 mL, 1.1 mmol, (c) 1 mL and, (d) Starting material observed and an indication of the desired product was also observed.

Scheme 122

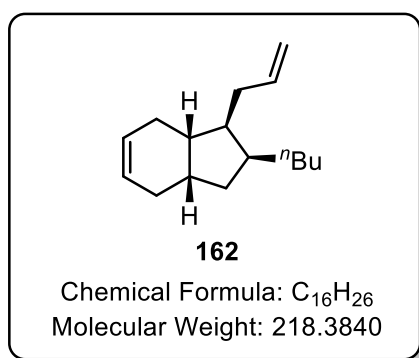
(a) 153 mg, 1.68 mmol (b) 1.32 mL, 3.3 mmol, (c) 3 mL and, (d) No starting material or desired product observed.

Scheme 124

The reaction was carried out as documented in the literature procedure.⁵³

In air, CuI (9.5mg, 0.05 mmol), LiO^tBu (80mg, 1 mmol), and ⁿbutyl BPin (138 mg, 0.75 mmol) were added to a Schlenk tube equipped with a stirrer bar. The vessel was evacuated and filled with argon (3x). The alkyl bromide **169** (120 mg, 0.5mmol), and DMF (0.5 mL) were added in turn. The resulting reaction mixture was stirred vigorously at 0 °C for 12 h. The reaction mixture was then diluted with Et₂O, filtered through silica gel with Et₂O, and concentrated in vacuo to give a colourless residue. ¹H NMR analysis gave no indication of the formation of the desired product or of remaining starting material.

Attempted Synthesis of (1S,2R,3aS,7aS)-1-allyl-2-butyl-2,3,3a,4,7,7a-hexahydro-1H-indene.



Scheme 124

The reaction was carried out as documented in the literature procedure.⁵⁴

In air, CuI (9.5 mg, 0.05 mmol), 2,2-bipyridyl (31 mg, 0.2 mmol) and LiOMe (19 mg, 0.5 mmol) were added to a Schlenk tube equipped with a stirrer bar. The vessel was then evacuated and filled with argon (3x). The alkyl tosylate **170** (121 mg, 0.5 mmol) and ⁿbutylmagnesium bromide (0.99 M in THF, 1 mL) were added in turn, under an atmosphere of argon at 0 °C. The resulting reaction mixture was stirred vigorously at °C for 24 h. The reaction mixture was then quenched by the addition of a saturated aqueous solution of NH₄Cl. The resulting solution mixture was then extracted with Et₂O (3x). The combined organic extracts were then subsequently dried over Na₂SO₄, filtered and had the solvent

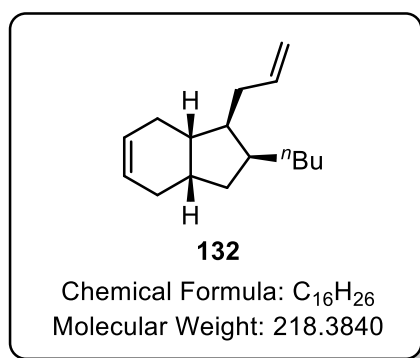
removed *in vacuo* to give a yellow oil. ^1H NMR analysis gave no indication of the formation of the desired product or remaining starting material.

Scheme 125

The reaction was carried out as documented in the literature procedure.⁵⁵

In air, CuI (9.5 mg, 0.05 mmol) and LiOMe (19 mg, 0.5 mmol) were added to a Schlenk tube equipped with a stirrer bar. The vessel was then evacuated and filled with argon (3x). The alkyl tosylate **170** (121 mg, 0.5 mmol), TMEDA (15 μL , 0.1 mmol) and *n*-butylmagnesium bromide (0.99 M in THF, 1 mL) were added in turn, under an atmosphere of argon at 0 $^\circ\text{C}$. The resulting reaction mixture was stirred vigorously at $^\circ\text{C}$ for 24 h. The reaction mixture was then quenched by the addition of a saturated aqueous solution of NH_4Cl . The resulting mixture was then extracted with Et_2O (3x). The combined organic extracts were then subsequently dried over Na_2SO_4 , filtered and the solvent removed *in vacuo* to give a yellow oil. The yellow oil was applied to a silica column and eluted with 1 % Et_2O / Petroleum ether (3 CV) and 30 % Et_2O /Petroleum ether (3 CV). The appropriate fractions were combined and had the solvent removed *in vacuo* to give an unidentifiable mixture (10 mg) and returned starting material (20 mg, 0.06 mmol, 12 % yield).

Attempted Synthesis of (1S,2R,3aS,7aS)-1-allyl-2-butyl-2,3,3a,4,7,7a-hexahydro-1H-indene.



Scheme 126

The reaction was carried out as documented in the literature procedure.⁵⁵

In air, CuI (9.5 mg, 0.05 mmol) and LiOMe (19 mg, 0.5 mmol) were added to a Schlenk tube equipped with a stirrer bar. The vessel was then evacuated and filled with argon (3x). The alkyl bromide **169** (120 mg, 0.5 mmol), TMEDA (15 μL , 0.1 mmol) and *n*-butylmagnesium bromide (0.99 M in THF, 1 mL) were added in turn, under an atmosphere of argon at 0 $^\circ\text{C}$. The resulting reaction mixture was stirred vigorously at $^\circ\text{C}$ for 24 h. The reaction mixture was then quenched by the addition of a saturated

aqueous solution of NH_4Cl . The resulting solution mixture was then extracted with Et_2O (3x). The combined organic extracts were then subsequently dried over Na_2SO_4 , filtered and had the solvent removed *in vacuo* to give a yellow oil. The yellow oil was applied to a silica column and eluted with 1 % Et_2O / Petroleum ether (3 CV) and 30 % Et_2O /Petroleum ether (3 CV). The appropriate fractions were combined and had the solvent removed *in vacuo* to give an unidentifiable mixture (17 mg).

1.5. References

- (1) Stephenson, G. R. *Advanced Asymmetric Synthesis: State-of-the-Art and Future Trends in Feature Technology*; Chapman & Hall, 1996.
- (2) Kende, A. S.; Fujii, Y.; Mendoza, J. S. *J. Am. Chem. Soc.* **1990**, *112*, 9645.
- (3) Heravi, M. M.; Zadsirjan, V.; Farajpour, B. *RSC Adv.* **2016**, *6*, 30498.
- (4) Shimizu, A.; Nishiyama, S. *Tetrahedron Lett.* **1997**, *38*, 6011.
- (5) Paterson, I.; Goodman, J. M.; Anne Lister, M.; Schumann, R. C.; McClure, C. K.; Norcross, R. D. *Tetrahedron* **1990**, *46*, 4663.
- (6) Nelson, S. G.; Cheung, W. S.; Kassick, A. J.; Hilfiker, M. A. *J. Am. Chem. Soc.* **2002**, *124*, 13654.
- (7) Jacobsen, E. N.; Marko, I.; Mungall, W.; Schroder, G.; Sharpless, K. B. *J. Am. Chem. Soc.* **1988**, *110*, 1968.
- (8) Paterson, I.; De Savi, C.; Tudge, M. *Org. Lett.* **2001**, *3*, 3149.
- (9) Jefford, C. W.; Bernardinelli, G.; Tanaka, J.-I.; Higa, T. *Tetrahedron Lett.* **1996**, *37*, 159.
- (10) Clayden, J.; Greeves, N.; Warren, S.; Wothers, P. *Organic Chemistry*; 2001.
- (11) Deslongchamps, P. *Stereoelectronic Effects in Organic Chemistry*; 1983.
- (12) Shirai, R.; Tanaka, M.; Koga, K. *J. Am. Chem. Soc.* **1986**, *108*, 543.
- (13) Simpkins, N. S. *J. Chem. Soc. Chem. Commun.* **1986**, No. 1, 88.
- (14) Kimbrough, R.; Gaines, T. B. *Nature* **1966**, *211*, 146.
- (15) Cousins, R. P. C.; Simpkins, N. S. *Tetrahedron Lett.* **1989**, *30*, 7241.
- (16) Cox, P. J.; Simpkins, N. S. *Synlett* **1991**, *1991*, 321.
- (17) Bunn, B. J.; Simpkins, N. S. *J. Org. Chem.* **1993**, *58*, 533.
- (18) Majewski, M.; Lazny, R.; Nowak, P. *Tetrahedron Lett.* **1995**, *36*, 5465.
- (19) Sugasawa, K.; Shindo, M.; Noguchi, H.; Koga, K. *Tetrahedron Lett.* **1996**, *37*, 7377.
- (20) Romesberg, F. E.; Gilchrist, J. H.; Harrison, A. T.; Fuller, D. J.; Collum, D. B. *J. Am. Chem. Soc.* **1991**, *113*, 5751.

- (21) Hall, P. L.; Gilchrist, J. H.; Harrison, A. T.; Fuller, D. J.; Collum, D. B. *J. Am. Chem. Soc.* **1991**, *113*, 9575.
- (22) Bennie, L. S.; Kerr, W. J.; Middleditch, M.; Watson, A. J. B. *Chem. Commun.* **2011**, *47*, 2264.
- (23) Henderson, K. W.; Kerr, W. J.; Moir, J. H. *Chem. Commun.* **2000**, No. 6, 479.
- (24) Anderson, J. D.; García García, P.; Hayes, D.; Henderson, K. W.; Kerr, W. J.; Moir, J. H.; Fondekar, K. P. *Tetrahedron Lett.* **2001**, *42*, 7111.
- (25) Henderson, K. W.; Kerr, W. J.; Moir, J. H. *Synlett* **2001**, *2001*, 1253.
- (26) Kerr, W. J.; Watson, A. J. B.; Hayes, D. *Chem. Commun.* **2007**, *46*, 5049.
- (27) Kowalski, C.; Creary, X.; Rollin, A. J.; Burke, M. C. *J. Org. Chem.* **1978**, *43*, 2601.
- (28) Kerr, W. J.; Watson, A. J. B.; Hayes, D. *Org. Biomol. Chem.* **2008**, *6*, 1238.
- (29) Kerr, W.; Watson, A.; Hayes, D. *Synlett* **2008**, *2008*, 1386.
- (30) Kerr, W. J.; Lindsay, D. M.; Patel, V. K.; Rajamanickam, M. *Org. Biomol. Chem.* **2015**, *13*, 10131.
- (31) Chen, H.; Huang, Z.; Hu, X.; Tang, G.; Xu, P.; Zhao, Y.; Cheng, C.-H. *J. Org. Chem.* **2011**, *76*, 2338.
- (32) Sellars, J. D.; Steel, P. G. *Chem. Soc. Rev.* **2011**, *40*, 5170.
- (33) Rajamanickam, M. *The Asymmetric Synthesis of Enol Phosphates and Their Application in Total Synthesis*, University of Strathclyde, 2015.
- (34) Casapullo, A.; Scognamiglio, G.; Cimino, G. *Tetrahedron Lett.* **1997**, *38*, 3643.
- (35) Henderson, A. R.; Stec, J.; Owen, D. R.; Whitby, R. J. *Chem. Commun.* **2012**, *48*, 3409.
- (36) Rousset, C. J.; Swanson, D. R.; Lamaty, F.; Negishi, E. *Tetrahedron Lett.* **1989**, *30*, 5105.
- (37) Gallantree-Smith, H. C.; Antonsen, S. G.; Görbitz, C. H.; Hansen, T. V.; Nolsøe, J. M. J.; Stenstrøm, Y. H. *Org. Biomol. Chem.* **2016**, *14*, 8433.
- (38) Antonsen, S.; Gallantree-Smith, H.; Görbitz, C.; Hansen, T.; Stenstrøm, Y.; Nolsøe, J. *Molecules* **2017**, *22*, 1720.
- (39) Nolsøe, J. M. J.; Antonsen, S.; Görbitz, C. H.; Hansen, T. V.; Nesman, J. I.; Røhr, Å. K.; Stenstrøm, Y. H. *J. Org. Chem.* **2018**, *83*, 15066.
- (40) Friedrich Marks, G. F. *Prostaglandins, Leukotrienes, and Other Eicosanoids: From Biogenesis to*

- Clinical Application*; Wiley-VCH, 1999.
- (41) Bennie, L. S. The Development and Application of Magnesium Amide Bases in Asymmetric Synthesis, University of Strathclyde, 2012.
- (42) Weber, T. The Development and Application of Magnesium Base-Mediated Transformations., University of Strathclyde, 2013.
- (43) Mundy, B. P.; Theodore, J. J. *J. Am. Chem. Soc.* **1980**, *102*, 2005.
- (44) Takano, S.; Moriya, M.; Ogasawara, K. *Tetrahedron Lett.* **1992**, *33*, 1909.
- (45) Boeckman, R. K.; Wang, H.; Rugg, K. W.; Genung, N. E.; Chen, K.; Ryder, T. R. *Org. Lett.* **2016**, *18*, 6136.
- (46) Netherton, M. R.; Dai, C.; Neuschütz, K.; Fu, G. C. *J. Am. Chem. Soc.* **2001**, *123*, 10099.
- (47) Terao, J.; Naitoh, Y.; Kuniyasu, H.; Kambe, N. *Chem. Lett.* **2003**, *32*, 890.
- (48) Hoeller, C.; Reznicek, G.; Huefner, A. *Monatshefte für Chemie / Chem. Mon.* **2004**, *135*, 447.
- (49) Lutz, V.; Baro, A.; Fischer, P.; Laschat, S. *European J. Org. Chem.* **2010**, *2010*, 1149.
- (50) Lipshutz, B. H.; Wilhelm, R. S.; Kozlowski, J. A.; Parker, D. *J. Org. Chem.* **1984**, *49*, 3928.
- (51) Noda, D.; Sunada, Y.; Hatakeyama, T.; Nakamura, M.; Nagashima, H. *J. Am. Chem. Soc.* **2009**, *131*, 6078.
- (52) Bedford, R. B.; Brenner, P. B.; Carter, E.; Cogswell, P. M.; Haddow, M. F.; Harvey, J. N.; Murphy, D. M.; Nunn, J.; Woodall, C. H. *Angew. Chemie Int. Ed.* **2014**, *53*, 1804.
- (53) Yang, C.-T.; Zhang, Z.-Q.; Liu, Y.-C.; Liu, L. *Angew. Chemie Int. Ed.* **2011**, *50*, 3904.
- (54) Liu, J.-H.; Yang, C.-T.; Lu, X.-Y.; Zhang, Z.-Q.; Xu, L.; Cui, M.; Lu, X.; Xiao, B.; Fu, Y.; Liu, L. *Chem. - A Eur. J.* **2014**, *20*, 15334.
- (55) Xu, S.; Oda, A.; Bobinski, T.; Li, H.; Matsueda, Y.; Negishi, E. *Angew. Chemie Int. Ed.* **2015**, *54*, 9319.
- (56) Love, B. E.; Jones, E. G. *J. Org. Chem.*, **1999**, *64*, 3755.
- (57) Krasovskiy, A.; Knochel, P. *Synthesis.* **2006**, *2006*, 890.
- (58) de Mier-Vinue, J.; Montana, a M.; Moreno, V.; Prieto, M. J. *Zeitschrift für Anorg. und Allg. Chemie* **2005**, *631*, 2054.

- (59) Hickmann, V.; Kondoh, A.; Gabor, B.; Alcarazo, M.; Fürstner, A. *J. Am. Chem. Soc.* **2011**, *133*, 13471.
- (60) Reid, B. T.; Mailyan, A. K.; Zakarian, A. *J. Org. Chem.* **2018**, *83*, 9492.
- (61) Seifert, T.; Malo, M.; Kokkola, T.; Engen, K.; Fridén-Saxin, M.; Wallén, E. A. A.; Lahtela-Kakkonen, M.; Jarho, E. M.; Luthman, K. *J. Med. Chem.* **2014**, *57*, 9870.
- (62) Egger, J.; Bretscher, P.; Freigang, S.; Kopf, M.; Carreira, E. M. *J. Am. Chem. Soc.* **2014**, *136*, 17382.
- (63) Kislukhin, A. A.; Hong, V. P.; Breitenkamp, K. E.; Finn, M. G. *Bioconjug. Chem.* **2013**, *24*, 684.
- (64) Alexakis, A.; Gille, S.; Prian, F.; Rosset, S.; Ditrach, K. *Tetrahedron Lett.* **2004**, *45*, 1449.
- (65) Hong, A. Y.; Krout, M. R.; Jensen, T.; Bennett, N. B.; Harned, A. M.; Stoltz, B. M. *Angew. Chemie Int. Ed.* **2011**, *50*, 2756.
- (66) Sloan, G. Extended Application of Magnesium Amide Base Reagents in Target Synthesis, University of Strathclyde, 2014.
- (67) Bonafoux, D.; Bordeau, M.; Biran, C.; Cazeau, P.; Dunogues, J.; Iversen, S. *Tetrahedron* **1996**, *3263*, 5532.
- (68) Benohoud, M.; Tuokko, S.; Pihko, P. M. *Chem. - A Eur. J.* **2011**, *17*, 8404.
- (69) Slade, D. J.; Pelz, N. F.; Bodnar, W.; Lampe, J. W.; Watson, P. S. *J. Org. Chem.* **2009**, *74*, 6331.
- (70) Parmar, D.; Price, K.; Spain, M.; Matsubara, H.; Bradley, P. A.; Procter, D. J. *J. Am. Chem. Soc.* **2011**, *133*, 2418.
- (71) Stork, G.; Brizzolara, A.; Landesman, H.; Szmuszkovicz, J.; Terrell, R. *J. Am. Chem. Soc.* **1963**, *85*, 207.
- (72) Cahiez, G.; Gager, O.; Habiak, V. *Synthesis*. **2008**, *2008*, 2636.
- (73) Starostin, E. K.; Furman, D. B.; Ignatenko, A. V.; Barkova, A. P.; Nikishin, G. I. *Russ. Chem. Bull.* **2006**, *55*, 2016.

Chapter Two

Structural Elucidation of Mucosin *via*

Computational Chemistry

2.1. Introduction

Typically, structural elucidation of natural products and their derivatives can be achieved by X-ray crystallography, allowing for unambiguous determination of their structure and relative stereochemistry.^{1,2} However, natural products with a high degree of conformational flexibility are often isolated as oils and therefore cannot be crystallised, meaning that the assignment of their structure and relative stereochemistry can only be carried out *via* NMR spectroscopy. Despite NMR spectroscopy being a very powerful tool in structural determination, it has often led to the misassignment of the relative stereochemistry in some natural products, typically discovered through, often arduous, total synthesis.^{3,4,5} As a result, new methods to aid structural elucidation of such natural products have been highly sought. Recently, computational methods have gained popularity for correctly assigning the relative stereochemistry of several natural products, *via* the computation of spectroscopic properties.^{6,7}

2.1.1. Calculation of NMR Chemical Shifts

Obtaining accurately calculated chemical shifts is a multi-step process. Initially, the geometry of a candidate structure needs to be obtained. Bifulco and co-workers noted that for conformationally rigid structures it is possible to obtain accurate chemical shifts by performing NMR GIAO calculations on the global minimum, easily achieved using DFT calculations alone.⁸ However, Bifulco identified that for highly flexible molecules, that may exist as multiple conformers in equilibrium, NMR GIAO (Gauge-Independent Atomic Orbital) calculations on the global minimum, alone, would not allow for accurately calculated chemical shifts.⁹ Indeed, to achieve accurately calculated chemical shifts for highly flexible chemical systems, Bifulco *et al.* propose that NMR GIAO calculations are carried out on all low energy conformers for the candidate structure. Having obtained the calculated shielding tensor for the low energy conformers a Boltzmann weighting can be applied to obtain averaged shielding tensors for each nucleus; this is represented in Equation 2.

$$\sigma^x = \frac{\sum_i \sigma_i^x \exp\left(\frac{-E_i}{RT}\right)}{\sum_i \exp\left(\frac{-E_i}{RT}\right)}$$

σ^x is the Boltzmann-averaged shielding tensor for nucleus x .

σ_i^x is the shielding tensor for nucleus x in conformer i .

E_i is the potential energy of conformer i (relative to the global minimum), obtained from the single-point *ab initio* calculation.

Equation 2 - Boltzmann-averaged shielding tensors

Having calculated shielding tensors, to obtain chemical shifts they need to be referenced to the shielding tensor of a suitable reference compound, typically tetramethylsilane. It has also been demonstrated by Sarotti and co-workers that the use of multiple reference compounds can increase the accuracy of calculated chemical shifts, by using benzene as the reference for sp^2 hybridised nuclei and methanol for sp^3 hybridised nuclei.¹⁰ This multi-standard method appears not to be widely adopted and tetramethylsilane is typically used. Shielding tensors can be converted into chemical shifts using Equation 3.

δ_{calc}^x is the calculated shift for nucleus x (in ppm).

σ^x is the shielding constant for nucleus x .

$$\delta_{calc}^x = \frac{\sigma^o - \sigma^x}{1 - \sigma^o/10^6}$$

σ^o is the shielding constant for the carbon nuclei in tetramethyl silane, which was obtained from a NMR GIAO calculation on tetramethyl silane.

Equation 3 - Calculating chemical shifts from shielding tensors

Despite significant improvements in NMR GIAO calculations, calculated NMR chemical shifts contain a significant degree of error, with average errors as high as 0.4 ppm for ^1H resonances and 10 ppm for ^{13}C resonance, which are clearly unusable for most applications.^{11,12} Considering this, it becomes necessary to correct calculated chemical shifts to remove the systematic error associated with the calculation of chemical shifts. Empirical scaling has proven to be a general method in correcting calculated shifts to achieve accurate data. This can be carried out in two ways; if experimental data is available for the calculated structure, a correction can be carried out *via* linear regression of the experimental vs the calculated chemical shifts. From this, linear regression values of the slope, m , and

y-intercept, c , which are referred to as scaling factors, can be obtained and used to scale chemical shifts using Equation 4.

$$\delta_{scaled} = (\delta_{unscaled} - c) / m$$

Equation 4- Scaling chemical shifts

Alternatively, if experimental data is unavailable it is possible to use generalised scaling factors which have been determined from a test-set of compounds at a specific level of computational theory. From the test-set, it is possible to extract the linear regression values for the slope, m , and y-intercept, c , and scale calculated chemical shifts using the previously mentioned equation. The main drawback of generalised scaling factors is that the shielding tensors need to be calculated, at the specific level of computational theory, for every compound in the given test-set before the scaling factors can be extracted and applied to the calculated chemical shifts of the computed molecule of interest. Fortunately, the CHEmical SHift REpository (CHESHIRE), a vast online resource, exists containing scaling factors across numerous levels of computational theory, allowing the computational chemist to scale calculated chemical shifts with ease.¹³ It has been shown within the chemical literature that scaling calculated chemical shifts allows for a significant reduction in error.¹¹ The application of scaled chemical shifts has been demonstrated within the literature, highlighting the utility of these methods.¹⁴

2.1.2. Elatenyne

In 2008, Burton and co-workers published their research on the originally proposed structure of elatenyne **176**, consisting of a fused tetrahydropyran ring system bearing an enyne appendage (Figure 17).¹⁵

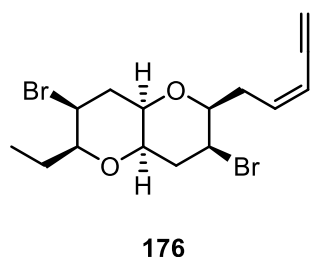


Figure 17 - Originally proposed structure for elatenyne

Through their valiant total synthesis efforts, it became evident that the natural product elatenyne was unlikely to feature the pyrano[3,2]pyran ring system, as first proposed during its isolation and initial

characterisation. Indeed, Burton and co-workers suggested it was more probable the gross structure of elatenyne contained a 2,2'-bifuranyl system **177** (Figure 18).¹⁶

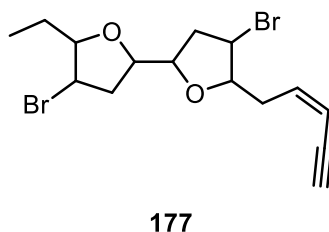


Figure 18 - Reassigned gross structure for elatenyne

Having reassigned the gross structure of elatenyne **177**, at this point, the total synthesis and structural reassignment of elatenyne seemed an insurmountable challenge, with 32 possible diastereomers, without re-isolation and independent characterisation of the natural product. Despite this, Goodman proposed that computation could prove a valuable tool in the structural elucidation of elatenyne.¹⁶ Having computed ¹³C NMR spectra for the 32 possible diastereomers of elatenyne, Goodman then compared the computed spectra of each diastereomer to that of the experimental data obtained from the isolation. Through the use of a variety of statistical parameters in order to quantify the probability that one or more of the computed ¹³C spectra matched the experimental data, Goodman was able to narrow down the number of likely candidates for synthesis. The correlation coefficients between the respective diastereomer and the experimental data identified three possible structures for elatenyne **178-180** (Figure 19).

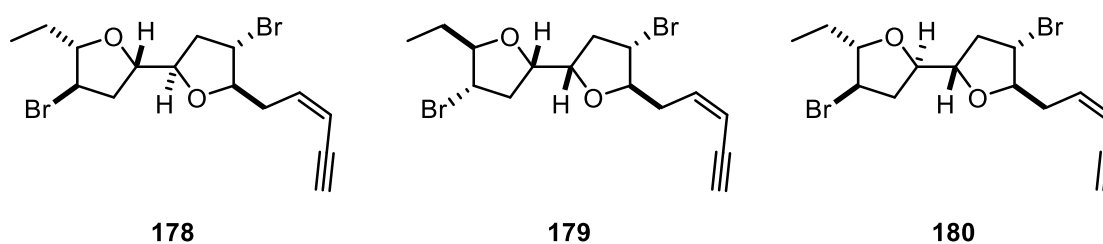


Figure 19 - Probable candidates for the structure of elatenyne based on correlation coefficients

In addition, mean absolute error (MAE) values were calculated for each computed ¹³C spectrum, identifying the three same probable structures **178-180**, along with an additional structure **181**, that was likely to be the natural product based on low MAE values (Figure 20).

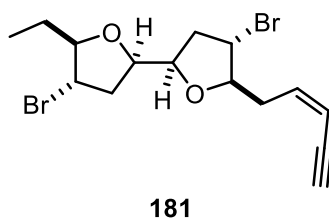


Figure 20 - Candidate structure for elatenyne based on MAE

With Goodman having identified four candidate structures from a possible 32, Burton *et al.* revisited the total synthesis of elatenyne, targeting the most likely structure predicted by Goodman and corroborated by Burton's biosynthetic reasoning.¹⁷ In 2012, Burton and Kim completed the total synthesis of elatenyne **182** (Figure 21) and its enantiomer demonstrating that DFT-computed NMR spectra can allow for the structure elucidation of relatively flexible molecules, ultimately, shortening the synthetic time required for the structural elucidation of molecules with a large number of possible stereochemical isomers.

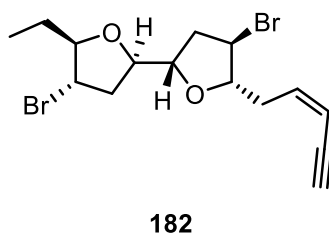


Figure 21 - Revised structure of elatenyne

The use of computational modelling to identify the correct diastereomer from the potential candidate stereoisomers was proven to be effective in the elucidation of elatenyne **182**. It also highlighted the need for more robust quantification of the probability that computed spectral data match the experimental data. The use of correlation coefficients and MAE resulted in four likely candidates from a possible 32 and despite being a significant advance, improvements in this methodology that could allow for the correct identification of a single stereoisomer from numerous candidate stereoisomers, would clearly be advantageous.

2.1.3. DP4

In 2010, Goodman *et al.* developed the DP4 methodology, which was designed to allow for a reliable assignment of stereochemistry with quantifiable probability when only a single experimental dataset is available.¹⁸ Using empirically scaled chemical shifts for each candidate structure, the difference between the scaled shifts and experimental shifts gives the error e . An assumption is then made that the error for each nucleus obeys a single t -distribution with a mean μ , standard deviation σ and

degrees of freedom ν . The probabilities of each observed error are then multiplied together to give the probability for that candidate structure, which is then, in turn, converted into the probability that each candidate structure is the correct one *via* Bayes's theorem. This can be described mathematically by Equation 5.

$$P = \frac{\prod \left(T^{\nu} \left(\frac{|\delta_{scaled} - \delta_{exp}| - \mu}{\sigma} \right) \right)}{\sum \left[\prod \left(T^{\nu} \left(\frac{|\delta_{scaled} - \delta_{exp}| - \mu}{\sigma} \right) \right) \right]}$$

Equation 5 - DP4 probability

To obtain values of μ , σ and ν for determining the probability that a calculated candidate structure matches the experimental data, a test-set of molecules, which cover 1717 ^{13}C shifts and 1794 ^1H shifts, had their ^1H and ^{13}C NMR spectra calculated using the computationally inexpensive B3LYP^{19–22} functional and 6-31G(d,p) basis set.²³ The mean μ has a value of 0, as a result of the empirical scaling of calculated chemical shifts. The standard deviation σ was calculated to be 2.306 ppm for ^{13}C chemical shifts and 0.185 ppm for ^1H chemical shifts. Finally, for the value of ν , the calculated data from the test-set was fitted to a *t*-distribution and the ν was recorded.¹⁸

To exemplify the power DP4 has in assigning a single stereoisomer to an experimental dataset, several natural products had their ^{13}C and ^1H NMR spectra calculated, and a variety of statistical approaches were benchmarked (Figure 22).

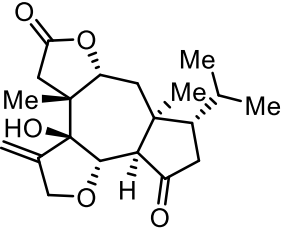
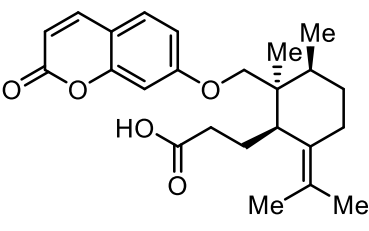
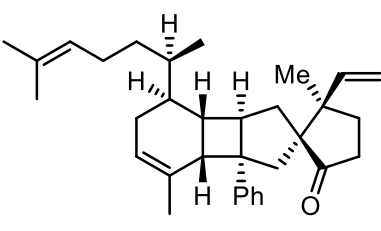
		
Tricholomalide A	Galbanic Acid	Biyouyanagin A
183	184	185
Correlation Coefficient: 36.77 %	Correlation Coefficient: 29.39 %	Correlation Coefficient: 43.08 %
MAE: 13.21 %	MAE: 23.89 %	MAE: 40.19 %
CMAE: 46.01 %	CMAE: 39.60 %	CMAE: 43.62 %
DP4: >99.99 %	DP4: 99.37 %	DP4: 49.97 %

Figure 22 - Exemplar molecules and their respective probabilities

In the case of Tricholomalide A **183**, which has 64 possible diastereomers, all statistical treatments of the data identified the correct structure as the most probable structure, with MAE performing the worst. Improved confidence is observed with the correlation coefficient and CMAE (corrected mean absolute error), but DP4 displayed exceptional confidence, in predicting the correct diastereomer with >99.99% probability, highlighting the power DP4 can have with such rigid structures. A similar story is observed with Galbanic acid **184**, a natural product featuring a greater number of rotatable bonds in comparison to Tricholomalide A **183**, with MAE performing poorly in comparison to the other statistical approaches. Despite the relatively poor performances using the correlation coefficient, MAE and CMAE, DP4 once again demonstrates excellent performance in selecting the correct diastereomer with >99 % probability. However, Goodman's publication highlights some examples where DP4 performs poorly, and one such example is Biyouyanagin A **185**. In the case of Biyouyanagin A **185**, DP4 only gives a 49.97 % probability for the correct diastereomer, which is only slightly better than the approximately 40 % probability observed with the other methods. The mediocre performance of DP4 with Biyouyanagin A **185** demonstrates that Goodman's initial iteration of DP4 was far from a general tool, as of 2010.

2.1.4. DP4+

In 2015, Sarotti *et al.* published their research on an improved DP4-like methodology.²⁴ Their modifications addressed two major shortcomings from Goodman's initial DP4 publication: 1) the level of computational theory utilised and 2) the exclusive use of scaled chemical shifts in calculating probability. Sarotti acknowledged that Goodman's use of B3LYP/6-31G(d,p) and no DFT geometry optimisation was used to keep computational costs low but raised concerns regarding the accuracy of the calculated NMR spectra obtained from this approach. Comparing the respective CMAE values of the ¹H and ¹³C computed chemical shifts, for two compounds **186** and **187** calculated at different levels of theory, demonstrated the varying levels of accuracy that can be achieved at different levels of computational theory.

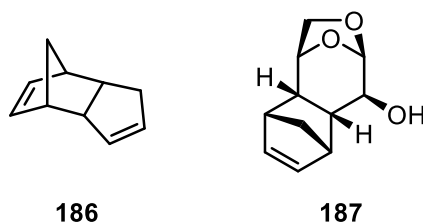


Figure 23 - Example compounds for accuracy comparison

Table 30 - Sarroti's comparison of the accuracy of calculated chemicals shifts

Entry	Level of Theory	Compound 186		Compound 187	
		¹ H	¹³ C	¹ H	¹³ C
1	B3LYP/6-31G(d,p)//MMFF	0.12	1.5	0.21	1.9
2	B3LYP/6-31G(d,p)//B3LYP/6-31G(d)	0.08	0.9	0.12	1.2
3	PCM/mPW1PW91/6-31+G(d,p)//B3LYP/6-31G(d)	0.06	0.6	0.09	1.1

Sarroti *et al.* demonstrated that for the two compounds **186** and **187**, the calculated ¹H and ¹³C spectra have a reduced CMAE when DFT level optimisation is carried out on each conformer (Table 30, Entry 2). This reduced CMAE highlights that the accuracy of NMR shift calculations can increase when switching from MMFF optimised geometries to B3LYP optimised geometries. Additionally, the inclusion of solvent and greater levels of theory for the NMR shift calculations afforded a further reduction of the CMAE (Table 30, Entry 3). Sarroti proposed that the inclusion of DFT optimised geometries and greater levels of computational theory in the NMR shift calculations would prove beneficial in improving the performance of DP4.

Goodman's treatment of the associated errors of each calculated shift assumed they followed a single *t*-distribution.¹⁸ However, Sarroti discusses how the distribution of errors associated with unscaled chemical shifts was best described by two overlapping *t*-distributions and was observed for both ¹H and ¹³C shifts under numerous levels of theory.²⁴ It is postulated that the two *t*-distributions represent sp² and sp³ chemical environments. As a result, Sarroti suggests the DP4 probability calculation should include unscaled chemical shifts to ascertain accurate probabilities and refers to this modification as the DP4+ probability. This is represented mathematically by Equation 6.

$$P = \frac{\prod \left(T^v \left(\frac{|\delta_{scaled} - \delta_{exp} - \mu|}{\sigma_{scaled}} \right) \right) \left(T^v \left(\frac{|\delta_{unscaled} - \delta_{exp} - \mu|}{\sigma_{unscaled}} \right) \right)}{\sum \left[\prod \left(T^v \left(\frac{|\delta_{scaled} - \delta_{exp} - \mu|}{\sigma_{scaled}} \right) \right) \left(T^v \left(\frac{|\delta_{unscaled} - \delta_{exp} - \mu|}{\sigma_{unscaled}} \right) \right) \right]}$$

Equation 6 - DP4+ probability

The cumulative effect of Sarroti's modifications to the DP4 methodology was showcased in the probabilities obtained from the correlation of experimental data with the calculated structures of cryptomoscatone D1 and cryptomoscatone D2. Cryptomoscatone D1 and D2 were isolated from the

bark of *Cryptocarya mandiocanna* by Yoshida *et al.*, who were able to determine the absolute configuration of the dihydropyran-2-one stereocentre but were unable to elucidate the relative stereochemistry of the remaining two alcohol-bearing stereocentres.²⁵ The stereochemical elucidation was, ultimately, solved *via* traditional synthetic methods.²⁶ However, using computational methods, Sarotti demonstrated the increased effectiveness of DP4+ in a case study where the traditional DP4 methodology, developed by Goodman *et al.*, had failed.²⁴ The experimental data obtained from both, cryptomoscatone D1 **188** and D2 **189** was assigned to the incorrect stereoisomer when DP4 was employed (Figure 24).

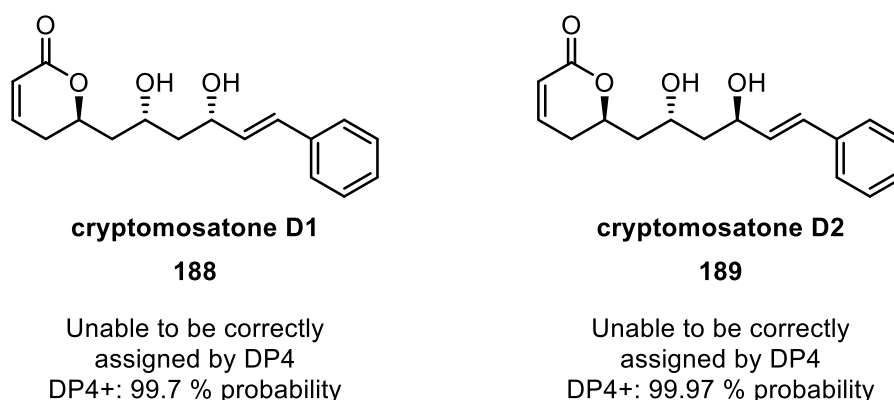


Figure 24 - Cryptomoscatone D1 and D2 and their respective DP4 and DP4+ performances

In stark contrast, DP4+, developed by Sarotti and co-workers, shows excellent agreement of the experimental data with the correct diastereomer with both cryptomoscatone D1 **188** and D2 **189**. This highlights another tool that can be used by the computational chemist, when DP4 has failed to confirm the correct structure. Additionally, Sarotti *et al.* also demonstrate potential pitfalls associated with DP4 methodology, in the case of potentially inadequate geometry optimisation and exclusion of unscaled chemical shifts in probability calculations.

2.1.5. DP4.2

In 2017, Goodman reported further improvements on his DP4 methodology, mainly addressing the drawbacks identified and demonstrated by Sarotti *et al.* in their publication.^{27,24} Goodman understood the criticism surrounding use of a single distribution to describe the errors associated with calculated chemical shifts, and sought to employ a more robust distribution. Initial attempts were made to not only describe the distribution of errors associated with calculated chemical shifts but also, dividing the chemical shift range into regions and examining how most effectively describe each region. Goodman also explored the use of greater levels of theory for both the energy calculations and the NMR GIAO calculations. Despite exploring higher levels of computational theory, Goodman opted to avoid

performing DFT level optimisations due to the computational cost and time-consuming nature, especially with compounds that generate several conformers. It was apparent to Goodman that different levels of computational theory could give differing distributions. Indeed, this was observed when comparing the distribution of errors obtained from the calculated shifts of the test-set compounds using B3LYP, M06-2X²⁸ and mPW1PW91²⁹ functionals. Ultimately, the hybrid mPW1PW91 functional proved to be well behaved as the distribution of errors could be well described using a 1-region, 2-Gaussian statistical model. However, the popular M06-2X functional, albeit better performing than B3LYP, requires a more sophisticated statistical model to perform as effectively as mPW1PW91. With these observations, Goodman proposed that by calculating the energy of the respective conformers using M06-2X/6-31G(d,p) and the NMR GIAO calculations using mPW1PW91/6-311G(d), would allow the computational chemist to obtain accurate probabilities when used in conjunction with a 1-region, 2-Gaussian statistical model. Goodman also provided numerous examples of compounds where DP4.2 outperformed the original DP4 methodology in assigning the correct diastereomers (Figure 25).

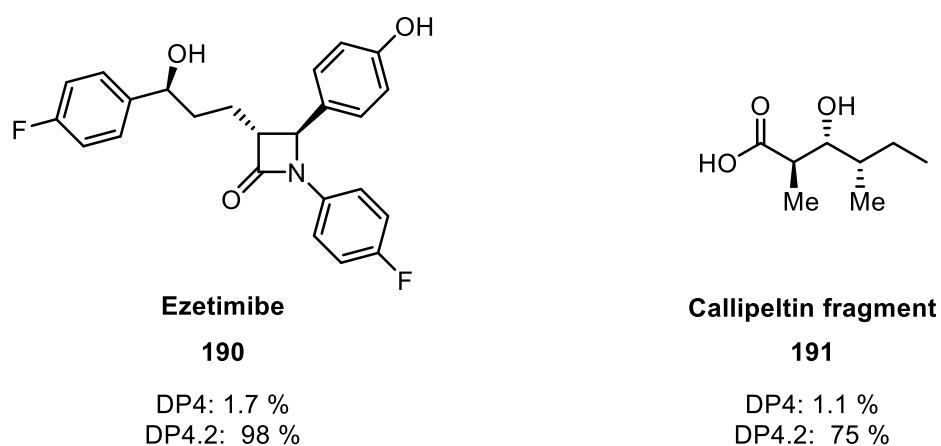


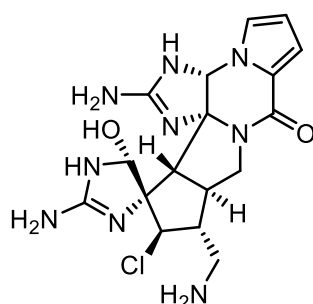
Figure 25 - Ezetimibe and Callipeltin and their respective DP4 and DP4.2 performances

Ezetimibe **190**, a drug used to treat high cholesterol levels, features three stereocentres and an sp^2 rich structure.³⁰ Using the original DP4 methodology, the correct diastereomer for Ezetimibe **190** was assigned with only a 1.7 % probability, not unsurprising when we consider Sarotti's criticisms surrounding the use of a single t -distribution to describe the errors of both sp^2 and sp^3 chemical environments. When the improved DP4.2 is employed, the NMR spectral data for Ezetimibe is assigned to the correct diastereomer with an exceptionally high 98 % probability. A similar trend is observed in the case of the Callipeltin fragment **191**, a smaller carboxylic acid bearing three stereocentres, highlighting the increased performance DP4.2 delivers when compared with the original DP4 methodology. However, no comparison to the performance of DP4+ was investigated in

Goodman's 2017 publication. Indeed, to date, unbiased benchmarking of the various DP4 methodologies is lacking in the chemical literature.

2.1.6. DiCE

More recent advances in DP4 methodology have been published in the chemical literature, notably Diastereomeric *in silico* Chiral Elucidation (DiCE) from Gonnella and co-workers.³¹ DiCE utilises a low level of computational theory and a single *t*-distribution in the probability calculation, despite the trends observed with DP4+ and DP4.2 advising against this.^{24,27} Interestingly, DiCE includes the use of calculated ¹⁵N chemical shifts to allow for improved performance with nitrogen-rich compounds, such as Palau'amine **192**, a guanidine-containing alkaloid possessing antifungal and antibiotic activity (Figure 26).³²



192

Figure 26 - Palau'amine

The authors demonstrate that DiCE has a performance similar to DP4+, and better than the original DP4 methodology but no comparison to DP4.2 is made.³¹

Thus, the comparison of calculated NMR chemical shifts to experimental NMR data has been utilised in the stereo-assignment of a range of natural products with a broad range of structures. With improvements in the statistical approaches, it is now possible, in numerous cases, for a computational chemist to narrow down to a single candidate that fits the experimental data. This is a significant improvement to the case of elatenyne, where Goodman was able to limit the candidate stereoisomers for synthesis from 32 to four.¹⁶ With this impressive utility in structural assignment, we investigated the application of DP4-type methodology to the structural elucidation of (–)-mucosin.

2.1.7. Proposed Work

As it became evident through Stenstrøm and co-worker's total synthesis efforts that (-)-mucosin had been misassigned by Casapulo, the need to identify the true structure of (-)-mucosin became increasingly imperative, in relation to our synthetic work.^{33,34} With recent advances in stereochemical assignment *via* computational chemistry, we proposed that by employing DP4 methodology, we could propose a probable structure for (-)-mucosin as a target for our total synthesis.

Initially, work focused on calculating the ¹³C chemical shifts for the eight (-)-mucosin methyl ester stereoisomers, and then utilising DP4 methodologies to obtain probabilities for all the candidate structures (Figure 27). It should be noted that due to the convoluted nature of the ¹H NMR spectra of mucosin and its stereopermutations, any computed ¹H chemical shifts will not be utilised in DP4 probability calculations.

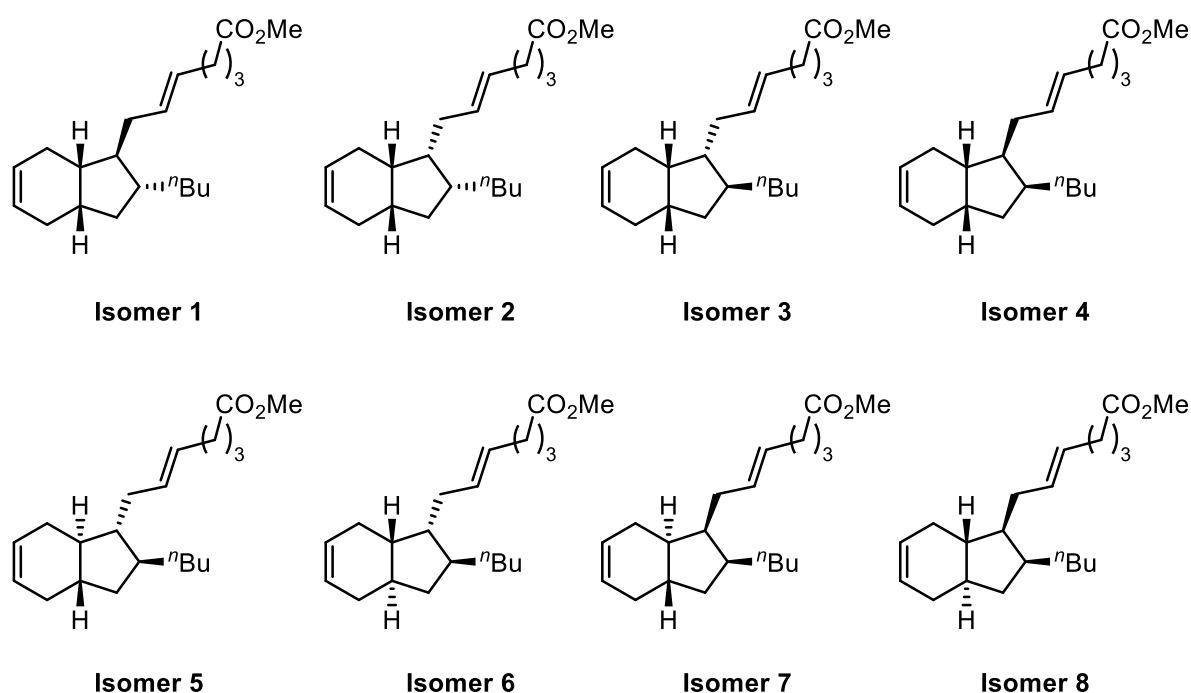


Figure 27 - Candidate structures for (-)-mucosin methyl ester

To ensure the ensure that DP4 is a reliable system for these extremely flexible oxylipin structures, it was possible to use the experimental data from Stenstrøm's synthesis of *cis*- and *exo*-mucosin to ensure a good correlation with the predicted structure. Should DP4 not prove successful in predicting the correct structures for *cis*- and *exo*-mucosin, other DP4 methodologies will be trialled, including DP4+ and DP4.2. This will allow us an opportunity to independently assess the performance of the

three DP4 methodologies, in assigning the correct stereoisomer in such a conformationally dynamic and therefore challenging system.

If good correlation of the available experimental spectra for *cis*- and *exo*-mucosin methyl esters is observed with their respective calculated ^{13}C NMR spectra, this will lend greater confidence to the structure that is predicted to match the experimental data obtained from the initial isolation and ultimately, influence our synthetic work going forward.

2.2. Results and Discussion

Under the assumption that Whitby's synthesis of (+)-mucosin featured a *cis*-bridgehead, the isotropic ^{13}C NMR shielding constants were computed for the four possible (-)-mucosin methyl ester stereoisomers containing the *cis*-bridgehead.³⁵ These initial calculations were performed using MMFF to identify the low energy conformers, and the subsequent energy and NMR GIAO calculations were computed using B3LYP/6-31G(d,p), as is required by DP4. The methyl ester of (-)-mucosin was chosen for computational modelling as the ^{13}C NMR shifts for mucosin methyl ester already have been extensively compared within the chemical literature.^{33,34}

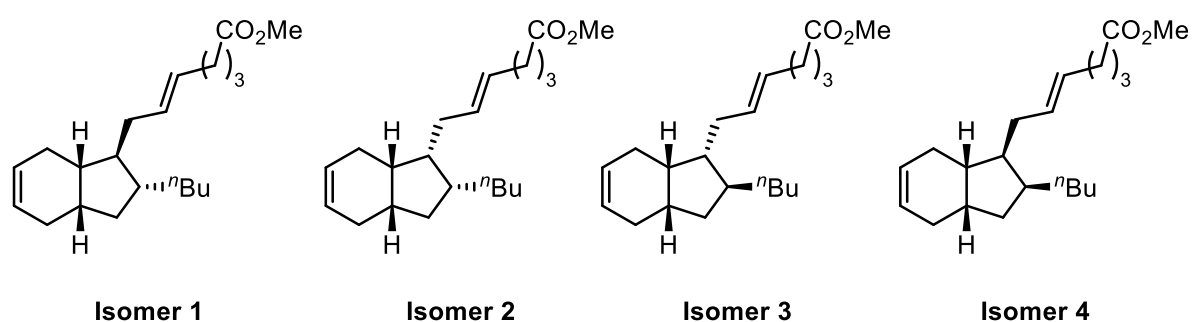


Figure 28 - Initial candidate structures of (-)-mucosin methyl ester

Once the shielding tensors were obtained, they were scaled against the, assigned, ^{13}C NMR spectrum recorded in Casapullo's isolation. The DP4 probability was then calculated, leading to the probabilities shown in Figure 29.

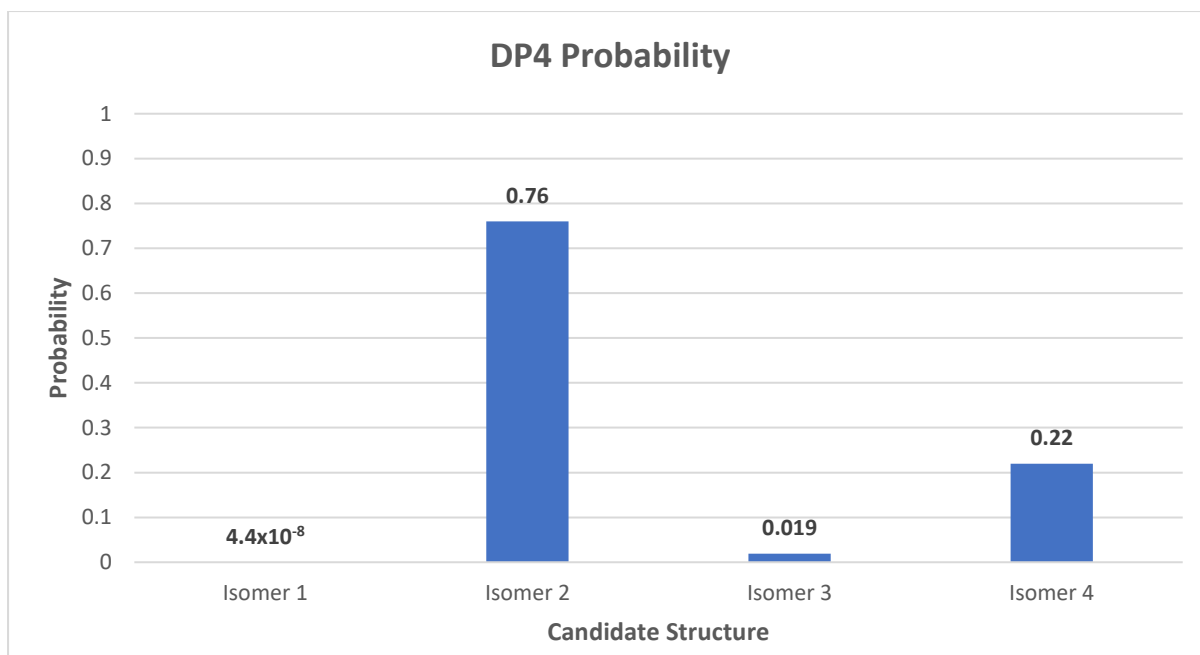


Figure 29 - DP4 Probabilities for the candidate structures of (-)-mucosin, containing a *cis*-bridgehead.

From this initial foray into structural assignment *via* DP4, two potential structures, **isomer 2** with 76 % probability, and **isomer 4** with 22 % probability, were identified as being likely candidates for the structure of (-)-mucosin methyl ester. These two structures have not been synthesised within the chemical literature, which seemed promising. However, these two structures do have the sidechains in a *syn*- relationship. In particular, **isomer 2** has both appendages pointing into the concave face of the molecule – an energetically unfavourable situation. Nevertheless, with these results in hand, the structures of **isomer 2** and **isomer 4** were targeted for synthesis (*vide supra*). However, shortly after identifying these probable structures for (-)-mucosin, Stenstrøm and co-workers confirmed the structure of the natural product, in their 2018 publication, as **isomer 5**.³⁶ It had become axiomatic that Whitby *et al.* had synthesised a structure containing a *cis*-bridgehead, but this assumption now appeared incorrect. The further four structures containing a *trans*-bridgehead had their ¹³C NMR spectra calculated and the DP4 probability of each computed structure representing the experimental data was reassessed (Figure 30, Figure 31).

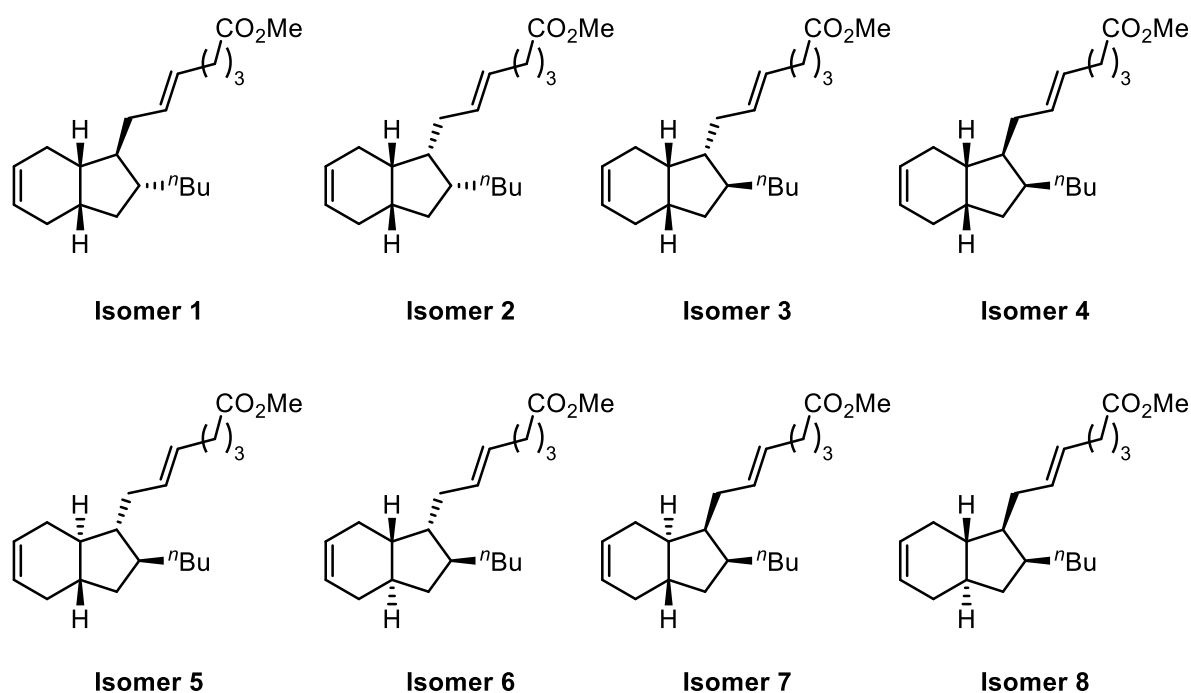


Figure 30 - Candidate structures of (-)-mucosin methyl ester

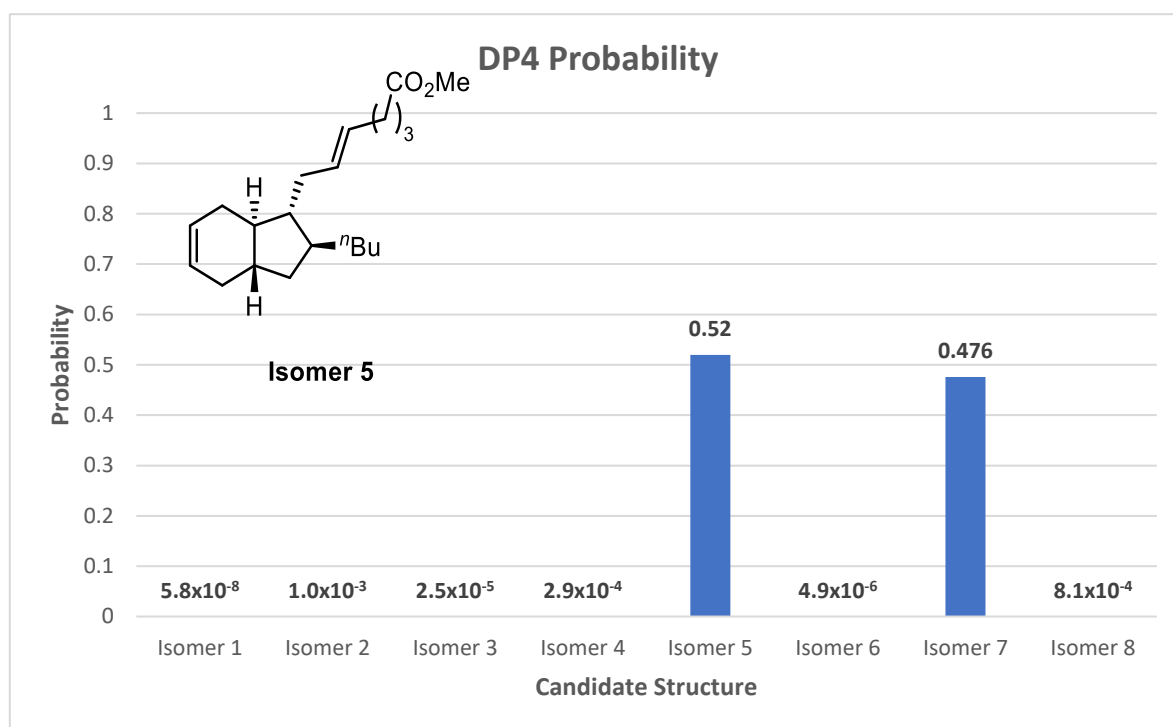


Figure 31 - DP4 Probabilities for the candidate structure of (-)-mucosin methyl ester

When considering all potential candidate structures for (-)-mucosin methyl ester, DP4 analysis suggests that the true structure of (-)-mucosin methyl ester, **isomer 5**, has a 52 % probability of being the natural product but also has high confidence in **isomer 7** with just less than 48 % probability. With

such a small margin between the two candidate structures, **isomer 5** and **isomer 7**, work then focused on understanding how to improve the DP4 probability performance.

With highly flexible oxylinin structures, such as (–)-mucosin, conformational flexibility plays a major role in the accurate calculation of NMR spectra as detailed by Bifulco.⁹ Considering this, the generation of conformers during the conformational search was revisited. Previously, the conformational search was carried out using an MCMM search and 10,000 steps. However, further investigation into the number of low energy conformers found within 10 kJmol⁻¹ of the global minimum identified that 200,000 steps were necessary for the conformational search to ensure all low energy conformers were found. With this knowledge, the conformational search was carried out using an MCMM search and 200,000 steps for each candidate structure, and the subsequent NMR GIAO and energy calculations were carried out, as previously, this resulted in newly calculated ¹³C spectra and, as a result, new probabilities for each candidate structure of (–)-mucosin methyl ester (Figure 32).

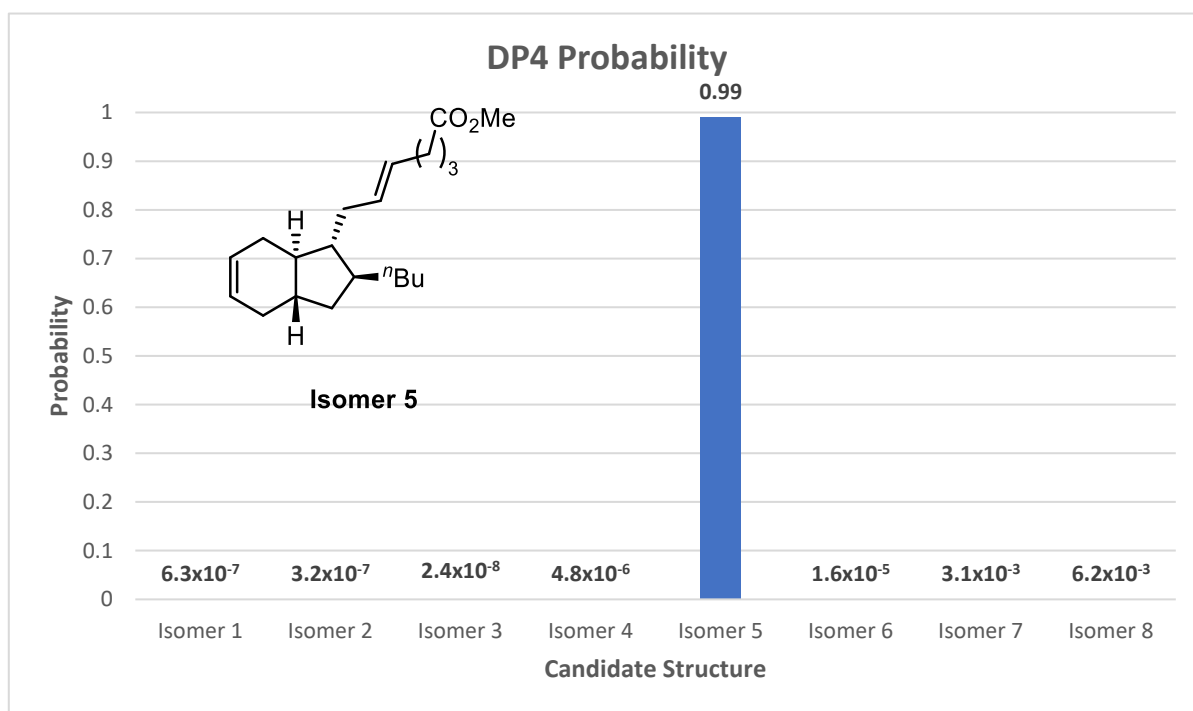


Figure 32 - DP4 probabilities generated from a more thorough conformational search

Gratifyingly, with a more thorough search of the conformational space, DP4 was able to identify **isomer 5** with 99% probability as being the correct structure of (–)-mucosin methyl ester; which Stenstrøm has supported through synthesis.³⁶ This process highlights a key issue surrounding accurate NMR spectra computation of highly flexible structures, as we were unable to obtain computed data of sufficient accuracy to allow for a nearly unanimous prediction, when an inadequate search of the conformational space was performed. To ensure the robustness of the DP4 methodology, the

computed isotropic shielding constants for each candidate structure were also scaled with the experimental data obtained from the synthesis of *cis*- and *exo*-mucosin methyl ester and their respective probabilities calculated (Table 31, Figure 33, Figure 34).

Table 31 - Stenstrøm's ¹³C comparison table between *cis*- and *exo*-mucosin methyl ester and the isolated data from Casapullo.

Casapullo et al.	<i>Cis</i>-Mucosin	<i>Exo</i>-mucosin
174.2	174.2	174.2
130.0	130.4	131.2
129.8	129.9	129.0
127.0	126.3	125.3
127.0	126.1	125.1
52.1	51.4	51.6
51.4	51.0	51.4
47.1	44.0	41.3
42.1	40.3	37.2
39.9	38.1	36.2
36.7	37.7	35.5
36.5	37.1	35.4
36.4	34.9	33.4
33.2	33.4	33.0
32.0	31.9	31.9
31.7	31.0	31.0
31.5	27.8	26.9
30.7	27.7	24.7
24.5	24.8	23.0
22.6	22.9	21.7
13.8	14.1	14.1

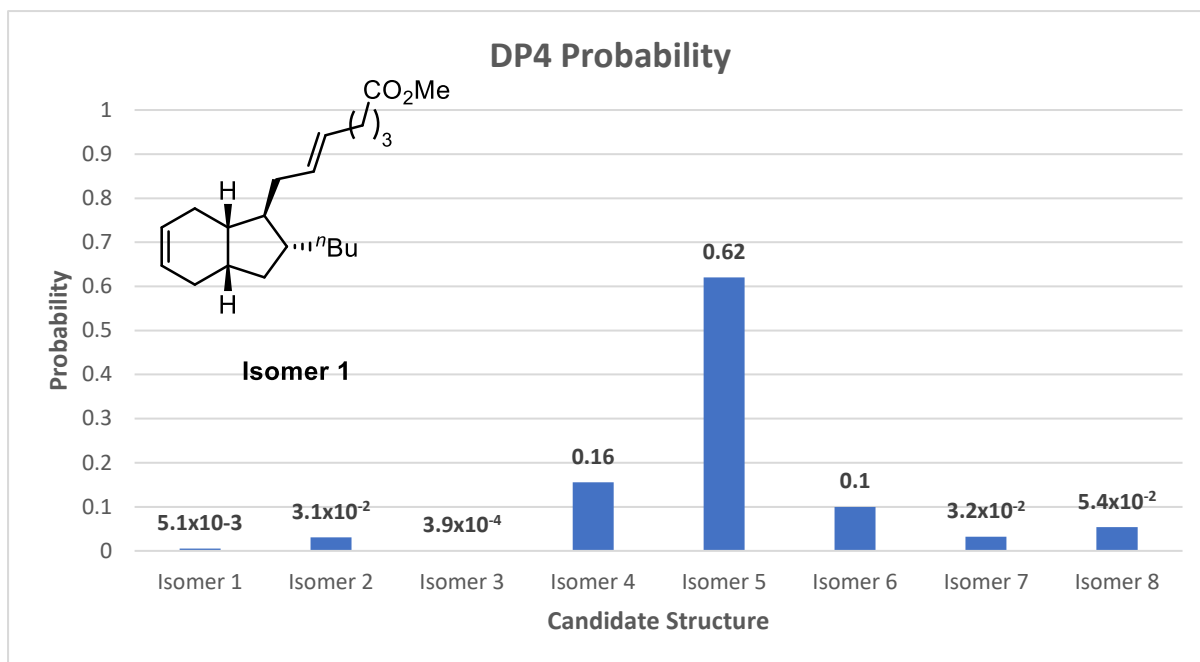


Figure 33 - DP4 probabilities generated upon the comparison of computed structures to the ^{13}C spectra obtained from the synthesis of *cis*-mucosin methyl ester

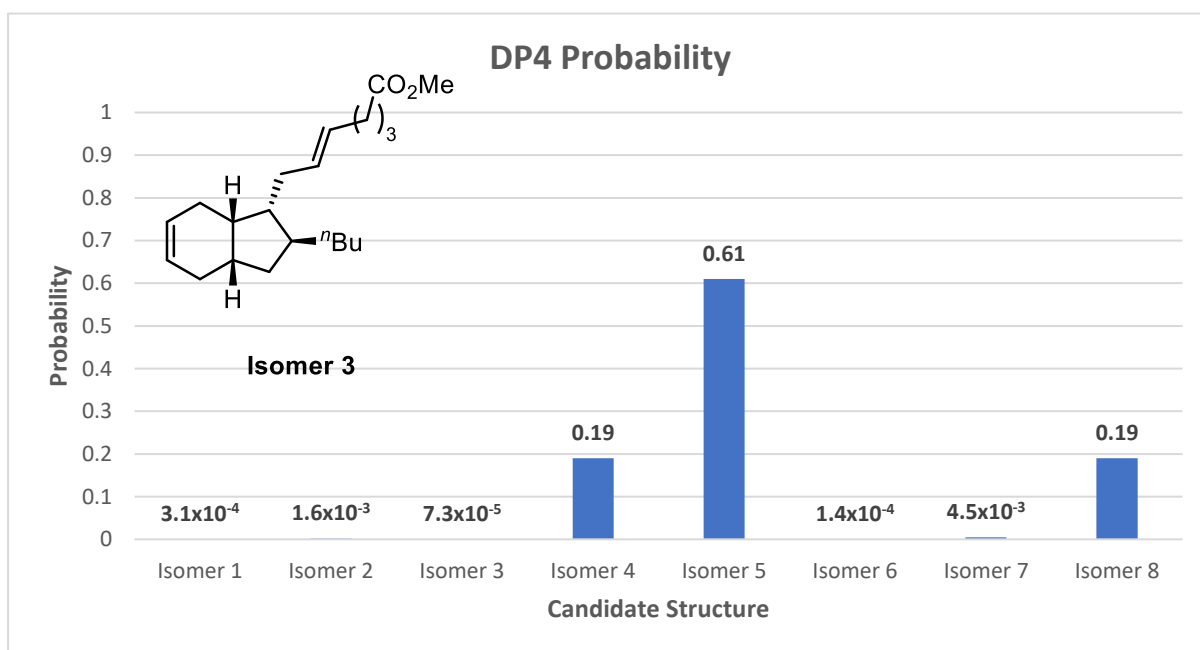


Figure 34 - DP4 probabilities generated upon the comparison of computed structures to the ^{13}C spectra obtained from the synthesis of *exo*-mucosin ester

It became evident that despite the success in identifying **isomer 5** as the candidate structure that matched the experimental data obtained from mucosin's isolation, DP4 was not able to identify the correct structure of *cis*-mucosin and *exo*-mucosin as **isomer 1** and **isomer 3**, respectively. It was then proposed that the multi-distribution error handling of DP4+ and DP4.2, and higher levels of

computational theory, might allow for the correct assignment of *cis*-mucosin methyl ester and *exo*-mucosin methyl ester.^{24,27} Considering this, energy calculations and optimisations were computed using B3LYP/6-31G(d). Subsequently, NMR GIAO calculations were computed using mPW1PW91/6-31+G(d,p), as is required by DP4+, for each candidate structure and their DP4+ probabilities calculated.²⁴ Additionally, further calculations were performed using M06-2X/6-31G(d,p) for energy calculations on all previously generated low-energy conformers for each candidate structure. NMR GIAO calculations were computed using mPW1PW91/6-311G(d), as is required by DP4.2, for each candidate structure and their respective DP4.2 probabilities calculated. With the DP4, DP4+ and DP4.2 probabilities for each candidate structure in hand, comparisons were made between the DP4-like methodologies (Figure 35).²⁷

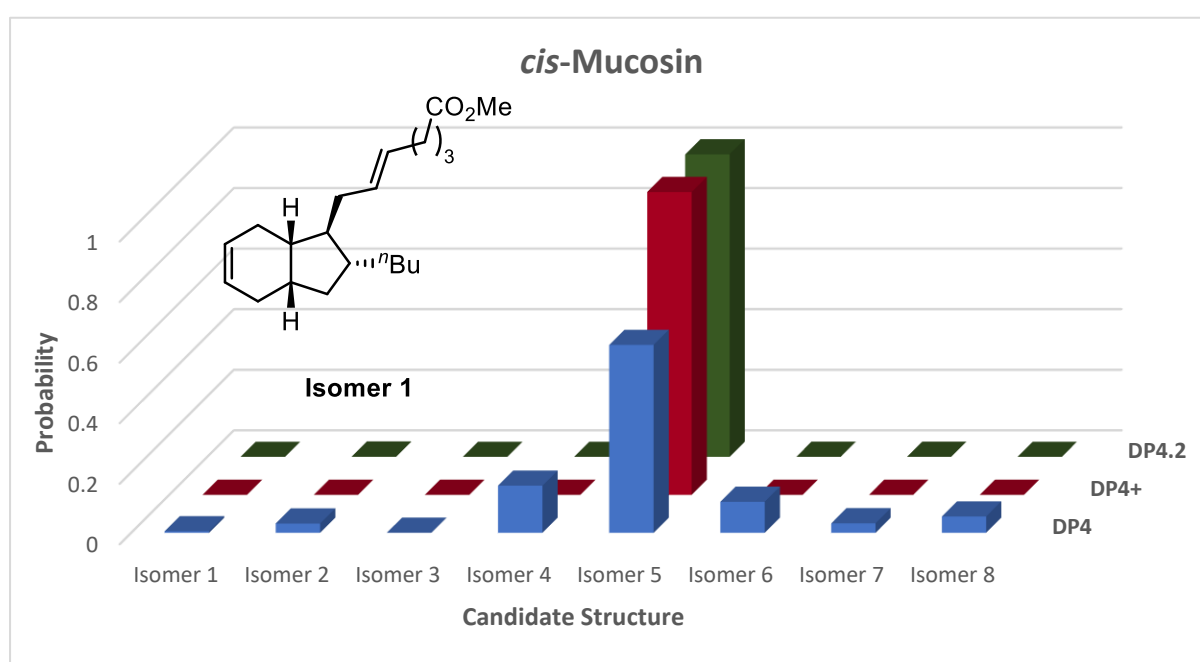


Figure 35 - Performance comparison of DP4-like methodologies using the spectral data from *cis*-Mucosin

Sarotti's DP4+ incorrectly identified **isomer 5** as the most probable candidate structure that matched the ¹³C spectral data from Stenstrøm's synthesis of *cis*-mucosin.³³ Additionally, Goodman's improved multi-gaussian statistical approach also incorrectly identified **isomer 5** as the most probable candidate. Indeed, it is alarming that all three trialled DP4-like methodologies identified **isomer 5** as the most probable structure for *cis*-mucosin methyl ester when **isomer 1** is the correct structure for *cis*-mucosin methyl ester, with DP4+ and DP4.2 displaying gross over-confidence in **isomer 5**.

The experimental data published by Stenstrøm *et al.* for their synthesis of *exo*-mucosin methyl ester was used in the various DP4-type analyses, and the results were compared (Figure 36).³⁴

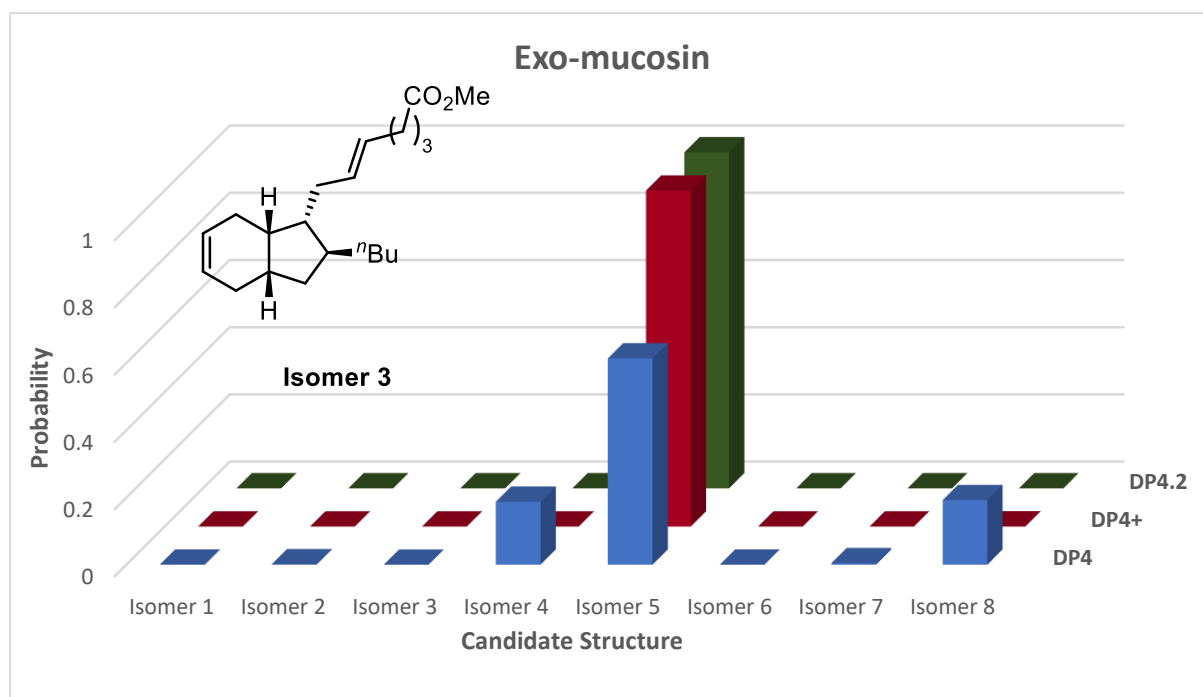


Figure 36 - Performance comparison of DP4-like methodologies using the spectral data from *exo-Mucosin*

Strangely, the ^{13}C NMR data reported by Stenstrøm for *exo-mucosin* methyl ester, when compared with the computed candidate structures for mucosin methyl ester through DP4-like analysis, indicates that **isomer 5** is, once again, the most probable candidate. This is especially peculiar considering that DP4+ and DP4.2 suggest **isomer 5** as the only probable structure whereas DP4 is less confident. DP4 also indicates **isomer 4** and **isomer 8** as possible structures with reduced probability. Regardless, none of the DP4 methodologies indicates **isomer 3** with any degree of probability as being the likely structure, which Stenstrøm and co-workers have demonstrated through synthesis.³⁴

As all the DP4 methodologies rely on scaled chemical shifts, the experimental data that is being used to scale the calculated shifts and ultimately used by DP4 analysis is a key element in obtaining robust probabilities. As a consequence, if the ^{13}C spectrum being used is misassigned or is unassigned, then it is likely that the computational chemist will obtain unreliable results from a DP4-like analysis.

Re-evaluating the ^{13}C spectra comparison table published by Stenstrøm, it became apparent that Stenstrøm and co-workers may not have fully assigned the ^{13}C spectra for both *cis*- and *exo-mucosin* methyl ester (Table 31).^{33,34} Indeed, the comparison table lists the ^{13}C chemical shifts for all three structures in descending order.^{33,34,37} As the work thus far had been carried out under the assumption that Stenstrøm had matched the chemical shifts to the resonances that had been fully assigned by Casapullo with the aid of 2D NMR experiments, it is possible this has negatively affected our previous efforts in assigning *cis*- and *exo-mucosin* methyl esters using DP4.³⁷ Upon contacting Stenstrøm *et al.*,

it was confirmed that no previous ^{13}C NMR assignment had been carried out within their laboratories. Graciously, Stenstrøm and co-workers had run the necessary 2D NMR experiments and shared the obtained data with us, to allow us to take this raw data and correctly assign the ^{13}C spectra for *cis*- and *exo*-mucosin methyl esters, to aid our computational work. Initially, work focused on the ^{13}C assignment of *cis*-mucosin methyl ester, with the data obtained from the HSQC, HMBC and NOESY NMR experiments carried out by Stenstrøm and co-workers. Using the 2D datasets, the following reassignment of *cis*-mucosin methyl ester was made through numerous correlations in the HSQC and HMBC spectra in analogy to the assignment, Casapullo carried out in the original characterisation of mucosin methyl ester (Figure 37, Table 32, Figure 38).³⁷

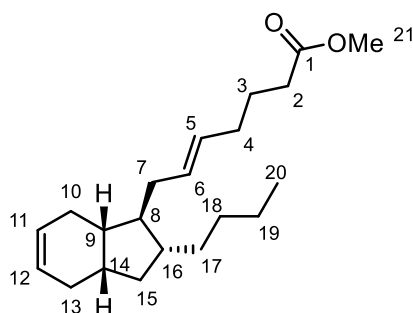


Figure 37 - Structure of *cis*-mucosin methyl ester and nuclei numbering scheme

Table 32 - ^{13}C assignment of *cis*-mucosin methyl ester

Position	^{13}C Assignment	HSQC	HMBC	NOESY
1	174.2		H21, H3, H2	
2	33.5	2.30	H21, H4, H3	
3	24.9	1.69	H5, H4, H2, H1	
4	32.1	2.02	H6, H5, H3, H2	
5	129.9	5.37	H7, H4, H3	
6	130.4	5.41	H8, H7, H4, H3	
7	37.8	2.03	H17, H8, H6, H3	H9
8	51.1	1.25	H13, H4, H3	H15
9	40.4	1.67	H16, H14, H11, H10, H8	H14
10	27.8	2.16, 2.07	H14, H13, H12, H11, H9, H8	H17
11	126.1	5.66	H13, H12, H10, H9	
12	126.3	5.66	H13, H11, H10, H9	
13	27.9	1.85, 1.81	H17, H12, H11, H10, H9, H8	
14	34.9	2.05	H17, H13, H10, H9	H9, H8, H13
15	37.2	1.51	-5H16, H14, H10	
16	44.1	1.48	H17, H15, H13, H9, H8	H17, H14
17	38.1	1.85, 1.07	H20, H19, H16, H7	
18	31.1	1.19	H20, H19, H16, H8	
19	23.1	1.28	H20, H18, H17, H16	
20	14.1	0.87	H19, H18	
21	51.4	3.66	H3, H2	

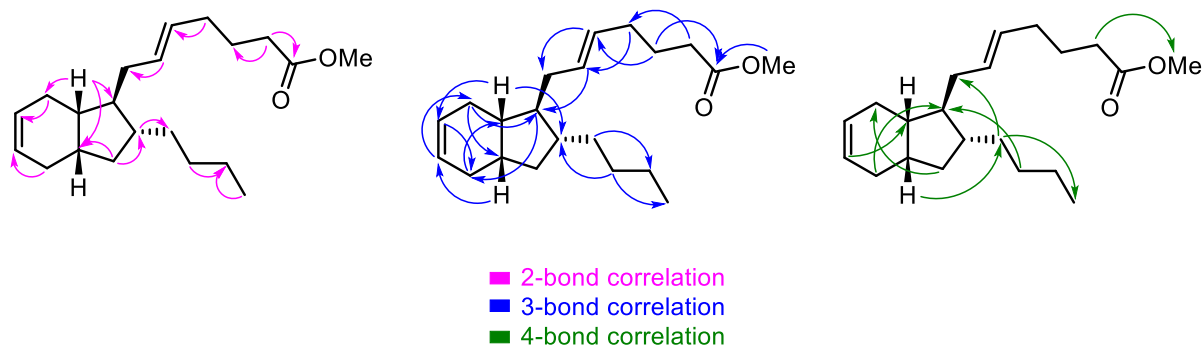


Figure 38 - The observed multiple bond correlations in *cis*-mucosin methyl ester

The ^{13}C assignment of the butyl chain was possible due to a distinctive resonance in the ^1H NMR spectrum (δ_{H} 0.87 (t, 3H)) indicative of the methyl group at C-20, and the connectivity of the butyl chain was then assigned in the ^{13}C NMR spectrum as δ_{C} 14.1 (C-20), 23.1 (C-19), 31.1 (C-18) and 38.1 (C-17). These assignments were confirmed by 2J -HMBC correlations between H-18/H-20 and C-19 and additionally by 3J -HMBC correlations between H-18 and C-20 and H-17 and C-20. The methyl ester-bearing side chain was represented by the ^{13}C signals at δ_{C} 51.4 (C-21), 174.2 (C-1), 33.5 (C-2), 24.9 (C-3), 32.1 (C-4), 129.9 (C-5), 130.4 (C-6) and 37.8 (C-7). These assignments were supported by 2J -HMBC correlations between H-2 and C-1/C-3, H-4 and C-5 and H-6 and C-7. Additionally, 3J -HMBC correlations between H-21/H-3 and C-1, H-2 and C-4, H-3 and C-5, H-4 and C-6, and H-5 and C-7, aided in the ^{13}C assignment of the methyl ester-bearing appendage in *cis*-mucosin methyl ester. Finally, a 4J -HMBC correlation between H-2 and C-21 indicated δ_{C} 33.5 (C-2) was α to the carbonyl of the methyl ester, confirmed by the correlation in the HSQC experiment to δ_{H} 2.30 (t, 2H). With both appendages assigned, the 5,6 bicyclic core, containing six methine groups and three methyldene groups, which are distinguishable from one another in the HSQC experiment, remained to be assigned. It was especially crucial that the ^{13}C assignment of the core structure was correct, as this structure contains the four contiguous stereocentres and any wrong assignment would likely give false positives in any DP4-like analysis. ^{13}C assignment of the stereocentre bearing the butyl sidechain δ_{C} 44.1 (C-16) was aided by a 3J -HMBC correlation between H-18 and C-16, and an additional 2J -HMBC correlation between H-16 and C-17. The remaining ^{13}C resonances were given the following assignments δ_{C} 51.1 (C-8), 40.4 (C-9), 27.8 (C-10), 126.1 (C-11), 126.3 (C-12), 27.9 (C-13), 34.9 (C-14) and 37.2 (C-15). Crucially, the methyl ester bearing sidechain was connected at C-8, based on a 3J -HMBC correlation between H-6 and C-8. The assignment of δ_{C} 40.4 (C-9) was supported by a 2J -HMBC correlation between H-9 and C-8 and an additional 3J -HMBC correlation between H-9 and C-16. The remaining ^{13}C assignment was confirmed by numerous 2J -HMBC correlations between H-9 and C-10/C-14, H-10 and

C-11, H-13 and C-12 and H-15 and C-14/C-16. Additionally, ³J-HMBC correlations between H-9 and C-11, H-10 and C-8/C-14, H-11 and C-13, H-12 and C-10, H-13 and C-9.

Having completed the ¹³C assignment of *cis*-mucosin methyl ester, *exo*-mucosin methyl ester was reassigned in a similar fashion (Figure 39, Table 33, Figure 40).

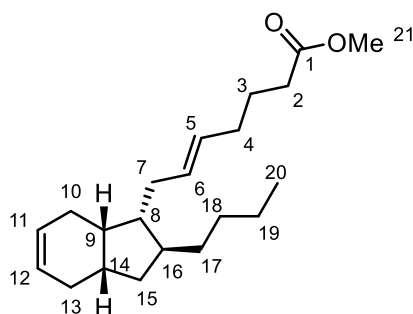


Figure 39 - Structure of *exo*-mucosin methyl ester and nuclei numbering scheme

Table 33 - ¹³C assignment of *exo*-mucosin methyl ester

Position	¹³ C Assignment	HSQC	HMBC	NOESY
1	174.3		H21, H3	
2	33.5	2.30	H21, H4	
3	24.9	1.68	H5, H4, H1	
4	32	2.00	H6, H5, H3, H2	
5	129.1	5.38	H7, H4, H3	
6	131.3	5.42	H7, H4	
7	33.6	1.96	H17, H8, H6	
8	51.8	1.53	H16,	H9
9	35.7	2.07	H16, H14, H10	H14, H10, H8
10	21.8	1.77,1.88	H12, H11, H9,	H9
11	125.3	5.65	H13, H10, H9	
12	125.1	5.60	H12, H11, H9	
13	27	1.85, 2.25	H15, H12, H11, H9	H14
14	37.4	1.93	H15, H10, H9	H15, H13, H9
15	35.6	1.36, 1.63	H16, H14, H13	H17
16	41.4	1.59	H18, H17, H15, H8	
17	36.3	1.44	H20, H19, H16, H7	H15
18	31.1	1.19	H20, H19, H16	
19	23.1	1.29	H20, H18, H17, H16	
20	14.3	0.88	H19, H18, H17	
21	51.5	3.66	H1, H2	

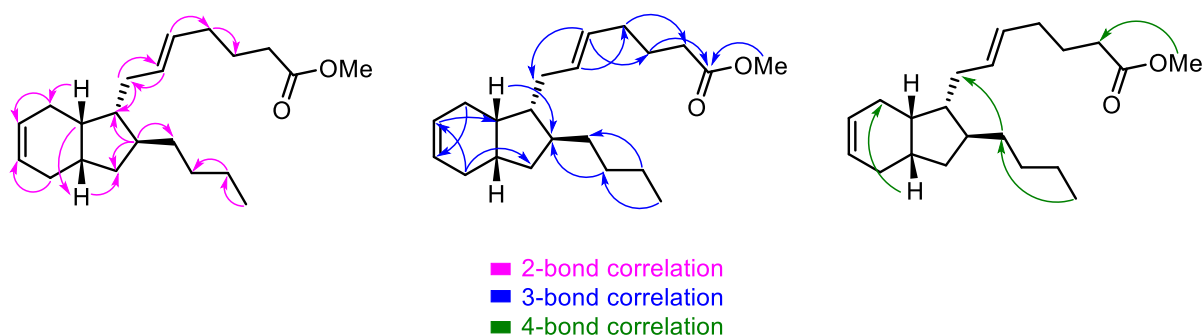


Figure 40 - The observed multiple bond correlations in *exo*-mucosin methyl ester

As before, the ^{13}C NMR spectrum assignment of the butyl chain was initiated by identifying δ_{H} 0.88 (t, 3H) as the methyl group at C-20. This led to the following ^{13}C assignment for the butyl chain: δ_{C} 14.3 (C-20), 23.1 (C-19), 31.1 (C-18) and 36.3 (C-17). These assignments were supported by 2J -HMBC correlations between H-20 and C-19, H-19 and C-18, and additionally by 3J -HMBC correlations between H-20 and C-18, and H-19 and C-17. A further 4J -HMBC correlation was also observed between H-20 and C-17. The second sidechain, bearing the methyl ester moiety was found to have the resulting ^{13}C assignment, δ_{C} 51.5 (C-21), 174.3 (C-1), 33.5 (C-2), 24.9 (C-3), 32.0 (C-4), 129.1 (C-5), 131.3 (C-6) and 33.6 (C-7). These assignments were confirmed by 2J -HMBC correlations between H-4 and C-3/C-5, H-6 and C-7, and H-7 and C-6. Additionally, 3J -HMBC correlations between H-21/H-3 and C-1, H-4 and C-2, H-5 and C-3/C-7, and H-6 and C-4, supported the ^{13}C assignment of the methyl ester-bearing sidechain in *exo*-mucosin methyl ester. With the assignment of both appendages in *cis*- and *exo*-mucosin methyl esters, it was noted that the vast majority of the ^{13}C assignment is relatively insensitive to changes in the stereochemical environment, and it was only C-7 and C-17 that displayed any dramatic variance, between the two structures. This further highlights the importance of obtaining the correct ^{13}C assignments of the core structure for reliable DP4-analysis. The stereocentre bearing the butyl chain δ_{C} 41.4 (C-16) was identified *via* a 3J -HMBC correlation between H-18 and C-16. The remaining ^{13}C chemical shifts were assigned to the following carbons: δ_{C} 51.8 (C-8), 35.7 (C-9), 21.8 (C-10), 125.3 (C-11), 125.1 (C-12), 27.0 (C-13), 37.4 (C-14) and 35.6 (C-15). The methyl ester-bearing side-chain was connected at C-8 based on 2J -HMBC correlations between H-7 and C-8 and H-16 and C-8. The 3J -HMBC correlations between H-9 and C-16, and H-11 and C-9, aided in the assignment of δ_{C} 35.7 (C-9). The remaining ^{13}C assignment was confirmed by numerous 2J -HMBC correlations between H-9 and C-10/C-14, H-10 and C-11, H-13 and C-12, H-14 and C-15, and H-16 and C-15. Additionally, 3J -HMBC correlations between H-9 and C-16, H-10 and C-12 and H-13 and C-11/C-15 were observed.

With the ^{13}C reassignments of both *cis*- and *exo*-mucosin methyl esters complete, attention focused on reassessing the power of stereochemical assignment within the cases of *cis*- and *exo*-mucosin methyl ester *via* DP4-like analysis. Initially, the reassigned *cis*-mucosin methyl ester experimental ^{13}C data was compared with each of the computed candidate structures and the respective probabilities were assessed using DP4, DP4+ and DP4.2 (Figure 41).

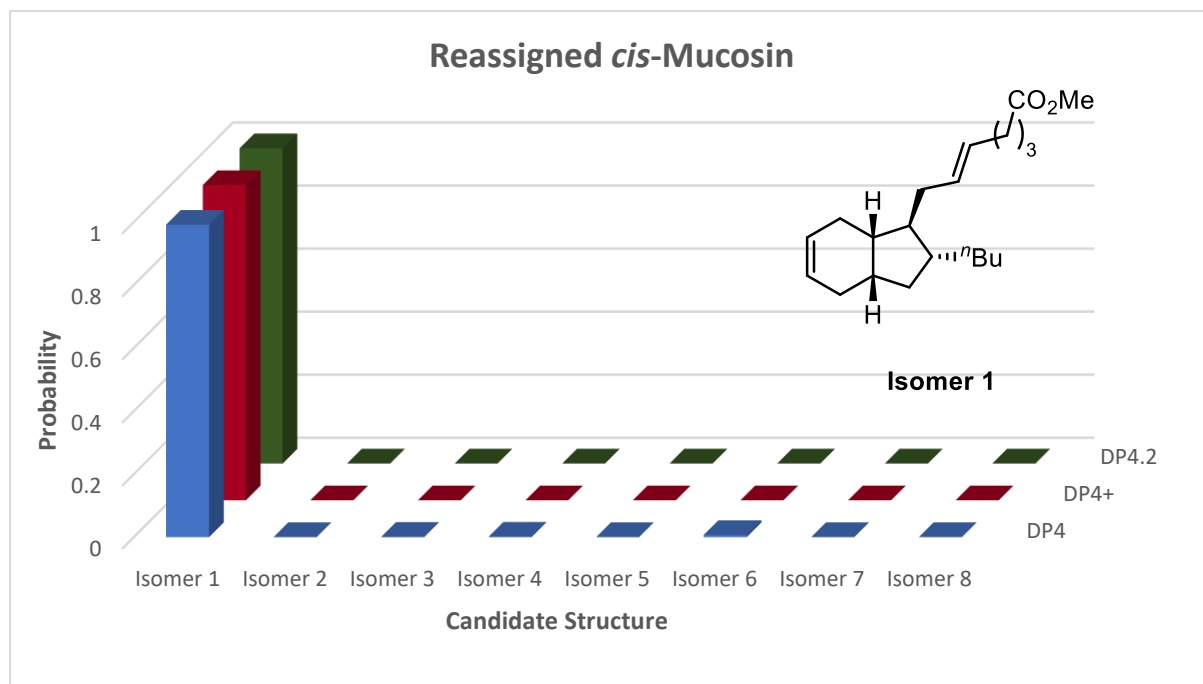


Figure 41 - Performance comparison of DP4-like methodologies using the reassigned spectral data from *cis*-Mucosin

Pleasingly, DP4, DP4+ and DP4.2 all unanimously identify **isomer 1** as the correct structure for *cis*-mucosin methyl ester using the newly assigned ^{13}C NMR experimental spectrum, of a structure established through synthesis within the literature. This is in stark contrast to the previous DP4 analysis, using the ^{13}C NMR data before assignment, which consistently identified **isomer 5** as the probable structure with DP4 displaying lower performance (Figure 35). With success in correctly identifying the structure of *cis*-mucosin methyl ester, the newly assigned *exo*-mucosin methyl ester experimental ^{13}C NMR spectral data was compared with each of the computed candidate structures, and the respective probabilities were assessed using DP4, DP4+ and DP4.2 (Figure 42).

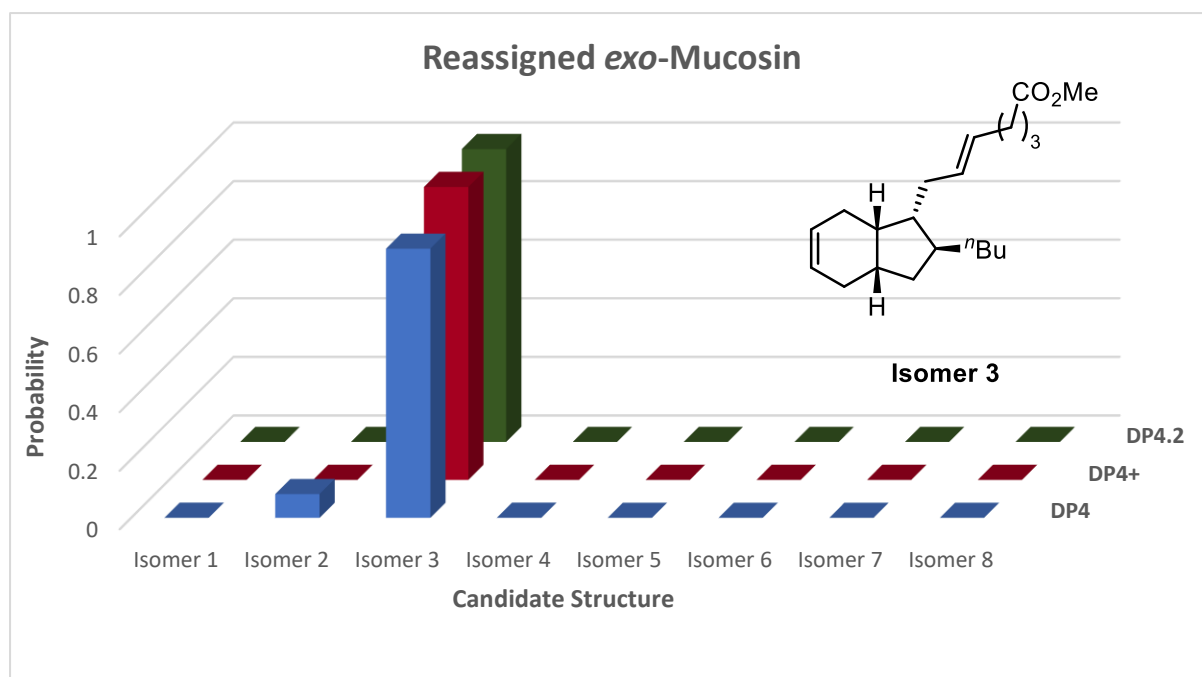


Figure 42 - Performance comparison of DP4-like methodologies using the reassigned spectral data from *exo*-Mucosin

When using the newly reassigned ^{13}C spectral data, DP4+ and DP4.2 correctly assign *exo*-mucosin methyl ester as **isomer 3** with >99 % probability. However, DP4 also assigns **isomer 3** as the most probable structure of *exo*-mucosin methyl ester but with a lower 92 % probability, and also identifies **isomer 2** with an 8 % probability. This potentially demonstrates the lower performance of the single distribution approach DP4 utilises to describe the likelihood of an error between the scaled shifts and experimental shifts being obtained. This work highlights that highly flexible oxylipin structures such as mucosin are amenable to DP4-like analysis with correctly assigned ^{13}C experimental data.

2.3. Conclusion

At the outset of this work, it was proposed that computational methodology combined with DP4-like probability approaches could further our work towards the structural elucidation and total synthesis of (-)-mucosin. However, having obtained our preliminary results, which identified **isomer 2** and **isomer 4** as being the likely stereoisomers of a *cis*-bridgehead mucosin methyl ester, as this work was in progress, Stenstrøm *et al.* published their work, which strongly supports **isomer 5** as the correct structure of mucosin methyl ester (Figure 43).³⁶

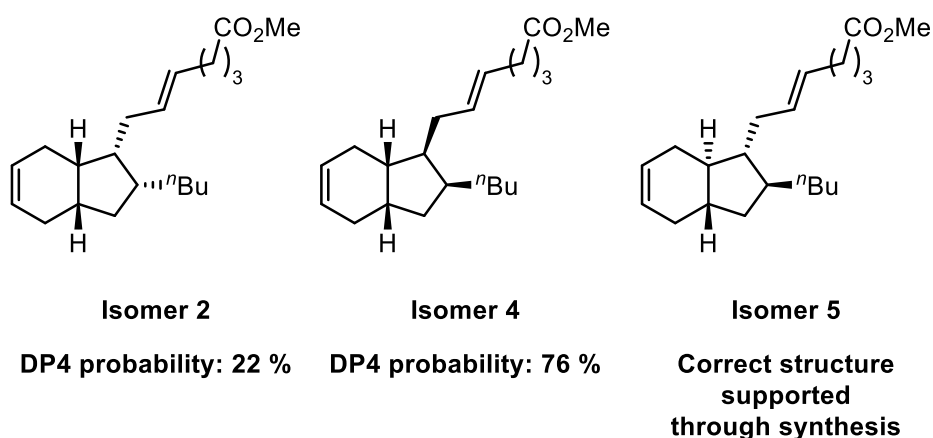


Figure 43 - Preliminary results

This ultimately brought our synthetic research toward this natural product to an end (*vide supra*), but raised questions regarding the reliability of computationally-aided structural assignment in our work. Through the subsequent investigation, the importance of the conformer generation step in order to achieve excellent DP4 performance, was highlighted. As a result, of a more thorough conformational search, **isomer 5** was correctly identified as the structure of mucosin methyl ester with a 99 % probability (Figure 44).

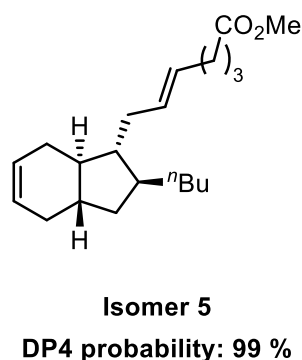


Figure 44 - Optimised results

Inspired by this outcome, the ^{13}C spectral data obtained from the Stenstrøm synthesis of *cis*- and *exo*-mucosin methyl esters were then subjected to DP4 treatment, and likely candidates were then identified. However, through the use of DP4 and the more sophisticated DP4+ and DP4.2 methodologies, *cis*- and *exo*-mucosin methyl esters were consistently wrongly identified. Further examination of the spectral data published by Stenstrøm led to the hypothesis that the resonances in these datasets had not been assigned to respective nuclei. In collaboration with Stenstrøm, we were able to obtain 2D NMR spectra of these products, allowing for us to completely assign the ^{13}C NMR spectra of both *cis*- and *exo*-mucosin methyl esters. Having assigned these ^{13}C spectra, pleasingly, all DP4-like analysis attempted within this work correctly identified *cis*-mucosin methyl ester and *exo*-mucosin methyl ester as **isomer 1** and **isomer 3**, respectively. These successful results identify that exceedingly flexible oxylipin structures such as mucosin can have their structure elucidated *via* the use of tools such as DP4. With the knowledge gained from this work, research would now focus on the potential structural elucidation of a similar natural product target.

2.4. Experimental

2.4.1. Details of Computational Methods

Conformer Generation

Molecular mechanics was employed to generate low-energy conformers for each candidate structure being investigated. All molecular mechanics calculations were performed using Macromodel³⁸ (Version 9.1, 9.5, or 9.7) interfaced to the Maestro³⁹ (Version 11.5) program. All conformational searches used the Monte Carlo Multiple Minimum⁴⁰ (MCM) method and the MMFF forcefield.⁴¹⁻⁴⁷ The searches were done in the gas phase, with a 50 kJmol⁻¹ upper energy limit and with the number of steps large enough to find all low-energy conformers at least 5-10 times. All conformers >10 kJmol⁻¹, with respect to the global minimum, were discounted.

DP4 Frequency and NMR GIAO Calculations¹⁸

Density functional theory (DFT) was employed to calculate the gas-phase energies for all generated conformers for each candidate structure. All frequency and NMR GIAO^{48,49} shielding tensor calculations were carried out using the B3LYP¹⁹⁻²² functional with the 6-31G(d,p) basis set.²³ All calculations using the B3LYP functional have been performed using Gaussian 09 quantum chemistry program package⁵⁰ (version D.01) or Jaguar⁵¹ (version 9.9).

DP4+ Frequency, Optimisation and NMR GIAO Calculations²⁴

Density functional theory (DFT) was employed to calculate the gas-phase geometries and energies for all generated conformers, for each candidate structure. All frequency and geometry calculations were carried out using the B3LYP¹⁹⁻²² functional with the 6-31G(d) basis set.²³ NMR GIAO^{48,49} shielding tensor calculations were carried out using the mPW1PW91²⁹ functional with the 6-31+G(d,p) basis set. The NMR GIAO^{48,49} shielding calculations were carried out in solution (using the polarizable continuum model, PCM, with chloroform as the solvent). All calculations using the B3LYP¹⁹⁻²² or mPW1PW91²⁹ functional have been performed using Gaussian 09 quantum chemistry program package (version D.01).⁵⁰

DP4.2 Frequency and NMR GIAO Calculations²⁷

Density functional theory (DFT) was employed to calculate the gas-phase energies and NMR GIAO^{48,49} shielding constant calculations for all generated conformers, for each candidate structure. All

frequency calculations were carried out using the M06-2X²⁸ functional with the 6-31G(d,p) basis set.²³ NMR GIAO^{48,49} shielding tensor calculations were carried out using the mPW1PW91²⁹ functional with the 6-311G(d) basis set.²³ The NMR GIAO^{48,49} shielding calculations were carried out in the gas-phase. All calculations using the B3LYP¹⁹⁻²² or mPW1PW91²⁹ functional have been performed using Gaussian 09 quantum chemistry program package (version D.01).⁵⁰

To calculate NMR shifts for a candidate structure, the shielding tensors were first averaged over symmetry-related positions in each conformer and then subjected to Boltzmann averaging over the conformers according to:

$$\sigma^x = \frac{\sum_i \sigma_i^x \exp\left(\frac{-E_i}{RT}\right)}{\sum_i \exp\left(\frac{-E_i}{RT}\right)}$$

Where σ^x is the Boltzmann-averaged shielding tensor for nucleus x , σ_i^x is the shielding constant for nucleus x in conformer i , and E_i is the potential energy of conformer i (relative to the global minimum), obtained from the single-point *ab initio* calculation. The temperature (T) was taken as 298 K. Chemical shifts were calculated according to:

$$\delta_{unscaled}^x = \frac{\sigma^o - \sigma^x}{1 - \sigma^o/10^6}$$

where δ_{calc}^x is the calculated shift for nucleus x (in ppm). σ^x is the shielding tensor for nucleus x . σ^o is the shielding tensor for the carbon nuclei in tetramethyl silane, which was obtained from a NMR GIAO calculation on *tetra*-methyl silane.

All NMR GIAO data extraction from Gaussian 09 output files and Boltzmann averaging was handled *via* the use of Python scripting.

2.4.2. Details of Statistical Analysis

DP4 Probability Calculations¹⁸

All calculated shifts were scaled against their respective experimental shifts *via* linear regression and scaled shifts were calculated according to:

$$\delta_{scaled} = (\delta_{unscaled} - c)/m$$

Where δ_{scaled} is the calculated scaled shift for nucleus x , (in ppm), $\delta_{unscaled}$ is the unscaled shift for nucleus x , C is the y-intercept from the linear regression, and m is the gradient from the linear regression.

The probability for each candidate structure was then calculated using the following equation:

$$P = \frac{\Pi \left(T^{\nu} \left(\frac{|\delta_{scaled} - \delta_{exp} - \mu|}{\sigma} \right) \right)}{\Sigma \left[\Pi \left(T^{\nu} \left(\frac{|\delta_{scaled} - \delta_{exp} - \mu|}{\sigma} \right) \right) \right]}$$

where P is the probability that a candidate structure is the correct one from the experimental shifts. δ_{scaled} is the calculated scaled shift for nucleus x (in ppm), δ_{exp} is the experimental shift for nucleus x (in ppm), μ is the mean, which is taken as 0 as a result of the empirical scaling and σ is the standard deviation which is 2.306 ppm for ¹³C NMR shifts. The respective t -distribution has degrees of freedom (ν) of 11.38. Values of σ and ν were determined by Goodman and co-workers.¹⁸

DP4+ Probability Calculations²⁴

All calculated shifts were scaled against their respective experimental shifts *via* linear regression and scaled shifts were calculated according to:

$$\delta_{scaled} = (\delta_{unscaled} - c)/m$$

where δ_{scaled} is the calculated scaled shift for nucleus x (in ppm), $\delta_{unscaled}$ is the unscaled shift for nucleus x , C is the y-intercept from the linear regression, and m is the gradient from the linear regression.

The probability for each candidate structure was then calculated using the following equation:

$$P = \frac{\prod \left(T^{\nu}_{scaled} \left(\frac{|\delta_{scaled} - \delta_{exp}| - \mu_{scaled}}{\sigma_{scaled}} \right) \right) \left(T^{\nu}_{unscaled} \left(\frac{|\delta_{unscaled} - \delta_{exp}| - \mu_{unscaled}}{\sigma_{unscaled}} \right) \right)}{\sum \left[\prod \left(T^{\nu}_{scaled} \left(\frac{|\delta_{scaled} - \delta_{exp}| - \mu_{scaled}}{\sigma_{scaled}} \right) \right) \left(T^{\nu}_{unscaled} \left(\frac{|\delta_{unscaled} - \delta_{exp}| - \mu_{unscaled}}{\sigma_{unscaled}} \right) \right) \right]}$$

where P is the probability that a candidate structure is the correct one from the experimental shifts, δ_{scaled} is the calculated scaled shift for nucleus x (in ppm), δ_{exp} is the experimental shift for nucleus x (in ppm), $\delta_{unscaled}$ is the unscaled shift for nucleus x , μ is the mean, which is taken as 0 as a result of the empirical scaling, and σ_{scaled} is the standard deviation for the scaled shifts, which is 0.122 ppm for ^{13}C shifts. The t -distribution T^{ν}_{scaled} has degrees of freedom (ν) of 4.318. $\mu_{unscaled}$ is the mean for the unscaled shifts, which has a value of -0.075 or 0.239 for sp^3 or sp^2 nuclei, respectively. $\sigma_{unscaled}$ is the standard deviation for the unscaled shifts, which has a value of 0.127 or 0.149 for sp^3 or sp^2 nuclei, respectively. The t -distribution $T^{\nu}_{unscaled}$ has degrees of freedom (ν) of 3.684 or 5.840 for sp^3 or sp^2 nuclei, respectively. Values of σ , μ and ν were determined by Sarotti and co-workers.²⁴

DP4.2 Probability Calculations²⁷

All calculated shifts were scaled against their respective experimental shifts *via* linear regression and scaled shifts were calculated according to:

$$\delta_{scaled} = (\delta_{unscaled} - c)/m$$

Where δ_{scaled} is the calculated scaled shift for nucleus x (in ppm), $\delta_{unscaled}$ is the unscaled shift for nucleus x , C is the y-intercept from the linear regression, and m is the gradient from the linear regression.

The probability for each candidate structure was then calculated using the following equation:

$$P = \frac{\prod \left(N_{(\mu_1, \sigma_1)}(\delta_{scaled} - \delta_{exp}) \right) \left(N_{(\mu_2, \sigma_2)}(\delta_{scaled} - \delta_{exp}) \right)}{\sum \left[\prod \left(N_{(\mu_1, \sigma_1)}(\delta_{scaled} - \delta_{exp}) \right) \left(N_{(\mu_2, \sigma_2)}(\delta_{scaled} - \delta_{exp}) \right) \right]}$$

where P is the probability that a candidate structure is the correct one from the experimental shifts. δ_{scaled} is the calculated scaled shift for nucleus x (in ppm), δ_{exp} is the experimental shift for nucleus x (in ppm), μ_1 is the mean for the first distribution, which is taken as -0.012304, σ_1 is the

standard deviation for the first distribution, which is 2.821282 ppm for ^{13}C shifts. μ_2 is the mean for the second distribution, which has a value of 0.00095, and $\sigma_{unscaled}$ is the standard deviation for the second distribution, which has a value of 1.361471. Values of σ_1 , σ_2 , μ_1 and μ_2 were determined by Goodman and co-workers.²⁷

All probability calculations relied on Microsoft Excel for Office 365, version 1906.

2.4.3. Tables of Calculated Isotropic Shielding Constants and Probabilities

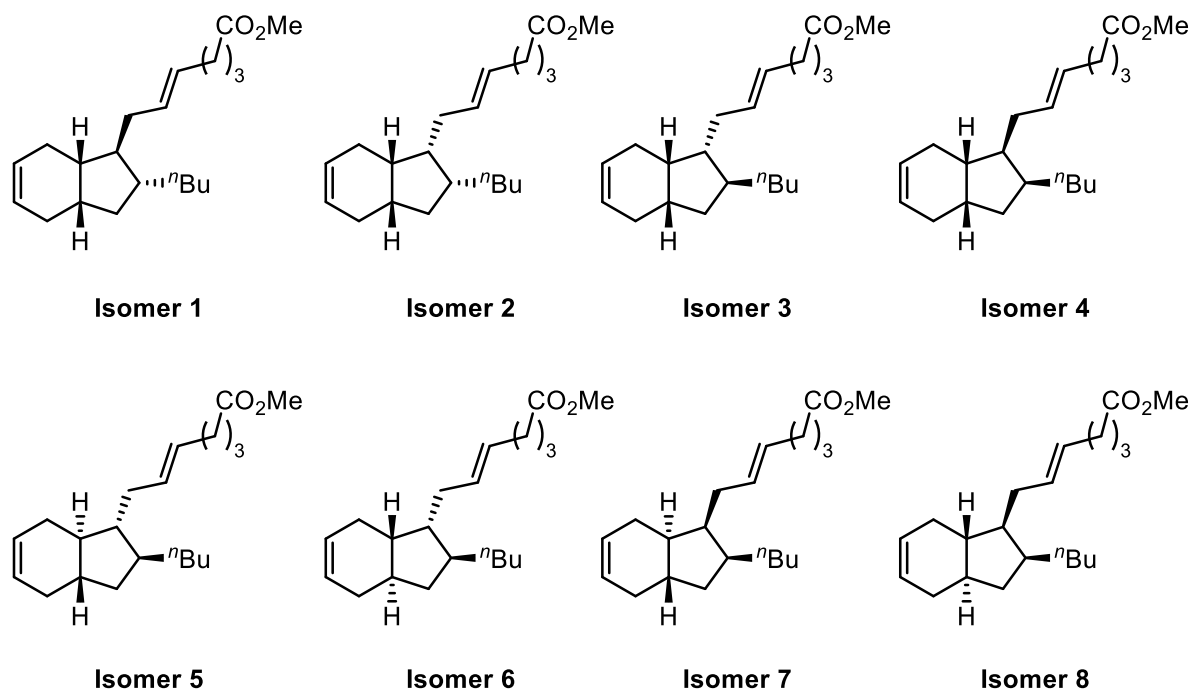


Figure 45 - Candidate structures for (-)-mucosin methyl ester

Figure 29

Table 34 – Calculated shielding tensors for the candidate structures of (–)-mucosin methyl ester containing a cis-bridgehead, after a 10,000 step MCMM search, and associated DP4 probabilities.

Nucleus Label	Isomer 1	Isomer 2	Isomer 3	Isomer 4
1	-15.23	-14.88	-14.73	-17.22
2	-155.49	-155.98	-159.24	-160.88
3	-161.85	-162.32	-164.81	-164.18
4	-154.59	-154.46	-157.03	-157.57
5	-55.39	-56.28	-57.55	-55.84
6	-55.36	-55.65	-52.89	-53.99
7	-146.93	-155.76	-153.69	-153.95
8	-133.35	-139.20	-134.41	-137.47
9	-150.37	-149.05	-149.39	-148.09
10	-158.28	-165.00	-166.02	-160.42
11	-62.30	-62.55	-62.29	-61.52
12	-62.01	-62.69	-62.39	-60.81
13	-160.92	-160.83	-161.00	-160.84
14	-151.17	-149.41	-150.06	-154.08
15	-150.03	-149.93	-152.67	-151.67
16	-139.88	-146.03	-144.78	-147.29
17	-147.67	-150.43	-150.17	-154.24
18	-155.41	-155.58	-154.98	-154.64
19	-162.96	-162.92	-163.04	-163.00
20	-174.18	-174.04	-174.10	-174.06
21	-137.26	-137.29	-137.43	-134.53
Probability	4.4x10 ⁻⁸	0.76	0.019	0.22

Figure 31

Table 35 - Calculated shielding tensors for all candidate structures of (-)-mucosin methyl ester, after a 10,000 step MCM search, and associated DP4 probabilities.

Nucleus Label	Isomer 1	Isomer 2	Isomer 3	Isomer 4	Isomer 5	Isomer 6	Isomer 7	Isomer 8
1	-15.23	-14.88	-14.73	-17.22	-14.35	-14.86	-14.71	-14.41
2	-155.49	-155.98	-159.24	-160.88	-158.84	-159.23	-158.27	-158.33
3	-161.85	-162.32	-164.81	-164.18	-164.76	-164.72	-164.04	-164.38
4	-154.59	-154.46	-157.03	-157.57	-156.69	-157.08	-156.86	-156.96
5	-55.39	-56.28	-57.55	-55.84	-56.99	-56.37	-57.96	-56.42
6	-55.36	-55.65	-52.89	-53.99	-53.85	-54.61	-50.21	-54.78
7	-146.93	-155.76	-153.69	-153.95	-146.69	-150.01	-157.95	-149.62
8	-133.35	-139.20	-134.41	-137.47	-134.05	-140.93	-139.93	-142.90
9	-150.37	-149.05	-149.39	-148.09	-139.89	-144.36	-140.27	-138.80
10	-158.28	-165.00	-166.02	-160.42	-155.57	-160.06	-157.57	-153.49
11	-62.30	-62.55	-62.29	-61.52	-59.97	-60.10	-58.56	-59.62
12	-62.01	-62.69	-62.39	-60.81	-60.02	-60.68	-60.75	-58.48
13	-160.92	-160.83	-161.00	-160.84	-155.70	-155.23	-153.17	-155.56
14	-151.17	-149.41	-150.06	-154.08	-148.07	-148.35	-149.04	-145.32
15	-150.03	-149.93	-152.67	-151.67	-152.76	-148.02	-152.43	-151.31
16	-139.88	-146.03	-144.78	-147.29	-143.49	-156.08	-142.09	-142.23
17	-147.67	-150.43	-150.17	-154.24	-149.41	-148.73	-153.28	-155.52
18	-155.41	-155.58	-154.98	-154.64	-155.29	-156.08	-155.11	-154.68
19	-162.96	-162.92	-163.04	-163.00	-164.54	-163.07	-162.95	-162.86
20	-174.18	-174.04	-174.10	-174.06	-174.02	-174.07	-174.14	-174.10
21	-137.26	-137.29	-137.43	-134.53	-137.19	-137.35	-137.30	-137.10
Probability	5.8x10 ⁻⁸	1.0x10 ⁻³	2.5x10 ⁻⁵	2.9x10 ⁻⁴	0.52	4.9x10 ⁻⁶	0.476	8.1x10 ⁻⁴

Figure 32

Table 36 - Calculated shielding tensors for all candidate structures of (-)-mucosin methyl ester, after a 200,000 step MCM search, and associated DP4 probabilities.

Nucleus Label	Isomer 1	Isomer 2	Isomer 3	Isomer 4	Isomer 5	Isomer 6	Isomer 7	Isomer 8
1	155.00	153.26	153.48	156.83	150.10	151.49	152.83	150.12
2	162.06	163.25	163.25	162.68	157.26	157.26	155.68	157.40
3	69.61	69.54	69.52	69.98	66.63	67.31	66.90	67.00
4	69.88	70.39	70.02	69.13	67.02	66.83	66.03	66.95
5	162.35	166.80	167.34	162.97	158.69	162.31	160.89	157.79
6	149.34	152.33	152.32	151.57	145.92	147.18	144.13	145.12
7	140.56	143.50	137.63	142.56	137.88	144.52	145.46	142.27
8	151.40	158.31	155.30	157.86	154.70	153.01	160.14	156.50
9	63.36	60.25	62.27	62.35	62.63	62.40	60.14	61.47
10	63.60	65.24	63.77	64.05	63.80	63.74	64.24	65.94
11	158.01	158.09	157.65	156.78	158.38	157.47	157.85	157.64
12	166.44	165.13	164.53	166.48	165.98	164.18	164.87	164.78
13	158.57	157.89	158.98	158.15	158.57	157.41	158.12	157.68
14	22.07	22.49	22.17	21.96	22.30	22.12	22.30	22.07
15	141.44	141.64	141.67	141.30	141.51	141.55	141.59	141.42
16	148.20	150.41	148.14	151.56	148.71	145.74	145.61	151.29
17	150.61	154.97	152.36	157.14	155.07	151.61	156.29	157.78
18	157.77	158.61	156.93	157.93	159.15	158.58	157.93	159.21
19	165.80	165.74	164.87	165.38	166.48	166.01	165.53	166.02
20	175.41	175.81	175.34	175.54	176.26	175.41	175.86	175.71
21	152.21	152.66	154.57	152.86	154.63	150.53	154.84	151.80
Probability	6.3x10 ⁻⁷	3.2x10 ⁻⁷	2.4x10 ⁻⁸	4.8x10 ⁻⁶	0.99	1.6x10 ⁻⁵	3.1x10 ⁻³	6.2x10 ⁻³

Figure 33

Table 37 – DP4 probabilities associated with the cis-mucosin methyl ester experimental data

	Isomer 1	Isomer 2	Isomer 3	Isomer 4	Isomer 5	Isomer 6	Isomer 7	Isomer 8
Probability	5.1x10 ⁻³	3.1x10 ⁻²	3.9x10 ⁻⁴	0.16	0.62	0.10	3.2x10 ⁻²	5.4x10 ⁻²

Figure 34

Table 38 - DP4 probabilities associated with the exo-mucosin methyl ester experimental data

	Isomer 1	Isomer 2	Isomer 3	Isomer 4	Isomer 5	Isomer 6	Isomer 7	Isomer 8
Probability	3.1x10 ⁻⁴	1.6x10 ⁻³	7.3x10 ⁻⁵	0.19	0.61	1.4x10 ⁻⁴	4.5x10 ⁻³	0.19

Figure 35

Table 8 - Calculated shielding tensors for the candidate structures of (-)-mucosin methyl ester and DP4.2 probabilities associated with the cis-mucosin methyl ester experimental data

Nucleus Label	Isomer 1	Isomer 2	Isomer 3	Isomer 4	Isomer 5	Isomer 6	Isomer 7	Isomer 8
1	1.20	1.50	1.14	1.27	1.38	1.26	1.00	1.42
2	153.79	153.67	152.86	152.19	153.46	153.83	152.91	153.67
3	162.38	162.11	162.10	161.20	162.19	162.15	161.53	162.03
4	152.98	153.61	152.12	152.25	153.21	153.22	152.72	153.31
5	49.05	50.53	50.26	52.11	49.17	49.02	49.48	50.82
6	47.00	45.14	46.12	45.47	47.37	47.11	45.01	45.92
7	145.13	154.15	151.53	153.62	148.77	148.68	155.40	152.31
8	133.66	138.88	132.90	144.22	132.37	139.15	140.17	138.37
9	145.13	147.60	148.24	143.98	139.80	141.74	139.16	139.97
10	157.27	163.20	164.23	160.46	154.03	158.42	157.09	153.56
11	55.16	55.56	54.69	54.88	51.98	51.87	51.11	51.85
12	55.09	55.14	55.46	54.52	51.76	52.34	51.40	51.76
13	158.08	158.59	158.55	157.08	152.80	152.48	151.02	152.68
14	150.21	148.73	149.26	150.54	145.48	146.52	148.28	144.76
15	147.33	148.60	149.95	146.96	148.84	145.02	149.88	146.62
16	141.74	147.07	142.96	147.90	144.08	141.05	141.44	145.67
17	146.05	152.36	148.38	153.41	148.69	146.58	151.84	153.46
18	153.24	155.35	152.16	154.26	154.39	153.68	152.84	153.98
19	161.25	163.02	160.33	161.20	161.71	160.95	160.98	161.29
20	172.10	172.71	171.90	172.04	172.46	172.06	172.02	172.02
21	135.83	135.97	135.85	135.73	135.84	135.94	135.75	135.94
Probability	2.6x10 ⁻⁶	8.3x10 ⁻⁴	7.8x10 ⁻⁸	7.3x10 ⁻¹²	0.99	5.0x10 ⁻⁵	8.3x10 ⁻⁵	1.3x10 ⁻⁵

Table 9- Calculated shielding tensors for the candidate structures of (-)-mucosin methyl ester and DP4+ probabilities associated with the cis-mucosin methyl ester experimental data

Nucleus Label	Isomer 1	Isomer 2	Isomer 3	Isomer 4	Isomer 5	Isomer 6	Isomer 7	Isomer 8
1	22.93	22.97	22.93	22.88	22.83	22.79	22.81	22.84
2	162.95	161.60	162.74	162.20	162.51	162.49	161.90	162.25
3	170.25	169.19	170.16	170.09	169.83	169.45	169.51	169.82
4	162.14	161.26	162.09	161.37	161.75	161.91	161.37	161.57
5	66.32	67.65	67.40	67.52	66.20	66.58	67.71	67.75
6	65.53	63.70	64.55	64.23	65.85	65.00	62.58	64.09
7	155.79	162.63	159.84	160.88	158.71	157.19	164.79	160.41
8	143.78	146.36	142.06	149.07	141.80	147.40	148.21	146.43
9	153.64	156.31	156.23	153.22	149.86	150.93	147.47	149.03
10	166.06	170.11	171.31	166.71	162.25	165.89	164.15	161.34
11	71.52	71.80	71.33	70.71	69.57	69.31	68.52	69.36
12	71.37	71.81	71.84	70.89	69.32	70.10	69.46	69.27
13	165.38	166.19	166.24	165.58	161.12	160.75	159.44	160.91
14	157.92	156.58	157.12	158.70	154.30	155.10	156.59	152.93
15	157.07	156.84	159.43	156.34	158.19	154.51	159.01	156.53
16	151.30	153.53	152.53	155.40	153.12	150.69	149.84	154.47
17	156.66	159.12	158.17	162.60	158.09	156.86	161.80	162.56
18	163.39	162.89	162.86	163.47	163.62	163.84	162.85	163.84
19	170.83	170.24	170.24	170.60	170.41	170.37	170.00	170.54
20	181.15	180.93	180.82	180.90	181.07	181.07	181.13	180.95
21	143.98	144.01	144.02	143.92	144.04	143.99	143.89	144.00
Probability	5.1×10^{-20}	1.4×10^{-25}	8.7×10^{-22}	7.0×10^{-18}	0.99	1.0×10^{-9}	5.4×10^{-20}	1.3×10^{-12}

Figure 36

Table 10 - DP4.2 probabilities associated with the exo-mucosin methyl ester experimental data

	Isomer 1	Isomer 2	Isomer 3	Isomer 4	Isomer 5	Isomer 6	Isomer 7	Isomer 8
Probability	6.4×10^{-8}	3.4×10^{-8}	3.8×10^{-14}	1.3×10^{-15}	0.99	1.7×10^{-11}	2.6×10^{-7}	1.9×10^{-05}

Table 11- DP4+ probabilities associated with the exo-mucosin methyl ester experimental data

	Isomer 1	Isomer 2	Isomer 3	Isomer 4	Isomer 5	Isomer 6	Isomer 7	Isomer 8
Probability	1.1×10^{-16}	5.3×10^{-20}	7.1×10^{-18}	5.7×10^{-17}	0.99	6.2×10^{-6}	3.1×10^{-17}	3.9×10^{-4}

Figure 41

Table 12 – DP4 probabilities associated with the reassigned cis-mucosin methyl ester experimental data

	Isomer 1	Isomer 2	Isomer 3	Isomer 4	Isomer 5	Isomer 6	Isomer 7	Isomer 8
Probability	0.99	8.2×10^{-5}	7.4×10^{-4}	1.5×10^{-3}	1.0×10^{-5}	6.7×10^{-3}	4.6×10^{-9}	1.5×10^{-8}

Table 13 – DP4+ probabilities associated with the reassigned cis-mucosin methyl ester experimental data

	Isomer 1	Isomer 2	Isomer 3	Isomer 4	Isomer 5	Isomer 6	Isomer 7	Isomer 8
Probability	0.99	1.6×10^{-28}	3.4×10^{-22}	3.9×10^{-25}	5.9×10^{-5}	2.5×10^{-7}	2.8×10^{-26}	7.1×10^{-19}

Table 14 – DP4.2 probabilities associated with the reassigned cis-mucosin methyl ester experimental data

	Isomer 1	Isomer 2	Isomer 3	Isomer 4	Isomer 5	Isomer 6	Isomer 7	Isomer 8
Probability	0.99	3.8×10^{-8}	5.8×10^{-6}	1.6×10^{-19}	7.1×10^{-6}	4.5×10^{-7}	2.7×10^{-17}	9.5×10^{-17}

Figure 42

Table 15 – DP4 probabilities associated with the reassigned exo-mucosin methyl ester experimental data

	Isomer 1	Isomer 2	Isomer 3	Isomer 4	Isomer 5	Isomer 6	Isomer 7	Isomer 8
Probability	5.3×10^{-5}	0.08	0.92	3.9×10^{-4}	8.7×10^{-8}	3.1×10^{-7}	9.3×10^{-11}	1.7×10^{-9}

Table 16 – DP4+ probabilities associated with the reassigned exo-mucosin methyl ester experimental data

	Isomer 1	Isomer 2	Isomer 3	Isomer 4	Isomer 5	Isomer 6	Isomer 7	Isomer 8
Probability	3.4×10^{-16}	1.22×10^{-11}	0.99	1.1×10^{-14}	4.7×10^{-29}	1.4×10^{-21}	3.5×10^{-40}	3.8×10^{-39}

Table 17 – DP4.2 probabilities associated with the reassigned exo-mucosin methyl ester experimental data

	Isomer 1	Isomer 2	Isomer 3	Isomer 4	Isomer 5	Isomer 6	Isomer 7	Isomer 8
Probability	2.1×10^{-7}	8.3×10^{-5}	0.99	5.0×10^{-21}	3.4×10^{-10}	1.5×10^{-14}	3.0×10^{-19}	9.3×10^{-19}

2.5. References

- (1) Jia, Y.-L.; Wei, M.-Y.; Chen, H.-Y.; Guan, F.-F.; Wang, C.-Y.; Shao, C.-L. *Org. Lett.* **2015**, *17*, 4216.
- (2) Wang, Q.; Tang, X.; Luo, X.; de Voogd, N. J.; Li, P.; Li, G. *Org. Lett.* **2015**, *17*, 3458.
- (3) Narayan, R. S.; Borhan, B. *J. Org. Chem.* **2006**, *71*, 1416.
- (4) Hattori, H.; Hoff, L. V.; Gademann, K. *Org. Lett.* **2019**, *21*, 3456.
- (5) Davoren, J. E.; Martin, S. F. *J. Am. Chem. Soc.* **2007**, *129*, 510.
- (6) Reddy, D. S.; Kutateladze, A. G. *Tetrahedron Lett.* **2016**, *57*, 4727.
- (7) Wu, J.; Lorenzo, P.; Zhong, S.; Ali, M.; Butts, C. P.; Myers, E. L.; Aggarwal, V. K. *Nature* **2017**, *547*, 436.
- (8) Barone, G.; Gomez-Paloma, L.; Duca, D.; Silvestri, A.; Riccio, R.; Bifulco, G. *Chem. - A Eur. J.* **2002**, *8*, 3233.
- (9) Barone, G.; Duca, D.; Silvestri, A.; Gomez-Paloma, L.; Riccio, R.; Bifulco, G. *Chem. - A Eur. J.* **2002**, *8*, 3240.
- (10) Sarotti, A. M.; Pellegrinet, S. C. *J. Org. Chem.* **2012**, *77*, 6059.
- (11) Jain, R.; Bally, T.; Rablen, P. R. *J. Org. Chem.* **2009**, *74*, 4017.
- (12) Forsyth, D. A.; Sebag, A. B. *J. Am. Chem. Soc.* **1997**, *119*, 9483.
- (13) Tantillo, D. J. Chemical Shift Repository <http://cheshirenmr.info/index.htm> (accessed Jul 9, 2019).
- (14) Lodewyk, M. W.; Soldi, C.; Jones, P. B.; Olmstead, M. M.; Rita, J.; Shaw, J. T.; Tantillo, D. J. *J. Am. Chem. Soc.* **2012**, *134*, 18550.
- (15) Sheldrake, H. M.; Jamieson, C.; Burton, J. W. *Angew. Chemie Int. Ed.* **2006**, *45*, 7199.
- (16) Smith, S. G.; Paton, R. S.; Burton, J. W.; Goodman, J. M. *J. Org. Chem.* **2008**, *73*, 4053.
- (17) Dyson, B. S.; Burton, J. W.; Sohn, T.; Kim, B.; Bae, H.; Kim, D. *J. Am. Chem. Soc.* **2012**, *134*, 11781.
- (18) Smith, S. G.; Goodman, J. M. *J. Am. Chem. Soc.* **2010**, *132*, 12946.
- (19) Stephens, P. J.; Devlin, F. J.; Chabalowski, C. F.; Frisch, M. J. *J. Phys. Chem.* **1994**, *98*, 11623.

- (20) Becke, A. D. *Phys. Rev. A* **1988**, *38*, 3098.
- (21) Becke, A. D. *J. Chem. Phys.* **1993**, *98*, 5648.
- (22) Lee, C.; Yang, W.; Parr, R. G. *Phys. Rev. B* **1988**, *37*, 785.
- (23) Hehre, W. J.; Radom, L.; P. v. R. Schleyer; Pople, J. A. *Ab Initio Molecular Orbital Theory*; John Wiley & Sons, Ltd: New York, 1986; Vol. 7.
- (24) Grimblat, N.; Zanardi, M. M.; Sarotti, A. M. *J. Org. Chem.* **2015**, *80*, 12526.
- (25) Cavalheiro, A. J.; Yoshida, M. *Phytochemistry* **2000**, *53*, 811.
- (26) Toneto Novaes, L. F.; Drekenner, R. L.; Avila, C. M.; Pilli, R. A. *Tetrahedron* **2014**, *70*, 6467.
- (27) Ermanis, K.; Parkes, K. E. B.; Agback, T.; Goodman, J. M. *Org. Biomol. Chem.* **2017**, *15*, 8998.
- (28) Zhao, Y.; Truhlar, D. G. *Theor. Chem. Acc.* **2008**, *120*, 215.
- (29) Adamo, C.; Barone, V. *J. Chem. Phys.* **1998**, *108*, 664.
- (30) Awad, K.; Mikhailidis, D. P.; Katsiki, N.; Muntner, P.; Banach, M. *Drugs* **2018**, *78*, 453.
- (31) Xin, D.; Jones, P.-J.; Gonnella, N. C. *J. Org. Chem.* **2018**, *83*, 5035.
- (32) Kinnel, R. B.; Gehrken, H. P.; Scheuer, P. J. *J. Am. Chem. Soc.* **1993**, *115*, 3376.
- (33) Gallantree-Smith, H. C.; Antonsen, S. G.; Görbitz, C. H.; Hansen, T. V.; Nolsøe, J. M. J.; Stenstrøm, Y. H. *Org. Biomol. Chem.* **2016**, *14*, 8433.
- (34) Antonsen, S.; Gallantree-Smith, H.; Görbitz, C.; Hansen, T.; Stenstrøm, Y.; Nolsøe, J. *Molecules* **2017**, *22*, 1720.
- (35) Henderson, A. R.; Stec, J.; Owen, D. R.; Whitby, R. J. *Chem. Commun.* **2012**, *48*, 3409.
- (36) Nolsøe, J. M. J.; Antonsen, S.; Görbitz, C. H.; Hansen, T. V.; Nesman, J. I.; Røhr, Å. K.; Stenstrøm, Y. H. *J. Org. Chem.* **2018**, *83*, 15066.
- (37) Casapullo, A.; Scognamiglio, G.; Cimino, G. *Tetrahedron Lett.* **1997**, *38*, 3643.
- (38) Mohamadi, F.; Richards, N. G. J.; Guida, W. C.; Liskamp, R.; Lipton, M.; Caufield, C.; Chang, G.; Hendrickson, T.; Still, W. C. *J. Comput. Chem.* **1990**, *11*, 440.
- (39) Maestro (Version 11.5). Schrödinger, LLC: New York 2018.
- (40) Chang, G.; Guida, W. C.; Still, W. C. *J. Am. Chem. Soc.* **1989**, *111*, 4379.

- (41) Halgren, T. A. *J. Comput. Chem.* **1996**, *17*, 490.
- (42) Halgren, T. A. *J. Comput. Chem.* **1996**, *17*, 520.
- (43) Halgren, T. A. *J. Comput. Chem.* **1996**, *17*, 553.
- (44) Halgren, T. A. *J. Comput. Chem.* **1999**, *20*, 730.
- (45) Halgren, T. A. *J. Comput. Chem.* **1996**, *17*, 616.
- (46) Halgren, T. A. *J. Comput. Chem.* **1999**, *20*, 720.
- (47) Halgren, T. A.; Nachbar, R. B. *J. Comput. Chem.* **1996**, *17*, 587.
- (48) Ditchfield, R. *J. Chem. Phys.* **1972**, *56*, 5688.
- (49) Wolinski, K.; Hinton, J. F.; Pulay, P. *J. Am. Chem. Soc.* **1990**, *112*, 8251.
- (50) Frisch, M. J.; Trucks, G. W.; Schlegel, H. B.; Scuseria, G. E.; Robb, M. A.; Cheeseman, J. R.; Scalmani, G.; Barone, V.; Petersson, G. A.; Nakatsuji, H.; Li, X.; Caricato, M.; Marenich, A.; Bloino, J.; Janesko, B. G.; Gomperts, R.; Mennucci, B.; Hratchian, H. P.; Ortiz, J. V.; Izmaylov, A. F.; Sonnenberg, J. L.; Williams-Young, D.; Ding, F.; Lipparini, F.; Egidi, F.; Goings, J.; Peng, B.; Petrone, A.; Henderson, T.; Ranasinghe, D.; Zakrzewski, V. G.; Gao, J.; Rega, N.; Zheng, G.; Liang, W.; Hada, M.; Ehara, M.; Toyota, K.; Fukuda, R.; Hasegawa, J.; Ishida, M.; Nakajima, T.; Honda, Y.; Kitao, O.; Nakai, H.; Vreven, T.; Throssell, K.; Montgomery, J. A.; Jr., J. E. P.; Ogliaro, F.; Bearpark, M.; Heyd, J. J.; Brothers, E.; Kudin, K. N.; Staroverov, V. N.; Keith, T.; Kobayashi, R.; Normand, J.; Raghavachari, K.; Rendell, A.; Burant, J. C.; Iyengar, S. S.; Tomasi, J.; Cossi, M.; Millam, J. M.; Klene, M.; Adamo, C.; Cammi, R.; Ochterski, J. W.; Martin, R. L.; Morokuma, K.; Farkas, O.; Foresman, J. B.; Fox, D. J. Gaussian 09, Revision A.02. Gaussian, Inc.: Wallingford CT 2016.
- (51) Jaguar (Version 9.9). Schrödinger, LLC: New York 2018.

Chapter Three

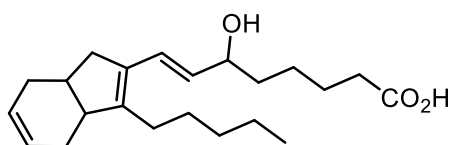
The Computationally-Guided Structural
Elucidation of Dictyosphaerin and the Total
Synthesis of Dictyosphaerin Methyl Ester

“But it ain’t how hard you hit; it’s about how hard you can get hit, and keep moving forward. How much you can take, and keep moving forward.” – Rocky Balboa

3.1. Introduction

3.1.1. Dictyosphaerin

In the previous chapter, it has been demonstrated that conformationally-flexible natural product, mucosin, can have the relative stereochemistry effectively assigned *via* computation. Consequently, a similar target natural product was sought that has suffered from stereochemical ambiguity, within the chemical literature, with the intention of proposing a probable structure then confirming it through subsequent synthesis. Indeed, dictyosphaerin is a structurally similar natural product where the absolute and relative stereochemistry remains undetermined (Figure 46).



193

Figure 46 - Proposed structure of dictyosphaerin

Dictyosphaerin **193** was isolated by Capon and co-workers in 1996 from *Dictyosphaeria sericea*, a marine green alga found in southern Australia.¹ Capon et al. identified key structural features in dictyosphaerin, such as the secondary allylic alcohol and carboxylic acid functionality, through their distinctive IR absorptions and ¹³C NMR resonances. Additionally, six olefinic ¹³C NMR resonances indicated the presence of three double bonds. Interestingly, a distinctive UV absorption provided evidence for the presence of a conjugated diene. Loss of butadiene was observed during mass spectrometry analysis, due to the fragmentation of a cyclohexene *via* a retro Diels-Alder reaction. However, due to overlapping ¹H NMR resonances, assigning the structure of dictyosphaerin **193** or dictyosphaerin methyl ester appeared too challenging. Fortunately, Capon and co-workers were able to propose a skeletal structure, containing three stereocentres, after further chemical transformations and subsequent analysis. Despite establishing the overall connectivity, the absolute and relative stereochemistry of dictyosphaerin **193** remain unassigned, and no efforts towards its synthesis or structural elucidation have been reported, within the chemical literature.

3.1.2. Proposed Work

The stereochemical assignment and structure confirmation of dictyosphaerin could be achieved entirely through synthetic efforts alone. However, as the structure of dictyosphaerin contained three

stereocentres, it is possible that the synthesis of four diastereomers would have to be achieved to identify the true structure of the natural product. With our research into correctly identifying the relative stereochemistry of mucosin, which is a similarly conformationally-flexible oxylipin structure, and its stereopermutations *via* computation and DP4-like analysis, we proposed to utilise this technique to aid our synthetic work towards dictyosphaerin. Initially, the candidate structures for dictyosphaerin will have their shielding tensors calculated *via* NMR GIAO calculations and the probabilities of matching the experimental data from Capon's characterisation assessed, using DP4-like analysis (Figure 47).

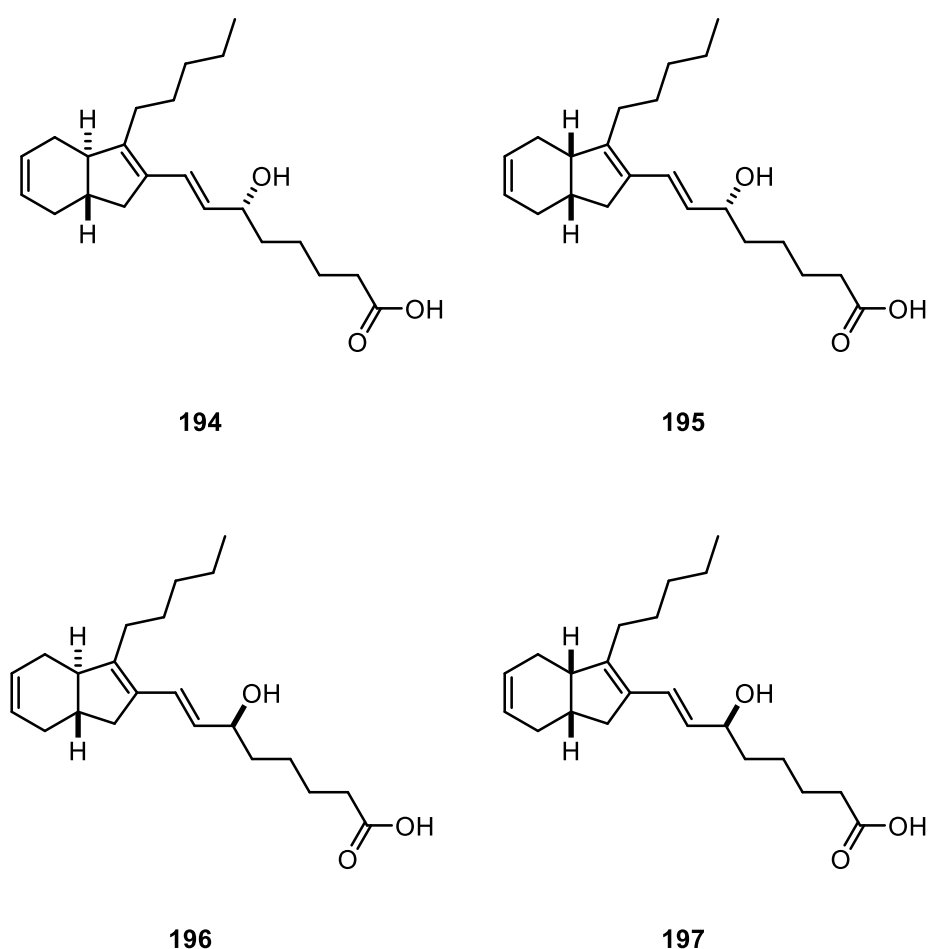
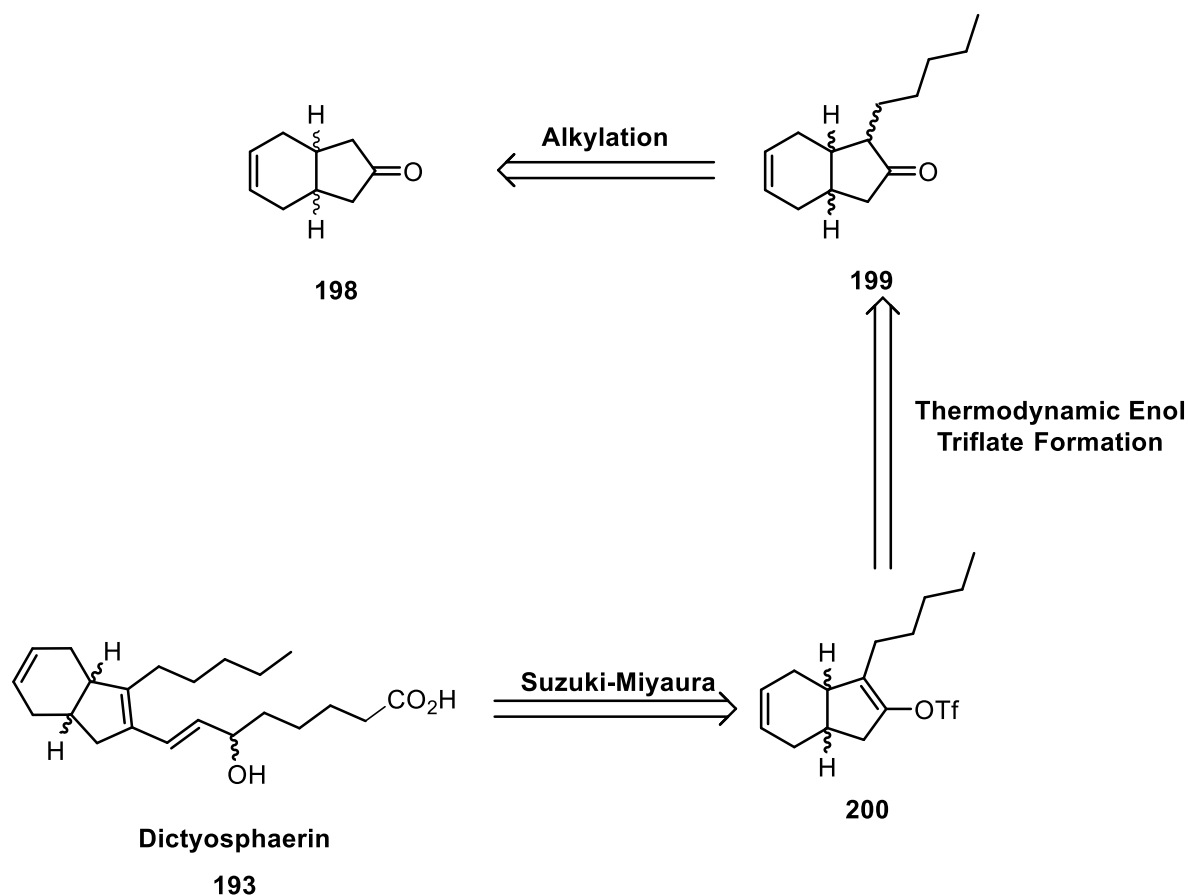


Figure 47 - Candidate structures for dictyosphaerin

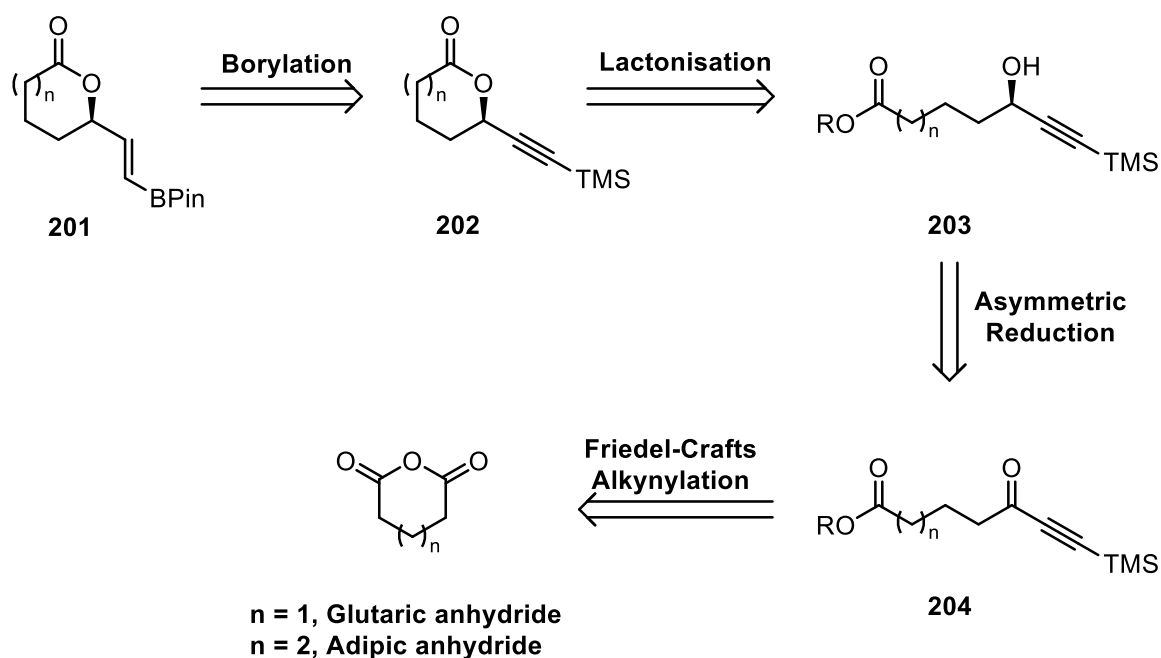
Having identified a probable candidate structure, work would then focus on its synthesis to ultimately prove the utility of DP4-analysis in the structural elucidation of a highly flexible, complex natural product, such as dictyosphaerin **193**. The proposed synthetic strategy towards the synthesis of dictyosphaerin **193** is detailed below in Scheme 139.



Scheme 139 - Proposed retrosynthesis of dictyosphaerin

Retrosynthetically, a convergent strategy towards dictyosphaerin **193** could be envisioned *via* a late stage Suzuki-Miyaura cross-coupling reaction to deliver the chiral allylic alcohol-bearing sidechain from the thermodynamic enol triflate **200**. The thermodynamic enol triflate **200** would be synthesised through the formation of the thermodynamic enolate generated from the alkylated ketone **199**, and subsequent quench with the appropriate electrophile. Alkylated ketone **199** could be made from ketone **198**, following a similar strategy utilised in our synthetic efforts towards (-)-mucosin. Desymmetrisation of the ketone containing a *cis*-bridgehead will be possible, as we have previously shown (*vide supra*). However, if dictyosphaerin **193** is indicated as possessing a *trans*-bridgehead, the synthetic strategy will need to be adapted, as the racemic *trans*-ketone is chiral and racemic, and thus is not suitable for asymmetric desymmetrisation.

As it is proposed to install the alcohol-bearing sidechain from a Suzuki-Miyaura cross-coupling, an appropriate boronic ester would need to be synthesised to facilitate this transformation. The proposed retrosynthesis of boronic ester is detailed in Scheme 140.



Scheme 140 - Proposed retrosynthesis of boronic ester

It is proposed that boronic ester **201** could be synthesised *via* the borylation of the deprotected silyl-protected alkyne lactone **202**. The lactone would be prepared from a lactonization process from the respective chiral propargylic alcohol **203**. The asymmetry inducing transformation would allow for the synthesis of the chiral propargylic alcohol **203** from the ynone **204**. The ynone **204** could be rapidly synthesised from a Friedel-Crafts alkynylation from adipic anhydride, or the commercially available glutaric anhydride. Obviously, if this synthesis cannot be achieved with adipic anhydride and instead it is undertaken with glutamic anhydride, a homologation procedure would likely need to be invoked after the cross coupling to afford dictyosphaerin **193**, the desired natural product.

If the convergent strategy proves successful, and access to the dictyosphaerin **193** is achieved, allowing us to confirm the proposed gross structure. It would be at this point that comparison to Capon's optical rotation and NMR characterisation would be undertaken. This would ensure that our proposed synthetic route has allowed access to (–)-dictyosphaerin. Additionally, the synthetic studies could confirm that DP4-like analysis is a viable tool in the structural elucidation of conformationally-flexible natural product targets, such as dictyosphaerin.

3.2. Results and Discussion

3.2.1. DP4 Analysis of Dictyosphaerin

Prior to any synthetic work, computational studies focused on determining a candidate stereoisomer for dictyosphaerin to direct our practical efforts. As was shown with (–)-mucosin and its stereopermutations, DP4-like analysis proved exceedingly effective in determining the correct relative stereochemistry for these highly-flexible oxylipins (*vide supra*). As dictyosphaerin is structurally similar to mucosin, it was thought that DP4-like analysis could also prove effective in the correct identification of its relative stereochemistry. We had previously demonstrated that DP4+ and DP4.2 were the highest performing methodologies with mucosin, and as a result our research would focus on these methodologies.

The ^{13}C NMR shielding tensors were computed for the four possible dictyosphaerin stereoisomers (Figure 48). These initial calculations were performed using MMFF to identify the low energy conformers and the subsequent energy calculations and optimisations were computed using B3LYP/6-31G(d). NMR GIAO calculations were computed using mPW1PW91/6-31+G(d,p), as is required by DP4+.² Due to numerous overlapping signals observed in the ^1H NMR spectrum obtained by Capon, it seemed sensible to only consider ^{13}C chemical shifts in any DP4-like analysis being undertaken.¹

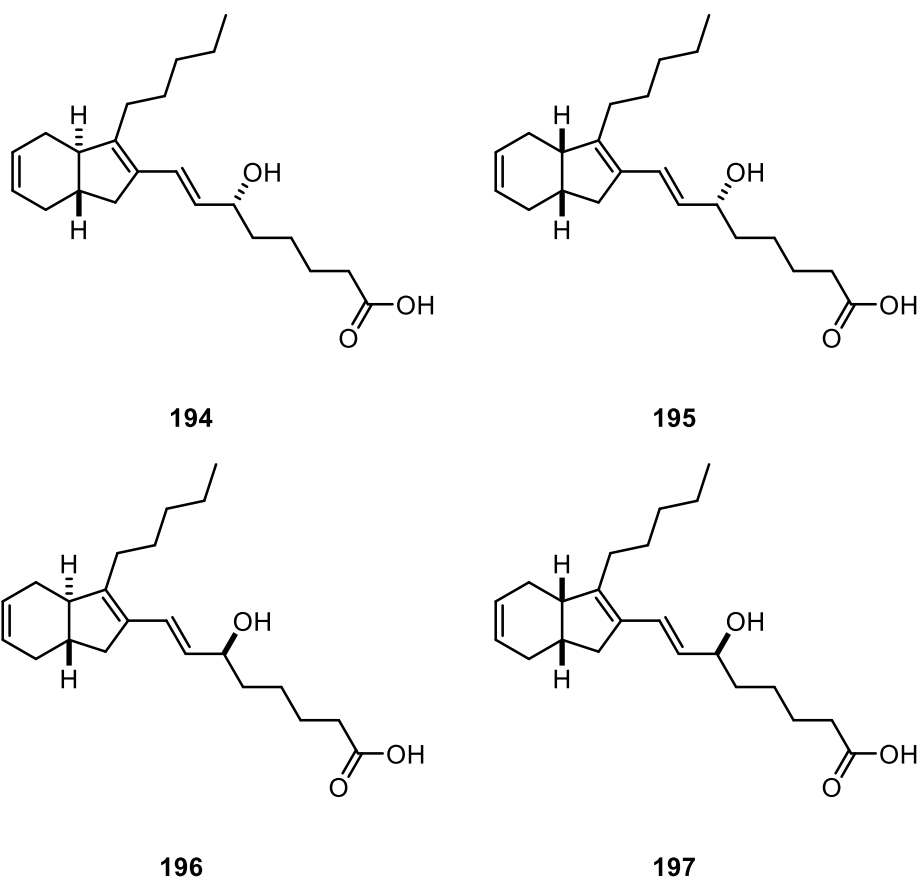


Figure 48 - Dictyosphaerin candidate structures

Having obtained the shielding tensors, they were scaled against the assigned ^{13}C spectrum recorded in Capon's isolation and the DP4+ probability was calculated leading to the probabilities shown in Figure 49.

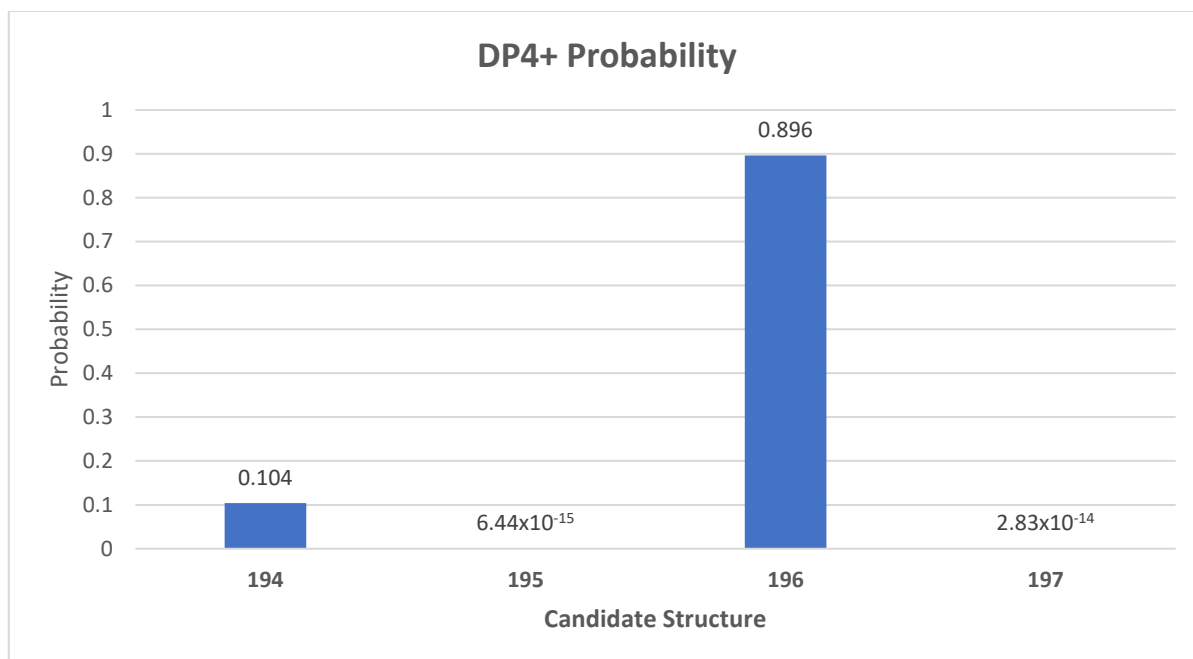


Figure 49 - DP4+ Probabilities for the candidate structures of dictyosphaerin

DP4+ analysis indicated two potential candidate structures, **194** and **196**. However, DP4+ had overwhelming confidence in **196** with approximately 90 % probability that the candidate structure matched the experimental ¹³C NMR spectral data obtained in Capon's characterisation.¹ Additionally, **194** was identified with approximately 10 % confidence. These results strongly suggest that the natural product contains a *trans*-bridgehead, similar to that observed with mucosin.³ The other high-performing DP4-like methodology, DP4.2, was also investigated to evaluate any differences in stereoisomer assignment. Further calculations were performed using M06-2X/6-31G(d,p) for energy calculations on all previously generated low-energy conformers for each candidate structure. NMR GIAO calculations were computed using mPW1PW91/6-311G(d), as is required by DP4.2.⁴ Having obtained the shielding tensors, they were scaled against the assigned ¹³C NMR spectra recorded in Capon's isolation, and the DP4.2 probability was calculated, leading to the probabilities shown in Figure 50.

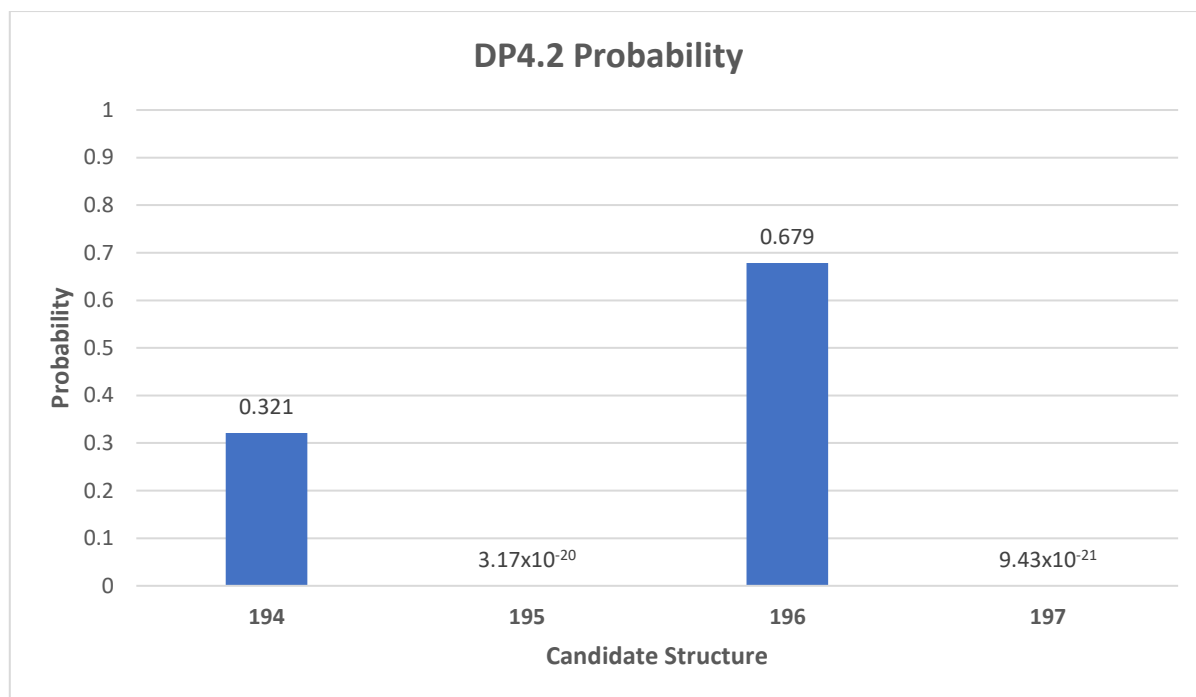


Figure 50 - DP4.2 Probabilities for the candidate structures of dictyosphaerin

Similarly, to DP4+, DP4.2 also discards *cis*-bridgehead structures and identifies two potential candidate structures for the structure of dictyosphaerin, **194** and **196**. In contrast however, DP4.2 displays reduced confidence in **196**, with respect to DP4+ analysis, with an approximately 68 % probability. As a consequence, **194** has an increased probability of being the structure of dictyosphaerin according to DP4.2 analysis. With this result, it becomes harder to exclude **194** from any synthetic efforts moving forward. Although, with both DP4+ and DP4.2 lending confidence only to the candidate structures containing a *trans*-bridgehead in the 5,6-bicyclic ring system, we can already exclude two of the possible four stereoisomers in our proposed synthetic work. With these results in hand, the syntheses of **194** and **196** will be investigated (Figure 51).

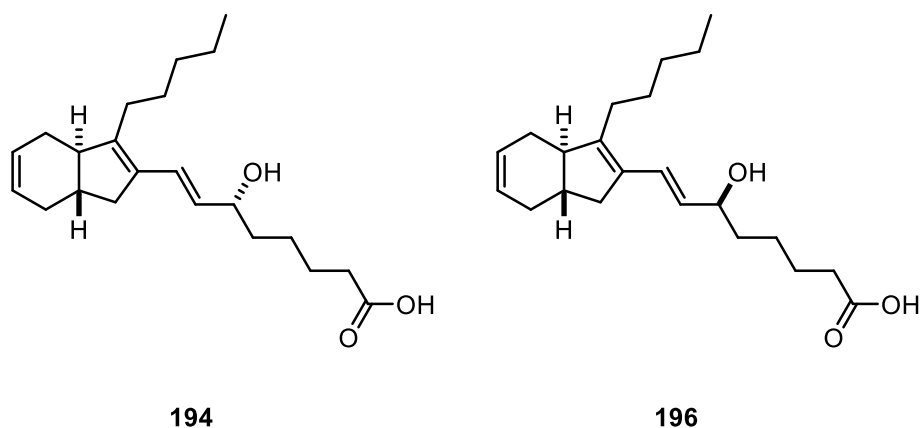
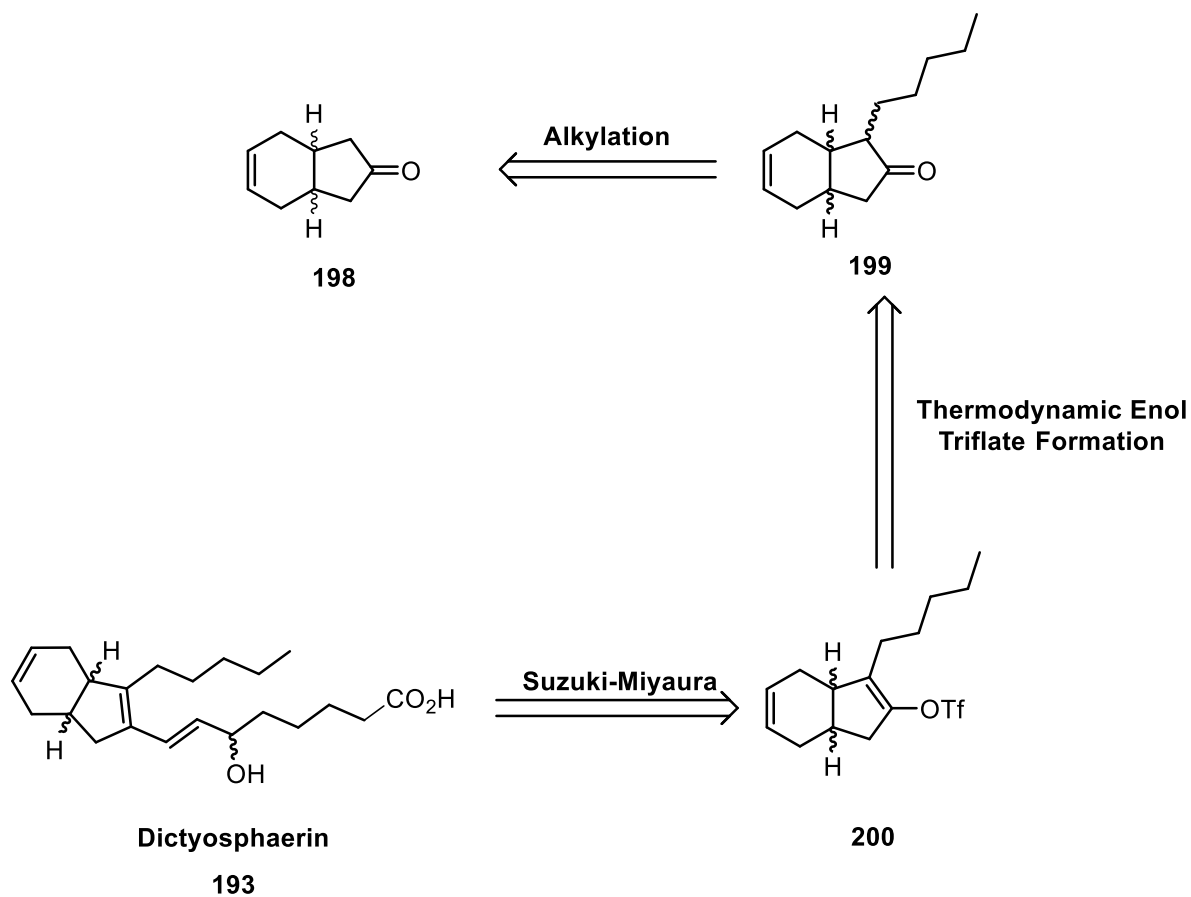


Figure 51 - Candidate structures targeted for the synthesis of dictyosphaerin

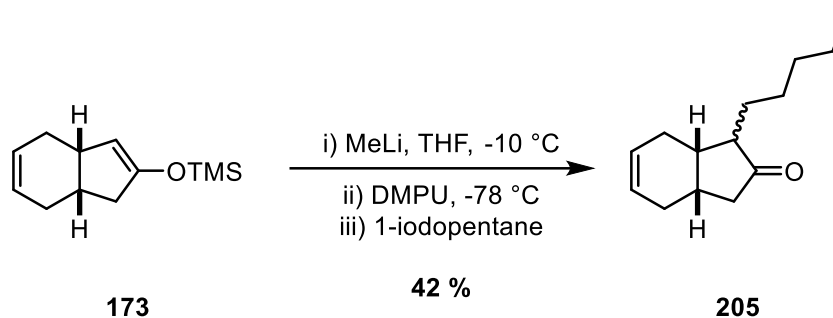
3.2.2. Synthesis of the Enol Triflate

As previously discussed, the synthesis of the enol triflate **200** is required for the key Suzuki-Miyaura cross-coupling in the proposed synthetic strategy towards dictyosphaerin, as highlighted below (Figure 55).



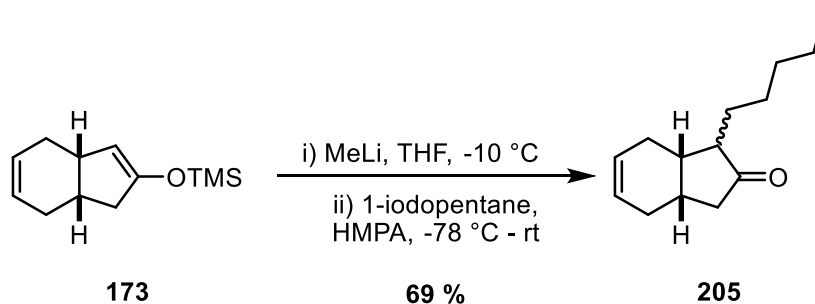
Scheme 141 - Proposed retrosynthesis for dictyosphaerin

The synthesis of the silyl enol ether **173** containing the *cis*-bridgehead was previously discussed in our synthetic efforts towards the total synthesis of mucosin (*vide supra*). As such, this system was used to model the alkylation to allow for the installation of the ⁿpentyl chain (Scheme 142).



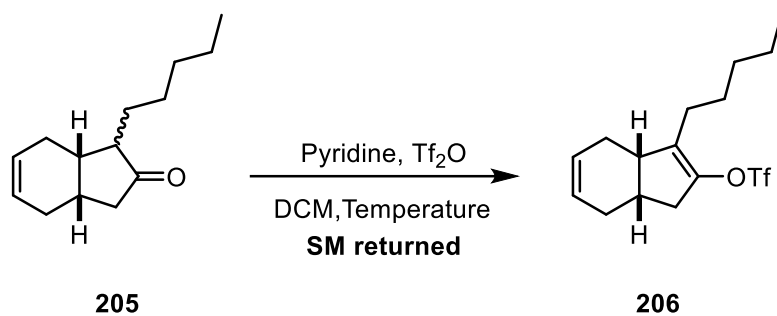
Scheme 142 - Alkylation performed with 1-iodopentane

Initial attempts to carry out this alkylation *via* the generation of a lithium enolate and subsequent quench with 1-iodopentane proved disappointing, with a modest 42 % yield of the desired alkylated ketone **205** being isolated. The observed result is likely due to the reduced reactivity of 1-iodopentane in comparison to the other electrophiles successfully employed in this reaction, such as allyl iodide (*vide supra*). Considering this, improving the reactivity of the generated lithium enolate towards the desired alkylation could overcome the lower reactivity observed when using 1-iodopentane as an electrophile. Indeed, it has been shown that the inclusion of HMPA as an additive can increase the observed reactivity in challenging alkylation reactions.⁵ As such, HMPA was employed in the desired alkylation of silyl enol ether **173** (Scheme 143).



Scheme 143 - Alkylation employing HMPA

Pleasingly, improved reactivity was indeed observed when employing HMPA as an additive, and the desired alkylated ketone **205** was obtained in a very good 69 % yield, as what would prove to be an inconsequential mix of diastereomers, after subsequent planarisation at this carbon centre. Having achieved the synthesis of the alkylated ketone **205** in good yield, work now focused towards the synthesis of the thermodynamic enol triflate **206**. It was initially thought that the desired enol triflate could be formed by employing an organic base (Scheme 144).

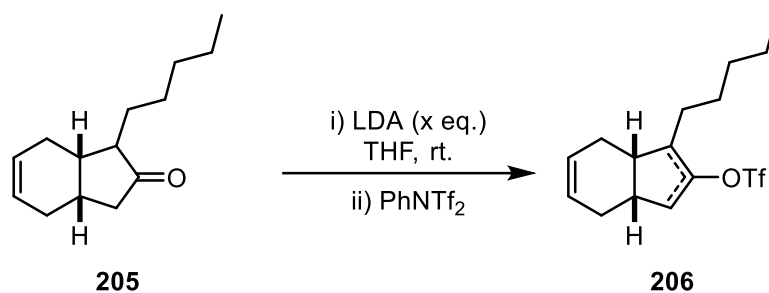


Scheme 144 - Attempted enol triflate formation

Table 39 - Attempted reaction conditions

Entry	Temperature	Result
1	-78 °C - rt	Starting material returned
2	0 °C - rt	Decomposition

Initially, the formation of the thermodynamic triflate **206** was attempted with pyridine and triflic anhydride at -78 °C (Table 39, Entry 1). These conditions resulted in no desired reaction and the starting material was returned, perhaps due to the low starting temperature hampering reactivity. Taking this into consideration, the reaction was attempted at a higher starting temperature of 0 °C and was then allowed to warm to room temperature (Table 39, Entry 2). Unfortunately, no discernible products relating to the starting material or the desired product could be identified by ¹H NMR spectroscopy. The decomposition observed in this reaction could be due to the use of the highly reactive triflic anhydride as an electrophile. Further work explored next the use of the less reactive triflating agent, *N*-phenyltriflimide, in an attempt to afford the desired thermodynamic enol triflate **206**.⁶ The use of strong organometallic bases are typically used to deliver kinetic enolates upon reaction with ketones. However, the generation of thermodynamic triflates has been achieved with the implementation of Hauser bases or LDA with *N*-phenyltriflimide, as reported in the literature.⁷ With this knowledge, the formation of the thermodynamic enol triflate **206** was revisited (Scheme 145, Table 40).



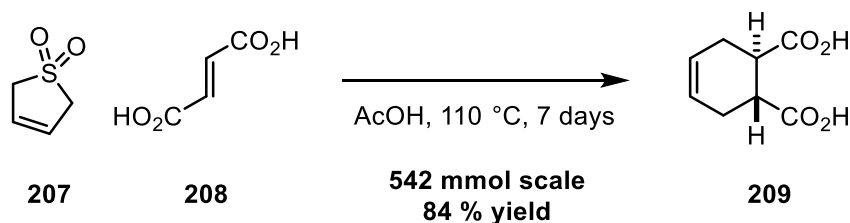
Scheme 145 - Formation of thermodynamic enol triflate with LDA

Table 40 - Thermodynamic triflate formation results

Entry	Conditions	Yield (%)	Thermodynamic: Kinetic
1	LDA (1 eq.), THF, PhNTf ₂ , rt	40	91:9
2	LDA (0.95 eq.), THF, PhNTf ₂ , rt	30	92:8

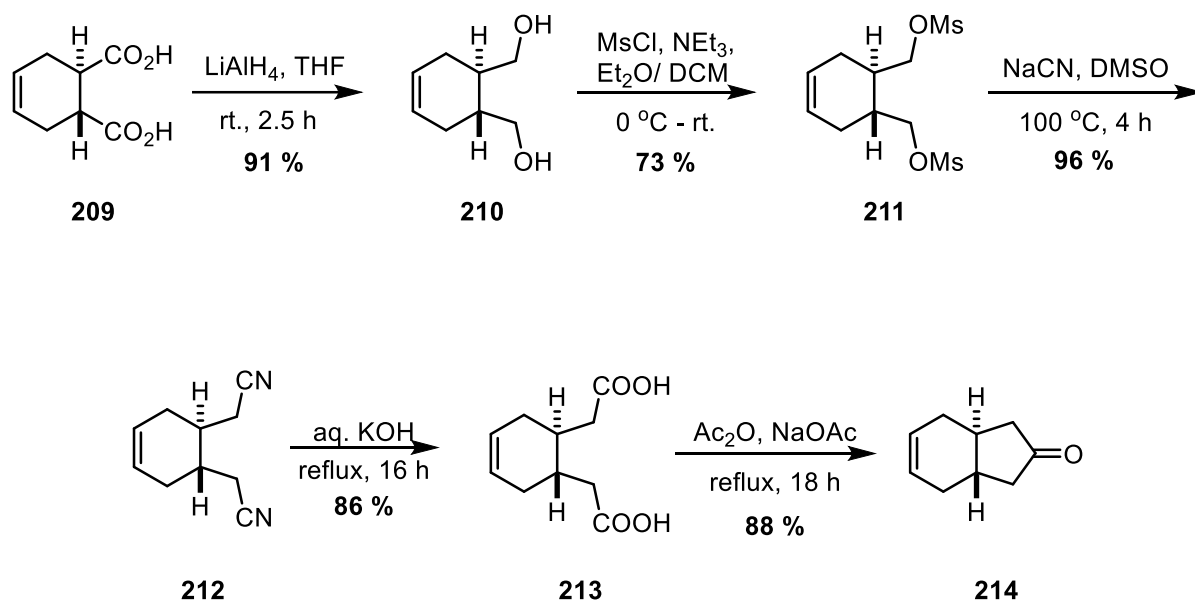
Pleasingly, a successful outcome was observed when employing one equivalent of LDA at room temperature, followed by a subsequent quench with *N*-phenyltriflimide, and the desired product **206** was isolated in a 40 % yield with a 91:9 thermodynamic to kinetic product ratio (Table 40, Entry 1). In order to obtain the thermodynamic enol triflate **206** as the sole product, a reduction in the stoichiometry of the base was investigated (Table 40, Entry 2). Upon reducing the equivalents of base, a reduction in yield was observed, with only 30 % of the desired product being isolated with a negligible increase in the thermodynamic product being observed. No further work was carried out to optimise the yield or increase the amount of the thermodynamic product at this stage. Instead, work focused on the synthesis of the *trans*-bridgehead containing enol triflate.

To verify the presence of a *trans*-bridgehead in dictyosphaerin, the synthesis of the racemic *trans*-ketone was pursued in a similar fashion to our synthesis of the *cis*-bridgehead containing ketone (*vide supra*). To commence this synthesis, a large quantity of the dicarboxylic acid **209** was synthesised via a Diels-Alder reaction (Scheme 146).



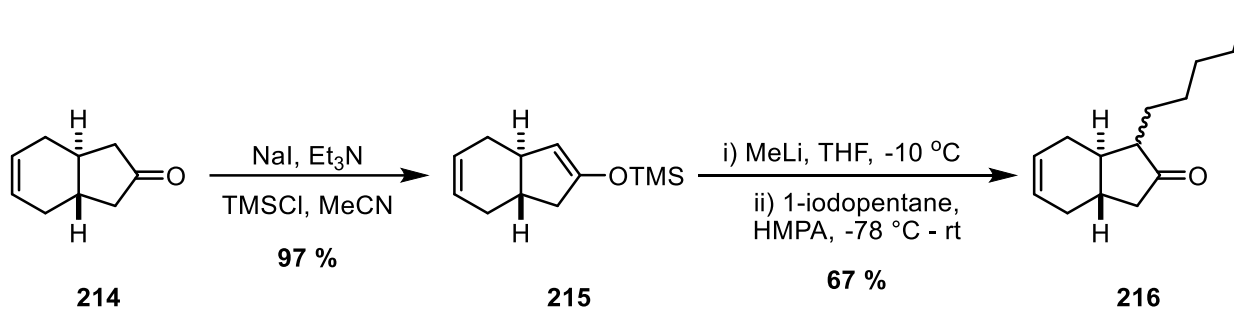
Scheme 146 - Diels-Alder reaction

Employing 3-sulfolene **207** and *E*-fumaric acid **208**, the desired cyclohexene was prepared an excellent 84 % yield, despite a lengthy reaction time. With large quantities of diacid **209** in hand, the synthesis of the *trans*-bridgehead containing ketone **214** was undertaken (Scheme 147).



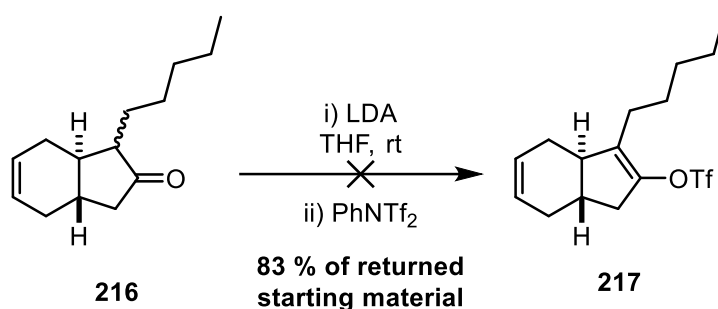
Scheme 147 - Synthesis of racemic trans-ketone

Reduction of the dicarboxylic acid **209** to the diol **210** proceeded efficiently when LiAlH_4 was employed, giving an excellent 91 % yield. With the diol **210** in hand, the homologation procedure commenced with mesylation, which proceeds in 75 % yield, followed by an $\text{S}_{\text{N}}2$ displacement with NaCN , which furnished the dinitrile **212** compound in a quantitative yield. Hydrolysis of the dinitrile **212** with aqueous KOH affords the diacid **213** in an excellent 90 % yield. Finally, the *trans*-bicyclic ketone **214** is synthesised *via* a Dieckmann condensation of diacid **213**. Having synthesised the racemic *trans*-ketone **214** work towards the synthesis of the desired enol triflate **217** continued. The pentyl side chain was installed using the previously optimised alkylation reaction, as described in Scheme 148.



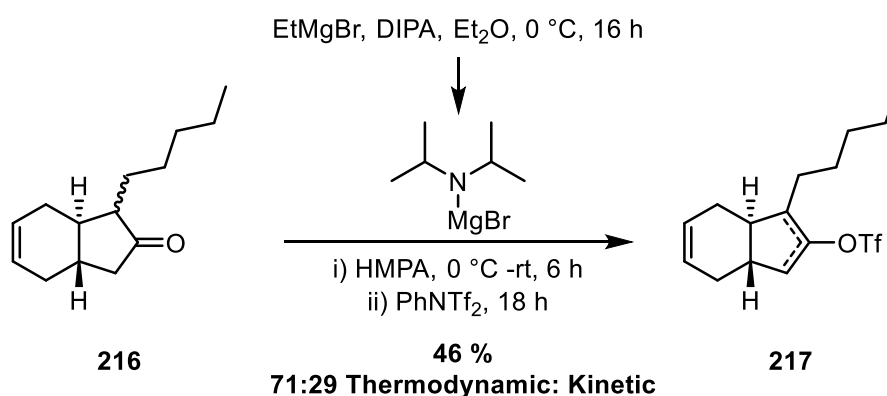
Scheme 148 - Synthesis of the trans-bridgehead alkylated ketone

The formation of the silyl enol ether **215** proceeded in an excellent 97 % yield using an *in situ* Finklestein process to generate the more reactive trimethylsilyl iodide. Having synthesised the required silyl enol ether **214**, alkylation with 1-iodopentane afforded the desired product, as expected, in a very good 67 % yield. The diastereoselectivity of this reaction could not be determined by ^1H NMR analysis due to overlapping resonances. However, this diastereoselectivity would become inconsequential due to the formation of the thermodynamic enol triflate **216**, resulting in the formation of an sp^2 centre at the diastereomeric carbon. The previously utilised conditions for the enol triflate formation were then applied to the alkylated ketone **216**, bearing a *trans*-bridgehead, as shown in Scheme 149.



Scheme 149 - Attempted synthesis of enol triflate

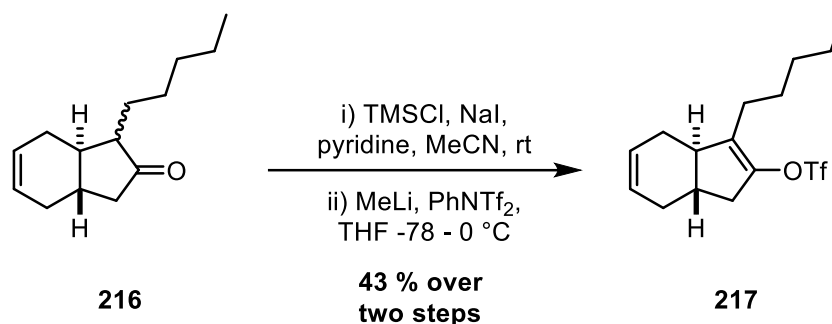
Incongruously, when applying the previously developed conditions, the use of LDA did not furnish the desired enol triflate **217** and starting material was returned. As such, the more thermally stable Hauser base was then employed in an attempt to afford the desired enol triflate **217** (Scheme 150).



Scheme 150 - Use of Hauser base to form enol triflate

The use of a Hauser base to facilitate the deprotonation of alkylated ketone **216** and subsequent electrophilic quench with *N*-phenyltriflimide did afford the desired enol triflate **217** in a moderate

yield. Despite this success, the ratio of the desired thermodynamic product was reduced in comparison to the *cis*-bridgehead-containing enol triflate **206**. A change of strategy was then sought to afford the desired thermodynamic enol triflate **217**. Synthesis of the thermodynamic silyl enol ether, which is well preceded within the chemical literature, could allow an opportunity to subsequently generate the respective thermodynamic lithium enolate.⁸ As a result, this could allow efficient access to the desired thermodynamic enol triflate **217**. Taking this into consideration, the enol triflate formation was reinvestigated.

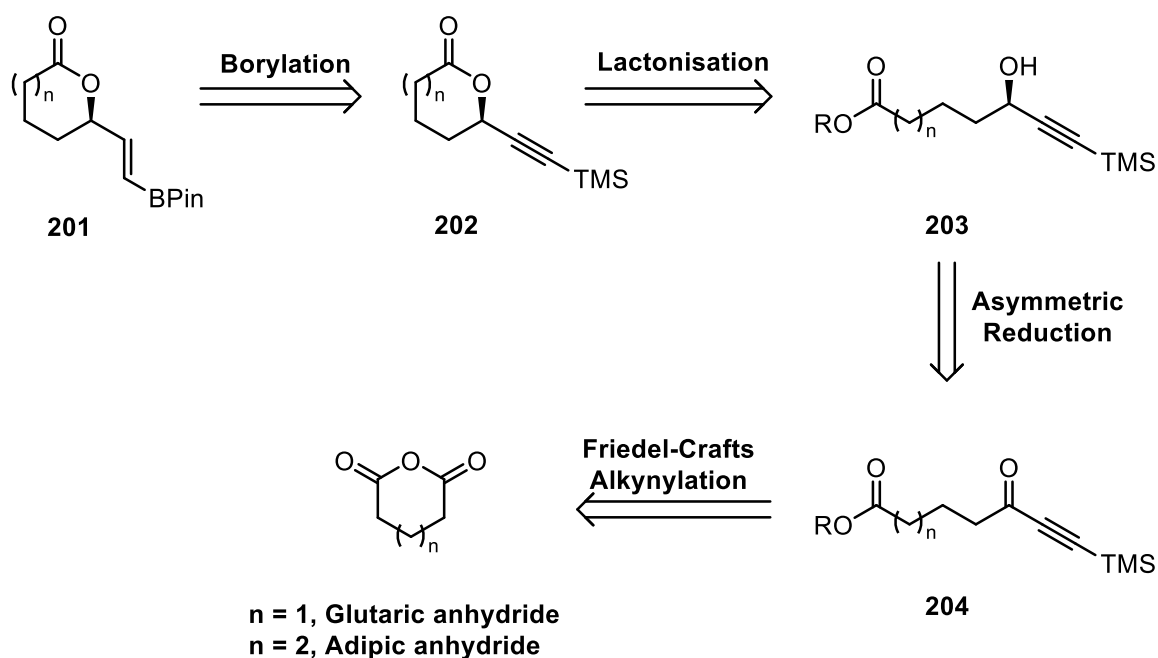


Scheme 151 - Enol triflate formation via a silyl enol ether

Pleasingly, when employing pyridine as a base, the silyl enol ether formation gave the exclusive thermodynamic enol ether when using conditions previously employed within mucosin. Upon treatment of the crude silyl enol ether with methyl lithium and quenching with *N*-phenyltriflimide, the desired thermodynamic enol triflate **217** was formed as the exclusive product in a 43 % yield over the two steps. With the desired thermodynamic enol triflate **217** now in hand, our focus shifted to the synthesis of the boronic ester **201** partner for the key cross-coupling in this convergent synthesis.

3.2.3. Synthesis of the Boronic Ester

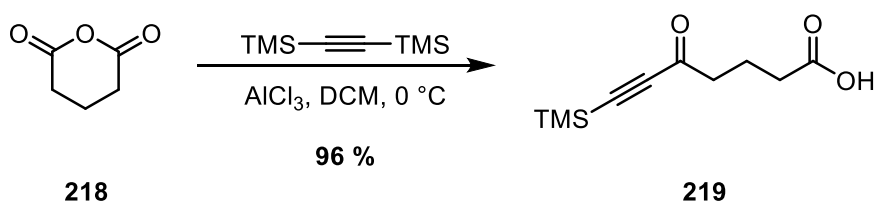
Having established the synthetic route towards the enol triflate intermediate, attention now focused on the synthesis of the requisite boronic ester coupling partner. The retrosynthesis of the boronic ester **201** is highlighted in Scheme 152.



Scheme 152 - Retrosynthesis of boronic ester

As previously discussed, targeting the six-membered lactone is potentially possible from the commercially available glutaric anhydride as highlighted above. However, for the total synthesis of dictyosphaerin, after cross-coupling and hydrolysis to give the free acid, a homologation would need to be performed. A more elegant solution would be to synthesise the boronic ester from adipic anhydride, circumventing the need for this inefficient homologation. However, adipic anhydride is commercially expensive and would have to be prepared within the laboratory. With this in mind, work initially focused on the synthesis of the boronic ester bearing the six-membered lactone.

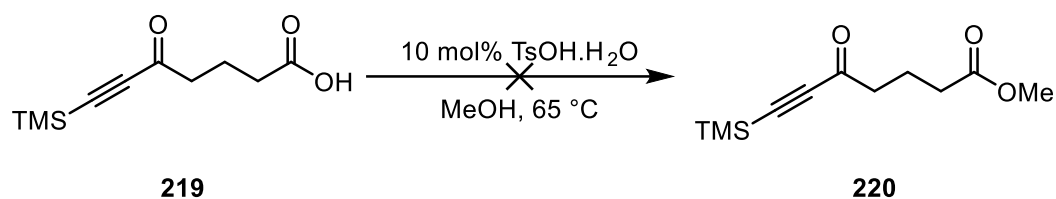
The first synthetic step towards the desired boronic ester was the ring opening of glutaric anhydride **218** to afford the keto-acid **219** (Scheme 153).⁹



Scheme 153 - Friedel-Crafts alkynylation

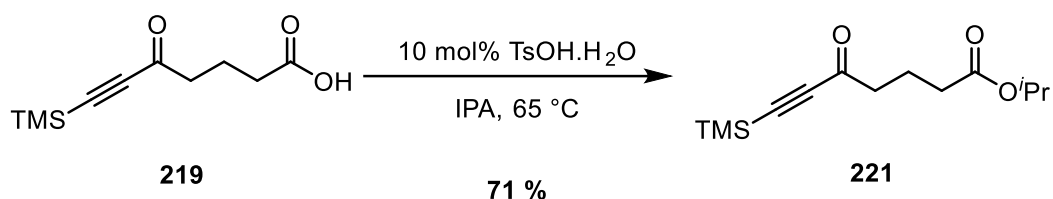
When employing a Lewis acid-mediated Friedel-Crafts alkynylation, the desired keto-acid **219** was isolated in an excellent yield of 96 %. Prior to the reduction of the ynone functionality, the free acid was converted into an ester to ensure the subsequent compounds were easy to purify. Initially,

esterification of the keto-acid **219** was carried out in methanol to afford the methyl ester **220** (Scheme 154).



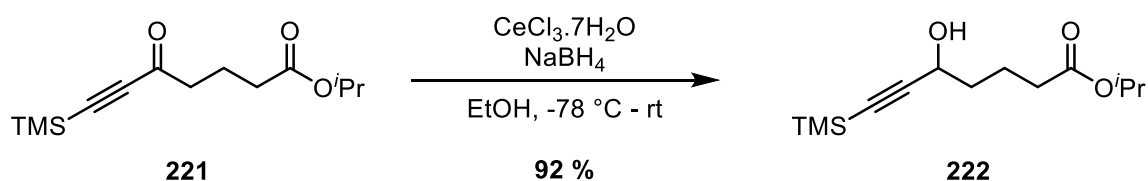
Scheme 154 - Esterification with methanol

Frustratingly, when employing an acid catalysed esterification using 10 mol% *p*-tolylsulfonic acid, the desired methyl ester **220**, was not isolated. The ¹H NMR spectroscopic analysis indicated the partial removal of the silyl protecting group, which is undesired at this stage. In order to circumvent this undesired deprotection, the sterically bulkier *iso*-propanol was utilised in the esterification to afford the *iso*-propyl ester **221** (Scheme 155).



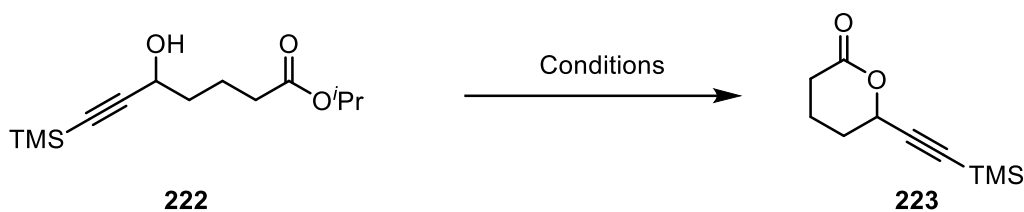
Scheme 155 - Esterification with isopropanol

Indeed, the *iso*-propyl ester **221** was isolated in a very good 71 % yield. With the keto-ester **221** now in hand, the racemic reduction of the ynone functionality was carried out using the 1,2-selective Luche reduction (Scheme 156).



Scheme 156 - Luche reduction of ynone

Pleasingly, the Luche reduction delivered only 1,2-reduction of the ynone functionality to afford the desired propargylic alcohol **222** in an excellent 92 % yield. At this stage, the asymmetric reduction was not explored as the route towards the desired boronic ester was yet to be established. Preparation of lactone **223** was investigated *via* an acid catalysed lactonization (Scheme 157).

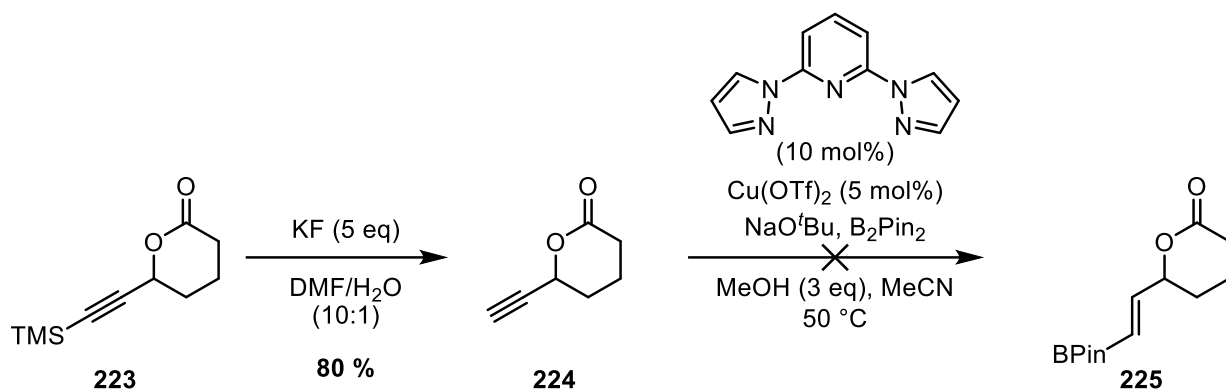


Scheme 157 - Lactonisation

Table 41 - Lactonisation conditions

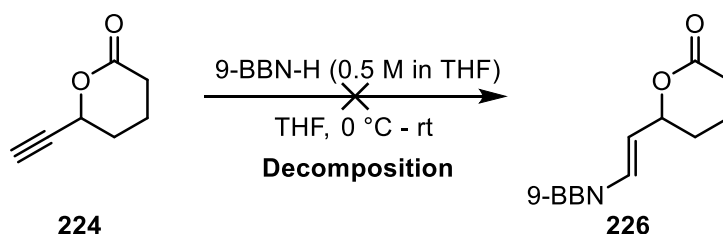
Entry	Conditions	Yield (%)
1	20 mol% TsOH.H ₂ O, Toluene, 70 °C, 72 h	55
2	20 mol% TsOH.H ₂ O, Toluene, Δ, 72 h	67
3	20 mol% TsOH.H ₂ O, Toluene, Δ, Dean-Stark with sodium pieces in trap, 6 h	91

Initially, the lactonization was performed at 70 °C, and after 72 hours, no further conversion was indicated by TLC. Upon isolation, only a 55 % yield of the desired lactone **223** was obtained. To increase the yield of this transformation, the reaction was heated to reflux for 72 hours. Disappointingly, a similar result was obtained after 72 hours with only a 67 % yield obtained. It was thought that the liberated *iso*-propanol from the lactonisation was causing the product lactone **223** to ring-open in solution with the system reaching an equilibrium. In order to drive the equilibrium towards the product, the *iso*-propanol would need to be sequestered from the system. The inclusion of sodium metal in the trap of a Dean-Stark apparatus would react with the *iso*-propanol to form sodium *iso*-propoxide, which is insoluble in toluene, and thus force the equilibrium towards the desired product **223**. Indeed, with the inclusion of sodium pieces in a Dean-Stark apparatus, the lactonisation proceeded to give an excellent 91 % yield of the desired product. With the desired six-membered lactone **223** in hand, work then focused on installation of the boronic ester. The synthesis of the desired boronic ester **225** required the removal of the silyl protecting group in **223** and then subsequent alkyne borylation (Scheme 158).



Scheme 158 - Synthesis towards boronic ester

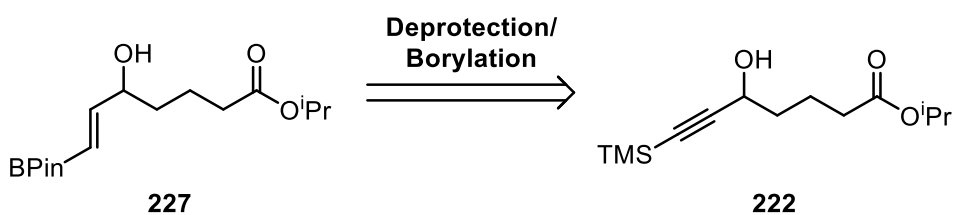
The deprotection of the TMS alkyne proceeded in an 80 % yield to deliver the terminal alkynyl lactone **224**, using potassium fluoride in DMF. Having successfully obtained the desired alkyne **224**, the borylation, *via* cupro-boration, did not deliver the desired boronic ester **225**. In fact, no discernible product could be identified by ^1H NMR spectroscopic analysis. It was possible that the alkynyl lactone **224** was unstable towards the reaction conditions as no starting material was observed by ^1H NMR spectroscopic analysis. Alternatively, it was proposed that hydroboration could deliver the corresponding vinyl borane **226**, which are known to also be competent nucleophiles in the Suzuki-Miyaura reaction.¹⁰ Considering this, the alkynyl lactone **224** was subjected to 9-BBN-H, in an attempt at hydroboration (Scheme 159).



Scheme 159 - Attempted hydroboration

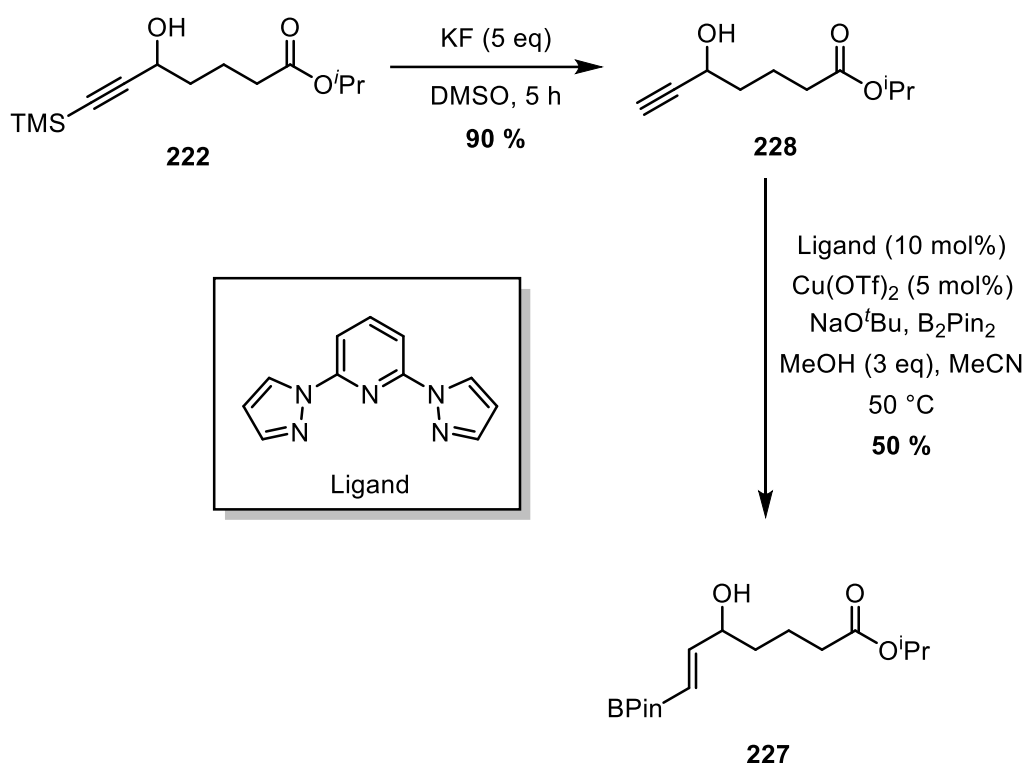
Unfortunately, the attempted hydroboration resulted in no desired product **226** by ^1H NMR analysis. This result lent more credence to the hypothesis that the lactone moiety was sensitive towards borylation conditions. At this point, work towards the lactone-containing boronic ester ceased and an alternative boronic ester was targeted to facilitate the synthesis of dictyosphaerin.

As the lactone functionality appeared to be sensitive towards borylation, it was hypothesised that avoiding the lactonisation and performing the borylation on the unprotected propargylic alcohol ester could provide access to a suitable coupling partner, as shown in Scheme 160.



Scheme 160 - Proposed synthesis of boronic ester

Proceeding with this strategy, the synthesis of the now desired boronic ester **227** required the removal of the silyl protecting group in ester **222**. Following the deprotection, borylation would then allow for the synthesis of the desired boronic ester.

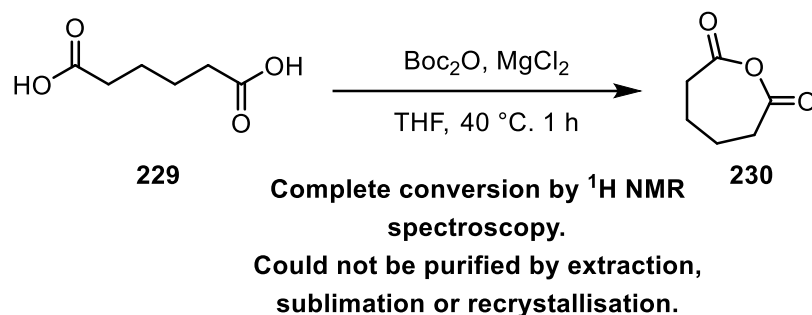


Scheme 161 - Synthesis of the desired boronic ester

As demonstrated previously, potassium fluoride in DMF performs the desired desilylation to afford the free terminal alkyne **228** in an excellent 90 % yield. Pleasingly, now performing the previously unsuccessful borylation, the terminal alkyne **228** was converted to the desired boronic ester **227** and isolated in a moderate 50 % yield.

With the synthetic route towards the desired boronic ester established, further work focused on the synthesis of a homologated boronic ester. As previously discussed, the synthesis of a homologated boronic ester would circumvent the need for a potentially challenging late-stage homologation to

afford dictyosphaerin (*vide supra*). Initially, the synthesis of the requisite adipic anhydride **230** was attempted *via* the cyclisation of the commercially available adipic acid **229**.



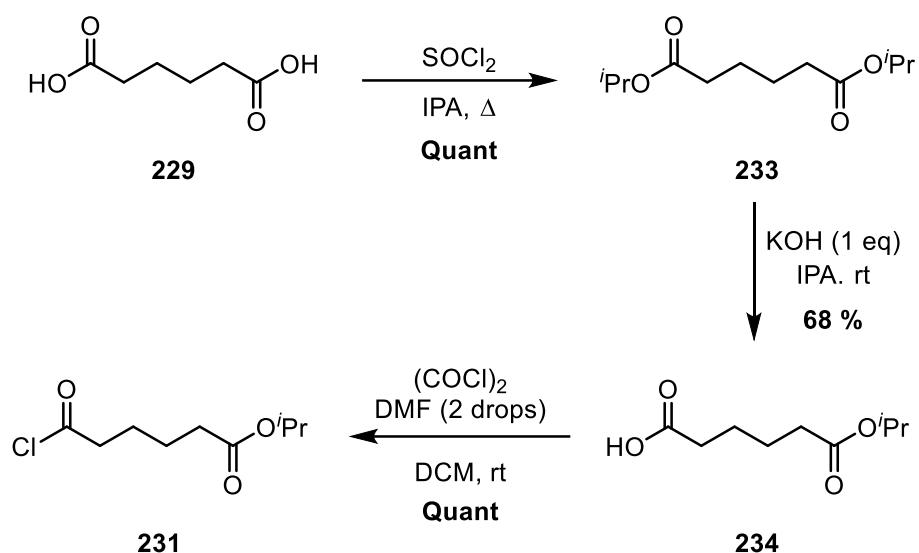
Scheme 162 - Cyclisation of adipic acid

Using, di-*tert*-butyl dicarbonate and MgCl_2 catalyst, the synthesis of adipic anhydride **230** was realised and confirmed by ^1H NMR spectroscopic analysis. However, isolation of the pure adipic anhydride **230** proved challenging. Initially, purification by extraction was problematic due to the insolubility of crude adipic anhydride **230**. This insolubility also made purification by recrystallisation or column chromatography impossible. Finally, sublimation of the crude material could not be realised without significant decomposition of the material. Without access to adipic anhydride **230**, the route towards the boronic ester would need to be modified. It was proposed that, the Friedel-Crafts alkylation could be performed on an acyclic acid chloride instead of the cyclic anhydride **230**, as has been demonstrated previously.¹¹ This modification would allow for minimal changes to the synthetic route already in place for the synthesis of the targeted boronic esters (Scheme 163).



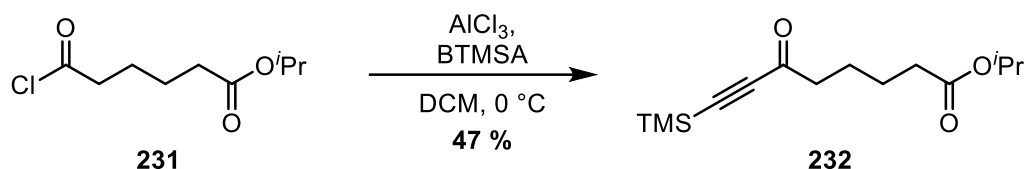
Scheme 163 - Newly proposed Friedel-Crafts alkylation

The synthesis of the requisite acid chloride **231** was realised from the commercially available adipic acid **229**, as shown in Scheme 164.



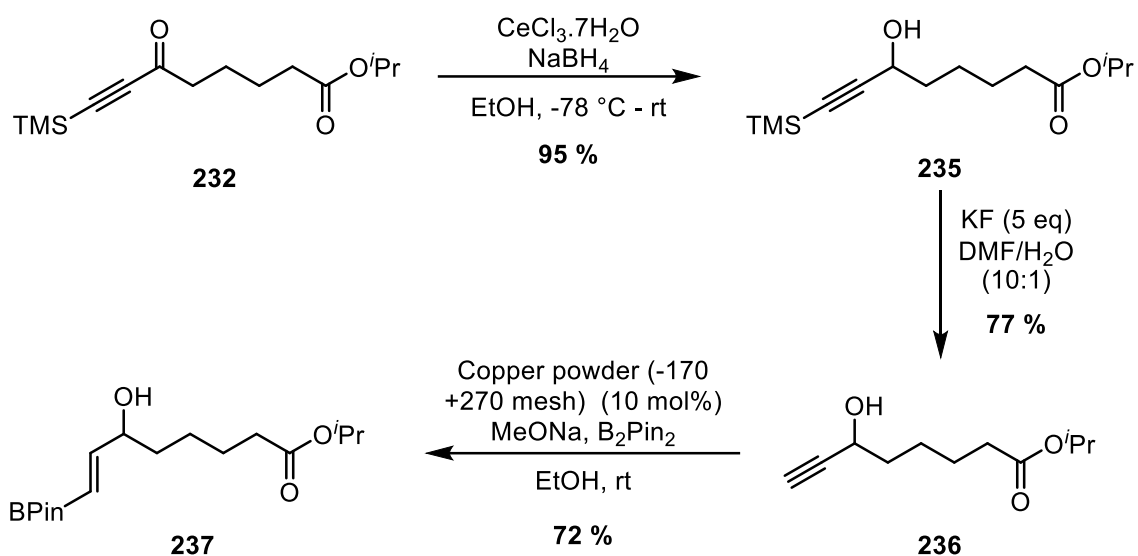
Scheme 164 - Synthesis of acid chloride

Initially, the synthesis of di-*iso*-propyl adipate **233** was achieved in a quantitative yield from adipic acid **229** using thionyl chloride in refluxing *iso*-propanol. The di-*iso*-propyl adipate **233** then underwent mono hydrolysis, using a single equivalent of base, to afford the desired carboxylic acid **234** in a good 68 % yield. The corresponding acid chloride **231** was then synthesised using oxalyl chloride and DMF as a catalyst. This allowed for an excellent quantitative yield of the desired acid chloride **231**. With the requisite acid chloride **231** in hand, the proposed alkylation was attempted (Scheme 165).



Scheme 165 - Friedel-Crafts alkylation

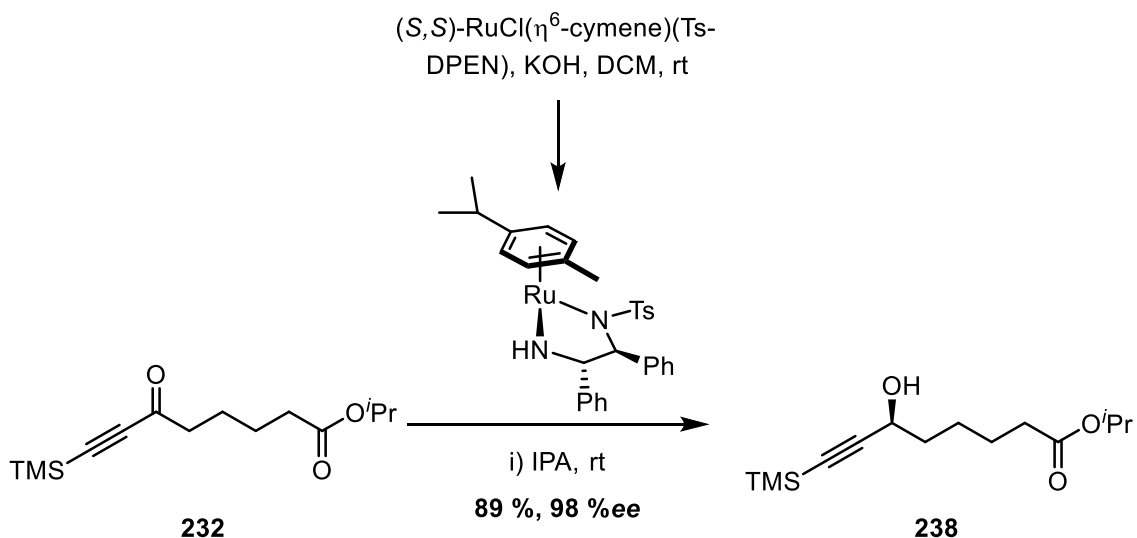
Indeed, the proposed alkylation afforded the desired ynone **232** in a moderate 47 % yield. Despite only a moderate yield, the reaction was carried out on a large scale, allowing access to sufficient material to proceed with the synthesis of the desired boronic ester **237**, as described in Scheme 166.



Scheme 166 - Synthesis of boronic ester

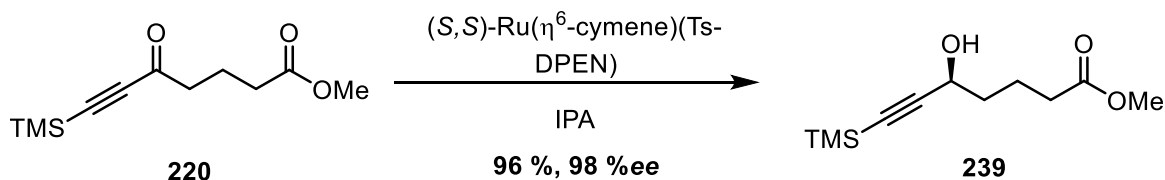
Pleasingly, the ynone **232** was reduced using the 1,2-selective Luche reduction to afford the propargylic alcohol **235** in an excellent 95 % yield. Subsequently, the trimethylsilyl protecting group was cleaved using potassium fluoride in DMF to deliver the terminal alkyne **236** in an *isolated* yield of 77 %. In contrast to the previously used borylation conditions, which utilised homogenous catalysis, heterogeneous catalysis allowed for the borylation of terminal alkyne **236** in a very good 72 % yield.¹²

Having established the synthetic strategy towards the boronic esters bearing the racemic allylic alcohol **237**, work focused next on installing the alcohol moiety as a single enantiomer. Asymmetric reduction was clearly an attractive strategy to follow, especially for the silyl protected ynone structures, which are prevalent in the asymmetric reduction literature.^{13,14} A popular and robust method for the asymmetric reduction of ynones, is through asymmetric transfer hydrogenation, employing the Nobel prize winning Noyori catalysts.^{15,16} As such, this asymmetric reduction method was applied to ynone **232** (Scheme 167).



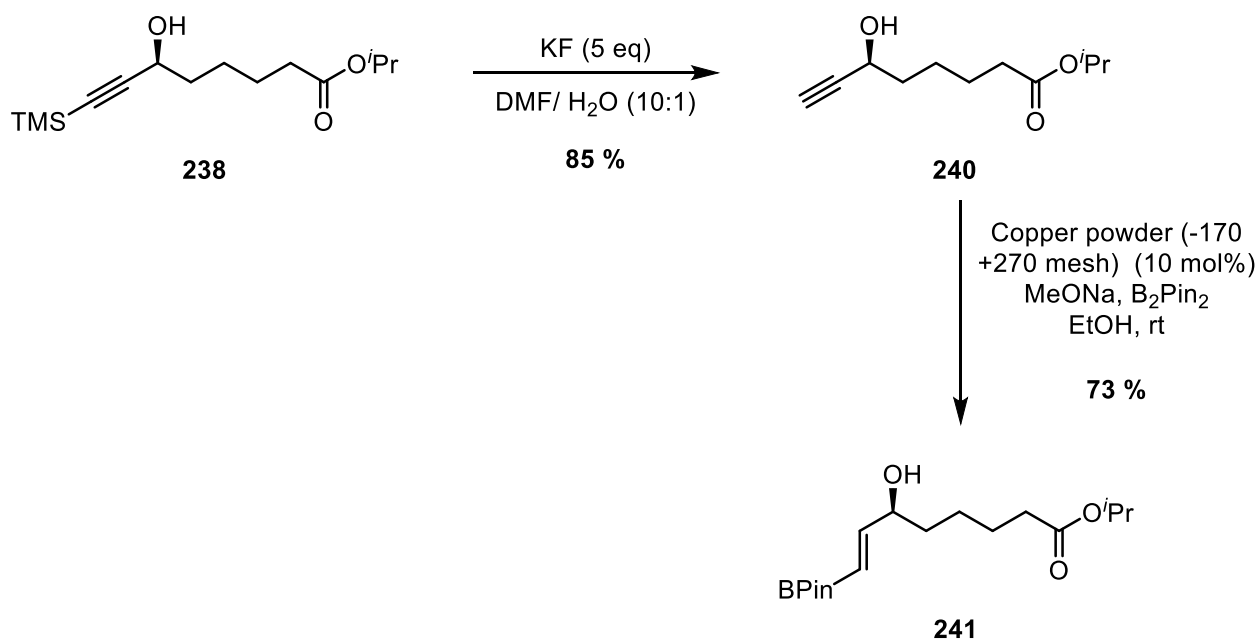
Scheme 167 - Asymmetric transfer hydrogenation

Asymmetric transfer hydrogenation of ynone **232** using the (S,S)-RuCl(η^6 -cymene)(Ts-DPEN) precatalyst delivered the (S)-propargylic alcohol **238** in an excellent 89 % yield and with impeccable enantioselectivity. The enantiomer ratio was determined by derivatisation to the *p*-nitrobenzoate ester and comparison to the derivatised racemic material by chiral HPLC (see experimental for details). The absolute stereochemistry of the alcohol product was determined by analogy from the asymmetric reduction, with the same catalyst system, of similar structures as described in the literature (Scheme 168).¹¹



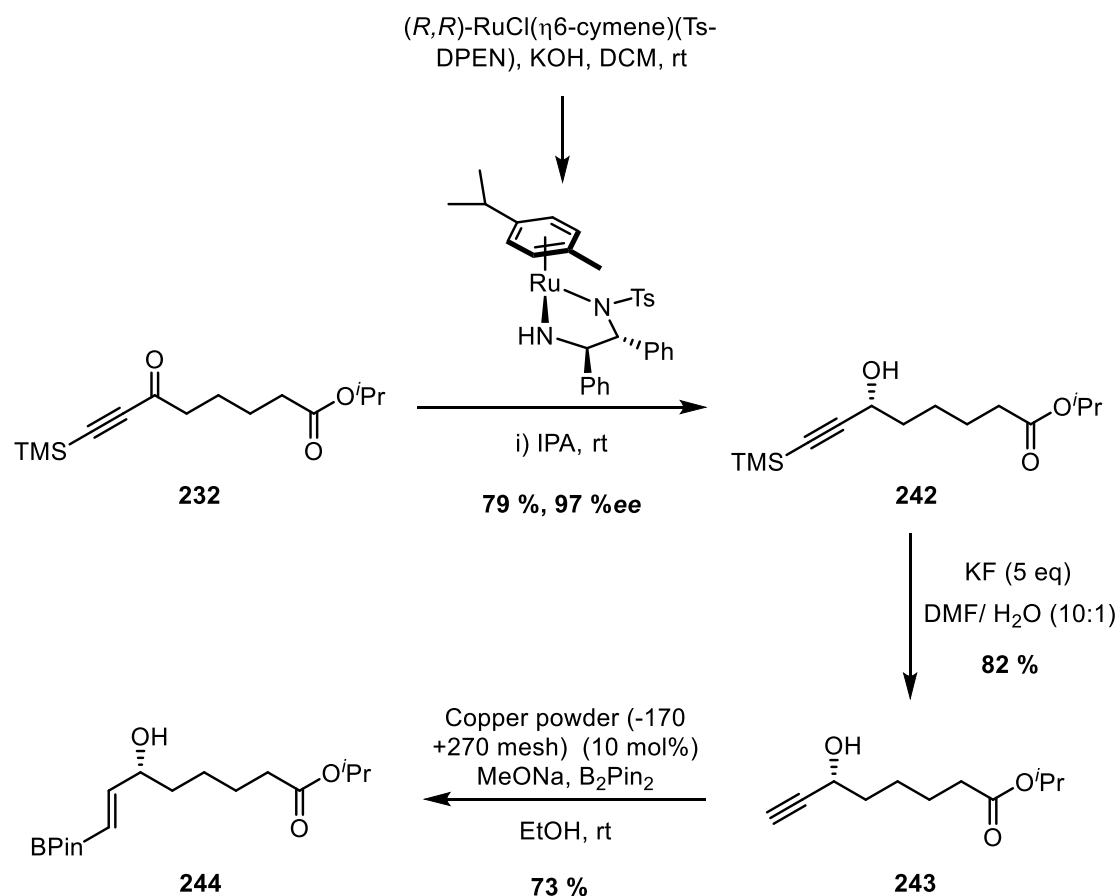
Scheme 168 - Literature precedent for absolute stereochemistry from asymmetric reduction

With the (S)-propargylic alcohol **238** in hand, the synthesis towards the desired chiral boronic esters was performed as shown previously (Scheme 169).



Scheme 169 - Synthesis of chiral boronic ester

The desired (*S*)-hydroxy boronic ester **241** was synthesised from the (*S*)-propargylic alcohol **238** via a deprotection of the silyl protecting group in an excellent yield of 85 %, with the resulting terminal alkyne **240** subjected to the previously demonstrated heterogenous borylation conditions to deliver the desired (*S*)-hydroxy boronic ester **241** in a good yield of 73 %. In addition to the (*S*)-hydroxy boronic ester **241**, the (*R*)-hydroxy boronic ester **244** was also synthesised using an identical strategy, with the asymmetric transfer hydrogenation performed utilising the (*R,R*)-RuCl(η^6 -cymene)(Ts-DPEN) precatalyst to afford the requisite (*R*)-propargylic alcohol **242** (Scheme 170).

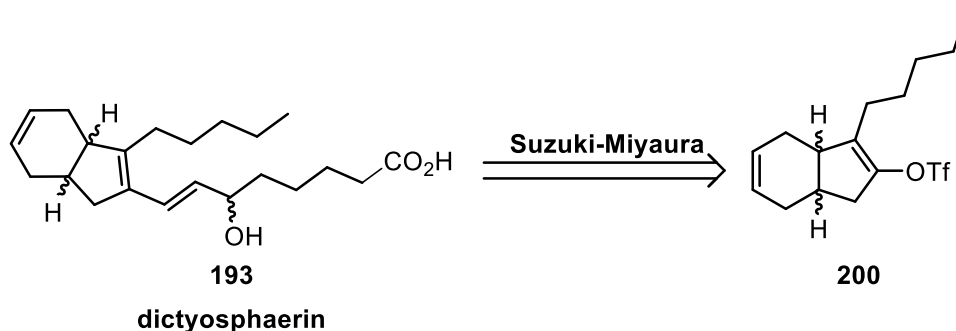


Scheme 170 - Synthesis of (R)-hydroxy boronic ester

Having both enantiomers of the required boronic ester in hand, the key Suzuki-Miyaura cross-coupling, to afford the skeletal structure of dictyosphaerin, was investigated.

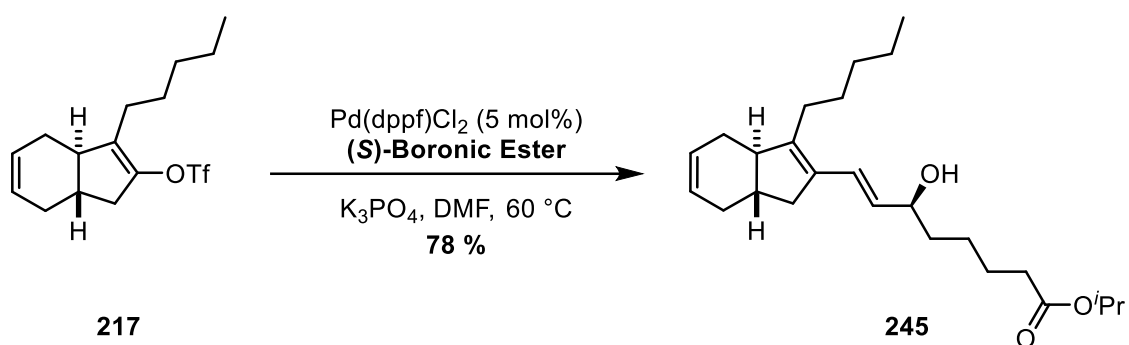
3.2.4. Completing the Convergent Strategy

With both the racemic enol triflate and both enantiomeric boronic esters in hand, research focused on the key Suzuki-Miyaura cross-coupling. This reaction would allow access to the skeletal structure of dictyosphaerin **193** and prove the viability of our proposed convergent strategy towards dictyosphaerin (Scheme 171).



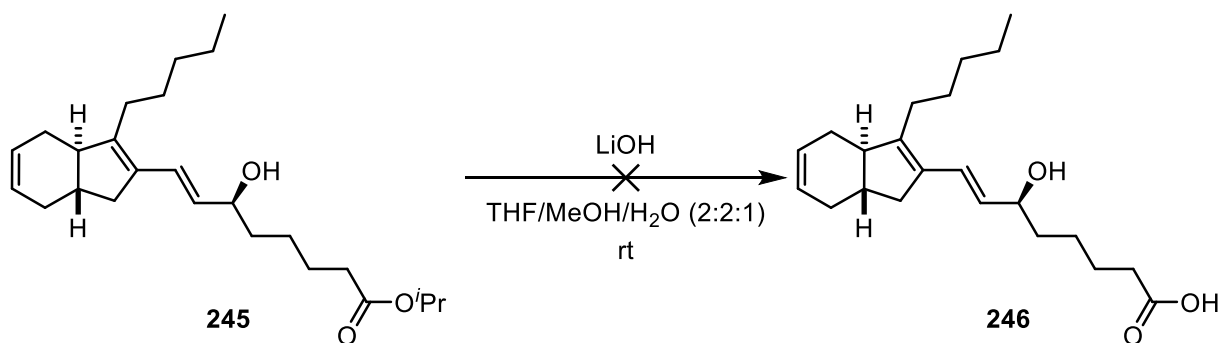
Scheme 171 - Retrosynthesis highlighting the key convergent step

To provide evidence for a *trans*-bridgehead in dictyosphaerin, as predicted by our theoretical work (*vide supra*), the racemic *trans*-bridged enol triflate **217** was cross-coupled with the (*S*)-hydroxy chiral boronic ester **241** (Scheme 172).



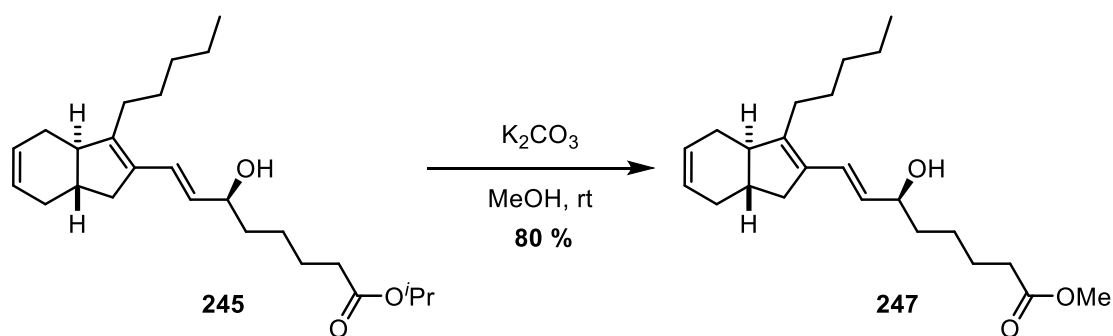
Scheme 172 - Suzuki-Miyaura reaction

Under relatively standard Suzuki-Miyaura conditions using Pd(dppf)Cl₂ as a pre catalyst, potassium triphosphate as an inorganic base and DMF as the solvent we were elated to observe for formation of dictyosphaerin *iso*-propyl ester **245**, albeit with a racemic bridgehead, in a 78 % yield. With this excellent result in hand, only the seemingly trivial hydrolysis of dictyosphaerin *iso*-propyl ester **245** to deliver dictyosphaerin itself, remained (Scheme 173).



Scheme 173 - Hydrolysis of dictyosphaerin iso-propyl ester

Unfortunately, the hydrolysis of dictyosphaerin *iso*-propyl ester **245** using lithium hydroxide resulted in significant decomposition of the material, with numerous new spots appearing by TLC analysis. Additionally, the ^1H NMR analysis showed only trace amounts of the desired product. This result proved not too surprising as in the isolation of dictyosphaerin, it is described as an unstable oil. As a result, Capon and co-workers synthesised and characterised the methyl ester to allow for extended storage of the natural product.¹ As transesterification would avoid unveiling the unstable free acid, synthesis of the methyl ester **247** from dictyosphaerin *iso*-propyl ester **245** was proposed. In order to confirm the presence of a *trans*-bridgehead in dictyosphaerin, the transesterification to afford dictyosphaerin methyl ester **247** was attempted (Scheme 174).

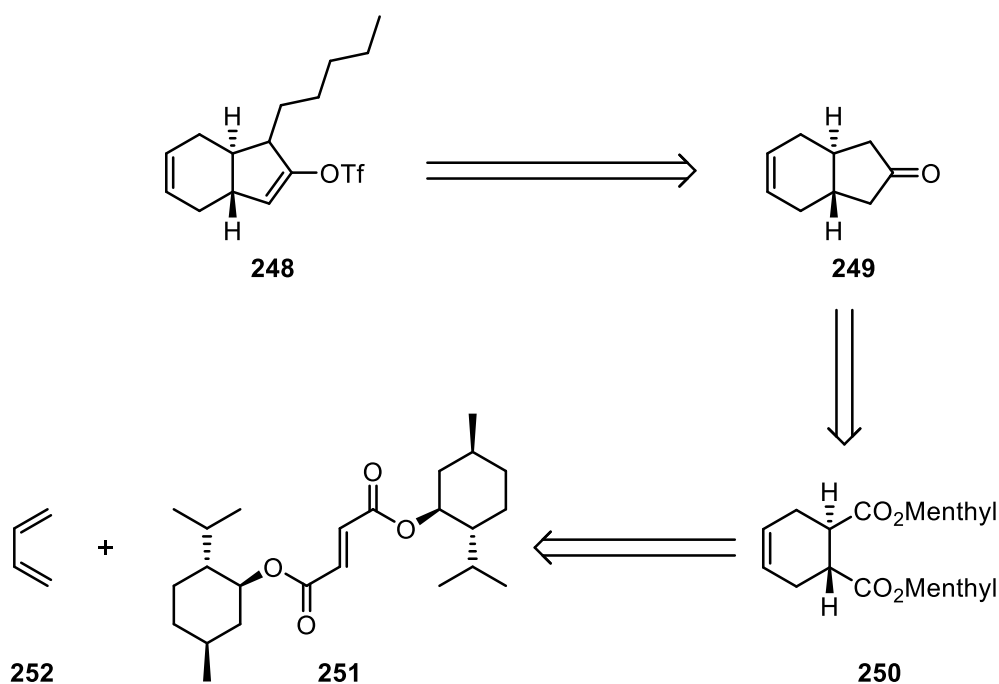


Scheme 174 - Transesterification to provide dictyosphaerin methyl ester

Pleasingly, transesterification, using potassium carbonate and methanol, afforded the desired methyl ester **247**, as the expected mixture of diastereomers, in an excellent 80 % yield. Additionally, upon comparison of the ^{13}C NMR spectrum to that of Capon's characterised dictyosphaerin methyl ester, indicated that this mixture of diastereomers likely contained the methyl ester of the natural product. This observation tentatively suggests that dictyosphaerin does contain a *trans*-bridgehead in the structure, as predicted by our computational work (*vide supra*), and confirms for the first time Capon's proposed structure. Interestingly, the mixture of diastereomers were incredibly similar by ^1H and ^{13}C spectroscopic NMR analysis, with only six extra ^{13}C resonances when compared with Capon's data. Considering this similarity, it was surprising that DP4-like analysis indicated preference for **196** over **194** at all. With this consideration, it was evident that the discrete synthesis of both **194** and **196** was required, to confidently assign the structure of dictyosphaerin *via* comparison of their ^{13}C NMR spectra and optical rotations to those obtained by Capon and co-workers.

3.2.5. Structural Determination of Dictyosphaerin

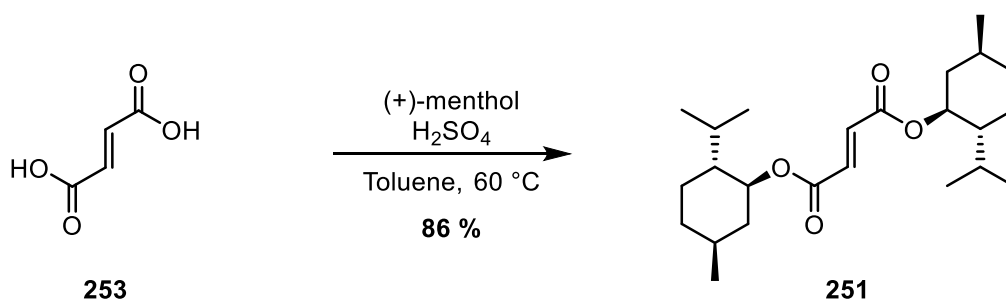
In order to elucidate the structure of dictyosphaerin, by analogy from dictyosphaerin methyl ester, a single enantiomer of the *trans*-bridged enol triflate would have to be synthesised. The previous strategy to install the stereocentres featured in the enol triflate was a Diels-Alder reaction between 3-sulfolene and fumaric acid. In the chemical literature, the use of menthol as a chiral auxiliary allows for diastereoselective Diels-Alder reactions, which would allow for access to the required stereoisomer in an asymmetric manner (Scheme 175).¹⁷



Scheme 175 - Retrosynthesis of the single enantiomer enol triflate

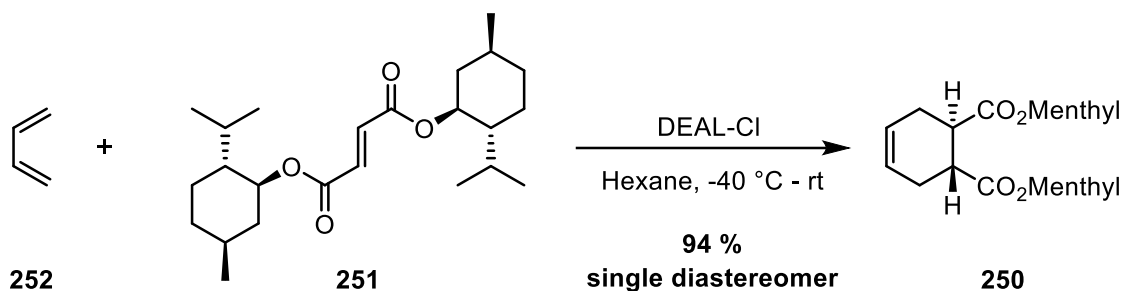
Prior to synthesis, we considered which enantiomer of bicyclic ketone **249** to select, and therefore which enantiomer of menthol to employ. Based on Stenstrom's elucidation of the correct absolute stereochemistry of mucosin, and given mucosin's structural and therefore biosynthetic similarity to dictyosphaerin, we made the assumption that the absolute stereochemistry of the ring junction in both natural products would be the same.³

To allow for the diastereoselective Diels-Alder reaction, the requisite dimethyl fumarate **251** was prepared by a simple acid-catalysed esterification employing (+)-menthol and fumaric acid **253** (Scheme 176).



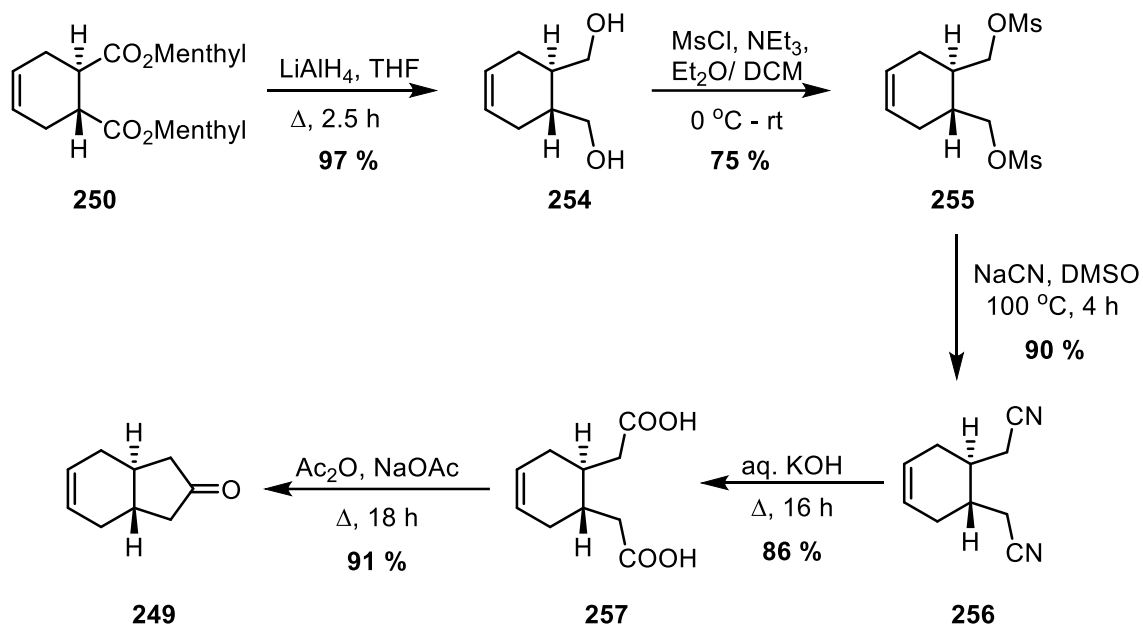
Scheme 176 - Synthesis of dimethyl fumarate

Pleasingly, the desired dimethyl fumarate **251** was synthesised in an excellent yield of 86 %. With sufficient quantities of the chiral auxiliary-derivatised fumarate **251** in hand, the diastereoselective Diels-Alder reaction was attempted, as shown in Scheme 177.



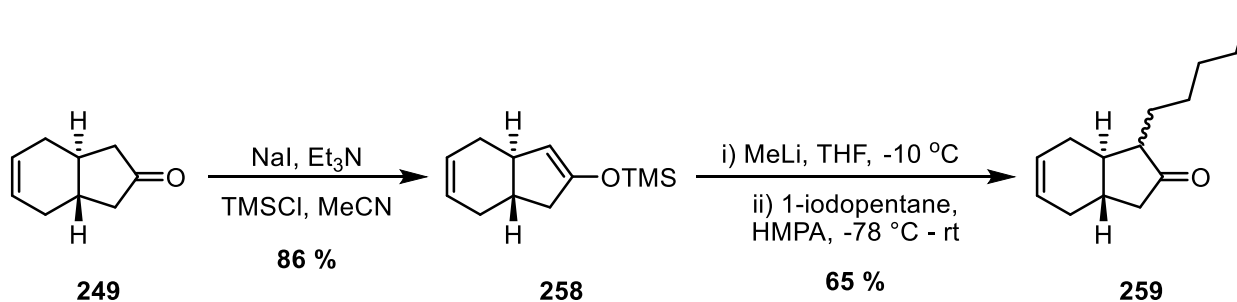
Scheme 177 - Diastereoselective Diels-Alder

When employing diethyl aluminium chloride as a Lewis acid, the Diels-Alder reaction delivered the chiral diester **250** in an excellent yield of 94 % as a single diastereomer. With the required stereocentres of the bridgehead in place, work towards the synthesis of the chiral ketone **249** was performed (Scheme 178).



Scheme 178 - Synthesis of ketone

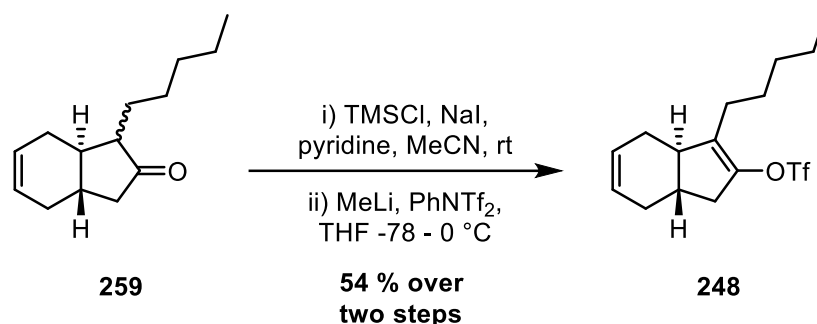
Reduction of the dimethyl ester **250** to the diol **254** proceeded efficiently when LiAlH_4 was employed, giving an excellent 97 % yield. With the diol **254** in hand, the homologation procedure commenced with mesylation, which proceeds in 75 % yield, followed by an $\text{S}_{\text{N}}2$ displacement with NaCN , which furnished the dinitrile **256** compound in a 90 % yield. Hydrolysis of the dinitrile **256** with aqueous KOH affords the diacid **257** in an excellent 86 % yield. Finally, the *trans*-ketone **249** is synthesised *via* a Dieckmann condensation of diacid **257** in an excellent 91 % yield. Having prepared significant quantities of the enantioenriched *trans*-ketone **249**, work towards the synthesis of the desired enol triflate continued. The previously established alkylation strategy was then applied to ketone **249**, to deliver the alkylated ketone **259**, as shown in Scheme 179.



Scheme 179 - Synthesis of alkylated ketone

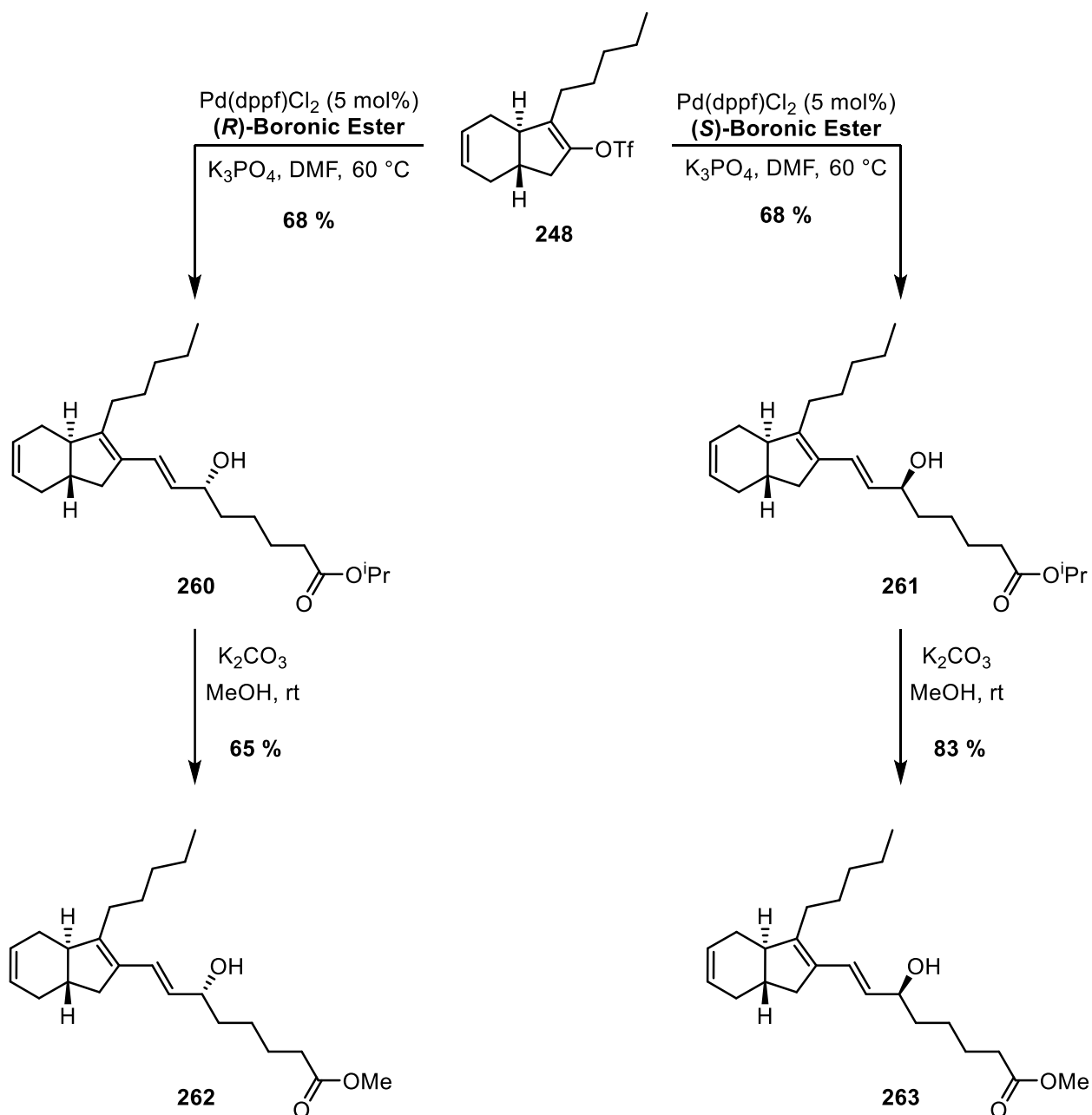
As before, the ketone **249** was converted into the trimethylsilyl enol ether **258** *via in situ* formation for trimethylsilyl iodide, in an excellent yield of 86 %. With the enolate equivalent in hand, the previously established conditions for the alkylation with 1-iodopentane efficiently delivered the

desired alkylated ketone **259** in a good yield of 65 %. As before, the alkylation gave a mixture of diastereomers which would prove inconsequential when the thermodynamic triflate was installed. Finally, the thermodynamic enol triflate **248** was obtained in a moderate yield from the enantioenriched alkylated ketone **259** (Scheme 180).



Scheme 180 - Synthesis of enol triflate

Indeed, *via* the synthesis of the thermodynamic silyl enol ether and the subsequent generation of the thermodynamic lithium enolate, the thermodynamic triflate **248** was afforded in a good yield of 54 % over two steps. With both the enantioenriched enol triflate **248** and enantioenriched chiral boronic esters **241** and **244** in hand, research then focused on the synthesis of the two candidate diastereomers of dictyosphaerin methyl ester. These were prepared by performing the already established Suzuki-Miyaura reaction of the enantioenriched thermodynamic enol triflate **248** with both chiral boronic esters **241** and **244** to give the respective dictyosphaerin *iso*-propyl esters **260** and **261**. Subsequently, the *iso*-propyl esters **260** and **261** were transesterified to the corresponding dictyosphaerin methyl esters **262** and **263**, as shown in Scheme 181.



Scheme 181 - Synthesis of dictyosphaerin methyl ester and epi-dictyosphaerin methyl ester

Pleasingly, both Suzuki-Miyaura reactions gave the same good yield of 68 %, affording both required diastereomers independently. Successively, both diastereomers were converted to the required methyl esters **262** and **263** in good yield. With both diastereomers in hand, their respective ¹³C NMR spectra and specific rotation values were measured and then compared with the data available from Capon's isolation (Figure 52, Table 42).¹

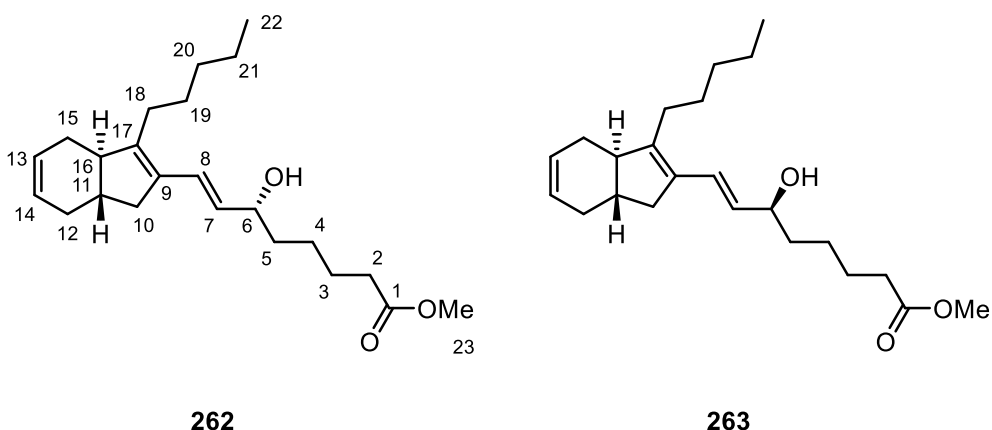


Figure 52 - Computationally predicted methyl esters and nuclei numbering scheme

Table 42 - Comparison table

Nuclei	Capon <i>et al.</i> ¹	262	263
1	174.1	174.2	174.2
2	34	34.1	34.1
3	24.8	24.9	24.9
4	25.1	25.2	25.2
5	37	37.2	37.1
6	73.2	73.4	73.3
7	131.1	131.3	131.3
8	125.4	125.5	125.5
9	133.7	133.8	133.9
10	36.9	37.1	37.0
11	42.4	42.6	42.5
12	31.3	31.4	31.4
13	128.4	128.5	128.5
14	127	127.1	127.1
15	29.8	29.9	29.9
16	49.4	49.5	49.5
17	145.7	145.8	145.8
18	26.5	26.6	26.6
19	28.3	28.5	28.4
20	31.8	31.9	31.9
21	22.5	22.6	22.6
22	14.0	14.1	14.1
23	51.5	51.6	51.6
Specific Rotation	-47°	-41.14°	-47.23°

As shown in Table 42, only six ¹³C NMR resonances (highlighted in red) display any variation between the two diastereomers. The ¹³C NMR data alone could indeed be considered inconclusive in determining which diastereomer represents the relative stereochemistry of dictyosphaerin methyl ester, despite the chemical shifts in the **263** ¹³C NMR spectrum being closer to that of dictyosphaerin

methyl ester, by a small margin. However, upon obtaining the specific rotations for both isomers, it was evident that **263** was more likely representative of not only the relative stereochemistry, but, importantly, the absolute stereochemistry, of the natural product (Figure 53).

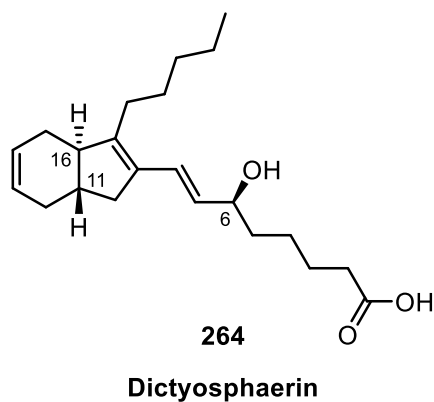


Figure 53 - Elucidated structure of dictyosphaerin

This result was most pleasing, as our synergistic use of computation, DP4-methodology and synthesis, has resulted in us establishing a compelling case that the natural dictyosphaerin **264** has the 6*S*,11*S*,16*R* stereochemistry as well as confirming Capon's proposed overall gross structure.¹

3.3. Conclusion

At the beginning of this work, dictyosphaerin, a conformationally flexible natural product, had not had its absolute or relative stereochemistry assigned – due to the complexity of its NMR spectral data and its lack of crystal form precluding X-ray analysis. In the initial stages of this work we were able to utilise DP4-like analysis to propose two candidate structures of dictyosphaerin (Figure 54).

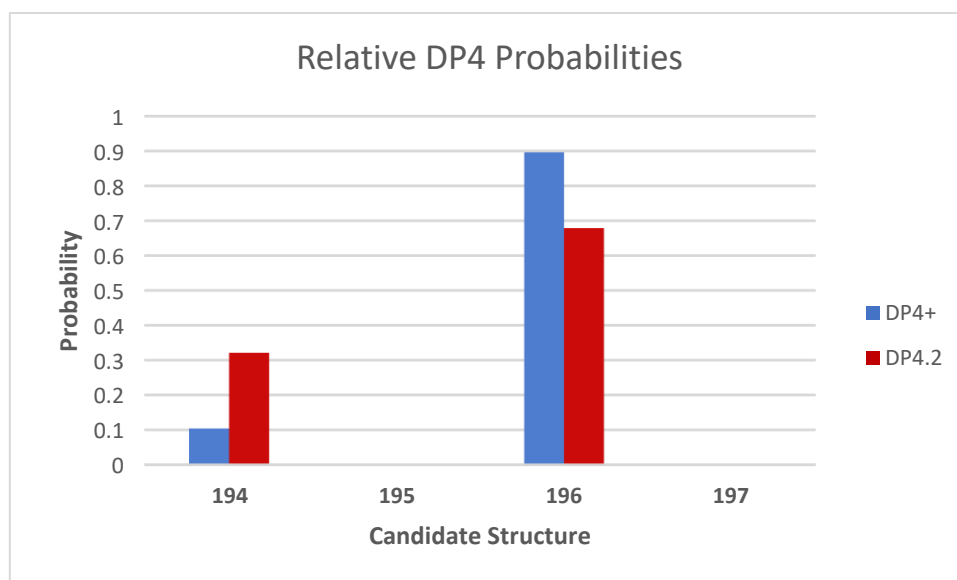
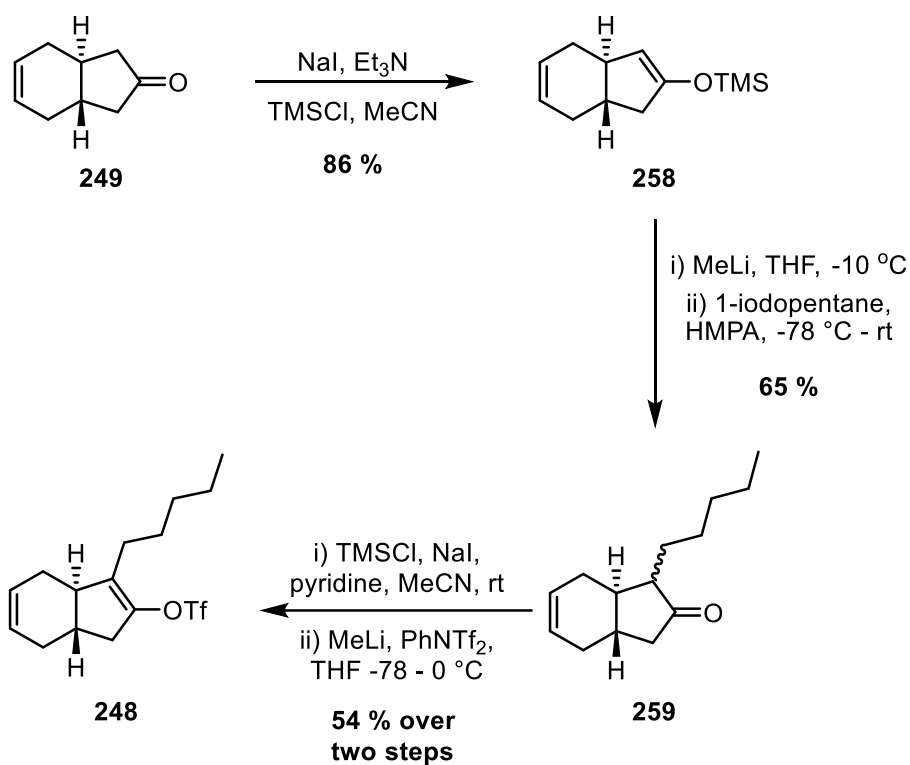


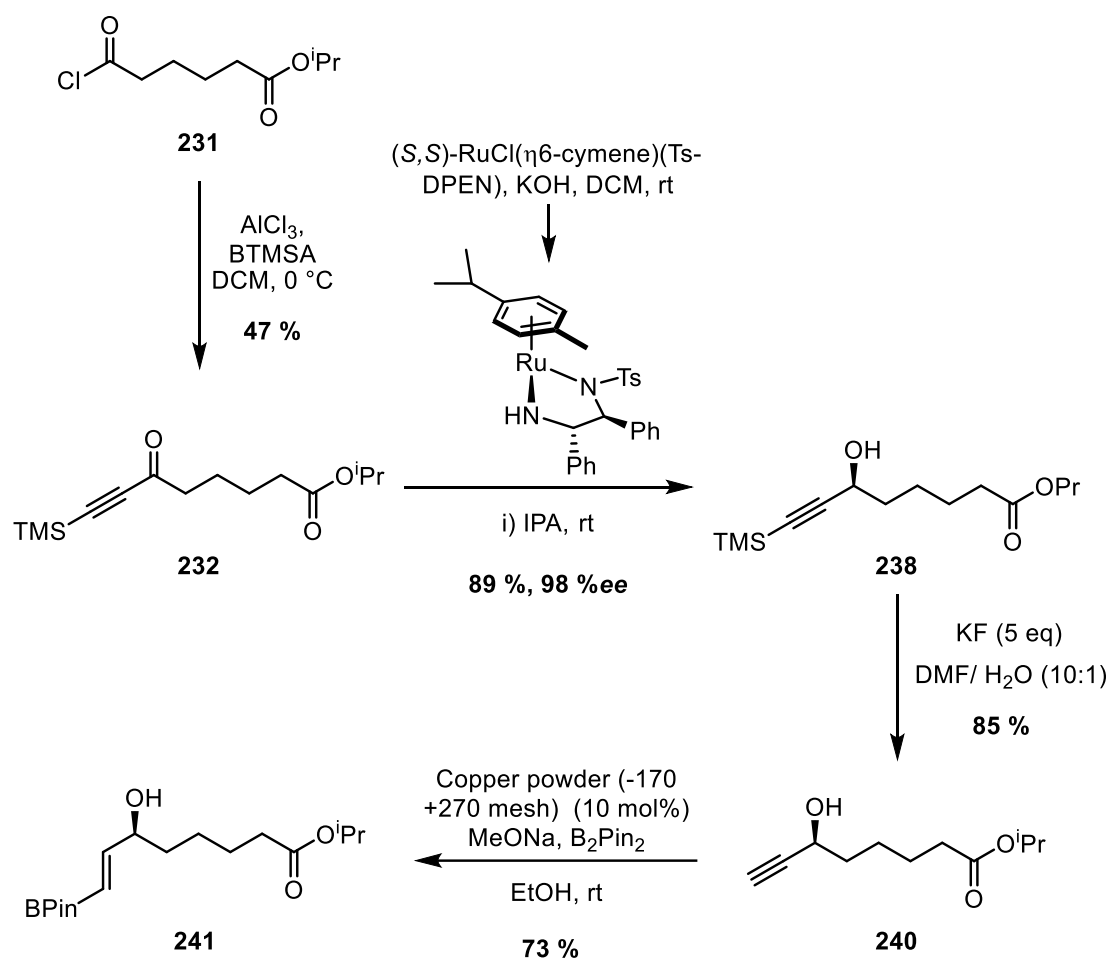
Figure 54 - Relative DP4 probabilities

Having identified **194** and **196** as possible structures for dictyosphaerin, DP4-like analysis had discounted any structure bearing a *cis*-bridgehead in the bicyclic ring system. As a result, work towards the synthesis of the proposed enol triflate with the *trans*-bridgehead proceeded. The requisite single enantiomer enol triflate **248** was synthesised from the chiral ketone **249**, which was in turn synthesised from the dimethyl fumarate, allowing for asymmetric induction (Scheme 182).



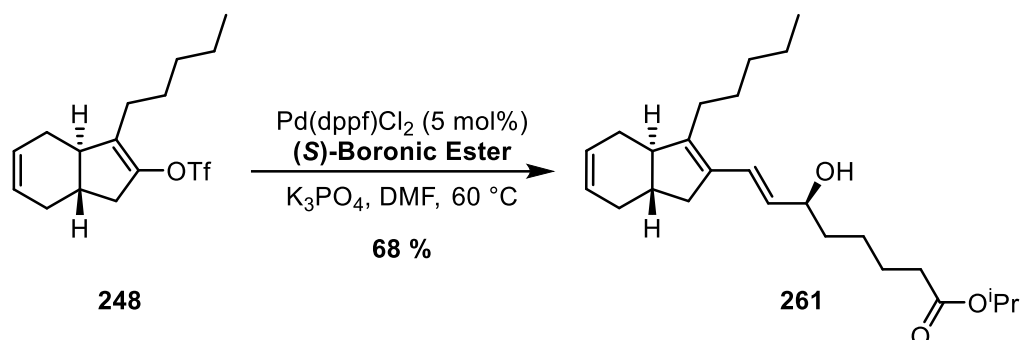
Scheme 182- Synthesis of enol triflate

In order to complete the synthesis of dictyosphaerin, the requisite boronic esters **241** and **244** were synthesised in preparation for the key Suzuki-Miyaura reaction in the proposed convergent strategy. Both enantiomers of the boronic esters were synthesised from the acid chloride **231**, which was prepared, in turn, from adipic acid (Scheme 183).



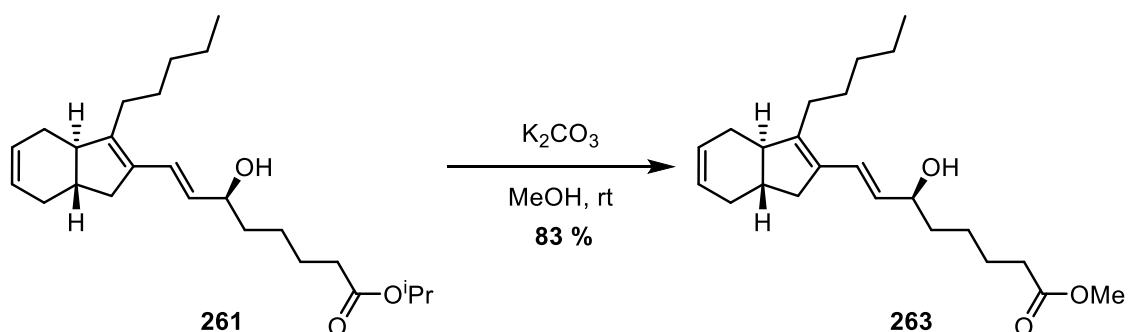
Scheme 183 - Synthesis of chiral boronic ester

From the acid chloride **231**, a Friedel-Crafts alkylation delivered the desired ynone **232** in a moderate yield. This ynone **232** was a suitable precursor for an asymmetric reduction, which would allow for the installation of the chiral allylic alcohol present in dictyosphaerin. The use of Noyori's asymmetric transfer hydrogenation catalysts allowed for an excellent yield and enantiomeric excess of the desired chiral propargylic alcohol **238**. With efficient access to the chiral component of the desired boronic ester, a deprotection and borylation strategy was explored. After deprotection of the TMS alkyne, heterogeneous Cu-catalysed borylation allowed for the installation of the desired boronic ester **241** in a good 73 % yield. With the requisite fragments in hand for the proposed convergent strategy towards dictyosphaerin's candidate structures, the key Suzuki-Miyaura reaction was then explored (Scheme 184).



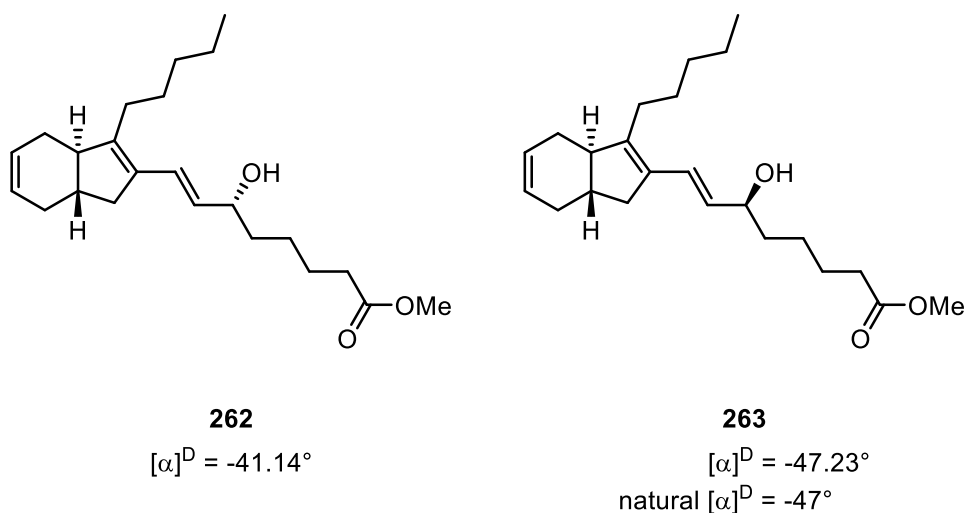
Scheme 184 - Key Suzuki-Miyaura reaction

Gratifyingly, the Suzuki-Miyaura reaction allowed for efficient access to the desired *iso*-propyl ester for both candidate structures of dictyosphaerin, with an 68 % yield for both diastereomers. To obtain access to dictyosphaerin, a seemingly trivial hydrolysis was attempted on the *iso*-propyl ester. However, it appeared that dictyosphaerin itself proved too unstable to isolate from the basic hydrolysis. However, Capon and co-workers had synthesised and characterised the respective methyl ester of dictyosphaerin in their reported isolation.¹ Instead, the transesterification of the *iso*-propyl ester **261** to the methyl ester **263** was investigated (Scheme 185).



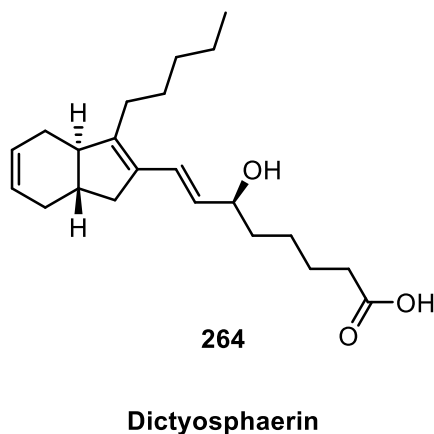
Scheme 185 - Synthesis of dictyosphaerin methyl ester

Pleasingly, methanolic potassium carbonate afforded the desired methyl ester **263** in an 83 % yield. The transesterification was performed on both diastereomers to deliver the respective methyl esters of each candidate structure. Once the respective syntheses were complete, comparison of the ¹³C NMR spectral data and optical rotations from Capon's report and the data obtained through our synthesis, was carried out (Scheme 186).



Scheme 186 - Optical rotations data for 260 and 261

Surprisingly, the ¹³C spectral data for both synthesised diastereomers **262** and **263** were exceptionally similar and thus relatively inconclusive, in elucidating the structure of dictyosphaerin methyl ester. However, the specific rotations for **263** matched the specific rotation obtained by Capon and co-workers for the methyl ester of the isolated natural product. From this result, it is possible to confirm, for the first time, that the relative stereochemistry of dictyosphaerin does indeed match the proposed candidate structure from the DP4+ and DP4.2 analysis as shown below in Scheme 187. Additionally, we have also confirmed the absolute stereochemistry of dictyosphaerin by comparison of the specific rotation obtained through synthesis to that of the one obtained from the isolation of dictyosphaerin.



Scheme 187 - Proposed structure of dictyosphaerin

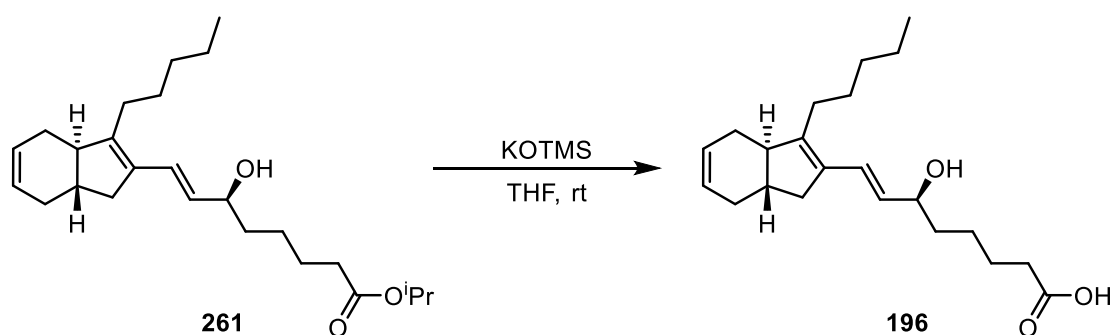
Interestingly, both DP4+ and DP4.2 gave strong agreements on the correct relative stereochemistry for dictyosphaerin. However, DP4+ displayed superior performance to that of Goodman's DP4.2 for these flexible oxylipin structures. It is possible that the DFT-level geometry optimisation that is required by DP4+ allows for this superior performance observed in the DP4-like analysis, when

considering highly flexible candidate structures. Additionally, DP4-like analysis in combination with experimentally obtained data for methyl esters **262** and **263** give strong evidence to support that **264** is the structure of the natural product.

3.4. Future Work

Total Synthesis of Dictyosphaerin

Despite, having provided a strong case for structure of dictyosphaerin *via* the synthesis of dictyosphaerin methyl ester, the total synthesis of dictyosphaerin has yet to be realised. Our attempt using lithium hydroxide to unveil the natural product from dictyosphaerin *iso*-propyl ester proved unsuccessful. However, using more mild conditions such as a basic hydrolysis employing potassium trimethylsilanoate could prove successful in isolating the unstable dictyosphaerin natural product.¹⁸



Scheme 188 - Hydrolysis employing potassium trimethylsilanoate

Indeed, if synthesis and isolation of dictyosphaerin **196** is achieved, this would be the first total synthesis of dictyosphaerin. Additionally, enzymatic hydrolysis of the *iso*-propyl ester **261** may be achieved using lipase enzymes. This could provide the mild hydrolysis conditions required for the synthesis and isolation of dictyosphaerin **196**.

DP4 Analysis Benchmarking

We have successfully shown that DP4-like methodologies can aid in structural elucidation of dictyosphaerin and in chapter two we also examined three varieties of DP4-like analysis; DP4, DP4+ and DP4.2. Without benchmarking, the chemist is unable to make an informed decision on which DP4 analysis to use when trying to propose a possible structure for a molecule of unknown stereochemistry. To this date however, there lacks an unbiased benchmarking of the available DP4-like methodologies within the literature. Examining the performance of the various DP4 analyses across a breadth of natural product structures and pharmaceutically relevant compounds, then comparing how well they assign the right stereoisomer to compounds of known stereochemistry, could allow for conclusions to be made on the appropriate application for each methodology based on structural features. This could then allow the chemist to make an informed decision on which DP4 methodology to use when presented with a molecule of unknown stereochemistry.

3.5. Experimental

3.5.1. Details of Computational Methods

Conformer Generation

Molecular mechanics was employed to generate low-energy conformers for each candidate structure being investigated. All molecular mechanics calculations were performed using Macromodel¹⁹ (Version 9.1, 9.5, or 9.7) interfaced to the Maestro²⁰ (Version 11.5) program. All conformational searches used the Monte Carlo Multiple Minimum²¹ (MCMM) method and the MMFF forcefield.²²⁻²⁸ The searches were done in the gas phase, with a 50 kJmol⁻¹ upper energy limit and with 200,000 steps. All conformers >10 kJ mol⁻¹, with respect to the global minimum, were discounted.

DP4+ Frequency, Optimisation and NMR GIAO Calculations²

Density functional theory (DFT) was employed to calculate the gas-phase geometries and energies for all generated conformers, for each candidate structure. All frequency and geometry calculations were carried out using the B3LYP²⁹⁻³² functional with the 6-31G(d) basis set.³³ NMR GIAO^{34,35} shielding tensor calculations were carried out using the mPW1PW91³⁶ functional with the 6-31+G(d,p) basis set. The NMR GIAO^{34,35} shielding calculations were carried out in solution (using the polarizable continuum model, PCM, with chloroform as the solvent). All calculations using the B3LYP²⁹⁻³² or mPW1PW91³⁶ functional have been performed using Gaussian 09 quantum chemistry program package (version D.06).³⁷

DP4.2 Frequency and NMR GIAO Calculations⁴

Density functional theory (DFT) was employed to calculate the gas-phase energies and NMR GIAO^{34,35} shielding constant calculations for all generated conformers, for each candidate structure. All frequency calculations were carried out using the M06-2X³⁸ functional with the 6-31G(d,p) basis set.³³ NMR GIAO^{34,35} shielding tensor calculations were carried out using the mPW1PW91³⁶ functional with the 6-311G(d) basis set.³³ The NMR GIAO^{34,35} shielding calculations were carried out in the gas-phase. All calculations using the B3LYP²⁹⁻³² or mPW1PW91³⁶ functional have been performed using Gaussian 09 quantum chemistry program package (version D.06).³⁷

To calculate NMR shifts for a candidate structure, the shielding tensors were first averaged over symmetry-related positions in each conformer and then subjected to Boltzmann averaging over the conformers according to:

$$\sigma^x = \frac{\sum_i \sigma_i^x \exp\left(\frac{-E_i}{RT}\right)}{\sum_i \exp\left(\frac{-E_i}{RT}\right)}$$

Where σ^x is the Boltzmann-averaged shielding tensor for nucleus x , σ_i^x is the shielding constant for nucleus x in conformer i , and E_i is the potential energy of conformer i (relative to the global minimum), obtained from the single-point *ab initio* calculation. The temperature (T) was taken as 298 K. Chemical shifts were calculated according to:

$$\delta_{unscaled}^x = \frac{\sigma^0 - \sigma^x}{1 - \sigma^0/10^6}$$

Where δ_{calc}^x is the calculated shift for nucleus x (in ppm), σ^x is the shielding tensor for nucleus x , and σ^0 is the shielding tensor for the carbon nuclei in tetramethylsilane, which was obtained from a NMR GIAO calculation on tetramethylsilane.

All NMR GIAO data extraction from Gaussian 09 output files and Boltzmann averaging was handled *via* the use of Python scripting.

3.5.2. Details of Statistical Analysis

DP4+ Probability Calculations²

All calculated shifts were scaled against their respective experimental shifts *via* linear regression and scaled shifts were calculated according to:

$$\delta_{scaled} = (\delta_{unscaled} - c)/m$$

where δ_{scaled} is the calculated scaled shift for nucleus x (in ppm), $\delta_{unscaled}$ is the unscaled shift for nucleus x , c is the y-intercept from the linear regression, and m is the gradient from the linear regression.

The probability for each candidate structure was then calculated using the following equation:

$$P = \frac{\prod \left(T^{\nu}_{scaled} \left(\frac{|\delta_{scaled} - \delta_{exp} - \mu_{scaled}|}{\sigma_{scaled}} \right) \right) \left(T^{\nu}_{unscaled} \left(\frac{|\delta_{unscaled} - \delta_{exp} - \mu_{unscaled}|}{\sigma_{unscaled}} \right) \right)}{\sum \left[\prod \left(T^{\nu}_{scaled} \left(\frac{|\delta_{scaled} - \delta_{exp} - \mu_{scaled}|}{\sigma_{scaled}} \right) \right) \left(T^{\nu}_{unscaled} \left(\frac{|\delta_{unscaled} - \delta_{exp} - \mu_{unscaled}|}{\sigma_{unscaled}} \right) \right) \right]}$$

where P is the probability that a candidate structure is the correct one from the experimental shifts, δ_{scaled} is the calculated scaled shift for nucleus x (in ppm), δ_{exp} is the experimental shift for nucleus x (in ppm), $\delta_{unscaled}$ is the unscaled shift for nucleus x . μ is the mean, which is taken as 0 as a result of the empirical scaling, and σ_{scaled} is the standard deviation for the scaled shifts, which is 0.122 ppm for ^{13}C shifts. The t -distribution T^{ν}_{scaled} has degrees of freedom (ν) of 4.318. $\mu_{unscaled}$ is the mean for the unscaled shifts, which has a value of -0.075 or 0.239 for sp^3 or sp^2 nuclei, respectively. $\sigma_{unscaled}$ is the standard deviation for the unscaled shifts, which has a value of 0.127 or 0.149 for sp^3 or sp^2 nuclei, respectively. The t -distribution $T^{\nu}_{unscaled}$ has degrees of freedom (ν) of 3.684 or 5.840 for sp^3 or sp^2 nuclei, respectively. Values of σ , μ and ν were determined by Sarotti and co-workers.²

DP4.2 Probability Calculations⁴

All calculated shifts were scaled against their respective experimental shifts *via* linear regression and scaled shifts were calculated according to:

$$\delta_{scaled} = (\delta_{unscaled} - c)/m$$

where δ_{scaled} is the calculated scaled shift for nucleus x (in ppm), $\delta_{unscaled}$ is the unscaled shift for nucleus x . C is the y -intercept from the linear regression, and m is the gradient from the linear regression.

The probability for each candidate structure was then calculated using the following equation:

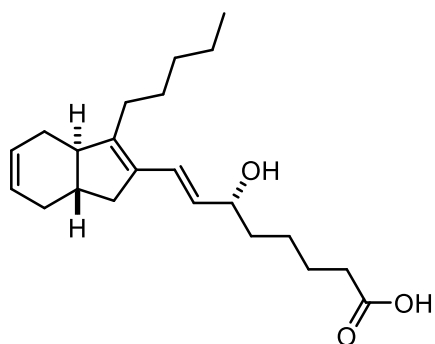
$$P = \frac{\prod \left(N_{(\mu_1, \sigma_1)}(\delta_{scaled} - \delta_{exp}) \right) \left(N_{(\mu_2, \sigma_2)}(\delta_{scaled} - \delta_{exp}) \right)}{\sum \left[\prod \left(N_{(\mu_1, \sigma_1)}(\delta_{scaled} - \delta_{exp}) \right) \left(N_{(\mu_2, \sigma_2)}(\delta_{scaled} - \delta_{exp}) \right) \right]}$$

where P is the probability that a candidate structure is the correct one from the experimental shifts, δ_{scaled} is the calculated scaled shift for nucleus x (in ppm), δ_{exp} is the experimental shift for nucleus x (in ppm), μ_1 is the mean for the first distribution, which is taken as -0.012304, σ_1 is the

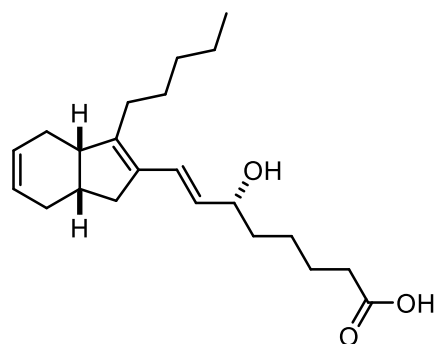
standard deviation for the first distribution, which is 2.821282 ppm for ^{13}C shifts, μ_2 is the mean for the second distribution, which has a value of 0.00095, and $\sigma_{unscaled}$ is the standard deviation for the second distribution, which has a value of 1.361471. Values of σ_1 , σ_2 , μ_1 and μ_2 were determined by Goodman and co-workers.⁴

All probability calculations relied on Microsoft Excel for Office 365, version 1906.

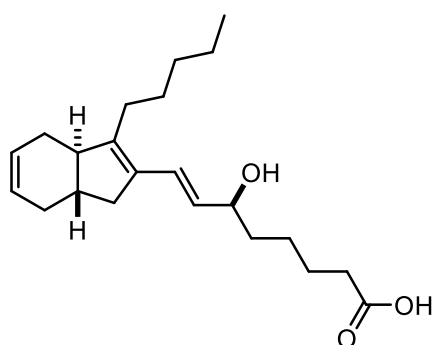
3.5.3. Tables of Calculated Shielding Tensors and Probabilities



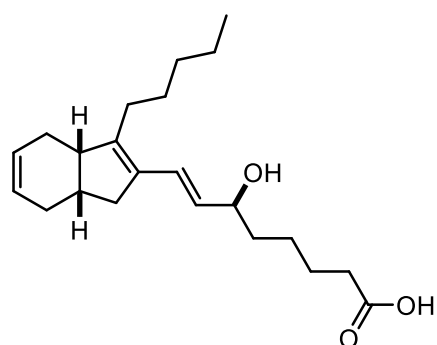
194



195



196



197

Figure 55 - Candidate structures for dictyosphaerin

Figure 49*Table 43 - Calculated shielding tensors for all candidate structures of dictyosphaerin and associated DP4+ probabilities*

Nuclei Label	194	195	196	197
1	5.99356	6.21274	5.83945	5.81741
2	152.78527	152.88891	153.14171	153.22201
3	160.73183	160.76888	161.46781	161.42747
4	160.77134	160.58471	160.89629	160.74900
5	149.84389	149.65880	149.83376	149.95510
6	110.58075	110.19545	110.38793	110.72167
7	50.63258	50.51559	50.88385	50.62619
8	57.34246	57.03216	56.67673	57.12835
9	45.66516	46.83566	45.83604	46.90480
10	148.33701	147.74589	148.40239	147.65010
11	142.90269	148.54675	142.93423	148.72481
12	153.69212	158.50496	153.69609	158.41757
13	51.84588	55.59823	51.81707	55.41175
14	53.20425	55.18358	53.21404	55.14459
15	155.09308	156.89583	155.14006	157.03158
16	135.24261	141.73839	135.29189	141.69782
17	30.96068	25.08885	30.84804	25.48918
18	158.57639	158.12631	158.68024	157.72072
19	156.81010	156.39335	156.43650	156.60744
20	154.44901	154.32581	153.99504	154.02563
21	161.93599	161.79157	161.86039	161.86095
22	172.84880	172.54169	172.58492	172.87815
Probability	0.104	6.44x10 ⁻¹⁵	0.896	2.83x10 ⁻¹⁴

Figure 50*Table 44 - Calculated shielding tensors for all candidate structures of dictyosphaerin and associated DP4.2 probabilities*

Nuclei Label	194	195	196	197
1	4.71857	4.94065	4.87663	4.91495
2	154.00774	154.39277	153.59235	154.15078
3	159.86401	160.94268	160.70718	159.72149
4	161.51918	160.03578	159.97949	159.34695
5	151.30347	151.57494	151.65050	148.95404
6	111.17165	111.39921	111.46226	112.28857
7	51.82853	50.83902	51.64500	50.51897
8	58.23535	58.32746	57.53357	60.46578
9	49.00758	49.74357	47.57963	50.37299
10	149.48451	148.51077	149.49726	148.35921
11	141.70608	148.05082	141.72412	148.21276
12	153.27146	159.09168	153.28547	159.05754
13	50.08051	55.84815	50.07751	55.87139
14	52.43706	54.41353	52.41892	54.36319
15	156.10107	158.02983	155.81656	158.05619
16	137.42371	144.28429	136.82247	144.31377
17	29.34780	25.85643	31.40972	26.26893
18	158.93417	158.02408	159.52956	157.70341
19	156.37921	157.57833	156.61911	156.50795
20	152.59632	153.46654	153.49488	152.79677
21	162.30260	162.03621	162.11749	161.50698
22	172.12432	172.81958	172.28737	172.55154
Probability	0.321	3.17x10 ⁻²⁰	0.679	9.43x10 ⁻²¹

Reagents

All reagents were obtained from commercial suppliers and used without further purification, unless otherwise stated. All reactions were carried out under an inert, dry argon atmosphere, unless otherwise stated. Purification was carried out according to standard laboratory methods.³⁹

- Tetrahydrofuran was dried by heating to reflux over sodium wire, using benzophenone ketyl as an indicator, then distilled under nitrogen.
- Dichloromethane was dried by heating to reflux over calcium hydride then distilled under nitrogen.
- Dry Et₂O, Hexane and PhMe were obtained from an Innovative Technology, Pure Solv, SPS-400-5 solvent purification system. All other solvents were used as purchased unless required dry, wherein distillation under argon, and over calcium hydride, was performed prior to use.
- MeLi was obtained as a solution in Et₂O, and standardised using diphenyl acetic acid in THF.³⁹
- ⁿBuLi was obtained as a solution in Hexane, and standardised using diphenyl acetic acid in THF.³⁹
- ⁿBu₂Mg was obtained as a solution in Et₂O and standardised using Iodine and LiCl in THF.³⁹
- Petroleum ether refers to petroleum ether in the boiling point (b.p.) range 40-60 °C unless otherwise stated.
- (+)-Menthol (optical purity 96 %*ee* by GLC) was purchased from Sigma-Aldrich.

Instrumentation and Data

Thin layer chromatography was carried out using Merck silica gel plates coated with fluorescent indicator UV254 and was analysed using a Mineralight UVGL-25 lamp or developed using a vanillin or potassium permanganate solution.

Flash column chromatography was carried out using Prolabo silica gel (230-400 mesh).

Melting points were obtained (uncorrected) on a Gallenkamp Griffin melting point apparatus.

IR spectra were obtained on a Shimadzu IR Affinity-1 Spectrophotometer machine and data are reported in cm⁻¹ unless stated otherwise.

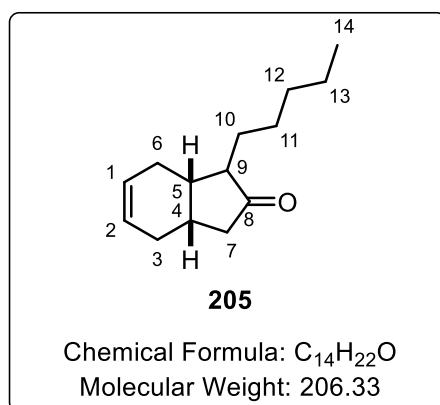
¹H, ¹³C NMR, ¹⁹F NMR and ¹¹B NMR spectra were recorded on a Bruker DPX spectrometer at 400 MHz, 101 MHz, 376 MHz and 128 MHz respectively. ¹H NMR and ¹³C NMR were also recorded on a Bruker DPX spectrometer at 600 MHz and 151 MHz, respectively. Unless otherwise stated, chemical shifts are reported in ppm. Coupling constants are reported in Hz and refer to ³J_{HH} interactions unless reported otherwise.

Chiral HPLC was carried out using a Chiralcel OJ-H column using a Gilson Model 302 pump, a Milton Roy Spectromonitor 3100 tuneable absorbance detector (set at 254 nm), and processed using a Dionex Advanced computer interface module.

Optical rotation measurements were carried out using a Perkin Elmer Polarimeter 341 or Rudolph Research Analytical Autopol III Automatic Polarimeter. Optical rotation values are quoted in 10^{-1} deg $\text{cm}^2 \text{g}^{-1}$ and concentrations are expressed in g ml^{-1} .

3.5.4. Synthesis of the Enol Triflate

Preparation of *rac*-(3*aS*,7*aS*)-1-pentyl-1,3,3*a*,4,7,7*a*-hexahydro-2*H*-inden-2-one.



Scheme 142

An oven-dried Schlenk tube was allowed to cool under an argon atmosphere and then flame-dried under vacuum before, once again, being cooled under an argon atmosphere. This cycle was repeated three times. To the now cool Schlenk tube was added silyl enol ether **173** (350 mg, 1.68 mmol) and THF (8 mL). The resulting colourless solution was cooled to -10 °C, with stirring, before the dropwise addition of MeLi (1.6 M in Et₂O) (1 mL, 1.6 mmol). After this, the resulting solution was allowed to stir at -10 °C for 20 min. The resulting solution was then cooled to -78 °C before the addition of DMPU (0.81 mL, 6.72 mmol), and the reaction mixture was allowed to stir at -78 °C for a further 60 min. To the resulting mixture was added 1-iodopentane (0.88 mL, 6.72 mmol) at -78 °C and the stirring was continued overnight. The resulting yellow solution was quenched by addition of a saturated aqueous solution of NH₄Cl and extracted with Et₂O (x3). The organic extracts were collected, combined and dried over Na₂SO₄. The resulting solution was concentrated *in vacuo* to provide the crude mixture as a colourless liquid. The crude was then applied to a silica column which was subsequently eluted with 5 % Et₂O/petroleum ether (40-60 °C) (2CV), then 10 % Et₂O/petroleum ether (40-60 °C) (2CV). The appropriate fractions were combined and concentrated *in vacuo* to yield the alkylated ketone **205** (145 mg, 0.7 mmol, 42 %) as a colourless oil.

Scheme 143

An oven-dried Schlenk tube was allowed to cool under an argon atmosphere and then flame-dried under vacuum before, once again, being cooled under an argon atmosphere. This cycle was repeated three times. To the now cool Schlenk tube was added silyl enol ether **173** (738 mg, 3.50 mmol) and THF (26 mL). The resulting colourless solution was cooled to -10 °C, with stirring, before the dropwise

addition of MeLi (1.67 M in Et₂O) (2.1 mL, 3.50 mmol). After this, the resulting solution was allowed to stir at -10 °C for 20 min. The resulting solution was then cooled to -78 °C before the rapid addition of a solution of 1-iodopentane (1.14 mmol, 8.75 mmol) in HMPA (8.75 mL), and the slurry was allowed to warm to room temperature overnight with stirring. The resulting yellow solution was then quenched by the addition of a saturated aqueous solution of NH₄Cl and extracted with Et₂O (x3). The organic extracts were collected, combined and dried over Na₂SO₄. The resulting solution was concentrated *in vacuo* to provide the crude mixture as a colourless liquid. The crude was then applied to a silica column, which was subsequently eluted with 5 % Et₂O/petroleum ether (40-60 °C) (2CV), and 10 % Et₂O/petroleum ether (40-60 °C) (2CV). The appropriate fractions were combined and concentrated *in vacuo* to yield the alkylated ketone **205** (495 mg, 2.40 mmol, 69 %) as a colourless oil.

Compound *isolated* as a mix of diastereomers.

IR ν (neat, cm⁻¹): 1735, 2856, 2924, 2953, 3024.

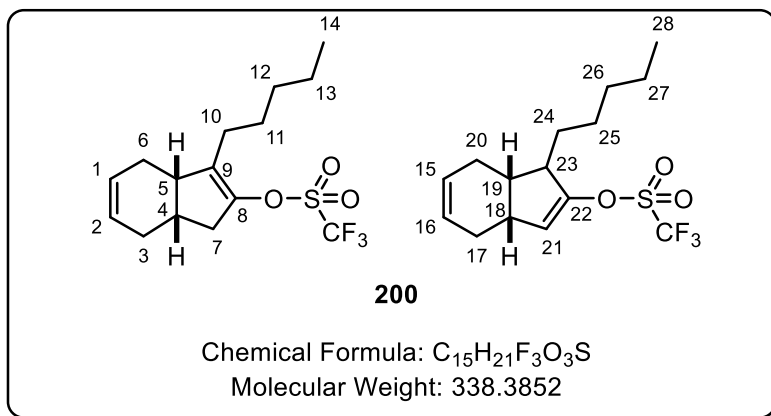
¹H NMR (400 MHz, Chloroform-*d*) δ 5.72 – 5.63 (m, 2H, H-1 and H-2), 2.45 – 2.18 (m, 4H, aliphatic protons), 2.18 – 1.87 (m, 4H, aliphatic protons), 1.79 – 1.64 (m, 1H, aliphatic protons), 1.57 – 1.37 (m, 3H, aliphatic protons), 1.36 – 1.18 (m, 5H, aliphatic protons), 0.91 – 0.83 (m, 3H, H-14).

¹³C NMR (101 MHz, Chloroform-*d*) δ 221.6, 125.1, 124.8, 124.6, 57.9, 51.4, 46.0, 41.2, 37.7, 34.1, 32.2, 31.9, 29.9, 28.4, 27.8, 27.1, 26.8, 26.2, 25.8, 24.2, 22.6, 22.1, 14.1.

HRMS (ESI) m/z calculated for C₁₄H₂₃O [M+H]⁺: 207.1749. Found: 207.1746.

R_f = 0.30 (10% Et₂O/ Petroleum ether)

Preparation of *rac*-(3*aR*,7*aS*)-1-pentyl-3*a*,4,7,7*a*-tetrahydro-1*H*-inden-2-yl trifluoromethanesulfonate.



General Procedure A:

A stirred solution of ketone **205** (90 mg, 0.44 mmol) and pyridine (0.04 mL, 0.55 mmol) in DCM (1 mL) was cooled to the appropriate temperature under an atmosphere of argon. To the stirred solution was added triflic anhydride (0.09 mL, 0.55 mmol) dropwise and the reaction mixture was allowed to gently warm to room temperature over 6 h. TLC analysis indicated no consumption of the starting material. The reaction was diluted with DCM (5 mL), washed with a saturated aqueous solution of NaHCO₃ and washed with a 1M solution of HCl. The collected organic extracts were dried over Na₂SO₄, filtered and half the filtrate had the solvent removed *in vacuo* to give a yellow residue. The yellow residue was applied to a silica column and eluted with 10 % Et₂O/ Petroleum ether. The appropriate fractions were combined and had the solvent removed *in vacuo* to give returned starting material **205** as a colourless oil.

Following the above **General Procedure A**, data are presented as a) temperature and b) amount, mmol and yield of returned starting material **205**.

Table 39, Entry 1

a) -78 °C and b) 82 mg, 0.40 mmol, 91 %.

Table 39, Entry 2

a) 0 °C and b) 0 mg.

General Procedure B:

A solution of di-*iso*-propylamine in THF was cooled to -78 °C under an atmosphere of argon after which, ⁿBuLi (2.4 M in hexanes) was added dropwise and the reaction mixture was allowed to stir for 0.5 h. Ketone **205** (50 mg, 0.24 mmol) in a solution of THF (1 mL) was added dropwise to the reaction mixture which was then allowed to warm to room temperature and stirred for 16 h, resulting in an orange solution. *N*-Phenyltriflimide (107 mg, 0.3 mmol) was then added to the reaction mixture, which was then allowed to warm to stir for a further 16 h. The reaction mixture was quenched by the addition of a saturated aqueous solution of NH₄Cl and extracted with Et₂O (3x). The combined organic extracts were dried with Na₂SO₄, filtered and the filtrate concentrated *in vacuo* to give a yellow residue. The crude was absorbed onto silica and applied to a silica column, eluting with petroleum ether (2 CV) and then with 5% Et₂O/petroleum ether (3 CV). The appropriate fractions were combined and reduced *in vacuo* to give the enol triflate **200** as a colourless oil.

Following the above **General Procedure B**, data are presented as a) amount of di-*iso*-propylamine, b) amount of ⁿBuLi and c) amount, mmol and yield of enol triflate **200**.

Table 40, Entry 1

a) 0.04 mL, 0.24 mmol, b) 0.1 mL, 0.24 mmol, and c) 32 mg, 0.095 mmol, 40 % yield, 91:9 thermodynamic:kinetic.

Table 40, Entry 2

a) 0.038 mL, 0.23 mmol, b) 0.095 mL, 0.23 mmol, and c) 24 mg, 0.071 mmol, 30 % yield, 92:8 thermodynamic:kinetic

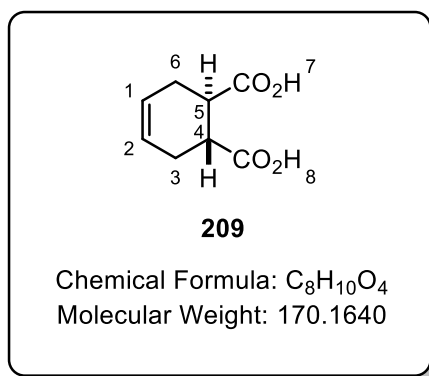
¹H NMR (400 MHz, Chloroform-*d*) δ 6.01 – 5.74 (m, 2H, H-1, H-2, H-15 and H-16), 5.55 – 5.47 (m, 0.09H, H-21), 2.93 – 2.83 (m, 0.09H, H-18), 2.82 – 2.68 (m, 1.91H, H-5), 2.60 – 2.41 (m, 1H, Aliphatic protons), 2.37 – 2.14 (m, 4H, Aliphatic protons), 2.02 – 1.79 (m, 3H, Aliphatic protons), 1.52 – 1.20 (m, 6H, Aliphatic protons), 0.89 (t, *J* = 7.0 Hz, 3H, H-14 and H-28).

¹³C NMR (101 MHz, Chloroform-*d*) δ 142.3, 135.9, 128.6, 128.3, 127.8, 127.8, 127.5, 127.5, 121.2, 120.6, 120.1, 116.9, 50.6, 40.0, 38.2, 37.7, 32.5, 32.0, 31.8, 28.7, 28.3, 27.4, 26.6, 26.4, 25.4, 24.7, 22.6, 22.5, 14.0.

¹⁹F NMR (376 MHz, Chloroform-*d*) δ -73.5, -74.4.

R_f = 1.00 (1% Et₂O/ Petroleum ether)

Preparation of *rac*-(1*R*,2*R*)-cyclohex-4-ene-1,2-dicarboxylic acid.⁴⁰



Scheme 146

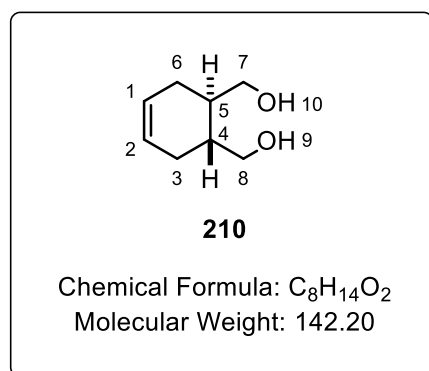
To a mixture of 3-sulfolene **207** (100 g, 846 mmol) and (*E*)-fumaric acid **208** (63 g, 542 mmol) was added acetic acid (650 mL), and the resulting mixture was warmed to 110 °C, with stirring for 7 days. The reaction mixture was then allowed to cool to room temperature, and the solvent was removed *in vacuo* to give a dark residue. The dark residue was washed with water until the remaining solid appeared grey. The grey solid was then triturated with boiling Et₂O to give a cream solid, which was dried *in vacuo* to give the diacid **209** (77 g, 453 mmol, 84 %) as a cream solid.

M.p.: 215-217 °C. lit.⁴¹: 217-221 °C

¹H NMR (400 MHz, DMSO-*d*₆) δ 12.23 (s, 2H, H-7 and H-8), 5.81 – 5.56 (m, 2H, H-1 and H-2), 2.63 – 2.54 (m, 2H, H-4 and H-5), 2.40 – 2.26 (m, 2H, H-3 or H-6), 2.12 – 2.00 (m, 2H, H-3 or H-6).

¹³C NMR (101 MHz, DMSO-*d*₆) δ 175.8, 125.1, 40.8, 27.5.

Preparation of *rac*-((1*S*,2*S*)-cyclohex-4-ene-1,2-diyl)dimethanol.³



Scheme 147

The reaction was carried out as documented in the literature procedure.^{42,43}

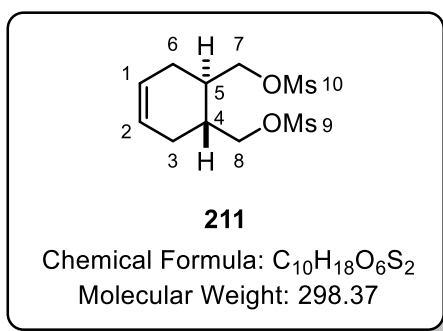
To a flame-dried flask fitted with a condenser was added distilled THF (350 mL), which was cooled in an ice-bath, before the addition of LiAlH₄ (14 g, 369 mmol) to give a grey suspension. To the resulting suspension had, a solution of diacid **209** (25 g, 146 mmol) in THF (150 mL) was added in a dropwise manner, and the resulting mixture was allowed to warm to room temperature, with stirring, under an atmosphere of argon, for 6 h. After this time, the reaction mixture was quenched by the addition of Na₂SO₄·10H₂O until the reaction mixture turned from a grey suspension to a white suspension. The white solid was filtered, and the filtrate was concentrated *in vacuo* to give the diol **210** (18.8 g, 132.2 mmol, 91 %) as a colourless oil.

IR (neat, cm⁻¹): 2887,3020, 3280 (br).

¹H NMR (400 MHz, Chloroform-*d*) δ 5.73 – 5.54 (m, 2H, H-1 and H-2), 3.73 (dd, *J* = 11.1, 2.8 Hz, 2H, H-7 or H-8), 3.63 – 3.56 (m, 2H, H-7 or H-8), 2.84 (s, 2H, H-9 and H-10), 2.08 – 1.97 (m, 2H, aliphatic protons), 1.92 – 1.80 (m, 2H, aliphatic protons), 1.73 – 1.66 (m, 2H, aliphatic protons).

¹³C NMR (101 MHz, Chloroform-*d*) δ 125.8, 66.1, 39.5, 28.3.

Preparation of *rac*-((1*R*,2*R*)-cyclohex-4-ene-1,2-diyl)bis(methylene) dimethanesulfonate.



Scheme 147

The reaction was carried out as documented in the literature procedure.^{42,43}

To a solution of diol **210** (20.0 g, 141 mmol) in DCM (170 mL) and Et₂O (510 mL) was added Et₃N (59 mL, 423 mmol) and the reaction mixture was cooled to 0 °C and MsCl (22.9 mL, 296.1 mmol) was added in a dropwise manner. The reaction mixture was then allowed to warm to room temperature and stirred for 18 h. The reaction mixture was concentrated *in vacuo* to deliver an orange residue which was then dissolved in DCM and H₂O. The layers were separated, the aqueous phase extracted with DCM (x3), and the organic extracts were washed with brine and then subsequently dried over Na₂SO₄ and filtered. The resulting solution was concentrated *in vacuo* to give a yellow oil, which was triturated with MeOH to provide the mesylate **211** (30.7 g, 103 mmol, 73 %) as a white solid.

M.p.: 76-78 °C

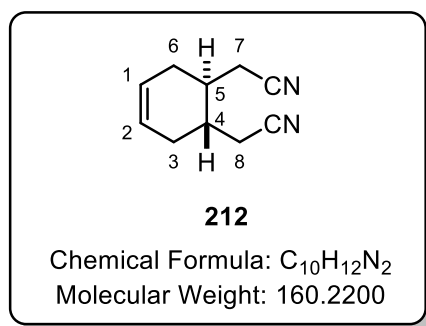
IR ν (neat, cm⁻¹): 1342, 2846, 2929, 3024.

¹H NMR (400 MHz, Chloroform-*d*) δ 5.64 (d, *J* = 1.8 Hz, 2H, H-1 and H-2), 4.24 (m, 4H, H-7 and H-8), 3.03 (s, 6H, H-9 and H-10), 2.24 – 2.11 (m, 4H, H-3 and H-6), 2.08 – 1.96 (m, 2H, H-5 and H-4).

¹³C NMR (101 MHz, Chloroform-*d*) δ 124.8, 70.8, 37.4, 33.7, 25.9.

HRMS (ESI) *m/z* calculated for C₁₀H₁₉O₆S₂ [M+H]⁺: 299.0618 Found: 299.0607

Preparation of *rac*-2,2'-((1*R*,2*R*)-cyclohex-4-ene-1,2-diyl)diacetonitrile.³



Scheme 147

The reaction was carried out as documented in the literature procedure.^{42,43}

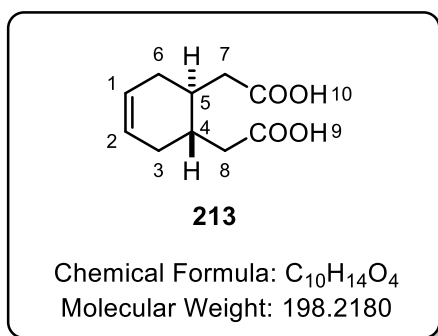
Under an argon atmosphere, a flame-dried flask fitted with a condenser, was charged with NaCN (14.3 g, 292 mmol) and a solution of dimesylate **211** (21.8 g, 73 mmol) in freshly distilled DMSO (220 mL). The resulting mixture was heated to 100 °C and allowed to stir for 18 h. After this time, the reaction mixture was allowed to cool to room temperature and water (400 mL) was added. The mixture was then extracted with EtOAc (3x) and the combined organic extracts were dried over Na₂SO₄ and filtered. The filtrate was concentrated *in vacuo* to yield the dinitrile **212** (11.2 g, 70 mmol, 96 %) as a yellow solid.

IR ν (neat, cm⁻¹): 2241, 2843, 2910, 3039.

¹H NMR (400 MHz, Chloroform-*d*) δ 5.72 – 5.60 (m, 2H, H-1 and H-2), 2.53 – 2.41 (m, 4H, H-7 and H-8), 2.36 – 2.23 (m, 2H, Aliphatic protons), 2.17 – 2.05 (m, 4H, Aliphatic protons).

¹³C NMR (101 MHz, Chloroform-*d*) δ 124.5, 117.7, 32.8, 28.4, 21.2.

Preparation of *rac*-2,2'-((1*S*,2*S*)-cyclohex-4-ene-1,2-diyl)diacetic acid.⁴⁴



Scheme 147

The reaction was carried out as documented in the literature procedure.^{42,43}

Dinitrile **212** (11.2 g, 70 mmol) was added to a solution of aq. 30 % KOH (120 mL) and heated to reflux with vigorous stirring for 18 h. The reaction mixture was then allowed to cool in an ice bath, after which, concentrated HCl was added dropwise until the pH was approximately 2. The precipitated solid thus formed was filtered off and dried in the vacuum oven to yield the diacid **213** (11.9 g, 60 mmol, 86 %) as a white solid.

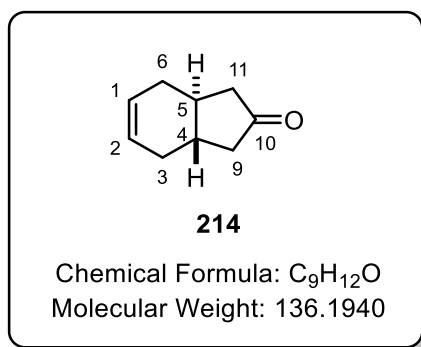
M.p.: 156-158 °C. lit.⁴⁴: 153-155 °C

IR (neat, cm^{-1}): 1685, 2549, 2646, 2895, 3034 (br).

^1H NMR (400 MHz, $\text{DMSO-}d_6$) δ 12.07 (s, 2H, H-9 and H-10), 5.57 (s, 2H, H-1 and H-2), 2.33 (dd, $J = 15.1$, $^2J = 4.6$ Hz, 2H, H-7 or H-8), 2.20 – 2.03 (m, 4H, Aliphatic protons), 2.00 – 1.85 (m, 2H, Aliphatic protons), 1.83 – 1.65 (m, 2H, Aliphatic protons).

^{13}C NMR (101 MHz, DMSO) δ 173.9, 125.0, 38.0, 32.9, 28.1.

Preparation of *rac*-(3*aS*,7*aS*)-1,3,3*a*,4,7,7*a*-hexahydro-2*H*-inden-2-one.⁴⁴



Scheme 147

The reaction was carried out as documented in the literature procedure.^{42,43}

A flame-dried flask fitted, with a condenser was charged with diacid **213** (11.8 g, 59.5 mmol) to which was added distilled Ac_2O (140 mL). The resulting mixture was heated to reflux, with stirring, under argon for 2.5 h. After this time, NaOAc (17.1 g, 208 mmol) was added, and the resulting mixture continued to reflux, with stirring, under argon for a further 16 h. The reaction mixture was then allowed to cool and was quenched by addition of a saturated aqueous NaHCO_3 solution then extracted

with Et₂O. The combined organic extracts were concentrated *in vacuo* to give an orange oil. The crude was further purified via column chromatography, eluting the silica gel column with 40 % Et₂O/petroleum ether. The appropriate fractions were combined and concentrated *in vacuo* to yield the ketone **214** (7.1 g, 52.2 mmol, 88 %) as a white solid.

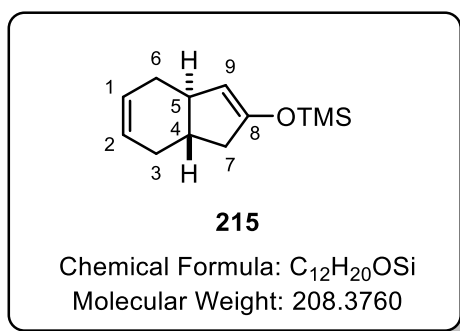
M.p.: 65-67 °C. lit.⁴⁴: 66-67 °C

IR (neat, cm⁻¹): 1726, 1737, 2831, 2891, 2962, 3022.

¹H NMR (400 MHz, Chloroform-*d*) δ 5.76 (d, *J* = 3.6 Hz, 2H, H-1 and H-2), 2.52 – 2.36 (m, 4H, H-9 and H-11), 2.00 – 1.83 (m, 6H, H-3, H-4, H-5 and H-6).

¹³C NMR (101 MHz, Chloroform-*d*) δ 217.9, 126.9, 45.6, 39.1, 31.6.

Preparation of *rac*-trimethyl(((3*aS*,7*aR*)-3*a*,4,7,7*a*-tetrahydro-1*H*-inden-2-yl)oxy)silane.



Scheme 148

The reaction was carried out as documented in the literature procedure.⁴⁵

A flask equipped with a stirrer bar was charged with NaI (1.36 g, 9.1 mmol), then gently flame-dried and allowed to cool under an atmosphere of argon. To the now cooled flask was added MeCN (13 mL), and the mixture was allowed to stir until the NaI had dissolved. To the resulting solution was added *trans*-bicyclic ketone **214** (500 mg, 3.7 mmol), Et₃N (1.3 mL, 9.1 mmol) and TMSCl (1.1 mL, 8.3 mmol), and the reaction mixture was allowed to stir for 16 h. The reaction mixture then was extracted with hexane (x3) and the combined hexane extracts were washed with a saturated aqueous solution of NaHCO₃. The solution was then were dried over Na₂SO₄, filtered and concentrated *in vacuo* to give the TMS enol ether **215** (750 mg, 3.60 mmol, 97 %) as a colourless oil.

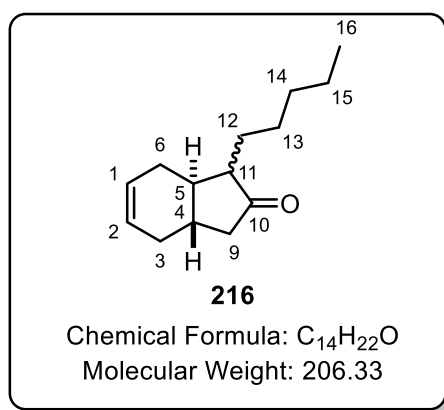
IR (neat, cm⁻¹): 1620, 2835, 2891, 2958, 3021 cm⁻¹.

^1H NMR (400 MHz, Chloroform-*d*) δ 5.79 – 5.59 (m, 2H, H-1 and H-2), 4.69 (s, 1H, H-9), 2.32 – 2.07 (m, 5H, Aliphatic protons), 2.05 – 1.72 (m, 3H, Aliphatic protons), 0.21 (s, 9H, Si(CH₃)₃).

^{13}C NMR (101 MHz, Chloroform-*d*) δ 156.2, 128.1, 127.4, 106.4, 44.3, 43.1, 39.6, 32.1, 30.6, 0.1.

HRMS (ESI) *m/z* calculated for C₁₂H₂₀OSi [M]: 208.1278 Found: 208.1284

Preparation of *rac*-(3*aS*,7*aR*)-1-pentyl-1,3,3*a*,4,7,7*a*-hexahydro-2*H*-inden-2-one.



Scheme 148

The reaction was carried out as documented in the literature procedure.⁵

An oven-dried Schlenk tube was allowed to cool under an argon atmosphere and then flame-dried under vacuum before, once again, being cooled under an argon atmosphere. This cycle was repeated three times. To the now cool Schlenk tube was added silyl enol ether **215** (550 mg, 2.64 mmol) and THF (18 mL). The resulting colourless solution was cooled to -10 °C, with stirring, before the dropwise addition of MeLi (1.65 mL, 1.6 M in Et₂O, 2.64 mmol). After this, the resulting solution was allowed to stir at -10 °C for 20 min. The solution was then cooled to -78 °C before the rapid addition of a solution of 1-iodopentane (0.86 mL, 6.60 mmol) in HMPA (6 mL). The resulting slurry was then allowed to warm to room temperature, with stirring, overnight. The resulting yellow solution was quenched by the addition of a saturated aqueous solution of NH₄Cl and extracted with Et₂O (x3). The organic extracts were collected, combined and dried over Na₂SO₄. The resulting solution was concentrated *in vacuo* to provide the crude mixture as a colourless liquid. The crude was then applied to a silica column which was subsequently eluted with 5 % Et₂O/petroleum ether (40-60 °C) (2CV), 10 % Et₂O/petroleum ether (40-60 °C) (2CV). The appropriate fractions were combined and concentrated *in vacuo* to yield the alkylated ketone **216** (365 mg, 1.77 mmol, 67 %) as a colourless oil.

The compound was isolated as a mixture of diastereomers.

IR ν (neat, cm^{-1}): 1674, 1707, 2900, 2960, 3039

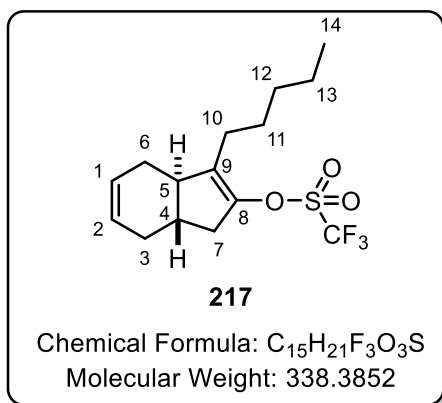
^1H NMR (400 MHz, Chloroform-*d*) δ 5.84 – 5.51 (m, 2H, H-1 and H-2), 2.47 – 2.27 (m, 2H, Aliphatic protons), 2.23 – 2.02 (m, 2H, Aliphatic protons), 2.02 – 1.69 (m, 4H, Aliphatic protons), 1.66 – 1.51 (m, 1H, Aliphatic protons), 1.46 – 1.13 (m, 8H, Aliphatic protons), 0.81 (t, $J = 6.9$ Hz, 3H, H-16).

^{13}C NMR (101 MHz, Chloroform-*d*) δ 221.6, 125.1, 124.8, 124.6, 57.9, 51.4, 46.0, 41.2, 37.8, 34.1, 32.2, 32.0, 32.0, 29.9, 28.4, 27.8, 27.1, 26.8, 26.2, 25.8, 24.2, 22.6, 22.2, 14.1.

HRMS (ESI) m/z calculated for $\text{C}_{14}\text{H}_{23}\text{O}$ $[\text{M}+\text{H}]^+$: 207.1749. Found: 207.1746.

$R_f = 0.30$ (10% Et_2O / Petroleum ether)

Preparation of *rac*-(3*aR*,7*aS*)-3-pentyl-3*a*,4,7,7*a*-tetrahydro-1*H*-inden-2-yl trifluoromethanesulfonate.



Scheme 149

A solution of di-*iso*-propylamine (0.04 mL, 0.24 mmol) in THF (1 mL) was cooled to -78 °C under an atmosphere of argon, after which, a solution of $n\text{BuLi}$ (0.1 mL, 2.4 M in hexane, 0.24 mmol) was added dropwise and the reaction mixture was allowed to stir for 0.5 h. A solution of ketone **216** (50 mg, 0.24 mmol) in THF (1 mL) was added dropwise to the reaction mixture, which was then allowed to warm to room temperature and stirred for 16 h to give an orange solution. *N*-Phenyltriflimide (107 mg, 0.3 mmol) was then added to the reaction mixture, which was allowed to stir for a further 16 h. TLC analysis indicated only starting material, with no conversion to the desired product. The reaction mixture was quenched by the addition of a saturated aqueous solution of NH_4Cl and extracted with

Et₂O (3x). The combined organic extracts were dried with Na₂SO₄, filtered and solvent removed *in vacuo* to give a yellow residue. The yellow residue was absorbed onto silica and applied to a silica column, eluting with petroleum ether (2 CV) and then with 5% Et₂O/petroleum ether (3 CV). The appropriate fractions were combined and reduced *in vacuo* to return the starting material **216** (42 mg, 0.20 mmol, 83 %) as a colourless oil.

Scheme 150

The reaction was carried out as documented in the literature procedure.⁶

A solution of di-*iso*-propylamine (0.04 mL, 0.24 mmol) in Et₂O (2.5 mL) was cooled to 0 °C under an atmosphere of argon, after which, EtMgBr (0.15 mL, 1.6 M in Et₂O, 0.24 mmol) was added dropwise and the reaction mixture was allowed to stir for 18 h. To the resulting white suspension was added HMPA (0.8 mL) and a solution of ketone **216** (50 mg, 0.24 mmol) in Et₂O (1 mL) and the suspension was allowed to warm to room temperature and stir for a further 6 h. To the suspension was added *N*-Phenyltriflimide (86 mg, 0.24 mmol) and the reaction mixture was allowed to stir at room temperature for a further 18 h. The reaction mixture was then quenched by the addition of a saturated aqueous solution of NH₄Cl and extracted with Et₂O (3x). The combined organic extracts were dried with Na₂SO₄, filtered and concentrated *in vacuo* to give a yellow residue. The yellow residue was absorbed onto silica and applied to a silica column, eluting with petroleum ether (2 CV) and then with 2.5% Et₂O/petroleum ether (3 CV). The appropriate fractions were combined and reduced *in vacuo* to give the enol triflate **217** (38 mg, 0.11 mmol, 46 %, 71:29 Thermodynamic: Kinetic product) as a colourless oil.

Scheme 151

The formation of the silyl enol ether intermediate was carried out as documented in the literature procedure.⁸

To a flask equipped with a stirrer bar was added NaI (43 mg, 0.29 mmol). The flask was placed under vacuum and flame dried. Once the flask had cooled, under argon, MeCN (0.5 mL) was added and the mixture stirred until the NaI dissolved after which ketone **216** (50 mg, 0.24 mmol), pyridine (0.022 mL, 0.29 mmol) and TMSCl (0.04 mL, 0.29 mmol) were then added and the mixture was allowed to stir under an atmosphere of argon for 18 h. The reaction mixture was extracted with hexane (3x) and the combined hexane extracts were then washed with a saturated aqueous solution of NaHCO₃, dried with Na₂SO₄, filtered and concentrated *in vacuo* to give the crude silyl enol ether. The crude silyl enol ether was dissolved in THF (1 mL) and cooled to 0 °C under an atmosphere of argon before the

dropwise addition of MeLi (0.15 mL, 1.6 M in Et₂O, 0.22 mmol) and stirring for a further 15 min. The resulting yellow solution was then cooled to -78 °C, and a solution of PhNTf₂ (107 mg, 0.3 mmol) in THF (0.5 mL) was added dropwise, and the reaction mixture was allowed to stir for 1.5 h then warmed to 0 °C for 0.5 h. The reaction mixture was quenched by the addition of a saturated aqueous solution of NH₄Cl and extracted with Et₂O (3x). The combined extracts were dried with Na₂SO₄, filtered and concentrated *in vacuo* to give a yellow residue. The crude was applied to a silica column and eluted with 1 % Et₂O/ Petroleum ether. The appropriate fractions were combined to give the enol triflate **217** (35 mg, 0.103 mmol, 43 % over two steps) as a colourless oil.

IR ν (neat, cm⁻¹): 1417, 1636, 1674, 2860, 2914, 3024.

¹H NMR (400 MHz, Chloroform-*d*) δ 5.82 – 5.68 (m, 2H, H-1 and H-2), 2.64 – 2.54 (m, 1H, H-5), 2.48 – 2.18 (m, 5H, aliphatic protons), 2.15 – 1.89 (m, 3H, aliphatic protons), 1.52 – 1.23 (m, 7H, aliphatic protons), 0.92 (t, *J* = 6.9 Hz, 3H, H-14).

¹³C NMR (101 MHz, Chloroform-*d*) δ 143.0, 134.6, 127.3, 125.8, 117.95 (q, ¹*J*_{CF} = 320.1 Hz), 44.3, 40.9, 35.4, 31.2, 29.7, 28.7, 26.5, 24.2, 21.8, 13.4.

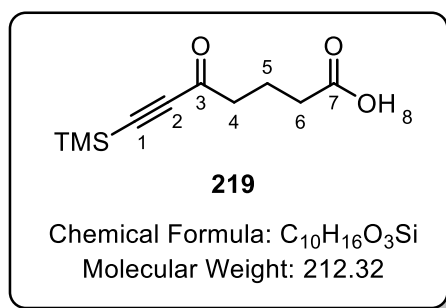
¹⁹F NMR (376 MHz, Chloroform-*d*) δ -74.4.

HRMS (ESI) *m/z* calculated for C₁₅H₂₁O₃F₃S₁ [M]: 338.1161 Found: 338.1158

R_f = 1.00 (1 % Et₂O/ Petroleum ether)

3.5.5. Synthesis of the Boronic Ester

Preparation of 5-oxo-7-(trimethylsilyl)hept-6-ynoic acid.⁹



Scheme 153

The reaction was carried out as documented in the literature procedure.⁹

To a stirred solution of glutaric anhydride **218** (2.86 g, 25 mmol) in DCM (212 mL) was added BTMSA (5.65 mL, 26.3 mmol), and the resulting solution was allowed to cool to 0 °C. Once cooled, AlCl₃ (3.5 g, 26.3 mmol) was added portion-wise and the solution was then allowed to warm to room temperature over 16 h. The resulting brown solution was cooled to 0 °C and quenched slowly by the addition of 1M HCl (200 mL), then the organic phase was separated and washed with 1M HCl (200 mL), water (200 mL) and brine (200 mL). The organic phase was dried over Na₂SO₄, filtered and the solvent was removed *in vacuo* to give the ketoacid **219** (5.1 g, 24 mmol, 96 %) as a yellow oil, which was taken on without further purification.

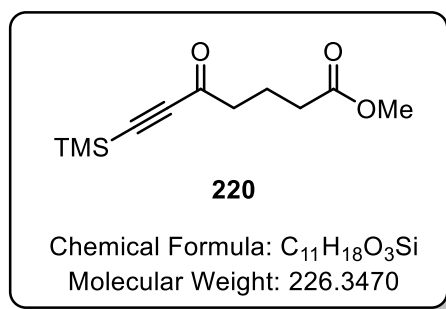
IR ν (neat, cm⁻¹): 1674, 1707, 2901, 2960, 3040 (br).

¹H NMR (400 MHz, Chloroform-*d*) δ 2.71 (t, *J* = 7.2 Hz, 2H, H-4), 2.46 (t, *J* = 7.3 Hz, 2H, H-6), 2.01 (p, *J* = 7.3 Hz, 2H, H-5), 0.27 (s, 9H, Si(CH₃)₃).

¹³C NMR (101 MHz, Chloroform-*d*) δ 186.7, 178.0, 101.8, 98.4, 44.1, 32.6, 18.7, -0.7.

R_f = 0.5 (50% Et₂O/ Petroleum ether)

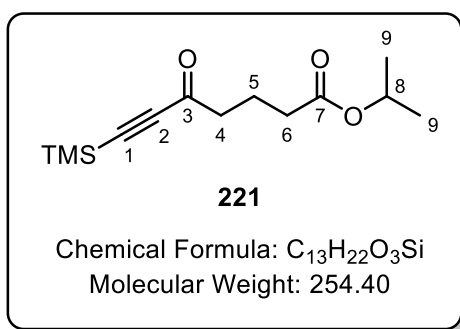
Attempted synthesis of methyl 5-oxo-7-(trimethylsilyl)hept-6-ynoate.



Scheme 154

To a stirred solution of ketoacid **219** (6 g, 28.3 mmol) in methanol (36 mL) was added TsOH.H₂O (540 mg, 3.1 mmol) and the reaction mixture was warmed to 55 °C for 16 h. The reaction mixture was cooled and had the solvent removed *in vacuo* to give a yellow gum. The yellow gum was redissolved in Et₂O and washed with a saturated aqueous solution of NaHCO₃. The collected organic phase was dried over Na₂SO₄, filtered and had the solvent removed *in vacuo* to give a yellow oil. ¹H NMR analysis indicated only partial removal of the silyl protecting group.

Preparation of *iso*-propyl 5-oxo-7-(trimethylsilyl)hept-6-ynoate.



Scheme 155

To a stirred solution of ketoacid **219** (6 g, 28.3 mmol) in *iso*-propanol (36 mL), was added TsOH.H₂O (540 mg, 3.1 mmol) and the reaction mixture was warmed to 55 °C for 16 h. The reaction mixture was then cooled and the solvent removed *in vacuo* to give a yellow gum. The yellow gum was redissolved in Et₂O and washed with a saturated aqueous solution of NaHCO₃. The collected organic phase was dried over Na₂SO₄, filtered and the solvent removed *in vacuo* to give a yellow oil. The yellow oil was applied to a silica column and eluted with 10 % Et₂O/ Petroleum ether. The appropriate fractions were combined and the solvent removed *in vacuo* to give the *iso*-propyl ester **221** (5.1 g, 20.1 mmol, 71 %) as a colourless oil.

IR ν (neat, cm⁻¹): 1718, 2873, 2937, 2960, 3290, 3439.

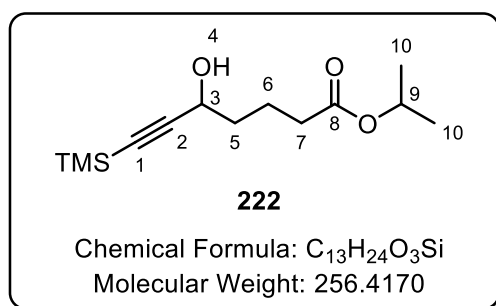
¹H NMR (400 MHz, Chloroform-*d*) δ 5.04 (sept, *J* = 6.3 Hz, 1H, H-8), 2.67 (t, *J* = 7.2 Hz, 2H, H-4), 2.35 (t, *J* = 7.3 Hz, 2H, H-6), 1.99 (p, *J* = 6.5 Hz, 2H, H-5), 1.26 (d, *J* = 6.3 Hz, 6H, H-9), 0.27 (s, 9H, Si(CH₃)₃).

¹³C NMR (101 MHz, Chloroform-*d*) δ 187.2, 172.8, 102.2, 98.5, 68.2, 44.6, 33.8, 22.2, 19.4, -0.4.

HRMS (ESI) *m/z* calculated for C₁₃H₂₃O₃Si [M+H]⁺: 255.1411. Found: 255.1414

R_f = 0.60 (10% Et₂O/ Petroleum ether)

Preparation of *iso*-propyl 5-hydroxy-7-(trimethylsilyl)hept-6-ynoate.



Scheme 156

To a solution of ketoester **221** (1 g, 3.9 mmol) in ethanol (30 mL), was added cerium chloride heptahydrate (1.9 g, 5.1 mmol) and the mixture was allowed to stir until the cerium chloride heptahydrate completely dissolved. The resulting colourless solution was then cooled to -78 °C, after which NaBH₄ (386 mg, 10.2 mmol) was added portion-wise over 1 h and the resulting reaction mixture was then warmed to room temperature and allowed to stir for a further 1 h. The reaction mixture was quenched by the addition of 1M HCl and extracted with DCM (3x). The combined organic extracts were dried over Na₂SO₄, filtered and the solvent removed *in vacuo* to give a yellow gum. The yellow gum was applied to a silica column and eluted with (30 % Et₂O/ Petroleum ether) (3 CV). The appropriate fractions were combined and had the solvent removed *in vacuo* to give the propargylic alcohol **222** (927 mg, 3.6 mmol, 92 %) as a colourless oil.

IR ν (neat, cm⁻¹): 1712, 1730, 2960, 3423.

¹H NMR (400 MHz, Chloroform-*d*) δ 5.02 (p, *J* = 6.3 Hz, 1H, H-9), 4.38 (t, *J* = 6.0 Hz, 1H, H-3), 2.34 (t, *J* = 7.1 Hz, 2H, H-7), 1.90 (s, 1H, H-4), 1.87 – 1.66 (m, 4H, H-5 and H-6), 1.24 (d, *J* = 6.3 Hz, 6H, H-10), 0.18 (s, 9H, Si(CH₃)₃).

¹³C NMR (101 MHz, Chloroform-*d*) δ 173.0, 106.4, 89.8, 67.7, 62.5, 37.0, 34.3, 21.9, 20.7, -0.1.

HRMS (ESI) *m/z* calculated for C₁₃H₂₅O₃Si [M+H]⁺: 257.1567. Found: 257.1570.

R_f = 0.35 (30% Et₂O/ Petroleum ether)

Preparation of 6-((trimethylsilyl)ethynyl)tetrahydro-2H-pyran-2-one.

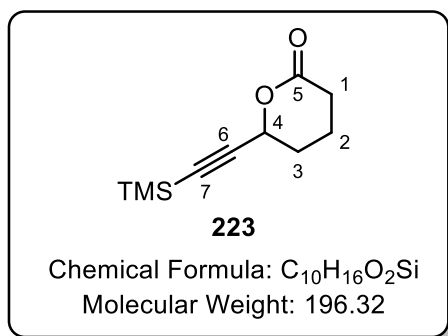


Table 41, Entry 1

To a solution of alcohol **222** (500 mg, 1.95 mmol) in toluene (60 mL) was added TsOH.H₂O (67 mg, 0.39 mmol), and the resulting mixture was allowed to stir at 70 °C, under an atmosphere of argon for 72 h. The reaction mixture was allowed to cool to room temperature and quenched by the addition of a saturated aqueous NaHCO₃ solution then extracted with Et₂O (3x). The collected organic extracts were combined, dried with Na₂SO₄, filtered and the solvent removed *in vacuo* to give a brown residue. The brown residue was applied to a silica column and eluted with (30 % Et₂O/ Petroleum) (3 CV). The appropriate fractions were combined and had the solvent removed *in vacuo* to give the alkynyl lactone **223** (210 mg, 1.07 mmol, 55 %) as a colourless oil.

Table 41, Entry 2

To a solution of alcohol **222** (100 mg, 0.39 mmol) in toluene (11 mL) was added TsOH.H₂O (15 mg, 0.08 mmol) and the resulting mixture was heated to reflux, under an atmosphere of argon for 72 h. The reaction mixture was allowed to cool to room temperature and quenched by the addition of saturated aqueous NaHCO₃ solution then extracted with Et₂O (3x). The collected organic extracts were combined, dried with Na₂SO₄, filtered and the solvent removed *in vacuo* to give a brown residue. The brown residue was applied to a silica column and eluted with (30 % Et₂O/ Petroleum) (3 CV). The appropriate fractions were combined and had the solvent removed *in vacuo* to give the alkynyl lactone **223** (51 mg, 0.26 mmol, 67 %) as a colourless oil.

Table 41, Entry 3

A flame-dried flask was fitted with a Dean-Stark apparatus, and sodium pieces added to the Dean-Stark trap. To this flask was added a solution of alcohol **222** (500 mg, 1.95 mmol) in toluene (60 mL)

then TsOH.H₂O (67 mg, 0.39 mmol) was added. The resulting mixture was heated to reflux, under an atmosphere of argon, for 6 h. The reaction mixture was allowed to cool to room temperature and quenched by the addition of saturated aqueous NaHCO₃ solution then extracted with Et₂O (3x). The collected organic extracts were combined, dried with Na₂SO₄, filtered and concentrated *in vacuo* to give a brown residue. The brown residue was applied to a silica column and eluted with (30 % Et₂O/ Petroleum) (3 CV). The appropriate fractions were combined and had the solvent removed *in vacuo* to give the alkynyl lactone **223** (351 mg, 1.78 mmol, 91 %) as a colourless oil.

IR ν (neat, cm⁻¹): 1737, 2958.

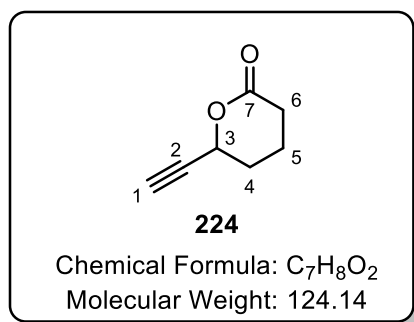
¹H NMR (400 MHz, Chloroform-*d*) δ 5.18 – 5.02 (m, 1H, H-4), 2.70 – 2.48 (m, 2H, H-1), 2.19 – 1.79 (m, 4H, H-2 and H-3), 0.19 (s, 9H, Si(CH₃)₃).

¹³C NMR (101 MHz, Chloroform-*d*) δ 170.4, 101.5, 92.8, 70.1, 29.7, 28.8, 17.8, 0.0.

HRMS (ESI) *m/z* calculated for C₁₀H₁₇O₂Si [M+H]⁺: 197.0998. Found: 197.0996.

R_f = 0.25 (30% Et₂O/ Petroleum ether)

Preparation 6-ethynyltetrahydro-2H-pyran-2-one.



Scheme 158

The reaction was carried out as documented in the literature procedure.⁴⁶

To a solution of TMS-alkyne **223** (100 mg, 0.51 mmol) in DMF (1 mL) was added water (0.1 mL) and KF (148 mg, 2.55 mmol) and the reaction was allowed to stir at room temperature for 5 min. The reaction was quenched with water and extracted with Et₂O (3x), the combined organic extracts were washed with brine (3x) after which the organic layer was dried with Na₂SO₄, filtered and had the solvent

removed *in vacuo* to give a colourless residue. The colourless residue was then applied to a silica column and eluted with (40 % Et₂O/ Petroleum ether). The appropriate fractions were combined to give the terminal alkyne **224** (51 mg, 0.41 mmol, 80 %) as a colourless oil.

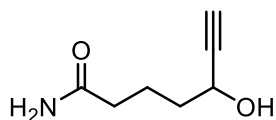
IR ν (neat, cm⁻¹): 1705, 2931, 3286.

¹H NMR (400 MHz, Chloroform-*d*) δ 5.21 – 5.10 (m, 1H, H-3), 2.74 – 2.51 (m, 3H, H-1 and H-6), 2.23 – 2.07 (m, 2H, H-4 or H-5), 2.04 – 1.86 (m, 2H, H-4 or H-5).

¹³C NMR (101 MHz, Chloroform-*d*) δ 169.8, 80.1, 75.5, 69.1, 29.4, 28.4, 17.4.

HRMS (ESI) *m/z* for C₇H₈O₂ could not be found. See below.

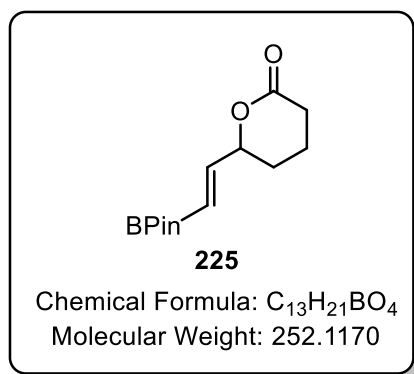
HRMS did not identify the parent ion. However, the amide below was identified, possibly formed *via* ring-opening by ammonia present in the mobile phase during analysis. HRMS (ESI) *m/z* calculated for C₇H₁₂NO₂ [M+H]⁺ = 142.0863. Found: 142.0865.



Chemical Formula: C₇H₁₁NO₂
Molecular Weight: 141.1700

R_f = 0.10 (40% Et₂O/ Petroleum ether)

Attempted preparation of (*E*)-6-(2-(4,4,5,5-tetramethyl-1,3,2-dioxaborolan-2-yl)vinyl)tetrahydro-2H-pyran-2-one.

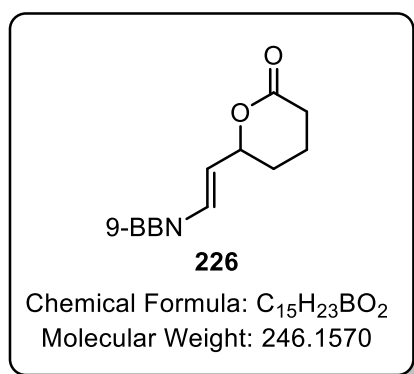


Scheme 158

The reaction was carried out as documented in the literature procedure.⁴⁷

To an oven-dried microwave vial was added Cu(OTf)₂ (5 mg, 15 μmol), tri-dentate mono-pyridine-dipyrzole (6 mg, 30 μmol), NaO^tBu (2mg, 30 μmol), B₂Pin₂ (91 mg, 0.36 mmol), MeCN (2mL) and MeOH (30 μL), and this mixture was allowed to stir for 30 min under an atmosphere of argon. Subsequently, a solution of alkyne **224** (37 mg, 0.3 mmol) in MeCN (1 mL), was added and the resulting mixture was stirred at 50 °C for 3 h. The reaction was diluted with Et₂O and washed with H₂O. The aqueous layer was extracted with further Et₂O (3x). The combined organic extracts were dried with Na₂SO₄, filtered and the solvent removed *in vacuo* to give a yellow residue. ¹H NMR spectroscopic analysis gave no indication of the formation of desired product.

Attempted preparation of 6-((E)-2-((1s,5s)-9-borabicyclo[3.3.1]nonan-9-yl)vinyl)tetrahydro-2H-pyran-2-one.

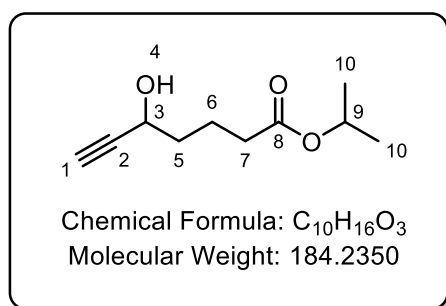


Scheme 159

The reaction was carried out as documented in the literature procedure.⁴⁸

A stirred solution of alkyne **224** (50 mg, 0.4 mmol) in THF (1 mL) was cooled to 0 °C under an atmosphere of argon. A solution of 9-BBN-H (0.9 mL, 0.5 M in THF, 0.45 mmol) was added dropwise and the reaction mixture was stirred for 3 h. TLC and ¹H NMR spectroscopic analysis did not indicate any remaining starting material or formation of the desired product.

Preparation of *iso*-propyl 5-hydroxyhept-6-ynoate.



Scheme 161

The reaction was carried out as documented in the literature procedure.⁴⁶

To a solution of TMS-alkyne **222** (100 mg, 0.39 mmol) in DMF (1 mL) was added water (0.1 mL) and KF (113 mg, 1.95 mmol), and the reaction mixture was allowed to stir at room temperature for 5 h. The reaction mixture was then quenched by the addition of water and extracted with Et₂O (3x). The combined organic extracts were washed with brine (3x), dried with Na₂SO₄, filtered and the solvent removed *in vacuo* to give a colourless residue. The colourless residue was then applied to a silica column and eluted with (40 % Et₂O/ Petroleum ether). The appropriate fractions were combined to give the terminal alkyne **228** (65 mg, 0.35 mmol, 90 %) as a colourless oil.

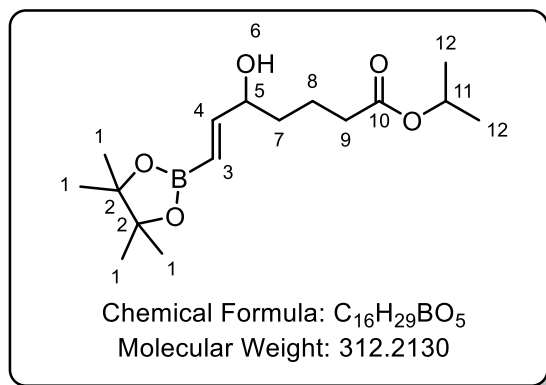
IR ν (neat, cm⁻¹): 1718, 2873, 2937, 2980, 3290, 3439 (br).

¹H NMR (400 MHz, Chloroform-*d*) δ 5.02 (sept, *J* = 6.3 Hz, 1H, H-9), 4.47 – 4.27 (m, 1H, H-3), 2.48 (d, ⁴*J* = 2.1 Hz, 1H, H-1), 2.35 (t, *J* = 7.0 Hz, 2H, H-7), 2.29 (s, 1H, H-4), 1.87 – 1.72 (m, 4H, H-5 and H-6), 1.25 (d, *J* = 6.3 Hz, 6H, H-10).

¹³C NMR (101 MHz, Chloroform-*d*) δ 172.5, 84.1, 72.5, 67.2, 61.3, 36.4, 33.6, 21.3, 20.0.

R_f = 0.25 (40 % Et₂O/ Petroleum ether)

Preparation of *iso*-propyl (*E*)-5-hydroxy-7-(4,4,5,5-tetramethyl-1,3,2-dioxaborolan-2-yl)hept-6-enoate.



Scheme 161

To an oven-dried microwave vial was added Cu(OTf)₂ (5 mg, 15 μmol), tri-dentate mono-pyridine-dipyrzole (6 mg, 30 μmol), NaO^tBu (2mg, 20 μmol), B₂Pin₂ (91 mg, 0.36 mmol), MeCN (2mL) and MeOH (30 μL), and this mixture was allowed to stir for 30 min under an atmosphere of argon. Subsequently, a solution of terminal alkyne **228** (55 mg, 0.3 mmol) in MeCN (1 mL) was added and the resulting mixture was stirred at 50 °C for 3 h. The reaction mixture was diluted with Et₂O, H₂O was added, and the mixture extracted with Et₂O (3x). The combined organic extracts were dried with Na₂SO₄, filtered and the solvent removed *in vacuo* to give a yellow residue. The yellow residue was applied to a silica column and eluted with (40% Et₂O/ Petroleum ether). The appropriate fractions were combined and had the solvent removed *in vacuo* to give the boronic ester **227** (47 mg, 0.15 mmol, 50 %) as a colourless oil.

IR ν (neat, cm⁻¹): 1641, 1728, 2864, 2933, 2978, 3435 (br).

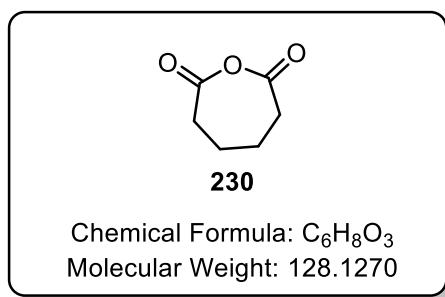
¹H NMR (400 MHz, Chloroform-*d*) δ 6.63 (dd, *J* = 18.1, 5.2 Hz, 1H, H-4), 5.66 (dd, *J* = 18.1, ⁴*J* = 1.4 Hz, 1H, H-2), 5.02 (sept, *J* = 6.3 Hz, 1H, H-11), 4.19 (m, 1H, H-5), 2.32 (t, *J* = 7.4 Hz, 2H, H-9), 1.85 – 1.51 (m, 4H, H-7 and H-8), 1.29 (s, 12H, H-1), 1.25 (d, *J* = 6.3 Hz, 6H, H-12).

¹³C NMR (101 MHz, CDCl₃) δ 173.2, 154.8, 83.4, 73.3, 67.7, 36.0, 34.5, 25.0, 24.9, 21.9, 20.9. Vinylic carbon attached to boron was not observed.

¹¹B NMR (128 MHz, Chloroform-*d*) δ 30.4.

R_f = 0.25 (50% Et₂O/ Petroleum ether)

Attempted synthesis of adipic anhydride

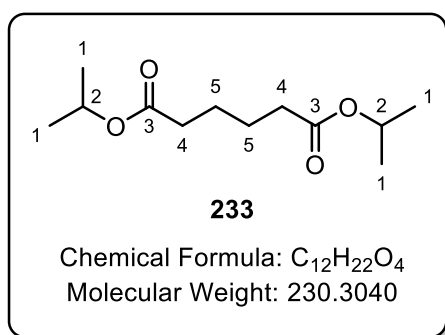


Scheme 162

The reaction was carried out as documented in the literature procedure.⁴⁹

To a stirred suspension of adipic acid **229** (1.46 g, 10 mmol) in THF (10 mL) was added Boc₂O (2.2g, 10.1 mmol) and MgCl₂ (20 mg, 0.21 mmol) and the resulting mixture was allowed to heated to 40 °C for 1 h. TLC analysis indicated conversion to adipic anhydride **230**. The solvent was removed *in vacuo* to give the crude material as a white residue. The crude material could not be purified by extraction, recrystallisation or sublimation.

Synthesis of di-*iso*-propyl adipate.



Scheme 164

The reaction was carried out as a modified procedure documented in the literature.⁵⁰

To a solution of adipic acid **229** (10 g, 68.3 mmol) in *i*PrOH (60 mL) was added SOCl₂ (24 mL, 331 mmol). The reaction mixture was then warmed to reflux and allowed to stir for 3 h. The reaction mixture was then concentrated *in vacuo* to give a yellow residue which was diluted with a saturated aqueous

solution of NaHCO₃ and extracted with Et₂O (3x). The combined organic extracts were dried with Na₂SO₄, filtered and the solvent removed *in vacuo* to give the di-*iso*-propyl adipate **233** (15.8 g, 68.3 mmol, Quantitative) as a colourless oil.

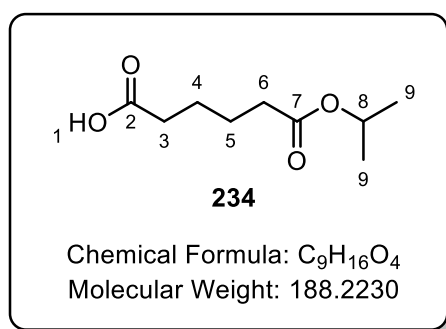
IR ν (neat, cm⁻¹): 1726, 2939, 2978.

¹H NMR (400 MHz, Chloroform-*d*) δ 5.01 (d, *J* = 6.2 Hz, 2H, H-2), 2.35 – 2.22 (m, 4H, H-4), 1.73 – 1.61 (m, 4H, H-5), 1.24 (d, *J* = 6.1 Hz, 12H, H-1).

¹³C NMR (101 MHz, Chloroform-*d*) δ 173.0, 67.6, 34.4, 24.5, 21.9.

HRMS (ESI) *m/z* calculated for C₁₂H₂₂O₄ [M]: 230.1513. Found: 230.1519.

Synthesis of 6-*iso*-propoxy-6-oxohexanoic acid.⁵¹



Scheme 164

The reaction was carried out as documented in the literature procedure.⁵⁰

To a solution of di-*iso*-propyl adipate **233** (15.8 g, 68.4 mmol) in *i*PrOH (160 mL) was added freshly-ground KOH (3.8 g, 68.4 mmol), and the reaction mixture allowed to stir for 16 h. The solvent was then removed *in vacuo* to give a white residue, which was dissolved in water and extracted with Et₂O. The aqueous layer was then adjusted to pH ~ 4 by addition of 2M HCl and extracted with EtOAc (3x). The combined EtOAc extracts were dried with Na₂SO₄, filtered and the solvent removed *in vacuo* to give the mono acid **234** (8.8 g, 46.7 mmol, 68 %) as a colourless oil.

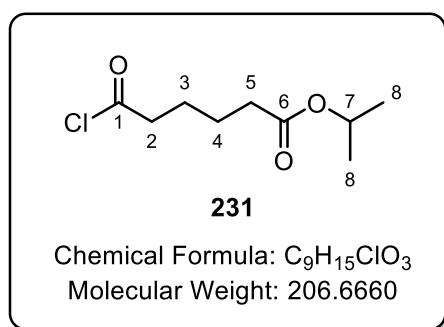
IR ν (neat, cm⁻¹): 1704, 1726, 2939, 2980, 3091(br).

^1H NMR (400 MHz, Chloroform-*d*) δ 5.02 (sept, $J = 6.2$ Hz, 1H, H-8), 2.45 – 2.36 (m, 2H, H-3), 2.36 – 2.26 (m, 2H, H-6), 1.79 – 1.60 (m, 4H, H-4 and H-5), 1.25 (d, $J = 6.6$ Hz, 6H, H-9).

^{13}C NMR (101 MHz, Chloroform-*d*) δ 178.6, 172.4, 67.1, 33.7, 33.1, 23.9, 23.6, 21.3.

$R_f = 0.40$ (50 % Et₂O/ Petroleum ether)

Synthesis of *iso*-propyl 6-chloro-6-oxohexanoate.



Scheme 164

The reaction was carried out as documented in the literature procedure.⁵⁰

To a solution of 6-*iso*-propoxy-6-oxohexanoic acid **234** (7.8 g, 41.4 mmol) in DCM (60 mL) was added oxalyl chloride (12.0 mL, 140.1 mmol) and DMF (2 drops) and the reaction mixture was allowed to stir under argon until the effervescence had ceased. The reaction mixture was then concentrated *in vacuo* to give the acid chloride **231** (8.55 g, 41.4 mmol, Quantitative) as a yellow oil.

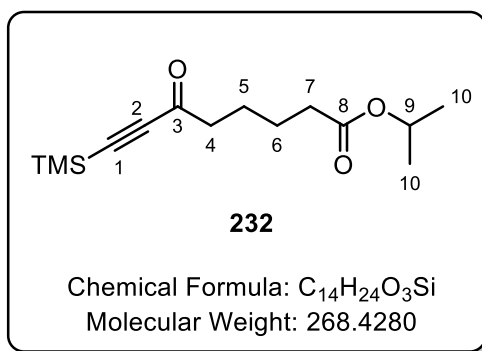
IR ν (neat, cm⁻¹): 1466, 1724, 1796, 2874, 2938, 2980.

^1H NMR (400 MHz, Chloroform-*d*) δ 5.03 (q, $J = 6.6$ Hz, 1H, H-7), 2.93 (t, $J = 6.7$ Hz, 2H, H-2), 2.32 (t, $J = 7.0$ Hz, 2H, H-5), 1.84 – 1.66 (m, 4H, H-3 and H-4), 1.25 (d, $J = 6.8$ Hz, 6H, H-8).

^{13}C NMR (101 MHz, Chloroform-*d*) δ 173.0, 171.9, 67.3, 46.2, 33.5, 24.0, 23.2, 21.3.

HRMS (ESI) m/z calculated for C₉H₁₆O₃Cl [M+H]⁺: 207.0783. Found: 207.0759.

Synthesis of *iso*-propyl 6-oxo-8-(trimethylsilyl)oct-7-ynoate.



Scheme 165

The reaction was carried out as documented in the literature procedure.¹¹

To a suspension of AlCl₃ (6.65 g, 49.9 mmol) in DCM (60 mL), cooled to 0 °C, was added a solution of BTMSA (10.3 mL, 47.8 mmol) and a solution acid chloride **231** (8.6 g, 41.6 mmol) in DCM (70 mL) was added dropwise. After stirring under an atmosphere of argon for 30 min, the reaction mixture was quenched by the addition of a 10 % aqueous solution of citric acid. The organic phase was separated and washed with further 10 % aqueous solution of citric acid, followed by water and then brine. The organic layer was then dried with Na₂SO₄, filtered and the solvent removed *in vacuo* to give a brown residue. The brown residue was applied to a silica column and eluted with 5 % Et₂O/Petroleum ether (3 CV) and then 10 % Et₂O/Petroleum ether (3 CV). The appropriate fractions were combined and the solvent removed *in vacuo* to give the ynone **232** (5.2 g, 19.4 mmol, 47 %) as a yellow oil.

IR ν (neat, cm⁻¹): 1676, 1728, 2873, 2900, 2930.

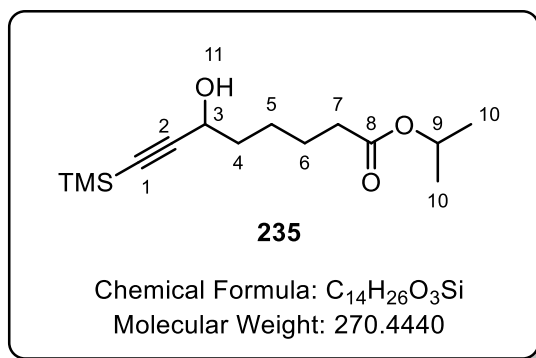
¹H NMR (400 MHz, Chloroform-*d*) δ 5.03 (sept, *J* = 6.5 Hz, 1H, H-9), 2.61 (t, *J* = 5.8 Hz, 2H, H-4), 2.31 (t, *J* = 6.7 Hz, 2H, H-7), 1.77 – 1.63 (m, 4H, H-5 and H-6), 1.25 (d, *J* = 6.7 Hz, 6H, H-10), 0.26 (s, 9H, Si(CH₃)₃).

¹³C NMR (101 MHz, Chloroform-*d*) δ 187.4, 172.9, 102.0, 98.0, 67.7, 44.9, 34.4, 24.4, 23.4, 21.9, -0.7.

HRMS (ESI) *m/z* calculated for C₁₄H₂₄O₃Si [M]: 268.1489. Found: 268.1495.

R_f = 0.60 (10 % Et₂O/ Petroleum ether)

Synthesis of *iso*-propyl 6-hydroxy-8-(trimethylsilyl)oct-7-ynoate.



Scheme 166

To a solution of ynone **232** (1.5 g, 5.6 mmol) in EtOH (50 mL) was added CeCl₃·7H₂O (2.7 g, 7.3 mmol) and the mixture was stirred until the cerium salt was completely dissolved. The solution was then cooled to -78 °C and NaBH₄ (0.636 g, 16.8 mmol) portion wise over 1 h and the reaction mixture was allowed to stir for a further 1 h. The reaction mixture was quenched with 2M aqueous solution of HCl and extracted with Et₂O (3x). The combined organic extracts were dried with Na₂SO₄, filtered and had the solvent removed *in vacuo* to give a colourless residue. The colourless residue was then applied to a silica column and eluted with 20 % Et₂O/Petroleum ether (3 CV) and 30 % Et₂O/Petroleum ether (3 CV). The appropriate fractions were combined and had the solvent removed *in vacuo* to give the propargylic alcohol **235** (1.42 g, 5.3 mmol, 95 %) as a colourless oil.

IR ν (neat, cm⁻¹): 1715, 1730, 2866, 2943, 2978, 3446.

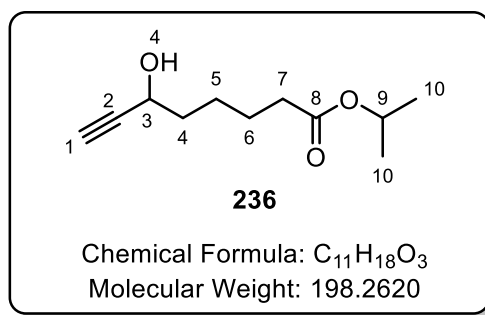
¹H NMR (400 MHz, Chloroform-*d*) δ 5.01 (p, *J* = 6.6 Hz, 1H, H-9), 4.36 (t, *J* = 6.8 Hz, 1H, H-3), 2.29 (t, *J* = 7.7 Hz, 2H, H-7), 1.82 – 1.61 (m, 5H, H-4, H-6 and H-11), 1.57 – 1.43 (m, 2H, H-5), 1.23 (d, *J* = 6.5 Hz, 6H, H-10), 0.17 (s, 9H, Si(CH₃)₃).

¹³C NMR (101 MHz, Chloroform-*d*) δ 173.2, 106.7, 89.6, 67.6, 62.7, 37.4, 34.7, 24.7, 21.9, 0.0.

HRMS (ESI) *m/z* calculated for C₁₄H₂₇O₃Si [M+H]⁺: 271.1724. Found: 271.1722.

R_f = 0.31 (30 % Et₂O/ Petroleum ether)

Synthesis of *iso*-propyl 6-hydroxyoct-7-ynoate.



Scheme 166

The reaction was carried out as documented in the literature procedure.⁴⁶

To a stirred solution of propargylic alcohol **235** (800 mg, 2.98 mmol), in DMF (5 mL) and H₂O (0.5 mL) was added KF (1.4 g, 24.1 mmol) and the resulting mixture was stirred for 5 h. The reaction mixture was diluted with water and extracted with Et₂O (3x). The combined organic extracts were dried with Na₂SO₄, filtered and the solvent removed *in vacuo* to give a colourless residue. The crude was then applied to a silica column and eluted with 25 % Et₂O/Petroleum ether (3 CV) and 35 % Et₂O/Petroleum ether (3 CV). The appropriate fractions were combined and had the solvent removed *in vacuo* to give the terminal alkyne **236** (456 mg, 2.3 mmol, 77%), as a colourless oil.

IR ν (neat, cm⁻¹): 1718, 2868, 2941, 2980, 3290, 3446 (br).

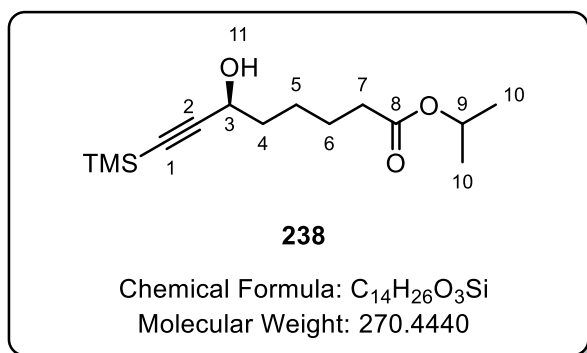
¹H NMR (400 MHz, Chloroform-*d*) δ 5.03 (sept, *J* = 6.3 Hz, 1H, H-9), 4.45 – 4.36 (m, 1H, H-3), 2.48 (d, ⁴*J* = 2.1 Hz, 1H, H-1), 2.31 (t, *J* = 7.4 Hz, 2H, H-7), 1.82 – 1.63 (m, 4H, H-4 and H-6), 1.57 – 1.48 (m, 2H, H-5), 1.25 (d, *J* = 6.3 Hz, 6H, H-10).

¹³C NMR (101 MHz, CDCl₃) δ 173.2, 87.9, 84.9, 73.1, 67.6, 62.2, 37.3, 34.6, 24.7, 21.9.

HRMS (ESI) *m/z* calculated for C₁₁H₁₉O₃ [M+H]⁺: 199.1329. Found: 199.1339.

R_f = 0.15 (40 % Et₂O/ Petroleum ether)

Synthesis of (*S*)-*iso*-propyl 6-hydroxy-8-(trimethylsilyl)oct-7-ynoate.



Scheme 167

The reaction was carried out as documented in the literature procedure.⁵²

To a flame-dried flask was added (*S,S*)-RuCl(η^6 -cymene)(Ts-DPEN) (60 mg, 94 μ mol), degassed DCM (5 mL) and freshly ground KOH (65 mg, 1.16 mmol). The reaction mixture was then allowed to stir under an atmosphere of argon for 1 h. The resulting purple reaction mixture was diluted with water (5 mL), filtered through a hydrophobic frit and washed with DCM (2 x 5 mL). The filtrate was concentrated *in vacuo* to give a purple residue. In an additional flame-dried flask was added ynone **232** (500 mg, 1.97 mmol) and IPA (5 mL), and the solution was subsequently degassed. The solution of ynone in IPA was added to the purple residue under an atmosphere of argon, and the resulting mixture was allowed to stir for 16 h. The reaction mixture was then concentrated *in vacuo* to give a brown residue. The crude was then applied to a silica column and eluted with 30% Et₂O/Petroleum ether (5 CV). The appropriate fractions were combined and had the solvent removed *in vacuo* to give the (*S*)-propargylic alcohol **238** (452 mg, 1.76 mmol, 89 %, 98 %*ee*) as a colourless oil.

Enantiomeric excess was determined by chiral HPLC analysis after derivatisation to the *p*-nitro benzoate (*vide infra*).

IR ν (neat, cm⁻¹): 1714, 2864, 2943, 3441 (br).

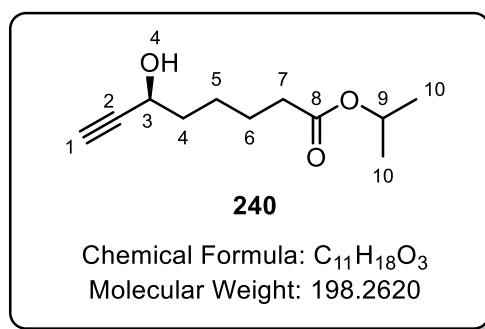
¹H NMR (400 MHz, Chloroform-*d*) δ 5.01 (p, *J* = 6.6 Hz, 1H, H-9), 4.36 (t, *J* = 6.8 Hz, 1H, H-3), 2.29 (t, *J* = 7.7 Hz, 2H, H-7), 1.82 – 1.61 (m, 5H, H-4, H-6 and H-11), 1.57 – 1.43 (m, 2H, H-5), 1.23 (d, *J* = 6.5 Hz, 6H, H-10), 0.17 (s, 9H, Si(CH₃)₃).

¹³C NMR (101 MHz, Chloroform-*d*) δ 173.2, 106.7, 89.6, 67.6, 62.7, 37.4, 34.7, 24.7, 21.9, 0.0.

HRMS (ESI) m/z calculated for $C_{14}H_{27}O_3Si$ $[M+H]^+$: 271.1724. Found: 271.1722.

R_f = 0.31 (30 % Et_2O / Petroleum ether)

Synthesis of (*S*)-iso-propyl 6-hydroxyoct-7-ynoate.



Scheme 169

The reaction was carried out as documented in the literature procedure.⁴⁶

To a stirred solution of (*S*)-propargylic alcohol **238** (412 mg, 1.52 mmol), in DMF (5 mL) and H_2O (0.5 mL) was added KF (441 mg, 7.6 mmol) and the resulting mixture was stirred for 5 h. The reaction mixture was diluted with water and extracted with Et_2O (3x). The combined organic extracts were dried with Na_2SO_4 , filtered and the solvent removed *in vacuo* to give a colourless residue. The colourless residue was then applied to a silica column and eluted with 25 % Et_2O /Petroleum ether (3 CV) and 35 % Et_2O /Petroleum ether (3 CV). The appropriate fractions were combined and had the solvent removed *in vacuo* to give the 6-(*S*)-hydroxy terminal alkyne **240** (255 mg, 1.29 mmol, 85 %) as a colourless oil.

IR ν (neat, cm^{-1}): 1724, 2866, 2939, 2980, 3286, 3433 (br).

1H NMR (400 MHz, Chloroform-*d*) δ 5.03 (sept, J = 6.3 Hz, 1H, H-9), 4.45 – 4.36 (m, 1H, H-3), 2.48 (d, 4J = 2.1 Hz, 1H, H-1), 2.31 (t, J = 7.4 Hz, 2H, H-7), 1.82 – 1.63 (m, 4H, H-4 and H-6), 1.57 – 1.48 (m, 2H, H-5), 1.25 (d, J = 6.3 Hz, 6H, H-10).

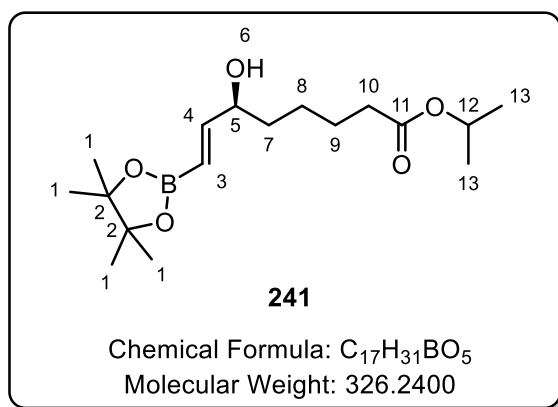
^{13}C NMR (101 MHz, Chloroform-*d*) δ 173.2, 87.9, 84.9, 73.1, 67.6, 62.2, 37.3, 34.6, 24.7, 21.9.

HRMS (ESI) m/z calculated for $C_{11}H_{19}O_3$ $[M+H]^+$: 199.1329. Found: 199.1339.

$R_f = 0.15$ (40 % Et₂O/ Petroleum ether)

$[\alpha]_D^{20} = -14.1^\circ$ (c 1.0, Chloroform)

Synthesis of *iso*-propyl (*S,E*)-6-hydroxy-8-(4,4,5,5-tetramethyl-1,3,2-dioxaborolan-2-yl)oct-7-enoate



Scheme 169

The reaction was carried out as documented in the literature procedure.¹²

To a flame-dried Schlenk flask was added copper powder (spherical, -170+270 mesh, Alfa Aesar) (8.8 mg, 0.14 mmol), sodium methoxide (14.9 mg, 0.28 mmol) and B₂Pin₂ (520 mg, 2.04 mmol). The Schlenk flask was evacuated and back-filled with argon (3x) before the addition of alkyne **240** (270 mg, 1.38 mmol) as a solution in EtOH (6 mL) and allowed to stir under argon for 18 h. The reaction mixture then concentrated to give a brown residue which was then applied to a silica column and eluted with 30 % Et₂O/Petroleum ether (3 CV) and 40 % Et₂O/Petroleum ether (3 CV). The appropriate fractions were combined, and the solvent removed *in vacuo* to give the 6-(*S*)-hydroxy boronic ester **241** (329 mg, 1.01 mmol, 73 %) as a colourless oil.

IR ν (neat, cm⁻¹): 1641, 1728, 2864, 2933, 2978, 3435 (br).

¹H NMR (400 MHz, Chloroform-*d*) δ 6.62 (dd, $J = 18.1, 5.3$ Hz, 1H, H-4), 5.64 (dd, $J = 18.1, {}^4J = 1.5$ Hz, 1H, H-3), 5.02 (sept, $J = 6.3$ Hz, 1H, H-12), 4.23 – 4.14 (m, 1H, H-5), 2.29 (t, $J = 7.4$ Hz, 2H, H-10), 1.70 – 1.54 (m, 4H, H-7 and H-9), 1.52 – 1.36 (m, 2H, H-8), 1.29 (s, 12H, H-1), 1.24 (d, $J = 6.3$ Hz, 6H, H-13).

¹³C NMR (101 MHz, Chloroform-*d*) δ 172.7, 154.5, 82.8, 73.0, 66.9, 35.7, 34.1, 24.4, 24.3, 21.4. Vinylic carbon attached to boron cannot be observed.

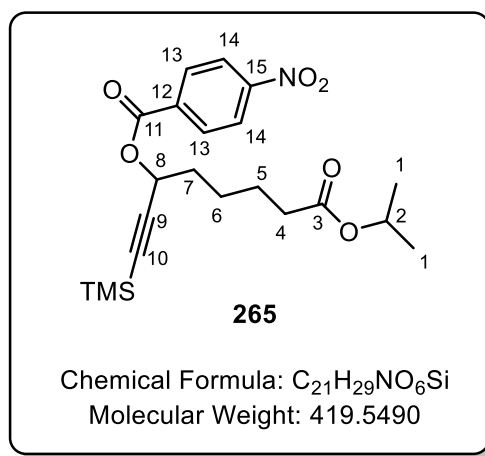
^{11}B NMR (128 MHz, Chloroform-*d*) δ 30.4 ppm.

HRMS (ESI) m/z calculated for $\text{C}_{17}\text{H}_{31}\text{O}_5\text{B}$ [M]: 326.2259. Found: 326.2240.

$R_f = 0.20$ (50 % Et_2O / Petroleum ether)

$[\alpha]_D^{20} = -3.92^\circ$ (c 1.0, Chloroform)

Synthesis of *8-iso-propoxy-8-oxo-1-(trimethylsilyl)oct-1-yn-3-yl 4-nitrobenzoate*.



To a solution of propargylic alcohol **235** (50 mg, 0.18 mmol) in DCM (2 mL) was added *p*-nitrobenzoylchloride (167 mg, 0.90 mmol), Et_3N (0.25 mL, 1.8 mmol) and a single crystal of DMAP. The resulting mixture was allowed to stir for 2 h. The reaction mixture then had the solvent removed *in vacuo* to give a yellow residue. The yellow residue was applied to a silica column and eluted with 20 % Et_2O / Petroleum ether. The appropriate fractions were combined, and the solvent removed *in vacuo* to give the *p*-nitrobenzoate ester **265** (73 mg, 0.17 mmol, 94 %) as a colourless oil.

IR ν (neat, cm^{-1}): 1528, 1606, 1728, 2866, 2953.

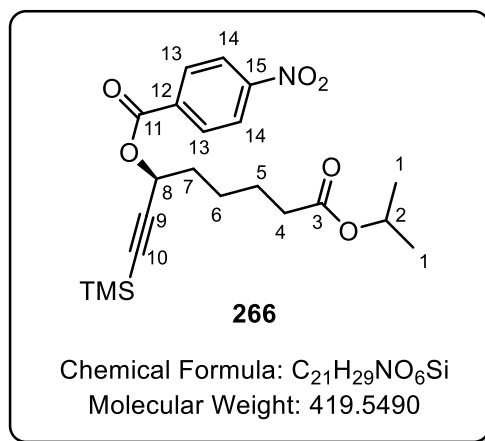
^1H NMR (400 MHz, Chloroform-*d*) δ 8.34 – 8.30 (m, 2H, H-14), 8.28 – 8.24 (m, 2H, H-13), 5.67 (t, $J = 6.5$ Hz, 1H, H-8), 5.02 (sept, $J = 6.3$ Hz, 1H, H-2), 2.33 (t, $J = 7.4$ Hz, 2H, H-4), 2.01 – 1.91 (m, 2H, Aliphatic protons), 1.73 (p, $J = 7.3$ Hz, 2H, Aliphatic protons), 1.64 – 1.52 (m, 2H, H-6), 1.24 (dd, $J = 6.2, 2.7$ Hz, 6H, H-1), 0.20 (s, 9H, $\text{Si}(\text{CH}_3)_3$).

^{13}C NMR (101 MHz, Chloroform-*d*) δ 173.0, 163.7, 150.7, 135.5, 131.0, 123.6, 101.7, 91.7, 67.6, 65.9, 34.6, 34.5, 24.7, 24.6, 21.9, -0.2.

HRMS (ESI) m/z calculated for $C_{21}H_{29}NO_6Si$ [M]: 419.1759. Found: 419.1769.

CHIRAL HPLC: Chiralcel OJ-H column, 50 % EtOH/0.1 % *iso*-propyl amine/ hexane, 254 nm, 0.7 ml/min, $RT_1 = 11.62$ min, $RT_2 = 13.82$ min.

Synthesis of (*S*)-8-*iso*-propoxy-8-oxo-1-(trimethylsilyl)oct-1-yn-3-yl 4-nitrobenzoate.



To a solution of (*S*)-propargylic alcohol **238** (100 mg, 0.36 mmol) in DCM (2 mL) was added *p*-nitrobenzoylchloride (334mg, 1.8 mmol), Et_3N (0.5 mL, 3.6 mmol) and a single crystal of DMAP. The resulting mixture was allowed to stir for 2 h. The reaction mixture then had the solvent removed *in vacuo* to give a yellow residue. The yellow residue was applied to a silica column and eluted with 20 % Et_2O / Petroleum ether. The appropriate fractions were combined, and the solvent removed *in vacuo* to give the *p*-nitrobenzoate ester **266** (124 mg, 0.30 mmol, 83 %, 98 %*ee*) as a colourless oil.

IR ν (neat, cm^{-1}): 1528, 1606, 1727, 2868, 2953.

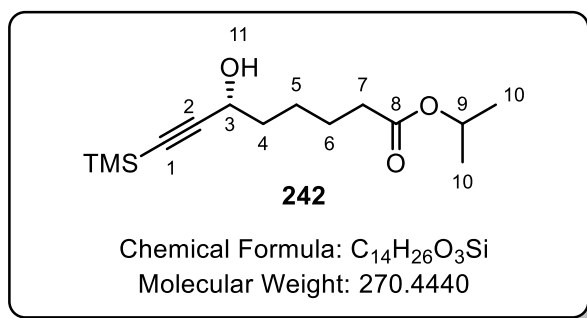
1H NMR (400 MHz, Chloroform-*d*) δ 8.34 – 8.30 (m, 2H, H-14), 8.28 – 8.24 (m, 2H, H-13), 5.67 (t, $J = 6.5$ Hz, 1H, H-8), 5.02 (sept, $J = 6.3$ Hz, 1H, H-2), 2.33 (t, $J = 7.4$ Hz, 2H, H-4), 2.01 – 1.91 (m, 2H, Aliphatic protons), 1.73 (p, $J = 7.3$ Hz, 2H, Aliphatic protons), 1.64 – 1.52 (m, 2H, H-6), 1.24 (dd, $J = 6.2, 2.7$ Hz, 6H, H-1), 0.20 (s, 9H, $Si(CH_3)_3$).

^{13}C NMR (101 MHz, Chloroform-*d*) δ 172.9, 163.7, 150.7, 135.5, 131.0, 123.6, 101.7, 91.7, 67.6, 65.9, 34.6, 34.6, 24.7, 24.6, 21.9, -0.2.

HRMS (ESI) m/z calculated for $C_{21}H_{29}NO_6Si$ [M]: 419.1759. Found: 419.1769.

CHIRAL HPLC: Chiralcel OJ-H column, 50 % EtOH/0.1 % *iso*-propyl amine/ hexane, 254 nm, 0.7 ml/min, RT₁ = 11.62 min, RT₂ = 13.83 min, RT₁ = 1 % RT₂ = 99 %.

Synthesis of (*R*)-*iso*-propyl 6-hydroxy-8-(trimethylsilyl)oct-7-ynoate.



Scheme 170

The reaction was carried out as documented in the literature procedure.⁵²

To a flame-dried flask was added (*R,R*)-RuCl(η^6 -cymene)(Ts-DPEN) (60 mg, 94 μ mol), degassed DCM (5 mL) and freshly ground KOH (65 mg, 1.16 mmol). The reaction mixture was then allowed to stir under an atmosphere of argon for 1 h. The resulting purple reaction mixture was diluted with water (5 mL), and filtered through a hydrophobic frit and washed with DCM (2 x 5 mL). The filtrate was concentrated *in vacuo* to give a purple residue. In an additional flame-dried flask was added ynone **232** (500 mg, 1.97 mmol), and IPA (5 mL), and the solution was subsequently degassed. The solution of ynone in IPA was added to the purple residue under an atmosphere of argon, and the resulting mixture was allowed to stir for 16 h. The reaction mixture was then concentrated *in vacuo* to give a brown residue. The crude was applied to a silica column and eluted with 30% Et₂O/Petroleum ether (5 CV). The appropriate fractions were combined and had the solvent removed *in vacuo* to give the (*R*)-propargylic alcohol **242** (423 mg, 1.56 mmol, 79 %, 97 %*ee*) as a colourless oil.

Enantiomeric excess was determined by chiral HPLC analysis after derivatisation to the *p*-nitro benzoate (*vide infra*).

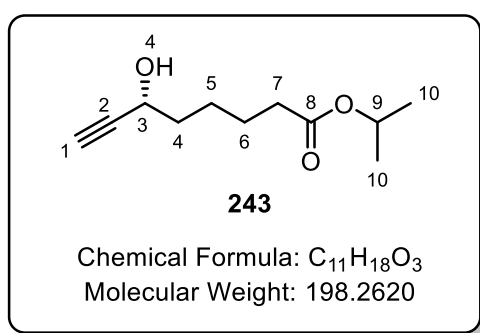
IR ν (neat, cm⁻¹): 1714, 2864, 2943, 3441 (br).

^1H NMR (400 MHz, Chloroform-*d*) δ 5.00 (sept, $J = 6.3$ Hz, 1H, H-9), 4.36 (q, $J = 5.6$ Hz, 1H, H-3), 2.28 (t, $J = 7.5$ Hz, 2H, H-7) 1.81 (d, $J = 4.9$ Hz, 1H, H-11), 1.76 – 1.61 (m, 4H, H-4 and H-6), 1.53 – 1.42 (m, 2H, H-5), 1.23 (d, $J = 6.3$ Hz, 6H, H-10), 0.16 (s, 9H, Si(CH₃)₃).

^{13}C NMR (101 MHz, Chloroform-*d*) δ 173.2, 106.7, 89.6, 67.6, 62.7, 37.4, 34.7, 24.7, 21.9, 0.0.

HRMS (ESI) m/z calculated for C₁₄H₂₇O₃Si [M+H]⁺: 271.1724. Found: 271.1722.

Synthesis of (*R*)-iso-propyl 6-hydroxyoct-7-ynoate.



Scheme 170

The reaction was carried out as documented in the literature procedure.⁴⁶

To a stirred solution of (*R*)-propargylic alcohol **242** (405 mg, 1.50 mmol), in DMF (4 mL) and H₂O (0.4 mL) was added KF (450 mg, 7.7 mmol) and the resulting mixture was stirred for 5 h. The reaction mixture was diluted with water and extracted with Et₂O (3x). The combined organic extracts were dried with Na₂SO₄, filtered and had the solvent removed *in vacuo* to give a colourless residue. The colourless residue was then applied to a silica column and eluted with 25 % Et₂O/Petroleum ether (3 CV) and 35 % Et₂O/Petroleum ether (3 CV). The appropriate fractions were combined and had the solvent removed *in vacuo* to give the (*R*)-terminal alkyne **243** (243 mg, 1.23 mmol, 82 %) as a colourless oil.

IR ν (neat, cm⁻¹): 1724, 2866, 2939, 2980, 3286, 3433 (br).

^1H NMR (400 MHz, Chloroform-*d*) δ 5.01 (sept, $J = 6.3$ Hz, 1H, H-9), 4.45 – 4.36 (m, 1H, H-3), 2.46 (d, $^4J = 2.1$ Hz, 1H, H-1), 2.29 (t, $J = 7.4$ Hz, 2H, H-7), 1.87 (d, $J = 5.5$ Hz, 1H, H-4), 1.77 – 1.62 (m, 4H, H-4 and H-6), 1.55 – 1.46 (m, 2H, H-5), 1.23 (d, $J = 6.3$ Hz, 6H, H-10).

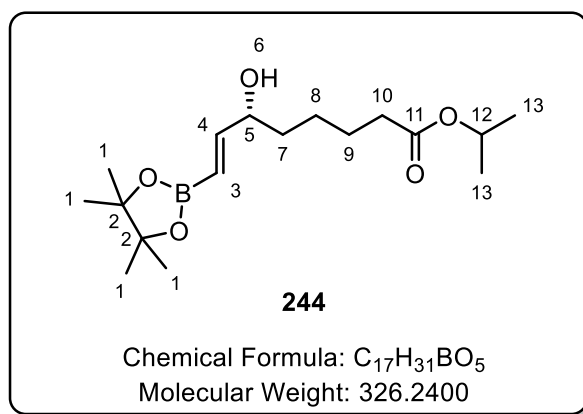
^{13}C NMR (101 MHz, Chloroform-*d*) δ 173.2, 87.9, 84.9, 73.1, 67.6, 62.2, 37.3, 34.6, 24.7, 21.9.

HRMS (ESI) m/z calculated for $\text{C}_{11}\text{H}_{19}\text{O}_3$ $[\text{M}+\text{H}]^+$: 199.1329. Found: 199.1339.

$R_f = 0.15$ (40 % Et_2O / Petroleum ether)

$[\alpha]_D^{20} = +13.9^\circ$ (c 1.0, Chloroform)

Synthesis of *iso*-propyl (*R,E*)-6-hydroxy-8-(4,4,5,5-tetramethyl-1,3,2-dioxaborolan-2-yl)oct-7-enoate.



Scheme 170

The reaction was carried out as documented in the literature procedure.¹²

To a flame-dried Schlenk flask was added copper powder (spherical, -170+270 mesh, Alfa Aesar) (8.7 mg, 0.14 mmol), sodium methoxide (14.7 mg, 0.28 mmol) and B_2Pin_2 (518 mg, 2.04 mmol). The Schlenk flask was evacuated and back-filled with argon (3x) before the addition of (*R*)-alkyne **243** (230 mg, 1.16 mmol) as a solution in EtOH (6 mL) which was allowed to stir under argon for 18 h. The reaction mixture was then concentrated to give a brown residue, which was then applied to a silica column and eluted with 30 % Et_2O /Petroleum ether (3 CV) and 40 % Et_2O /Petroleum ether (3 CV). The appropriate fractions were combined, and the solvent removed *in vacuo* to give the 6-(*R*)-hydroxy boronic ester **244** (321 mg, 0.98 mmol, 73 %) as a colourless oil.

IR ν (neat, cm^{-1}): 1641, 1728, 2864, 2933, 2978, 3435 (br).

^1H NMR (400 MHz, Chloroform-*d*) δ 6.62 (dd, $J = 18.1, 5.3$ Hz, 1H, H-4), 5.64 (dd, $J = 18.1, ^4J = 1.5$ Hz, 1H, H-3), 5.02 (sept, $J = 6.3$ Hz, 1H, H-12), 4.23 – 4.14 (m, 1H, H-5), 2.29 (t, $J = 7.4$ Hz, 2H, H-10), 1.70 – 1.54 (m, 4H, H-7 and H-9), 1.52 – 1.36 (m, 2H, H-8), 1.29 (s, 12H, H-1), 1.24 (d, $J = 6.3$ Hz, 6H, H-13).

^{13}C NMR (101 MHz, Chloroform-*d*) δ 172.7, 154.5, 82.8, 73.0, 66.9, 35.7, 34.1, 24.4, 24.3, 21.4. Vinyl carbon attached to boron was not observed.

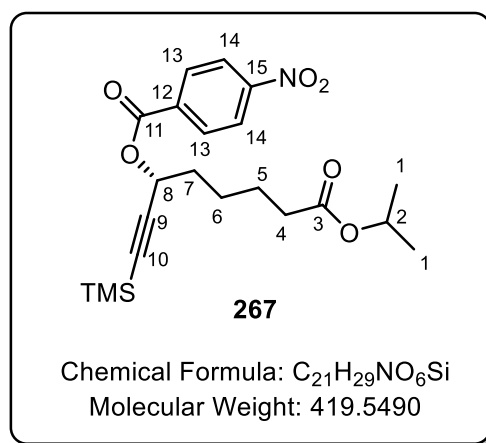
^{11}B NMR (128 MHz, Chloroform-*d*) δ 30.4.

HRMS (ESI) m/z calculated for $\text{C}_{17}\text{H}_{31}\text{O}_5\text{B}$ [M]: 326.2259. Found: 326.2240.

$R_f = 0.20$ (50 % Et_2O / Petroleum ether)

$[\alpha]_{\text{D}}^{20} = +3.85^\circ$ (c 1.0, Chloroform)

Synthesis of (*R*)-8-iso-propoxy-8-oxo-1-(trimethylsilyl)oct-1-yn-3-yl 4-nitrobenzoate.



To a solution of (*R*)-propargylic alcohol **242** (100 mg, 0.36 mmol) in DCM (2 mL) was added *p*-nitrobenzoylchloride (334mg, 1.8 mmol), Et_3N (0.5 mL, 3.6 mmol) and a single crystal of DMAP. The resulting mixture was allowed to stir for 2 h. The reaction mixture then had the solvent removed *in vacuo* to give a yellow residue. The yellow residue was applied to a silica column and eluted with 20 % Et_2O / Petroleum ether. The appropriate fractions were combined, and the solvent removed *in vacuo* to give the *p*-nitrobenzoate ester **267** (126 mg, 0.30 mmol, 83 %, 97 %*ee*) as a colourless oil.

IR ν (neat, cm^{-1}): 1528, 1606, 1727, 2868, 2953.

^1H NMR (400 MHz, Chloroform-*d*) δ 8.34 – 8.30 (m, 2H, H-14), 8.28 – 8.24 (m, 2H, H-13), 5.67 (t, $J = 6.5$

Hz, 1H, H-8), 5.02 (sept, $J = 6.3$ Hz, 1H, H-2), 2.33 (t, $J = 7.4$ Hz, 2H, H-4), 2.01 – 1.91 (m, 2H, Aliphatic protons), 1.73 (p, $J = 7.3$ Hz, 2H, Aliphatic protons), 1.64 – 1.52 (m, 2H, H-6), 1.24 (dd, $J = 6.2, 2.7$ Hz, 6H, H-1), 0.20 (s, 9H, Si(CH₃)₃).

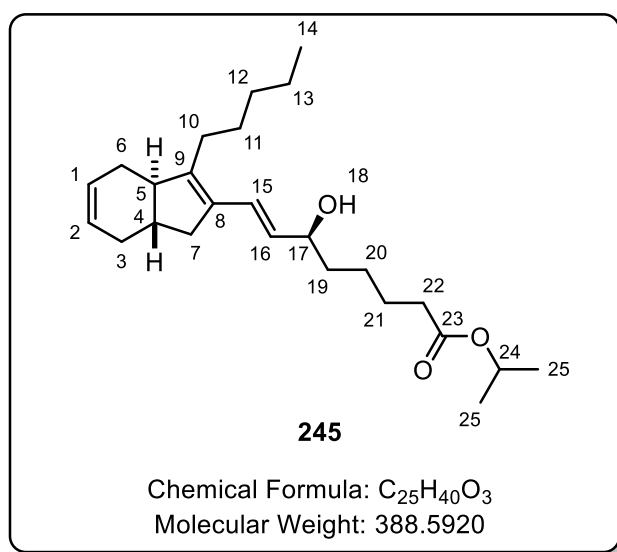
¹³C NMR (101 MHz, Chloroform-*d*) δ 172.9, 163.7, 150.7, 135.5, 131.0, 123.6, 101.7, 91.7, 67.6, 65.9, 34.6, 34.6, 24.7, 24.6, 21.9, -0.2.

HRMS (ESI) m/z calculated for C₂₁H₂₉NO₆Si [M]: 419.1759. Found: 419.1769.

CHIRAL HPLC: Chiracel OJ-H column, 50 % EtOH/0.1 % *iso*-propyl amine/ hexane, 254 nm, 0.7 ml/min, RT₁ = 11.63 min, RT₂ = 13.85 min, RT₁ = 98.5 % RT₂ = 1.5 %.

3.5.6. Completing the Convergent Strategy

Preparation of *iso*-propyl (*E*)-6-hydroxy-8-((3*aS*,7*aS*)-3-pentyl-3*a*,4,7,7*a*-tetrahydro-1*H*-inden-2-yl)oct-7-enoate.



Scheme 172

To a solution of enol triflate **217** (20 mg, 0.06 mmol) and (*S*)-hydroxy boronic ester **241** (38 mg, 0.12 mmol) in DMF (0.6 mL) was added Pd(dppf)Cl₂ (2 mg, 2.8 μ mol) and subsequently K₃PO₄ (38 mg, 0.18 mmol). The resulting mixture was warmed to 60 °C, with stirring under an atmosphere of argon, for 16 h. The reaction mixture was then diluted with water and extracted with Et₂O (3x). The combined organic extracts were dried with Na₂SO₄, filtered and the filtrate had the solvent removed *in vacuo* to give a red residue. The crude was absorbed onto silica and applied to a silica column, eluting with petroleum ether (2 CV) and then with 20% Et₂O/petroleum ether (3 CV). The appropriate fractions

were combined and reduced *in vacuo* to yield the dictyosphaerin *iso*-propyl ester **245** (18 mg, 0.046 mmol, 78 %) as a colourless oil.

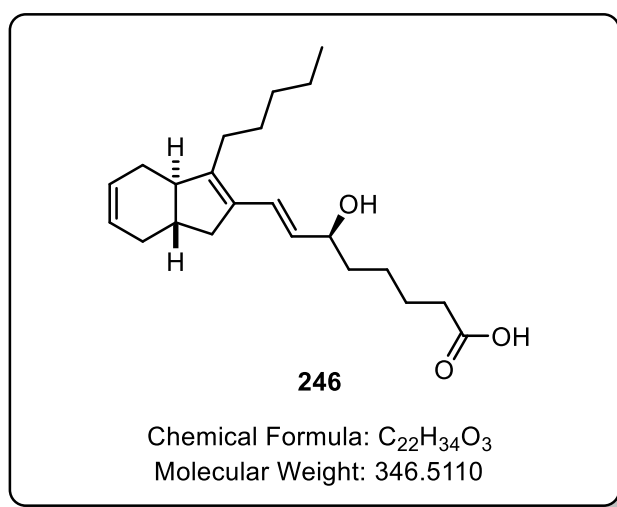
IR ν (neat, cm^{-1}): 1730, 2856, 2926, 3477 (br).

^1H NMR (400 MHz, Chloroform-*d*) δ 6.51 (d, $J = 15.5$ Hz, 1H, H-15), 5.83 – 5.65 (m, 2H, H-1 and H-2), 5.54 (dd, $J = 15.5, 7.2$ Hz, 1H, H-16), 5.00 (sept, $J = 6.3$ Hz, 1H, H-24), 4.18 (m, 1H, H-17), 2.53 (m, 1H, H-5), 2.38 – 2.22 (m, 6H, aliphatic protons), 2.13 – 1.82 (m, 4H, aliphatic protons), 1.77 – 1.50 (m, 6H, aliphatic protons), 1.48 – 1.27 (m, 5H, aliphatic protons), 1.25 – 1.19 (m, 8H, aliphatic protons), 0.88 (t, $J = 7.2$ Hz, 3H, H-25). Hydroxyl proton was not observed.

^{13}C NMR (101 MHz, Chloroform-*d*) δ ^{13}C NMR (101 MHz, CDCl_3) δ 173.3, 145.8, 145.7, 133.9, 133.8, 131.3, 128.5, 127.1, 125.5, 73.4, 73.3, 67.5, 49.5, 42.6, 42.5, 37.2, 37.2, 37.1, 37.0, 34.7, 32.0, 31.9, 31.4, 29.9, 28.5, 26.6, 26.6, 25.1, 25.0, 22.6, 21.9, 14.1.

HRMS (ESI) m/z calculated for $\text{C}_{25}\text{H}_{40}\text{O}_3$ [M]: 388.2972 Found: 388.2999

Attempted synthesis of dictyosphaerin.



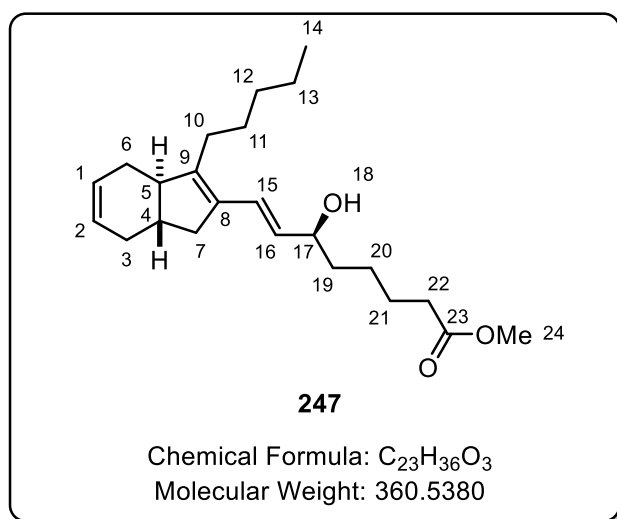
Scheme 173

The reaction was carried out as documented in the literature procedure.⁵³

To a stirred solution of dictyosphaerin *iso*-propyl ester **245** (15 mg, 0.039 mmol) in MeOH (0.5 mL), THF (0.5 mL) and H_2O (0.25 mL) was added $\text{LiOH}\cdot\text{H}_2\text{O}$ (4.5 mg, 0.19 mmol) and the resulting solution was allowed to stir for 30 min. TLC analysis indicated consumption of starting material and formation

of multiple new spots. The reaction mixture was quenched by the addition of 10 % aqueous solution of citric acid and extracted with Et₂O (3x). The combined organic extracts were dried over Na₂SO₄, filtered and the filtrate concentrated *in vacuo* to give a colourless residue. ¹H NMR analysis of the clear residue indicated minimal amounts of the desired product.

Preparation of dictyosphaerin methyl ester.¹



Scheme 174

The reaction was carried out as documented in the literature procedure.⁵⁴

To a stirred solution of dictyosphaerin *iso*-propyl ester **245** (19 mg, 0.049 mmol) in MeOH (0.5 mL) was added K₂CO₃ (33 mg, 0.24 mmol) and the resulting solution was allowed to stir for 6 h. The reaction mixture was quenched by the addition of a 10 % aqueous solution of citric acid, and extracted with Et₂O (3x). The combined organic extracts were dried over Na₂SO₄, filtered and the filtrate had the solvent removed *in vacuo* to give a colourless residue. The crude was absorbed onto silica and applied to a silica column, eluting with petroleum ether (2 CV) and then with 20% Et₂O/petroleum ether (3 CV). The appropriate fractions were combined and reduced *in vacuo* to yield the dictyosphaerin methyl ester **247** (14 mg, 0.039 mmol, 80 %) as a colourless oil. Hydroxyl proton was not observed.

IR ν (neat, cm⁻¹): 1647, 1739, 2835, 2854, 2924, 2951, 3019, 3450 (br).

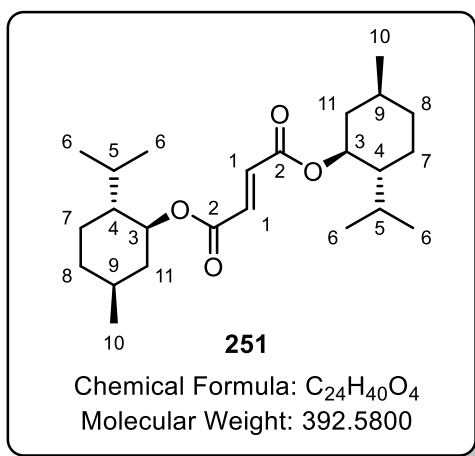
¹H NMR (600 MHz, Chloroform-*d*) δ 6.52 (d, *J* = 15.5 Hz, 1H, H-15), 5.83 – 5.64 (m, 2H, H-1 and H-2), 5.54 (dd, *J* = 15.4, 7.2 Hz, 1H, H-16), 4.19 (q, *J* = 6.7 Hz, 1H, H-17), 3.66 (s, 3H, H-24), 2.64 – 2.48 (m,

^1H , H-5), 2.38 – 2.21 (m, 6H, Aliphatic protons), 2.18 – 1.84 (m, 4H, Aliphatic protons), 1.75 – 1.50 (m, 2H, Aliphatic protons), 1.50 – 1.18 (m, 9H, Aliphatic protons), 0.88 (t, $J = 7.1$ Hz, 3H, H-14).

^{13}C NMR (151 MHz, Chloroform-*d*) δ 174.2, 145.9, 145.8, 133.9, 133.8, 131.3, 128.5, 127.1, 125.5, 73.4, 73.3, 51.6, 49.5, 49.5, 42.6, 42.5, 37.2, 37.1, 37.1, 37.0, 34.1, 32.0, 31.9, 31.4, 29.9, 28.5, 28.5, 26.6, 26.6, 25.2, 24.9, 22.6, 22.6, 14.1.

3.5.7. Structural Determination of Dictyosphaerin

Preparation of bis((1*S*,2*R*,5*S*)-2-*iso*-propyl-5-methylcyclohexyl) fumarate.³



Scheme 176

The reaction was carried out as documented in the literature procedure.³

A mixture of (*E*)-fumaric acid **253** (4.89 g, 42.2 mmol) and (+)-menthol (37.5 g, 240 mmol) was dissolved in toluene (50 mL). To the resulting solution was added concentrated H₂SO₄ (2 mL), and the reaction mixture was warmed to 60 °C, with stirring, for 16 h. The reaction mixture was allowed to cool, and then washed with a saturated aqueous solution of NaHCO₃. The organic phase was dried with Na₂SO₄, filtered and the filtrate concentrated *in vacuo* to give a yellow residue. The crude was applied to a silica column and eluted with 2.5 % Et₂O/ Petroleum Ether (5 CV). The appropriate fractions were combined and had the solvent removed *in vacuo* to give the dimethyl ester **251** (14.2 g, 36.2 mmol, 86 %) as a colourless oil.

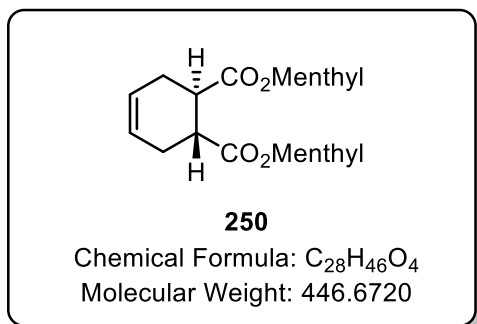
IR ν (neat, cm⁻¹): 1643, 1717, 2868, 2928, 2953.

¹H NMR (400 MHz, Chloroform-*d*) δ 6.82 (s, 2H, H-1), 4.79 (td, *J* = 10.9, 4.4 Hz, 2H, H-3), 2.08 – 1.94 (m, 2H, Aliphatic protons), 1.92 – 1.81 (m, 2H, Aliphatic protons), 1.75 – 1.65 (m, 4H, Aliphatic protons), 1.54 – 1.39 (m, 4H, Aliphatic protons), 1.16 – 0.96 (m, 4H, Aliphatic protons), 0.96 – 0.86 (m, 14H, Aliphatic protons), 0.76 (d, *J* = 7.0 Hz, 6H, H-10).

¹³C NMR (101 MHz, Chloroform-*d*) δ 164.8, 134.0, 75.5, 47.1, 40.8, 34.3, 31.5, 26.3, 23.5, 22.1, 20.8, 16.4.

$[\alpha]_{\text{D}}^{20} = +98.9^\circ$ (c 1.7, Chloroform)

Preparation of bis((2*R*,5*S*)-2-*iso*-propyl-5-methylcyclohexyl) (1*R*,2*R*)-cyclohex-4-ene-1,2-dicarboxylate.¹



Scheme 177

The reaction was carried out as documented in the literature procedure.³

Dimethyl ester **251** (14.1 g, 36.0 mmol) was azeotropically dried with hexane (2 x 100 mL) then dissolved in dry hexane (225 mL), and the solution was cooled to -40 °C. To the cooled solution, diethyl aluminium chloride (72 mL, 1 M in hexane, 72 mmol) was added dropwise to the stirred solution. The resulting red solution was allowed to stir at -40 °C for 30 min. In parallel, in a separate flask at -78 °C, was added 1,3-butadiene (120 mL, 15 wt% in hexane, 151 mmol), and the solution was cooled to -78 °C, for 30 min. The precooled diene was added dropwise to the red solution and completion of the addition, the reaction mixture was allowed to warm to -30 °C and then stirred for 18 h. The now yellow solution was allowed to warm to room temperature, and a 1M aqueous solution of HCl (200 mL) was added dropwise. Saturated aqueous Rochelle's salt (50 mL) was then added, the resulting suspension was filtered, and the filtrate was extracted with Et₂O (3x). The combined organic extracts were dried with Na₂SO₄, filtered and concentrated *in vacuo* to give a colourless residue. The crude was applied to a silica column and eluted with 1% Et₂O/Petroleum ether (10 CV). The appropriate fractions were combined and had the solvent removed *in vacuo* to give the chiral cyclohexene **250** (15.2, 34.0 mmol, 94 %, single diastereomer) as a colourless syrup.

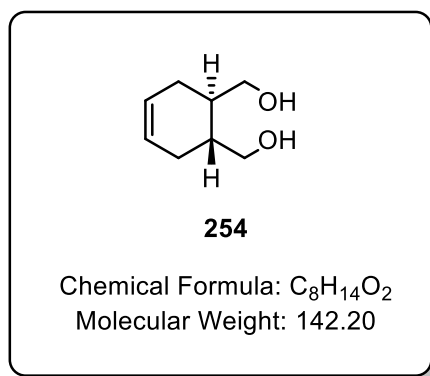
IR ν (neat, cm⁻¹): 1726, 2868, 2924, 2953, 3030.

¹H NMR (400 MHz, Chloroform-*d*) δ 5.70 (d, *J* = 2.5 Hz, 2H, HC=CH), 4.69 (td, *J* = 10.9, 4.3 Hz, 2H, 2x CHOC(O)), 3.01 – 2.79 (m, 2H, Aliphatic protons), 2.51 – 2.38 (m, 2H, Aliphatic protons), 2.24 – 2.11 (m, 2H, Aliphatic protons), 2.08 – 1.97 (m, 2H, Aliphatic protons), 1.96 – 1.83 (m, 2H, Aliphatic protons), 1.73 – 1.65 (m, 4H, Aliphatic protons), 1.56 – 1.25 (m, 4H, Aliphatic protons), 1.21 – 0.96 (m, 4H, Aliphatic protons), 0.95 – 0.87 (m, 14H, Aliphatic protons), 0.76 (d, *J* = 7.0 Hz, 6H, Aliphatic protons).

^{13}C NMR (101 MHz, Chloroform-*d*) δ 174.6, 125.1, 74.4, 47.1, 41.3, 40.8, 34.4, 31.5, 28.0, 26.1, 23.3, 22.1, 21.0, 16.0.

$[\alpha]_{\text{D}}^{20} = +28.7^\circ$ (c 2.05, Chloroform)

Preparation of ((1*S*,2*S*)-cyclohex-4-ene-1,2-diyl)dimethanol.³



Scheme 177

The reaction was carried out as documented in the literature procedure.³

To a flame-dried flask fitted with a condenser, under an atmosphere of argon, was added distilled THF (35 mL), which was cooled in an ice-bath, before the addition of LiAlH_4 (2.14 g, 56.5 mmol) to give a grey suspension. To the resulting suspension, a solution of diester **250** (12 g, 27.8 mmol) in THF (70 mL) was added in a dropwise manner, and the resulting mixture was heated to reflux, with stirring, for 2.5 h. After this time, the reaction mixture cooled to room temperature and quenched by the addition of $\text{Na}_2\text{SO}_4 \cdot 10\text{H}_2\text{O}$ until the reaction mixture turned from a grey suspension to a white suspension. The white suspension was filtered, and the filtrate was concentrated *in vacuo* to give the diol **254** (3.85 g, 27.1 mmol, 97 %) as a colourless oil.

M.p.: 52-54°C, lit.³: 52-54 °C

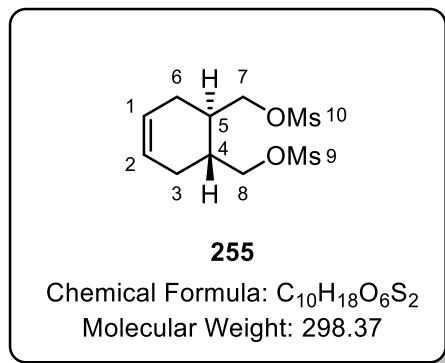
IR (neat, cm^{-1}): 2887,3020, 3280 (br).

^1H NMR (400 MHz, Chloroform-*d*) δ 5.73 – 5.54 (m, 2H, $\text{CH}=\text{CH}$), 3.73 (dd, $J = 11.1$, $^2J = 2.8$ Hz, 2H, CH_2OH), 3.63 – 3.56 (m, 2H, CH_2OH), 2.84 (s, 2H, OH), 2.08 – 1.97 (m, 2H, aliphatic protons), 1.92 – 1.80 (m, 2H, aliphatic protons), 1.73 – 1.66 (m, 2H, aliphatic protons).

^{13}C NMR (101 MHz, Chloroform-*d*) δ 125.8, 66.1, 39.5, 28.3.

$[\alpha]_D^{20} = -64.3^\circ$ (c 1.50, Chloroform)

Preparation of ((1*S*,2*S*)-cyclohex-4-ene-1,2-diyl)bis(methylene) dimethanesulfonate.



Scheme 177

To a solution of diol **254** (1.6 g, 11.2 mmol) in DCM (20 mL) and Et₂O (40 mL), was added Et₃N (4.7 mL, 33.6 mmol) followed by MsCl (1.9 mL, 24.0 mmol) dropwise at 0 °C. The reaction mixture was then allowed to warm to room temperature and stirred for 18 h. The reaction mixture was concentrated *in vacuo* to deliver an orange residue which was then dissolved in DCM and H₂O. The layers were separated, and the organic phase was washed with brine, dried over Na₂SO₄, and filtered. The resulting solution was concentrated *in vacuo* to give a yellow oil, which was triturated with MeOH to provide the dimesylate **255** (2.5 g, 8.38 mmol, 75 %) as a white solid.

M.p.: 76-78°C

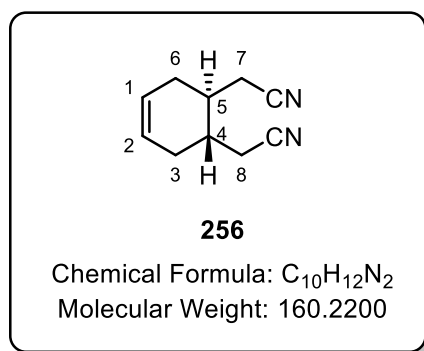
IR ν (neat, cm⁻¹): 1342, 2846, 2929, 3024.

¹H NMR (400 MHz, Chloroform-*d*) δ 5.64 (d, *J* = 1.8 Hz, 2H, H-1 and H-2), 4.24 (m, 4H, H-7 and H-8), 3.03 (s, 6H, H-9 and H-10), 2.24 – 2.11 (m, 4H, H-3 and H-6), 2.08 – 1.96 (m, 2H, H-4 and H-5).

¹³C NMR (101 MHz, Chloroform-*d*) δ 124.8, 70.8, 37.4, 33.7, 25.9.

HRMS (ESI) *m/z* calculated for C₁₀H₁₉O₆S₂ [M+H]⁺: 299.0618 Found: 299.0607

Preparation of 2,2'-((1S,2S)-cyclohex-4-ene-1,2-diyl)diacetonitrile.³



Scheme 177

The reaction was carried out as documented in the literature procedure.^{42,43}

Under an atmosphere of argon, a flame-dried flask fitted with a condenser, was charged with NaCN (1.5 g, 30.9 mmol) and a solution of dimesylate **255** (2.3 g, 7.7 mmol) in freshly distilled DMSO (20 mL). The resulting mixture was heated to 100 °C and allowed to stir for 18 h. After this time, the reaction mixture was allowed to cool to room temperature and water was added (40 mL). The mixture was then extracted with EtOAc and the combined organic extracts were dried over Na₂SO₄ and filtered. The filtrate was concentrated *in vacuo* to yield the dinitrile **256** (11.1 g, 6.9 mmol, 90 %) as a yellow solid.

M.p.: 84-86 °C, lit³: 86-89 °C

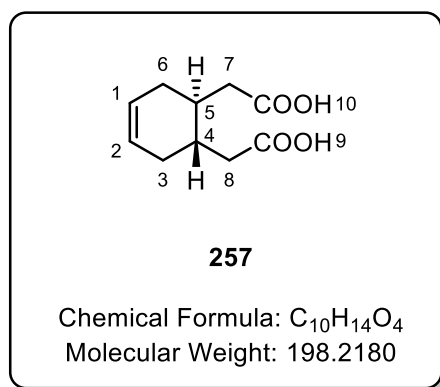
IR ν (neat, cm⁻¹): 2241, 2843, 2910, 3039.

¹H NMR (400 MHz, Chloroform-*d*) δ 5.72 – 5.60 (m, 2H, H-1 and H-2), 2.53 – 2.41 (m, 4H, H-7 and H-8), 2.36 – 2.23 (m, 2H, Aliphatic protons), 2.17 – 2.05 (m, 4H, Aliphatic protons).

¹³C NMR (101 MHz, Chloroform-*d*) δ 124.5, 117.7, 32.8, 28.4, 21.2.

$[\alpha]_D^{20} = -94.2^\circ$ (c 1.40, Chloroform)

Preparation of 2,2'-((1S,2S)-cyclohex-4-ene-1,2-diyl)diacetic acid.⁴⁴



Scheme 177

The reaction was carried out as documented in the literature procedure.^{42,43}

Dinitrile **256** (1.1 g, 6.90 mmol) was added to a solution of aq. 30 % KOH (30 mL) and the mixture was heated to reflux, with vigorous stirring for 18 h. The reaction mixture was then allowed to cool in an ice bath, and concentrated HCl was added dropwise until the pH was approximately 2. The precipitated solid thus formed was filtered and dried in the vacuum oven to yield the diacid **257** (1.18 g, 5.95 mmol, 86 %) as a white solid.

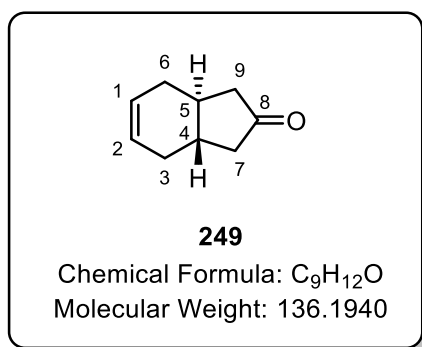
M.p.: 156-158 °C. lit.⁴⁴: 153-155 °C

IR (neat, cm⁻¹): 1685, 2549, 2646, 2895, 3034 (br).

¹H NMR (400 MHz, DMSO-*d*₆) δ 12.07 (s, 2H, H-9 and H-10), 5.57 (s, 2H, H-1 and H-2), 2.33 (dd, *J* = 15.1, ²*J* = 4.6 Hz, 2H, H-7 or H-8), 2.20 – 2.03 (m, 4H, Aliphatic protons), 2.00 – 1.85 (m, 2H, Aliphatic protons), 1.83 – 1.65 (m, 2H, Aliphatic protons).

¹³C NMR (101 MHz, DMSO-*d*₆) δ 173.9, 125.0, 38.0, 32.9, 28.1.

Preparation of (3a*S*,7a*S*)-1,3,3a,4,7,7a-hexahydro-2*H*-inden-2-one.⁴⁴



Scheme 177

The reaction was carried out as documented in the literature procedure.^{42,43}

A flame-dried flask fitted with a condenser, was charged with diacid **257** (800 mg, 4.04 mmol), and distilled Ac₂O (9.6 mL) was added. The resulting mixture was heated to reflux, with stirring, under argon for 2.5 h. After this time, NaOAc (1.16 g, 14.1 mmol) was added and the resulting mixture was allowed to continue to reflux, with stirring under argon for a further 16 h. The reaction mixture was then allowed to cool, and was quenched by addition of a saturated aqueous NaHCO₃ solution then extracted with Et₂O. The combined organic extracts were concentrated *in vacuo* to give an orange oil. The crude was further purified via column chromatography, eluting the silica gel column with 40 % Et₂O/petroleum ether. The appropriate fractions were combined and concentrated *in vacuo* to yield the chiral ketone **249** (497 mg, 3.65 mmol, 91 %) as a white solid.

M.p.: 65-67 °C. lit.⁴⁴: 66-67 °C

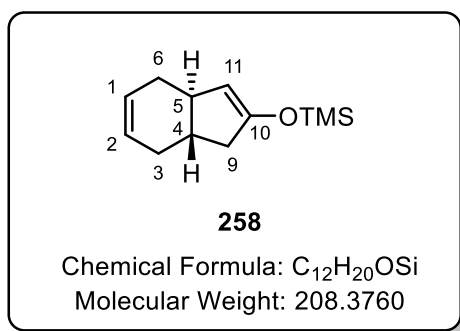
IR (neat, cm⁻¹): 1726, 1737, 2831, 2891, 2962, 3022.

¹H NMR (400 MHz, Chloroform-*d*) δ 5.76 (d, *J* = 3.6 Hz, 2H, H-1 and H-2), 2.52 – 2.36 (m, 4H, H-7 and H-9), 2.00 – 1.83 (m, 6H, H-3, H-4, H-5 and H-6).

¹³C NMR (101 MHz, Chloroform-*d*) δ 217.9, 126.9, 45.6, 39.1, 31.6.

[α]_D²⁰ = +96.7° (c 1.13, Ethanol)

Preparation of trimethyl(((3a*R*,7a*S*)-3a,4,7,7a-tetrahydro-1*H*-inden-2-yl)oxy)silane.



Scheme 179

The reaction was carried out as documented in the literature procedure.⁴⁵

A flask equipped with a stirrer bar was charged with NaI (525 mg, 3.5 mmol), then gently flame-dried and allowed to cool under an atmosphere of argon. To the now cooled flask was added MeCN (6 mL), and the mixture was allowed to stir until the NaI had dissolved. To the resulting solution was added *trans*-ketone **249** (400 mg, 2.9 mmol), Et₃N (0.49 mL, 3.5 mmol) and TMSCl (0.44 mL, 3.5 mmol) and the reaction mixture was allowed to stir for 16 h. The reaction mixture was then extracted with hexane (x3) and the combined hexane extracts were washed with a saturated aqueous solution of NaHCO₃. The hexane solution was then dried over Na₂SO₄, filtered and the filtrate concentrated *in vacuo* to give the TMS silyl enol ether **258** (521 mg, 2.50 mmol, 86 %) as a colourless oil.

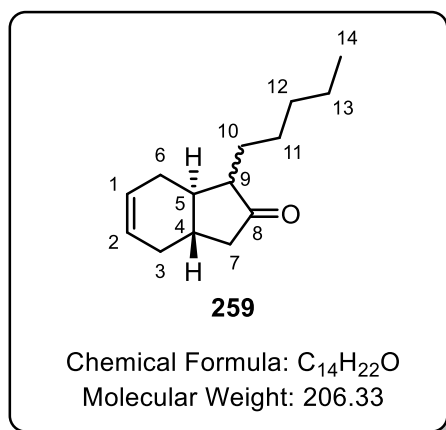
IR (neat, cm⁻¹): 1620, 2835, 2891, 2958, 3021 cm⁻¹.

¹H NMR (400 MHz, Chloroform-*d*) δ 5.79 – 5.59 (m, 2H, H-1 and H-2), 4.69 (s, 1H, H-11), 2.32 – 2.07 (m, 5H, Aliphatic protons), 2.05 – 1.72 (m, 3H, Aliphatic protons), 0.21 (s, 9H, Si(CH₃)₃).

¹³C NMR (101 MHz, Chloroform-*d*) δ 156.2, 128.1, 127.4, 106.4, 44.3, 43.1, 39.6, 32.1, 30.6, 0.1.

HRMS (ESI) *m/z* calculated for C₁₂H₂₀OSi [M]: 208.1278 Found: 208.1284

Preparation of (3a*S*,7a*R*)-1-pentyl-1,3,3a,4,7,7a-hexahydro-2*H*-inden-2-one.



Scheme 179

The reaction was carried out as documented in the literature procedure.⁵

An oven-dried Schlenk tube was allowed to cool under an argon atmosphere and then flame-dried under vacuum before, once again, being cooled under an argon atmosphere. This cycle was repeated three times. To the now cool Schlenk tube was added silyl enol ether **258** (410 mg, 1.97 mmol) and THF (15 mL). The resulting colourless solution was cooled to -10 °C, with stirring, before the dropwise addition of MeLi (1.3 mL, 1.5 M in Et₂O, 1.97 mmol). After this, the resulting solution was allowed to stir at -10 °C for 20 min. The solution was then cooled to -78 °C, before the rapid addition of a solution of 1-iodopentane (0.51 mL, 3.94 mmol) in HMPA (5 mL). The resulting slurry was then allowed to warm to room temperature overnight. The resulting yellow solution was quenched by the addition of a saturated aqueous solution of NH₄Cl and extracted with Et₂O (x3). The organic extracts were collected, combined and dried over Na₂SO₄. The solution was then concentrated *in vacuo* to provide the crude product as a colourless liquid. The crude was then applied to a silica column, which was subsequently eluted with 5 % Et₂O/petroleum ether (40-60 °C) (2CV), 10 % Et₂O/petroleum ether (40-60 °C) (2CV). The appropriate fractions were combined and concentrated *in vacuo* to yield the alkylated ketone **259** (266 mg, 1.29 mmol, 65 %) as a colourless oil.

The compound was isolated as a mixture of diastereomers.

IR ν (neat, cm⁻¹): 1674, 1707, 2900, 2960, 3039

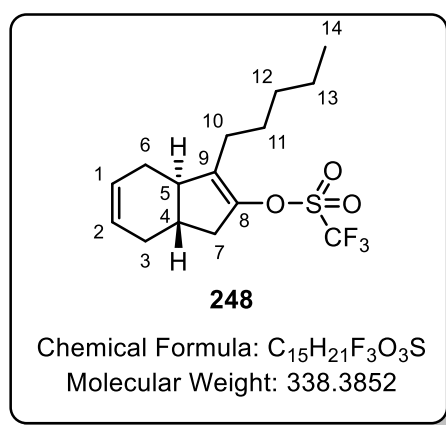
¹H NMR (400 MHz, Chloroform-*d*) δ 5.84 – 5.51 (m, 2H, H-1 and H-2), 2.47 – 2.27 (m, 2H, Aliphatic protons), 2.23 – 2.02 (m, 2H, Aliphatic protons), 2.02 – 1.69 (m, 4H, Aliphatic protons), 1.66 – 1.51 (m, 1H, Aliphatic protons), 1.46 – 1.13 (m, 8H, Aliphatic protons), 0.81 (t, *J* = 6.9 Hz, 3H, H-14).

^{13}C NMR (101 MHz, Chloroform-*d*) δ 221.6, 125.1, 124.8, 124.6, 57.9, 51.4, 46.0, 41.2, 37.8, 34.1, 32.2, 32.0, 32.0, 29.9, 28.4, 27.8, 27.1, 26.8, 26.2, 25.8, 24.2, 22.6, 22.2, 14.1.

HRMS (ESI) m/z calculated for $\text{C}_{14}\text{H}_{23}\text{O}$ $[\text{M}+\text{H}]^+$: 207.1749. Found: 207.1746.

R_f = 0.30 (10% Et_2O / Petroleum ether)

Preparation of (3*aR*,7*aS*)-3-pentyl-3*a*,4,7,7*a*-tetrahydro-1*H*-inden-2-yl trifluoromethanesulfonate.



Scheme 180

The formation of the silyl enol ether intermediate was carried out as documented in the literature procedure.⁸

To a flask was added NaI (94 mg, 0.63 mmol), and the flask then was placed under vacuum and flame dried. Once the flask had cooled, MeCN (1 mL) was added and the mixture stirred until the NaI dissolved. Ketone **259** (100 mg, 0.48 mmol), pyridine (0.05 mL, 0.63 mmol) and TMSCl (0.08 mL, 0.63 mmol) was added and the mixture allowed to stir under an atmosphere of argon for 18 h. The reaction mixture was extracted with hexane (3x) and the hexane extracts were then washed with a saturated aqueous solution of NaHCO_3 , dried with Na_2SO_4 , filtered and concentrated *in vacuo* to give the crude silyl enol ether. The crude silyl enol ether was dissolved in THF (1 mL) and cooled to 0 °C under an atmosphere of argon, before the dropwise addition of MeLi (0.3 mL, 1.6 M in Et_2O , 0.48 mmol) and stirring for a further 15 min. The resulting yellow solution was then cooled to -78 °C, a solution of PhNTf_2 (196 mg, 0.55 mmol) in THF (1 mL) was added dropwise, and the reaction mixture was allowed to stir for 1.5 h and warmed to 0 °C for 0.5 h. The reaction mixture was quenched by the addition of a saturated aqueous solution of NH_4Cl and extracted with Et_2O (3x). The combined organic extracts were dried with Na_2SO_4 , filtered and concentrated *in vacuo* to give a yellow residue. The yellow

residue was applied to a silica column and eluted with 1 % Et₂O/ Petroleum ether. The appropriate fractions were combined to give the chiral enol triflate **248** (90 mg, 0.26 mmol, 54 % over two steps) as a colourless oil.

IR ν (neat, cm⁻¹): 1417, 1636, 1674, 2860, 2914, 3024.

¹H NMR (400 MHz, Chloroform-*d*) δ 5.82 – 5.68 (m, 2H, H-1 and H-2), 2.64 – 2.54 (m, 1H, H-5), 2.48 – 2.18 (m, 5H, aliphatic protons), 2.15 – 1.89 (m, 3H, aliphatic protons), 1.52 – 1.23 (m, 7H, aliphatic protons), 0.92 (t, *J* = 6.9 Hz, 3H, H-14).

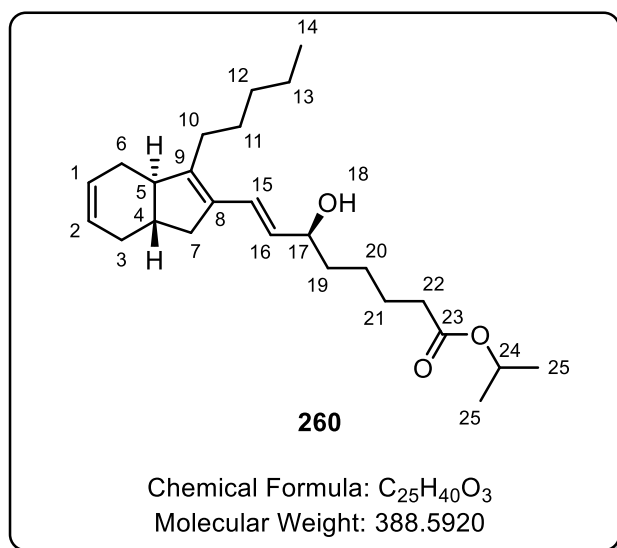
¹³C NMR (101 MHz, Chloroform-*d*) δ 143.0, 134.6, 127.3, 125.8, 117.95 (q, ¹*J*_{CF} = 320.1 Hz), 44.3, 40.9, 35.4, 31.2, 29.7, 28.7, 26.5, 24.2, 21.8, 13.4.

¹⁹F NMR (376 MHz, Chloroform-*d*) δ -74.4.

HRMS (ESI) *m/z* calculated for C₁₅H₂₁O₃F₃S₁ [M+H]⁺: 338.1161 Found: 338.1158

R_f = 1.00 (1 % Et₂O/ Petroleum ether)

Preparation of *iso*-propyl (*S,E*)-6-hydroxy-8-((3*aR*,7*aS*)-3-pentyl-3*a*,4,7,7*a*-tetrahydro-1*H*-inden-2-yl)oct-7-enoate



Scheme 181

To a solution of enol triflate **248** (40 mg, 0.12 mmol) and (*S*)-hydroxy boronic ester **241** (76 mg, 0.24 mmol) in DMF (1.2 mL) was added Pd(dppf)Cl₂ (4 mg, 5.6 μ mol) and subsequently K₃PO₄ (76 mg, 0.36 mmol). The resulting mixture was warmed to 60 °C, with stirring under, an atmosphere of argon. The

reaction mixture was then diluted with water and extracted with Et₂O (3x). The combined organic extracts were dried with Na₂SO₄, filtered and the filtrate concentrated *in vacuo* to give a red residue. The red residue was absorbed onto silica and applied to a silica column, eluting with petroleum ether (2 CV) and then with 20% Et₂O/petroleum ether (3 CV). The appropriate fractions were combined and reduced *in vacuo* to yield the dictyosphaerin *iso*-propyl ester **260** (32 mg, 0.082 mmol, 68 %) as a colourless oil.

IR ν (neat, cm⁻¹): 1730, 2856, 2926, 3477 (br).

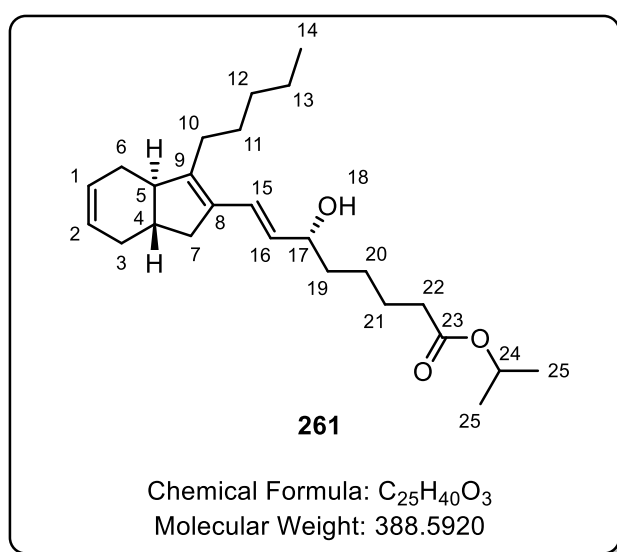
¹H NMR (600 MHz, Chloroform-*d*) δ 6.51 (d, *J* = 15.5 Hz, 1H, H-15), 5.78 – 5.70 (m, 2H, H-1 and H-2), 5.53 (dd, *J* = 15.5, 7.1 Hz, 1H, H-16), 4.99 (sept, *J* = 6.2 Hz, 1H, H-24), 4.18 (q, *J* = 6.6 Hz, 1H, H-17), 2.53 (dd, *J* = 14.1, 7.1 Hz, 1H, H-5), 2.38 – 2.20 (m, 6H, aliphatic protons), 2.13 – 1.93 (m, 3H, aliphatic protons), 1.88 (t, *J* = 13.3 Hz, 1H, aliphatic protons), 1.70 – 1.49 (m, 6H, aliphatic protons), 1.45 – 1.17 (m, 13H, aliphatic protons), 0.87 (t, *J* = 7.1 Hz, 3H, H-14). Hydroxyl proton was not observed.

¹³C NMR (151 MHz, Chloroform-*d*) δ 173.3, 145.7, 133.9, 131.3, 128.5, 127.0, 125.5, 73.3, 67.5, 49.5, 42.5, 37.2, 37.0, 34.7, 31.9, 31.4, 29.9, 28.4, 26.6, 25.1, 25.0, 22.6, 21.9, 14.1.

HRMS (ESI) *m/z* calculated for C₂₅H₄₀O₃ [M]: 388.2972 Found: 388.2999

$[\alpha]_D^{20}$ = -47.4° (c 1.5, Chloroform)

Preparation of *iso*-propyl (*R,E*)-6-hydroxy-8-((3*aR*,7*aS*)-3-pentyl-3*a*,4,7,7*a*-tetrahydro-1*H*-inden-2-yl)oct-7-enoate



Scheme 181

To a solution of enol triflate **248** (40 mg, 0.12 mmol) and (*R*)-hydroxy boronic ester **244** (76 mg, 0.24 mmol) in DMF (1.2 mL) was added Pd(dppf)Cl₂ (4 mg, 5.6 μmol) and subsequently K₃PO₄ (76 mg, 0.36 mmol). The resulting mixture was warmed to 60 °C, with stirring under, an atmosphere of argon. The reaction mixture was then diluted with water and extracted with Et₂O (3x). The combined organic extracts were dried with Na₂SO₄, filtered and the filtrate concentrated *in vacuo* to give a red residue. The red residue was absorbed onto silica and applied to a silica column, eluting with petroleum ether (2 CV) and then with 20% Et₂O/petroleum ether (3 CV). The appropriate fractions were combined and reduced *in vacuo* to yield the 6-epi-dictyosphaerin *iso*-propyl ester **261** (32 mg, 0.082 mmol, 68 %) as a colourless oil.

IR ν (neat, cm⁻¹): 1730, 2856, 2926, 3477 (br).

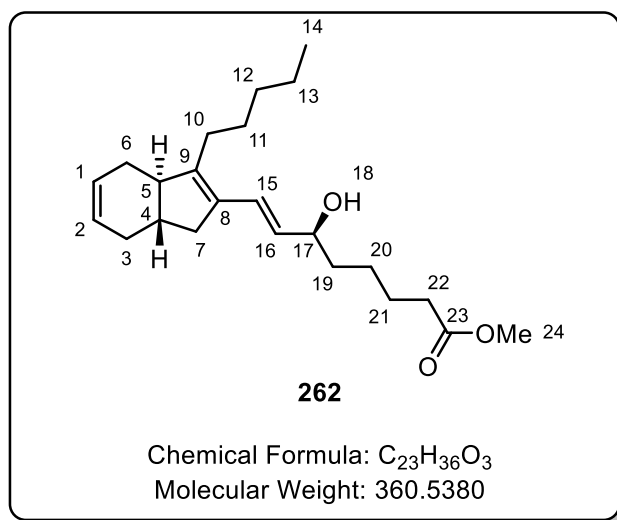
¹H NMR (600 MHz, Chloroform-*d*) δ 6.51 (d, *J* = 15.5 Hz, 1H, H-15), 5.80 – 5.69 (m, 2H, H-1 and H-2), 5.53 (dd, *J* = 15.5, 7.2 Hz, 1H, H-16), 4.99 (sept, *J* = 6.2 Hz, 1H, H-24), 4.18 (q, *J* = 6.7 Hz, 1H, H-17), 2.52 (dd, *J* = 14.1, 7.1 Hz, 1H, H-5), 2.35 – 2.21 (m, 6H, aliphatic protons), 2.09 – 1.95 (m, 3H, aliphatic protons), 1.89 (t, *J* = 13.3 Hz, 1H, aliphatic protons), 1.73 – 1.50 (m, 6H, aliphatic protons), 1.46 – 1.19 (m, 13H, aliphatic protons), 0.87 (d, *J* = 7.2 Hz, 3H, H-14). Hydroxyl proton was not observed.

¹³C NMR (151 MHz, Chloroform-*d*) δ 173.3, 145.8, 133.8, 131.3, 128.5, 127.0, 125.5, 73.3, 67.5, 49.5, 42.6, 37.2, 37.1, 34.7, 31.9, 31.4, 29.9, 28.5, 26.6, 25.1, 25.0, 22.6, 21.9, 14.1.

HRMS (ESI) *m/z* calculated for C₂₅H₄₀O₃ [M]: 388.2972 Found: 388.2999

$[\alpha]_D^{20}$ = -42.4° (c 1.5, Chloroform)

Preparation of dictyosphaerin methyl ester.¹



Scheme 181

The reaction was carried out as documented in the literature procedure.⁵⁴

To a stirred solution of dictyosphaerin *iso*-propyl ester **260** (30 mg, 0.077 mmol) in MeOH (0.75 mL) was added K₂CO₃ (54 mg, 0.39 mmol) and the resulting solution was allowed to stir for 6 h. The reaction mixture was quenched by the addition of a 10 % aqueous solution of citric acid and extracted with Et₂O (3x). The combined organic extracts were dried over Na₂SO₄, filtered and the filtrate concentrated *in vacuo* to give a colourless residue. The colourless residue was absorbed onto silica and applied to a silica column, eluting with petroleum ether (2 CV) and then with 20% Et₂O/petroleum ether (3 CV). The appropriate fractions were combined and reduced *in vacuo* to yield the dictyosphaerin methyl ester **262** (23 mg, 0.064 mmol, 83 %) as a colourless oil.

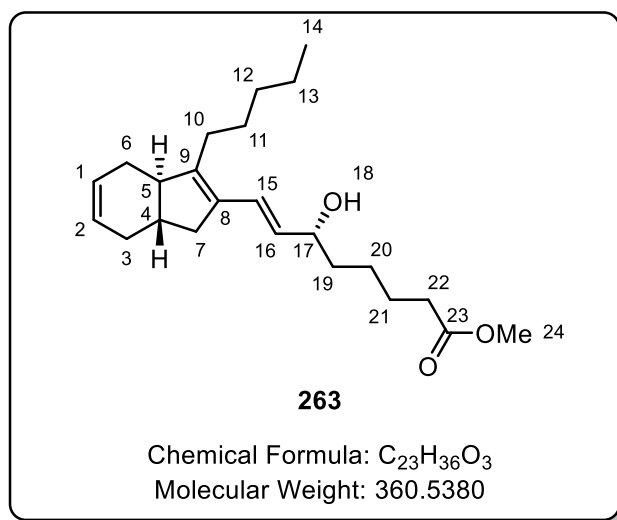
IR ν (neat, cm⁻¹): 1638, 1736, 2857, 2926, 3019, 3477 (br).

¹H NMR (600 MHz, Chloroform-*d*) δ 6.51 (d, *J* = 15.5 Hz, 1H, H-15), 5.84 – 5.65 (m, 2H, H-1 and H-2), 5.54 (dd, *J* = 15.5, 7.1 Hz, 1H, H-16), 4.18 (q, *J* = 6.6 Hz, 1H, H-17), 3.66 (s, 3H, H-24), 2.54 (dd, *J* = 14.1, 7.1 Hz, 1H, H-5), 2.41 – 2.21 (m, 5H, Aliphatic protons), 2.12 – 1.94 (m, 3H, Aliphatic protons), 1.89 (t, *J* = 13.2 Hz, 1H, Aliphatic protons), 1.71 – 1.50 (m, 6H, Aliphatic protons), 1.49 – 1.20 (m, 8H, Aliphatic protons), 0.88 (t, *J* = 7.0 Hz, 3H, H-14). Hydroxyl proton was not observed.

¹³C NMR (151 MHz, Chloroform-*d*) δ 174.2, 145.8, 133.9, 131.3, 128.5, 127.1, 125.5, 73.3, 51.6, 49.5, 42.5, 37.1, 37.0, 34.1, 31.9, 31.4, 29.9, 28.4, 26.6, 25.2, 24.9, 22.6, 14.1.

$[\alpha]_{\text{D}}^{20}$ = -47.26° (c 0.7, Chloroform)

Preparation of 6-*epi*-dictyosphaerin methyl ester.



Scheme 181

The reaction was carried out as documented in the literature procedure.⁵⁴

To a stirred solution of 6-*epi*-dictyosphaerin *iso*-propyl ester **261** (30 mg, 0.077 mmol) in MeOH (0.75 mL) was added K₂CO₃ (54 mg, 0.39 mmol) and the resulting solution was allowed to stir for 6 h. The reaction mixture was quenched by the addition of a 10 % aqueous solution of citric acid and extracted with Et₂O (3x). The combined organic extracts were dried over Na₂SO₄, filtered and the filtrate concentrated *in vacuo* to give a colourless residue. The colourless residue was absorbed onto silica and applied to a silica column, eluting with petroleum ether (2 CV) and then with 20% Et₂O/petroleum ether (3 CV). The appropriate fractions were combined and reduced *in vacuo* to yield the 6-*epi*-dictyosphaerin methyl ester **263** (18 mg, 0.050 mmol, 65 %) as a colourless oil.

IR ν (neat, cm⁻¹): 1638, 1736, 2857, 2926, 3019, 3437 (br).

¹H NMR (400 MHz, Chloroform-*d*) δ 6.51 (d, J = 15.5 Hz, 1H, H-15), 5.81 – 5.69 (m, 2H, H-1 and H-2), 5.54 (dd, J = 15.5, 7.2 Hz, 1H, H-16), 4.18 (q, J = 6.7 Hz, 1H, H-17), 3.66 (s, 3H, H-24), 2.53 (dd, J = 14.1, 7.1 Hz, 1H, H-5), 2.35 – 2.22 (m, 5H, Aliphatic protons), 2.12 – 1.96 (m, 3H, Aliphatic protons), 1.89 (t, J = 13.3 Hz, 1H, Aliphatic protons), 1.72 – 1.50 (m, 6H, Aliphatic protons), 1.47 – 1.23 (m, 8H, Aliphatic protons), 0.88 (t, J = 6.8 Hz, 3H, H-14). Hydroxyl proton was not observed.

¹³C NMR (101 MHz, Chloroform-*d*) δ 174.2, 145.8, 133.8, 131.3, 128.5, 127.1, 125.5, 73.4, 51.6, 49.5, 42.6, 37.2, 37.1, 34.1, 31.9, 31.4, 29.9, 28.5, 26.6, 25.2, 24.9, 22.6, 14.1.

$[\alpha]_D^{20}$ = -41.14° (c 0.7, Chloroform)

HRMS (ESI) m/z calculated for $C_{23}H_{35}O_3$ [M-H]⁻: 359.2581 Found: 359.2585

3.6. References

- (1) Rochfort, S. J.; Watson, R.; Capon, R. J. *J. Nat. Prod.* **1996**, *59*, 1154.
- (2) Grimblat, N.; Zanardi, M. M.; Sarotti, A. M. *J. Org. Chem.* **2015**, *80*, 12526.
- (3) Nolsøe, J. M. J.; Antonsen, S.; Görbitz, C. H.; Hansen, T. V.; Nesman, J. I.; Røhr, Å. K.; Stenstrøm, Y. H. *J. Org. Chem.* **2018**, *83*, 15066.
- (4) Ermanis, K.; Parkes, K. E. B.; Agback, T.; Goodman, J. M. *Org. Biomol. Chem.* **2017**, *15*, 8998.
- (5) Dudley, G. B.; Danishefsky, S. J. *Org. Lett.* **2001**, *3*, 2399.
- (6) Mc Murry, J. E.; Scott, W. J. *Tetrahedron Lett.* **1983**, *24*, 979.
- (7) Paquette, L. A.; Liang, S.; Wang, H.-L. *J. Org. Chem.* **1996**, *61*, 3268.
- (8) Cazeau, P.; Duboudin, F.; Moulines, F.; Babot, O.; Dunogues, J. *Tetrahedron* **1987**, *43*, 2075.
- (9) Nayyar, N. K.; Hutchison, D. R.; Martinelli, M. J. *J. Org. Chem.* **1997**, *62*, 982.
- (10) Ripin, D. H. B.; Bourassa, D. E.; Brandt, T.; Castaldi, M. J.; Frost, H. N.; Hawkins, J.; Johnson, P. J.; Massett, S. S.; Neumann, K.; Phillips, J.; Raggon, J. W.; Rose, P. R.; Rutherford, J. L.; Sitter, B.; Stewart, A. M.; Vetelino, M. G.; Wei, L. *Org. Process Res. Dev.* **2005**, *9*, 440.
- (11) Götz, K.; Liermann, J. C.; Thines, E.; Anke, H.; Opatz, T. *Org. Biomol. Chem.* **2010**, *8*, 2123.
- (12) Zhao, J.; Niu, Z.; Fu, H.; Li, Y. *Chem. Commun.* **2014**, *50*, 2058.
- (13) Parker, K. A.; Ledebøer, M. W. *J. Org. Chem.* **1996**, *61*, 3214.
- (14) Helal, C. J.; Magriotis, P. A.; Corey, E. J. *J. Am. Chem. Soc.* **1996**, *118*, 10938.
- (15) The Nobel Prize in Chemistry 2001
<https://www.nobelprize.org/prizes/chemistry/2001/summary/> (accessed Jul 22, 2019).
- (16) Matsumura, K.; Hashiguchi, S.; Ikariya, T.; Noyori, R. *J. Am. Chem. Soc.* **1997**, *119*, 8738.
- (17) Furuta, K.; Iwanaga, K.; Yamamoto, H. *Tetrahedron Lett.* **1986**, *27*, 4507.
- (18) Hrvatsko kemijsko društvo., M.; Hrvatsko prirodoslovno društvo., I.; Sveučilište u Zagrebu., M.; Bartolinčić, A.; Vinković, V. *Croat. Chem. Acta* **1956**, *80*, 109.
- (19) Mohamadi, F.; Richards, N. G. J.; Guida, W. C.; Liskamp, R.; Lipton, M.; Caufield, C.; Chang, G.; Hendrickson, T.; Still, W. C. *J. Comput. Chem.* **1990**, *11*, 440.

- (20) Maestro (Version 11.5). Schrödinger, LLC: New York 2018.
- (21) Chang, G.; Guida, W. C.; Still, W. C. *J. Am. Chem. Soc.* **1989**, *111*, 4379.
- (22) Halgren, T. A. *J. Comput. Chem.* **1996**, *17*, 490.
- (23) Halgren, T. A. *J. Comput. Chem.* **1996**, *17*, 520.
- (24) Halgren, T. A. *J. Comput. Chem.* **1996**, *17*, 553.
- (25) Halgren, T. A. *J. Comput. Chem.* **1999**, *20*, 730.
- (26) Halgren, T. A. *J. Comput. Chem.* **1996**, *17*, 616.
- (27) Halgren, T. A. *J. Comput. Chem.* **1999**, *20*, 720.
- (28) Halgren, T. A.; Nachbar, R. B. *J. Comput. Chem.* **1996**, *17*, 587.
- (29) Stephens, P. J.; Devlin, F. J.; Chabalowski, C. F.; Frisch, M. J. *J. Phys. Chem.* **1994**, *98*, 11623.
- (30) Lee, C.; Yang, W.; Parr, R. G. *Phys. Rev. B* **1988**, *37*, 785.
- (31) Becke, A. D. *Phys. Rev. A* **1988**, *38*, 3098.
- (32) Becke, A. D. *J. Chem. Phys.* **1993**, *98*, 5648.
- (33) Hehre, W. J.; Radom, L.; P. v. R. Schleyer; Pople, J. A. *Ab Initio Molecular Orbital Theory*; John Wiley & Sons, Ltd: New York, 1986; Vol. 7.
- (34) Ditchfield, R. *J. Chem. Phys.* **1972**, *56*, 5688.
- (35) Wolinski, K.; Hinton, J. F.; Pulay, P. *J. Am. Chem. Soc.* **1990**, *112*, 8251.
- (36) Adamo, C.; Barone, V. *J. Chem. Phys.* **1998**, *108*, 664.
- (37) Frisch, M. J.; Trucks, G. W.; Schlegel, H. B.; Scuseria, G. E.; Robb, M. A.; Cheeseman, J. R.; Scalmani, G.; Barone, V.; Petersson, G. A.; Nakatsuji, H.; Li, X.; Caricato, M.; Marenich, A.; Bloino, J.; Janesko, B. G.; Gomperts, R.; Mennucci, B.; Hratchian, H. P.; Ortiz, J. V.; Izmaylov, A. F.; Sonnenberg, J. L.; Williams-Young, D.; Ding, F.; Lipparini, F.; Egidi, F.; Goings, J.; Peng, B.; Petrone, A.; Henderson, T.; Ranasinghe, D.; Zakrzewski, V. G.; Gao, J.; Rega, N.; Zheng, G.; Liang, W.; Hada, M.; Ehara, M.; Toyota, K.; Fukuda, R.; Hasegawa, J.; Ishida, M.; Nakajima, T.; Honda, Y.; Kitao, O.; Nakai, H.; Vreven, T.; Throssell, K.; Montgomery, J. A.; Jr., J. E. P.; Ogliaro, F.; Bearpark, M.; Heyd, J. J.; Brothers, E.; Kudin, K. N.; Staroverov, V. N.; Keith, T.; Kobayashi, R.; Normand, J.; Raghavachari, K.; Rendell, A.; Burant, J. C.; Iyengar, S. S.; Tomasi, J.; Cossi, M.;

- Millam, J. M.; Klene, M.; Adamo, C.; Cammi, R.; Ochterski, J. W.; Martin, R. L.; Morokuma, K.; Farkas, O.; Foresman, J. B.; Fox, D. J. Gaussian 09, Revision A.02. Gaussian, Inc.: Wallingford CT 2016.
- (38) Zhao, Y.; Truhlar, D. G. *Theor. Chem. Acc.* **2008**, *120*, 215.
- (39) Love, B. E.; Jones, E. G. *J. Org. Chem.*, **1999**, *64*, 3755.
- (40) Mamedov, E. G. *Russ. J. Org. Chem.* **2007**, *43*, 184.
- (41) Hufford, D. L.; Tarbell, D. S.; Koszalka, T. R. *J. Am. Chem. Soc.* **1952**, *74*, 3014.
- (42) Bennie, L. S. The Development and Application of Magnesium Amide Bases in Asymmetric Synthesis, University of Strathclyde, 2012.
- (43) Weber, T. The Development and Application of Magnesium Base-Mediated Transformations., University of Strathclyde, 2013.
- (44) Aube, J.; Ghosh, S.; Tanol, M. *J. Am. Chem. Soc.* **1994**, *116*, 9009.
- (45) Sloan, G. Extended Application of Magnesium Amide Base Reagents in Target Synthesis, University of Strathclyde, 2014.
- (46) Goto, R.; Okura, K.; Sakazaki, H.; Sugawara, T.; Matsuoka, S.; Inoue, M. *Tetrahedron* **2011**, *67*, 6659.
- (47) Liu, S.; Zeng, X.; Xu, B. *Tetrahedron Lett.* **2016**, *57*, 3706.
- (48) Fang, G. Y.; Aggarwal, V. K. *Angew. Chemie Int. Ed.* **2007**, *46*, 359.
- (49) Robert, C.; de Montigny, F.; Thomas, C. M. *ACS Catal.* **2014**, *4*, 3586.
- (50) Shuttleworth, S. J.; Silva, F. A.; Tomassi, C. D.; Cecil, A. R. L.; Hill, T. J. Spiruchostatin Analogues and Their Therapeutic Use. GB20090008873 20090522, 2009.
- (51) Yan, J.; Travis, B. R.; Borhan, B. *J. Org. Chem.* **2004**, *69*, 9299.
- (52) Ungeheuer, F.; Fürstner, A. *Chem. - A Eur. J.* **2015**, *21*, 11387.
- (53) Gallantree-Smith, H. C.; Antonsen, S. G.; Görbitz, C. H.; Hansen, T. V.; Nolsøe, J. M. J.; Stenstrøm, Y. H. *Org. Biomol. Chem.* **2016**, *14*, 8433.
- (54) Shankar, M.; Mohan, H. R.; Prasad, U. V.; Krishna, M. H.; Rao, P. M.; Lakshmikumar, T.; Subbaraju, G. V. *Asian J. Chem.* **2013**, *25*, 913.